

2018 GIF Symposium Proceedings



THE GENERATION IV INTERNATIONAL FORUM

Established in 2001, the Generation IV International Forum (GIF) was created as a co-operative international endeavour seeking to develop the research necessary to test the feasibility and performance of fourth generation nuclear systems, and to make them available for industrial deployment by 2030. The GIF brings together 13 countries (Argentina, Australia, Brazil, Canada, China, France, Japan, Korea, Russia, South Africa, Switzerland, the United Kingdom and the United States), as well as Euratom – representing the 28 European Union members – to co-ordinate research and development on these systems. The GIF has selected six reactor technologies for further research and development: the gas-cooled fast reactor (GFR), the lead-cooled fast reactor (LFR), the molten salt reactor (MSR), the sodium-cooled fast reactor (SFR), the supercritical-water-cooled reactor (SCWR) and the very-high-temperature reactor (VHTR).

NUCLEAR ENERGY AGENCY

The OECD Nuclear Energy Agency (NEA) was established on 1 February 1958. Current NEA membership consists of 33 countries: Argentina, Australia, Austria, Belgium, Canada, the Czech Republic, Denmark, Finland, France, Germany, Greece, Hungary, Iceland, Ireland, Italy, Japan, Luxembourg, Mexico, the Netherlands, Norway, Poland, Portugal, Korea, Romania, Russia, the Slovak Republic, Slovenia, Spain, Sweden, Switzerland, Turkey, the United Kingdom and the United States. The European Commission and the International Atomic Energy Agency also take part in the work of the Agency.

The mission of the NEA is:

- to assist its member countries in maintaining and further developing, through international co-operation, the scientific, technological and legal bases required for a safe, environmentally sound and economical use of nuclear energy for peaceful purposes;
- to provide authoritative assessments and to forge common understandings on key issues as input to government decisions on nuclear energy policy and to broader OECD analyses in areas such as energy and the sustainable development of low-carbon economies.

Specific areas of competence of the NEA include the safety and regulation of nuclear activities, radioactive waste management and decommissioning, radiological protection, nuclear science, economic and technical analyses of the nuclear fuel cycle, nuclear law and liability, and public information. The NEA Data Bank provides nuclear data and computer program services for participating countries.

The Nuclear Energy Agency serves as technical secretariat to GIF.

Generation IV International Forum

2018 GIF SYMPOSIUM PROCEEDINGS

Foreword

With the adoption of the Paris Agreement in 2015, almost all signatories agreed to set nationally determined limits on greenhouse gas emissions, with the aim of limiting the increase of the global mean surface temperature at the end of the century to below 2°C relative to pre-industrial levels. To reach this goal, carbon dioxide (CO₂) emissions from electricity generation must fall to nearly zero by the middle of this century, even as electricity needs worldwide continue to grow and expand in end uses such as transportation, heating and industrial energy use.

The International Atomic Energy Agency (IAEA) has addressed the actual situation concerning the climate emergency and the need to promote nuclear power as part of the solution:

Nuclear power is a low-carbon source of energy. In 2018, nuclear power produced about 10% of the world's electricity. Together with the expansion of renewable energy sources and switching from coal to natural gas as fuel, higher nuclear power production contributed to the reduction of global CO₂ emissions. Clearly, nuclear power – as a low carbon source of electricity – can play a key role in the transition to a clean energy future.

Since the beginning of this century, we have worked within our Generation IV International Forum (GIF) organization to study and develop future nuclear systems based on technological innovation and strong international co-operation. Challenges faced by the nuclear industry were identified, include safety concerns as well as cost and regulatory uncertainties in an evolving context, attempting to define what the future energy mix will be...

In the 20-year history of the Forum, the first Symposium took place in 2009 and gathered the whole GIF community. Occurring every three years, the 2018 symposium was held in Paris, France, over 15-17 October.

The 2018 Symposium addressed classical topics like safety, security, research infrastructures, technology, operation, maintenance and simulation, as well as on-going studies regarding progresses on the different Generation IV systems.

Special aspects of the 2018 Symposium dealt with human capital development, such as webinars which were put in place. The integration of these Generation IV systems in the future low carbon energy mix was also addressed in a specific session.

On a personal note, it was an honor for me to have a leading role in organizing this Symposium. But I could not have done it alone. An international scientific program committee was established to achieve this goal and I am profoundly grateful to its members, who contributed to make this Symposium a success. I would also like to thank the OECD Nuclear Energy Agency (NEA) for their help as well as Pascal Terrasson, François Storrer and Gilles Rodriguez for their support and contribution.



Eric Abonneau

Table of contents

TRACKS 1 AND 2: PROGRESS ON GEN IV SYSTEMS.....	7
ADVANCES IN THE GIF VERY HIGH TEMPERATURE REACTOR SYSTEM (M. A. FÜTERER ET AL).....	9
THE GENERATION-IV LEAD-COOLED FAST REACTOR ACTIVITIES (A.ALEMBERTI ET AL).....	23
IMPLEMENTATION OF THE GEN-IV REQUIREMENTS IN THE BN-1200 DESIGN (B.VASILIEV ET AL).....	35
AN UPDATE ON THE DEVELOPMENT STATUS OF THE SUPER-CRITICAL WATER-COOLED REACTORS (L. K. H. LEUNG ET AL)	43
ADVANCEMENT IN THERMAL-HYDRAULICS AND SAFETY R&D SUPPORTING DEVELOPMENT OF SUPER-CRITICAL WATER-COOLED REACTORS (L. K. H. LEUNG ET AL).....	51
10 YEARS' OVERVIEW OF A SUCCESSFUL CONTRIBUTION OF EURATOM TO GENERATION IV INTERNATIONAL FORUM (S. ABOUSAHL ET AL).....	59
THERMAL-HYDRAULIC PERFORMANCE OF ALTERNATIVE NUCLEAR FUELS FOR THE HPLWR (L. CASTRO ET AL).....	75
THE SIGNIFICANT COLLABORATION OF JAPAN AND FRANCE ON THE DESIGN OF ASTRID SODIUM FAST REACTOR SINCE 2014 (F. VARAINE ET AL).....	85
ASTRID PROJECT, OVERVIEW AND STATUS PROGRESS (F. VARAINE ET AL).....	91
VHTR TECHNOLOGY DEVELOPMENT IN JAPAN – Progress of R&D Activities for GIF VHTR System – (T. SHIBATA ET AL).....	99
STATUS OF CURRENT KNOWLEDGE AND DEVELOPMENTS IN FRANCE ON MOLTEN SALT REACTORS (J. GUIDEZ ET AL).....	107
STRATEGY AND R&D STATUS OF CHINA LEAD-BASED REACTOR (Y. WU).....	117
MOLTEN-SALT REACTOR AS NECESSARY ELEMENT FOR THE CLOSURE OF THE NUCLEAR FUEL CYCLE FOR ALL ACTINIDES (V. IGNATIEV ET AL).....	123
THREE DIMENSIONAL TRANSIENT ANALYSIS FOR CONTROL RODS DROP INTO CSR1000 CORE (W. LIANJIET ET AL).....	131
PROGRESS IN GFR TECHNOLOGY (B. HATALA ET AL).....	137
PAST, PRESENT AND FUTURE OF SCWR DEVELOPMENT IN CANADA (L. K. H. LEUNG ET AL).....	143
CURRENT PROGRESS IN EXPERIMENTAL DEVELOPMENT OF MSR AND FHR TECHNOLOGIES (J. UHLIR ET AL).....	153
SUBCHANNEL ANALYSIS OF A LBE-COOLED FAST REACTOR BLESS (C. SUN ET AL).....	159
NUMERICAL AND EXPERIMENTAL THERMAL HYDRAULICS STUDIES OF HIGH TEMPERATURE MOLTEN SALTS FOR GENERATION IV NUCLEAR REACTORS (P. RUBIOLO ET AL).....	165
TRACK 3 : HUMAN CAPITAL DEVELOPMENT	175
GIF WEBINARS: AN ONLINE EDUCATIONAL RESOURCE (P. PAVIET ET AL).....	177
TEACHING SODIUM FAST REACTORS IN CEA (C. LATGE ET AL).....	183

TRACK 4: RESEARCH INFRASTRUCTURES	189
THE DEVELOPMENT AND COMMISSIONING OF THE LIQUID LEAD LABORATORY (LILLA) FOR MECHANICAL TESTING IN LIQUID LEAD (Z. SZARAZ ET AL)	191
R&D EXPERIMENTAL CAPABILITIES FOR ADVANCING GIF SCWR SYSTEM IN THE NEXT DECADE (L. K. H. LEUNG ET AL)	199
INTRODUCTION ON SOME EXPERIMENTAL FACILITIES FOR VHTR SYSTEM (Y. ZHENG)	209
DEVELOPMENT AND LICENSING OF A MOLTEN SALT TEST REACTOR, TMSR-LF1 (K. CHEN)	217
GENERATION-IV SYSTEMS' EXPERIMENTAL INFRASTRUCTURE NEEDS (R. GARBIL ET AL)	221
TRACK 5: SAFETY AND SECURITY	237
NEW SAFETY MEASURES PROPOSED FOR EUROPEAN SODIUM FAST REACTOR IN HORIZON-2020 ESFR-SMART PROJECT (J. GUIDEZ ET AL)	239
APPLICATION OF PRACTICAL ELIMINATION APPROACH FOR GEN IV REACTORS DESIGN (J. GUIDEZ ET AL)	249
GIF RISK AND SAFETY WORKING GROUP: APPLICATION OF THE ISAM METHODOLOGY TO GEN-IV NUCLEAR SYSTEMS (Y. OKANO ET AL)	253
TRACK 6: FUELS AND MATERIALS FOR GEN IV SYSTEMS	263
HTR-STAP PROGRAM PACKAGE: SOURCE TERM ANALYSIS CODES FOR PEBBLE-BED HIGH-TEMPERATURE GAS-COOLED REACTOR (H. CHEN ET AL)	265
THE GIF PROLIFERATION RESISTANCE AND PHYSICAL PROTECTION WORKING GROUP (PRPPWG): ACHIEVEMENTS AND PERSPECTIVES (G. G. M. COJAZZI ET AL)	275
REPORT ON MANUFACTURING EXPERIMENTAL APPARATUS TO INVESTIGATE SWR PHENOMENON IN THE PCSG (S. SEO ET AL)	285
STUDY ON RISK ANALYSIS METHODOLOGY OF FIRE BARRIER FAILURE CAUSED BY SEISMIC-INDUCED SODIUM FIRE IN SODIUM FAST REACTOR (J. JIANG ET AL)	293
DESIGN AND SAFETY STUDIES OF THE MOLTEN SALT FAST REACTOR CONCEPT IN THE FRAME OF THE SAMOFAR H2020 PROJECT (E. MERLE ET AL)	299
DEVELOPMENT OF ODS TEMPERED MARTENSITIC STEEL FOR HIGH BURN UP FUEL CLADDING TUBE OF SFR (S. OHTSUKA ET AL)	305
PHYSICAL PROPERTIES OF NON-STOICHIOMETRIC (U, PU)O₂ (M. WATANABE ET AL)	315
OXYGEN POTENTIAL AND SELF-IRRADIATION EFFECTS ON FUEL TEMPERATURE IN AM-MOX (Y. IKUSAWA ET AL)	321
HEAT CAPACITY OF UC FROM FIRST PRINCIPLES (D. LEGUT ET AL)	329
OPTIMISATION OF MANUFACTURING PROCESS OF FUNCTIONALLY GRADED COMPOSITE STEELS FOR LEAD-BISMUTH COOLED FAST REACTOR CLADDING APPLICATION (J. LEE ET AL)	333
EVALUATION OF PILGERING PROCESS OF FUNCTIONALLY GRADED COMPOSITE TUBE FOR LEAD-BISMUTH EUTECTIC COOLED FAST REACTOR THROUGH FINITE ELEMENT ANALYSIS (T. KIM ET AL)	339
DEVELOPMENT AND ASSESSMENT OF MATERIALS FOR THE GENERATION IV NUCLEAR REACTORS: A BRIEF OVERVIEW OF RESEARCH IN AUSTRALIA (O. MURANSKY ET AL)	345
TRACK 7: ADVANCED COMPONENTS	355
GEN WORKSHOP 64: AN INNOVATIVE WAY TO WORK ON A HARMONISED SET OF RULES FOR GEN-IV REACTORS (C. PETESCH ET AL)	357

USE OF CAD MODELS IN ESFR-SMART EU PROJECT (J. BODI ET AL)	363
STATUS OF THE ASTRID GAS POWER CONVERSION SYSTEM OPTION (D. PLANCQ ET AL)	369
CODES AND STANDARDS DEVELOPMENT FOR NEXT GENERATION SODIUM-COOLED FAST REACTORS IN JAPAN (T. ASAYAMA ET AL)	379
INNOVATIVE SODIUM FAST REACTORS CONTROL ROD DESIGNS (H. GUO ET AL)	385
TRACK 8: INTEGRATION OF GEN IV REACTORS IN LOW CARBON ENERGY SYSTEM	393
OPTIMAL ENERGY STORAGE SYSTEM FOR THE AHTR TECHNOLOGY (O. P. RAKERENG ET AL)	395
BASE-LOAD NUCLEAR REACTORS WITH HEAT STORAGE TO BUY AND SELL ELECTRICITY: INTEGRATING NUCLEAR AND RENEWABLES (C. FORSBERG)	403
SMALL MODULAR LFR: CONSTRUCTION COST FEATURES AND COMPARISON WITH PWR (S. BOARIN ET AL)	415
EMWG POSITION PAPER ON THE IMPACT OF INCREASING SHARE OF RENEWABLES ON THE DEPLOYMENT OF GENERATION IV NUCLEAR SYSTEMS (A. MENDOZA ET AL)	425
TRACK 9: DECOMMISSIONING & WASTE MANAGEMENT	437
TRACK 10: OPERATION, MAINTENANCE, SIMULATION, TRAINING	439
IN SERVICE INSPECTION AND REPAIR DEVELOPMENTS FOR SFRS (F. BAQUÉ ET AL)	441
PAPERS WITH NO TRACK	459
DEVELOPING A MOLTEN SALT REACTOR SAFEGUARDS MODEL (B. CIPITI ET AL)	461
CORROSION BEHAVIOR OF 310S IN SUPERCRITICAL WATER (B. GONG ET AL)	467
THE USA'S ADVANCED REACTOR TECHNOLOGIES (ART) GRAPHITE R&D PROGRAM (W. WINDES ET AL)	477
DEVELOPMENT OF SAFETY DESIGN GUIDELINES ON STRUCTURES, SYSTEMS AND COMPONENTS FOR GENERATION IV SODIUM-COOLED FAST REACTOR SYSTEMS (S. KUBO ET AL)	485
ECONOMIC AND FINANCIAL ANALYSIS OF A LEAD-COOLED SMALL MODULAR REACTOR (SMR) (C. PIETTE ET AL)	495
Appendix A: Financial Statements	519

TRACKS 1 AND 2: PROGRESS ON GEN IV SYSTEMS

ADVANCES IN THE GIF VERY HIGH TEMPERATURE REACTOR SYSTEM (M. A. FÜTERER ET AL)

Michael A. Fütterer⁽¹⁾, Fu Li⁽²⁾, Hans Gougar⁽³⁾, Lyndon Edwards⁽⁴⁾, Manuel A. Pouchon⁽⁵⁾,
Minhwan Kim⁽⁶⁾, Franck Carré⁽⁷⁾, Hiroyuki Sato⁽⁸⁾

(1) European Commission - Joint Research Centre, the Netherlands.

(2) INET, Tsinghua University, China.

(3) Idaho National Laboratory, United States.

(4) ANSTO, Australia.

(5) PSI, Switzerland.

(6) KAERI, Republic of Korea.

(7) CEA, DEN, France.

(8) JAEA, Japan.

Abstract

This paper provides an update on the international effort in the development of the Very High Temperature Reactor (VHTR) system pursued through international collaboration between 8 countries in the Generation IV International Forum (GIF), and an outlook on future R&D. The versatility of the VHTR enables it to be designed with inherent safety characteristics and optimised for both electric and non-electric applications, in particular for cogeneration of heat and power. Recent highlights from the four currently active GIF VHTR R&D projects are provided and placed into the context of the related national programs. Based on VHTR's relatively high technology readiness level, orientations for future R&D are outlined and will contribute to further enhancing the system's market readiness level.

I. Introduction

The VHTR system international collaboration pursues R&D towards technology demonstration between 8 countries in the Generation IV International Forum (GIF). The initial motivations to develop this reactor type are summarised and several of the more recent targeted cogeneration applications of VHTR power are addressed. The inherent safety characteristics of the VHTR are a precious asset enabling the technology to answer today's desire to further enhance nuclear safety and energy security as well as to reduce fossil fuel usage. Cooperation in the frame of GIF is clearly beneficial for all project partners. Initially, a wealth of historical experience was collected and shared in the form of documents, presentations at dedicated workshops, and even including fuel and material samples. In the further course of project execution, time, effort and scarce facilities (such as irradiation

space or hot cell equipment) are shared. These expedite progress and create synergies. Recent highlights from the four currently active GIF VHTR R&D projects (Materials, Fuel and Fuel Cycle, Hydrogen Production, Computational Methods Validation and Benchmarks) are then described and placed into the context of the related national programs. The majority of these programs currently focus on licensing requirements for demonstrators of near term steam production scenarios for power generation and industrial process heat applications while more aggressive, longer term and higher temperature applications are mainly pursued to enable thermochemical production of bulk hydrogen. Based on the VHTR's relatively high technology readiness level, orientations for future R&D are outlined that will enhance the system's market readiness level further. Focus is placed on System Integration and Assessment, Safety Analysis and Demonstration, Waste Minimisation and Cost Reductions.

Table 1. Market for HTGR process heat [28]

Region	Plug-in market	Total market	GDP 2011 (approx.)
Europe	~ 800 TWh/y (EUROPAIRS)	~ 3,000 TWh/y (EUROPAIRS)	17,000 bn€ / 25% of world
USA	~ 1,100 TWh/y (MPR Associates)	~ 3,600 TWh/y (MPR Associates)	15,000 bn€ / 22% of world
Japan		1,000 – 1,400 TWh/y (est.)	5,900 bn€ / 8% of world
China		1,200 – 1,700 TWh/y (est.)	7,000 bn€ / 10% of world
India		300 – 500 TWh/y (est.)	2,000 bn€ / 3% of world
Russia		300 – 500 TWh/y (est.)	2,000 bn€ / 3% of world
World total	3,000 – 5,000 TWh/y ~ 370 – 630 GWh	11,000 – 16,000 TWh/y	69,000 bn€

II. Technical Characteristics

High or Very High Temperature Reactors were developed and operated between the 1960s-1990s, two are currently operational (HTR-10 is running and HTTR is awaiting regulator approval to restart), and two reactors are under construction (HTR-PM). They are characterised by fully ceramic coated particle fuel, the use of graphite as neutron moderator and helium as coolant. All modern designs feature passive decay heat removal capability resulting in inherent safety. They are generally conceived as modular SMRs and are particularly suitable for the highly efficient cogeneration of process heat and power. Several such reactors have already operated routinely in the reactor outlet temperature range 700-850°C. Furthermore, operational experience has also been gained in two reactors for longer periods of time up to 950°C which is presently considered a limit for today's structural alloys. Beyond this temperature, new structural materials are required.

The initial driver for the VHTR in GIF was the desire of several signatories to develop a reactor capable of powering CO₂-free bulk hydrogen production facilities using the thermochemical iodine-sulphur cycle. This process consumes heat at a temperature of 850°C thus, taking due account of heat transfer cascades, it would require a reactor outlet temperature of approx. 1000°C. This remains a long-term target of the GIF VHTR System. At the same time, efforts are continuing to reduce the temperature

requirements of H₂ production (by using catalysts or different processes) and to apply innovative heat transfer technology such that the reactor itself can operate at the lowest possible temperature.

In addition to hydrogen production, more recent market research in several of the signatory countries has shown that process heat, mostly in the form of steam < 600°C ("plug-in" market, cf. Table 1), represents a very significant existing market in all industrialised countries, globally several hundred GWh, which today is almost entirely fossil-fueled. For such an application, a moderate reactor outlet temperature of approx. 750°C would be sufficient. The technology basis for the VHTR had been established in former high-temperature gas reactors such as Dragon (UK), the US Peach Bottom and Fort Saint-Vrain power plants, the German AVR and THTR prototypes, and the Japanese HTTR and Chinese HTR-10 test reactor. These reactors represent the two baseline concepts for the VHTR core: the prismatic block-type and the pebble-bed type. Initially, low-enriched uranium fuel at very-high burnup will be used in a once-through mode, while plutonium- or thorium-based fuels are longer term options. Several solutions are being investigated to adequately manage the back-end of the fuel cycle. The potential for a closed or symbiotic fuel cycle (of the U-Pu type or the Th-U type) was investigated in several studies (e.g. in the projects GT-MHR, Deep Burn, PUMA etc.) and will require the demonstration of reprocessing,

specifically a head-end process for making the TRISO coated particle fuel accessible [31], [32]. Although various fuel designs are considered in the VHTR systems, all exhibit similarities allowing for a coherent R&D approach with TRISO-coated particle fuel as the common denominator. This fuel form is composed of small kernels of fissile ceramic material (typically UO_2 or UCO), surrounded by a porous carbon buffer, and coated with three layers: pyrocarbon/silicon carbide/pyrocarbon. As demonstrated in many experimental and operational performance tests, this coating represents a very efficient barrier against fission product release under both normal and accident conditions.

In the past, both the AVR and HTTR reactors already demonstrated operation up to 950°C for long periods of time. A VHTR could currently be designed to deliver heat and electricity over a range of core outlet temperatures between 700 and 950°C , and possibly up to or more than 1000°C in the future. The available high-temperature alloys used for heat exchangers and metallic components determine the current temperature range of VHTR (700 - 950°C).

In current or near-term projects of VHTR design and construction, the reactor delivers heat to steam generators which feed an indirect Rankine cycle for power conversion using the latest available technology from conventional power plants. However, direct helium gas turbine or indirect (gas mixture turbine) Brayton-type cycles could be utilised in the future. The experimental reactors HTTR (Japan, 30 MWth, awaiting regulator approval for restart) and HTR-10 (China, 10 MWth, operating) support the advanced reactor concept development for the VHTR. They provide important information for the demonstration and analysis of safety and operational features. This allows improving the analytical tools for design and licensing of commercial-size demonstration VHTRs. The HTTR, in particular, will provide a platform for coupling advanced hydrogen production technologies with a nuclear heat source at temperatures as high as 950°C .

Globally, the technology is being advanced through near- and medium-term projects, such as HTR-PM, NGNP, GT-MHR, NHDD and GTHTR300C, led by several start-ups, plant vendors and national laboratories respectively in China, the United States, South Korea and Japan. The construction of the HTR-PM demonstration plant in China (two pebble-bed reactor modules with 250 MWth each delivering

steam to a single super-heated steam turbine generating 200 MWe) started on 9 December 2012. The reactor outlet temperature will be 750°C , which is well within the limits of the current state-of-the-art for materials and components, yet suitable for the generation of high-quality steam of 566°C . The HTR-PM demonstration plant is planned to be synchronised to the grid by the end of 2019, representing a major step towards the deployment of Generation IV technology.

III. The VHTR System in GIF

The GIF VHTR system is currently running four R&D projects, namely "Materials", "Fuel and Fuel Cycle", "Hydrogen Production", "Computational Methods, Validation and Benchmarking". Major R&D achievements in response to the R&D challenges as identified in the 2014 Technology Roadmap Update and in the 2018 GIF R&D Outlook are briefly summarised. References, documenting highlights, are given only indicatively and are not exhaustive. A comprehensive Status Report was published in 2014 [2] and more detail on project achievements is available in the GIF Annual Report 2017 [29].

In addition to the restricted information exchanged on the GIF platform, much of the progress made on the VHTR system internationally is reported since 2002 every two years in the HTR conference series [1], and several papers at this conference will provide technical details on progress.

III.A. Fuel and fuel cycle

The VHTR fuel cycle will initially be a once-through fuel cycle specified for high burn-up (150 - 200 GWd/tHM) using low enriched uranium. The used fuel, fuel cycle, enrichment and target burn-up are the result of an overall cost optimisation which may differ from one country to another. Solutions to improve the fuel cycle back-end have been developed, while the possible use of thorium for a closed thorium-uranium fuel cycle is considered a longer term option.

The two alternate (pebble or prismatic) fuel designs have many technologies in common that allow for a unified R&D approach. The well-known UO_2 TRISO-coated particle fuel (with a UO_2 kernel and SiC/PyC coatings) is the origin of the VHTR's benign safety performance and may be used in either, or it may be further enhanced with a UCO fuel kernel (as shown by

the US program) and/or advanced coatings through additional research.

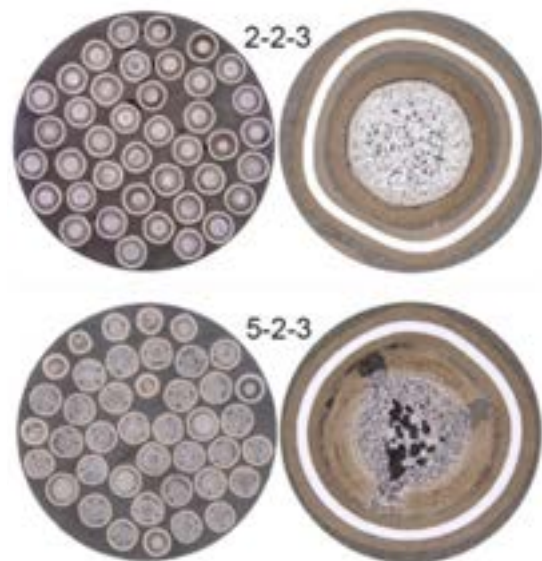
The primary emphasis in fuel development was on performance at high burn-up, power density, and temperature. The R&D broadly addressed manufacture and characterisation, quality assurance methods, irradiation performance and accident behavior. Irradiation tests provided the data on coated particle fuel and fuel element performance under irradiation necessary to support fabrication process development, to qualify the fuel design, and to support development and validation of models and computer codes on fission product transport which are relevant for safety assessment and licensing [3], [4], [5], [6], [7]. They also provided irradiated fuel and materials samples for post-irradiation and safety testing which is done to confirm that the fuel remains leak tight against fission product escape in all normal, transient or accident conditions (beyond design basis) where small fractions of the core can reach temperatures of the order of 1600°C.

In the US, PIE of the AGR-2 and AGR-3/4 experiments is still in progress both at Idaho National Laboratory (INL) and Oak Ridge National Laboratory (ORNL). Ongoing AGR-2 PIE consists of destructive compact examinations, including deconsolidation-leach-burn-leach analysis, gamma counting of individual particles, finding and analysing particles with failed SiC, non-destructive particle X-ray analysis, and particle microanalysis. UCO particle morphologies and microstructures generally have appeared similar to what was observed with the earlier AGR-1 irradiation experiment. Optical microscopy of a number of particles from different compacts indicated that the higher irradiation temperatures achieved in AGR-2 Capsule 2 resulted in less buffer fracture, presumably due to thermal creep allowing more stress relaxation than at lower temperatures. Figure 2 shows representative morphologies of particles from Compact 2-2-3 (time-average, volume-average irradiation temperature of 1261°C) and Compact 5-2-3 (1108°C). Note the increased occurrence of buffer fracture in Compact 5-2-3. In addition, detailed microanalysis of irradiated particles at relatively low length-scales using electron beam instruments is being performed to examine the migration of fission products in the coating layers.

The AGR-3/4 PIE currently in progress includes analysis of fission products on the capsule components to help quantify total fission

product release from the fuel, destructive examination of fuel compacts to examine the state of the particles and the distribution of fission products within the fuel, and heating tests to evaluate fission product transport at elevated temperatures. Fuel compact destructive examination begins with deconsolidation-leach-burn-leach analysis. This is more complex for the AGR-3/4 compacts than for standard cylindrical fuel compacts (such as those from the AGR-1 and AGR-2 experiments), because of the inclusion of “designed-to-fail” (DTF) particles in the AGR-3/4 compacts. Compacts must be deconsolidated such that the DTF particles are avoided, as they would be dissolved and overwhelm the solution activity, making measurement of fission product inventory in the compact matrix impossible. To achieve this, a method of radially deconsolidating the compacts has been developed and deployed in the hot cell at INL. This approach removes sequential, thin regions around the compact circumference, allowing intact TRISO particles to be collected and fission product inventory in the matrix to be measured while avoiding the DTF particles along the compact centerline. Three compacts have been deconsolidated to date.

Figure 1. Particle ensembles (left) and representative particles (right) from two AGR-2 compacts irradiated at time-average, volume-average temperatures of 1261°C (Compact 2-2-3, top) and 1108°C (Compact 5-2-3, bottom)



AGR-3/4 heating tests will include fuel compacts, fuel bodies (i.e., intact capsule internals consisting of fuel compacts surrounded by matrix and graphite rings), and individual matrix/graphite rings. The objective in all cases is to better understand fission product transport in the fuel and in matrix and graphite at elevated temperatures. Two AGR-3/4 compact heating tests in pure helium have been completed (one at an isothermal temperature of 1400°C, the other involving isothermal holds at 1600 and 1700°C). Additional tests are planned in the next several years.

The final fuel qualification irradiation for the AGR program is AGR-5/6/7. This experiment will consist of 194 fuel compacts and a total of approximately 575,000 particles. The AGR-5/6 portion of the test will irradiate the fuel over a broad range of burnup (approximately 6-18% FIMA), fast neutron fluence (1.5 to 7.5×10^{25} n/m², $E > 0.18$ MeV), and temperature (approximately 600-1350°C), to approximate the range of values that would be experienced by the fuel in an HTGR core. The AGR-7 portion of the experiment constitutes a fuel performance margin test, which will involve temperatures far in excess of those expected in a gas-cooled reactor during normal operation. Time-average peak fuel temperature in this capsule will reach approximately 1500°C, with burnups of approximately 18% FIMA. The AGR-5/6/7 fuel compacts were fabricated in 2017, and fabrication of the irradiation test train (5 individual capsules in total) is completed. The experiment was inserted into the Advanced Test Reactor at INL in February 2018.

In the EU, the PIE of the HFR-EU1 irradiation test performed in the High Flux Reactor at Petten containing Chinese and German fuel irradiated at typical pebble bed conditions has been completed.

For China, two HTR-10 pebbles irradiated in HFR-EU1 were transported from JRC Petten to JRC Karlsruhe in 2016, and one of them was tested there at the simulated accident temperature, after the PIE of the HTR-PM irradiated pebbles. One high temperature test was completed of an HTR-10 pebble, and two de-consolidations and coated particle examinations will be performed in 2018.

In Korea, the irradiation test in the High-flux Advanced Neutron Application Reactor (HANARO) had been conducted between August 2013 and March 2014 to a maximum burnup of 37344 MWd/MtU over 5 reactor cycles. Different fuel forms were irradiated: Kernel, coated

particles, fuel compacts and graphite. Irradiation was completed in March 2014 and the data analysis of the irradiation conditions is now finalised. Non-destructive experiments (NDE) on irradiated rods (measurement of the rod diameters, gamma-scanning, X-ray CT inspection, laser piercing, collection and analysis of fission gas), fuel compacts and graphite specimens (dimensional measurement, measurement of weights and densities, deconsolidation of fuel compacts, X-ray inspection, measurement of thermal diffusion coefficients of graphite disks) were performed. Destructive experiments were carried out on TRISO fuel particles (optical inspection, EPMA). Post irradiation examinations on IG-110 and A3-3 graphite were performed in 2017 (thermal conductivity, hardness and Young's modulus).

For licensing purposes, irradiated fuel is submitted to temperature transients as they would be expected in the case of a Low Pressure Conduction Cool-Down and in which case the fuel should not release radioactivity. For this purpose, several installations are being built by the project partners.

In China, the conceptual design of accident heating furnaces is underway. In China, conceptual designs of Key pieces of PIE equipment necessary to analyse TRISO fuel have been completed. In Korea, simulated heat-up test equipment has been constructed for a simulated heating test in a laboratory. Preliminary experiments were conducted in order to verify the design of the heat-up test equipment and the design of the cold fingers. Specimens of Ag (a fission product expected to be released through intact SiC coatings) in a graphite container were tested at a maximum temperature of 1700°C in an argon atmosphere.

AGR-2 fuel compact safety tests are in progress, with 8 UCO and 3 UO₂ tests completed at various temperatures. In general, the results continue to demonstrate the excellent performance of the fuel. The UCO fuel, in particular, exhibits very low incidence of coating failure at temperatures as high as 1800°C, and is similar in performance and behavior to the previously-tested AGR-1 fuel. The AGR-2 UO₂ fuel demonstrated excellent in-pile behavior to a burnup as high as 10.7% FIMA, but also exhibits notable degradation of the SiC layer due to CO attack at elevated temperatures (1600-1700°C) that is characteristic of the UO₂ fuel type.

The Neutron Radiography (NRAD) reactor in the INL Hot Fuel Examination Facility is being used

to re-irradiate AGR-2 fuel to generate short-lived fission products (^{131}I , ^{133}Xe) to evaluate release behavior in heating tests. Two tests have been performed to date involving the re-irradiation of loose Kernels, followed by heating in the FACS furnace in pure helium to observe iodine and xenon release. In addition, a method has been developed to mechanically crack loose, irradiated particles, such that these cracked particles can be re-irradiated in NRAD and heated in FACS to examine iodine and xenon release. Finally, the capability for re-irradiating whole AGR fuel compacts in the NRAD reactor is being developed, with similar tests on whole compacts expected to start next year. This will include the AGR-3/4 fuel compacts, which each contain 20 designed-to-fail particles with exposed Kernels, providing a source of fission products that will be released during the test and measured.

The US is also developing a furnace system that will be used to perform high-temperature tests of irradiated fuel specimens in oxidising conditions. The system will allow irradiated specimens to be heated to temperatures as high as 1600°C in gas mixtures containing air or moisture, while measuring possible fission product release from the fuel. The system will be installed in a hot cell at the Materials and Fuels Complex at INL.

In Japan, oxidation tests with SiC-TRISO are being carried out. The oxidation testing furnace was built in 2015. Oxidation tests are progressing using dummy SiC-TRISO particles with/without OPyC layer at ~1600°C with 20 ppm - 20% of O₂ atmosphere. Results will be available by December 2020.

A strategy for waste minimisation and waste management was established that considers among others sustainability criteria, economics, and proliferation issues. Different approaches for used fuel management are possible and were investigated [31], [32]:

- Direct disposal of fuel elements
- Separation of fuel element from graphite moderator
- Separation of coated particles from matrix graphite and treatment of both fractions
- Separation of Kernels from coatings and recycling of fuel

III.B. Materials and components

The following Key components some of which may be similar to those of a Gas Fast Reactor are required in a VHTR system. These include the reactor pressure vessel, circuit components such as valves or circulators, piping, thermal insulation, seals to minimise expensive helium leakage, helium handling and purification systems, instrumentation, intermediate heat exchangers, and Brayton cycle turbo machinery. The pressure vessels are unique due to their dimensions and depending on the reactor size they can range from road-transportable to larger than modern boiling water reactor vessels. Their development has included efforts in terms of welding and fabrication methods, as well as means to ensure high thermal emissivity of the outer vessel walls.

The intermediate heat exchanger must be a highly reliable, compact and thermally efficient boundary between the primary and the secondary coolants. Printed circuit heat exchangers or plate-fin type compact heat exchangers are favored because of their size and high efficiency, but high temperature materials, manufacturing processes and the components themselves need to be qualified together with the development of suitable design codes and standards for the required temperatures, thermal and/or pressure cycling and required lifetime in a potentially corrosive environment.

For core outlet temperatures up to about 950°C, existing materials can be used; however, temperatures above this, including safe operation during off-normal conditions, require the development and qualification of new materials. Research has focused on (1) graphite for the reactor core and internals [8], [9], [10]; (2) high-temperature metallic materials for internals, piping, valves, high-temperature heat exchangers [11], [12], and gas turbine components; and (3) ceramics and composites for control rod cladding and other core internals as well as for high-temperature heat exchangers and gas turbine components.

Research activities continue on near- and medium-term project needs (i.e., graphite and high-temperature metallic alloys) with limited long-term activities on ceramics and composites.

Characterisation of selected baseline data and the inherent scatter of candidate grades of graphite was performed by multiple members. Thermal conductivity, pore distribution (volume fraction and geometry), and fracture

behavior were examined for numerous grades. Graphite irradiations continued to provide data on property changes, especially at low doses and for irradiation-creep behavior, while related work on oxidation examined both short-term air and steam ingress, as well as the effects of their chronic exposure on graphite. Another area of significant multi-signatory interest is the oxidation resistance of graphite as a function of temperature and exposure conditions. A summary illustrating the strength of graphite following different types of oxidation is given in Figure 2.

Additionally, multiple signatories (Japan, Korea, US) continue to examine complementary approaches for improving the overall oxidation resistance of graphite by applying SiC, boron, and B₄C coatings to the graphite. Data to support graphite model development was generated in the areas of microstructural evolution, irradiation damage mechanisms, and creep. Support was provided for both ASTM and ASME development of the codes and standards required for use of nuclear graphite, which continue to be updated and improved. Multiaxial fracture testing, at both the laboratory and component scale, as well as analysis of graphite was performed. China has been particularly active in testing and analysing multi-block, large-scale-models of graphite core support structures.

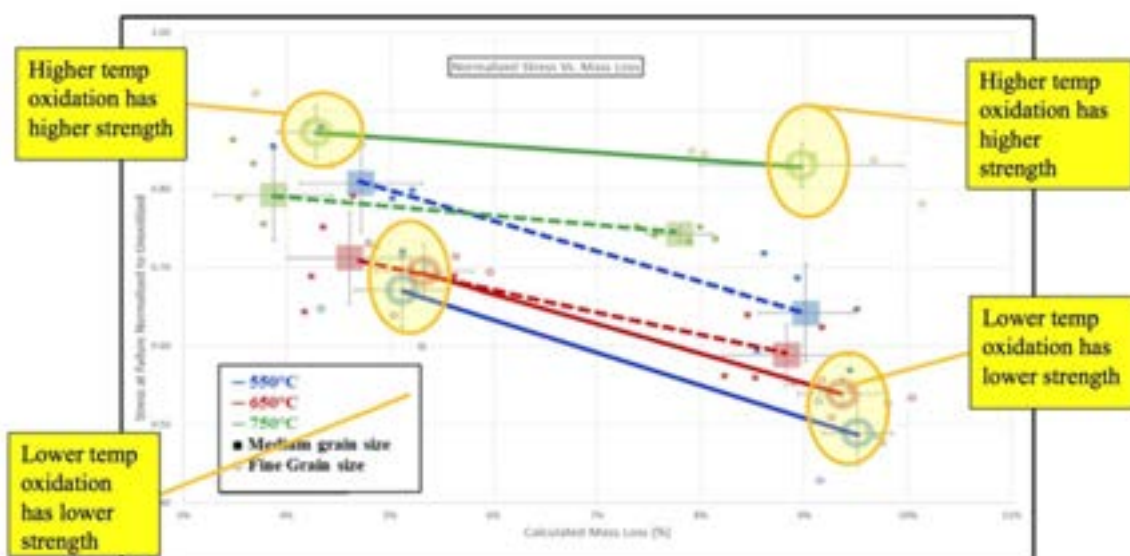
Examination of high-temperature alloys (800H and 617) provided very useful information for

their use in heat exchanger and steam generator applications. These studies included an evaluation of the existing data base and an extension of it through creep, creep-fatigue and creep crack growth rate testing to 950°C. The most significant outcome of this work was the development and submission of an ASME Code Case for the use of Alloy 617 as a new construction material for high temperature nuclear components at temperatures up to 950°C for 100,000 h. Data for the Code Case was contributed by the US, Korea and France. The lower temperature portion of the Code Case, allowing use of Alloy 617 at temperatures up to 371°C was approved by ASME and the high temperature portion is expected to be approved in 2018.

Work has also focused on the properties of welds including creep testing of Alloy 800H performed by KAERI comparing properties of base versus weldment showing that the strength of the weld metal is slightly higher than the base metal, but that its ductility is slightly lower.

Other metallic materials were also examined as part of the Project Arrangement. Irradiation and irradiation creep was studied on 9Cr-1Mo ferritic-martensitic steels and oxide-dispersion-strengthened steels, plus creep behaviour was examined in 2.25Cr-1Mo steel for steam generator applications.

Figure 2. Residual strength of graphite as a function of oxidation mass loss and temperature of exposure. Low temperature oxidation causes larger strength loss for similar oxidation levels



Future projects are considering the use of ceramics and ceramic composites where radiation doses, environmental challenges, or temperatures (up to or beyond 1000°C) will exceed capabilities of metallic materials. This is especially true for control rods, reactor internals, thermal insulation materials, and for gas-cooled fast reactor fuel cladding. Limited work continues to examine the irradiation and thermomechanical properties of SiC and SiC-SiC composites and oxidation in C-C composites. Here, as an example of combined effects, Switzerland and France are studying the temperature dependent irradiation in-situ creep of SiC-SiC materials. The influence of fabrication, architecture, and processing on the properties and fracture mechanisms of the composites is being investigated. The results of this work is being actively incorporated into developing testing standards and design codes for composite materials, and to examine irradiation effects on ceramic composites for these types of applications.

Another activity by Switzerland regards the additive manufacturing of ceramic components, mainly focusing on the production of innovative fuel, but also having the potential to introduce highly specific and functional structural parts [30].

VHTR reactors, in common with other Gen IV systems, could benefit from recent advances in both materials and manufacturing (e.g. EB additive manufacturing.) However, getting new materials or manufacturing processes qualified can be a long and tortuous process, and the long lead times involved produce an effective and consequent barrier to market entry of new or optimised materials and processes at an industrial scale. These considerations have led the GIF Policy Group to launch an Advanced Manufacturing and Materials Engineering Interim Task Force led by Australia to assess the interest in cross cutting activities supporting advanced materials and innovative manufacturing development to a high TRL and the GIF VHTR system is supporting this initiative.

III.C. Reactor systems and balance-of-plant

The VHTR has two established baselines for the core: pebble bed or prismatic block. Each system has its specific advantages. Several signatories of the VHTR system pursue their own design projects and much of the information is shared within GIF, however, there is currently no common design effort going on within the GIF VHTR system. For

power conversion, several nearer term (and lower temperature) VHTR projects use steam cycle technology [13], [14], since much of the process heat market can be captured with steam at these temperatures (<550°C) and because of the well-established commercial infrastructure supporting steam-based power conversion. Direct helium gas turbine or indirect (gas mixture turbine) Brayton-type cycles are also being considered by several countries [15], [16], especially with higher temperature (~950°C) VHTR concepts.

Regardless of the choice of power conversion, supply of process heat will require an intermediate heat exchanger connected to the primary circuit [17]. Near-term concepts for these components are being developed using existing materials, and more advanced concepts are stimulating the development of new materials. An intermediate heat exchanger is also required for thermo-chemical hydrogen production and may use a heat transfer fluid such as helium, a gas mixture, or a molten salt.

As a specific process heat application, the GIF VHTR system organises the collaborative development of hydrogen production processes [18], [19]. Several facilities combining the three elementary processes of the iodine-sulphur process to a thermo-chemical cycle were built and operated in Japan and China at continuous, stable operation at 20-60 l/h for up to 4 days. Progress was made in the area of materials, components, optimisation of elementary processes, process control, safety, system integration and cost evaluation. The main alternatives to the iodine-sulphur cycle are high-temperature electrolysis, hybrid cycles using various fractions of high temperature process heat and electricity, or the Copper-Chlorine process. The iodine-sulphur cycle and high-temperature electrolysis deserve further development in areas such as viability of the basic processes, materials for electrolysis cells or reaction vessels, and scale-up and control of large processes. Recent developments of the copper-chlorine process in Canada provided the impetus for an accelerated viability demonstration plan that includes an integrated lab-scale system of 50 l/h using an industrial heat source.

In Japan, JAEA has carried out demonstration tests of hydrogen production using the SI process. The goal has been to verify the integrity of process components and stability of the hydrogen production process. Following a 31 hour test in 2016 at a production rate of 20 l/h, the focus has been on quantitative

evaluation of engineering issues in reactor sections. Prevention methods for leakage of HI-containing solution are also being considered. A longer term stable operation of this hydrogen production process is expected from improvements achieved by these efforts.

In China, at INET, R&D activities on nuclear hydrogen production have been progressing well. In 2016, an evaluation of the progress and prospect of the two main technologies, the SI and HTSE processes, was conducted, and the SI process was selected for future scale-up and potential coupling to HTR-10. Consideration was given to the difficulties of scale-up, coupling technology and application scenarios of nuclear hydrogen production with HTR-PM600. INET has carried out fundamental studies of improving the efficiency of the SI process (Figure 3), including H₂ separation by membrane technology, novel design of the Electro-Electro Dialysis (EED) process for HI concentration, Kinetics of the Bunsen reaction, etc. In parallel, development studies of the Key prototype reactors have been carried out. In addition, INET has developed a two-step R&D plan for piloting the SI process over the next 10 years; the first step is on fully understanding the safety issues of nuclear hydrogen related to the Key technologies for pilot scale SI process by 2020, and the second step is the development of HTR-SI coupling technology by 2025.

Figure 3. INET's Sulphur-Iodine process for nuclear hydrogen production



In Korea, a new three-year project “VHTR Key technology performance improvement” was initiated in March 2017. Its purpose is to improve the level of Key technologies to support VHTR development and demonstration in the future. The key technologies to be

considered are the design analysis codes, thermo-fluid experiments, TRISO fuel, high-temperature materials database, and high temperature heat applications. As a part of this project, a high-temperature heat utilisation technology has been investigated. In 2017, material and heat balance analyses have been performed for high-temperature heat utilisation systems such as SI, HTSE, and Steam Methane Reforming processes in terms of hydrogen production efficiency, energy demand, and thermal utilisation. This effort will provide basic information for an evaluation of the performance of coupled systems and optimisation of the VHTR and High Temperature Heat Utilisation System.

In absence of a separate GIF VHTR project on System Integration and Assessment, several of the signatories investigate the integration of VHTR systems into electricity grids and heat networks with fossil and variable renewable fractions [21], [22], [23].

The US Department of Energy Energy (EERE) H2@Scale is funding Idaho National Laboratory to develop and build a 25 kW HTSE demonstration facility to study efficient H₂ production and energy integration (Figure 4).

Figure 4. Hydrogen generation and applications in an integrated energy system (source: INL)



This facility will support system integration studies within the Dynamic Energy Transport and Integration Laboratory (DETAIL) at INL. It will demonstrate thermal integration with co-located systems for steam production and will support transient and reversible operation for grid stabilisation studies via a microgrid and Real-Time Data Simulation (RTDS) systems. This facility will be operational in summer of 2018.

The Sol2Hy2 project, funded by the European Fuel-Cell and Hydrogen Joint Undertaking, has focused on the bottle-necks solving materials research and development challenges, and demonstration of the relevant Key components of the solar-powered, CO₂-free hybrid water splitting cycles, complemented by their advanced modelling and processes simulation with added conditions-specific technical-economical assessment, optimisation, quantification and evaluation. The main focus was on the Hybrid Sulphur Cycles (HyS). The main results and achievements of the project are reported in the analysis, development and validation of new process flowsheets to include solar power input for Key units of the plant, targeted at selected locations (specified by user) and allowing a flexible combination of different sources, inclusive of the new Outotec Open Cycle, where sulphuric acid is directed to be a commercial by-product to hydrogen rather than to be cracked and returned to the HyS cycle. This enables an increase of the renewable sources share, improves waste heat utilisation and ensures 24/7 plant operation, eliminating solar input instability, combined with reasonable capital costs and balance of the products streams. In the electrolyser unit - the core of H₂ generation - most of the challenges were solved - elimination of platinum-group metals catalysts, control of parasitic reactions, lowering the capital costs (e.g. ~3 times vs. existing analogues). The operation of the developed sulphuric acid cracking unit was successfully demonstrated at the solar tower Jülich (Germany). An extra development of the software for plant design and optimisation was also carried out allowing the user to analyse and optimise the hydrogen production process in an interactive and guided way, through the use of user-friendly graphical user interfaces. This enables any user to evaluate technical and economic performance of a hydrogen production plant in any feasible location well before field studies.

Significant technical progress has been achieved in the development of the steps of the Cu-Cl hybrid thermochemical cycle in Canada over the last year. Combined with the moderate temperature (<530°C) heat requirement of the process, the recent technical progress has provided the impetus for an accelerated development project to demonstrate an integrated process coupled to an industrial heat source. Process technical viability demonstration plans over a three year period include a lab-scale system of 50 l/h, already in progress during this year, to elucidate any

difficulties in the integration of the electrochemical, hydrolysis, thermolysis and separation/drying steps involved in the process. In parallel, a 1 ton/day capacity unit will be designed for demonstration in collaboration with industrial and academic partners.

Beyond the process equipment, research is ongoing into the coupling of a nuclear reactor with industrial processes [20]. This involves the analysis of safe and reliable control and operation, including combined effects of each of the systems. It also branches out into the conceptual design, the licensing and economics of systems for cogeneration of electricity and process heat in various petrochemical and other applications.

III.D. Computational tools and test facilities

In support to design and licensing, a project on Computational Methods, Validation and Benchmarking (CMVB) was prepared for signature in 2018. The project signatories have already exchanged significant information while the project was still provisional [24], [25]. The project encompasses neutronic and thermal fluid model validation using a number of experiments provided by the signatories. In 2017, the project was presented with the guidelines for validating system and computational fluid dynamics models that have been accepted by the US Nuclear Regulatory Commission. A common set of validation guidelines will be adopted and applied within the GIF research.

After in-depth discussion in several meetings, past, current, and new test facilities and projects have been proposed as potential resources to carry out the experiments for model development and benchmarking activities.

In China, experiments using sixteen separate engineering test facilities, including a helium circulator test facility (Figure 5) have been completed in support of HTR-PM development.

The component installation of the HTR-PM is proceeding toward start-up testing, likely before the end of 2018. Critical tests and start-up physics testing will also contribute valuable data to the code development and validation. China's HTR-10 was restarted to test the major components and system operation. It was operated at power to conduct a melt-wire experiment to measure in-core temperatures. A cold shuffling stage was started in order to discharge the measurement elements out of the core for later inspection.

Figure 5. HTR-PM Main Helium Circulator Test Facility



The European R&D focus is on demonstration-oriented technology. The ARCHER project was completed in January 2015 whilst the GEMINI+ project continues until 2020. Korea has focused its R&D on improvement and validation of VHTR passive safety features such as the hybrid air-cooled RCCS with water jacket. In the US, the Department of Energy's Advanced Reactor Technologies program supported the development and validation of core analysis tools, most notably with the construction and operation of thermal fluid test facilities (HTTF, NSTF, MIR, etc.). Data from Natural Circulation Shutdown Heat Removal Facility (NSTF) experiments is available for validation of air-cooled and water-cooled RCCS models.

The HTTF at Oregon State University was shut down after experiencing heater failures during startup. The re-designed heater elements will be installed in 2018 prior to start-up testing. All these research activities carried out in test facilities and reactors play an important role for V&V of computer codes and calculation methods, which will benefit the cmVB work.

III.E. Economics

Detailed economic studies have been performed for both electricity production and process heat applications by several GIF signatories, and they have been shared informally. The US results suggest that modular VHTRs are competitive with new LWRs for electricity production. For process heat and co-generation applications, the VHTR can be competitive with conventional combined cycle gas turbine systems producing steam and electricity when the cost of natural gas is higher than 8 USD/MMBtu. Carbon taxes may reduce

this threshold. Currently, the cost of natural gas varies widely across the globe. Thus, the economic viability depends largely on the financial and regulatory climate in individual countries. The inherent safety features of VHTR may benefit the economics index indirectly. Similar to certain other small and medium sized reactor concepts, the VHTR can also take credit for lower infrastructure requirements such as easier integration in weaker electricity grids, lower cooling requirements, and proximity to industrial sites and agglomerations.

Market research has also been performed by several of the GIF signatories [26], which were shared informally and corroborate the motivation for this system.

The VHTR System Steering Committee has worked together with several companies to provide technical and economic performance information on so far three different VHTR designs to the GIF Senior Industry Advisory Panel for analysis.

III.F. Safety objectives

A VHTR can be designed with a high degree of inherent safety with passive cooling and core/fuel integrity under all circumstances. The VHTR system has interacted closely with the GIF Risk and Safety Working Group to provide a White Paper and Safety Self-Assessment document. A further effort to generate a set of safety requirements [27] and safety design criteria for VHTRs is currently underway under the auspices of the IAEA (CRP to be finalised in 2018) and will be completed by the VHTR system. The VHTR system has also reported to the OECD/NEA Working Group on the Safety of Advanced Reactors (WGSAR) to consult regulators and TSOs for input.

IV. Path Forward

R&D objectives and needs, guiding the future VHTR system R&D efforts, have been identified. The GIF VHTR system is currently running four R&D projects for which the path forward is detailed and updated annually in the individual Project Plans. In the next years, the VHTR system will direct its work towards further improved Technology and Market Readiness and towards the demonstration of the technology in the following areas:

- Fuel testing and qualification capability (including fabrication, QA, irradiation, safety testing and PIE), to be completed

- in some countries. Waste reduction and fuel recycling.
- Qualification of graphite, hardening of graphite against air/water ingress, e.g. by SiC infiltration, management of graphite waste.
 - Coupling technology and related components (e.g. isolation valves, intermediate heat exchangers).
 - Establishment of Design Codes & Standards for new materials and components.
 - Advanced manufacturing methods and other cost cutting R&D.
 - Interaction with EMWG and industry to optimise VHTR design.
- Licensing and Siting: V&V of computer codes for design and licensing.
 - System Integration with other energy carriers in Hybrid Energy Systems.
 - Follow-up of HTR-PM demonstration tests, enhance information exchange with several start-ups, investors, new national programs.
 - HTTR: safety demonstration tests and coupling to H₂ production plant (subject to regulator approval for restart).

Publicly available details on results obtained within these GIF VHTR projects are available in the references.

References

- [1] HTR 2016 proceedings: www.ans.org/store/item-700409/ ISBN: 978-0-89448-732-3.
- [2] M. A. Fütterer, Fu Li, C. Sink, S. de Groot, M. Pouchon, Y.W. Kim, F. Carré, Y. Tachibana, Status of the Very High Temperature Reactor System, *Progress in Nuclear Energy* 77 (2014) 266-281.
- [3] S. Knol, S. de Groot, R. V. Salama, J. Best, K. Bakker, I. Bobeldijk, J. R. Westlake, M. A. Fütterer, M. Laurie, Chunhe Tang, Rongzheng Lui, Bing Liu, Honhsheng Zhao, HTR-PM Fuel Pebble Irradiation Qualification in the High Flux Reactor in Petten, *Proc. HTR 2016*, Las Vegas, NV, USA, 6-10 Nov. 2016.
- [4] Bong Goo Kim, Sunghwan Yeo, Kyung-Chai Jeong, Yeon-Ku Kim, Young Woo Lee, Moon Sung Cho The First Irradiation Testing and PIE of TRISO-Coated Particle Fuel in Korea, *Proc. HTR 2016*, Las Vegas, NV, USA, 6-10 Nov. 2016.
- [5] Shohei Ueta, Jun Aihara, Asset Shaimerdenov, Daulet Dyussambayev, Shamil Gizatulin, Petr Chakrov, Nariaki Sakaba Irradiation Test and Post Irradiation Examination of the High Burnup HTGR Fuel, *Proc. HTR 2016*, Las Vegas, NV, USA, 6-10 Nov. 2016.
- [6] M. Davenport, D. A. Petti, J. Palmer, Status of TRISO Fuel Irradiations in the Advanced Test Reactor Supporting High-Temperature Gas-Cooled Reactor Designs, *Proc. HTR 2016*, Las Vegas, NV, USA, 6-10 Nov. 2016.
- [7] P. A. Demkowicz, J. D. Hunn, D. A. Petti, R. N. Morris, Key Results from Irradiation and Post-Irradiation Examination of AGR-1 UCO TRISO Fuel, *Proc. HTR 2016*, Las Vegas, NV, USA, 6-10 Nov. 2016.
- [8] T. D. Burchell, W. E. Windes, A Comparison of the Irradiation Creep Behavior of Several Graphites, *Proc. HTR 2016*, Las Vegas, NV, USA, 6-10 Nov. 2016.

- [9] M. Davenport, D. A. Petti (INL), Preliminary Results of the AGC-4 Irradiation in the Advanced Test Reactor and Design of AGC-5, Proc. HTR 2016, Las Vegas, NV, USA, 6-10 Nov. 2016.
- [10] M. C. R. Heijna, J. A. Vreeling, The INNOGRAPH Irradiations; HTR Graphite Material Properties from 0 to 25 dpa, Proc. HTR 2016, Las Vegas, NV, USA, 6-10 Nov. 2016.
- [11] J. K. Wright, T. M. Lillo, R. N. Wright, Woo-Gon Kim, In Jin Sah, Eung Seon Kim, Ji Yeon Park, Min Hwan Kim, Creep and Creep-Rupture of Alloy 617, Proc. HTR 2016, Las Vegas, NV, USA, 6-10 Nov. 2016.
- [12] Ji Yeon Park, Woo Gon Kim, Weon Ju Kim, Dong Jin Kim, Se Hwan Chi, Eung Seon Kim, Min Hwan Kim, R&D Activities on VHTR Materials at KAERI, Proc. HTR 2016, Las Vegas, NV, USA, 6-10 Nov. 2016.
- [13] Zuoyi Zhang, Yujie Dong, Fu Li, Zhengming Zhang, Haitao Wang, Xiaojin Huang, Hong Li, Bing Liu, Xinxin Wu, Hong Wang, Xingzhong Diao, Haiquan Zhang, Jinhua Wang, The Shandong Shidao Bay 200 MWe High-Temperature Gas-Cooled Reactor Pebble-Bed Module (HTR-PM) Demonstration Power Plant: An Engineering and Technological Innovation, Engineering 2 (2016) 112–118.
- [14] F. Shahrokhi, L. Lommers, J. Mayer III, F. Southworth, AREVA Steam Cycle High Temperature Gas-Cooled Reactor Development and Deployment Plan, Proc. HTR 2016, Las Vegas, NV, USA, 6-10 Nov. 2016.
- [15] Hiroyuki Sato, Yasunobu Nomoto, Shoichi Horii, Junya Sumita, Xing Yan, Hirofumi Ohashi, HTTR-GT/H2 Test Plant—System Performance Evaluation for HTTR Gas Turbine Cogeneration Plant, Proc. HTR 2016, Las Vegas, NV, USA, 6-10 Nov. 2016.
- [16] H. Tsukamoto, S. Oyama, K. Suyama, Y. Mizokami, G. Totani, X. Yan, H. Sato, Y. Nomoto, S. Horri, J. Iwatsuki, HTTR-GT/H2 test plant - design study on helium gas turbine for the heat utilization system connected to JAEA's HTTR, Proc. HTR 2016, Las Vegas, NV, USA, 6-10 Nov. 2016.
- [17] Su-Jong Yoon, J. O'Brien, K. Wegman, Xiaodong Sun, Thermal-Hydraulic Performance of Printed Circuit Heat Exchangers: CFD Analysis with Experimental Validation, Proc. HTR 2016, Las Vegas, NV, USA, 6-10 Nov. 2016.
- [18] Seiji Kasahara, Yoshiyuki Imai, Koichi Suzuki, Jin Iwatsuki, Atsuhiko Terada, Xing L. Yan, Conceptual Design of Iodine-Sulfur Process Flowsheet with More Than 50% Thermal Efficiency for Hydrogen Production, Proc. HTR 2016, Las Vegas, NV, USA, 6-10 Nov. 2016.
- [19] Nobuyuki Tanaka, Hiroaki Takegami, Hiroki Noguchi, Yu Kamiji, Jin Iwatsuki, Hideki Aita, Seiji Kasahara, Shinji Kubo, IS Process Hydrogen Production Test for Components and System Made of Industrial Structural Material (I)—Bunsen and HI Concentration Section, Proc. HTR 2016, Las Vegas, NV, USA, 6-10 Nov. 2016.
- [20] T. Jackowski, A. Przybyszewska, G. Wrochna, O. Baudrand, M. A. Fütterer, P.-M. Plet, F. Roelofs, V. Chauvet, C. Auriault, D. Hittner, H. Tuomisto, R. Ståhl, Results from the European NC2I-R Project on Nuclear Cogeneration with High Temperature Reactors, Proc. HTR 2016, Las Vegas, NV, USA, 6-10 Nov. 2016.
- [21] S. Schröders, K. Verfondern, H.-J. Allelein, Energy Economic Evaluation of Hydrogen

- Production by HTGR and Solar Tower, Proc. HTR 2016, Las Vegas, NV, USA, 6-10 Nov. 2016.
- [22] C. Forsberg, Base-Load High-Temperature Reactors with Variable Electricity to the Grid using Brayton Cycles to Match Low-Carbon Electricity Markets, Proc. HTR 2016, Las Vegas, NV, USA, 6-10 Nov. 2016.
- [23] M. W. Patterson, Cogeneration of Electricity and Liquid Fuels using an HTGR as the Heat Source, Proc. HTR 2016, Las Vegas, NV, USA, 6-10 Nov. 2016.
- [24] Yangping Zhou, Pengfei Hao, Fu Li, Lei Shi, Yuan Liu, Feng He, Yujie Dong, Zuoyi Zhang, Effects of Bypass Flow and Power Change and Deviation on Performance of Thermal Mixing Structure of HTR-PM, Proc. HTR 2016, Las Vegas, NV, USA, 6-10 Nov. 2016.
- [25] S. Kassermann, A. Xhonneux, F. Tantilillo, A. Trabadelo, D. Lambertz, H.-J. Allelein, V&V of the HTR Code Package (HCP) as an Extensive HTR Steady State and Transient Safety Analysis Framework, Proc. HTR 2016, Las Vegas, NV, USA, 6-10 Nov. 2016.
- [26] M. A. Fütterer, A Glimpse on the Market for VHTR/HTGR products, presented at GIF Policy Group Meeting, Cape Town, South Africa, 19-20 Oct. 2017.
- [27] Hirofumi Ohashi, Hiroyuki Sato, Shigeaki Nakagawa, Kazumi Tokuhara, Tetsuo Nishihara, Kazuhiko Kunitomi, Development of Safety Requirements for HTGRs Design, Proc. HTR 2016, Las Vegas, NV, USA, 6-10 Nov. 2016.
- A. Bredimas, Results of a European industrial heat market analysis as a pre-requisite to evaluating the HTR market in Europe and elsewhere, Nuclear Engineering and Design, Volume 271, May 2014, Pages 41-45.
- [28] GIF Annual Report 2017, to be published on www.g4if.org.
- [29] M. A. Pouchon, Aqueous Additive Production Method for the Fabrication of Ceramic and/or Metallic Bodies, WO/2018/036813, 2 March 2018. <https://patentscope.wipo.int/search/en/detail.jsf?docId=WO2018036813>
- [30] D. Grenèche, P. Brossard, The Reprocessing Issue for HTR Spent Fuels, Proc. ICAPP'04, Pittsburgh, PA, USA, June 13-17, 2004.
- [31] M. A. Fütterer, F. von der Weid, P. Kilchmann, A High Voltage Head-End Process for Waste Minimization and Reprocessing of Coated Particle Fuel for High Temperature Reactors, Proc. ICAPP'10, paper 10219, San Diego, CA, USA, 13-17 June 2010.

THE GENERATION-IV LEAD-COOLED FAST REACTOR ACTIVITIES (A.ALEMBERTI ET AL)

Alessandro Alemberti⁽¹⁾; K. Tuček⁽²⁾; T. Obara⁽³⁾; M. Kondo⁽⁴⁾; A. Moiseev⁽⁵⁾; I.S. Hwang⁽⁶⁾; C. Smith⁽⁷⁾; Y. Wu⁽⁸⁾; M. Jin⁽⁸⁾

- (1) Ansaldo Nucleare SpA, Italy.
 (2) European Commission, Joint Research Center (JRC), the Netherlands.
 (3-4) Tokyo Institute of Technology (TIT), Japan.
 (5) JSC "NIKIET", Russian Federation.
 (6) Seoul National University, Republic of Korea.
 (7) Naval Postgraduate School, United States.
 (8) Institute of Nuclear Energy Safety Technology , Chinese Academy of Sciences, China.

Abstract

Since 2012 the Lead-cooled Fast Reactor provisional System Steering Committee (LFR-pSSC) of the Generation IV International Forum (GIF) has developed a number of top level strategic activities with the aim to assist and support development of Lead-cooled Fast Reactor technology in member countries and entities. The current full members of the GIF-LFR-pSSC (i.e., signatories of the GIF LFR Memorandum of Understanding /MoU/) are: Euratom, Japan, the Russian Federation, the Republic of Korea and the United States. The People's Republic of China participates in the pSSC in observer status.

The LFR concepts identified by GIF include three reference systems. The options considered are a large system rated at 600 MWe (ELFR EU), intended for central station power generation, a 300 MWe system of intermediate size (BREST-300 Russia), and a small transportable system of 10-100 MWe size (SSTAR US) that features a very long core life. It can be noted that the reference concepts for GIF-LFR systems cover the full range of power levels, including small, intermediate and large sizes. Important synergies exist among the different reference systems so that coordination of the efforts carried out by participating countries has been one of the Key objectives of the GIF-LFR-pSSC.

This paper highlights the main recent collaborative efforts and achievements of the LFR-pSSC, including the development of the LFR System Research Plan, the LFR White Paper on Safety, the LFR System Safety Assessment and the LFR Safety Design Criteria document. A brief overview of the main aspects of the above-mentioned reports is included in this paper to highlight the benefits of the collaborative work carried out inside GIF. Finally, the status of the development of LFRs in the GIF member countries and entities is briefly presented, making reference to the principal LFR initiatives taking place world-wide.

I. Introduction

This paper provides a history and overview of the activities carried out by the GIF-LFR-pSSC since 2012.

The activities carried out by pSSC-participating countries are then summarised in order to give a picture of the different scenarios and interests. New initiatives are also briefly mentioned in order to illustrate the potential of the LFR in the

near future. Research and development needs are then briefly summarised throughout the text with the aim assist research organisations in identifying priorities for the development of such a promising technology.

II. GIF-LFR Reference Designs

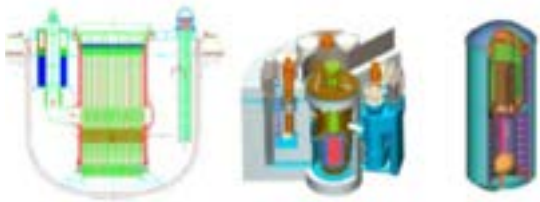
The LFR concepts identified by GIF include three reference systems. The options considered are a large system rated at 600 MWe

(ELFR, EU), intended for central station power generation, a 300 MWe system of intermediate size (BREST-OD-300, Russian Federation), and a small transportable system of 10-100 MWe size (SSTAR, US) that features a very long core life, cf. Figure 1.

It can be noted that the reference concepts for GIF-LFR systems cover the full range of power levels, including small, intermediate and large sizes.

Important synergies exist among the different reference systems so that a coordination of the efforts carried out by participating countries has been one of the Key points of LFR development.

Figure 1. GIF-LFR Reference Systems: ELFR (left), BREST-OD-300 (center) and SSTAR (right)



III. History of The GIF-LFR-PSSC

The GIF-LFR Provisional System Steering Committee (pSSC) was initially formed in 2005. The original membership included the EC, the US, Japan and Korea. With Korea primarily in observer status between 2005 and 2008, this initial committee, among its other activities, worked together to prepare a series of drafts of an initial LFR System Research Plan (LFR-SRP).

During this first phase of the GIF research planning effort, beginning in 2005 and culminating in the completion of the final draft System Research Plan (SRP), two main directions or research thrusts were envisioned: the first was a (relatively) large central station plant and the second was a small transportable LFR system.

In 2010, the GIF-LFR Memorandum of Understanding (MoU) was signed between EC and Japan, and this resulted in a reformulation of the pSSC. Then in 2011, the Russian Federation added its signature to the MoU. In April 2012, the reformulated pSSC met in Pisa, Italy and a number of actions were defined. The US was invited to participate in the activities of pSSC as an observer, and the process of

preparing a revised SRP was initiated. The new pSSC, with representatives of EC, Japan and Russia, envisioned various updates to the central station and small reactor thrusts while adding a mid-size LFR (i.e., the BREST-300) as a new thrust in the SRP.

The third meeting of the pSSC was hosted by OECD-NEA in Paris on March 7-8 2013, in conjunction with the IAEA conference on Fast Reactors, FR-13. This committee meeting saw an enlarged number of participants with additional observer representatives from China and Korea.

Following this first phase of the reformulated pSSC the activities continued with two meetings every year enlarging the scope of the collaboration and improving the relationship between partners by mutual support.

In December 2015 the Republic of Korea became a full member of the pSSC by signing the LFR-MoU, while in February 2018 the MoU was signed by the US. Currently, only China is attending the meetings in the observer status and the committee hopes that soon also this Country will sign the LFR-MoU and become a full member of the Committee.

Several initiatives have been promoted by the group and are briefly summarised in the following to provide an overview of the top-level activities.

IV. Main Activities of LFR-pssc

Since the formation of the pSSC, a number of significant activities have been performed. Some of these activities have been presented in earlier GIF symposium papers (e.g., [1]). In the following paragraphs, the most recent and ongoing activities of the pSSC are summarised.

LFR Safety Design Criteria (SDC): the development of the LFR SDC used the previously-developed SFR SDC report as a starting point. However, it was realised that the IAEA SSR-2/1 (on which the SFR SDC was based) did not require many of the features identified for the SFR to be adopted for the LFR due to fundamental differences between the two liquid metal-cooled fast reactors. The LFR-SDC has been recently updated taking into account inputs from RSWG as well as the European project ARCADIA, and was completely revised to comply with the new version of IAEA SSR-2/1 (revision 1) issued at the end of 2016. The report is presently under internal review and a revised version is expected to be provided and discussed with the RSWG before the end of 2018.

LFR System Safety Assessment: in 2014, the RSWG asked the SSC chairs to develop a report on their systems to analyse them systematically, assess their safety level and identify further safety-related R&D needs. The initial LFR assessment report was prepared by the LFR pSSC and a revision of the report addressing comments from the RSWG is now in preparation. Detailed discussions were conducted in early 2018, with the objective of bringing the report to a final and agreed form.

LFR-pSSC comments to the GENIV- IRSN report: in 2015, the pSSC took the initiative to analyse in detail the IRSN report on the safety of Generation IV reactors and provide comments. The Committee sincerely appreciated the technically comprehensive review of LFR safety aspects provided by IRSN. However, the Committee also felt that the results of recently-concluded as well as ongoing R&D efforts were possibly not fully considered by IRSN when drawing some of their conclusions. The comments provided by the pSSC are expected to form the basis for further discussions and possible update of the IRSN report in future.

Cooperation Agreement EURATOM-ROSATOM: following the signature in May 2014 of a Cooperation Agreement (CooA) between the BREST and LEADER projects, by NIKIET (on behalf of ROSATOM) and Ansaldo (on behalf of the LEADER consortium), two dedicated meetings were organised and conducted. Presently the two organisations (NIKIET and Ansaldo) are discussing the possibility for a renewal of the cooperation agreement.

US/EURATOM LFR INERI project: in March 2017 a new International Nuclear Energy Research Initiative (INERI) project was started. The title of the project is: "Small Modular Lead-cooled Fast Reactors in regional energy markets: safety, security, and economic assessments". The project facilitates collaboration between a USDOE-sponsored organisation, in this case the Naval Postgraduate School, Monterey, CA, and EURATOM R&D and Industrial organisations, led by the JRC. Other Key organisations involved are: Argonne National Laboratory (ANL), Lawrence Livermore National Laboratory (LLNL), Ansaldo Nucleare, ENEA, RATEN-ICN, SCK•CEN, Hydromine, Westinghouse, and LeadCold. This joint US/Euratom project is investigating the feasibility and assessing the potential deployment of Small Modular Lead-cooled Fast Reactors in regional energy markets and for insular applications. An INERI program review was held at Oak Ridge, TN, in July 2017, and an INERI Joint Project Plan was completed

in September 2017. The status of the project and further actions have been defined in a dedicated project meeting in April 2018 in Amsterdam.

IAEA FR-17 – Ekaterinburg (RU): The LFR community was widely represented at this very important event for Fast Reactors. Several papers were presented by our Russian Colleagues with topics ranging from fuel cycle, experimental facilities and results as well activities related to LFR design and licensing. Additionally, many researchers participated from Europe, Korea, China and the US and presented their work showing the increasing world-wide interest in heavy liquid metal (HLM) technology.

GLANST – Seoul (KR): The GIF-LFR-pSSC supported the organisation of the first Global Symposium on Lead and Lead Alloy Cooled Nuclear Energy Science and Technology (GLANST) in Seoul in September 2017. This new Global Symposium was launched in September 2017 with a five-year interval in order to provide an additional forum in parallel with the already successful HLMC. This first edition was also supported by the Korean Radioactive Waste Society and the Korea National Research Foundation. On this basis, the Scientific Committee of GLANST, including Key members of the GIF LFR-pSSC as well as Key members of HLMC, organised and convened the GLANST-2017 conference. The inaugural conference held at Seoul National University (SNU) was well received with the participation of about 50 participants from GIF member states with important Keynote speakers invited.

V. Activities in GIF-LFR Countries

This section summarises briefly the main activities carried out in the frame of GIF by Countries that signed the GIF-LFR-MoU or are participating in observer status.

Russian Federation: An innovative fast reactor BREST-OD-300 with inherent safety is being developed as a pilot and demonstration prototype of future nuclear power with a closed nuclear fuel cycle [2]. One of the BREST-OD-300 development objectives is the practical justification of the main design approaches applied to the reactor facility with lead coolant based on a closed nuclear fuel cycle, and confirmation of the foundations on which these approaches are based to ensure inherent safety [3, 4]. Special attention in the reactor development is paid to justification of the reactor core and its components. Mixed

uranium-plutonium nitride is used to ensure complete breeding of fuel in the core and a small reactivity margin preventing any prompt-neutron excursion during reactor operation [5]. A low-swelling ferrite-martensitic steel is used as fuel cladding.

To confirm fuel serviceability, radiation tests of fuel elements are being conducted in the BN-600 power reactor and in the BOR-60 research reactor. At the present time, eight FAs with nitride fuel elements are being irradiated in the BN-600 reactor, and the fuel elements from two previously withdrawn Fuel Assemblies (FAs) are being subjected to post-irradiation studies. Seven FAs with nitride fuel elements are currently being irradiated in the BOR-60 research reactor.

Figure 2. Full-scale FA mock-ups



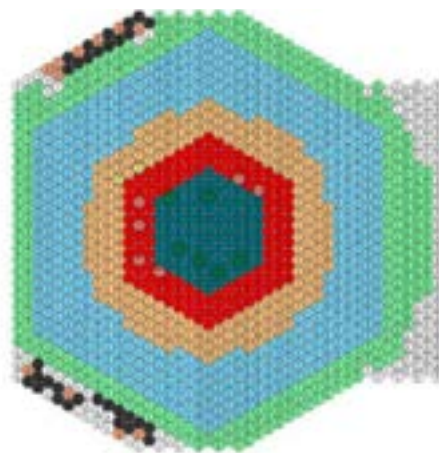
In designing the reactor core components, novelty was coupled with reference solutions. The FA has a shroud-less hexagonal design. Such a solution eliminates the possibility of fuel melting due to FA flow area blockage; even in the event that the flow area at the inlet of a 7-FA group is blocked, the safe operation limits of the fuel cladding temperature are not exceeded. Another positive point is a 30% reduction in the metal content of the shroud-less FA as compared to the shrouded option. Technologically, the adopted design is based on the experience gained when fabricating FAs for VVER reactors.

To justify the FA design serviceability, full-scale mock-ups (Fig. 2) were manufactured and subjected to mechanical, hydraulic and vibration tests in air and water environments. Mechanical tests included transverse bending, torsion, axial tension and compression. Vibration tests were conducted using running and stationary water.

Vibration tests were also performed in air. Hydraulic tests of FA mock-ups were conducted using lead coolant. In the reactor core composed of shroud-less FAs, Knowledge of local flow rates within hydraulic cells in terms of the fuel element temperature determination is important. To determine the inter-cell and inter-cassette mixing coefficients, specific experiments in liquid metal and air were carried out. A mock-up of 37-rod fuel bundle was used in the liquid metal experiments to refine the heat transfer coefficients. Thus, a large quantity of data was obtained and used for validation of the codes intended for thermal-hydraulic calculations of the reactor core.

To confirm the corrosion resistance of the FA elements in the lead coolant, tests using small-scale fuel-free mock-ups of the FAs at different temperatures were conducted. The absence of data from physical experiments with nitride fuel led to the necessity of carrying out additional experimentation using the BFS critical facility (Fig. 3).

Figure 3. Map of BFS critical assembly with BREST-type fuel composition



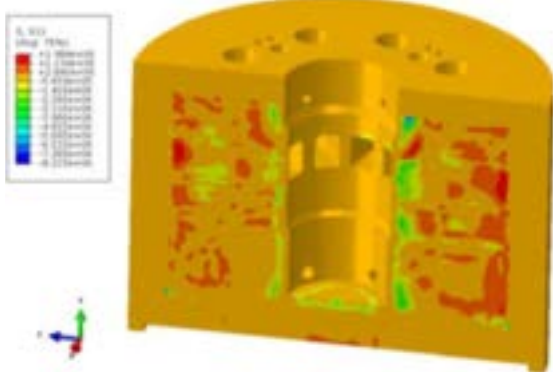
In the associated simulations lead, plutonium, and uranium nitride were used. Based on the results the calculation codes were validated for neutronic calculations. The results of the calculations carried out using the validated

software tools show the possibility to achieve a small reactivity margin during the reactor operation and provision of a practically stable power density field during the duration of the fuel lifetime.

An integral layout is used in the reactor facility to avoid coolant losses. The reactor vessel material is multilayer metal concrete; the lead coolant and the main components of the primary circuit are located in the reactor vessel.

A wide range of calculations and experimental studies were required to confirm the serviceability of such a vessel type (Fig. 4), which is novel for the nuclear power industry. The experimental justification is based on investigations and testing of the small- and full-scale components. Using the developed full-scale mockup of the vessel bottom a capability to ensure the required temperature of the building structures has been demonstrated, and joint thermal movements of the components have been determined. Using the developed full-scale mockup of the central part of the vessel, heating-up modes have been optimised, and the gas emission parameters have been determined. The analytical justification showed that the adopted vessel design ensures that the probability of formation of a leak with partial coolant loss would be no greater than 9.7×10^{-10} /year.

Figure 4. Distribution of first primary stresses 1 in concrete filler of reactor vessel by the end of heating-up



The integral layout with a steam generator (SG) located in the reactor unit vessel needs to be confirmed in terms of safety and serviceability of the SG. Therefore, a thorough justification of the steam generator components and the processes taking place in the steam generator

has been planned and is being carried out. In the course of the SG experimental justification several mock-ups have been developed, which were used to verify the parameters identified in the detailed design.

Because of the high density of lead, it was necessary to analyse the possibility of a secondary failure of the steam generator tubes if one of the tubes breaks. The dependent failure and the subsequent ingress of steam into the coolant may in turn affect the circulation in the circuit and consequently impair the thermal condition of the fuel elements. Based on a series of conducted experiments (Fig. 5), it was demonstrated that it is impossible for a single SG tube rupture (SGTR) to develop into a multiple tube rupture (dependent rupture exclusion).

Figure 5. Tube rupture experiment



The reactor main coolant pumps (MCPs) are intended to establish the lead coolant head and provide for its circulation in the circuit. To confirm serviceability of the MCPs, several mock-ups of the pump have been developed, as well as the test sections to check their performance. In the future, a test-bench base will be set up to enable testing of a full-scale prototype of the reactor coolant pump, including endurance tests. Other main and ancillary components are being justified at small- and medium-scale test benches; the properties of structural materials in the operating temperature ranges and rated operating conditions, including irradiation, are being obtained. The main (largest) components developed for the BREST reactor facility have been justified through the experiments and

calculations and are now being prepared for prototype testing. The whole detailed design of the BREST-OD-300 reactor facility has been carried out and supported by small- and medium-scale test benches and test sections, as well as validated software tools, showing that the design meets the Key parameter specifications. The licensing application for BREST has been completed and submitted to the licensing authority where it is currently under review.

Japan: Fundamental experimental and theoretical studies for the LFR have been carried out by the Tokyo Institute of Technology.

In the frame of material studies, material compatibility investigations for the LFR have been pursued. The corrosion characteristics of 13 Kinds of steels (e.g., 316 type austenitic steel, 9Cr martensitic steels, 12Cr martensitic steels, Si-rich martensitic steel, Al-rich ferritic steels and 18Cr ferritic steel) have been investigated by means of corrosion tests with a non-isothermal type forced convection loop with LBE as the coolant. The findings of these compatibility studies can be summarised as documented in references [6-9]. First, it was found that the occurrence of severe corrosion-erosion on the steels was induced by the destruction of their corroded surfaces in flowing Pb-Bi at low oxygen concentration [6]. However, this severe corrosion-erosion could be suppressed by the formation of protective oxide layers on the steel surfaces in the flowing Pb-Bi [7], and then corrosion losses were greatly mitigated, if the oxygen concentration was adequately controlled in the flowing Pb-Bi [8]. The formation of Si or Al-rich oxide layers, which had excellent stability, was effective in protecting the steel surfaces in the flowing Pb-Bi for long-term duration [9].

The oxygen sensor is one of the essential technologies for corrosion mitigation. The performance of solid electrolyte oxygen sensors [8] was improved as a result of refinement of the sensor structure [10, 11]. The in-situ corrosion monitor is also one of the Key technologies. An in-situ corrosion monitor was developed based on electrochemical impedance spectroscopy (EIS). The properties and the effectiveness of the oxide layers were analysed in-situ in static Pb. The EIS signals indicated that there were changes in the layer thickness related to the growth of the oxide layers in the liquid metal. Crack initiation and propagation in the protective oxide layers were also detected by the change of electrical resistance and capacitance in the EIS signals.

In the frame of theoretical studies, innovative LFR concepts have been studied. The use of Lead alloy (LBE) as a coolant favors the neutron economy in fast reactors. By using this characteristic, both breed and burn and CANDU burning reactor concepts have been studied. Such reactors need only natural uranium or depleted uranium for the fuel once they come into an equilibrium condition. It is also possible to achieve high burnup of fuel, up to 40%. Studies have been performed to investigate fuel integrity at high burnup, design of initial cores to start-up the reactor, and innovative design of reactor cores.

Republic of Korea: Under the present political/social environment in Korea, characterised by strong uncertainties related to the support of nuclear initiatives, the LFR R&D has been redirected towards marine propulsion and space power development, by taking advantage of the excellent safety, very long refueling intervals and economy of LFR. LFR R&D progress has been made mainly within university programs during the past twenty years, since the first Korean study began in 1996 at Seoul National University. LFR R&D has expanded into the Ulsan National Institute of Science and Technology (UNIST), the Korea Advanced Institute of Science and Technology (KAIST), Pohang Institute of Science and Technology (PosTech) as well as SungKyunKwan University (SKKU).

The Korean LFR Program has presently three main objectives: (i) development of micro-modular reactors for marine propulsion, including ice breakers, container ships and other remote station applications; (ii) technology development for sustainable power generation using energy produced during nuclear waste transmutation; and (iii) development of a new electricity generation unit to match the needs of economically and safe distributed power source.

To meet the first goal, a compact micro-modular reactor called HARMONIUM has been designed based on URANUS as the reference. HARMONIUM has innovative features including compact core with the help of pony pumps and the use of supercritical CO₂ cycle on the secondary side while Keeping the reactor core life of thirty years covering the entire lifecycle of ice-breakers and container ships without refueling.

To meet the second goal, the Korean first LFR-based burner PEACER (Proliferation-resistant Environment-friendly Accident-tolerant Continual-energy Economical Reactor) has

been developed to transmute long-lived wastes in spent nuclear fuel into short-lived low-intermediate level wastes, since 1996. In 2008, the Korean Ministry of Science and Technology selected the SFR as the technology for long-lived waste transmutation. Since then, LFR R&D for transmutation in Korea has turned its direction towards an ADS-driven Th-based transmutation system designated as TORIA (Thorium Optimised Radioisotope Incineration Arena) with the leadership of the Nuclear Transmutation Energy Research Centre of Korea (NUTRECK) at Seoul National University.

To meet the third goal for distributed power stations, URANUS has been developed. Based on the PEACER design, a small proliferation-resistant transportable power capsule designated as PASCAR has been developed at NUTRECK by capitalising on outstanding natural circulation and chemical stability of the lead-bismuth eutectic coolant. The PASCAR design employs a pool-type capsule including a core of U-TRU-Zr-alloy fuel rods in an open-square lattice and in-vessel steam generators with no pumps, while enriched uranium dioxide fuel can be used for near-term applications. Recently the core design has been changed to use fresh enriched UO_2 fuel rods in a hexagonal geometry. Like the PASCAR design, URANUS is targeted for 30 years of operation without on-site refueling at an electric power up to 100 MW and a Rankine cycle efficiency of 40%. The natural circulation capability, fast load-follow-capability, coolant chemistry management technique as well as steam generator tube leak-before-break features are considered to be promising solutions to meet the demand for passive safety and security at competitive levelised cost of electricity.

In the area of large-scale thermal-hydraulic test systems, the first large scale LFR test facility in Korea, HELIOS, has been moved from SNU to the Ulsan National Institute of Science and Technology where a new LFR development program has been started Government support. At SNU, a new mock-up, designated as PILLAR (Pool-type Integral Leading test facility for Lead-Alloy-cooled small modular Reactor), has been designed, built and operated since 2017 [12].

A new approach for reactor core design has been investigated with an inverted core concept that reverses the nuclear fuel region and coolant channel. With a preliminary neutronic study, it is found that the diameter of the active core can be reduced and a more compact design can be achieved. The reduction of the core diameter improves the economy, productivity

and transportability of small modular reactors (SMRs).

EURATOM: Following the signature of the FALCON (Fostering ALfred CONstruction) Consortium Agreement in December 2013 by Ansaldo, ENEA (Italy) and ICN (Romania), a new consortium agreement has been discussed and signed during 2017. The main motivation for this new formulation is to open the consortium to possible participation of new partners, not only within the European Community but also internationally.

In 2017 and 2018, the main activities related to the ALFRED [13] design development included: (i) development of a new conceptual design configuration for the primary side; (ii) evaluation of options for steam generator configurations; (iii) evaluation of different options for primary pumps; (iv) integration of a new Decay Heat Removal (DHR) system in the primary pool; (v) optimisation studies of core and FAs; and (vi) development of a new anti-freezing system for DHR systems. Design activities for a test facility of the DHR anti-freezing system (SIRIO) have been started thanks to a grant of the Italian government, and construction of the facility is expected to start at the beginning of 2018.

In 2018, a new facility became operational for conducting pre-normative, separate effect tests of candidate structural materials for LFRs in realistic environmental conditions with temperatures up to 650°C. The facility is a part of the JRC's Liquid Lead Laboratory (LILLA).

Concerning the Steam Generator Tube Rupture Event (SGTR), in the frame of the EURATOM MAXSIMA Project, an experimental campaign of four runs, investigating heavy liquid metal-water interaction, in a large configuration, was carried out at the CIRCE facility in 2017. Experimental runs provided new verifications that no propagation of the rupture to the surrounding tubes occurred (i.e., no "domino effect") during the tests. Post-test analysis was able to predict pressure and temperature time trends in agreement with experimental data, providing a contribution to code validation for water-HLM interaction scenarios in a large pool facility. The analyses performed provided the evidence that a suitable design of a depressurisation system (e.g., rupture discs) could allow for the mitigation of the postulated SGTR event in heavy liquid metal nuclear systems with confidence and safety. Figs. 6 and 7 illustrate the facilities and the results of the SGTR experimental campaign.

As regards the projects co-funded by the EURATOM H2020 program, SESAME (Thermal hydraulics simulations and experiments for the safety assessment of metal cooled reactors) and MYRTE (MYRRHA research and transmutation endeavor) continue their respective R&D activities with activities coordinated through the conduct of joint meetings to discuss and report progress. In 2017, three new collaborative projects of interest for Generation IV and LFR have been funded and already launched:

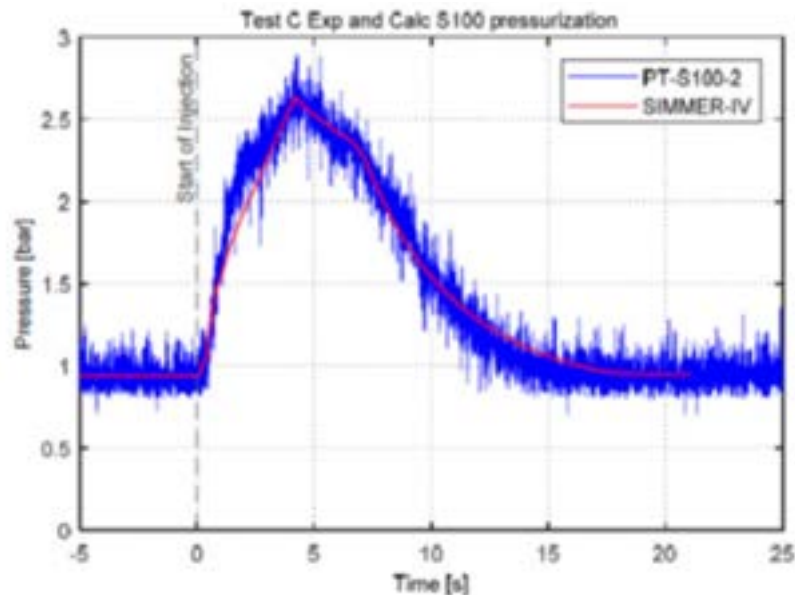
- **GEMMA** - materials for Gen IV/LFRs, with a total budget of 6.6 MEUR and coordinated by ENEA-Italy, started in June 2017;
- **INSPYRE** - fuel for fast reactors, with a total budget of 9.4 MEUR and coordinated by CEA-France, started in September 2017;
- **M4F** - materials for Gen IV and fusion, with a total budget of 6.5 MEUR and coordinated by CIEMAT-Spain, started in September 2017.

A new EURATOM H2020 call for project proposals has been published at the end of October 2017. In the call, project proposals related to safety and severe accident simulations of Gen IV reactors as well as projects related to innovation aspect of nuclear safety are sought.

Figure 6. SGTR Test Section in CIRCE facility (MAXSIMA Project, H2020)



Figure 7. SGTR Experiment in CIRCE facility (MAXSIMA Project, H2020). Calculated and experimental pressure time trends in the main vessel cover gas



United States: Work on LFR concepts and technology in the U.S. has been carried out since 1997. In addition to reactor design efforts, past activities included work on lead corrosion and thermal-hydraulic testing at a number of organisations and laboratories, and the development and testing of advanced materials suitable for use in lead or Pb-Bi environments. While current LFR activities in the US are limited, past and ongoing efforts and especially new efforts in the industrial sector demonstrate continued and growing interest in LFR technology.

With regard to design concepts, of particular relevance is the past development of the Small, Secure Transportable Autonomous Reactor (SSTAR), carried out by ANL, LLNL and other organisations over an extended period of time [14]. SSTAR is an SMR that can supply 20 MWe/45 MWt with a reactor system that is transportable. Some notable features include reliance on natural circulation for both operational and shutdown heat removal; a very long core life (15-30 years) with cassette refueling; and an innovative supercritical CO₂ (S-CO₂) Brayton cycle power conversion system. Although this system is a legacy concept without current developmental research, the concept represents one of the three reference designs of the GIF LFR pSSC in recognition of the potential for small LFRs to address growing interest in and promise of SMRs based on LFR technology. It is noted that several other small LFR concepts are currently being developed in the US and elsewhere.

Other more current efforts include university research on methods for in-service inspection and the implementation of autonomous load following in lead-cooled reactors, as well as ongoing research associated with the EU-US INERI project “Small Modular Lead-cooled Fast Reactors in Regional Energy Markets: Safety, Security, and Economic Assessments.”

In the US industrial sector, current LFR reactor initiatives include the new LFR reactor concept identified as LFR-AS (Amphora Shaped) by Hydromine, Inc. [15], and an ongoing initiative by Westinghouse Corporation to design and commercialise a new advanced LFR system [16]. Finally, it should be noted that, in February 2018, the US-DOE signed the GIF-LFR-MoU, supporting in this way the growing interest of US stakeholders in LFR technology.

People’s Republic of China (Observer): The government of China has provided continuous national support to develop lead-based reactors technology since 1986, under the auspices of

the Chinese Academy of Sciences (CAS), the Ministry of Science and Technology, the NSF, etc. Following the last 30 years of research on lead-based reactors, the China LEAD-based Reactor (CLEAR) was selected as the reference reactor for both accelerator-driven system (ADS) and fast reactor systems, and the program is being carried out by the Institute of Nuclear Energy Safety Technology (INEST/FDS Team), CAS.

The activities on CLEAR reactor design, reactor safety assessment, design and analysis software development, lead-bismuth experiment loop, and Key technologies and components R&D activities are being carried out as indicated in [17, 18].

Since 2016, the China Lead-based Mini Reactor CLEAR-M has been proposed for remote area power supply. The first step is to construct CLEAR-M10, which is a small module 1-10MW class lead-based reactor to demonstrate transportable small-scale energy supply system. The conceptual design of CLEAR-M10 has been fixed. An advanced external neutron-driven lead-based reactor (CLEAR-A) for energy production has also been designed as well.

In order to validate and test the Key components and operating technology of lead-based reactor, the lead-alloy cooled non-nuclear reactor CLEAR-S [19] with a main vessel of 2m diameter and 6.5m height, 2.5MW electric heating power and >200t LBE inventory (Fig. 8), and the lead-based zero power nuclear reactor CLEAR-0 have been constructed and operation started. The lead-based virtual reactor CLEAR-V has been developed as well. A series of experiments on thermal hydraulics, component testing, thermal-power conversion, etc. have been carried out to support the CLEAR series projects and LFR technology development.

Figure 8. Lead alloy cooled integrated non-nuclear test facility CLEAR-S



V. Conclusion

This paper summarises the main recent collaborative efforts and achievements of the LFR-pSSC. A brief overview of the main aspects is included in the paper to illustrate the benefits of the collaborative work carried out inside GIF. Finally, the status of the development of LFRs in the GIF member countries and entities is briefly presented, making reference to the world-wide LFR technology initiatives taking place which represent both societally and industrially promising technology innovation.

Acknowledgements

The Authors want to acknowledge the continuous support of their respective governments, member states, and organisations provided to the activities carried out as a part of the Generation IV International Forum.

Nomenclature

ADS	Accelerator-driven System
ALFRED	Advanced Lead Fast Reactor European Demonstrator
ANL	Argonne National Laboratory
AS	Amphora Shaped
BREST	Bystryi Reactor so Svintsovym Teplonositelem
CAS	Chinese Academy of Sciences
CLEAR	China LEAd-based Reactor
CooA	Cooperation Agreement
EIS	Electrochemical Impedance Spectroscopy
ELFR	European Lead Fast Reactor
ENHS	Encapsulated Nuclear Heat Source
EURATOM	European Atomic Energy Community
FA	Fuel Assembly
FALCON	Fostering Alfred Construction
G4M	Gen4 Module
GIF	Generation IV International Forum
GLANST	Global Symposium on Lead and Lead Alloy Cooled Nuclear Energy Science and Technology
H2020	EURATOM Horizon 2020 Framework Program for nuclear research and training

HLM	Heavy Liquid Metal
INERI	International Nuclear Energy Research Initiative
INEST	Institute of Nuclear Energy Safety Technology
JRC	Joint Research Center of the European Commission
KAIST	Korea Advanced Institute of Science and Technology
LFR	Lead Fast Reactor
LILLA	Liquid Lead Laboratory
LLNL	Lawrence Livermore National Laboratory
MCP	Main Coolant Pump
MoU	Memorandum of Understanding
NUTRECK	Nuclear Transmutation Energy Research Centre of Korea
PEACER	Proliferation-resistant Environment-friendly Accident-tolerant Continual-energy Economical Reactor
PILLAR	Pool-type Integral Leading test facility for Lead-Alloy-cooled small modular Reactor
POLAR	Passively Operated Lead Arctic Reactor
PosTech	Pohang Institute of Science and Technology
pSSC	provisional System Steering Committee
RSWG	Risk & Safety Working Group
SDC	Safety Design Criteria
SG	Steam Generator
SGTR	Steam Generator Tube Rupture
SKKU	SungKyunKwan University
SMR	Small Modular Reactor
SNU	Seoul National University
SRP	System Research Plan
SSA	System Safety Assessment
SSTAR	Small Secure Transportable Autonomous Reactor
TIT	Tokyo Institute of Technology
UNIST	Ulsan National Institute of Science and Technology

References

- [1] L. Cinotti, C.F. Smith and H. Sekimoto, "Lead-cooled Fast Reactor (LFR): Overview and Perspectives," Proceedings, GIF Symposium, Paris, France 9-10 September 2009.
- [2] E.O. Adamov "Closed fuel cycle technologies based on fast reactors as the corner stone for sustainable development of nuclear power" IAEA - FR17 Yekaterinburg, Russian Federation 26 – 29 June 2017.
- [3] Yu.G. Dragunov, V.V. Lemekhov, A.V. Moiseev, V.S. Smirnov, O.A. Yarmolenko, V.P. Vasyukhno, Yu.S. Cherepnin, D.A. Afremov, Yu.V. Lemekhov "BREST-OD-300 Reactor Facility: Development Stages and Justification" IAEA - FR17 Yekaterinburg, Russian Federation 26 – 29 June 2017.
- [4] V.V. Lemekhov, A.V. Moiseev, V.S. Smirnov et al "BREST-OD-300 Reactor: State of Development and Justification" GLANST - Global Symposium on Lead and Lead Alloy Cooled Nuclear Energy Science and Technology September 7-8, 2017, Seoul National University, Seoul, Korea.
- [5] A.F. Grachev, L.M. Zabudko, E.A. Zvir, D.V. Zozulya, Yu.A. Ivanov, F.N. Kryukov, Yu.S. Mochalov, M.V. Skupov "Development of innovative fast reactor nitride fuel in Russian Federation: state-of-art" IAEA - FR17 Yekaterinburg, Russian Federation 26 – 29 June 2017.
- [6] Masatoshi KONDO, Minoru TAKAHASHI, Tadashi SUZUKI, Kotaro ISHIKAWA, Koji. HATA, S. Qiu and Hiroshi SEKIMOTO, "Metallurgical study on erosion and corrosion behaviors of steels exposed to liquid lead bismuth flow", Journal of Nuclear Materials, 343, 349-359 (2005).
- [7] Masatoshi KONDO, Minoru TAKAHASHI, Naoki SAWADA and Koji HATA, "Corrosion of Steels in Lead-Bismuth Flow", Journal of Nuclear Science and Technology, 43, 2 107-116 (2005).
- [8] Masatoshi KONDO, Minoru TAKAHASHI, Kunimitu MIURA and Tatuya ONIZAWA, "Study on Control of Oxygen Concentration in Lead Bismuth Flow Using Lead Oxide Particles", Journal of Nuclear Materials, 357, 97-104 (2006).
- [9] Masatoshi KONDO and Minoru TAKAHASHI, "Corrosion Resistance of Si- and Al- Rich Steels in Lead Bismuth Flow", Journal of Nuclear Materials, 356, 203-212 (2006).
- [10] Pribadi Mumpuni ADHI, Masatoshi KONDO, Minoru TAKAHASHI, Performance of solid electrolyte oxygen sensor with solid and liquid reference electrode for liquid metal, Sensors and Actuators B 241, 1261-69 (2017).
- [11] Pribadi Mumpuni ADHI, Nariaki OKUBO, Atsushi KOMATSU, Masatoshi KONDO, Minoru TAKAHASHI, Electrochemical Impedance Analysis on Solid Electrolyte Oxygen Sensor with Gas and Liquid Reference Electrodes for Liquid LBE, Energy Procedia, 131C, pp. 420-427 (2017).
- [12] Yong-Hoon Shin, Il Soon Hwang, "Design of an integral experimental facility for lead-alloy cooled small modular reactor research: PILLAR", Global Symposium on Lead and Lead Alloy Cooled Nuclear Energy Science and Technology (GLANST-2017), Seoul, Republic of Korea, September 7-8, 2017.
- [13] M. Frignani, A. Alemberti "ALFRED: A Strategic Vision for LFR Deployment" ANS Winter meeting & EXPO October 29-November 2, 2017 Washington, D.C.
- [14] Smith, C.F., W. Halsey, N. Brown, D. Wade, "SSTAR: the US lead-cooled fast reactor (LFR)," Journal of Nuclear Materials 376(3):255-259, June 2008.
- [15] Cinotti, L., "The innovations of the LFR-AS-200 project," Small Modular Lead Fast Reactor (LFR-AS-200) Symposium, Imperial College, London, UK, July 12, 2016.
- [16] World Nuclear Association, "Westinghouse proposes LFR project," <http://www.world-nuclear-news.org/NN-Westinghouse-proposes-LFR-project-1410154.html>, 14 October 2015.

[17] Y. Wu, Y. Bai, Y. Song, et al, "Development strategy and conceptual design of China Lead-based Research Reactor", *Annals of Nuclear Energy*, 87(2): 511-516, 2016

[18] Y. Wu, "Design and R&D Progress of China Lead-Based Reactor for ADS Research Facility", *Engineering*, 2(1): 124-131, 2016

[19] Y. Wu, "CLEAR-S: an integrated non-nuclear test facility for China lead-based research reactor", 40(14): 1951-1956, 2016

IMPLEMENTATION OF THE GEN-IV REQUIREMENTS IN THE BN-1200 DESIGN (B.VASILIEV ET AL)

Boris Vasiliev⁽¹⁾, Aleksey Vasyaev⁽²⁾, Sergey Shepelev⁽³⁾, Iurii Ashurko⁽⁴⁾, Andrey Gulevich⁽⁵⁾,
Dmitry Klinov⁽⁶⁾

(1-3) JSC "Afrikantov OKBM", Russian Federation.

(4-6) JSC "SSC RF-IPPE", Russian Federation.

Abstract

The report analyses the BN-1200 design, the Russian commercial sodium-cooled fast reactor (SFR), in terms of its compliance with requirements for advanced Generation-IV nuclear energy systems (NES).

Basic conceptual technical decisions implemented in the BN-1200 design which allow satisfying requirements for the Generation-IV NES related to safety, sustainability, economics, proliferation resistance and physical protection are described.

A self-assessment of the BN-1200 concept based on 26 metrics developed within the framework of the Generation-IV International Forum (GIF) for the Generation-IV SFR is performed.

The analysis of compliance of the safety requirements applied for development of the BN-1200 design with the safety design criteria for the Generation-IV SFR developed within the GIF framework is presented.

I. Introduction

The BN-1200 reactor facility design has been developed within the framework of the Federal Target Program (FTP) "Nuclear power technologies of a new generation for the period of 2010-2015 and with outlook to 2020" aimed at the development and creation of new technological platform for nuclear power based on transition to closed nuclear fuel cycle with Generation-IV fast reactors.

Development of the design of the commercial power unit with BN-1200 reactor was carried out on the basis of all experience gained in Russia in the area of the sodium-cooled fast reactors (SFR) design, construction and operation: BR-5/10, BOR-60, BN-350, BN-600, BN-800.

In accordance with the FTP goals, the BN 1200 should meet the requirements for the Generation-IV NES. For this reason, the BN 1200 concept was submitted in 2017 by the State Corporation "Rosatom" for consideration within the framework of the GIF Project Arrangement on SFR System Integration and

Assessment (SIA) as a "design track" that meets the criteria for the Generation-IV SFR. According to the review procedure established within the framework of the SFR SIA Project Arrangement for "design track" evaluation, Russian specialists have carried out a self-assessment of the BN-1200 concept in terms of its compliance with the Generation-IV SFR parameters, formulated within the GIF framework as a set of 26 metrics on various aspects of reactor technologies: sustainability, safety, economics, proliferation resistance and physical protection. The results of the self-assessment, confirming the compliance of the BN-1200 concept with the parameters of the Generation-IV SFR, were approved by the members of this GIF Project Arrangement. They were presented in detail at the IAEA International Conference on Fast Reactors FR17 held in Yekaterinburg in 2017. [1]

A special working group was organised within the GIF to provide more detailed consideration of the GIF Key safety goals, those are of a general nature, by developing safety design criteria (SDC) for the Generation-IV SFR. This group (SDC Task Force) released a report

containing 83 safety design criteria for the Generation-IV SFR. [2]

We will follow the same order considering the extent of compliance between safety requirements used in the BN-1200 design and the listed safety design criteria.

The estimation of the level of compliance of the BN-1200 design with the Generation-IV SFR safety design criteria, developed by the SDC Task Force, was provided by means of comparison between the safety requirements applied for development of the BN-1200 design and the specified SDC for the Generation-IV SFR.

This report reviews the Key characteristics of the BN-1200 design and the approaches used to ensure its safety, as well as briefly describes the

main results of the above-mentioned studies that allow making conclusion about the degree of compliance of the BN-1200 with metrics and criteria for the Generation-IV SFR.

II. Description of the BN-1200

As noted above, the BN 1200 design was developed taking into account the previous SFR experience, and primarily the experience gained on design, construction and operation of the BN 600 and BN-800. In this regard, it would be interesting to follow the trends of changing technical solutions and characteristics adopted in the listed reactor facilities and in the BN-1200 design, which are presented in Table 1.

Table 1. Parameter trends in the Russian SFR

Parameter	BN-600	BN-800	BN-1200	
Thermal power, MW	1470	2100	2800	
Electric power, gross, MW	600	880	1220	
Efficiency, gross/net, %	42.5/40	41.9/38.8	43.5/40.7	
Fuel type	UO ₂	MOX ¹⁾	MNUP	MOX
Maximum burnup, % h.a.	11.2	11.5	7.6/10.9	11.8/14.5
Maximum damage dose, dpa	82	90	96/131	116/140
Fuel cladding material	Austenitic steel	Austenitic steel	Advanced austenitic steel/Ferritic-martensitic steel	
Fuel pin diameter, mm	6.9	6.9	9.3/10.5	9.3
Size across flats, mm	96	96	181	
Average core power density, MW/m ³	400	450	~ 230	
Mean residence time for fuel subassemblies (FSA), EFPD	560	465	920/1320	1060/1320
Breeding ratio	0.85	1.0	up to 1.4	up to 1.2
Integration of the primary system equipment	Partial	Partial	Complete	
SG configuration	Sectional-modular	Sectional-modular	Integral	
Technical solutions for safety: - Jacketing of pipes and vessels with radioactive Na - Emergency protection systems - Circuit of decay heat removal system location - Corium confinement system (core catcher) - Room to confine emergency releases	Partial SCRAM Tertiary - -	Partial SCRAM, PAZ-G Secondary + -	Complete SCRAM, PAZ-G, PAZ-T Primary ²⁾ + +	
Probability of severe accidents for SFR power unit per reactor-year	1.0·10 ⁻⁵	1.2·10 ⁻⁶	5.0·10 ⁻⁷	
Design lifetime, year	30 ³⁾	45	60	

1) – Hybrid core with UO₂/MOX at the initial phase; 2) – DHRS loops are connected to the primary circuit; 3) – 40 years (after design lifetime extension).

The main parameters of the BN-1200 heat removal loops are presented in Table 2.

Table 2. Main parameters of the BN-1200 heat removal loops

Parameter	Value
Number of primary loops	4
Number of secondary loops	4
Primary circuit sodium flowrate, kg/s	15784
Secondary circuit sodium flowrate, kg/s	12776
Primary circuit coolant temperature (IHX outlet/inlet), °C	410/550
Secondary circuit coolant temperature (SG outlet/inlet), °C	355/527
Tertiary circuit parameters:	
Live steam pressure, MPa	17.0
Live steam temperature, °C	510
Feedwater temperature, °C	275
Type of intermediate steam reheating	Steam

The BN-1200 core configuration is presented in Figure 1.

Figure 1. BN-1200 core

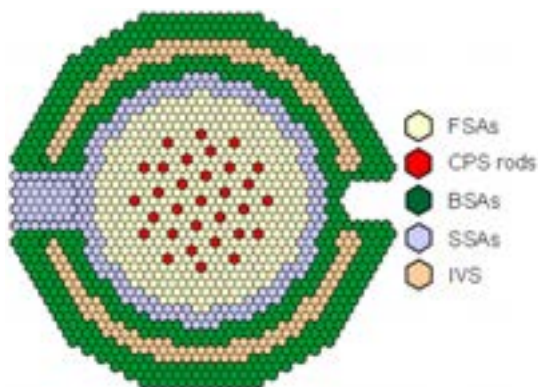
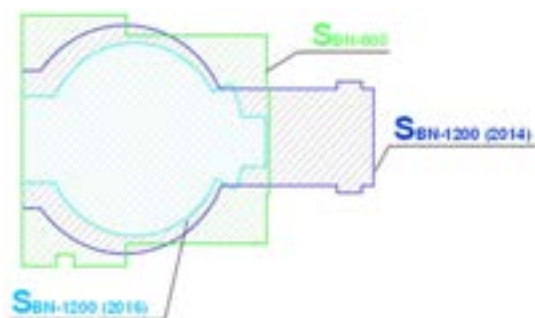


Figure 2. Evolution of the BN-1200 reactor building layout



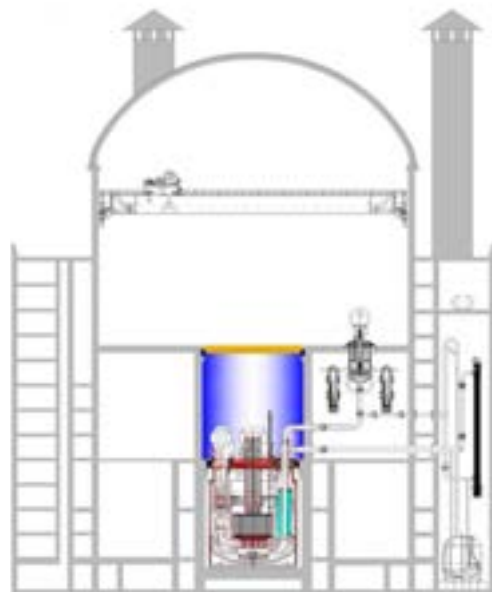
Enhancement of the BN-1200 technical-and-economic characteristics is one of the priorities for the design improvement. In particular, a significant reduction in the construction volumes of the BN-1200 reactor building was achieved compared to the BN-800 one (Figure 2).

A significant contribution to reduction of the metal consumption of the reactor facility and simplification of its systems is provided by:

- Integral layout of the primary circuit;
- Simplification of the refuelling system by exception of intermediate storage drums of fresh and spent FSAs (SFSAs) and organisation of a capacious in-vessel storage (IVS) for SFSAs, providing direct unloading of SFSAs (after their exposure in the IVS) from the IVS into washing cells and further into an exposure pool;
- Transition from sectional-modular SG scheme to integral one based on application of straight-tube large-capacity modules;
- Application of one turbo-generator per power unit.

The view of the BN-1200 reactor building is illustrated by Figure 3.

Figure 3. View of the BN-1200 reactor building



III. Safety Approach Applied to the BN-1200 Design

The BN-1200 design was developed in accordance with requirements of existing Russian regulatory documents in the field of NPP safety. Accordingly, approach to substantiation of the BN-1200 safety is dictated by these documents. The most important of these documents are:

- Federal Standards and Rules in the Field of Use of Atomic Energy "General Safety Assurance Provisions for Nuclear Power Plants" (NP-001-15), Moscow, 2015. [3]
- Federal Standards and Rules in the Field of Use of Atomic Energy "Nuclear Safety Rules for Reactor Installations of Nuclear Power Plants" (NP-082-07), Moscow, 2008. [4]

In accordance with paragraph (p.) 1.2.4 of the NP-001-15, the BN-1200 safety is ensured due to consistent implementation of the Defence in Depth (DiD), which provides for developing the NPP design documentation on the basis of a conservative approach with inherent safety features of the reactor facility and measures aimed at elimination of the cliff edge effect.

As mentioned above, the BN-1200 design focuses on maximum enhancement of inherent safety features of the reactor facility and application of safety systems based on passive principles of operation in order to ensure a high level of safety (p. 3.1.10 of the NP-001-15). In particular, in case of failure of standard emergency protection systems, the design provides for two independent passive reactor shutdown systems based on different principles of actuation:

- Passive shutdown system based on hydraulically suspended absorbing rods (PAZ-G);
- Passive shutdown system self-actuated due to increase of the reactor core outlet coolant temperature above a certain value (PAZ-T).

A passive decay heat removal system (DHRS) through air-sodium heat exchangers that is directly connected to the reactor vessel is applied in the BN-1200.

Deterministic and probabilistic safety analyses are applied for the BN-1200 safety analysis (p. 1.2.9 of the NP-001-15).

In order to mitigate possible core damage in case of a severe beyond-design basis accident (BDBA), the following solutions and requirements were implemented in the BN-1200 design:

- In accordance with p. 3.4 of the Appendix to the NP-082-07 reactivity coefficient values in terms of temperature and power of the reactor as well as a total coefficient of reactivity in terms of the coolant and fuel temperature are provided negative over the entire range of the reactor parameter changes during normal operation and anticipated operational occurrences including design basis accidents. For BDBAs, the permissible range of the sodium void reactivity effect (SVRE) is substantiated;
- Sodium cavity over the reactor core is designed to reduce SVRE in case of sodium boiling in the core;
- Decrease of core power density;
- Reduction of a burnup reactivity margin by use of mixed nitride uranium-plutonium (MNUP) fuel or by application of an axial layer in case of the mixed oxide (MOX) fuel.

As mentioned above, pool type arrangement of the primary circuit with location of all sodium systems including cold traps and chemical-engineering control systems within the reactor vessel is applied in the BN-1200 design (Figure 4). The reactor vessel, in turn, is surrounded by a guard vessel that practically eliminates a risk of radioactive sodium release outside the reactor vessel and its fire.

Figure 4. Integral layout of the BN-1200 primary circuit



The pipelines of the secondary loops are surrounded by safety jackets that mitigate consequences of sodium leaks in the secondary loops.

The following measures are provided for case of the core damage:

- Core catcher located at the bottom of the reactor vessel to eliminate release of failed core fragments outside the reactor vessel boundaries;
- A volume of the room located above the reactor and used as a containment analogue to localise radioactive products and to eliminate their release into the environment.

IV. Evaluation of the BN-1200 According to the GIF Metrics for the Generation-IV SFR

As part of the BN-1200 concept submission for consideration within the SFR SIA Project

Arrangement, a self-assessment of the BN-1200 concept was performed regarding its compliance with the Generation-IV SFR parameters. This self-assessment was carried out in accordance with the methodology developed by the GIF, which contains a list of 26 metrics related to the aspects of sustainability, safety, economics, proliferation resistance and physical protection. The values of these metrics obtained for the BN-1200 are presented in Table 3.

A detailed justification of the selected metric values for the BN-1200 is presented in the report to the IAEA Conference on fast reactors FR17 in Yekaterinburg. [1]

Here we will limit ourselves by the final results of this self-assessment, which are presented in Figure 5. These results are collected into four categories of sustainability, proliferation resistance and physical protection, safety and reliability, and economics.

Table 3. Values of the GIF metrics for the BN-1200 reactor

No	Metric	Value
1	Fuel makeup, MTU/GWe·year	< 10
2	Radwaste mass, MT/GWe·year	5–15
3	Radwaste volume, m ³ /GWe·year	5–15
4	Long-term energy generation, KW/GWe·year	< 0,1
5	Long-term radiotoxicity, MSv/GWe·year	< 20–100
6	Environmental impact	A little better than the basic one
7	Released materials	Fuel with LEU or intensive radiation
8	Spent nuclear fuel characteristics	Radiation level >50,000 MW·day/MT h.m.
9	Resistance to acts of terrorism/sabotage	Passive systems without an active startup
10	Reliability	Failure rate reduced by a factor of 5
11	Standard personnel irradiation	Standard irradiation considerably reduced
12	Emergency personnel/population irradiation	Emergency irradiation considerably reduced
13	Reactivity control reliability	Design characteristics prevent core damage
14	Heat removal reliability	DHRS does not require any energy source
15	Uncertainty of dominating phenomena	Full-scale study on phenomena in the entire range
16	Reactor thermal inertia	Longer thermal inertia of fuel/coolant
17	Scale of integral experiments	Integral testing on a prototype scale
18	Source terms	Limits of the relative release less by a factor of 10
19	Energy release mechanisms	Energy release less by a factor of 2
20	Time to core damage after the initial event	Core is damaged after 24 h following the initial event
21	Radioactivity confinement efficiency	Release fraction less by a factor of 10
22	Current specific capital costs, USD /kW	1400
23	Electricity cost, USD /MW·h	16–20
24	Construction period, month	45–65
25	Design cost, USD M	15–50
26	R&D cost, USD M	150–350

Figure 5. Summary diagrams of the GIF metrics for the BN 1200



Figure 5 shows that the BN-1200 has indicators related to sustainability, proliferation resistance and physical protection, safety and reliability categories higher than for the Generation-III light water reactors (LWRs). The BN-1200 indicators, corresponding to category of economics, are slightly worse than the LWR indicators. In certain degree, it can be explained by the fact that reference values of the economic indicators related to the LWR in the mentioned GIF methodology are not realistic in modern conditions.

The achieved results show that the BN 1200 design, on the whole, has good potential to meet the criteria related to Generation-IV NES. Regarding further improvement of the design, main attention should be focused on enhancement of its economic characteristics without decreasing the high level of its safety achieved.

V. Comparison of Safety Requirements to the BN-1200 Design With Safety Design Criteria for Generation-IV SFR

The development of the SDC for the Generation-IV SFR is based on the IAEA document regulating SDC for the LWR. [5] These criteria were analysed for their adaptation to the SFR, and they were added with criteria that take into account the specific features of these reactors, in particular the properties of the sodium coolant. As a result of this activity, the above-mentioned report [2] was issued, which was subsequently revised [6] taking into account the comments of experts from national nuclear regulatory authorities and international organisations, as well as the revised IAEA document for the LWR [7] reflecting the lessons learned from the Fukushima accident.

The safety design criteria developed by the SDC TF for the Generation-IV SFR are divided into the following categories:

- General criteria related to management of safety in design (Criteria 1-3);
- Principal technical criteria (Criteria 4-12);
- Set of criteria related to general plant design which is divided into five subsets:
 - Design basis (Criteria 13-28);
 - Design for safe operation over the lifetime of the plant (Criteria 29-31);
 - Human factors (Criterion 32);
 - Other design considerations (Criteria 33-41);
 - Safety analysis (Criterion 42);
- Group of criteria related to design of specific plant systems:
 - Overall plant system (Criterion 42bis);
 - Reactor core and associated features (Criteria 43-46);
 - Reactor coolant systems (Criteria 47-53);
 - Containment structure and containment system (Criteria 54-58);
 - Instrumentation and control systems (Criteria 59-67);
 - Emergency power supply (Criterion 68);
 - Supporting systems and auxiliary systems (Criteria 69-76);
 - Other power conversion systems (Criterion 77);
 - Treatment of radioactive effluents and radioactive waste (Criteria 78-79);
 - Fuel handling and storage systems (Criterion 80);
 - Radiation protection (Criteria 81-82).

In order to evaluate the degree of compliance of the BN-1200 design with the specified SDC for the Generation-IV SFR, Russian specialists performed a comparative analysis of the safety requirements that were applied for the BN 1200 design [3-4] and safety design criteria for the Generation-IV SFR. [8] Note that NP-001-15 issued in 2015 is revised taking into account lessons learned from Fukushima-1 accident.

A detailed comparative analysis for each individual criterion has been done in the paper presented at the 7th Joint IAEA-GIF Technical

Meeting/Workshop on the Safety of Liquid Metal Cooled Fast Reactors. [8] Summarising these results, we note that all SDC are taken into account to any extent in the Russian regulatory documents on safety.

However, it should be specially highlighted the implementation of the following basic safety approaches in the BN-1200 design that are formulated in SDC:

- Consistent implementation of the DiD principle;
- Maximum enhancement of inherent safety features and predominant application of safety systems based on passive principles of operation;
- Combination of deterministic and probabilistic approaches to safety analysis.

Measures adopted in the BN-1200 design allow practical eliminating:

- Occurrence of the severe BDBAs with large-scale reactor core damage;
- Radioactive sodium leaks.

But the deterministic analysis of postulated severe BDBAs with large-scale core damage, performed in the BN-1200 design, shows that even failure of all active and passive shutdown systems does not lead to excess of the permissible limits for radioactivity release outside the NPP site and does not require evacuation of the population accordingly.

VI. Conclusion

The results of the BN-1200 concept self-assessment performed in accordance with the GIF methodology show that the BN-1200 design has a good potential from the point of view of its correspondence to metrics for the Generation-IV NES.

Comparison of the safety requirements applied for development of the BN-1200 design with safety design criteria for the Generation-IV SFR developed by the GIF SDC Task Force indicates their compliance.

Thus, the analysis of implementation of the GIF metrics and design safety criteria for the Generation-IV SFR in the BN-1200 design allows making conclusion about its general correspondence to the mentioned metrics and criteria for the Generation-IV SFR.

Acknowledgements

This work was prepared with support of the Innovation Complex of the State Atomic Energy Corporation "Rosatom".

Nomenclature

BDBA	Beyond-Design-Basis-Accident
BSA	Boron shielding assembly
CPS	Control and protection system
DHRS	Decay heat removal system
DiD	Defence-in-Depth
EFPD	Effective full power day
FSA	Fuel subassembly
FTP	Federal Target Program
GIF	Generation IV International Forum
IAEA	International Atomic Energy Agency
IHX	Intermediate heat exchanger
IVS	In-vessel storage

LEU	Low enriched uranium
LWR	Light water reactor
MA	Minor actinides
MNUP	Mixed nitride uranium-plutonium fuel
MOX	Mixed oxide fuel
NES	Nuclear energy system
NPP	Nuclear power plant
PAZ-G	Passive shutdown system with hydraulically suspended rods
PAZ-T	Passive shutdown system based on temperature actuation principle
SDC	Safety design criteria
SFR	Sodium-cooled fast reactor
SG	Steam generator
SIA	System integration and assessment
SFSA	Spent fuel subassembly
SVRE	Sodium void reactivity effect
SSA	Steel shielding assembly

References

- [1] Shepelev S. F., Marova E. V., et al, «Evaluation Results of BN-1200 Compliance with the Requirements of GENERATION IV and INPRO», IAEA International Conference on Fast Reactors and Related Fuel Cycles: Next Generation Nuclear Systems for Sustainable Development FR17, Yekaterinburg, Russia, 26-29 June 2017, IAEA-CN-245-399.
- [2] Safety Design Criteria for Generation IV Sodium-cooled Fast Reactor System, SDC-TF/2013/01, May 1, 2013.
- [3] Federal Standards and Rules in the Field of Use of Atomic Energy "General Safety Assurance Provisions for Nuclear Power Plants" (NP-001-15), Moscow, 2015.
- [4] Federal Standards and Rules in the Field of Use of Atomic Energy "Nuclear Safety Rules for Reactor Installations of Nuclear Power Plants" (NP-082-07), Moscow, 2008.
- [5] Safety of Nuclear Power Plants: Design, IAEA Safety Standards Series No. SSR-2/1, 2012.
- [6] Safety Design Criteria for Generation IV Sodium-cooled Fast Reactor System (Rev. 1), SDC-TF/2017/02, September 30, 2017.
- [7] Safety of Nuclear Power Plants: Design, IAEA Safety Standards Series No. SSR-2/1 (Rev. 1), 2016.
- [8] I. Ashurko, «Implementation of Safety Design Criteria in the Large Power Size Sodium Cooled Fast Reactor BN-1200 Design», 7th Joint IAEA-GIF Technical Meeting/Workshop on the Safety of Liquid Metal Cooled Fast Reactors, Vienna, Austria, 27-29 March 2018.

AN UPDATE ON THE DEVELOPMENT STATUS OF THE SUPER-CRITICAL WATER-COOLED REACTORS (L. K. H. LEUNG ET AL)

L.K.H. Leung⁽¹⁾, Y.-P. Huang⁽²⁾, V. Dostal⁽³⁾, A. Yamaji⁽⁴⁾ and A. Sedov⁽⁵⁾

(1) Canadian Nuclear Laboratories, Canada.

(2) Nuclear Power Institute of China, China.

(3) Řež Research Centre, Czech Republic.

(4) Waseda University, Japan.

(5) NRC "Kurchatov Institute", Russian Federation.

Abstract

The Super-Critical Water-cooled Reactor (SCWR) is a high-temperature, high-pressure watercooled reactor that operates above the thermodynamic critical point of water (374°C, 22.1 MPa). Its main mission is to generate electricity efficiently, economically and safely. Furthermore, the high core outlet temperature of SCWRs (up to 625°C) facilitates co-generation, such as hydrogen production, space heating and steam production. The development of SCWRs has been advanced with the completion of three concepts and a few are being pursued within the Generation-IV International Forum. In addition, the development is being expanded to the SCW small modular reactor for deployment in small remote communities. Recent advancements and the future plan for the SCWR development are described.

I. Introduction

Advanced designs of nuclear power plants (NPPs) are being considered for future deployments to minimise the release of greenhouse gas, which is the primary cause for climate change. The Generation-IV International Forum (GIF) was established in 2000 to support joint research and development (R&D) in developing these advanced nuclear systems [1]. Six systems were selected among over 1000 potential candidates. Among the six selected options, the Super-Critical Water-cooled Reactor (SCWR) is the only one that is directly evolved from the current NPPs, which have been designed and operating over the past 50 years.

The main goals of using supercritical water (SCW) in nuclear reactors are to increase the efficiency of modern NPPs, decrease capital and operational costs, and finally decrease electrical energy costs [2]. This would enhance the sustainability of nuclear power as the fuel consumption is reduced for generating the power and subsequently a reduction in spent fuel for disposal. Furthermore, the safety characteristics of SCWR have been advanced from the introduction of additional passive safety systems. Depending on the concept

configuration, the aspects of proliferation resistance and physical protection have been improved.

Several SCWR concepts have been established for generating powers greater than 1000 MWe (except for Japan's fast-neutron spectrum SCWR) [3]. Table 1 lists the Key parameters for SCWR concepts. These concepts are considered too large for replacing coal-fire stations and excessive for small remote communities, small mining operations and steam/heat production. There are strong interests to develop a small SCWR concept for those applications. This paper describes the recent advancements and the future plan for the SCWR development within the GIF.

1000 MWe (except for Japan's fast-neutron spectrum SCWR) [3]. Table 1 lists the Key parameters for SCWR concepts. These concepts are considered too large for replacing coal-fire stations and excessive for small remote communities, small mining operations and steam/heat production. There are strong interests to develop a small SCWR concept for those applications. This paper describes the recent advancements and the future plan for the SCWR development within the GIF.

Table 1. Key Parameters of SCWR concepts

	Canada	China		EU	Japan		Russian Federation
Type	PT	PV	PV	PV	PV	PV	PV
Spectrum	Thermal	Thermal	Mixed	Thermal	Thermal	Fast	Fast
Pressure (MPa)	25	25	25	25	25	25	24.5
Inlet Temp. (°C)	350	280	280	280	290	280	290
Outlet Temp. (°C)	625	500	510	500	510	501	540
Thermal Power (MW)	2540	2300	3800	2300	4039	1602	3830
Efficiency (%)	48	43	44	43.5	43	44	45
Active Core Height (m)	5	3	4.5	4.2	4.2	2.4	4.07
Fuel	Pu-Th (UO ₂)	UO ₂	UO ₂ MOX	UO ₂	UO ₂	MOX	MOX
Moderator	D ₂ O	H ₂ O	H ₂ O/-	H ₂ O	H ₂ O	-/ZrH	-
# of Flow Passes	1	2	2	3	1/2	1/2	1/2

II. General Descriptions of SCWR

The SCWR is a high-temperature, high-pressure water-cooled reactor that operates above the thermodynamic critical point of water (374°C, 22.1 MPa) [1]. Two types of core configuration are being pursued: pressure vessel (PV) and pressure tube (PT). These core designs are based on thermal neutron, fast neutron or mixed (thermal and fast) spectra.

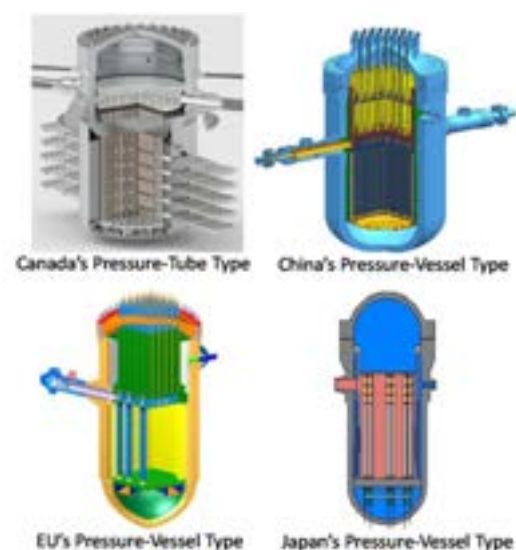
The majority of SCWR plants are developed for power generation higher than 1000 MWe at operating pressures of about 25 MPa and reactor outlet temperatures up to 625°C. Under these conditions, the coolant does not change phase (boil) in the reactor, the SCWR adopts the direct cycle eliminating moisture separator reheaters and recirculation pumps as in the boiling-water reactors, or steam generators as in the pressurised light-water and heavy-water reactors. This has significantly reduced the sizes and footprints of the containment, building and plant of SCWR. The balance-of-plant configuration is the same as that of the fossil-fuel power plant, which has been based on over 50 years of design and operation experience.

The main mission of the SCWR is to generate electricity efficiently, economically and safely. All SCWRs could generate electricity with thermal efficiencies ranging from 43 to 48%, which is better than 35% for the current fleet of nuclear reactor systems. The high core outlet temperature of SCWRs facilitates co-generation, such as hydrogen production, space heating and steam production [2].

III. SCWR Core Concepts

The SCWR thermal-spectrum core concepts have been based mainly on the pressure-vessel configuration [4]. However, the one developed in Canada is based on the pressure-tube configuration. Coolant is circulated from the bottom to the top of fuel assemblies in a single path for both Japan's and Canada's concepts. However, it passes through two zones of fuel assemblies (two-path system) in China's concept [5] and three zones (three-path system) in EU's concept. Figure 1 illustrates the thermal-spectrum core configurations.

Figure 1. Thermal-Spectrum SCWR Core Configurations



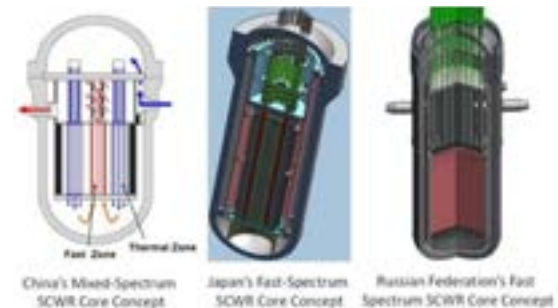
Canada's concept consists of an inlet plenum, where the coolant enters into the core and distributes to the fuel channels, and an outlet header, which collects the high-temperature coolant from the fuel channels and directs to the high-pressure turbine. The fuel channels are submerged within the low-pressure heavy-water moderator in the calandria vessel. Control and shutdown rods are inserted from the side of the calandria vessel into the low-pressure moderator.

Both China's and EU's core concepts have a similar configuration, except that China's core is divided into two zones, while the EU's core into three zones. Coolant enters the vessel from the inlet nozzles and is divided into two streams. In China's concept, the majority of coolant travels up the passage besides the vessel wall and down through the first zone of fuel assemblies. It mixes with the remaining coolant in the lower plenum and travels up through the second zone of fuel assemblies. The remaining coolant entering the vessel travels down to the lower plenum and mixes with the bulk coolant. In EU's concept, most of the coolant travels down the passage beside the vessel wall and up through the first zone of fuel assemblies. The remaining coolant flows up another passage to the top of the vessel, mixes with the coolant through the first zone, down through the second zone and up through the third zone of fuel assemblies. The hightemperature coolant collected at the outlet header is directed to the high-pressure turbine. Control and shutdown rods are inserted from the top of the vessel into the core.

Japan's core concept is similar to that of a boiling water reactor [6]. Coolant enters the vessel from the inlet nozzles and is divided into two streams. Most of the coolant travels down the passage beside the vessel wall. It mixes with the remaining coolant at the lower plenum and travels up through the fuel assemblies. The remaining coolant entering the vessel flows up another passage to the top of the vessel and then down to the bottom of the vessel along the wall mixing with the bulk coolant. It cools the vessel wall and maintains the wall at low temperatures. The hightemperature coolant exiting the fuel assemblies is collected in the outlet header and is directed to the high-pressure turbine. Control and shutdown rods are inserted from the bottom of the vessel into the core. There is an option for a two-path core configuration, which is similar to China's SCWR concept.

The flexibility of SCWRs facilitates the development of mixed- and fast-spectrum core concepts, as illustrated in Figure 2, other than thermal-spectrum core concepts. A mixed-spectrum SCWR core concept is being developed at the Shanghai Jiao Tong University in China [7]. Its configuration is similar to that of China's thermal-spectrum core. The first zone of fuel assemblies is the thermal-spectrum region while the second zone is the fast-spectrum region. Control and shutdown rods are also inserted from the top of the vessel to the core.

Figure 2. Mixed- and Fast-Spectrum SCWR Core Configurations



The configuration of Japan's fast-spectrum core concept differs from that of the thermal-spectrum core concept [4]. It is separated into two zones with a two-path flow pattern (similar to that of China's thermal-spectrum core configuration). The first zone consists of separated seed and blanket fuel assemblies with the downward coolant flow, while the second zone consists of seed fuel assemblies with the upward coolant flow. Control and shutdown rods are inserted through the top of the vessel into the core (unlike Japan's thermal-spectrum core where the rods are inserted through the bottom of the vessel).

Russian Federation's fast-spectrum core concept has the option of adopting the single-path or two-path flow pattern [8]. For the single-path core concept, the coolant entering the core travels to the top of the vessel and then directs to the bottom of the vessel. It flows upwards through the fuel assemblies and discharges to the highpressure turbine. For the two-path core concept, the coolant entering the core is separated into two streams. The majority of the coolant travels up to the top of the vessel and then downward through the outer zone of fuel assemblies. The remaining coolant flows down

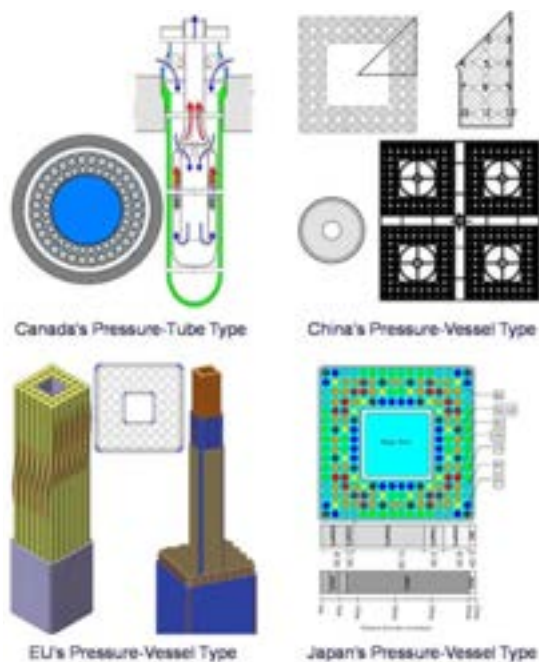
through the passage beside the vessel wall. It mixes with the bulk flow and travels upward through the inner zone of fuel assemblies. The high-temperature coolant is directed to the high-pressure turbine.

IV. SCWR Fuel Concepts

Fuel concepts for thermal-spectrum cores of the pressure-vessel type of SCWRs resemble closely to those of light water reactors [4], [5], [9].

Figure 3 illustrates the fuel assemblies for thermal-spectrum cores of SCWR. Uranium fuel with various levels of enrichment and neutron absorber has been included in the pellets. Differences are mainly in the spacing devices and the introduction of a water rod at the central region of the fuel assembly to enhance the moderation of the coolant at high pressure and high-temperature conditions.

Figure 3. Thermal-Spectrum SCWR Fuel Concepts



The fuel concept for Canada's SCWR consists of a "flask"-like structure that contains the fuel assembly and is connected to the outlet header [4]. Several nozzles are introduced for the coolant entering into the structure. These nozzles also serve as orifices to control the flow rate matching the power generation in the channel (another set of openings are also

installed at the top of the pressure tube). The fuel assembly resembles to fuel bundles of the heavy-water reactors with two rings of 32 fuel rods and an active length of 5 metres. Spacing between fuel rods is maintained with a wire-wrapped spacer. A central flow tube is installed for the coolant to travel down from the nozzles to the bottom of the fuel channel. Furthermore, it improves the moderation for the inner-ring rods resulting in a balanced radial power profile. The coolant travels upward through the fuel assembly to the outlet header, and is discharged to the high-pressure turbine. Pellets inside the fuel element consist of a mixture of thorium and plutonium (15wt% on average).

The fuel-assembly concept of China's thermal-spectrum SCWR is configured into a square array of 56 fuel rods [5]. Wire-wrapped spacers are introduced to maintain the gap size between fuel rods. A water rod is installed in the central region to increase the moderation. Pellets in the fuel rod consist of enriched uranium and are similar to those of light-water reactors. Each pellet has a central hole to reduce the fuel centreline temperature. Four assemblies are grouped together with a boiling-water-reactor type of control-rod configuration.

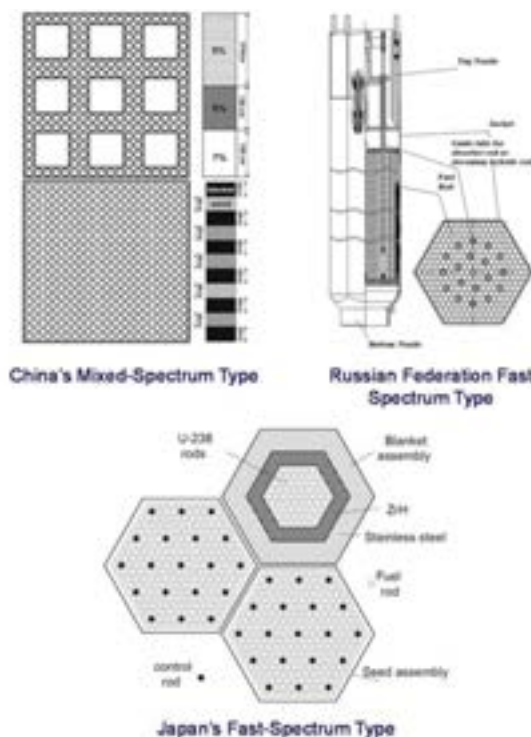
The fuel assembly concept of EU's thermal-spectrum SCWR has a square-array configuration with 40 fuel rods [4]. Wirewrapped spacers are also used to maintain the gap size between fuel rods. A water rod is installed in the central region to increase the moderation. Pellets in the fuel rod consist of enriched uranium and are similar to those of light-water reactors. Nine assemblies are grouped together with common head and foot pieces.

The fuel assembly concept of Japan's thermal-spectrum SCWR is the largest among all concepts [9]. It consists of 192 fuel rods and resembles closely to that of the boiling water reactor. Grid spacers are used to maintain the gap size between fuel rods. A water rod is installed in the central region to increase the moderation. Pellets in the fuel rod consist of uranium fuel of various levels of enrichment. Several rods contain only neutron absorbers for initial reactivity suppression. Four assemblies are grouped together with a boiling-water-reactor type of control-rod configuration.

Fuel assembly concepts for mixed- and fast-spectrum SCWRs are illustrated in Figure 4. Two separate fuel assemblies are proposed for China's mixed-spectrum SCWR; one for the thermal zone and the other for the fast zone [7]. The fuel assembly concept for the thermal zone consists of 180 fuel rods with nine water rods

distributed within the assembly. Wire-wrapped spacers are used to maintain the gap size between fuel rods. Pellets in the fuel rod consist of enriched uranium. Three grades of enriched uranium pellets are inserted at different levels of the fuel rod (i.e., lower grades at the top where the coolant temperature is the highest and higher grades at the bottom). The fuel assembly concept for the fast zone consists of 324 fuel rods. Wirewrapped spacers are used to maintain the gap size between fuel rods. Each fuel rod contains both the seed and blanket pellets wafered in different sections. Mixed oxide fuel is used for the seed pellet and depleted uranium fuel for the blanket pellet.

Figure 4. Mixed- and Fast-Spectrum SCWR Fuel Concepts



Two separate fuel-assembly types are introduced for Japan's fast-spectrum SCWR: seed assemblies each with 252 fuel rods and blanket assemblies each with 127 fuel rods [4]. These fuel assemblies are configured in hexagonal arrays. Mixed oxide fuel and stainless steel cladding are used for seed fuel rods, and depleted uranium and stainless steel cladding are used for blanket fuel rods. In the blanket assembly, the fuel rod region is surrounded by a solid moderator (Zirconia Hydride layer) so that fast neutrons coming

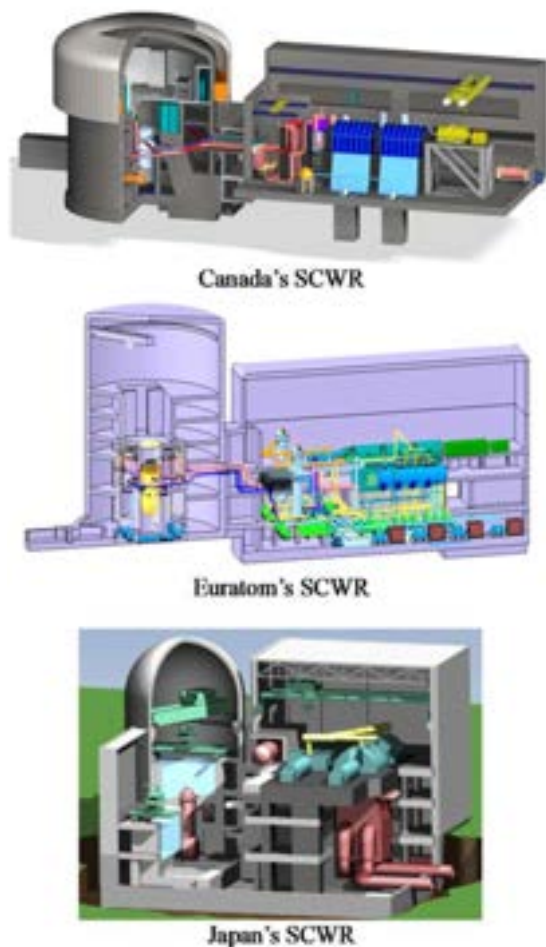
from the seed fuel are slowed down in the Zirconia Hydride layer and are absorbed by the blanket fuel without causing fast fissions. It enables the fast-spectrum SCWR to have a negative void reactivity without adopting flat core shape or additional devices. Nineteen control rods are inserted into each seed fuel assembly.

The fuel assembly concept for Russian Federation's fast-spectrum SCWR is configured into a similar array to that of Japan's seed fuel assembly (i.e., 252 fuel rod in a hexagonal array) [8]. However, only one fuel assembly is adopted with seed and blanket fuel layers wafered in each fuel rod. Mixed-oxide fuel is used for the seed layers and depleted uranium with zirconium hydride is used for the blanket layers. Nineteen absorber or zirconium hydride rods are inserted into the fuel assembly.

V. SCWR Plant Concepts

Canada, Euratom and Japan have successfully completed the development of their SCWR plant concepts, as shown in Figure 5 [10]. China and the Russian Federation are continuing their development. Most of these plant concepts were evolved from the Advanced Boiling Water Reactors (ABWRs), and included additional passive systems to improve their safety characteristics.

The inner core structure of the reactor building is the primary containment building, which is a cylindrical steel-lined concrete structure. It houses the reactor, high activity components and systems as well as the containment pool. The containment building contains all safety-related pressure boundary components. Inlet and outlet pipes penetrating the containment building are equipped with isolation valves so that the radiation release to environment can be isolated and confined inside the containment building. A suppression pool is used to limit the containment pressure. This has led to a reduction in the volume of the containment building compared to current fleet of nuclear reactors.

Figure 5. SCWR Plant Concepts

The containment building is enveloped within the shield building, which protects against external missiles, airplane crashes and natural hazards (such as tornados, tsunamis and floods). The shield building houses all lower radioactivity processes such as the containment pool filter system, drywell and steam tunnel cooling system, and fuel transfer pool cooling system. Both the containment building and the shield building are to be built on the same base slab, and are structurally decoupled except at the base in order to reduce loads induced by an external factor, such as missile or aircraft impact on the shield building. The physical separation of these two buildings also simplifies construction and limits the detrimental effect that might occur from deformations resulting from loads, temperature variations and differential settlement.

VI. Future Developments

Canada is focusing on the verification and validation of their SCWR core, fuel and plant components to improve the confident. China has developed the core concept for CSR-1000. An international peer review has been planned after completion. The development of the mixed spectrum core concept is continuing. Euratom focuses on improving their fuel concept with further studies on materials and heat transfer. Japan is continuing the development of their fast spectrum core concept. The Russian Federation has been progressing slowly in the development of their fast-spectrum core concept.

Nuclear Power Institute of China has proposed to design and construct a prototype SCWR, which simulates their CSR-1000 design. The power rating would match the minimal requirement for the super-critical pressure turbine. This small size prototype is representative to Euratom's High Performance Light Water Reactor, Japan's SCWR and a fuel channel of Canada's pressure-tube type SCWR. Therefore, a strong collaborative effort can be established for the design and construction.

As listed in Table 1, the majority of SCWR concepts were established for power generation greater than 1000 MWe (except for Japan's fastneutron spectrum SCWR), which have been considered too large and inflexible for small communities and developing countries. These SCWR concepts can be scaled down to reduce the power generation for meeting requirements of local deployment. Canada has developed a preliminary small SCWR concept, which is capable to generate power of 300 MWe. Optimisation of the core configuration is continuing. In addition, a strategy has been established to develop a very small SCWR concept for remote and mining communities and military bases. China has planned to design a small SCWR for generating 150-MWe power (CSR-150) after completing the design of the CSR-1000 SCWR. This small SCWR will also serve as a demonstration of the SCWR. The research team at Euratom has also expressed interest in developing a small SCWR referred to as the European Small Modular supercritical water Reactor Technology (or E-SMART). A proposal has been prepared for submission. Several commonalities (such as core outlet temperatures and flow paths) are envisioned for the small SCWR concepts facilitating joint development effort to expedite deployment.

VII. Conclusion

- Several SCWR concepts have been developed for generating powers higher than 1000 MWe (except for Japan's fast-spectrum SCWR). These concepts are based on the pressure vessel or pressure-tube configuration in thermal, fast and mixed spectra.
- The majority of these SCWR concepts adopt the uranium-based fuel, except for Canada's SCWR that uses a mix of thorium and plutonium fuel as reference.
- Canada, Euratom and Japan completed their thermal-spectrum SCWR concepts, which have been reviewed by international peers for their viability.
- China completed their development of the thermal-spectrum SCWR concept and is focusing on completing the plant concept. An international peer review of their concept has been planned.
- Nuclear Power Institute of China has proposed the design and construction of a prototype SCWR for the CSR-1000.
- Canada, China and Euratom are interested in designing small SCWRs for deployment in developing countries and small communities. These SCWRs are scaled-down versions of the reference designs, but would operate at less challenging conditions to expedite the deployment.

Acknowledgements

L. Leung would like to express his sincere appreciation of the support of the Natural Resources Canada and Atomic Energy of Canada Limited in developing the Canadian SCWR concept.

Nomenclature

ABWR	Advanced Boiling-Water Reactor
E-SMART	European Small Modular supercritical water Reactor Technology
EU	European Union
GIF	Generation IV International Forum
HPLWR	High Performance Light Water Reactor
NPP	Nuclear Power Plant
PT	Pressure Tube
PV	Pressure Vessel
SCW	Super-Critical Water
SCWR	Super-Critical Water-cooled Reactor

References

- [1] OECD Nuclear Energy Agency, "Technology Roadmap Update for Generation IV Nuclear Energy Systems", January 2014.
- [2] Duffey, R.B. and Leung, L.K.H., "Advanced Cycle Efficiency: Generating 40% More Power from the Nuclear Fuel", Proc. World Energy Congress (WEC), Montreal, Canada, September 12-16, 2010.
- [3] IAEA, "Heat Transfer Behaviour and Thermohydraulics Code Testing for Supercritical Water Cooled Reactors (SCWRs)", IAEA-TECDOC-1746, August 2014.
- [4] Schulenberg, T. and Leung, L. "Super-critical water-cooled reactors", Handbook of Generation IV Nuclear Reactors, Editor: I.L. Piro, Woodhead Publishing Series in Energy: 103, 2016.
- [5] IAEA, "Status Report - Chinese Supercritical Water-Cooled Reactor (CSR1000)", IAEA Advanced Reactors Information System (ARIS) Database, December, 2015.
- [6] Yamada, K. et al., "Overview of the Japanese SCWR Concept Developed under the GIF Collaboration", Proc. 5th International Symposium on Supercritical Water-cooled Reactors, Vancouver, Canada, March 13-17, 2011.

- [7] Cheng, X. et al., "A Mixed Core for Supercritical Water-cooled Reactors", *Nuclear Engineering and Technology*, 40(2), pp. 117-126, 2007.
- [8] Ryzhov, S. et al., "Concept of a Single-Circuit RP with Vessel Type Supercritical Water-Cooled Reactor", *Proc. 5th International Symposium on Supercritical Water-cooled Reactors*, Vancouver, Canada, March 13-17, 2011.
- [9] Sakurai, S. et al., "Japanese SCWR Fuel and Core Design Study", *Proc. 5th International Symposium on Supercritical Water-cooled Reactors*, Vancouver, Canada, March 13-17, 2011.
- [10] Schulenberg, T. et al., "Review of R&D for Supercritical Water Cooled Reactors Progress in Nuclear Energy", *Progress in Nuclear Energy*, Vol. 77, pp. 282-299, November, 2014.

ADVANCEMENT IN THERMAL-HYDRAULICS AND SAFETY R&D SUPPORTING DEVELOPMENT OF SUPER-CRITICAL WATER-COOLED REACTORS (L. K. H. LEUNG ET AL)

L.K.H. Leung⁽¹⁾, J.-G. Zang⁽²⁾ and X. Cheng⁽³⁾

(1) Canadian Nuclear Laboratories, Canada.

(2) Nuclear Power Institute of China, China.

(3) Karlsruhe Institute of Technology, Germany.

Abstract

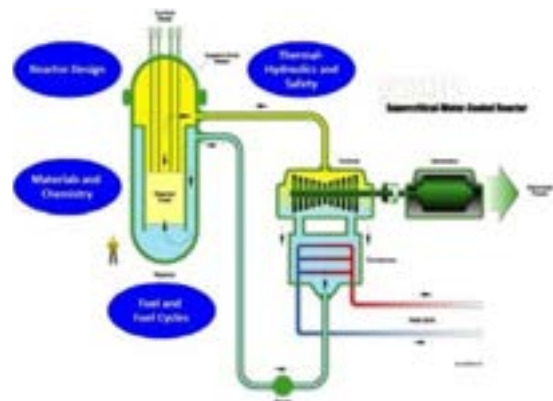
A collaborative R&D program has been established within the Thermal-Hydraulics and Safety Project Management Board to support the thermal-hydraulics design and safety analyses of Super-Critical Water-cooled Reactors (SCWRs). It covers both experimental and analytical studies at international research institutes and academia. A large amount of experimental data have been obtained with high pressure water or surrogate fluids (such as carbon dioxide and refrigerants) in simple test sections and bundle sub-assemblies. These data were applied in validating prediction methods and analytical tools. Analytical studies were performed to improve the prediction accuracy of thermal-hydraulics parameters. These studies cover the assessment of correlations and development of prediction method. Selected achievements from the collaborative R&D program are summarized.

I. Introduction

Advanced designs of nuclear power plants are being considered for future deployments to minimise the release of greenhouse gas, which is the primary cause for climate change. The Generation-IV International Forum (GIF) was established in 2000 to support joint research and development (R&D) in developing these advanced nuclear systems [1]. Six systems were selected among over 1000 potential candidates. Among the six selected options, the Super-Critical Water-cooled Reactor (SCWR) is the only one that is directly evolved from the current NPPs.

Several SCWR concepts have been developed from design and operation experience of light-water reactors and super-critical fossilfuel power plants [2]. The SCWR System Research Plan identifies Key technology areas in support of the development (see Figure 1).

Figure 1. Technology Areas supporting SCWR development



Thermal-hydraulics and safety are considered critical as these areas have significant impact on the operating power and the safety margin of SCWR concepts, and on the selection of cladding material and neutronic design.

Collaborative R&D effort is in place within the GIF SCWR Thermal-Hydraulics and Safety Project Management Board to enhance the Knowledge base, provide experimental data, and develop prediction methods and analytical tools. It is the objective of this paper to present recent advancements in thermal-hydraulics and safety R&D for SCWR.

II. Thermal-Hydraulics in SCWRs

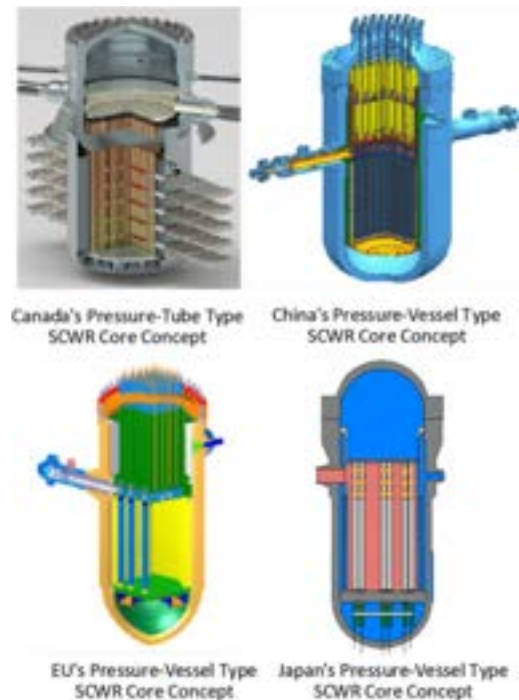
The SCWR is a high-temperature, high-pressure water-cooled reactor that operates above the thermodynamic critical point of water (374°C, 22.1 MPa). Its main mission is to generate electricity efficiently, economically and safely. In addition, the high core outlet temperature of SCWRs (up to 625°C) facilitates co-generation, such as hydrogen production, space heating and steam production [2].

Unlike the current generation of nuclear reactor systems, coolant in SCWRs does not undergo phase change with increasing temperature at supercritical pressures. Current safety criteria based on critical heat flux is no longer applicable for normal operations. In turn, fuel cladding and centreline temperatures have been adopted as the safety criteria for the SCWR. This would require accurate predictions of thermal-hydraulics parameters (such as heat transfer, hydraulics resistance, mixing, etc.) using verified analytical tools.

Several SCWR concepts adopt the multipasses configuration for coolant in the core to enhance mixing and reduce the cladding temperature [2]. Figure 2 illustrates core configurations of the thermal-spectrum SCWR concepts. Single-pass coolant-flow path is adopted in both Canada's and Japan's concepts, while two- and three-passes coolant-flow paths have been adopted in China's and European Union's (EU's) concepts, respectively. The increase in core complexity requires additional experimental studies on the effect of flow direction on thermal-hydraulics parameters.

Coolant in SCWR systems undergoes significant changes in density due to the increase from subcritical to supercritical temperatures over the core at supercritical pressures. These systems may be susceptible to dynamic instability. Knowledge base and experience acquired from analyses of the system in boiling water reactors have been applied for SCWRs. However, supplemental experiments and analyses are required to enhance the understanding the stability behaviours at supercritical pressures.

Figure 2. Thermal-Spectrum SCWR Core Configurations [2]

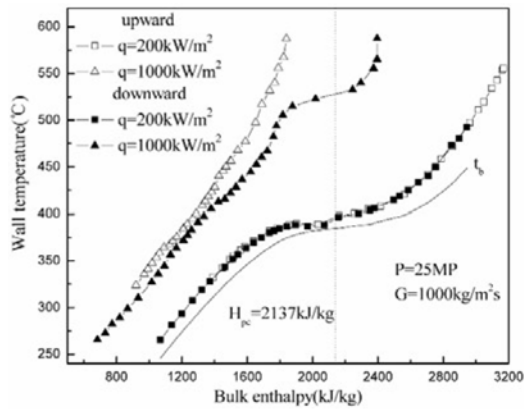


Safety systems of SCWRs consist of an automatic depressurization system that relieves the pressure rapidly to facilitate the injection of emergency coolant under accident scenarios. The critical-flow behaviours are essential in the design of the pressure relieve valve. Furthermore, these behaviours are also required in analyses of system responses to the postulated large-break loss-of-coolant accidents. Current critical-flow models implemented in safety analysis codes have been derived from experimental data obtained at subcritical pressures. Verification of these models is needed to ensure their applicability at supercritical pressures.

III. Heat Transfer

Heat-transfer experiments were performed with upward and downward flow of water at supercritical pressures inside a vertical annulus test section [3], [4]. The annulus test section consisted of an inner heater element having an outer diameter of 8 mm and an unheated outer tube having an inside diameter of 12 mm (i.e., 2 mm gap). Figure 3 compares wall-temperature measurements between upflow and downflow. Wall-temperature measurements are about the same between upflow and downflow at the heat flux of 200 KW/m² but are generally higher for upflow than downflow at the heat flux of 1000 KW/m².

Figure 3. Comparison of Wall-Temperature Measurements between Upward and Downward Flows of Supercritical Water in an Annulus [4]



Experiments were performed using three different test sections (i.e., an 8-mm tube, a 22mm tube, and a three-rod bundle) cooled with carbon-dioxide flow [5], [6], [7]. Figure 4 illustrates the wall temperature measurements obtained with the carbon dioxide flow inside an 8mm tube at various pressures and inlet fluid temperatures for the mass flux of 510 kg/m²s and the heat flux of 50 kW/m² [5]. Deteriorated heat transfer has been observed at some conditions, but not the others. Figure 5 compares experimental heat-transfer coefficients obtained in this study and those of Fewster and Jackson [8] at similar test conditions [6]. Very good agreement between these two sets of experimental data, hence improving the confident on the new data.

Figure 4. Wall Temperature Measurements Obtained with Carbon Dioxide Flow in an 8 mm Tube [5]

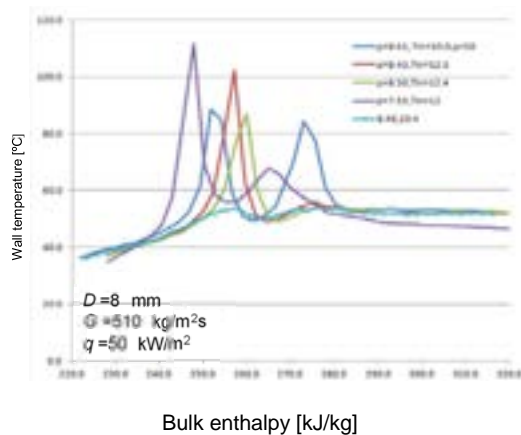
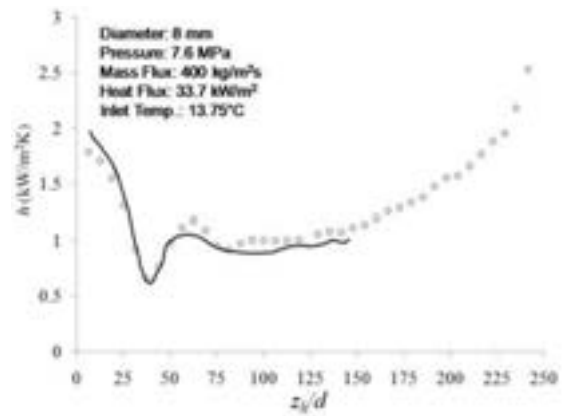


Figure 5. Comparison of Heat-Transfer Coefficients for Carbon Dioxide Flow [6]



The 3-rod bundle assembly was constructed with three 10-mm OD Inconel-600 tubes having a heated length of 1.5 metres [7]. Spacing between rods was maintained by wrapping a hypodermic stainless-steel tubing around each rod. Three unheated fillers were installed at the subchannels neighboring to the pressure tube to eliminate maldistribution of flow in various subchannels. A moveable thermocouple assembly was installed inside each heated rod. Thermocouples were rotated within the rod over 360° and traversed along the rod. Figure 6 illustrates the circumferential temperature variations around the three heated rods of the bundle. The circumferential temperatures are non-symmetrical with the peak temperature located at the subchannel between the heated rod and the unheated filler rod (insufficient data to confirm this observation for Rod C due to thermocouple malfunctions). The peak temperature locations for all rods appear tilting to one side, which is possibly attributed to the winding direction of the spacer along the heated rod.

Figure 6. Circumferential Temperature Maps obtained with the 3-Rod Bundle cooled with Carbon Dioxide Flow

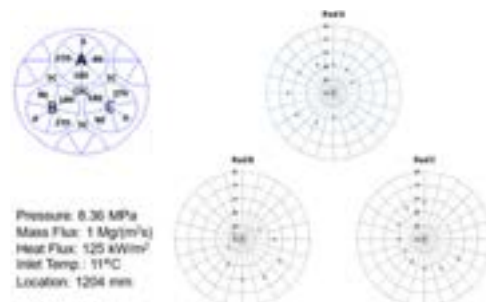
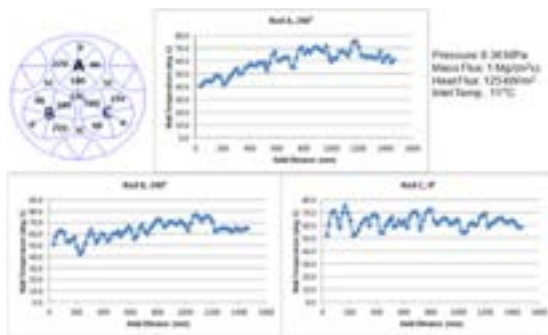


Figure 7 illustrates the axial surface temperature measurements at the peak temperature angle of each rod. Some fluctuations in surface temperature have been observed mainly due to the presence of the wire-wrapped spacer. It appears that no significant increases in wall temperature (corresponding to the deteriorated heat transfer phenomenon) were encountered over the heated rod. As indicated above, there are insufficient data to confirm the peak-temperature angle for Rod C. The peak-temperature angle of 0° was established from the available data only.

Figure 7. Axial Wall-Temperature Distributions at the Peak Temperature Angle of Each Rod in the Supercritical CO_2 Cooled 3-Rod Bundle



Heat-transfer experiments have been performed with supercritical water through a 4rod (2×2) bundle to provide circumferential walltemperature measurements around the heated rods [9], [10]. These experiments consist of two phases: the first phase focuses on the bundle configuration with no spacing device (i.e., bare bundle) and the second phase on the bundle configuration with the wrapped-wire spacers. Figure 8 illustrates the circumferential walltemperature distributions around the heated tubes of the 4-rod bundle without spacers [9]. The presented wall temperatures correspond to outersurface values calculated from inner-surface measurements obtained at a location 500 mm from the start of the heated length. Wall temperatures at the corner region (around 180°) are higher than those in other regions. The increase in wall temperature at the corner region is attributed to the small gap with low flows and high enthalpies lowering the heat-transfer coefficient. The temperature gradient between the corner and the centre

subchannels (where the lowest temperature is observed) regions is about 9°C . This signifies that the wall temperature at the corner region increases more rapidly than that at the centre subchannel region. Overall, the temperature variations from 0° - 180° and from 180° - 360° are relatively symmetrical. This signifies no tilting or bowing on the heated rod at this location. Measurements are similar between moveable and fixed thermocouples.

Figure 8. Circumferential Wall-Temperature Distributions around Two Heated Rods of the 4Rod Bundle without Spacers

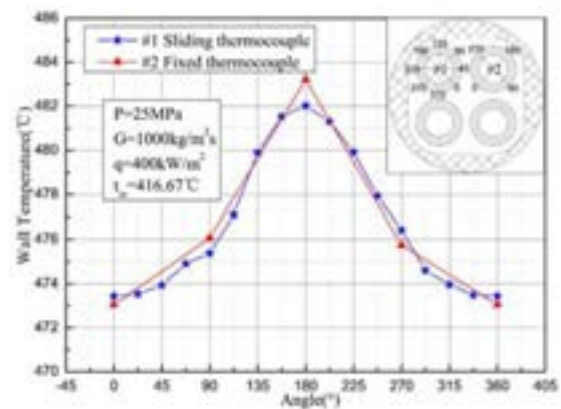
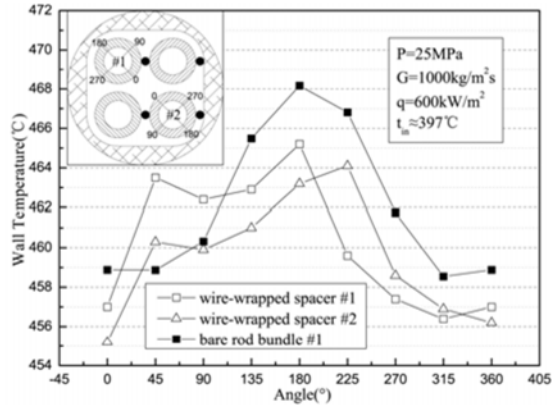


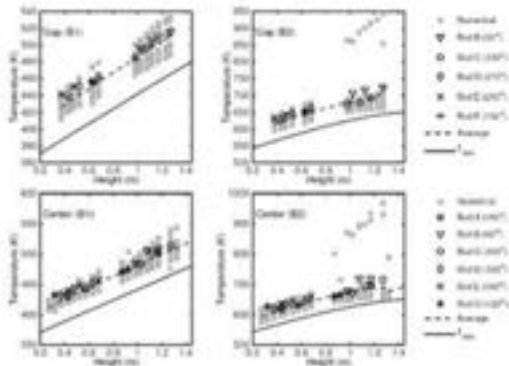
Figure 9 illustrates the circumferential wall-temperature distributions around the heated tubes of the 4-rod bundle with the wire-wrapped spacers [10]. The overall variations of the wall temperature around the wire-wrapped rods are similar to those around the bare (without the wire) rods. However, the wall temperatures for the wire-wrapped rods are mostly lower than those for the bare rods, especially at the peak-temperature location (i.e., around 180°). Areas, where higher temperatures were observed for the wire-wrapped rod, correspond to the location of the wire, which generated additional heat from the electrical resistance with direct joule heating. Peak temperature was also observed at the vicinity of the narrow-gap area (i.e., 180°).

Figure 9. Circumferential Wall-Temperature Distributions around Two Heated Rods of the 4Rod Bundle with Wire-Wrapped Spacers



An international benchmark study on supercritical heat transfer was held with participants performed *blind* calculations to predict cladding temperatures on a heated 7-rod bundle cooled with water flow at supercritical pressures [11]. The experiments were performed in a supercritical water test facility at Japan Atomic Energy Agency. The bundle consisted of seven hexagonally arranged heating rods, each of which was uniformly heated over a length of 1 500 mm by a Nickel-Chromium alloy heating element with a diameter of 4.2 mm that was embedded in Boron nitride. The thickness of the rod cladding was 1 mm. Spacing between the heating rods was 1 mm. Five honeycomb-shaped spacers were installed at an axial pitch of 25 mm. Wall temperatures at each rod were measured at six locations at different axial and azimuthal positions. Both subchannel codes and CFD tools with various turbulent models were applied. Figure 10 compares predictions of various analytical tools against experimental cladding temperatures at heated rods for two test cases. The grey squares show all numerical results for all gap facing locations, the other symbols indicate measured wall temperatures. The dashed line is a polynomial fit of the numerical results. Overall, a large scatter was observed among predictions of various analytical tools. The experimental cladding temperatures were close to the mean predictions of the scatter. However, none of these analytical tools were capable to capture the increasing cladding-temperature trend beyond the axial location of ~1 metre in Case B2. Deficiencies of these analytical tools have been identified for future improvements.

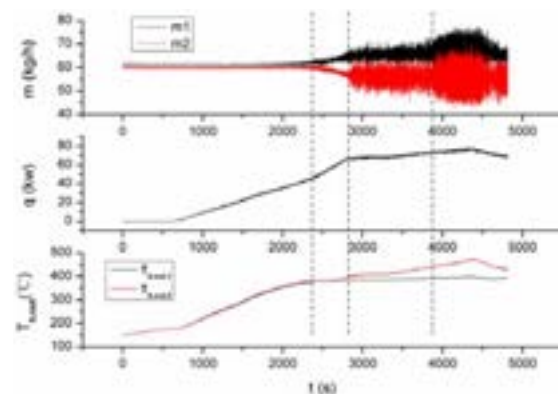
Figure 10. Rod Surface Temperatures Located at the Gap and Centre Regions



IV. Stability

An experiment was performed to examine the instability characteristics for water in two parallel channels at supercritical pressures [12]. The heated channels have a length of 3 000 mm and inner and outer diameters of 6 and 11 mm. Instability boundaries were established in the parallel channels with increasing power. Figure 11 illustrates the initiation of instability observed from the experiment. The asymmetry of flow rate between these parallel channels increases with increasing fluid temperature and mass flow rate. This has suppressed the occurrence of parallel flow instability. The flow becomes more stable with increasing pressure or decreasing inlet temperature.

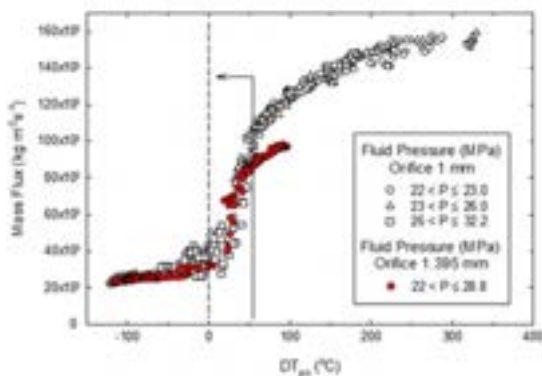
Figure 11. Initiation of Instability in Parallel Channels



V. Critical Flow

Experiments were performed to examine the choking flow characteristics at supercritical upstream pressures [13]. The test section consisted of a sharp-edged orifice, where flow was discharged from supercritical upstream pressures to a medium-pressure tank. Two different sizes of the orifice opening (1 and 1.395 mm in diameter) were tested. Figure 12 illustrates the variation of critical mass flux with differences between pseudo-critical temperature and fluid temperature ($DT_{pc}=T_{pc}-T_{fluid}$). The critical mass flux increases with decreasing temperature difference (or increasing fluid temperature).

Figure 12. Variations of Critical Mass Flux with Differences in Pseudo-Critical and Fluid Temperatures



VI. Conclusion

Thermal-hydraulics experiments have been performed with water or surrogate fluids (such as refrigerant and carbon dioxide) through tubes, annuli and bundles to support the development of SCWRs. Data from these experiments have been shared among partners in benchmarking exercises of analytical tools and in assessment of prediction methods. These efforts facilitated advancement in the understanding of the technology, reducing the

prediction uncertainties of thermal-hydraulics parameters (such as the maximum fuel cladding and fuel centreline temperatures) and improving the confidence of the developed SCWR concepts.

Acknowledgements

L. Leung would like to express his sincere appreciation of the support of the Natural Resources Canada and Atomic Energy of Canada Limited for the Canadian Thermal-Hydraulics and Safety R&D program.

Nomenclature

CFD	Computational Fluid Dynamics
D, d	Diameter (mm or m)
DT	Temperature Difference
EU	European Union
G	Mass Flux ($\text{kg}/\text{m}^2\text{s}$)
GIF	Generation IV International Forum
h	Heat-Transfer Coefficient ($\text{kW}/\text{m}^2\text{K}$)
H_{pc}	Pseudo-Critical Enthalpy (kJ/kg)
HPLWR	High Performance Light Water Reactor
m	Mass Flow Rate (kg/h)
OD	Outer Diameter
P, p	Pressure (MPa)
q	Heat Flux (kW/m^2)
R&D	Research and Development
SCWR	Super-Critical Water-cooled Reactor
$T_{b, out}$	Bulk-Fluid Temperature at Test-Section Outlet ($^{\circ}\text{C}$)
T_{fluid}	Bulk-Fluid Temperature ($^{\circ}\text{C}$)
T_{in}, t_{in}	Inlet-Fluid Temperature ($^{\circ}\text{C}$)
T_{pc}	Pseudo-Critical Temperature ($^{\circ}\text{C}$)
Z_h	Heated Distance (m)

References

- [1] OECD Nuclear Energy Agency, "Technology Roadmap Update for Generation IV Nuclear Energy Systems", January 2014.
- [2] L.K.H. Leung, Y.-P. Huang, V. Dostal, H. Matsui and A. Sedov, "An Update on the Development Status of the Super-Critical Water-Cooled Reactors", Proc. 4th GIF Symposium, Paris, France, 16-17 October, 2018.
- [3] Z. Yang, Q. Bi, H. Wang, G. Wu and, R. Hu, "Experiment of Heat Transfer to Supercritical Water Flowing in Vertical Annular Channels", J. Heat Transfer, Vol. 135, pp. 042504-1-042501-9, 2013.
- [4] H. Wang, Q. Bi, Z. Yang and L. Wang, "Experimental and numerical investigation of heat transfer from a narrow annulus to supercritical pressure water", Annals of Nuclear Energy, Vol. 80, pp. 416–428, 2015.
- [5] H. Zahlan, K. Jiang, S. Tavoularis and D.C. Groeneveld, "Measurements of heat transfer coefficient, CHF and heat transfer deterioration in flows of CO₂ at near-critical and supercritical pressures", Procs. 6th International Symposium on Supercritical Water-Cooled Reactors, Shenzhen, Guangdong, China, March 03–07, 2013.
- [6] H. Zahlan, D. Groeneveld and S. Tavoularis, "Measurements of convective heat transfer to vertical upward flows of CO₂ in circular tubes at near-critical and supercritical pressures", Nuclear Engineering Design, Vol. 289, pp. 92–107, 2015.
- [7] A. Eter, D. Groeneveld and S. Tavoularis, "An experimental investigation of supercritical heat transfer in a three-rod bundle equipped with wire-wrap and grid spacers and cooled by carbon dioxide", Nuclear Engineering Design, Vol. 303, pp. 173–191, 2016.
- [8] J. Fewster and J.D. Jackson, "Experiments on supercritical pressure convective heat transfer having relevance to SPWR", Procs. 4th International Congress on Advances in Nuclear Power Plants (ICAPP'04), Pittsburgh, PA, USA, June 13–17, 2004.
- [9] H. Wang, Q. Bi, L. Wang, H. Lv and L.K.H. Leung, "Experimental Investigation of Heat Transfer from a 2×2 Rod Bundle to Supercritical Pressure Water", Nuclear Engineering Design, Vol. 275, pp. 205– 218, 2014.
- [10] H. Wang, Q. Bi and L.K.H. Leung, "Heat Transfer from a 2×2 Wire-Wrapped Rod Bundle to Supercritical Pressure Water", Int. J. of Heat and Mass Transfer, Vol. 97, pp. 486–501, 2016.
- [11] M. Rohde, J.W.R. Peeters, A. Pucciarelli, A. Kiss, Y. Rao, E.N. Onder, P. Mühlbauer, A. Batta, M. Hartig, V. Chatoorgoon, R. Thiele, D. Chang, S. Tavoularis, D. Novog, D. McClure, M. Gradecka and K. Takase, "A Blind, Numerical Benchmark Study on Supercritical Water Heat Transfer Experiments in a 7Rod Bundle", Proc. 7th International Symposium on Supercritical Water-Cooled Reactors (ISSCWR-7), Helsinki, Finland, 15-18 March, 2015.
- [12] T. Xiong, X. Yan, Z. Xiao, Y. Li, Y. Huang and J. Yu, "Experimental study on flow instability in parallel channels with supercritical water", Annals of Nuclear Energy, Vol. 48, pp. 60–67, 2012.
- [13] A. Muftuoglu and A. Teysseidou, "Experimental study of abrupt discharge of water at supercritical conditions", Experimental Thermal and Fluid Science, Vol. 55, pp. 12–20, 2014.

10 YEARS' OVERVIEW OF A SUCCESSFUL CONTRIBUTION OF EURATOM TO GENERATION IV INTERNATIONAL FORUM (S. ABOUSAHL ET AL)

Authors: Said Abousahl⁽¹⁾, Andrea Bucalossi⁽¹⁾, Roger Garbil⁽²⁾
Co-Authors: Georges Van Goethem⁽²⁾, Pierre Frigola⁽¹⁾, Thomas Fanghaenel⁽¹⁾

(1) European Commission, Directorate General Joint Research Centre, DG JRC, Euratom, Belgium.

(2) European Commission, Directorate General for Research & Innovation, DG RTD, Euratom, Belgium.

I. Introduction

The European Atomic Energy Community (Euratom) Research and Training framework programmes of the European Union (EU) are benefitting from a consistent success in pursuing excellence in research and facilitating Pan European and International collaborative efforts across a broad range of nuclear science and technologies, nuclear fission and radiation protection.

To fulfil EU/Euratom R&D programmes (Horizon 2020, H2020) key objectives of maintaining high levels of nuclear knowledge and building a more dynamic and competitive European industry, joint research activities are implemented by co-financing Research and Innovation and Coordination and Support Actions, complemented by direct research performed by the Euratom laboratories and the promotion of Pan-European mobility of researchers and transnational access to research infrastructures (RIs).

Establishment by the research community of European technology platforms are being capitalised. Mapping of research infrastructures and Education and Training (E&T) capabilities is allowing a closer cooperation within the European Union and beyond, benefiting from multilateral international agreements between Euratom, OECD/NEA Nuclear Energy Agency, Generation-IV International Forum (GIF), International Atomic Energy Agency (IAEA) and relevant international fora.

EU/Euratom 'Achievements and Challenges' in facilitating pan-European and multi national collaborative efforts through Research and Training framework programmes show the

benefits of research efforts in key fields, of building an effective 'critical mass', of promoting the creation of 'centres of excellence' with an increased support for 'open access to key research infrastructures', exploitation of research results, management of knowledge, dissemination and sharing of learning outcomes. [6]

II. The European Landscape

Nuclear power plants (NPP) currently provide 30% of the overall European electricity generated and 15% of the primary energy consumed in the European Union. In 2017, 135 NPPs are in operation in Europe, representing a total installed electrical capacity of 137 GWe and a gross electricity generation of around 850 TWh per year. Nuclear fission is a major contributor already today as a low-carbon technology in the Energy Union's strategy to reduce its fossil fuel dependency and to fulfil its 2020/2030/2050/COP21 energy and climate policy objectives [1]. However the sector is currently facing several challenges: a) one concerns the plans of most EU Member States (MS) to extend the design lifetime of their nuclear power plants; b) other countries, such as France, Finland, the Czech Republic, Hungary and the UK, are planning new builds; c) while others, like Germany, are either considering or have excluded nuclear energy from their energy mix for now; d) a bigger share of renewables should be fostered at European level; and e) fierce international competition is taking place at a global level. Interest in nuclear power is boosted by the need to ensure a secure and competitive supply of energy and by concern over climate change. Finally, whether or not

Member States will continue to use nuclear for electricity production, for both energy and non-energy applications, Europe will need to keep and train highly qualified staff across the whole continent benefitting from hands-on training on key research infrastructures and share its knowledge worldwide. [1]

Figure 1. Nuclear Power Plants in Operation in Europe, November 2016 (ENS)



III. Euratom Treaty and EU/Euratom Legislative Framework

The Euratom Treaty provides a legal Framework to ensure a safe and sustainable use of peaceful nuclear energy across the EU and helps, providing financial support non-EU countries to meet equally high standards of safety and radiation protection, safeguards and security. With legally binding Nuclear Safety Directive (2009/71/Euratom) [18] and its latest amendment (2014/87/Euratom) [19], EU nuclear stress tests, including safety requirements of the Western European Nuclear Regulators Association (WENRA) and the International Atomic Energy Agency (IAEA), the EU became the first major regional nuclear actor with a legally binding regulatory framework as regards to nuclear safety. Furthermore, this legal framework has been recently complemented by the Directive (2011/70/Euratom) [20] that establishes a Community framework for the responsible and safe management of spent fuel and radioactive waste (both from fission and fusion systems), and the Directive (2013/59/Euratom) [21] laying down basic safety standards for protection against the dangers arising from exposure to ionising radiation.

Directives on Nuclear Installations' Safety (Art.7), Nuclear Waste Management (Art.8), Basic Safety Standards (Ch.4) and IAEA Convention on Nuclear Safety, all emphasise that each MS shall take the appropriate steps to ensure that sufficient numbers of qualified staff with appropriate education, training and re training are available for all safety-related activities in - or for each - nuclear installation throughout its life. In this context, 'Conclusions' were issued at: a) 'EU Competitiveness Council in November 2008 encouraging Member States and the EC to establish a 'review of EU professional qualifications and skills' in the nuclear field; and b) a 'Second Situation Report on EU E&T in the Nuclear Energy Field' was published in 2014 by the European Human Resources Observatory in the Nuclear Energy Sector (EHRO-N, the latest created in 2009 by the European Nuclear Energy Forum (ENEF)) underlining the amount of nuclear-educated qualified staff needed in the future. [2]

The European Commission (EC) promotes and facilitates through the Euratom Framework Programmes (FP) nuclear research and training activities within MS and complements them through its specific Community FP. Horizon 2020 European Atomic Energy Community's (Euratom) Research and Innovation Framework Programme other 2014-2018 has a budget of EUR 1,603 million to implement and is distributed as following: (a) indirect actions for RTD fusion research and development programme, EUR 728 million; (b) indirect actions for RTD nuclear fission, safety and radiation protection, EUR 318 million; and (c) Joint Research Centre (JRC) direct actions, EUR 559 million. In addition, at total of EUR 2 573 million is dedicated to the construction of ITER, one of the world's most ambitious research endeavour and an international collaborative project (EU, US, China, Japan, India, Russia, South Korea) to demonstrate the potential of nuclear fusion as an energy source. [3]

Research and Development (R&D) activities supporting the enhancement of the highest nuclear safety standards in Europe are mainly promoted by EC DG RTD indirect actions together with JRC direct actions.

The JRC has been providing internationally recognised scientific and technical support in the nuclear safety domain (fuel cycle, materials, nuclear data, waste and decommissioning) as well as in the field of nuclear safeguards for EU/Euratom Inspectors, (training courses, educational modules), the European Safeguards R&D Association (ESARDA). Furthermore the

JRC has supported the EU actions plans and initiatives related to the mitigation of risk associated with CBRN (chemical, biological, radiological and nuclear) materials. European and International safeguards authorities have benefited from JRC's dedicated R&D and operational support in collaboration with other EC Directorates General (DG)s, ENER, TRADE, DEVCO and EEAS.

Beyond EU borders, the EC- DG DEVCO manages the 'Instrument for Nuclear Safety Cooperation (INSC)' where among others an initiative on Training and Tutoring (T&T) provided post graduate professional education to expert staff at Nuclear Regulatory Authorities (NRA) and Technical Support Organisations (TSO), both in terms of management and of technical means in the areas of nuclear safety and radiation protection which proved to be very successful in strengthening local organisations and regional cooperation. DG-DEVCO manages also the 'Instrument contributing to Peace and Stability (IcPS)' where several security projects implemented outside EU borders are funded. A good example of initiatives funded by the instrument is the establishment of the EU CBRN Centres of excellences in 8 regions in the world with the participation of about 60 partner countries [4]

IV. Initiatives Are Being Capitalised

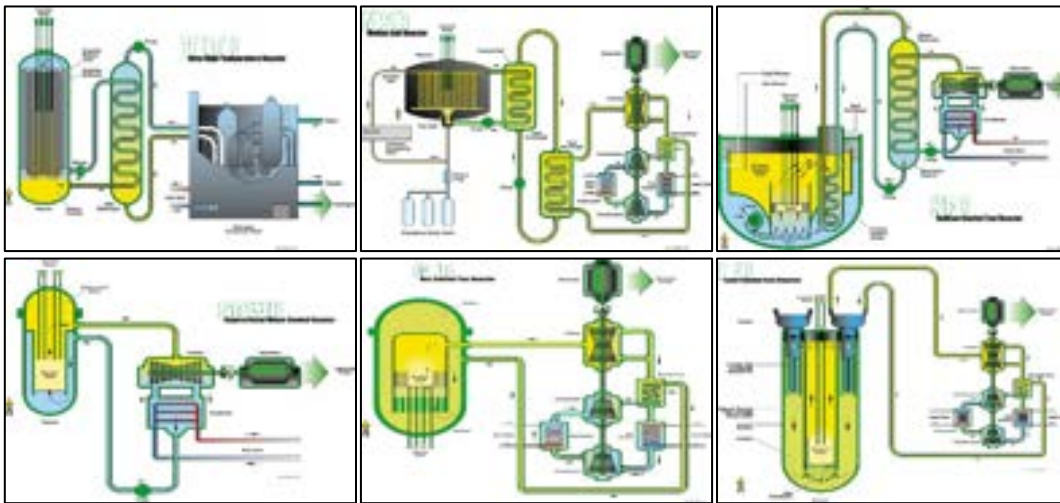
The European Commission helps to stimulate joint funding from Member States and/or enterprises, and benefits are being capitalised from the increasing interaction between European Technology Platforms (ETPs) launched during the 7th Framework Programme (2007-2013), namely the 'Sustainable Nuclear Energy Technology Platform' (SNETP incorporating NUGENIA Generation II III water cooled reactor technology, ESNII Generation IV fast reactors employing the closed fuel cycle, and NC2I Cogeneration of electricity and heat), the 'Implementing Geological Disposal of Radioactive Waste Technology Platform' (IGDTP), the 'Multidisciplinary European Low Dose Initiative' (MELODI association), the European Energy Research Alliance (EERA) Joint

Programme in Nuclear Materials (JPNM), the European Nuclear Education Network Association (ENEN), the Strategic Energy Technology Plan (SET-Plan) and other EU stakeholder fora (ENEF, ENSREG, WENRA, ETSON, FORATOM, etc.) as well as OECD/NEA, GIF and IAEA at international level. [5], [6], [7], [8]

The Generation IV International Forum (GIF) is a cooperative international framework which was launched in 2001, at the initiative of the Department of Energy DOE from USA, to carry out the research and development needed to establish the feasibility and performance capabilities of the next generation nuclear energy systems, in order to achieve GIF's four goals: Sustainability, Economics, Safety & Reliability, and Proliferation Resistance and Physical Protection (PR&PP). GIF is organised around three crosscutting methodology working groups (WG on economics, PR&PP, risk & safety), six reactor system arrangements and Memoranda of Understanding (SA or MoU) and within each system arrangement, specific project arrangements (PA) exist. The six reactor systems are Sodium-cooled Fast Reactor (SFR), Lead-cooled Fast Reactor (LFR), Very High-Temperature Reactor (VHTR), Gas-Cooled Fast Reactor (GFR); Supercritical Water-Cooled Reactor (SCWR) and Molten Salt Reactor (MSR).

On the basis of a EU/Euratom Commission Decision dated 2 November 2002, EU/Euratom acceded to Generation IV International Forum by signing in July 2003 the 'Charter of the Generation IV Forum' and the International 'Framework Agreement' existing between all GIF Members. The JRC is the Implementing Agent for EU/Euratom within GIF [22].

EU/Euratom has been contributing - to all six reactor systems, crosscutting working groups, Policy and Experts' groups - with the signature of system arrangements (SA for SFR, GFR, VHTR and SCWR in November 2006 and renewed in 2016) or Memoranda of Understanding (MoU for MSR in October 2010 and LFR in December 2010). They allow all European Member States to share and benefit from key research results within specific systems of their choice and under the GIF multi-national collaboration framework .

Figure 2. GIF Systems

V. A Decade of Progress Through International Cooperation

This 10 years' overview [23] is an assessment (2005-2014) of EU/Euratom safety Research, Development, Demonstration and Innovation (safety RD&D&I) dedicated to all six Generation IV systems and crosscutting activities. It is only providing the best estimation one could draw from the financial commitments (and technical contributions) between EU/Euratom and Member States' consortia towards EU/Euratom projects selected following open competitive call for proposals, within Framework Programme 6 and 7, FP6 (2002-2006) and FP7 (2007-2013). Please note that JRC is 'shown for this exercise' as any entity from MS (public or private), for the sake of clarity, transparency, and to avoid any double financial accounting, complemented by JRC direct funding, and as it was fully eligible to EC DG RTD indirect co-funding.

It gives a relevant illustration of the RD&D&I efforts – having a high European added value with the highest impact on building a European scientific Research Area (ERA) - made other a

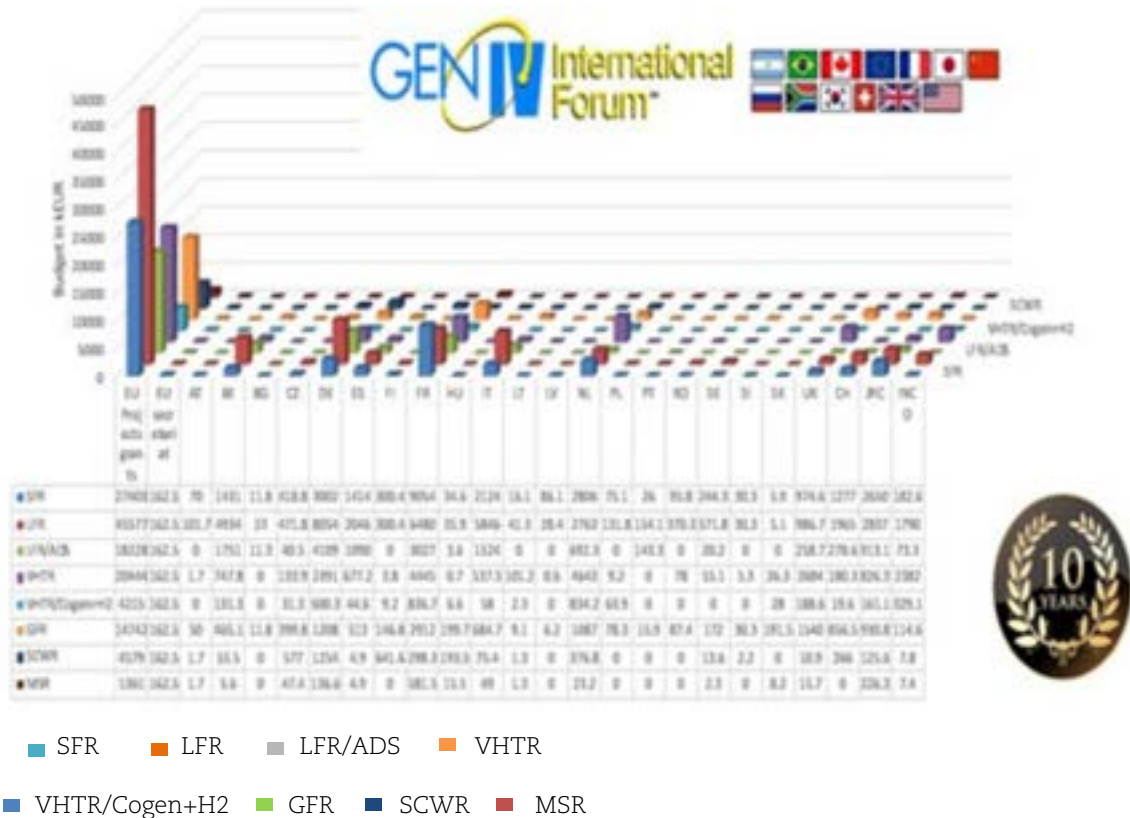
decade by the research community involved in European research programmes. It nevertheless does not include inherent direct costs of operation of usually unique small, medium or large-scale infrastructures, its staff involved for experimental works, construction or upgrading costs, in kind contributions towards specific projects and so on. In addition, given that France and Switzerland are participating as individual Member States to GIF, their respective contribution to GIF in this exercise covers only their financial contribution as a EU/Euratom MS partner within EU/Euratom projects.

All data were retrieved from European Commission's DG RTD / JRC projects co-financed by EU/Euratom and MS consortia including International Cooperation Organisations (INCO e.g. mainly from JP, KR, RU, USA but also ZA, AU, CA, CN, IN, UA and so on). All publicly available information on the projects was used such as from the European Commission R&D Information System (CORDIS), the latest European Research Participant Portal (PP), and the European Commission Budget Financial Transparency System (FTS). [9]

Figure 3. Euratom and MS estimated co funding of GIF related safety Research, Development, Deployment and Innovation (RD&D&I) FP6 and FP7 projects between 2005 and 2014, a tabular overview (mainly FR, DE, NL, IT, BE, JRC, ES, UK, INCO, and CH)

	SFR	LFR	LFR/ADS	VHTR	VHTR/Cogen+H2	GFR	SCWR	MSR	Total M€UR
EURATOM Projects	27403.3	45576.7	18227.6	20443.5	4214.9	14742.4	4579.2	1361.3	136548.9
EURATOM secretariat	162.5	162.5	162.5	162.5	162.5	162.5	162.5	162.5	1300
AT	70	101.7	0	1.7	0	50	1.7	1.7	226.7
BE	1431.3	4933.5	1750.7	747.8	131.3	465.1	55.5	5.6	9520.8
BG	11.8	23	11.3	0	0	11.8	0	0	57.8
CZ	418.8	471.8	40.5	133.9	31.3	399.8	577	47.4	2120.4
DE	3001.8	8053.8	4109.1	2390.5	500.3	1208	1253.7	136.6	20653.8
ES	1413.5	2046.1	1090.1	677.2	44.6	513	4.9	4.9	5794.5
FI	300.4	300.4	0	3.8	9.2	146.8	641.6	0	1402.2
FR	9054.2	6479.5	3026.5	4445.3	836.7	2911.9	298.3	581.5	27633.8
HU	34.6	35.9	3.6	0.7	6.6	199.7	193.5	15.5	490.1
IT	2124	5846.2	1524.2	537.5	58	684.7	75.4	49	10899
LT	16.1	41.3	0	101.2	2.3	9.1	1.3	1.3	172.7
LV	86.1	28.4	0	0.6	0	6.2	0	0	121.3
NL	2806.1	2763.4	692.3	4642.7	834.2	1086.7	376.8	23.2	13225.3
PL	75.1	131.8	0	9.2	63.9	78.3	0	0	358.1
PT	26	154.1	143.3	0	0	15.9	0	0	339.3
RO	95.8	370.3	0	78	0	87.4	0	0	631.4
SE	244.3	571.8	20.2	55.1	0	172	13.6	2.3	1079.3
SI	30.3	30.3	0	5.3	0	30.3	2.2	0	98.3
SK	5.9	5.1	0	26.3	28	191.5	0	8.2	264.9
UK	974.6	986.7	258.7	2683.9	188.6	1540.1	10.9	15.7	6659.2
CH	1276.6	1964.6	278.6	180.3	19.6	856.5	266	0	4842.3
JRC	2650.2	2837.1	913.1	826.3	161.1	930.8	125.6	226.3	8670.6
INCO	182.6	1790.4	73.3	2382.1	329.1	114.6	7.8	7.4	4887.4
Totals	53733.4	85543.8	32162.9	40372.8	7459.7	26452.4	8485.1	2487.8	256698.1

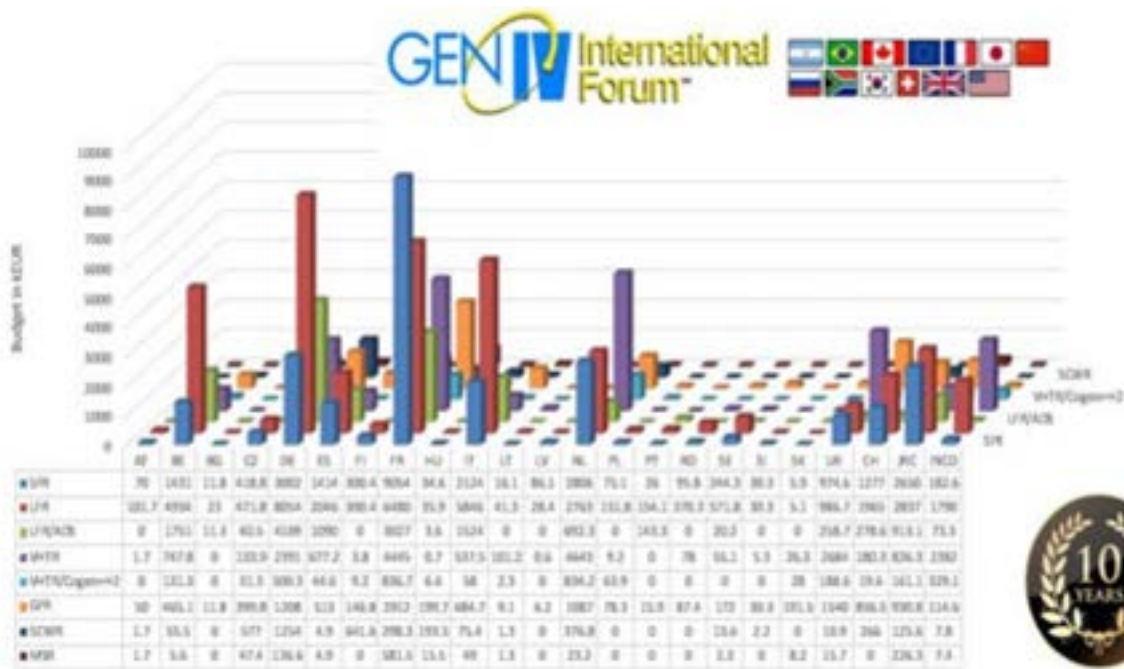
Figure 4. EU/Euratatom and MS contributions to GIF related and crosscutting EU/Euratatom Projects co-funded between 2005 and 2014 (including JRC and INCO), colour codes provided here below



A Member States’ feedback also followed a specific survey providing relevant information on any highly relevant RD&D&I from the main stakeholders. Out of 47 FP6 and FP7 projects identified, they are projects directly contributing to specific safety assessments of the respective GIF technology system arrangements. Most projects supported RD&D&I on key nuclear safety crosscutting fields, namely fuel developments, thermal hydraulics, materials research, numerical simulation and design activities of future reactor technologies, partitioning and transmutation, support to infrastructures, education, training and knowledge management, and international cooperation.

Such a decade of progress through International Cooperation (INCO) enabled – and highlighted potential future – activities such as : a) Networking activities, to foster a culture of co-operation between scientific communities, research infrastructures, industries and other stakeholders as appropriate, to help develop a more efficient and attractive research framework; b) Transnational access or virtual access activities, to support scientific communities in their access to any identified key research infrastructures; and c) Joint research activities, to improve, in quality and/or quantity, the integrated services provided at international level by these infrastructures.

Figure 5. MS RD&D&I priorities per GIF related and crosscutting technologies co funded within FP6 and FP7 EU/Euratom projects



Any summary of the related technical achievements and progress made over the last decade, activities performed, detailed analysis of the projects co-funded, deliverables exchanged within GIF system arrangements, are available within the respective GIF annual reports, and public summary or final reports available at the European Commission R&D Information System (CORDIS) of the projects co funded. One could also refer to regular systems' peer-reviewed papers together with a special edition of the scientific journal entitled 'Progress in Nuclear Energy, vol.77' published in November 2014, with a section dedicated to the 'Status of Generation IV Reactor Developments' and the respective system technologies. [10]

The share of safety RD&D&I GIF related and crosscutting projects was of around 15%, only 47 projects out of 240 EU/Euratom FP6 and FP7 projects. The latest were selected following yearly or bi annual competitive call for proposals in the framework of the EU/Euratom work programmes. It covered all six GIF systems throughout the decade within call topics such as to: a) 'innovative concepts' or 'other activities of nuclear technology and safety' during FP6; b) 'potential of advanced nuclear systems', 'Generation IV nuclear systems and the European Sustainable Nuclear

Industrial Initiative (ESNII)', 'Crosscutting activities and ESNII', but also 'Advanced reactor systems' and 'Transmutation of minor actinides, towards industrial applications' in FP7.

EU/Euratom financial support to the OECD/NEA GIF secretariat is also constantly provided on a yearly basis at a level of EUR 120k on average.

In proportion, the EU/Euratom projects were related to LFR technology (including LFR Pb-Bi Accelerator Driven System (LFR/ADS) being the project Multi-purpose hYbrid Research Reactor for High-tech Applications (MYRRHA) at SKC-CEN, in Mol, in Belgium today), then respectively VHTR, SFR and GFR. Activities on SCWR and MSR remained modest but they were evaluated as being key for the pan European and International community. The total budget of these 47 FP6 and FP7 projects identified was of around EUR 270 million (of which EUR 136 million co-funded by EU/Euratom grants). In line with the legal basis and European Commission FP6 and FP7 Communications following negotiations with Member States, EU/Euratom research and training work programmes mainly supported key crosscutting fields of RD&D&I nuclear safety. EU/Euratom projects dedicating only a large share (if not all) of their activities related

to GIF systems and crosscutting activities have been included. The authors tried to be as accurate as possible but one could argue there is some subjectivity in the allocation to any technology when providing such an assessment of the following projects:

FP6 GCFR (2005-09, The Gas Cooled Fast Reactor Project), RAPHAEL (2005-10, ReActor for Process heat, Hydrogen And Electricity generation), EUROTRANS (2005-10, EUROpean research programme for the TRANsmutation of high level nuclear waste in an accelerator-driven system), PATEROS (2006-08, Partitioning and Transmutation European Roadmap for Sustainable nuclear energy), PUMA (2006-09, Plutonium and Minor Actinides Management by Gas-Cooled Reactors), VELLA (2006-09, Virtual European Lead Laboratory), ELSY (2006-10, European Lead-cooled System), HPLWR Phase 2 (2006-10, High Performance Light Water Reactor - Phase 2), EISOFAR (2007-08, Roadmap for a European Innovative Sodium cooled Fast Reactor), and ALISIA (2007-08, Assessment of Liquid Salts for innovative applications);

FP7 F BRIDGE (2008-12, Basic Research for Innovative Fuels Design for GEN IV systems), HYCYCLES (2008-11, Materials and components for Hydrogen production by sulphur based thermochemical cycles), CARBOWASTE (2008-13, Treatment and Disposal of Irradiated Graphite and Other Carbonaceous Waste), GETMAT (2008-13, Gen IV and Transmutation MATerials), EUROPAIRS (2009-11, End User Requirement fOr Process heat Applications with Innovative Reactors for Sustainable energy supply), CDT (2009-12, Central Design Team for a fast-spectrum transmutation experimental facility), CP-ESFR (2009-13, Collaborative project on European sodium fast reactor), FAIRFUELS (2009 15, FABrication, Irradiation and Reprocessing of FUELS and targets for transmutation), ADRIANA (2010-11, ADvanced Reactor Initiative And Network Arrangement), HeLiMnet (2010-12, Heavy Liquid Metal Network), ANDES (2010-13, Accurate Nuclear Data for nuclear Energy Sustainability), LEADER (2010-13, Lead-cooled European Advanced Demonstration Reactor), ARCAS (2010-13, ADS and fast Reactor CompARison Study in support of Strategic Research Agenda of SNETP), GOFASTR (2010-13, European Gas Cooled Fast Reactor), EVOL (2010-13, Evaluation and Viability of Liquid Fuel Fast Reactor System), THINS (2010-15, Thermal-hydraulics of Innovative Nuclear Systems), ADEL (2011-13, ADvanced ELectrolyser for Hydrogen Production with Renewable Energy Sources), MAX (2011-14, MYRRHA Accelerator

eXperiment, research and development programme), SILER (2011-14, Seismic-Initiated events risk mitigation in Lead-cooled Reactors), MATTER (2011-14, MATerials TESting and Rules), SCWR-FQT (2011-14, Supercritical Water Reactor - Fuel Qualification Test), ARCHER (2011 15,), JASMIN (2011-15, Joint Advanced Severe accidents Modelling and Integration for Na-cooled fast neutron reactors), SEARCH (2011-15, Safe ExploitAtion Related CHEmistry for HLM reactors), FREYA (2011-16, Fast Reactor Experiments for hYbrid Applications), ALLIANCE (2012-15, Preparation of ALlegro - Implementing Advanced Nuclear Fuel Cycle in Central Europe), ASGARD (2012-16, Advanced fuels for Generation IV reActors: Reprocessing and Dissolution), SARGEN IV (2012-13,), PELGRIMM (2012-15), MAXSIMA (2012-18, Methodology, Analysis and eXperiments for the Safety In MYRRHA Assessment), NC2I R (2013-15,), ARCADIA (2013-16, Assessment of Regional CAPabilities for new reactors Development through an Integrated Approach), MARISA (2013-16, MyrrhA Research Infrastructure Support Action), SACSESS (2013-16, Safety of ACTinide Separation proceSSes), ESNII PLUS (2013-17, Preparing ESNII for HORIZON 2020), and MatISSE (2013-17, Materials' Innovations for a Safe and Sustainable nuclear in Europe).

In the 10 year reporting period the JRC has complemented EU/Euratom indirect actions by providing a contribution of around EUR 25 million from its own specific EC direct funding to the six GIF systems and mainly towards RD&D&I on SFR, LFR and VHTR. This amount rises to EUR 35-40 million when including infrastructure, maintenance and staff related costs .

Figure 6. EU/Euratom MS LFR safety RD&D&I (mainly DE, FR, IT, BE, JRC, ES, CH, INCO, SE, CZ, RO, FI), budget scale up to EUR 9.000k

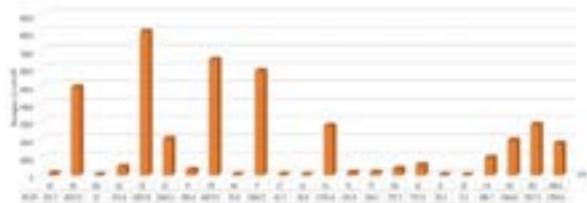
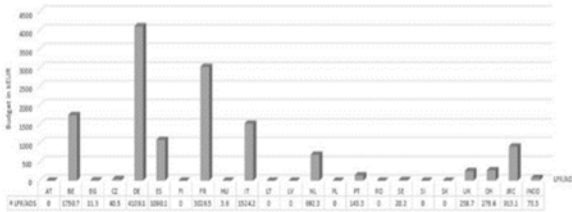
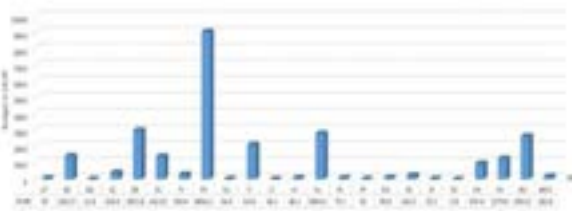


Figure 7. EU/Euratom MS LFR/ADS safety RD&D&I (DE, FR, BE, IT, ES, JRC, CH, UK, PT, INCO) budget scale up to EUR 4.500k



Belgium and Italy have mainly invested in Lead (or Lead-bismuth) technology. SCK-CEN nuclear research centre, located in Mol, Belgium, has also benefitted from a EUR 60 million grant from its government for the period 2010-14 and dedicated an additional EUR 30 million from its own budget towards MYRRHA RD&D&I (Pb-Bi LFR and ADS). Italy has also dedicated EUR 30 million to LFR technology and ALFRED reactor system.

Figure 8. EU/Euratom MS SFR safety RD&D&I (mainly FR, DE, NL, JRC, IT, BE, ES, CH, UK, CZ, FI, SE, INCO, RO), budget scale up to EUR 10.000k



During this reporting period, EU/Euratom MS such as France has, in the meantime invested mainly through its national research programmes in several different GIF systems. In a public report from the Cour des Comptes dated from 2012, investments on a yearly basis dedicated to Generation IV RD&D&I were estimated at EUR 75 million and increased to EUR 102 million from 2010. The Advanced Sodium Technological Reactor for Industrial Applications (ASTRID) SFR pre-conceptual design phase was the main focus due to a substantial technological and operational feedback experience. [11]

Figure 9. EU/Euratom MS VHTR safety R&D&I (NL, FR, UK, DE, INCO, JRC, BE, ES, IT, CH, LT), budget scale up to EUR 5.000k

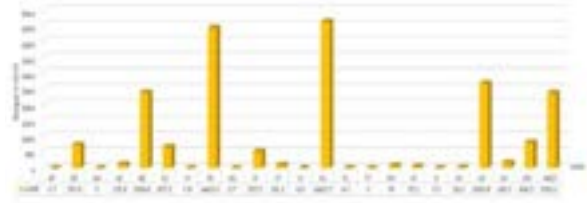
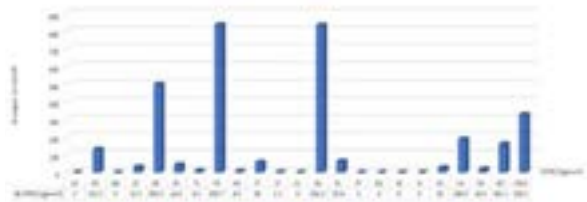


Figure 10. EU/Euratom MS VHTR-COGEN-H2 safety RD&D&I (FR, NL, DE, INCO, UK, JRC, BE, PL, ES, IT, CZ, SK, CH), budget scale up to EUR 900k



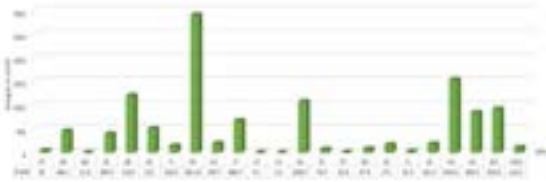
The main objective of nuclear co-generation is to make nuclear power present in a broader way in district heating and industrial heat supply. The European Nuclear Cogeneration Industrial Initiative (NC2I) is today the third pillar of the Sustainable Nuclear Energy Technology Platform (SNETP). It is dedicated to the demonstration of an innovative and competitive energy solution for a low carbon cogeneration of heat and electricity based on nuclear energy. Cogeneration technologies could extend the low carbon contribution from nuclear fission to the energy system by directly providing heat for different applications like: process heat; sea water desalination, contribution to transportation by synthetic fuels or hydrogen production, and district heating.

The best answer to nuclear electricity co-generation could be a reactor of small to medium power. VHTRs with power ranges up to 600 MWth, with the highest safety parameters, have the ability to provide heat at temperatures utilised by the 'Steam' market. For some part of the market, utilising lower temperatures, Small Modular Reactors (utilising light water technology) would also be suitable.

Germany has allocated EUR 3-4 million for each of the three fast reactors technologies and VHTR within EU/Euratom projects.

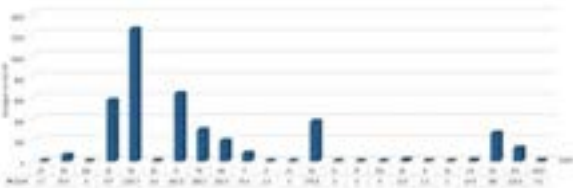
Finland has invested EUR 500k - 1 million for each of the three fast reactor systems, VHTR and SCWR within EU/Euratom projects.

Figure 11. EU/Euratom MS GFR safety RD&D&I (FR, UK, DE, NL, JRC, CH, IT, ES, BE, CZ, HU, SK, FI, SE, INCO, RO), budget scale up to EUR 3.000k



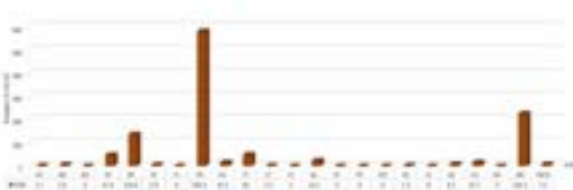
The Czech Republic has focused on SCWR (EUR 3 million) and LFR (EUR 1 million) within EU/Euratom projects.

Figure 12. EU/Euratom MS SCWR safety RD&D&I (DE, FI, CZ, NL, FR, CH, HU, JRC, IT, BE), budget scale up to EUR 1.400k



The Netherlands invested in SCWR, MSR and LFR with budgets of EUR 400 - 800k.

Figure 13. EU/Euratom MS MSR safety RD&D&I (mainly FR, JRC, DE, IT, CZ, NL, UK, HU, SK, INCO, BE), budget scale up to EUR 600k



(MSRs are seen in some countries as a promising advanced reactor technology because of the various benefits associated with them. They can adapt to a variety of nuclear fuel cycles (such as Uranium-Plutonium and

Thorium-Uranium cycles), which allow for the extension of fuel resources. They can also be designed as nuclear waste ‘burners’ or breeders. They operate at higher temperatures, which lead to increased efficiencies in generating electricity and use for other high-temperature process heat applications. In addition, low operating pressures can reduce the risk of a large break and loss of coolant as a result of an accident, thereby enhancing the safety of such a reactor.

VI. Additional Successful Initiatives and Recommendations

EU/Euratom also promotes research and training, development, demonstration, and innovation of nuclear fission technologies in order to achieve the Strategic Energy Technology plan (SET Plan) objectives of the nuclear initiative, namely:

- By 2020, (1) to maintain the safety and competitiveness in fission technology, and (2) to provide long-term waste management solutions; and
- By 2050, (3) to complete the demonstration of a new generation (Gen IV) of fission reactors with increased sustainability namely via the European Sustainable Nuclear Fission Industrial Initiative (ESNII), and (4) to enlarge nuclear fission applications beyond electricity production through the Nuclear Cogeneration Industrial Initiative (NC2I).

Within the European Sustainable Nuclear Industrial Initiative (ESNII), Sodium Fast Reactor (SFR) technology is considered to be the reference technology since it already has substantial technological and operations feedback in Europe. The ASTRID demonstrator should be operational by around 2030. Lead Fast Reactor (LFR) technology has significantly extended its technological base. MYRRHA, a Pb-Bi flexible irradiation facility, an Accelerator Driven System (ADS) supporting Fission/Fusion/radioisotope research is planned in Belgium by around 2030 as a European Technology Pilot plant. LFR can be considered as the shorter-term alternative technology, supported by FALCON consortium set up in December 2013 for the construction of an LFR demonstrator (ALFRED) and comprising Italy's National Agency for New Technologies, Energy and Sustainable Economic Development (ENEA), ANSALDO Nucleare, the Romanian Nuclear Research Institute (RATEN ICN) and

CV-řež (CZ). Gas Fast Reactor (GFR, ALLEGRO) technology is considered to be a longer-term alternative option supported by the Visegrad 4 countries (CZ, SK, HU and PL).

The Deployment Strategy of the Sustainable Nuclear Energy Technology Platform (SNETP) has confirmed in 2015 these priorities at EU level, and EU MS will continue to mainly invest through their national programmes in different GIF systems.


ASTRID SFR pre-conceptual design phase ended in December 2012 and approval was given by the French Government to continue all conceptual research activities - by providing a EUR 650 million grant managed by CEA - with nevertheless remaining options still opened such as an internal core-catcher, a core-catcher between two vessels or external core-catcher, and a Gas Power Conversion system. Today other 600 people are working on ASTRID from CEA, AREVA, EDF, ASTRUM, ALSTHOM, AMEC, COMEX NUCLEAIRE, CNIM, TOSHIBA, ROLLS-ROYCE, BOUYGUES and JACOB, JAEA, Mitsubishi Heavy Industries, Mitsubishi FBR systems. Belgium and Italy will continue

investing in Lead-Bismuth/ADS and Lead systems. Germany, although having a 2022 phase out policy (since 2011 following Fukushima events), continued supporting research in fast systems but also VHTR. Spain continued supporting materials developments, SFR, SCWR and LFR. The Czech Republic continued its research in SCWR and to a lesser extent MSR, GFR, VHTR and LFR systems. Finland has allocated resources for each of the three fast reactor systems, VHTR and SCWR. Sweden continued supporting SFR and LFR. The Netherlands continued supporting with a similar financial effort LFR and MSR.

National, European, International funding, financial and legal instruments can support the realisation of ESNII as a pan European and multi-national initiative by providing support to key research infrastructures. Investigations considered the latest respective progress of MS projects and national investment plans, a study from Deloitte dated from 2010, H2020 Research and Innovation, Cohesion Policy and European Regional Development Fund, and the 2014-2020 Multi-Financial Framework programmes. [12]

Figure 14. Financial assessments of a selection of ESNII projects, Deloitte Study (2010)

Financial assessments of a selection of ESNII projects



Source	Colour	Description	Criteria to include in the financial framework
EIB Loan (or Euratom)	Green	Financial support provided by EIB or through loans facility under Euratom Treaty	Gen-IV projects could be risky - promoter risk profile important. Revenue stream (e.g. sale of electricity) needed for repayments. In any case, loans will never exceed c.25% of forecast project value
Tax exemptions	Red	Joint Undertaking or ERIC schemes may allow exoneration of direct and/or indirect taxes.	Could represents between 14-15% of the total costs.
EU incentives & grants	Yellow	Financial support provided by Cohesion Policy Funds, Framework Programme, other subsidies, etc.	Cohesion funds: limited to max. 35% and will depend on host site Other subsidies: case by case according to the project/promoter characteristics.
Private investors	Cyan	Financial investments by nuclear industry - vendors, utilities, and other private sector energy players.	Information supplied by the companies concerned
National public research investors	Orange	Financial support provided by national nuclear organisations and other public R&D institutions.	Information supplied by the organisations concerned.
Hosting country public investment	Dark Orange	Financial support for improvements in local infrastructure (roads, housing, schools, etc.)	Funds from local / regional / natl. authorities hosting the project: max. 5% of the budget.

This section was created and with the collaboration of different experts, identifying the best possible situation in January 2010. It does not represent any financial commitment by the different project participants.

Such financial and legal assessment confirmed that several mechanisms could provide part of the necessary support. It could be either to

upgrade existing key supporting infrastructures, or to build new ones also contributing to ESNII industrial initiative and its specific large scale

projects through: a) European Investment Bank (EIB) loans, Euratom or H2020 InnovFin Risk Sharing Financial Facility (RSFF); b) tax exemptions benefitting from a Joint Undertaking (or equivalent such as an International non-profit association, Belgian AISBL); c) EU incentives or grants provided through Cohesion Policy funds and European Development Regional Funds (ERDF) dedicated to building research infrastructures, establishment of centres of excellence with potential support from EU/Euratom research Framework programmes for RD&D&I; d) Private investors, energy providers and research organisations; e) National public research organisations; f) Public investments from the hosting country towards basic infrastructures as a host of a new facility; and g) The European Fund for Strategic Investments (EFSI) where MYRRHA and ALLEGRO were indicated respectively by the Belgian and Slovak Governments as potential leading projects.

The European Commission approved in 2011 European Regional Development Fund (ERDF) funding support of EUR 5.5 million for the construction of a new research facility in Rez in the Czech Republic hosting today helium and supercritical water research loops. Early 2014, the Czech Republic obtained a further EU ERDF funding support of EUR 85 million (total costs of EUR 100 million) towards their SUSTAINABLE ENERGY project (SUSEN). Building such a research infrastructure extends their energy research possibilities with emphasis on nuclear technologies at the Research Center of Rez and at the Pilsen University of West Bohemia. It also allows them to act as a relevant research partner within the EC smart specialisation platforms promoted for cooperation in the field of energy with the establishment of partnerships and cooperation with other European research centres. [13]

To further increase the impact of the Euratom fission research programme, financial leveraging support through H2020 InnovFin instrument was promoted from 2017 onwards to foster further coordination, cross-border operation and possible integration of national research investment actions of pan-European interest in the specific field of research. With only a EUR 20 million contribution from Euratom, InnovFin could enable total loan investments of around EUR 300 million by 2020 for building new and/or upgrades of fission research infrastructures (applying InnovFin leverage of around 7 to this financial guarantee provided by EC and matched by EIB) out of a total investment of around EUR 1.2 billion (if

estimated at 20% on average of the overall investment on infrastructures). First projects (FR, BE, NL) should be promoted from 2018-20. [14]

In February 2017 the EU/Euratom Scientific and Technical Committee (STC), complementing FP7 Ex-post and H2020 mid-term evaluations of the EU/Euratom framework programme, prepared a broad-based technical opinion on issues within the scope of the Euratom Treaty, nuclear energy systems, nuclear safety, radiation protection, radioactive waste management, related research requirements, education & training and the future Euratom research and training programmes. In relation to evaluation findings, the key points of the STC opinion gave, among others, the following key recommendations:

- the significant role played by nuclear energy in certain Member States as a component of low carbon electricity supply and contributing to the competitiveness of European Industry;
- the importance of a European contribution, both as regards safety culture but also technological and industrial knowhow, in ensuring appropriate attention is paid to the safety, sustainability, non-proliferation and competitiveness aspects of advanced (so-called Generation-IV) systems as progress is made internationally towards industrial scale deployment of these systems around the middle of the 21st Century: [15];
- ensuring a vibrant education & training culture, involving basic academic education as well as continuous professional development, focused on advanced technology across all nuclear topics to guarantee a new generation of experts will be available when needed, and to maintain high levels of safety throughout the sector;
- the urgent need for a coordinated and coherent approach to infrastructure investment that must be undertaken if the EU is to ensure value for money, appropriate leverage both between and within the 'direct actions' and 'indirect actions' components of the Euratom research and training programme, and enduring capacity and capability in facilities that underpin nuclear technology and that are vital for Member States in all related fields, including

those essential for medicine and radiation protection, security and safeguards.

Nuclear fission technology public and private investments within European Member States are overall of the order of EUR 1200 million on a yearly basis. Euratom support is estimated at around 10% through collaborative R&D funding schemes leveraging public/private investments and international partnerships. Support to long term research joint programmes is provided when innovation, training, competence management and knowledge sharing have a high European added value and are promoted towards Gen-II-III-IV reactor technology, as well as waste management, geological disposal and radiation protection.

An additional total cost of large scale demonstrators towards sustainable innovative fission technologies including relevant supporting (e-)infrastructures (e.g. Jules Horowitz Reactor (JHR), PALLAS, and MYRRHA) is estimated at around EUR 12-15 billion over the next twenty years (industrial initiatives having a different level of maturity and gathering ASTRID, MYRRHA, ALFRED, ALLEGRO and HTR-NC2I are estimated at around EUR 9-10 billion (2015-2035), fuel cycle, partitioning and transmutation, supporting Infrastructures, JHR and PALLAS at EUR 3-5 billion (2015-2025)). National geological disposal estimated costs were given within the latest spent fuel and radioactive waste management directive implementing report based on EU Member States' programme (e.g. EUR 25 billion in France, EUR 3.5 billion in Finland, dated May 2017). The fusion community has also indicated in June 2017 that EU/Euratom budget needs would be of around EUR 5 billion between 2021 and 2025 (first plasma) for the construction of the International Thermonuclear Experimental Reactor (ITER) and a further EUR 5 billion for ITER operations till the first deuterium-tritium (D T) plasma which is scheduled by around 2035. [16]

VII. Conclusions and EU/Euratom Research Perspectives

The European Council decision dated 11 February 2016 extended by a qualified majority further participation of the European Atomic Energy Community (Euratom) in the Framework Agreement for international collaboration on research and development of Generation IV nuclear energy systems. The significant role played by nuclear energy in

certain Member States as a component of low carbon electricity supply and contributing to the competitiveness of European Industry is acknowledged. There is a common understanding that all EU Member States, even those with no nuclear power plants, have an interest in ensuring nuclear safety throughout the EU. [17]

Instruments used so far for EU/Euratom fission research are well suited for leveraging RD&D&I activities of high European added value in nuclear safety, radiation protection, and geological disposal. Completion of the European Research Area should lead to increased cooperation in research in Europe to ensure there is an effective 'critical mass' of research effort in key fields, the creation of 'centres of excellence', greater emphasis on competitiveness and public/private partnerships, increased support for research infrastructures and the exploitation and management of knowledge which contributes to maintaining high levels of knowledge and competitiveness of industry in the nuclear fields. EU/Euratom feedback is that today's Euratom support to all six systems is highly appreciated with a high impact as of pan European added value.

Considering EU/Euratom Scientific and Technical Committee (STC) opinion, FP7 Ex-post and H2020 mid-term evaluations, EU technology platforms and Fora recommendations, investments are however insufficient for RD&D&I development of more safe and sustainable advanced systems; these technologies carry significant risks and require an integrated approach to the whole innovation process.

The lack of new investment and unavailability of appropriate large-scale research infrastructures in fission would be major hindrance. Some EUR 12-15 billion in investment (public and private) is needed over the next 20 years to fully implement ESNII industrial initiative. There is therefore a real need to pool resources at all levels (EU, national and international) and to commit and sustain financing for these technologies with agreed multi-annual strategies otherwise it will either not happen or take too long, resulting in delays in technology development. The risks inherent in continued underinvestment in advanced nuclear systems, and failure to grasp opportunities at either the European level or in support of leading Member States will mean that the EU will no longer be able to fulfil its

potential and occupy its rightful position in the evolving international initiatives in this field.

There is an urgent need for a coordinated and coherent approach to infrastructures' investment. Generation IV innovative nuclear reactors still remain very attractive to young students, scientists and engineers engaging in a nuclear career thanks to its related scientific innovative challenges.

GIF's ambitious goals drive RD&D&I, but approaches differ by system and the six systems do not all compete within the same niche. While each member country has national programmes that exceed its level of participation in the Generation IV International Forum, collaboration is an essential element of

ultimately achieving a globally accepted, reliable advanced reactor system ready for licensing and commercialisation.

Acknowledgements

This research was supported by institutions, companies or individuals involved in EU/Euratom research projects. We are also thankful to colleagues who provided expertise that greatly assisted the research

Nomenclature

Within the text of the paper.

References

- [1] European Energy Strategy: Secure, competitive, and sustainable energy
<http://ec.europa.eu/energy/en/topics/energy-strategy>
- [2] EU/Euratom legislative framework
<http://ec.europa.eu/energy/en/topics/nuclear-energy>
- EHRO-N, European Human Resources Observatory for the Nuclear sector, Perspective report
http://ehron.jrc.ec.europa.eu/sites/ehron/files/documents/public/ehron_putting_into_perspective_report_2012_05_25_0.pdf
- [3] EU Multiannual Financial Framework (MFF)
http://ec.europa.eu/budget/mff/index_en.cfm
- Horizon 2020 European Research Framework Programmes
http://ec.europa.eu/research/horizon2020/index_en.cfm
<http://ec.europa.eu/programmes/horizon2020/h2020-sections>
- [4] European Commission Departments (Directorates-General) and services
http://ec.europa.eu/about/ds_en.htm
- [5] European Technology Platforms (ETPs)
<http://cordis.europa.eu/technology-platforms/>
SNETP Sustainable Nuclear Energy Technology Platform <http://www.snetp.eu/>
IGDTP Implementing Geological Disposal of Radioactive Waste <http://www.igdtp.eu/>
MELODI Multi-disciplinary European Low Dose Initiative <http://www.melodi-online.eu/>
- [6] Independent authoritative expert body with regulatory backgrounds for the stress tests
ENSREG European Nuclear Safety Regulator Group
http://ec.europa.eu/energy/nuclear/ensreg/ensreg_en.htm
ENEF European Nuclear Forum Energy
http://ec.europa.eu/energy/nuclear/forum/forum_en.htm
- [7] Strategic Energy Technology Plan (SET-Plan)
http://ec.europa.eu/energy/technology/set_plan/set_plan_en.htm
EERA European Energy Research Alliance
<https://www.eera-set.eu/>
EIT KIC InnoEnergy MSc EMINE – European Master in Nuclear Energy

- www.innoenergy.com/education/master-school/msc-emine-european-master-in-nuclear-energy/
- ENEN European Nuclear Education Network Association <http://www.enen.eu>
- [8] OECD/NEA Nuclear Energy Agency <http://www.oecd-nea.org/>
- GIF Generation-IV International Forum <http://www.gen-4.org/>
- IAEA International Atomic Energy Agency <http://www.iaea.org/>
- [9] CORDIS, European Community Research and Development Information Service http://cordis.europa.eu/home_en.html EU Participant Portal <http://ec.europa.eu/research/participants/portal/desktop/en/home.html>
- EU Financial Transparency System http://ec.europa.eu/budget/fts/index_en.htm
- [10] GIF annual reports www.gen-4.org/gif/jcms/c_44720/annual-reports
- Progress in Nuclear Energy, volume 77 <http://www.sciencedirect.com/science/journal/01491970/77>
- [11] Rapport Cour des comptes sur les coûts de la filière électronucléaire française, 31/01/2012 <https://www.ccomptes.fr/fr/publications/les-couts-de-la-filiere-electro-nucleaire>
- [12] Deloitte study, Funding opportunities and legal status options for the future European Sustainable Nuclear Industrial Initiative of the Strategic Energy Technology Plan, February 2010, Executive summary <http://collections.internetmemory.org/haeu/20161215121151/http://cordis.europa.eu/pub/fp7/euratom-fission/docs/deloitte-gen4-022010-executive-summary.pdf>
- Full report <http://collections.internetmemory.org/haeu/20161215121151/http://cordis.europa.eu/pub/fp7/euratom-fission/docs/deloitte-gen4-022010-full-report.pdf>
- [13] EU Regional Policy, European Regional Development Fund ERDF http://ec.europa.eu/regional_policy/en/funding/erdf/
- The Sustainable Energy Project (SUSustainable ENergy, SUSEN) project <http://susen2020.cz/en/>
- EC JRC Smart Specialisation Platform <http://s3platform.jrc.ec.europa.eu/>
- [14] EIB RSFF InnovFin <http://www.eib.org/products/blending/innovfin/index.htm>
- EIB EFSI European Fund for Strategic Investments <http://www.eib.org/efsi/>
- [15] Horizon 2020 Evaluation, input studies and evaluation methods <https://ec.europa.eu/research/evaluations/index.cfm?pg=h2020evaluation>
- [16] JHR Jules Horowitz Reactor <http://www-rjh.cea.fr/general-description.html>
- MYRRHA Multi-purpose hYbrid Research Reactor for High-tech Applications http://sckcen.be/en/Technology_future/MYRRHA
- PALLAS reactor <http://www.pallasreactor.com/?lang=en>
- Horizon Europe - the next research and innovation framework programme https://ec.europa.eu/info/designing-next-research-and-innovation-framework-programme/what-shapes-next-framework-programme_en
- Legal texts and factsheets https://ec.europa.eu/commission/publications/research-and-innovation-including-horizon-europe-iter-and-euratom-legal-texts-and-factsheets_en,
- ITER <http://www.iter.org/>, EUROfusion <https://www.euro-fusion.org/> and JET Tokamak <http://www.ccf.ac.uk/JET.aspx>
- [17] COUNCIL DECISION (Euratom) 2016/2116 of 12 February 2016 approving the conclusion by the European Commission, on behalf of the European Atomic Energy Community, of the Agreement extending the Framework Agreement for International Collaboration on Research and Development of Generation IV nuclear Energy systems <https://eur-lex.europa.eu/legal-content/en/TXT/?uri=CELEX:32016D2116>
- [18] Council Directive 2009/71/Euratom of 25 June 2009 establishing a Community framework for the nuclear safety of nuclear installations

- <https://eur-lex.europa.eu/legal-content/EN/TXT/?uri=celex%3A32009L0071>
- [19] Council Directive 2014/87/Euratom of 8 July 2014 amending Directive 2009/71/Euratom establishing a Community framework for the nuclear safety of nuclear installations https://eur-lex.europa.eu/legal-content/EN/TXT/?uri=uriserv%3AOJ.L_.2014.219.01.0042.01.ENG
- [20] Council Directive 2011/70/Euratom of 19 July 2011 establishing a Community framework for the responsible and safe management of spent fuel and radioactive waste <https://eur-lex.europa.eu/legal-content/EN/TXT/?uri=celex%3A32011L0070>
- [21] Council Directive 2013/59/Euratom of 5 December 2013 laying down basic safety standards for protection against the dangers arising from exposure to ionising radiation, and repealing Directives 89/618/Euratom, 90/641/Euratom, 96/29/Euratom, 97/43/Euratom and 2003/122/Euratom <https://eur-lex.europa.eu/legal-content/EN/TXT/?uri=CELEX%3A32013L0059>
- [22] Commission Decision C(2006) 7
- [23] Euratom Contribution to the Generation IV International Forum Systems in the period 2005-2014 and future outlook, Publications Office of the European Union, 2017

THERMAL-HYDRAULIC PERFORMANCE OF ALTERNATIVE NUCLEAR FUELS FOR THE HPLWR (L. CASTRO ET AL)

Landy Castro⁽¹⁾, Genrry Delgado⁽²⁾, Rogelio Alfonso⁽²⁾, Carlos García⁽²⁾, Dany S. Domínguez⁽³⁾

(1) Facultad de Ingeniería, Universidad Nacional Autónoma de México, México.

(2) Instituto Superior de Ciencias y Tecnologías Nucleares, La Habana, Cuba.

(3) Universidade Estadual de Santa Cruz, Brazil.

Abstract

The High Performance Light Water Reactor (HPLWR) is one of the most promising designs of the Super-Critical Water-Cooled Reactor (SCWR). The use of uranium nitride (UN) and uranium carbide (UC), as alternative nuclear fuels for the SCWR, offer the advantage of high thermal conductivity compared to uranium dioxide (UO₂). For the analysis of these alternative nuclear fuels in SCWRs, some important design features must be considered. One of them is the porosity; the nuclear fuel is manufactured with different porosity values, as high as 20%, to reduce its hardness and swelling, influencing its thermal conductivity. Another issue is related to the chemical reactivity of UN and UC with water and nickel, which forces the use of coatings for fuel pellets. In this paper, a CFD analysis of thermal-hydraulic behavior in the HPLWR fuel assembly, using alternative fuels, was carried out. The use of UN coated with zirconium carbide layers and UC coated with titanium nitride layers were analysed. The impact of porosity induced changes in fuel temperature profiles was analysed. The radial and axial fuel temperature distributions were obtained for all cases. It was found that the maximum temperature values obtained using UN and UC, both coated and uncoated, were lower than those obtained with UO₂. It was found that the porosity changes on the proposed fuels have a small influence on the maximum fuel temperature.

I. Introduction

Within the concepts of Generation IV nuclear reactors, the Supercritical Water-Cooled Reactor (SCWR) is one of the most viable designs. It is based on two proven technologies: the design and operation of the current Light Water-cooled Reactors (LWR) and the coal-fired power plants that operate with supercritical water. The SCWR is basically an LWR that operates at pressures and temperatures above the critical point of water (374°C and 22.1 MPa), and with a direct energy conversion cycle.

The High Performance Light Water Reactor (HPLWR), European proposal of SCWR, is a pressurised vessel design that operates with supercritical water at 25 MPa, able to reach a core outlet temperature of 500°C. The conceptual design of this reactor aims to produce an electric power of 1000 MWe with a

net efficiency of about 44%. Also, the plant construction costs will be reduced to EUR 1000/kWe [1]. The proposed fuel is UO₂ with 5% enrichment on weight [2].

Despite the advantages of using UO₂, its application in high temperature reactors is limited due to its low thermal conductivity [2]. It has been found that temperatures above the accepted limit of 2123.15 K can be reached using UO₂ in SCWRs [3]. The above has led to the study of new fuel alternatives among which uranium nitride (UN) and uranium carbide (UC) are being considered as viable options.

The thermal conductivity of UN and UC is several times higher than those of conventional UO₂, ThO₂ and MOX fuels. In general, UN and UC offer several advantages that are significant concerning UO₂, due to their high densities and high thermal conductivities. However, both fuels have a reactive nature with water; also,

the uranium nitride reacts with nickel, which is one of the cladding constituent components. To solve this problem, several coatings have been proposed for the fuel pellets [4]–[6]. Usually, the fuel pellet is coated with two layers in the radial direction. Some of the proposed coat materials are zirconium carbide (ZrC) and titanium nitride (TiN). The purpose of the first layer is to support the linear expansion of the fuel, without exerting an unacceptable amount of pressure on the outer layer. The outer coating provides structural integrity and retains the fission products. Therefore, according to the defense in depth concept, the coated fuel pellets adds another barrier against the radioactivity release [6].

It is expected that to reduce the hardness and swelling of uranium nitride and uranium carbide pellets, they will be manufactured with porosities up to 20%, which in turn affects the thermal conductivity and the temperature distribution in the fuel. Generally, the solid thermal conductivity decreases when the voids (pores) increase within its structure. Hence low porosity is desirable to maximise the conductivity. However, the fission gases produced during burning results in internal pressures that may swell the fuel and hence deform it. Thus some porosity degree is desirable to accommodate the fission gases and limit the swelling potential [7].

There is not enough experimental data to evaluate the thermal-hydraulic performance of the different alternative nuclear fuels in supercritical conditions, considering different porosities and coating layers [8].

Several numerical investigations have been carried out to predict the heat transfer behavior in supercritical conditions. Some fuel proposals have been analysed for the SCWRs, using various thermal-hydraulic codes and taking into account multiple geometrical configurations, different mass flow, power and fuel enrichment regimes [2], [9]. A coupled neutron-thermal-hydraulic analysis, using the MCNP and SACoS codes in a supercritical water-cooled thermal reactor was carried out by Chaudri et al. [6]. This study, proposed the use of UN coated with zirconium carbide (ZrC) and UC coated with silicon carbide (SiC) as alternatives to uranium dioxide. They showed that by using UN-ZrC and UC-SiC, instead of UO_2 , the fuel center-line temperature decreased approximately of 500 K and the radial power density became uniform. Carbide and nitride ceramic fuels without coating showed a higher value of linear power density compared to UO_2

and coated fuel pellets. Coated fuel pellets achieved maximum value of linear power density very close to the UO_2 fuel. They verified that when the coating thickness increases and the radius and distance between the fuel rods are constants, the percent of thermal neutrons increases, then the hardness of the neutron spectrum decreases. The authors assumed constant and conservative values of fuel thermal conductivity.

Traditional thermal-hydraulic codes, like SACoS, COBRA, RELAP, etc., calculate heat transfer by using heat transfer coefficients obtained from empirical correlations. These codes do not provide detailed information neither on the complex mechanism of heat transfer in supercritical water nor of the spatial temperature distributions throughout the domain [10].

Recently, the use of Computational Fluid Dynamics codes (CFD) for numerical studies in nuclear reactors has become relevant. With these codes, it is possible to obtain consistent results and provide a better description of heat transfer mechanisms in supercritical conditions. For example, a partially coupled neutronic-thermal-hydraulic calculation of the HPLWR fuel assembly, using the MCNP code and the CFD code, ANSYS-CFX 13 was performed by Xi et al. [11]. In that work, the authors considered constant material properties, and disregard the temperature changes and the influence of fuel porosity in heat transfer.

In general, different alternative fuels have been studied to be used in SCWRs, but the influence of manufactured fuel porosity on the fuel temperature profiles has not been well analysed. Similarly, many studies, disregard the effect of the temperature changes on the fuel thermal conductivity.

In this paper, a comparative study of new alternative fuels for the HPLWR is performed, using the CFD code ANSYS-CFX. A thermal-hydraulic calculation of the HPLWR fuel assembly is carried out using UN fuel uncoated and coated with ZrC, and UC fuel uncoated and coated with TiN. The thickness of the coating layers changes from 0.3 mm to 0.5 mm. The analysis was carried out considering the changes in the fuel thermal conductivity due to manufactured porosity and temperature variations. The manufactured fuel porosity was limited up to 20%. The axial and radial temperature profiles were obtained for all configurations of both proposed fuels and compared with the ones obtained for the UO_2 .

II. Physical and Computational Models

HPLWR's fuel assembly

Several HPLWR core designs have been proposed [1], one of their biggest differences is in the number of passes through the core, which influences coolant, moderator, and fuel behavior. There are one, two and three pass core designs, which indicate the change of the coolant flow direction through the reactor core. A one-pass core is a simpler design. However, a huge increase in enthalpy along the channel may lead to overheating of fuel elements. In a multi-pass flow in the core, the flow mixes to avoid fuel rod hot spots from the high rise of enthalpy. The drawback of this concept is the large pressure drop that reduces the effectiveness of natural circulation [12]. In addition, it has not been proven that such a sophisticated flow path is mechanically feasible.

In this work, the one-pass core configuration proposed by Hofmeister et al. [13] is used, this is the simplest core design and where, in theory, the coolant and the fuel elements highest axial temperature gradients are observed.

The HPLWR's fuel assembly analysed is a square arrangement of 40 fuel rods with a box in it, through which water flows with moderator functions.

In this design, the feed water enters the reactor pressure vessel at 553.15 K. Approximately the 25% of the water flows to the upper plenum, from where it descends as a moderator through the assembly gaps and moderator boxes to the lower plenum. Around 75% of the feed water goes through the down-comer to the lower plenum, where it is mixed with the moderator water and rises as coolant through the sub-channels, between the fuel elements and heating up to a temperature of approximately 773 K.

Since the fuel assembly is symmetric, in this study, only one-eighth part is modeled, as can be seen in Figure 1.

In the cases where the coated UN and UC, respectively, are analysed, two layers are added to the fuel, maintaining the same fuel rod diameter. Table 1 shows the geometrical data of the fuel assembly.

Figure 1. One-eighth of the square fuel assembly

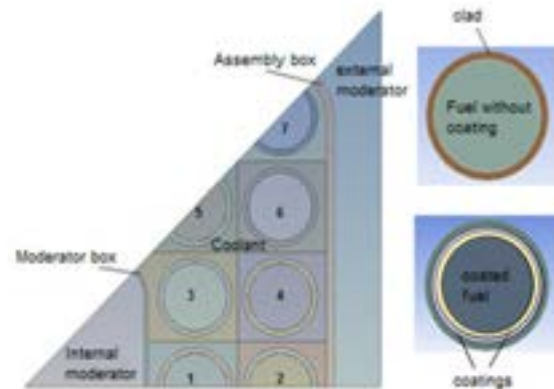


Table 1. Dimensions of the HPLWR fuel assembly without coated fuels

Parameters	Dimensions [mm]
Fuel gap	0.15
Fuel rod diameter	8
Cladding thickness	0.5
Pitch	9.2
Thickness of the moderator box	0.3
Thickness of the assembly box	0.9
Size of the moderator box	25.8
Distance between fuel assemblies	10
Size of the assembly box	66.8
Active core height	4200

Study cases

The study was conducted for 3 cases, in which the fuels thermal conductivity is affected by several factors (Table 2). In the first case, the thermal-hydraulic behavior of uncoated fuels was analysed, taking into account the variations in thermal conductivity with respect to temperature. In the second case, the effect of fuel porosity is analysed in addition. In the third case, the thermal-hydraulic calculation of the HPLWR fuel assembly is carried out using UN fuel coated with ZrC and UC fuel coated with TiN. For both, a porosity of 10% is assumed. The coating thickness is varied from 0.3 mm to 0.5 mm. The results are compared with those obtained for uncoated UN and UC with a porosity of 10% and UO₂ with a porosity of 0% (Maximum conductivity capacity).

Table 2. Study Cases

Cases	Fuel	Porosity	Coating thickness [mm]
No. 1	UO ₂ UN, UC	0	-
No. 2	UO ₂ UN,UC	0: 0.05; 0.1; 0.15; 0.2	-
No.3	UN-ZrC	0.1	0.3/0.4/0.5
	UC-TiN	0.1	0.3/0.4/0.5

Computational model

The CFD codes solve the equations of a fluid flow over a region of interest, with certain conditions at the border of the region. Basically, the set of equations ANSYS CFX solves are the conservation equations (1;2;3).

$$\frac{\partial \bar{\rho}}{\partial t} + \frac{\partial}{\partial x_i} (\bar{\rho} \bar{u}_i) = 0 \quad (1)$$

$$\frac{\partial}{\partial t} (\bar{\rho} \bar{u}_i) + \frac{\partial}{\partial x_j} (\bar{\rho} \bar{u}_i \bar{u}_j) = -\frac{\partial \bar{p}}{\partial x_i} - \frac{\partial}{\partial x_j} (\bar{\tau}_{ij} - \bar{\rho} \bar{u}_i \bar{u}_j') \quad (2)$$

$$\frac{\partial}{\partial t} (\bar{\rho} \bar{H}) + \frac{\partial}{\partial x_j} (\bar{\rho} \bar{u}_j \bar{H}) = \frac{\partial}{\partial x_j} \left(k \frac{\partial \bar{T}}{\partial x_j} - \bar{\rho} \bar{u}_j \bar{h}' + \bar{\tau}_{ij} \bar{u}_i' - \bar{\rho} \bar{u}_j \bar{h} \right) + \frac{\partial}{\partial x_j} \left[\bar{u}_j (\bar{\tau}_{ij} - \bar{\rho} \bar{u}_i \bar{u}_j') \right] \quad (3)$$

Where ρ, u, p are respectively density, velocity and pressure of the fluid, k is the turbulent Kinetic energy, τ is the shear stress, T represents the temperature and H is the total effective enthalpy [8].

Spatial discretisation

A mesh sensitivity study was carried out, and the independence was obtained from a mesh with elements of 12 mm in the axial direction and 0.4 mm in the radial direction for a total of 2 591 050 elements in the cases where fuels are not covered and 3 015 400 elements when it is coated.

Boundary conditions

The boundary conditions of the model are shown in Table 3.

To determine the coolant inlet temperature, an energy balance is made at the boundary of the lower plenum, equation (4), where moderator water is mixed with the rest of the feed water.

$$H_{TOT} = \frac{\dot{m}_{MB} * H_{MB} + \dot{m}_{AG} * H_{AG} + \dot{m}_{DC} * H_{DC}}{\dot{m}_{TOT}} \quad [J/kg]$$

where H is enthalpy, \dot{m} is the mass flow, the subscript TOT stands for the coolant, MB represents the moderator box, AG represents

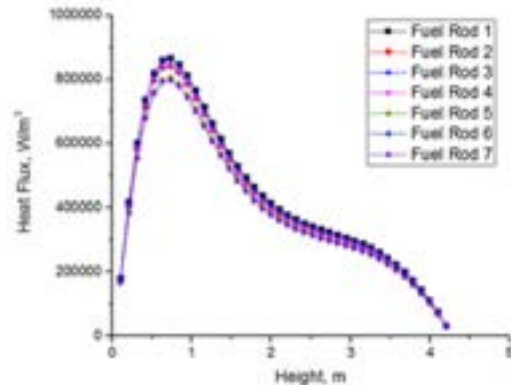
assembly gap and DC represent the water flowing through the down-comer.

Table 3. Boundary conditions

Parameters	Value
System pressure	25 MPa
T_{ent} (moderator)	280°C
\dot{m}_{ent} coolant	0.167 kg/s
\dot{m}_{ent} moderator box	0.01336 kg/s
\dot{m}_{ent} assembly gap	0.02672 kg/s

As shown in Figure 2, the power profile generated by the fuel elements without coating is taken from the results of the coupled neutronic/thermal-hydraulic calculation performed by Castro et al. [14].

Figure 2. Heat flux generated in one-eighth of the HPLWR fuel assembly [14]



Other works [6] have obtained that the overall shape of the linear power profile is similar for uncoated and coated fuels. The higher peak near the bottom of the fuel rod and a smaller peak near the top of fuel rod are reproduced due to the moderator/fuel ratio remains practically the same for coated ceramic fuel and UO₂. For the study cases of the coated fuel (UN-ZrC and UC-TiN), the same shape of the power profiles generated in uncoated fuels was assumed. The factor (F) is used to adjust the same generated power for all cases. Since the fuel pellet diameter is reduced, the volumetric power density has to be increased. Table 4 shows the adjustment factors for the power profiles of the coated fuels.

Table 4. Adjustment factor for the heat flux profiles of the coated fuels

Coating thickness [mm]	0.3	0.4	0.5
Fuel pellet diameter [mm]	5.7	5.3	4.9
Fuel rod diameter [mm]	8	8	8
F	1.465	1.695	1.983

Material properties

The properties of the water were taken from the International Association for Water Properties [15]. The IAPWS-IF97 was chosen from the library of materials available in CFX.

The fuel cladding is a steel alloy (SS316L), its properties were taken according to the Thermophysical Properties of Materials for Nuclear Engineering: A Tutorial and Collection of Data [16]. Nuclear fuel properties were also taken from [16]. To take into account the effect of porosity (P) on fuel density (ρ_{fuel}), it was used the expression (5):

$$\rho_{fuel}(T, P) = \rho_{fuel}(T) \cdot (1 - P) \text{ [kg/m}^3\text{]} \quad (5)$$

Where P stands for fuel porosity in volume fraction. To take into account the changes in the fuel thermal conductivity due to changes in the manufactured porosity, equations (7) for UO_2 , (8) for UN and (9) for UC were used.

$$k_{UO_2}(T, P) = k_{UO_2}(T) \cdot (1 - (2.6 - 5 \cdot 10^{-4}) \cdot P) \text{ [W/mK]} \quad (7)$$

$$k_{UN}(T, P) = 1.864 \cdot e^{-2.14 \cdot P} \cdot T^{0.361} \text{ [W/mK]} \quad (8)$$

$$k_{UC}(T, P) = k_{UC}(T) \cdot \frac{1-P}{1+P} \text{ [W/mK]} \quad (9)$$

The properties of the selected external and internal coatings are shown in Table 5:

Table 5. Properties of coatings (ZrC and TiN)

Properties	ZrC	TiN
Density [kg/m ³]	6.59	5.4
Specific heat [J/kg K]	366.155	545.302
Thermal conductivity [W/m K]	20.5	19.2

III. Results and Discussion**Uncoated fuels without porosity**

In this case, it is considered the fuel thermal conductivity only affected by temperature changes. The average axial thermal conductivity profile of the UO_2 , the UC and the UN fuels in one-eighth of the HPLWR fuel assembly is shown in Figure 3. Using UC and UN fuels, the thermal conductivity increases with height, but from 0.8 m it remains practically constant through the active core. The thermal conductivity of UO_2 first decreases and then remains constant.

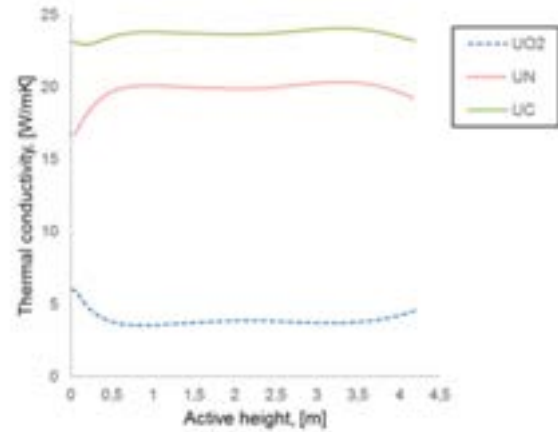
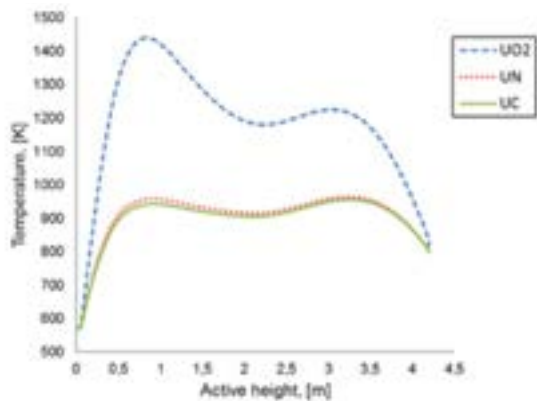
Figure 3. Axial profile of the average fuel thermal conductivity

Figure 4 shows the axial profiles of the maximum fuel temperature averaged over the seven fuel rods of the one-eighth of the fuel assembly for each fuel alternative. Due to the large differences of thermal conductivity between analysed fuels (figure 3), a difference of about 476 K is present in the maximum average value of temperature for UO_2 and UN fuels, and about 484 K for UO_2 and UC fuels.

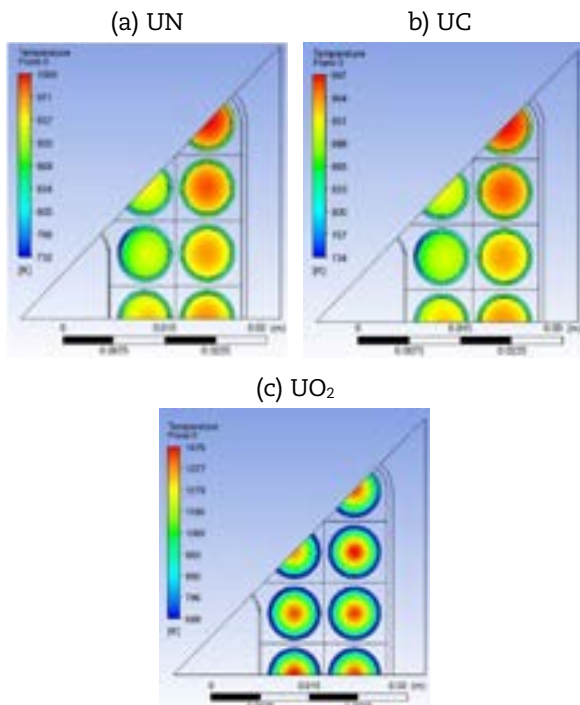
In the case of UO_2 , a maximum average temperature value of 1441 K is reached in the lower region of the fuel assembly, while for UN and UC it is obtained in the upper zone, with a value of 964 K for UN and 956 K for UC. For UO_2 the maximum individual temperature value encountered was 1475 K in fuel rod No. 6, for UN was 1005 K, and for UC was 997 K, both in fuel rod No. 7.

Figure 4. Axial profile of the maximum fuel temperature



In the colorimetric scheme of Figure 5, the temperature is shown in the hottest planes for each fuel studied. For UN (Figure 5a) and UC (Figure 5b), the temperature in the centre of the fuel rod next to the inner moderator box is lower than that of the external fuel rod in the upper area of the fuel assembly.

Figure 5. Radial distribution of fuel temperature (Planes where the maximum temperature is reached)

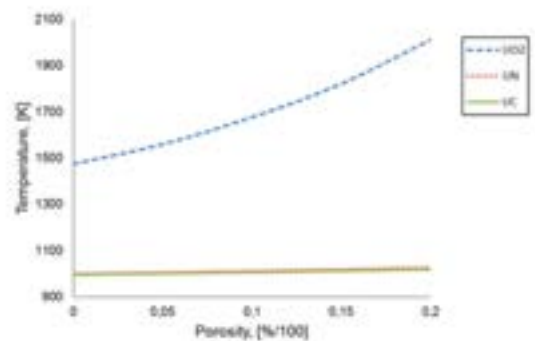


As can be seen in Figure 5c, using UO₂, a maximum temperature value of 1476 K is obtained in the fuel rod No. 6 at an axial distance of 0.83 m. The UN and the UC show maximum temperatures of 1005 K and 997 K respectively, both located in the fuel element No. 7 in the upper zone of the fuel assembly.

Uncoated fuels with porosity. Influence of porosity on maximum fuel temperature

To reduce the hardness and swelling of ceramics fuels, it is recommended to make them with porosities in some cases up to 20% [4]. Figure 6 shows the dependence of the maximum temperature of UO₂, UN and UC with the porosity, in a range of 0 to 20%. It is observed that for UO₂, with a porosity of 20% a temperature of 1952 K is obtained, this value is close to the accepted temperature limit of 2123.15 K. With UC, lower temperature values of around 984 K are achieved. It is important pointing that the temperature of the UN and the UC is not strongly influenced by porosity, at least for the range of 0 to 20%, however, for UO₂ the temperature increases by 511 K.

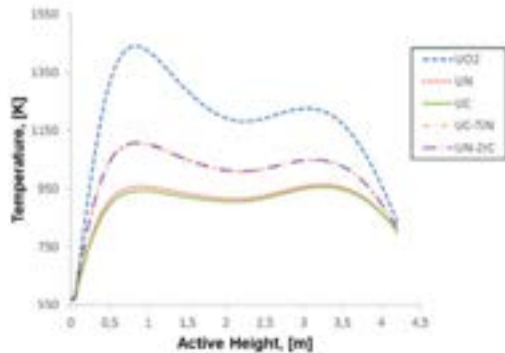
Figure 6. Maximum temperature of UO₂, UN y UC as a function of porosity Coated fuels



This section shows the results of the thermal-hydraulic calculation of the HPLWR fuel assembly using UN coated with ZrC and UC coated with TiN.

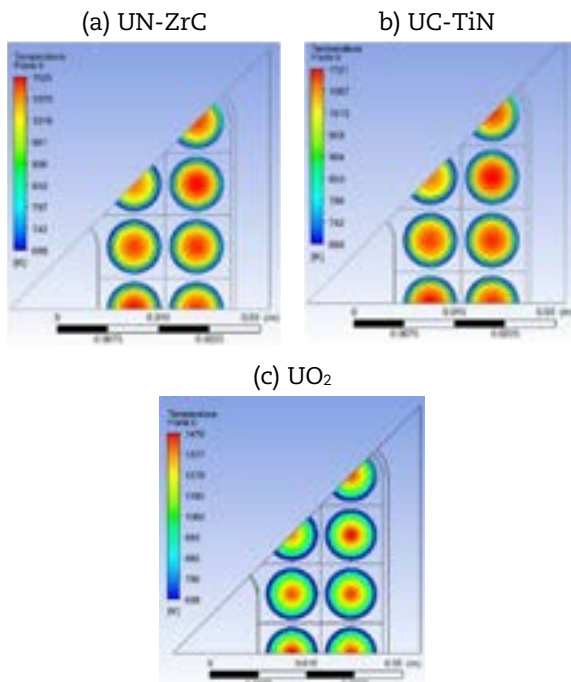
In Figure 7 can be seen a comparison of the axial profiles for the fuel centerline temperature, UO₂ is assumed at its highest heat conduction capacity (porosity 0%). A porosity of 10% is used for UN and UC coated and uncoated.

Figure 7. Axial profile for the maximum temperature of UO_2 , UN, UC, UN-ZrC, and UC-TiN



The maximum in the axial temperature profile for UN-ZrC and UC-TiN is reached in the lower zone of the fuel assembly, with values of 1108 K and 1104 K respectively. It is observed that the temperature values for the coated fuels are higher than those obtained without coating. However, these temperature values are lower than those obtained with UO_2 .

Figure 8. Radial distribution of fuel temperature (Planes where the maximum temperature is reached)



In Figure 8, the radial temperature distributions of UN-ZrC, UC-TiN, and UO_2 ($P = 0\%$) are shown in the plane where the maximum value for the

fuel temperature is obtained. The maximum temperature values are reached in fuel rod No. 6 for UN-ZrC and UC-TiN, with values of 1125 K and 1121 K respectively. It can be seen that the radial distribution of temperature in the UN-ZrC and the UC-TiN is more uniform than that found in the UO_2 . The temperature difference between the centerline of the UO_2 and its external surface is around 600 K, while for UN and UC it is around 100 K and 85 K, correspondingly.

Influence of coating thickness

Increasing the coating thickness, the maximum fuel temperature values rise. As can be seen in Figure 9 and 10, a growth up to 142 K can be seen in the central line for UC-ZrC and 136 K for UN-TiN respectively. For both cases the thickness of the layers was varied from 0.3 to 0.5 mm, the fuel rods diameter (8 mm) was kept constant.

Figure 9. Axial profiles of the maximum temperature for UN-ZrC (Coating thickness from 0.3 to 0.5 mm)

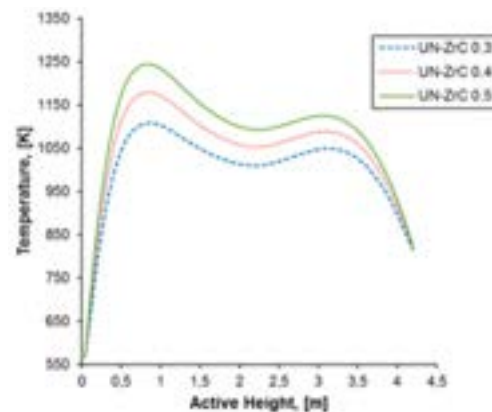


Figure 10. Axial profiles of the maximum temperature for UC-TiN (Coating thickness from 0.3 to 0.5 mm)

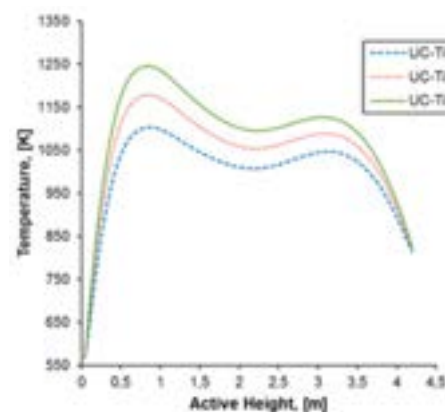


Figure 11 and 12 shows the axial average temperature profile of the external layer (EL) and the internal layer (IL) of the ZrC and the TiN respectively. With the increase in thickness of the coating layers, the temperature of the outer layers of ZrC and TiN remains practically constant, while the temperature of the inner layers, increases. The greatest temperature differences were observed in the lower zone of the fuel assembly. The outer coating maximum temperature value is approximately 1006 K for the ZrC and 1016 K for the TiN.

Figure 11. Axial temperature profiles for ZrC layers with different thicknesses

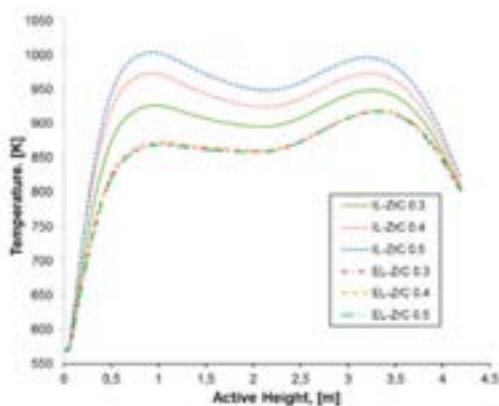
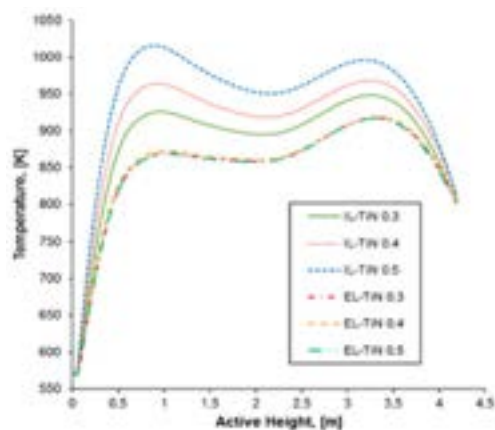


Figure 12. Axial temperature profiles for TiN layers with different thicknesses



V. Conclusion

The high values for thermal conductivity of uranium nitride and uranium carbide make them an excellent option to be used as nuclear fuels in supercritical water cooled reactors. It was found that by using these fuels, instead of the conventional UO_2 , the maximum temperatures in the fuel are remarkably reduced. The radial and axial temperature distributions for UN, UC, and UO_2 were obtained, taking into account the variations of the fuel thermal conductivity concerning the temperature and manufactured porosity. In all cases, lower temperature values were obtained in the fuel rods using UN and UC. The fuel porosity variation has little influence on the maximum temperature reached for UN and UC, while the maximum temperature of UO_2 is strongly affected by this parameter. It was observed that the maximum temperature values for the coated fuels are higher than those obtained without coating. However, these temperature values are lower than those obtained with UO_2 . By increasing the thickness of the coating layers from 0.3 up to 5 mm and maintaining the same rod radius, the maximum fuel temperature increases about 140 K. Also, the external coating layers remain practically at the same temperature, while the inner coating layers were heated with increasing thickness.

Acknowledgements

The authors acknowledge the financial support of the UNAM postdoctoral fellowships

References

- [1] T. Schulenberg, J. Starflinger, P. Marsault, D. Bittermann, C. Maráczy, E. Laurien, J. A. Lycklama, H. Anglart, M. Andreani, M. Ruzickova, and A. Toivonen, "European supercritical water cooled reactor," *Nucl. Eng. Des.*, vol. 241, no. 9, pp. 3505–3513, 2011.
- [2] L. C. Grande, "Thermal Aspects of Using Alternative Nuclear Fuels in Supercritical Water-Cooled Reactors.," 2010.
- [3] I. Pioro, M. Khan, V. Hopps, C. Jacobs, R. Patkunam, S. Gopaul, and K. Bakan, "SCWR Pressure-Channel Nuclear Reactor Some Design Features.," pp. 874–888, 2008.
- [4] H. Ahmed, K. S. Chaudri, and S. M. Mirza, "Comparative analyses of coated and composite UN fuel – Monte Carlo based full core LWR study," *Prog. Nucl. Energy*, vol. 93, pp. 260–266, 2016.
- [5] H. Zhao, D. Zhu, K. S. Chaudri, S. Qiu, W. Tian, and G. Su, "Preliminary transient thermal-hydraulic analysis for new coated UN and UC fuel options in SCWR," *Prog. Nucl. Energy*, vol. 71, pp. 152–159, 2014.
- [6] K. S. Chaudri, W. Tian, Y. Su, H. Zhao, D. Zhu, G. Su, and S. Qiu, "Coupled analysis for new fuel design using un and UC for SCWR," *Prog. Nucl. Energy*, vol. 63, pp. 57–65, 2013.
- [7] N. E. Todreas and M. S. Kazimi, *Nuclear Systems I - Thermal Hydraulic Fundamentals*. 1990.
- [8] L. Castro, L. Rojas, C. García, and C. B. de Olivera, "Metodología para el cálculo acoplado neutrónico-termohidráulico del reactor nuclear de agua ligera de alto desempeño.," *IngenieríaEnergética*, 2015.
- [9] M. K. Saadi and B. Bashiri, "Neutronic and thermal-hydraulic analysis of alternative ceramic fuels in the next-generation of light water reactors," *Prog. Nucl. Energy*, vol. 87, pp. 89–96, 2016.
- [10] K. Podila and Y. Rao, "CFD modelling of supercritical water flow and heat transfer in a 2x2 fuel rod bundle," *Nucl. Eng. Des.*, vol. 301, pp. 279–289, 2016.
- [11] X. Xi, Z. Xiao, X. Yan, Y. Li, and Y. Huang, "The axial power distribution validation of the SCWR fuel assembly with coupled neutronics-thermal hydraulics method," vol. 258, pp. 157–163, 2013.
- [12] M. K. Rowinski, J. Zhao, T. J. White, and Y. C. Soh, "Safety analysis of Super-Critical Water Reactors–A review," *Prog. Nucl. Energy*, vol. 106, no. February, pp. 87–101, 2018.
- [13] J. Hofmeister, C. Waata, J. Starflinger, T. Schulenberg, and E. Laurien, "Fuel assembly design study for a reactor with supercritical water," *Nucl. Eng. Des.*, vol. 237, no. 14, pp. 1513–1521, 2007.
- [14] L. Castro, R. Alfonso, C. R. García, J. Rosales, and D. S. Dominguez, "CFD analysis of thermal-hydraulic behaviour of the high performance light water reactor fuel assembly," *Int. J. Nucl. Energy Sci. Technol.*, vol. 11, no. 3, pp. 229–250, 2017.
- [15] IAPWS, *International Association for the Properties of Water and Steam, Revised Release on the IAPWS Industrial Formulation 1997 for the Properties of Water and Steam*. Switzerland, 2007.
- [16] IAEA, *Thermophysical Properties of Materials for Nuclear Engineering: A Tutorial and Collection of Data*. Viena, 2008.

THE SIGNIFICANT COLLABORATION OF JAPAN AND FRANCE ON THE DESIGN OF ASTRID SODIUM FAST REACTOR SINCE 2014 (F. VARAINE ET AL)

F. Varaine⁽¹⁾, G. Rodriguez⁽¹⁾, J. M. Hamy⁽²⁾, S. Kubo⁽³⁾, T. Iitsuka⁽⁴⁾, H. Mochida⁽⁵⁾

(1) French Atomic Energy and Alternative Energies Commission (CEA), France.

(2) Framatome, France.

(3) Japan Atomic Energy Agency (JAEA), Japan.

(4) Mitsubishi Heavy Industry (MHI), Japan.

(5) Mitsubishi Fast Breeder Reactors (MFBR), Japan.

I. Introduction

After 6 years of Conceptual Design phase (called AVP Phase), the Advanced Sodium Technological Reactor for Industrial Demonstration (ASTRID) Project entered in January 2016 its Basic Design Phase. Since the beginning (2010), the management of ASTRID project was organised around a strong involvement of industrial partners in the reactor design [1].

Since 2014, a partnership with Japanese nuclear institutes and industries is effective on two main items: ASTRID reactor design studies and R&D in support of Sodium Fast Reactors (SFR) [2]. This French-Japanese collaboration on ASTRID Program and Sodium Fast Reactor has been set up in two steps: the signature of a General Arrangement between CEA and the representatives of MEXT and METI on May 5th, 2014; in a second step, an Implementing Arrangement was signed the same year on August 7th by CEA, AREVA NP, JAEA, MHI and MFBR.

This collaboration of a significant level is foreseen to run at least up to the end of 2019. At the beginning, the collaborative work (input data, planning and deliverables) was divided in 29 Task Sheets covering ASTRID design (3 Task Sheets) and R&D (26 Tasks Sheets). Since 2016, the contribution of JAEA/MHI-MFBR to the ASTRID reactor engineering studies has increased, passing from three to twelve Design Task Sheets. Therefore the cooperation between CEA, AREVA NP, JAEA, MHI-MFBR is fruitful and it has been complemented by all parties since July 2017 by an additional

contribution to enlarge Japanese involvement in a process called “Joint Evaluation” to prepare a future potential Common Design.

Japan’s contribution to ASTRID program is very significant. Except CEA (which acts as the industrial architect of the project), JAEA-MHIMFBR became in 2015 the 2nd largest contributor to the ASTRID program - behind Framatome - in terms of involved staff and related financial contribution. It means that ASTRID project has to adapt its project management to integer this important partnership.

After a brief recall of the ASTRID context and the genesis of this collaboration, this paper aims at a presentation of the significant involvement of JAEA / MHI – MFBR in the ASTRID design studies through the “Design Task Sheets” and through the “Joint evaluation”.

II. ASTRID Project Partnership

As defined in the French Law of 28 June 2006 on the sustainable management of radioactive materials and waste, CEA’s Nuclear Energy Division is responsible for the ASTRID project.

For the Basic Design phase, CEA has renewed the bilateral partnerships for this new step, reflecting the determination of the different partners to be involved in the ASTRID project. As shown in Fig. 1, it was settled of 14 bi-lateral partnerships connected to CEA at the beginning of the Basic Design phase.

Figure 1. Set of ASTRID Partnership

Since beginning of the project, CEA acts as the Project manager from the definition of the main functional requirements to the assembly of the 3D mock up including performance control, configuration and interface management between elementary products. Since the AVP phase, the project management is entirely based on a Product Breakdown Structure (PBS), which is in constant evolution.

II.A. Japan and France Cooperation in the Nuclear SFR Field before ASTRID Project

Japan and France have been involved for a long time in the peaceful use of nuclear energy and dispose of many nuclear power plants to produce electricity. Each of the two countries has been developing the technology of Sodium Fast Reactors for several decades. Japan with JOYO and MONJU reactors, and France with RAPSODIE, PHENIX and SUPERPHENIX reactors have both significantly gained skills and experimental feedback in operating sodium fast reactors. Collaborative R&D arrangements have been existing for a long time, based on a mutual interest in the respective design and related safety approach. Indeed, even if Japan chose the concept of a loop type reactor when France considers a pool type, cross-analyses have brought to light many similarities in design, technology, materials, fuel, safety approach, etc. It has been the subject of exchange of company employees between SFR reactor and the detachment of CEA sodium specialists on MONJU site. Several common publications can illustrate these fruitful exchanges [3], [4], [5], [6].

III. The ASTRID Project Partnership With Japan

The history of, and the rules governing the ASTRID Project partnership with Japan have been extensively explained in [2]. This chapter will just recall the main milestones.

First exchanges on a possible involvement of Japan in the ASTRID project took place in 2010, but no further action was engaged because the priority for France was to structure ASTRID project which had just been launched.

In 2013, Japan and France initiated the discussion for an entry in the ASTRID project. Five working groups were created: 1/Definition of the terms of the agreement and of its principles of governance, 2/ASTRID design activity, 3/R&D on severe accidents, 4/R&D on fuel, 5/Other R&D items (Na technology, ISI&R, Instrumentation).

Figure 2. Preparatory meeting of the design activity at Tokyo, June 2014

In 2014, these discussions led to a two-level partnership:

The "General arrangement", which establishes the main principles of collaboration; the signatories are the Japanese Ministry of economy, trade and industry (METI) and Ministry of education, culture, sports, science and technology (MEXT) on Japan side, and the CEA by delegation of the French government. It was signed on May 5th, during the visit of the Japanese Prime Minister in Paris.

The "implementing arrangement", signed by JAEA, MHI, its subsidiary Mitsubishi FBR Systems (MFBR), AREVA (now Framatome) and CEA. It specifies in detail the principles and the governance of the R&D and design activities,

the intellectual property and rights of use, the transfer of information to third parties, the rights after 2019 etc. At the starting point, 29 Task Sheets were approved, three for ASTRID design and 26 for R&D.

Figure 3. First face to face meeting at Lyon, September 2014



The Executive Committee is responsible for proposing the creation of new implementing arrangements, follow their progress and solve the related difficulties (face-to-face meeting every semester). The Joint Team is in charge of the day-to-day control of design and R&D work (monthly meeting). This organisation is fully embedded and coherent with the organisation set-up with the other partners of the ASTRID project.

III.A. Collaborative Works on Design Studies Related to ASTRID

In the design field, Japanese team first contributed directly to the ASTRID Preliminary Design phase on three topics coherently with the ASTRID Master Plan. They concerned the design of an active decay heat removal system, a control rod system with Curie point electro magnets, and a seismic isolation system for the Reactor Building.

Design activities increased sharply during the year 2016 from three Task Sheets to nine, then to ten in 2017. Up to now, the current list of design activities is as follows:

- Astrid Active Decay Heat Removal System (DHRS),
- Curie Point Electro Magnet (CPEM) for diversified Astrid control rods,
- Seismic Isolation System (SIS) of the Astrid Nuclear Island (Benchmark),

- Fabricability and thermo-mechanical calculations of the Astrid Above Core Structure (ACS),
- Fabricability studies of the Astrid Polar Table,
- Contribution to propose technical solutions of the Astrid Core Catcher,
- Transient evaluation and benchmark of Astrid plant,
- Thermomechanical analyses of Astrid main and inner vessel,
- Evaluation of Astrid Core characteristics and core shielding,
- General discussions on the Astrid reactor system, for preparation of future Design Task Sheet or Joint Evaluation.

An overview of the technical progress of these design Task Sheets can be found in [7].

III.B. Reinforcement of the Collaboration: Common View of a Future SFR

In the frame of the Franco-Japanese collaboration in nuclear reactor field, the first collaborative agreement on ASTRID signed in 2014 has been reinforced by a bilateral collaboration agreement on nuclear energy including a specific chapter dedicated to the ASTRID signed the 21st of March 2017 (see Fig. 4). This agreement is setting the framework to start deeper bilateral discussion. As specified in this signed collaborative agreement: "This discussion aims at:

- Deepening the exchanges in order to define more clearly a common technical design of the ASTRID demonstrator, especially the means to integrate adjustments of French and Japanese technology to the current design study carried out since 2010;

- Identifying a potential new collaboration framework relating to the Know-how and experience of both partners, ensuring a fair and appropriate management of the Intellectual Property and taking into account the reflection carried out by the French part on a new organisation for the next coming steps of this project;

- Identifying in France and in Japan, facilities that shall be used to proceed to the validation of the design and R&D works.

Both partners will make all possible efforts to achieve their discussion at the end of 2018, or sooner if possible, in order to settle the new phase of their collaboration."

Figure 4. Picture of Ms Ségolène Royal and Mr Hiroshige Sekō signing the 21st of March 2017 the New Fr-Jp collaboration agreement on Nuclear Energy



The project organisation is performed in two steps. It started with a series of Face-to-Face meetings performed during the first semester of 2017 to understand the fundamental specifications from each part and the technical points of convergence and those to be further discussed for a deeper exchange and explanation. Then, according to this first step of evaluation, Working Groups were created to be able to achieve a better common view for a SFR common design reactor.

These Working groups are presented in Fig. 5.

Figure 5. Table of the joint Working Group items

Group N°	Subject Name
WG1	Top Level Requirements
WG2	Core & Fuel
WG3	Reactor Shutdown
WG4	CDA Mitigation
WG5	Reactor structure / Primary system (HPD)
WG6	Secondary / tertiary systems
WG7	DHRS
WG8	Fuel Handling
WG9	Containment
WG10	System Consistency & Costs
WG11	Joint road map for common SFR technological qualification
WG12	Joint road map for common SFR numerical simulation

Each of them was composed of a board of specialists coming from CEA/Framatome/JAEA/MHI-MFBR. Each of these working groups (except WG10) had to respect the following rules:

- They have to initiate their respective collaborative project with a Workplan accepted by all parts.
- They have to perform several regular meeting by visio-conference (see Fig. 6).
- They have to perform regular Progress of Technical Work report to the WG10 plus a final written synthesis at the end of 2017; and the same process is reproduced for 2018.

The objective is to confirm by each working group the requirements and expectation for ASTRID project and SFR simulation program for extrapolation to future commercial SFR. Conclusions of this joint study have to be reported to the respective national government board.

Figure 6. The efficient use of the video conference system to exchange at 10 000 Km distance



Acknowledgements

Many people are involved in this collaboration and it was impossible to put all of them as co-authors. Nonetheless, the authors would like to thank all persons involved in the different Task Sheets, coming from ASTRID project team, Project and Engineering teams from Japan (JAEA / MHI - MFBR) and France (FRAMATOME).

Nomenclature

ACS	Above Core Structure
ASTRID	Advanced Sodium Technological Reactor for Industrial Demonstration
AVP1/2	Conceptual design studies, phase 1/2 of ASTRID project

BD	Basic Design	MEXT	Japanese Ministry of education, culture, sports, science and technology
CEA	French Atomic Energy Commission	MHI	MITSUBISHI Heavy Industry
CFD	Computational Fluid Dynamic	MFBR	Mitsubishi FBR Systems
CPEM	Curie Point Electro-Magnetic system	PBS	Product Breakdown Structure
DHRS	Decay Heat Removal System	R&D	Research and Development
FBR	Fast Breeder Reactor	SASS	Self Actuated Shutdown System
GEN IV	Fourth Generation Reactor	SFR	Sodium Fast Reactor
HFD	High Frequency Design	SIS	Seismic Isolation System
ISI&R	In-Service Inspection & Repair	SPX	Superphenix (French SFR)
JAEA	Japan Atomic Energy Agency	TH	Thermal Hydraulic
JSFR	Japan Sodium Fast Reactor	TS	Task Sheet
METI	Japanese Ministry of economy, trade and industry	WG	Working Group
		3D	Three-Dimensional

References

- [1] J. ROUAULT, ASTRID the SFR GEN 4 Technology Demonstrator Project: Where we are, where do we stand for ?, ICAPP2015, Nice France, 3-6 may 2015, Paper 15439.
- [2] J. ROUAULT et al., Japan-France Collaboration on the ASTRID program and Sodium Fast Reactor, ICAPP2015, Nice France, 3-6 may 2015, Paper 15440.
- [3] N. DEVICTOR et al., Pool and Loop type Sodium-cooled Fast Reactors – Identification of cooperation possibilities - ICAPP2011 Nice, France, May 2-5, 2011, Paper 11378.
- [4] Y. CHIKAZAWA et al., R&D in support of ASTRID and JSFR: cross-analysis and identification of possible areas of cooperation – Nuclear Technology VOL. 182 MAY 2013.
- [5] G. RODRIGUEZ et al., Monju as an international asset: international assistance and cooperation, ANES 2004, American Nuclear Energy Symposium 2004, October 3-6, Miami Beach, Florida, USA.
- [6] F. BEAUCHAMP et al., Cooperation on impingement wastage experiment of Mod. 9Cr-1Mo steel, using SWAT-1R sodium-water reaction test facility, FR13 IAEA International Conference, Paris, France, March 4-7, 2013.
- [7] G. RODRIGUEZ et al., The collaboration of Japan and France on the design of ASTRID sodium fast reactor, ICAPP2017. Fukui and Kyoto, Japan, April 24-28, 2017, Paper 17428.

ASTRID PROJECT, OVERVIEW AND STATUS PROGRESS (F. VARAINE ET AL)

F. Varaine⁽¹⁾, G. Rodriguez⁽¹⁾, J. M. Hamy⁽²⁾, S. Kubo⁽³⁾, H. Mochida⁽⁴⁾, U. Yukinori⁽⁵⁾, J. P. Helle⁽⁶⁾, A. Remy⁽⁷⁾, T. Chauveau⁽⁸⁾, J. L. Mazel⁽⁹⁾, M. Libessart⁽¹⁰⁾, R. P. Benard⁽¹¹⁾, M. Fukuie⁽¹²⁾, D. Settimo⁽¹³⁾, V. Gautier⁽¹⁴⁾, Y. Lhor⁽¹⁵⁾, M. Lefrançois⁽¹⁶⁾.

- (1) CEA, Atomic Energy Commission, Cadarache Research Center, France
 (2) FRAMATOME, France.
 (3) JAEA, Japan Atomic Energy Agency, Japan.
 (4) MFBR, Mitsubishi FBR Systems, Japan
 (5) MHI, Mitsubishi Heavy Industries, Japan.
 (6) NOX, France.
 (7) GE, General Electrics, United States.
 (8) BOUYGUES, France.
 (9) VELAN, France.
 (10) ARIANE Group, France.
 (11) SEIV ALCEN, France.
 (12) TOSHIBA, Japan.
 (13) EDF, Electricité de France, France.
 (14) CNIM, Constructions industrielles de la Méditerranée, France.
 (15) ONET Technologies, France.
 (16) TECHNETICS.

Abstract

After 6 years of conceptual design phase, the French Advanced Sodium Technological Reactor for Industrial Demonstration (ASTRID) project has started at the beginning of 2016, a 4 years basic design phase. The objective of this paper is to show and underline ASTRID progress and status. The ASTRID project is based on a very efficient partnership, allowing versatility and manageability. Very high level and up-to-date project management methods are performed, including technical control with engineering System tools and 3D mock-up consolidation.

All the industrials partners involved in the project during the last phase have decided to pursue in the ASTRID project, and the strategic partnership with Japan is going to be reinforced.

ASTRID design has also evolved, taking into account new progresses on design to reach better consistency according to high level of reliability and safety, consistent with Generation IV objectives. A cost Killing methodology is provided and feedbacks will be expected during 2018 and 2019 years. In the same time, an ongoing effort started two years ago is underway to map all the qualification needs and define all associated processes consistent with safety regulator requirement.

I. Introduction

As a prototype of SFR technology ASTRID has the main objective of demonstrating advances on an industrial scale by qualifying innovative options. ASTRID must integrate in its own design French and also international SFRs feedback.

As GEN IV system, ASTRID must answer to main requirements and objectives devoted to these concepts with a mastered investment cost and non-proliferation warranty:

- Safety level is targeted according to GEN IV requirements and at least equivalent to GEN III concepts, taking into account Fukushima Daichi accident feedback with improvement against external hazards compared with previous SFRs, including progresses on SFR specificities with a robustness of safety demonstrations.
- Durability aspects in order to preserve natural resources using Pu multi-recycling from spent PWR MOX fuel [1]

along with utilisation of natural depleted uranium which allow in France, producing electricity for few thousands of years.

- Operability demonstration with load factor of 80% or more after first “learning” years associated to significant progress concerning In Service Inspection & Repair (ISI&R).
- Capabilities on minor actinides transmutation demonstrations.

The Genesis of the ASTRID Project was done in the frame of the French Act of 28 June 2006 on sustainable management of radioactive materials and wastes, French Government entrusted CEA (French Commission for Atomic Energy and Alternative Energy) to conduct design studies of ASTRID (Advanced Sodium Technological Reactor for Industrial Demonstration) prototype. After a first period of studies and R&D jointly performed by the CEA, EDF and FRAMATOME to investigate a range of innovative solutions, the project itself so-called ASTRID was launched in late 2009 and a project team was set up in the first half of 2010. Funding was granted through an agreement between the French Government and CEA within the scope of the “investments for the future” program published in the Official Journal on 11th September 2010 [2].

Since 2010, when the first studies were launched to define the ASTRID project, over 3000 technical documents were produced to design the ASTRID reactor.

After 6 years of conceptual design phase, the French 600MWe ASTRID reactor has started at the beginning of 2016, a 4 years Basic Design phase (BD). The project is now at mid-term of this phase and significant milestones were achieved.

This four-year BD phase has for objective at the end of 2019:

- To achieve a consistent definition of all ASTRID systems and components.
- To provide an optimised reactor design.
- To provide all the documents required for the continuation of the project, aiming to increase, as priority, the level of maturity of the most innovative components.

From January 2016 to October 2016, the Confirmation of Configuration Phase (P2C) for Basic Design took place. During this period, it was necessary to integrate in the design studies

the gas (nitrogen) PCS and, in particular, the opportunities for techno-economic optimisations which can result from this integration. On the other hand, optimisation and targeted risk reduction on some end of preliminary design options was reached. Around fifteen thematic working groups have been set up to deal with these issues in order to converge towards stabilised choices that were approved during a design review in October 2016.

All the working groups carried out around a hundred technical meetings in total and more than 300 technical points were analysed. Finally, an expert group carried out an evaluation to ensure that the objectives of this P2C phase were reached, in particular in regards with cost-mastering, operability, safety and extrapolability to a commercial power reactor.

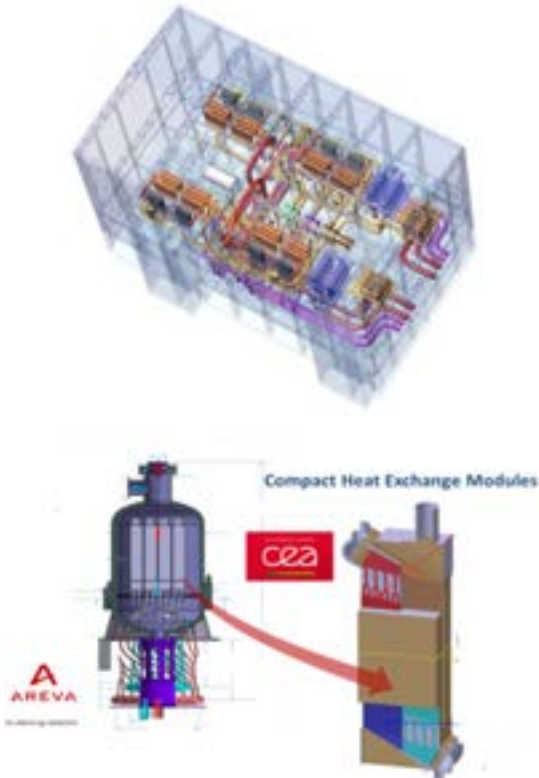
II. ASTRID Configuration for Basic Design

The new configuration was endorsed by the CEA “4th Generation” program during the configuration confirmation review held in Cadarache on 18 and 19 October 2016. This new configuration changed a lot compared to the previous one [3], [4].

II.A. Gas PCS

The Gas PCS in its completeness: Integration and industrialisation of compact sodium-gas heat exchangers (power unit ~190 thMW) integrating innovative exchange modules. Eight exchangers are required, two per secondary loop. Two machine rooms (see Figure 1), each with a gas turbine with three compression stages, are located on each side of the exchanger buildings, so as to minimise the pipes length. Under these turbine halls are placed the storage tanks for the nitrogen inventory (~ 130 tons) [5].

Figure 1. 3D View of Machine Hall and detail of Compact Na-Gas Heat Exchanger
(© CEA-FRAMATOME-GE)



II.B. Fuel Handling and Storage

It was decided to add an external Buffer Storage Vessel in sodium to decouple the handling phases for fuel loading/unloading from those of fuel cleaning and storage. This choice makes it possible to reduce the handling time around 9 days whereas it was previously 20 days [6].

The choice has been made to limit, for cost reasons, both the storage capacity around 100 subassemblies and to limit the residual power of each assembly by only discharging it, after a phase of decay heat of one cycle in a limited internal storage in the primary vessel.

Mutualised storage for fresh and spent fuel subassemblies in the same pool was designed. The fresh subassemblies being stored in gas cask themselves are placed in the pool. This solution limits the footprint of the storage areas and makes it possible to share some common resources (see Figure 2). It allows storage allocation to be adapted to the needs of the plant. The nominal capacity is set to 300 fresh subassemblies (~ 1 core) and 900 spent subassemblies (~ 3 cores).

Figure 2. View of primary and secondary fuel handling and mutualised pool storage
(© CEA-FRAMATOME)



II.C. Main Vessel and Components

ASTRID reactor is a pool type reactor with a conical inner vessel with an internal core catcher (see Figure 3).

The main core catcher function is to collect and manage the corium (melted fuel and metallic structure) coming from the 21 corium guides after a hypothetical Core Disruptive Accident scenario.

Three primary pumps are devoted to the circulation of the sodium from the cold plenum to the diagrid to ensure sodium supply of the core. Four Intermediate Heat Exchangers (IHX and secondary loop), four diversified in-vessel decay heat removal circuits (two passives and two actives) and one circuit in the reactor pit were designed.

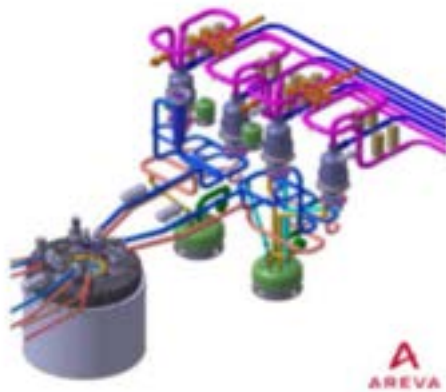
Figure 3. View of reactor vessel (© CEA-FRAMATOME)



II.D. Secondary Loops

The secondary loops transfer the thermal power from the primary circuit to the Power Conversion System (PCS) (see Figure 4). They ensure a forced circulation of the secondary sodium from the IHX to the sodium-gas heat exchanger according to the Brayton gas. Secondary loops must be designed to ensure natural convection onset in the primary circuit in case of loss of supply station power.

Figure 4. 3D View of secondary loops (© CEA-FRAMATOME)



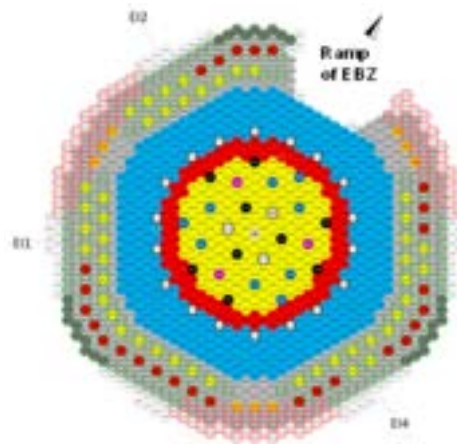
II.D. Core

The reactor configuration at the end of 2017 includes a CFV core (low void sodium worth) (see Fig. 5) referenced 'CFV BD 16-10' (Ref. 5). In CFV core, low sodium void effect is achieved by an heterogeneous fissile zone with sodium plenum in the upper part of the assemblies, Upper Neutron Shielding in boron carbide and an axial fertile plate in the internal core.

Complementary safety devices for prevention (DCS-P) and for severe accidents mitigation (DCS-M) have been implemented in the core:

- three hydraulic absorber rods which fall if the core sodium flow decreases under a given threshold (DCS-P-H);
- Curie point electromagnet will release Diversified control rods by loss of bearing capacity if the core temperature increases too much;
- 21 crossing tubes (DCS-M-TT) to discharge the corium towards the core catcher in case of a hypothetical core disruptive accident scenario.

Figure 5. CFV BD 16-10 (© CEA-FRAMATOME)

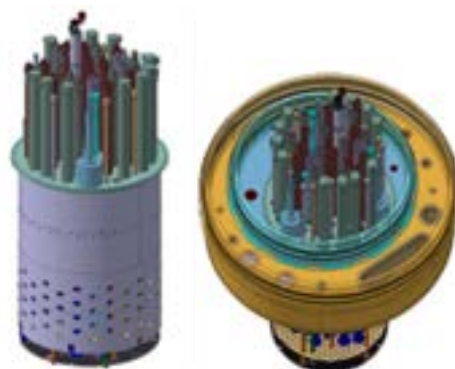


II.E. ACS and Polar Table

Upper closures complete the envelope of the primary circuit at the top of the main vessel and participate in the confinement of the cover gas.

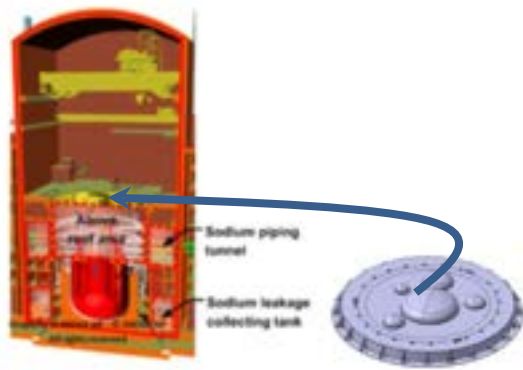
The Above Core Structure (ACS) (see Figure 6) supports the twenty-one control rod drive mechanisms, all the core instrumentation and the Direct Lift Charge Machine. Instrumentation supported by the ACS includes 351 temperature and flowrate measuring poles, high temperature fission chambers to detect local reactivity effect, tubes for sodium sampling over each fuel subassembly to localise fuel cladding failure and high Temperature Ultra-Sonic Transducers (active and passive detection).

Figure 6. 3D view of the ASTRID ACS (© CEA-FRAMATOME)



The general arrangement of ASTRID reactor building has determined a closed space between the ASTRID upper closure and the reactor building: it is called the above roof area. This area (see Figure 7) is delimited on its lower part by the upper reactor closure (also called the reactor roof) and on its upper part by the Polar table. This polar table is conceived to limit the pressure loading in the reactor building in case of sodium fire in the above roof area. In addition, it prevents from the risk of heavy charge fall on the reactor roof.

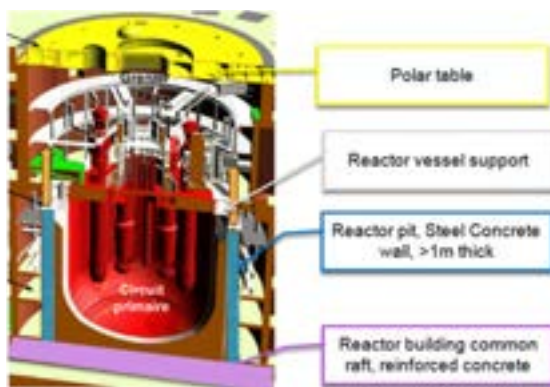
Figure 7. Reactor Building and Polar Table
(© CEA-FRAMATOME)



II.F. Reactor Pit

The concrete reactor pit withstands the dead weight of the reactor vessel and the primary circuit (Figure 8). Its design is governed by the severe accident load case scenario, applying a huge upward tensile force.

Figure 8. Steel Concrete Reactor pit (in blue) in the reactor vessel environment (© CEA-FRAMATOME-BOUYGUES)

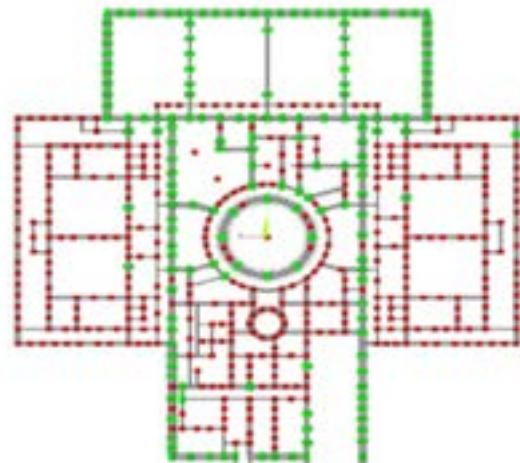


II.G. Seismic Insulation

For ASTRID, preliminary studies concluded to isolate directly all the buildings of the nuclear island on a para-seismic raft equipped with para-seismic pads (see Figure 9). The goal on ASTRID project is to decrease the horizontal building accelerations from 5 to 10 times.

Based on European standards, based on previous solutions used elastomeric rubber with metallic parts pads. ASTRID Project and its partners (BOUYGUES and CNIM) have chosen to improve the material, using polyurethane material instead of natural rubber. Several advantages are expected [7].

Figure 9. Plan view of the location of the seismic pads (© CEA-FRAMATOME-BOUYGUES)

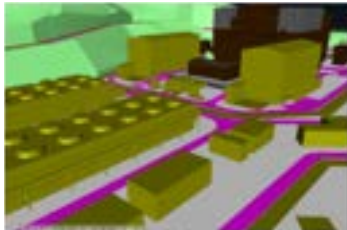


II.H. Balance-Of-Plant and General Layout

To implement studies in real conditions, a reference site was selected as a possible one. That makes it possible to apprehend the whole of the site interfaces with the installation design. A project management process ensures impacts follow-up on the reference site (geology, seismic conditions, climatology, external aggression, plugin to networks and so on) in order to manage and quantify them during studies. This approach allows to identify clearly all the design options linked to the reference site and to compare several sites between them.

The present reference site is located at Marcoule CEA Center. [8], and a global layout is presented in the Figure 10.

Figure 10. Global layout of ASTRID environment and East/West cutting view of the nuclear island (© CEA-NOX)



III. Partnership

All of the partnerships around ASTRID, established during the Conceptual Design phase, were renewed (except for Rolls Royce), with some changes or modification of the scope.

III.A. Industrial Partnership

The main scopes for the Basic Design are recalled below for each industrial partner (see Figure 11):

- FRAMATOME: Engineering of the nuclear island, I&C, industrialisation of the sodium-gas compact exchanger.
- EDF: Operation and project management feedback from Phenix and SUPERPHENIX operation.
- SEIV: Hot cell design.
- CNIM: Industrialisation and fabricability of large components, gas cycle heat exchangers, seismic pads.
- BOUYGUES: Civil engineering, seismic pads.
- NOX: General layout and site infrastructure.
- GENERAL ELECTRIC: Tertiary energy conversion system.
- VELAN: Sodium isolation valve for secondary circuits.
- TOSHIBA: Secondary circuit electromagnetic pump.
- ARIANE GROUP: Operability, waste management.
- JAEA/MHI/MFBR: see Japan Partnership sub-chapter.

- ONET TECHNOLOGIES: Inspection carrier system, concept of innovative control rod mechanism.
- TECHNETHICS: Insulation seals for several reactor areas and in particular for the rotating plugs.

It will be noted that the responsibility for the engineering of the core and associated subassemblies is carried over to the CEA through the core design engineering and is not formalised through a specific endorsement.

Figure 11. The ASTRID Project engineering and partnership organisation



III.B. Japanese Partnership

In the framework of the Implementing Arrangement of August 7th, 2014 signed between Japan Atomic Energy Agency (JAEA), Mitsubishi Heavy Industry (MHI) Mitsubishi FBR Systems (MFBR), FRAMATOME and CEA, contribution, of ASTRID Design activities increased significantly during the year 2016 from three Task Sheets to nine, then ten in 2018. [9] [10]. Subjects treated in Design Task sheets are:

- Task Sheet D1: Astrid Active Decay Heat Removal System (DHRS),
- Task sheet D2: Curie Point Electro Magnet (CPEM) for diversified Astrid control rods,
- Task Sheet D3: Seismic Isolation System of Astrid reactor (SIS),
- Task Sheet D4: Fabricability and thermo-mechanical calculations of the Astrid Above Core Structure (ACS),
- Task sheet D5: Fabricability of the Astrid Polar Table,
- Task Sheet D6: Contribution to propose technical solutions of the design of the Astrid Core Catcher,

- Task Sheet D7: Transient evaluation of Astrid plant,
- Task sheet D8: Thermomechanical analyses of Astrid main and inner vessel,
- Task sheet D11: Evaluation of Astrid Core characteristics and core shielding,
- Task Sheet D12: General discussions on the Astrid reactor system.

In addition, a Declaration of Intent between France and Japan including the proposal to strengthen future ASTRID collaboration was signed in March 2017. Thus, in addition to working groups, a special effort was made at the end of 2017 to share and converge on the requirements of possible common specifications.

IV. Conclusions

After 6 years of conceptual design phase, the French 600 MWe ASTRID project has started at the beginning of 2016, a 4 years basic design phase. The project is now at mid-term of this phase, The ASTRID project is based on a very efficient partnership, allowing versatility and manageability. Very high level and up-to-date project management methods are performed. All the Industrials partners involved in the project during the last phase have decided to pursue in the ASTRID project, and the strategic partnership with Japan is going to be reinforced.

ASTRID design had also evolved, taking into account new advanced on design to reach better consistency according to high level of reliability and safety, consistent with Generation IV objectives.

For 2018, the project is launching a phase of design to cost to allow cost reduction. In the same time an ongoing effort started two years ago is underway to map all the qualification needs and define associated processes consistent with safety regulator requirement. A more realistic planning has been prepared, adding a four years consolidation phase between basic design and detailed design, in order to increase the level of confidence and progress on the technology feasibility including experimental validations of the ASTRID's main innovative options.

Acknowledgements

Many people are involved in the ASTRID Project and it is a very good opportunity to thank them for the quality of the work produced and their involvement in this great project. The ASTRID

project team is very grateful to all engineers, researchers, SFR specialists and experts coming from ASTRID partners (FRAMATOME, ARIANE GROUP, BOUYGUES, CEA, CNIM, EDF, GENERAL ELECTRIC, JAEA, MFBR, MHI, NOX, ONET TECHNOLOGIES, SEIV, TECHNETICS, TOSHIBA, VELAN) without whom all this work could not be presented here.

Nomenclature

ACS	Above Core Structure
ASTRID	Advanced Sodium Technological Reactor for Industrial Demonstration
BD	Basic Design
CEA	French Atomic Energy Commission
CFV	Low Void sodium worth Core
CPEM	Curie Point Electro-Magnetic system
DCS-M	Complementary Safety Device for Mitigation
DCS-M-TT	Complementary Safety Device for Mitigation – Transfer Tube
DCS-P	Complementary Safety Device for Prevention
DHRS	Decay Heat Removal System
FBR	Fast Breeder Reactor
GEN IV	Fourth Generation Reactor
IHX	Intermediate Heat Exchanger
ISI&R	In-Service Inspection & Repair
JAEA	Japan Atomic Energy Agency
MHI	MITSUBISHI Heavy Industries
MFBR	Mitsubishi FBR Systems
MW	MegaWatt
PCS	Power Conversion System
P2C	Confirmation of Configuration Phase
PWR	Pressurised Water Reactor
R&D	Research and Development
SC	Steel Concrete structure
SFR	Sodium Fast Reactor
SIS	Seismic Isolation System
SPX	Superphenix (French SFR)
TS	Task Sheet
WG	Working Group
3D	Three Dimension

References

- [1] J. P. GROUILLER et al; “Plutonium recycling capabilities of ASTRID reactor”; Proceedings of International Conference on Fast Reactors and Related Fuel Cycles, Yekaterinburg, Russian Federation, 2017, IAEA-CN 245-348.
- [2] F. GAUCHE; “The French Prototype of 4th Generation Reactor: ASTRID”; Proceedings of Annual meeting on nuclear technology, Berlin, May 17&18th, (2011).
- [3] F. CHANTECLAIR et al.; “ASTRID reactor - Design overview and main innovative options for Basic Design”; Proceedings of International Conference on Fast Reactors and Related Fuel Cycles, Yekaterinburg, Russian Federation, 2017, IAEA CN 245-400.
- [4] MS. CHENAUD et al ; “Progress in the design of the ASTRID nuclear island”; Proceedings of ICAPP 2018, Charlotte, NC, USA, April 8-11, 2018 #23890.
- [5] D. PLANCQ et al., “Progress in ASTRID Sodium Gas Heat Exchanger Development”, Proceedings of International Conference on Fast Reactors and Related Fuel Cycles, Yekaterinburg, Russian Federation, (2017), IAEA-CN-245-285.
- [6] F. DECHELETTE et al., “The fuel handling route of ASTRID at the beginning of the basic design”, Proceedings of International Conference on Fast Reactors and Related Fuel Cycles, Yekaterinburg, Russian Federation, (2017), IAEA-CN-245-395.
- [7] P. SAUNIER et al.; “Seismic isolation system in civil work design of Gen IV nuclear power plant buildings”; Proceedings of ICAPP 2018, Charlotte, NC, USA, April 8-11, 2018 #23845.
- [8] P. AMPHOUX et al.; “Status of ASTRID architecture in starting of Basic Design phase”; Proceedings of ICAPP 2017, Fukui and Kyoto, Japan, April 24-28, 2017, a90408.
- [9] F. VARAINE et al; “The Collaboration of Japan and France on the design of ASTRID Sodium Fast Reactor”; Proceedings of ICAPP 2017, Fukui and Kyoto, Japan, April 24-28, 2017, a90428.
- [10] F. VARAINE et al., “The significant collaboration of Japan and France on the design of ASTRID Sodium Fast Reactor since 2014”, Proceedings of GIF Symposium, Paris, France, 16-17 October, 2018.

VHTR TECHNOLOGY DEVELOPMENT IN JAPAN
– Progress of R&D Activities for GIF VHTR System – (T. SHIBATA ET AL)

Shibata Taiju, Sato Hiroyuki, Ueta Shohei, Takegami Hiroaki, Takada Shoji,
 Kunitomi Kazuhiko

Japan Atomic Energy Agency (JAEA), Japan.

Abstract

Very High Temperature Reactor (VHTR) of Generation IV nuclear reactor system is expected to extend the use of nuclear heat to a wider spectrum of industrial applications such as hydrogen production, high efficiency power generation, etc., due largely to high temperature heat supply capability as well as inherent safe characteristics. An interest in VHTR as an advanced nuclear power source for the next generation reactor, therefore, has been increasing more and more. Japan Atomic Energy Agency (JAEA) joins the research projects for the VHTR system in the Generation IV International Forum (GIF).

JAEA has been conducting research and development under the HTTR (High-Temperature Engineering Test Reactor) project. The project aims to establish both HTGR technology and heat application technology.

As for the HTGR technology, the HTTR, a first VHTR system constructed at the Oarai Research and Development Institute of JAEA, is used to demonstrate reactor performance and safety. The HTTR achieved a continuous reactor operation with reactor outlet temperature of 950°C for 50 days in 2010. During the operation, the SiC-TRISO (tri-structural isotropic) coated fuel particle (CFP) for HTTR showed excellent quality to retain fission gas. Researches on burnup extension and on ZrC coating for CFP were carried out for upgrading fuel technologies. Neutron irradiation effect on SiC coated oxidation-resistant graphite is carried out. Some specimens showed excellent stability. JAEA has been pursuing an activity to establish an international safety standard for licensing of commercial HTGR cogeneration systems considering safety characteristics of HTGRs. The HTTR is preparing for the restart to obtain the license following the new regulation standard. The restart is expected in FY2019.

As for the heat application technology, world's first continuous hydrogen production by IS (Iodine-Sulfur) process was successfully demonstrated in 2004. JAEA also achieved 31 hours of hydrogen production by a test facility made of industrial materials in 2016. JAEA is planning a demonstration of heat application technologies on the HTTR. The basic design of test plant, HTTR-GT/H₂, consists of a Brayton-cycle helium gas turbine power conversion system and an IS-process hydrogen cogenerating plant has been completed.

I. Introduction

High Temperature Gas-cooled Reactor (HTGR) is a graphite-moderated, helium-cooled reactor and heat resistant ceramic coated fuel particles are used. HTGR has excellent inherent safety characteristics and can meet the energy demand for various industries.

VHTR is a next step of HTGR and can supply high temperature helium gas in the range between 700 and 950°C or higher to the reactor outside. This high temperature energy can meet various heat application requirements

such as hydrogen production by thermo-chemical processes and power generation by helium gas turbine. Japan Atomic Energy Agency (JAEA) has been conducting research and development for VHTR (HTGR) system under the HTTR (High-Temperature Engineering Test Reactor) project. HTTR is the pin-in block type first HTGR constructed at the Oarai Research and Development Institute of JAEA. The project aims to establish both HTGR technology and heat application technology.

Japan's basic philosophy is to advance nuclear-energy utilisation under ensuring safety. Japanese "The Strategic Energy Plan" and "The

Growth Strategy” indicate the promotion of research and development of HTGR. Ministry of Education, Culture, Sports, Science and Technology (MEXT) established an HTGR committee with industries and academia in Japan to discuss roadmap and conceptual design for the first demonstration plant of HTGR. The overseas deployment strategy for domestic HTGR technologies was discussed by a working group under the committee.

JAEA joins the research projects for the VHTR system in the Generation IV International Forum(GIF). This paper describes the major ongoing activities on research and development for the VHTR system pursued in JAEA.

II. Research and Development for VHTR System

(1) Reactor technologies

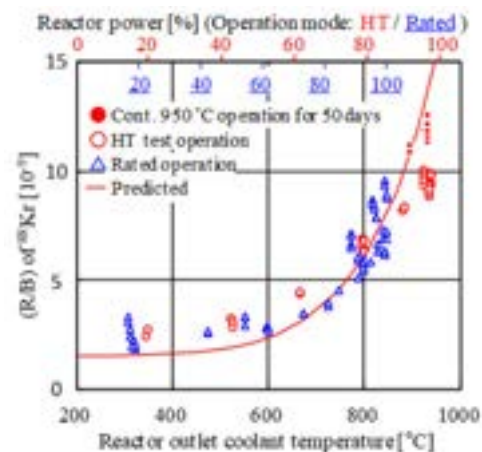
(1-1) R&D on VHTR fuel in Japan

As a reference concept of VHTR to attain higher outlet coolant temperature up to above 1000°C [1], fuel temperature of VHTR would be higher than that of the HTTR. Then, it is important for VHTR to use highly qualified SiC-TRISO (tri-structural isotropic) coated fuel particle (CFP) to prevent unexpected additional failure during operations. In JAEA, fuel fabrication technologies have been developed with the collaboration of the Nuclear Fuel Industry Co., Ltd. since the early 1970’s, and the first and second loading fuels of the HTTR have been fabricated with totally 1,800 kg of uranium [2, 3]. Average through-coatings and SiC defective fractions for the first and second loading fuels were 2×10^{-6} and 8×10^{-5} , and 8×10^{-5} and 1.7×10^{-4} , respectively [2, 3]. It was concluded that these values were quite lower than the criteria, 1.5×10^{-4} for through-coatings failure and 1.5×10^{-3} for SiC-defective fractions [2, 3], and the HTTR fuel has been fabricated successfully, whose quality attained as high as or higher than the mass-produced HTGR fuels in the world [4].

With regard to evaluation of fuel integrity, a highly accurate and sensitive method shall be needed for the VHTR operation, because diffusional release of fission gas from as-fabricated uranium contamination of the VHTR fuel could make it difficult to detect a low level of additional fuel failure at an early stage due to higher fuel temperature than that of the conventional HTGR. Through testing operations of the HTTR, an evaluation method for fuel integrity during operations has been

established with high accuracy and sensitivity by measuring fission gases quantitatively in the primary coolant. Figure 1 shows the predicted (R/B)s of ^{88}Kr as a function of the reactor power during the continuous reactor operation with reactor outlet temperature of near 950°C for 50 days [4]. The prediction was carried out assuming as-fabricated through-coatings failure fraction (2×10^{-6}) and as-fabricated uranium contamination fraction (2.5×10^{-6}) in fuel compact matrix and no additional fuel failure during operations [4]. It was concluded that the fission gas release fraction was as low as that from the diffusion from the contaminated uranium in fuel compact matrix. Finally, it was concluded that the HTTR fuel demonstrated excellent quality during the continuous high temperature operation.

Figure 1. Release rate to birth rate (R/B) ratio of ^{88}Kr as a function of reactor outlet coolant temperature. [4]



For upgrading of HTGR technologies, JAEA has developed new SiC-TRISO CFP designed for burnup extension, and also an advanced type of coated fuel particle, where ZrC replaces SiC, in order to raise the operating temperature. For the former, new SiC-TRISO CFP targets the burnup at 100Gwd/t for a 50 MWt small-sized HTGR for multiple heat applications, named HTR50S, with the reactor outlet coolant temperature of 750°C and 900°C. Table 1 shows the comparison of TRISO between HTTR and new types. The new SiC-TRISO CFP has been fabricated by NFI and irradiated in WWR-K research reactor in Kazakhstan. As the result, level of fission gas release by additional failure corresponded to that from as-fabricated SiC-defective fuel at about 93.3 GWd/t of burnup,

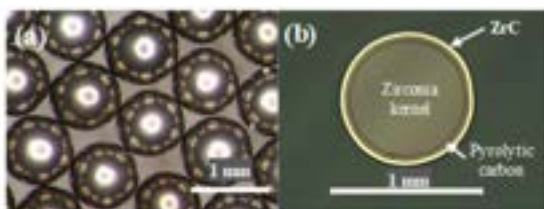
and finally, integrity of new TRISO under irradiation has been demonstrated.

Table 1. Specifications of TRISO of HTTR and new types.

Size (μm)	HTTR (Spec.)	New TRISO (Spec.)
Kernel dia	600	500
Buffer thick	60	95
IPyC thick	30	40
SiC thick	25	35
IPyC thick	45	40

For the latter to upgrade HTGR fuel technologies, ZrC-TRISO is expected to be applied as the VHTR fuel as an alternative to SiC-TRISO CFP to take advantage of ZrC's excellent properties, which will be used under high temperature and extended burnup conditions. To have optimum performance, stoichiometric ZrC, whose quantity ratio of Zr to C is 1, should be deposited. We have constructed a ZrC coater applying an original fabrication technique using zirconium bromide and methane gases, and also developed ZrC layer inspection techniques [5]. Finally, stoichiometric ZrC has been obtained as shown in Figure 2 and its fabrication conditions for high quality stoichiometric ZrC has been successfully determined [5].

Figure 2. Appearance (a) and cross section (b) of ZrC coating on the dummy particle.



(1-2) R&D on oxidation-resistant graphite

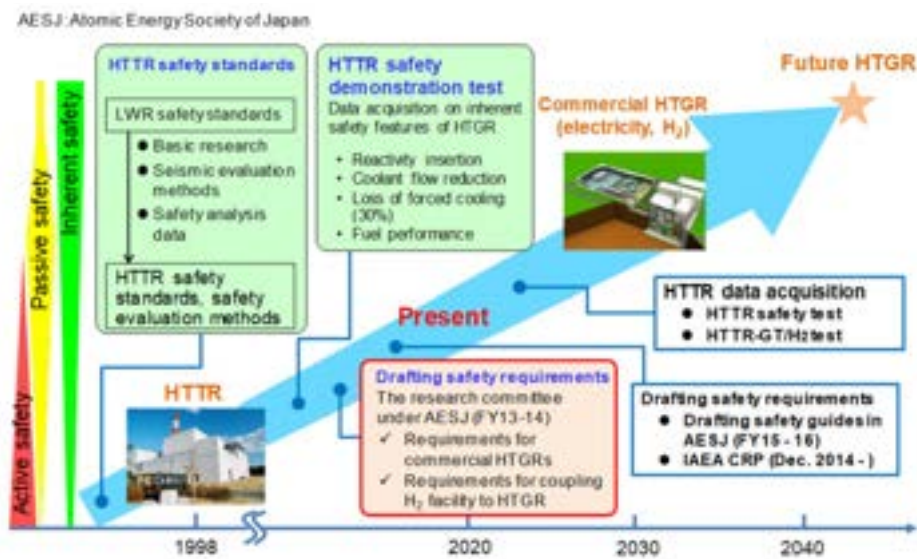
Graphite materials are used for in-core components of VHTR(HTGR). For the graphite components, it is necessary to keep their geometry against oxidation damage in air and water ingress accidents. Although severe oxidation damage could be prevented by using purified graphite materials, it is desirable to enhance oxidation resistance to keep much safety margin. SiC coating on graphite surface is the candidate method for this purpose.

JAEA, Japanese four graphite companies (Toyo Tanso Co., Ltd., IBIDEN CO., LTD., TOKAI CARBON CO., LTD. and Nippon Techno-Carbon Co., Ltd.) and Institute of Nuclear Physics of the Republic of Kazakhstan (INP) are carrying out the R&Ds to develop oxidation-resistant graphite to apply the in-core graphite components [6]. The irradiation test was carried out by WWR-K reactor in INP through the ISTC partner project. Irradiation test about oxidation-resistant graphite specimens was completed with 200 days at irradiation temperature about 1200oC. The maximum fast neutron fluence($E>0.18\text{MeV}$) were calculated as 1.2×10^{25} and $4.2 \times 10^{24} \text{ m}^{-2}$ for two irradiation capsules [6]. After the irradiation, the irradiated specimens were heated up about 1100°C or 1200°C in an electric furnace and exposed at mixed gas ($\text{He}+20\%\text{O}_2$) to evaluate the integrity of SiC coating against oxidation. The change of the gas contents flown through the irradiated specimen in the electric furnace was measured. Also, the change of the specimen weight before and after the gas injection test was measured. As a result, some specimens showed excellent stability against neutron irradiation and subsequent oxidation. Detailed evaluation is underway.

(1-3) Establishment of safety standards

JAEA has been pursuing an activity to establish an international safety standard for licensing of commercial HTGR cogeneration systems considering safety characteristics of HTGRs based on construction and operational experiences accumulated in the HTTR. A roadmap for the activity is shown in Figure 3.

Figure 3. Road map for establishment of safety standards



Draft safety requirements for commercial HTGR systems were developed under the research committee in Atomic Energy Society of Japan (AESJ) based on top-level safety approaches shown as follows:

- Plant conditions with massive releases of radionuclides from the plant to environment should be practically eliminated.
- Integrity of radionuclide retention barrier of coated fuel particle should be protected in all plant conditions.
- Safety functions should be relied on inherent and passive safety features.

In addition, basic concepts of safety guides including evaluation items to fulfil safety requirements, design basis event selection approaches and acceptance criteria were investigated in the AESJ research committee.

The draft safety standards are provided to the Coordinated Research Project (CRP) of International Atomic Energy Agency (IAEA) as a basis for discussion. The project members are from 8 countries; China, Germany, Indonesia, Kazakhstan, Korea, Ukraine, United States and Japan. The project is scheduled to be completed in the end of 2018 and the results of the discussion are planned to be documented in NE technical report series and TECDOC. Key elements in the safety standards may considered to be reviewed under the framework

of Generation IV International Forum (GIF) for further elaboration. The outcome of these results is expected to be the basis for safety standards for licensing of modular cogeneration HTGRs to be deployed in newcomer countries such as Poland, etc.

(1-4) Restart of HTTR

Almost three years and 7 months have passed since JAEA submitted the evaluation results satisfying the new regulation standard to the Nuclear Regulation Authority (NRA) in Japan on Nov. 26, 2014. Two hundred one pre-review meetings and 61 review meetings have been carried out by the Groups of Research Reactor and Earthquake and Tsunami. The review by the Research Reactor Group was completed in October, 2017. Concerning the review by the Earthquake and Tsunami Group, the design seismic motion in Oarai area was fixed in June, 2017. Review on evaluation of foundation ground and near slope was completed in November, 2017 as same as that of volcano. The design seismic motion was enlarged than the estimated one at the time of application as the results of review as same as that of LWRs by NRA. Then, the tentative target schedule toward the restart of HTTR was revised because additional seismic evaluation is necessary based on the new enlarged design seismic motion, although countermeasures against seismic integrity are considered unnecessary. JAEA has reported the revised tentative target schedule to the NRA on January 24, 2018 as

shown in Figure 4. After the restart of HTTR, the loss of forced cooling tests will be carried out. The restart is expected in FY2019.

Figure 4. Tentative target schedule toward restart of HTTR

	FY2014	FY2015	FY2016	FY2017	FY2018	FY2019
Evaluation of natural phenomena						
Re-evaluation of seismic design classification						
Seismic evaluation						
Documentation of verification results, including evaluation of BOEA						
Evaluation by NRA						
Periodic inspection	Application Nov. 23					

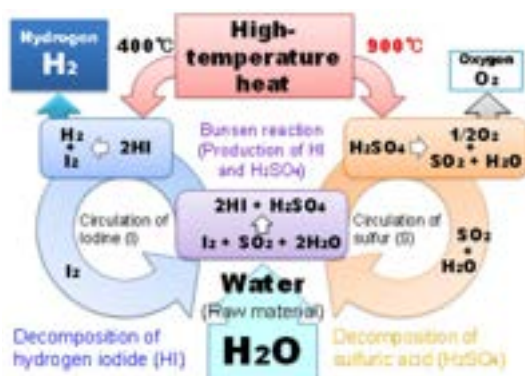
(2) Heat utilisation technologies

(2-1) Hydrogen production test by Iodine-Sulfur process

JAEA has been conducting research and development on the thermochemical iodine-sulfur (IS) process for nuclear hydrogen production. The IS process is one of the most attractive high-temperature heat application of VHTR [7, 8].

Figure 5 shows a schematic of the IS process. In the IS process, hydrogen (H_2) is produced by water-splitting through the three chemical reactions: Bunsen reaction, sulfuric acid (H_2SO_4) decomposition and hydriodic acid (HI) decomposition.

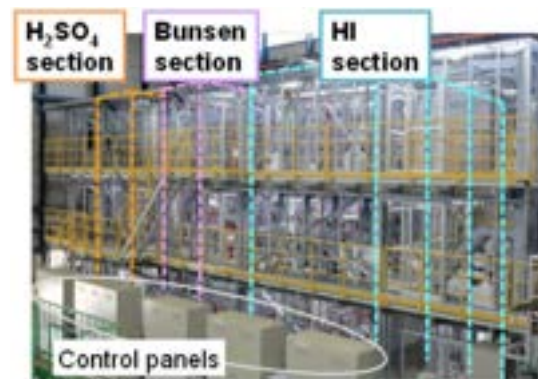
Figure 5. Schematic of thermochemical IS process



JAEA successfully achieved world's first continuous hydrogen production by the IS process with a glass and fluoro-resin made apparatus in 2004 [9]. We then conducted integrity tests of three main components made of industrial material for practical use during 2010-14 [10, 11]. Based on the test results, a hydrogen production test-facility made of industrial material was fabricated for integrity verification of all components and stability of hydrogen production in 2014 [12]. Figure 6 shows an appearance of the test-facility, which can produce H_2 of 100 NL/h-scale with an electric heating.

After the individually performance test of each section during 2014-15 [13, 14], we conducted hydrogen production test twice. The objective of the first test, in February 2016, was to verify integrated operation of the all sections, and the second one, in October 2016, was to carry out long-term stable operation and verify the reliability of the facility.

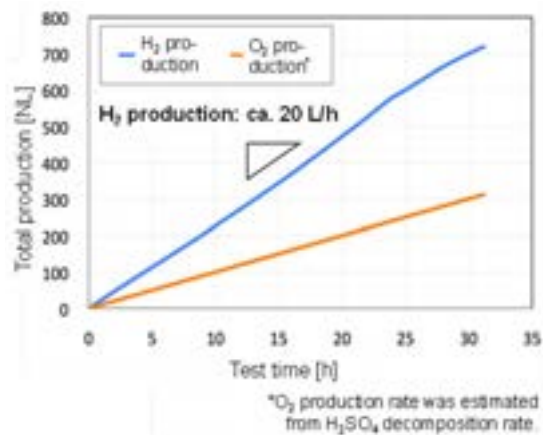
Figure 6. Appearance of hydrogen production test-facility



Draft chamber: W 18.5 x D 5 x H 8.1 (m)

In the first test, we succeeded hydrogen production of 10 L/h- H_2 rate for 8 hours with integration of the all sections. The result of this test revealed that some component was required to be modified for stable operation. The second test was therefore conducted after improvement of technologies for stably operating: transport technology of HIX solution and prevention technology of I_2 precipitation. The improved technologies were confirmed successfully, and made it possible to increase test duration up to 31 hours of 20 L/h- H_2 rate, as shown in Figure 7. The production ratios of H_2 and O_2 of the two tests were around a stoichiometric ratio of H_2O decomposition.

Figure 7. Result of hydrogen production test in Oct. 2016



After the second tests, the condition of components material was investigated by overhaul inspection of corrosion-resistance components. Serious damage or corrosion was not found in the inspection. We will conduct the next hydrogen production test to confirm operation stability and components reliability, which have been improving by reflecting the results of the hydrogen production tests and the inspection. These results including future hydrogen production tests will be utilised for the design of hydrogen production system with VHTR.

(2-2) HTTR cogeneration demonstration program

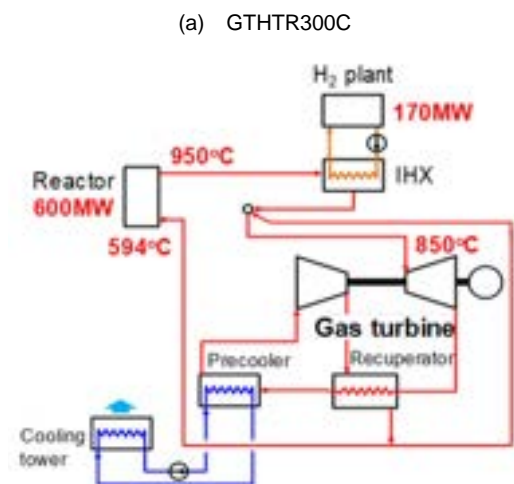
On the basis of reactor and heat application technologies developed under the HTTR project, JAEA launched HTTR cogeneration demonstration program with the aim of completing the system technology of HTGR hydrogen cogeneration for commercial plant construction. The HTTR cogeneration demonstration program has following objectives:

- Obtain first-of-a-kind license for nuclear-heated helium gas turbine power and hydrogen cogeneration plant.
- Demonstrate unique system economical and reliable operation as a prerequisite for construction of the commercial plant.

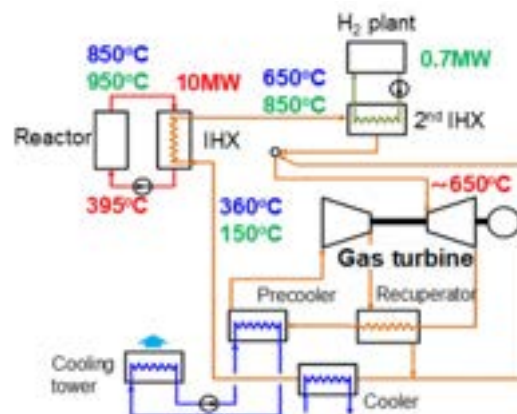
A comparison of system layouts between the commercial HTGR plant, GTHTR300C, and the HTTR gas turbine cogeneration test plant (HTTR-GT/H₂ plant) [15] is shown in Figure 8. The GTHTR300C employs direct cycle gas turbine system and installs an intermediate

heat exchanger (IHX) between the reactor and the gas turbine to provide heat to a hydrogen production plant in a secondary helium cooling system. On the other hand, it is not practical for the HTTR-GT/H₂ plant to device a heat application system in the same manner as the commercial plant because it requires extensive modification in the nuclear facility including the penetration of primary piping through the containment vessel. Instead, the helium gas turbine and a second IHX are installed in cascade in the secondary system whereas the hydrogen production plant is located in the tertiary loop. Such configuration enables to demonstrate the series operation of hydrogen production plant and helium gas turbine in the GTHTR300C.

Figure 8. Comparison of system layout between (a)GTHTR300C and (b)HTTR-GT/H₂ plant



(a) HTTR-GT/H₂ plant



We have been conducting system and component design for the HTTR-GT/H₂ plant since 2015. As a result, we have completed pre-licensing of the basic design with a power output of 1 MW and a hydrogen production rate of 30 Nm³/h. We expect the completion of the project in the middle of 2030s. The project begins with connecting the helium gas turbine to the HTTR and expands by adding the hydrogen production plant to enable cogeneration.

Toward the realisation of the HTTR demonstration test, it is important to share program goals and construction cost with foreign entities utilising international collaboration. A further direction of study is to investigate a detailed test plan with countries interested in a joint demonstration program.

III. Summary

JAEA joins the research projects for the VHTR system in the GIF. To develop VHTR system, JAEA has been conducting research and development under the HTTR project. The project aims to establish both HTGR technology

and heat application technology. As for the reactor technology, upgrading of fuel performance, development of SiC coated oxidation-resistant graphite, establishment of international safety standards, etc. are under way. The HTTR is preparing for the restart to obtain the license following the new regulation standard. The restart is expected in FY2019.

As for the heat application technology, IS-process hydrogen production test facility successfully achieved 31 hours continuous hydrogen production. JAEA is planning a demonstration of heat application technologies on the HTTR, a Brayton-cycle helium gas turbine and an IS-process hydrogen cogenerating plant.

Acknowledgements

The authors would like to express their thanks to D. S. Kasahara for the contribution to the hydrogen production project in GIF VHTR system and to Dr. H. Ohashi for the provision of information about the international safety standard.

References

- [1] OECD Nuclear Energy Agency, Technology Roadmap update for Generation IV Nuclear Energy Systems, January 2014.
- [2] K. Sawa, T. Tobita, H. Mogi, et al., Fabrication of the First-Loading Fuel of the High Temperature Engineering Test Reactor, *J. Nucl. Sci. Technol.* 36 (8), 683-690 (1999).
- [3] S. Ueta, T. Izumiya, et al., Database of fabrication characteristics of the second-loading-fuel for the High Temperature Engineering Test Reactor, 1; Fuel kernels, coated fuel particles and fuel compacts, JAEA-Data/Code 2006-009, Japan Atomic Energy Agency (2006) [written in Japanese].
- [4] S.Ueta, J. Aihara, N. Sakaba, et al., Fuel performance under continuous high-temperature operation of the HTTR, *J. Nucl. Sci. Technol.* 51(11-12) 1345-1354 (2014).
- [5] S. Ueta, J. Aihara, A. Yasuda, et al., Fabrication of uniform ZrC coating layer for the coated fuel particle of the very high temperature reactor, *J. Nucl. Mater.* 376 (2), 146-151 (2008).
- [6] T. Shibata, J. Sumita, N. Sakaba, T. Osaki, H. Kato, S. Izawa, T. Muto, S. Gizatulina, A. Shaimerdenov, D. Dyussambayev, P. Chakrov, Irradiation test about oxidation-resistant graphite in WWR-K Research Reactor, Proc. HTR 2016, 6-10 Nov. 2016.
- [7] A. Terada, J. Iwatsuki, S. Ishikura, H. Noguchi, S. Kubo, H. Okuda, S. Kasahara, N. Tanaka, H. Ota, K. Onuki, R. Hino, Development of Hydrogen Production Technology by Thermochemical Water splitting IS Process, *J. Nucl. Sci. Technol.*, v44, 3, p.477, 2007.
- [8] S. Kubo, N. Tanaka, J. Iwatsuki, S. Kasahara, Y. Imai, H. Noguchi and K. Onuki, R&D Status on Thermochemical IS Process for Hydrogen Production at JAEA, *Energy Procedia*, v29, p.308 2012.
- [9] S. Kubo, H. Nakajima, S. Kasahara, S. Higashi, T. Masaki, H. Abe, A demonstration study on a closed-cycle hydrogen production by the thermochemical water-splitting

- iodinesulfur process, Nuclear Engineering and Design, v233, p.47, 2004.
- [10] S. Kasahara, N. Tanaka, H. Noguchi, J. Iwatsuki, H. Takegami, S. Kubo, JAEA's R&D on the Thermochemical Hydrogen Production IS Process, Paper HTR2014-21233, Proc. HTR 2014, Weihai, China, 27-31 Oct. 2014.
- [11] S. Kubo, N. Tanaka, H. Noguchi, J. Iwatsuki, S. Kasahara, Y. Imai, K. Onuki, R&D progress in thermochemical water-splitting iodine-sulfur process at JAEA, Paper HTR2012-2-005, Proc. HTR 2012, Tokyo, Japan, 28 Oct. - 1 Nov. 2012.
- [12] H. Noguchi, S. Kubo, J. Iwatsuki, S. Kasahara, N. Tanaka, Y. Imai, A. Terada, H. Takegami, Y. Kamiji, K. Onuki, Y. Inagaki, Components for Sulfuric Acid Processing in the IS process, Nuclear Engineering and Design, v271, p.201, 2014.
- [13] N. Tanaka, H. Takegami, H. Noguchi, Y. Kamiji, J. Iwatsuki, H. Aita, S. Kasahara, S. Kubo, IS process hydrogen production test for components and system made of industrial structural material, 1; Bunsen and HI concentration section, p.1022, Proc. HTR 2016, 6-10 Nov. 2016.
- [14] H. Noguchi, H. Takegami, Y. Kamiji, N. Tanaka, J. Iwatsuki, S. Kasahara, S. Kubo, IS process hydrogen production test for components and system made of industrial structural material, 2; H₂SO₄ decomposition, HI Distillation, and HI Decomposition Section, p.1029, Proc. HTR 2016, 6-10 Nov. 2016.
- [15] X. L. Yan, et al., Design of HTTR-GT/H₂ test plant, Nuclear Engineering and Design, 329, 223-233 (2018).

STATUS OF CURRENT KNOWLEDGE AND DEVELOPMENTS IN FRANCE ON MOLTEN SALT REACTORS (J. GUIDEZ ET AL)

J. Guidez et al.

CEA, Direction de l'Energie Nucléaire, Saclay, France.

Abstract

The present presentation is focused on a brief state of art on Molten Salt Reactors around the world with a focus on the French developments in 2018.

Many reactor concepts using molten salts are currently being studied around the world. Some of these concepts simply use molten salt as coolant, but keep a solid fuel. These concepts are not currently studied in France. Similarly, a large number of projects using a liquid fuel salt are thermal reactor concepts. The current research in France is not focused on such concepts because the need is to close the fuel cycle, using the products obtained and available after reprocessing, as Plutonium and Uranium, while minimising the waste production. The studies carried out in France therefore focus on fast reactors allowing both to use these products as fuel and to minimise the final production of waste and its radiotoxicity. Such reactors also make possible to develop nuclear power using thorium, or other actinides, and calculations performed on the subject will be presented.

This search for a fast reactor leads to a reactor design without solid moderator as graphite, where criticality is reached in the core area and where the thermal energy produced is then removed by a secondary molten salt circuit, to conventional electricity production or a calogenic use.

This concept of fast reactor presents some important advantages such as much lower reprocessing needs, significant incineration possibilities, minimisation of final waste, strong negative temperature coefficient ... but also some challenges such as the development and qualification of materials subjected to high irradiation levels, or the final choice of salt between the two chlorides and fluorides families. Each of these families has advantages and disadvantages that will be discussed.

Finally, the potential benefits of this type of liquid fuel reactor are recalled as well as the remaining open issues for which developments would be required.

Introduction

Molten Salt Reactors (with fuel dissolved in molten salt) were studied in the USA in the 1960s and a large REX is available on the operation of the ARE and MSRE reactors. (Ref 1,2,3 and 4). All necessary documentation can be found in ref 5.

This paper is a reminder of recent developments on the subject in the world, and on the main technical choices made today on the projects under study in France.

This paper does not talk about fuel reprocessing and therefore the corresponding technical choices. These choices would require another paper on this very complex subject. So we are talking, in this paper, only about technical choices at the level of the reactor itself.

National Programs in the World in 2018

China

It is the country with the largest and most structured program.

All means have been allocated to a research center, SINAP located in Shanghai, which must develop the whole concept in all its forms: research on the concept, codes, materials, technology, reprocessing, etc. It is estimated that about 1000 people work in this center, with operational molten salt loops, technological research and the announcement of a small prototype.

As usual, China is part of the acquis that is to say on the initial basis of the concept MSRE, and with the same initial options, namely a thermal reactor, fluoride salts, with moderator graphite.

Russia

In Russia, a small team is working at the Kurchatov Institute on the 1000 MWe reactor MOSART project. Here too, research is carried out around the concept in different fields. On the materials, research is continuing to obtain materials supporting corrosion without higher temperatures. In the field of reprocessing, research is also continuing. Finally, valuable baseline studies have been performed on the dissolution values of different products in salts.

The MOSART concept is more innovative: it is a fast reactor with fluoride salts, aiming to use the available waste (U/Pu/Actinides) while integrating the possibilities of thorium.

Some provisions are specific as the use, at the heart level, of a graphite wall to play a role of neutron reflectors and protectors of the wall to increase the service life.

India

A smaller national program exists. It is a fast reactor, with fluoride salts, and valorising thorium. So consistent with the national strategy of closing the cycle and using thorium.

Start-up Projects

In the Anglo-Saxon and European world, many start-up companies are now proposing reactor concepts using molten salts, of which here is a list that is not necessarily exhaustive! Note that some projects use molten salt only as coolant and continue to use a solid fuel. They are therefore not concerned by this paper (for example: MOLTEX which combines a heat transfer salt with a fuel that becomes liquid in operation, inside pencils assembled in square assemblies).

Among the liquid fuel reactor projects, we find:

- Integral Molten Salt Reactor 400 (Terrestrial Energy, Canada) thermal,
- Molten Fast Chloride Salt Fast Reactor (Terrapower and co, USA),
- Transatomic Power Reactor (Transatomic + MIT, USA) thermal,
- ThorCon (Martingale, USA) thermal,
- Liquid Fluoride Thorium Reactor (Flibe Energy, USA) thermal,
- Molten Chloride Fast Reactor (Elysium Industries, USA) fast,
- Seaborg Waste Burner (Seaborg Technologies, Denmark) thermal,
- Copenhagen Atomic Waste Burner (Copenhagen Atomics, Denmark) thermal,
- Thorenco Process Heat Reactor, etc.

These start-ups often have relatively small means, make little basic developments, benefit from state aids (eg the DOE GAIN program) and also operate on the principle of filing patents or a license for them to be marketable. However, the number of developing projects shows the dynamism of R & D on MSR, and illustrates the interests of the industry in breaking with the use of solid fuel. Among those developing a liquid fuel concept, the best known are discussed below.

Terrestrial energy's ISRM 400 in Canada

This project is a 400 MWt thermal reactor based on fluoride and using graphite. It is a concept with passive capacities for the evacuation of residual power, burning of uranium (LEU). The developed concept is passive (natural convection) and is directly inspired by the MSRE, which it wants to be a direct extension. They announce USD 17.2 million in funding and a pre-licensing review underway in Canada.

The Terra power molten chloride fast reactor.

Terra Power presents a prototype reactor of 30MWt, fast but with chloride salts. This reactor has been studied with both cycles Regenerators: U / Pu and Th / U. In 2016, Terrapower would have received USD 40 million from DOE for this project.

The molten chloride salt fast reactor (MCSFR) from Elysium industry

This 1000 MWe reactor aims at a closed fuel cycle by using spent fuel. He therefore chose a fast spectrum and a chloride salt.

The transatomic power reactor (MIT project)

This project takes the line of the MSRE (thermal reactor) but trying to replace the graphite with zirconium hydride.

Thorcon de martingale

There we are still in a thermal project close to the MSRE, but in a form of modular concepts.

Liquid Fluorid thorium reactor by Flibe energy

Still a thermal concept close to the MSRE, but more focused on the use of thorium.

Analysis of the Different Concepts

First of all, we notice a great variety in the technical choices offered, which shows the current lack of a consensus solution but also shows the versatility of the concept. There are many thermal generating concepts that are often similar to MSRE, with a moderator (often graphite), and many fast concepts that have all the potential benefits of rapids, especially for cycle closures. For the choice of salts, fluorides are often retained, but chlorides which also have certain advantages, are not definitively excluded. For the choice of fuel, the U / Pu cycle is often found, the use of spent fuel, but the possibilities of the thorium cycle are often presented in addition as well as the possibilities of incineration of actinide type waste (for example the reactor developed by Terra Power). The reprocessing of the liquid fuel, when provided, is presented either online or in batch. Some projects have modular versions (cost savings on the mass production of modules). In fact, it is the choice of objectives which determines certain basic technical choices, in particular between the thermal spectrum or fast: if the objectives are favoring the closing of the cycle, it leads always to the choice of a fast spectrum.

And in France ?

The national objective is the closure of the cycle and the minimisation of waste

In this context, previous studies were carried out at two periods of time by the CEA and EDF:

- from 1970 to 1983, design studies around the MSBR reactor;

- in 2000, CEA and EDF focused on RSF with the primary objective of incinerating Pu and / or minor actinides (TASSE concept at CEA, AMSTER concept at EDF(ref 6)), before highlighting breeder concepts: a breeder AMSTER version in thermal spectrum and thorium cycle, and the REBUS fast breeder REBUS concept, U / Pu cycle and chloride salt.

Since then, there have not been a lot of test loops. One, conducted at EDF, was a facility to study the corrosion of nickel-based alloys in fluoride. And an inactive molten salt test loop was built and used at the CNRS / LPSC in Grenoble for technological research. (ref 7, 8, 9).

More recently, the CNRS (LPSC - Grenoble) has carried out studies on a fast-spectrum MSR fluoride salt MSR project: The MSFR is designed to close the cycle using the "waste" produced by the current nuclear industry (U and Pu) and to incinerate actinides. Numerous calculations have been also made with the thorium cycle.(ref 10, 11, 12, 13 , 14)

This type of reactor is potentially capable of transforming all our waste (depleted U, reprocessing U, Thorium, Pu, or even later actinides) into energy production; so to close the cycle and minimise our final waste. The chosen power is 3 GWt. The consolidation of the MSFR project is important, which is why this "paper reactor" served as a reference for the European EVOL and then SAMOFAR studies. And a new European project dedicated to the safety analysis of the MSFR is currently in preparation (SAMOSAFER). The documentation on the MSFR can be found in ref 15.

Main Technical Choices of MSFR

Choice of the salt

The main constraints are that the salts must not be activated, have a good resistance under irradiation, be transparent to neutrons, have a good chemical stability at high temperature (> 1300°C), not produce radioelements that are difficult to manage, have a low vapor pressure, have good thermal characteristics (conductivity and capacity), have good thermohydraulic properties, be able to solubilise fissile and fertile materials (uranium, plutonium, thorium), and facilitate reprocessing and redox control.

Two major families of salts can be used: chlorides and fluorides. It is usually the fluorides that are proposed in the different projects (as on the MSRE) but some concepts

like that of Terrapower (USA) use chlorides. These chlorides have certain advantages that may explain this choice:

- A melting temperature for some eutectics (around 400/500°C) lower than that of fluorides,
- A better solubility of Pu and fission products depending on the salt retained (eg the NaCl-UCl₃ binary).

Nevertheless, chlorides have drawbacks that limit the above advantages:

- A significant production of chlorine 36. This isotope is particularly troublesome. It has a period of 300 000 years and is very difficult to manage and store.
- A harder spectrum, which may have some neutron advantages for a quick release, but which is inconvenient for holding materials close to the active zone (axial reflector, fertile covers).
- For the reprocessing, the UCl_n and PuCl_n compounds are much less volatile (and therefore less recoverable by this process) than the fluorinated compounds.
- A hygroscopic character (water absorption) much more pronounced than for fluorides and aggressive corrosion by pitting.
- Soluble in water : in case of contact, possibility of entrainment of the elements present in the salt.
- A larger "migration area" which leads to a neutron leak requiring either a bigger heart or the placement of reflectors.

Most projects therefore propose fluorides for which we already have a first REX on the MSRE, which have good behavior under irradiation, whose neutron properties are good and whose melting temperatures remain correct if the eutectic is well chosen. (ref 16, 17) They also simplify certain phases of reprocessing thanks to the volatility of UF₆.

On the other hand, they have certain disadvantages:

- The temperatures of use are higher (rather between 600 and 700°C),
- The Li⁶ is generator of tritium²,
- The Li⁶ is also a neutron poison,

- If the PuF₅ is also very volatile, its fluorination is more difficult to achieve (but it is feasible).

In practice, the enrichment of Li⁷ is necessary (typically 99.995%) in order to be critical and to limit the production of tritium (NB: EDF already uses Li⁷-enriched lithium industrially to manage the PH of water). This being done, there is a wide range of possible fluorides: the mixture LiF and BeF₂ (FliBe) was used on the MSRE. But KF, NaF are also possible.

As part of the MSFR, and after choice of fluorides, it has been proposed: LiF-ThF₄-UF₄-(TRU) F₃, that is to say a LiF-based salt (with about 22 mol% heavy nuclei). For a U / Pu cycle, LiF-UF₄-PuF₃ can be used with approximately 22 mol% of heavy nuclei.

Following elements were avoided as a secondary component of the fuel salt, in the MSFR project :

- BeF₂ because Beryllium and its compounds are toxic. It has the property of lowering the melting temperature and increasing the thermalisation of neutrons.
- KF because it is difficult to dehydrate and it can lead to the formation of K gas during high temperature reductions.
- + NaF because it does not bring much net benefit in terms of melting temperature (it lowers the temperature of 50°C) or solubility, and is less chemically stable than LiF.
- ZrF₄ decreases strongly melting temperature and captures oxygen before actinides, but it lowers the solubility of Pu, and its extraction is necessary because its concentration increases (it is one of the main FP).
- The RbF is very transparent to neutrons and lowers the melting temperature, but it may be problematic during reprocessing using any chemical reduction process.

In conclusion, LiF is the final product retained by the project as a salt base for the MSFR project. The melting temperature of the mixture with the heavy cores is 585°C. LiF has the advantage of being a mono-constituent base for the fuel salt thus formed, which simplifies the reprocessing of the fuel salt. On the other hand, lithium 7 enrichment is necessary to minimise the production of tritium and to reach criticality (the lithium 6 being a neutron poison).

NB: The solubility of PuF₃ in alkaline fluoride-based salts is high in the absence of 4-valent constituents (such as UF₄), but it drops very strongly for valence 4 concentrations of about 22 mol% which correspond to more often at the lowest melting points of the mixtures. When the valencies of U and Pu are the same, the solubility of Pu is very strong. Its solubility is very low in the salts containing BeF₂.

Choice of materials

Following the initial setbacks with Inconel on the ARE, the MSRE project had developed a new material based on nickel and molybdenum: the Hastelloy-N which will be used for the tank and exchangers and for which therefore has an operating REX. This REX has shown that, subject to control of the redox potential, corrosion was limited at 650°C to about 2.5 microns / year. In fact, pure salt would not be the corrosive agent but pollutants (water, residual oxides, and PF) dissolved in it. The REX of the MSRE thus identified a beginning of corrosion by tellurium. The metallic Te forms with the Cr of the alloy an intermetallic compound which concentrates at the grain boundaries and weakens the alloy. To avoid this phenomenon, it suffices to reduce the metallic Te to telluride ions Te²⁻ which is soluble in the salt. This reduction is ensured by the presence of a U⁴⁺ + / U³⁺ + chemical buffer. This buffer maintains the chemical potential of the salt in a range where corrosion is very limited. Moreover, the fission reactions have an oxidising character. Indeed, when the fissions make disappear a U⁴⁺ ion to replace it by a set of fission products whose average load is close to 3+, the medium becomes more oxidising thus requiring the control of the redox potential in order to avoid corrosion. It is thus seen that subject to a control of the redox potential, one can hope to be able to limit these corrosion problems.

It should also be noted that the Hastelloy-N was certified at that time (pressurised and nuclear enclosure) for operation up to 704°C. However, and in addition to corrosion, a material under fast spectrum will be subjected to a strong irradiation in dpa and a production of helium (reaction n, α on the Ni) which will weaken it. These effects are poorly known, even though high temperatures could allow diffusion defects to heal and eliminate helium.

Other degradation factors are creep and cyclic fatigue due to temperature fluctuations (shutdown and restart phases) and free level.

For these reasons, the use of materials that would be even more efficient is studied: new alloys still based on nickel (EM 819 Aubert and Duval), with Molybdenum and / or Tungsten. The company Aubert and Duval had produced the EM721 and EM722, and the Russians tested the EM721 provided. But none of these new materials are available and validated. (ref 18 and 19)

Concerning the protective materials of the tank, graphite poses problems of change of volume according to the temperature and the received fluency. Its use is therefore simpler in heat flow than in fast flow. However, it was retained by the Russian on the fast project MOSART to protect the material of the tank. Its life is also limited (Terrestrial Energy in its thermal version, announces a duration of 7 years). Note also that the management of irradiated graphite remains problematic. For all these reasons, it has been excluded from the design of the MSFR.

Finally, SiC is another interesting material (ceramic type), both for the thermal protection of the walls directly in contact with the combustible salt (axial reflector and fertile cover) and to make the exchangers. It has a good mechanical strength up to 2000°C, a good resistance to corrosion if it is quite pure, and a good resistance to irradiation. On the other hand, it poses certain industrial problems (mode of assembly, connection with metals, etc.) and presents at these temperatures the risk of rupture of the "fragile" type (propagation of the crack in case of rupture, even if the material is otherwise very solid). It should be noted that the use of SiC-SiC-fiber composites makes it possible to eliminate this "fragile" type of fracture appearance. Finally, its thermal conductivity is much greater than that of steels (about a factor of 5).

If we compare to the available materials, we arrive at the following assessment: In conclusion, research is in progress on promising materials, but today the only material available and validated still seems the Hastelloy-N used on the MSRE (and of his Chinese counterpart the GH3535). Its use on a new reactor would require either a decrease in power density to reach lower operating temperatures and closer to its validation area, an extension of its certification area of + 50°C (which involves testing to achieve). It is also possible to envisage a thermal protection material at the level of the walls of the heart. Finally, the effects of irradiation during a long time also remain to be validated.

Salt chemistry

If LiF is retained as a fuel salt for MSFR, after fluorination of U, Pu (or even Th), the products are dissolved in LiF for starting the reactor. A large number of products will then be created by nuclear reactions during operation. Tables giving the solubility in LiF of the main products concerned exist, in particular published by the Kurchatov Institute and JRC Karlsruhe. However, it is necessary to be able to monitor in time the actual chemical composition of the combustible fluid. In addition, the rise in concentration of certain fission products (such as Lanthanides or zirconium) will make them reach their solubility limit and lead to the risk of deposition (possibly co-deposition with PuF₃). This is one of the points that require the reprocessing of the combustible salt for their extraction. (ref 20) From the point of view of safety, it will certainly be necessary to have in the fuel circuit a line sample, with continuous circulation (for example on a cold trap, of the type of online purifications of the RNR-Na). If this system works for MSR, it should make it possible both to be sure of where the products will be deposited and to be able to extract and process them (either for recycling or as waste). It should be noted that the operating temperature adopted for the cold trap would then be the temperature to be taken into account for the initial solubilisation and that the validation of this innovative concept remains to be done. Finally, the risks associated with selective solidification of particular isotopes will have to be studied, as well as the reheating procedures for melting and returning the salt to the fuel circuit during operation.

In conclusion, the operation of a reactor will lead to the creation of many products in the fuel salt, which must be managed to prevent inadvertent deposition.

Insoluble fission products

Neutron reactions lead to the continuous formation of insoluble fission products. Some are metallic and could lead to untimely depositions, especially in exchangers. Others are gaseous (Kr, Xe) and will naturally go back to free levels. It is preferable that they be extracted and processed continuously. On the MSRE, this extraction of PF gases was by bubbling with a neutral gas (generally helium or argon, or Kr / Xe recycled). (ref 1 , 2)Once this extraction is carried out, it would be possible to make selective separations to be defined according to the gases produced. These separations are fairly standard provisions on all

reactors (PWR, RNR-Na, ...) but which, as for all sectors, need to be defined, depending on the products to be separated, up to the final waste management mode. This management can range from simple rejection (inactive gas with a low krypton type period), to storage in decay tanks for short-lived products, and to definitive storage for other products (activated carbon, etc.). On the MSRE, the imperviousness at the shaft of the primary mechanical pump was ensured by a continuous injection of helium. It is this helium that caused the fission gases to their final treatment. In the REX MSRE some filter clogging and the strong influence of gas entrainment variations on the reactivity of the core, this because of the thermal spectrum since the gas contains absorbent PF (nonexistent effect in fast spectrum).

Choice of the intermediate fluid

An intermediate fluid is necessary to evacuate the heat of the intermediate exchangers, to the energy conversion circuit (in water or gas).

This fluid must have the following characteristics:

- Be liquid at operating temperatures with the necessary margins for solidification and vaporisation,
- Support significant irradiation levels without activating. The activation data must also be confirmed (if there is radiolysis or creation of radioisotopes by activation the management of the intermediate fluid circuit is made more complex),
- Do not be corrosive with regard to the materials used, in particular, the material of the intermediate heat exchanger which must support the combustible and intermediate fluids,
- Do not cause significant disturbances in case of fuel leakage,
- Be able to manage the consequences of a water leak in the intermediate circuit, in the case a water / steam energy conversion system (detection and mitigation). The detection of a water vapor entry and consequence management remains a delicate point, and it is to be specified.

For all these reasons, but also of chemical neutrality, it is also a liquid salt which is generally used as an intermediate fluid. Usually, a mixture of fluorides is proposed because they

meet the needs (LiF-NaF-BeF₂, LiF-NaF-ZrF₄, LiF-NaF-BF₃, LiF-NaF-KF). Studies done on the MSBR had proposed sodium fluoro borate (NaBF₄ with 8% NaF) which has the advantage of not being activated and capturing tritium.

Note also that this assessment does not close the door in search of a fluid, even other than a salt, which would respond even better to all the criteria.

Neutronics

The initial studies focused on comparisons between thermal, epithermal and fast spectra. Very quickly, the choice fell on a fast spectrum that better meets the needs of the French industry, and has many advantages:

- Very negative feedback coefficients (advantages from the point of view of safety and reactor management);
- Better fission / transmutation capacity (advantages from the point of view of incineration of waste);
- Absence of graphite whose lifetime would be limited and which today constitutes a waste without an outlet.

The design of the MSFR foresees a central zone of the tank where, due to the critical geometry, the chain reaction with heat generation takes place. The combustible fluid heats up and then continues its course to cool in the exchangers (where geometry is no longer critical). At the outlet of the exchangers, the salt returns to the central zone. The complete circuit is composed of independent sectors immersed in the tank: the salt never leaves the tank.

A first peculiarity of the concept is the absence of control bars. Indeed, the very high coefficients of thermal counter-reaction and the absence of thermal inertia (unlike a solid fuel) make it possible to control the power by the thermal with a very great speed of response. The control is then performed by cooling the intermediate fluid. A priori, there would be no need for control rods (if we must put one it is necessary to define its usefulness with respect to the risk in case of malfunction). Note that the shutdown situation of this reactor is similar to a zero power model reactor: the salt inlet temperature corresponds to its outlet temperature: no power is drawn from the fuel salt which remains hot. Note also that drain the fuel salt (in a subcritical geometry) by emptying the tank is also possible.

Another point is the need for calculations with Neutronic / Thermohydraulic coupling to simulate the nominal state. (ref 21) Indeed, it is the high expansion of the salt that induces the counter-reaction coefficients for controlling the reactor. Current calculations have already taken into account this coupling and it has also been validated experimentally on all reactors and liquid fuel experiments. This specificity of liquid fuel is one of the fundamental points of the interest of the concept. Finally, some of the delayed neutrons (necessary for the overall neutron stability) are entrained in the combustible fluid leaving the central zone to circulate in the exchangers. This point specific to the MSR is of course to be taken into account in the calculations since it decreases the effective beta. It should be noted, however, that this reduction in the effective beta increases the speed of the counter reactions and thus increases the stability of the reactor.

Several very interesting points emerge from the calculations already carried out:

- Efficiency in a reduced volume: we arrive for the MSFR (1400 MWe) at 18 m³ with 330 W/cm³ with an initial inventory of 3.5 t/GWe⁴. It should be noted, however, that our Russian and American colleagues have chosen a lower power density. Indeed, the high power density makes of course the attractive concept in terms of compactness and use of the material (and therefore capacity of deployment of a sector) but introduces more constraints on the capacity of the exchangers to evacuate the power. It should be noted that the power density for MOSART is at least one third of the value of the MSFR. The level of this power density is a design choice.
- A high efficiency of waste combustion.
- A very big advantage of the fast spectrum vis-à-vis a thermal spectrum is the ability to operate without being poisoned by PF (low reserve of reactivity required).
- The possibility of fissioning all actinides (for example: americium) since they are preserved in the heart.
- The fast spectrum leads to much smaller reprocessing needs (between 10 and 40 liters per day). However it should be noted that Zirconium is a neutron poison and that its production can cause

difficulties after a few years. It will therefore be necessary to find a way to extract it (for the moment this extraction process is not yet available).

Moreover, the design is based on the choice of the specific power which conditions the capacity of the exchangers to extract the heat produced. This remains the same regardless of the nominal power required for the reactor. In short, a reactor with a volume twice as small has a nominal power half as much (there are half as many exchangers).

Finally, an interesting point for all MSR, is that a neutron excursion does not result in the melting of a solid core and its interaction with the cooling fluid, but by a simple expansion of the fluid. The central zone of the heart causing the increase of the neutron leak and thus the decrease of the reactivity. Therefore, and with certain reservations (existence of a free surface, etc.), the potential release of mechanical energy is much lower (or almost zero) which is an advantage in terms of safety analysis and acceptability of the reactor.(ref 22, 23)

MSFR Potential for the Fuel Cycle

A fast MSR can operate with a wide variety of fuels: natural or depleted or enriched U, thorium, Pu, actinides, etc. The only constraint is that this mixture of fissile, fertile, even waste, must allow to reach the criticality to guarantee the functioning. This flexibility is a huge asset since it allows mixing all types of isotopes in the fuel salt. In the case of the U / Pu cycle, it is the Pu that will be the preferred fissile element because already available in large quantities; likewise depleted or reprocessed uranium serves as a fertile element.

This U / Pu cycle has the following advantages:

- It is the best-known regeneration cycle,
- France already has operational skills and industrial equipment,
- France has almost 300 000 tons of depleted uranium (without counting the reprocessed uranium),
- If thorium (fertile element) is introduced, the production of U233 makes it possible to dispose of a complementary fissile element little by little. Note, however, that the solubility of Pu in a combustible salt with Thorium is lower.

The U / Pu cycle is therefore the one that seems to have the highest priority for MSR in the

French context. Note, however, that the thorium cycle has several long-term interests(ref 10, 11, 12):

- Thorium is available (around 10,000 tons in France),
- The Th / U cycle is one of only two regeneration cycles available,
- Thorium is produced of the U233 which is an excellent fissile.

The fertile elements currently available in France are uranium (natural or enriched or depleted or reprocessing) and thorium. But minor actinides are also candidates for incineration in an MSR. Indeed, during the salt reprocessing phase in the reactor unit simply put they back into the heart (with Pu and U). Note that it is possible to start a reactor with various mixtures of fissile depending on availability, which makes the concept very flexible depending on the conditions of the moment. Similarly, the power supply during operation has the same flexibility, the main thing being to maintain criticality. For example: in the deliverable EVOL (European project), the starting composition comprises 77.5% of LiF, 6.6% of ThF₄, 12.3% of UF₄ containing enriched uranium at 13% and 3%, 6% transuranians (TRUF3: UO_x irradiated at 60 GWd / t, cooled 5 years). The big advantage over solid fuel reactors is avoiding long and expensive cycles, from manufacturing / storage / use / decay / reprocessing / re-manufacturing / transport / etc.

Let us also note that if we do not seek the regeneration, it is enough not to put a fertile element and we then have a reactor of type "burner" whose only function will be the consumption of fissile isotopes in the spectrum fast.

Conclusion

This paper does not deal with the problems of reprocessing the molten fuel, which is necessary for the overall operation of the reactor. It allows locating, in relation to all the projects develop in the world, the studies carried out in France and the main technical choices currently retained at the level of the reactor himself.

The short-term priorities for research and development seem today to be in this context:

- Zirconium extraction process: it is necessary but there is currently no identified process,
- Development of processes and reprocessing steps online,
- Technical study of a cold trap,
- Development of operating and instrumentation devices for the reactor,
- Study of the corrosion of materials,
- Study of the effects due to irradiation over extended periods,
- Development of components (pumps, exchangers, etc.),
- Study of the natural convection operation of the fuel circuit in all the possible operating conditions (normal, starting, stopping, incident, etc.).
- Economic prospective study (allowing to have more elements on the impact of the specific characteristics of MSR and design options).

References

- [1] Experience with the molten salt reactor experiment - P.H.Haubenreich, J.R.Engel - Nuclear applications & Technology, vol.8, February 1970.
- [2] ORNL/ER-341. Program management plan for the Molten Salt Reactor Experiment remediation project at Oak ridge National Laboratory.
- [3] STJ-02MSRE-D992 - Molten Salt Reactor Experiment Engineering Evaluation and Extended Life Study, URS | CH2M Oak Ridge LLC, Oak Ridge, Tennessee.
- [4] DOE/OR/01-2496&D1 - Engineering Evaluation of Options for Molten Salt Reactor Experiment Defueled Coolant Salts, Oak Ridge, Tennessee.
- [5] Documentation MSRE (Oak Ridge): <http://energyfromthorium.com/pdf/>.
- [6] David LECARPENTIER, "Le concept AMSTER, aspects physiques et sûreté", EDF and CNAM, Paris, France (2001).
- [7] P. Rubiolo, M. Tano Retamales, V. Ghetta and J. Giraud, J. Blanco, O. Doche, N. Capellan, "Design of close and open channel experiments to study molten salt flows", 2018 International Congress on Advances in Nuclear Power Plants (ICAPP 18).
- [8] Pablo Rubiolo, Mauricio Tanoa, Julien Giraudb, Véronique Ghettab, Juan Blancoa, Olivier Dochea, Nicolas Capellana « Design of close and open channel experiments to study molten salt flows LPSC, Univ. Grenoble Alpes, Grenoble INP, 53 rue des Martyrs, F-38026 Grenoble, France.
- [9] J. Giraud, V. Ghetta, P. Rubiolo, M. Tano-Retamales, "Development and Test of a Cold Plug Valve with Fluoride Salt", 12th International Topical Meeting on Reactor Thermal-Hydraulics, Operation, and Safety (NUTHOS-12) will take place in Qingdao City, Shandong Province, China, on October 14-18, 2018.
- [10] Davide RODRIGUES, "Solvatation du thorium par les fluorures en milieu sel fondu à haute température : application au procédé d'extraction réductrice pour le concept MSFR", PhD Thesis, Paris Sud University (2015).
- [11] Elsa MERLE-LUCOTTE, "Le cycle Thorium en réacteurs à sels fondus peut-il être une solution au problème énergétique du XXIème siècle ? Le concept de TMSR-NM", Habilitation à Diriger les Recherches, Grenoble INP, France (2008).
- [12] Ludovic MATHIEU, "Cycle Thorium et Réacteurs à Sel Fondu: Exploration du champ des Paramètres et des Contraintes définissant le Thorium Molten Salt Reactor", PhD Thesis, Grenoble Institute of Technology and EDF, France (2005).
- [13] Alexis NUTTIN, "Potentialités du concept de réactEUR à sels fondus pour une production durable d'énergie nucléaire basée sur le cycle thorium en spectre épithermique", PhD Thesis, Grenoble I University and EDF, France (2002).

- [14] P.R. Rubiolo, M. Tano Retamales, V. Ghetta and J. Giraud, "High temperature thermal hydraulics modeling of a molten salt: application to a molten salt fast reactor (MSFR)", ESAIM: Proceedings and surveys, 58, p. 98-117 (2017).
- [15] Documentation sur le MSFR : <http://lpsc.in2p3.fr/index.php/fr/groupe-de-physique/enjeux-societaux/msfr/rsf-reacteurs-a-sels-fondus/lang-fr-msfr-bibliographie-lang-lang-en-msfr-bibliography-lang>.
- [16] Molten salt reactor chemistry – W.R.Grimes – Nuclear Applications & technology, vol.8, February 1970.
- [17] Assessment of properties of candidate liquid salt coolants for the AHTR – D.F.Williams, L.M.Toth, K.T.Clarno, C.W.Forsberg – ORNL/GEN4/LTR-05-001, June 30 2005.
- [18] Thèse de R. Cury : "Etude métallurgique des alliages Ni-W et Ni-W-CR : relation entre ordre à courte distance et durcissement", université paris XII – 2007.
- [19] Thèse de Stéphanie Fabre le 25 septembre 2009 à l'université de Toulouse - Titre : « Comportement de métaux et alliages en milieux fluorures fondus ».
- [20] Jorgen FINNE, "Chimie des mélanges de sels fondus - Application à l'extraction réductrice d'actinides et de lanthanides par un métal liquide", PhD Thesis, EDF-CEA-ENSCP, Paris, France (2005).
- [21] Axel LAUREAU, "Développement de modèles neutroniques pour le couplage thermohydraulique du MSFR et le calcul de paramètres cinétiques effectifs", PhD Thesis, Grenoble Alpes University, France (2015).
- [22] Thèse de Delphine Gérardin – « développement d'outils numériques et réalisation d'études pour le pilotage et la sûreté du réacteur à sels fondus MSFR », Université Grenoble-Alpes – 2017.
- [23] Mariya BROVCHENKO, "Etudes préliminaires de sûreté du réacteur à sels fondus MSFR", PhD Thesis, Grenoble Institute of Technology, France (2013).

STRATEGY AND R&D STATUS OF CHINA LEAD-BASED REACTOR (Y. WU)

Yican Wu

Key Laboratory of Neutronics and Radiation Safety, Institute of Nuclear Energy Safety Technology, China.

Abstract

Lead-based reactor is one of the most promising nuclear energy systems for Generation-IV reactor and Accelerator Driven subcritical System (ADS). Institute of Nuclear Energy Safety Technology, Chinese Academy of Sciences (INEST/FDS Team) placed more emphases on China LEAd-based Reactor (CLEAR) design and R&D for more than 30 years. In this contribution, the design of lead-based mini-reactor CLEAR-M for energy production and advanced external neutron source driven nuclear energy system CLEAR-A for multi-purpose will be introduced. The technologies to support the CLEAR lead-based reactor projects will be presented, and test facilities have been constructed, including the lead alloy integrated non-nuclear test facility CLEAR-S, the lead-based zero power critical/subcritical reactor CLEAR-0, the lead-based virtual reactor CLEAR-V will be introduced as well.

Introduction

Lead-based reactor has many attractive features and may play an important role in the future energy supply, which is one of the most promising nuclear energy systems for Generation-IV reactor and ADS system[1]. Chinese government has provided a continuous national support to develop lead-based reactors technology since 1986, by Chinese Academy of Sciences (CAS), Minister of Science and Technology, NSF etc. In the last 30 years' research on lead-based reactor, Institute of Nuclear Energy Safety Technology, Chinese Academy of Sciences (INEST/FDS Team) places more emphases on China LEAd-based Reactor (CLEAR) design [2-6], materials [7,8], liquid metal technology [9-11], and software and simulation [12]. In this contribution, the design and R&D activities and progress will be introduced.

Design Activities and Status

China LEAd-based Reactor (CLEAR) series was proposed, such as, China Lead-based Mini-reactor CLEAR-M for independent power supply, Advanced External Neutron Source Driven

Nuclear Energy System (CLEAR-A) for multi-purpose, and so on. In first step, we are carrying out three projects in parallel named CLEAR-M10a, CLEAR-A10 and CLEAR-I to construct 10MWth experimental reactors to support CLEAR-M and CLEAR-A projects.

CLEAR-M

CLEAR-M project aiming at construction of small module energy supply system has been launched. The main purpose of this system is to provide electric as a flexible power system for wide application such as island, remote districts and industrial park etc.

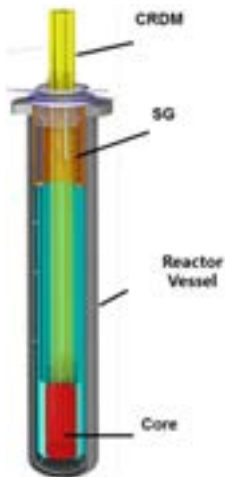
The typical design of CLEAR-M is CLEAR-M10, which is a 10MW level electric power reactor. With the characteristics of small modular, long refueling cycle, inherent safety and Combined Heat and Power (CHP), CLEAR-M10 can flexibly meet various electric needs. The main parameters of CLEAR-M10 are shown in table 1. As shown in figure 1, CLEAR-M10 is a pool-type reactor cooled by pure Lead. The natural circulation heat transport has been adopted to reduce maintenance requirements of main equipment and enhance the reliability and safety. The use of <20% UO₂ has been chosen to

realise long refueling period while four radial regions with different fuel enrichments were designed to decrease the power peaking factor. CLEAR-M10 incorporated two independent and redundant residual heat removal system among which the emergency heat removal system is the Reactor Vessel Air Cooling System (RVACS).

Table 1. Main design parameters of CLEAR-M

Item	Parameter
Thermal power	35MWth
Electrical power	14MWe 10MWe+17MWt
Fuel	Ave.18.5% UO ₂
Core life	20 years
Core inlet / outlet temperatures	375/495°C
Turbine inlet pressure	13MPa
Reactor vessel	Φ2.2m/H 8.5m

Figure 1. Overall view of CLEAR-M reactor

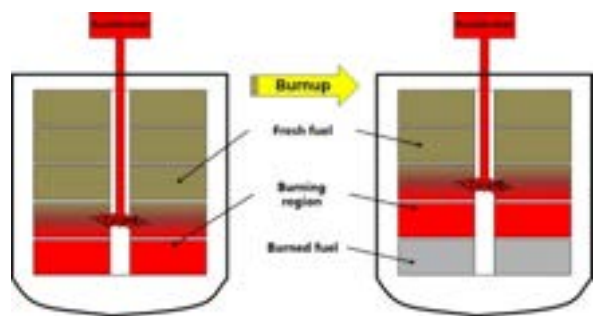


The engineering design for the first step as prototype mini-reactor CLEAR-M10a with 10MWth are underway. The existing technology has been used to accelerate the implementation progress. For example, the Lead Bismuth Eutectic (LBE) coolant has been chosen and the outlet temperature was set to 380°C. The cladding material will be chosen as 15-15Ti, which has already been tested.

CLEAR-A

Advanced External Neutron Source Driven Nuclear Energy System (CLEAR-A) has been proposed, the principle of which is an external neutron source driven subcritical lead-based reactor. The main purpose is to make use of depleted uranium, thorium or spent fuel from PWR as fuel to achieve high fuel utilisation and nuclear waste minimisation while producing energy. The principle of CLEAR-A is shown in Fig. 2.

Figure 2. CLEAR-A principle diagram



The typical fuel cycle scheme of CLEAR-A is shown in Fig. 3. Only some low-enriched uranium is needed in the first core, then depleted uranium, natural uranium, and spent fuel from PWR are consumed. The spent fuel discharged from in CLEAR-A can be reprocessed and serve as starting fuel for a new CLEAR-A type reactor.

Figure 3. Typical CLEAR-A U-Pu fuel cycle scheme



The typical design of CLEAR-A is CLEAR-A100, which is Advanced External Neutron Source Driven Nuclear Energy Demonstration System with output of 100 MWe. CLEAR-A100 mainly consists of an accelerator system, a spallation target system and a subcritical lead-based reactor. The ignition zone loaded with low enrichment U-Zr alloy or transuranium fuels and breeding zone loaded with depleted uranium or thorium. The overall layout of

CLEAR-A100 is shown in Fig.4 and the system parameters of CLEAR-A100 are shown in Tab.2.

Figure 4. The overall layout of CLEAR-A100 reactor system

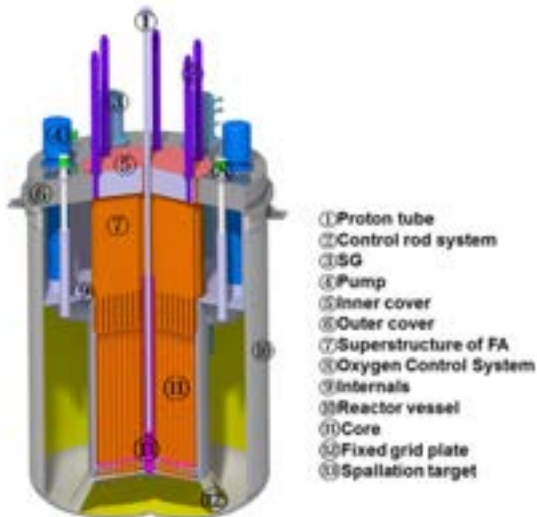


Table 2. System Parameters of CLEAR-A100

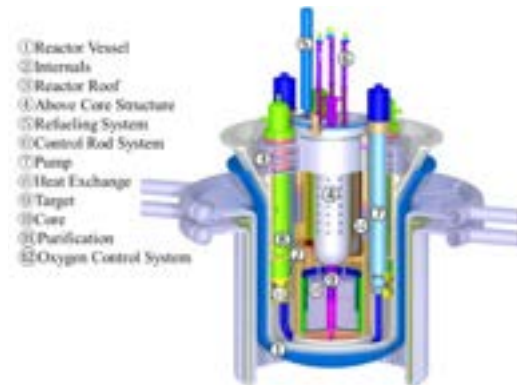
Items		Values
Power		400MW/150MWe
Neutron Source	Driver	900MeV/10mA
	Target	Pb
	Neutron Intensity	$\sim 10^{18}$ (n/s)
K_{eff}		0.97
Coolant		Pb
Neutron Spectrum		Fast
Fuel		12% UZr+DU/ TRU+Th
Refueling Cycle		15 yrs

In order to validate the engineering technology of the external neutron source driven nuclear energy system, a 10 MW Advanced External Neutron Source Driven Nuclear Energy Experimental System (CLEAR-A10) proposed to be built in the near future. CLEAR-A10 is for lead-cooled experimental reactor to test the nuclear breeding, nuclear waste transmutation and energy production technology.

Another 10MWth accelerator-driven lead-bismuth cooled subcritical experimental system named China LEAd-based Research Reactor CLEAR-I was also developed supported by CAS ADS project for nuclear waste transmutation research, which was launched in 2011. CLEAR-I is innovatively designed with

dual-mode operation capacity. The core can be operated in both critical and sub-critical mode, which is loaded with 19.75% UO_2 . The configuration of the primary system is pool-type with 600t LBE coolant inventory, as illustrated in Fig.1. The coolant is circulated by two primary pumps. Four primary heat exchangers are directly immersed into the pool. The secondary coolant is pressurised water without electricity generation.

Figure 5. Overall view of CLEAR-I reactor system



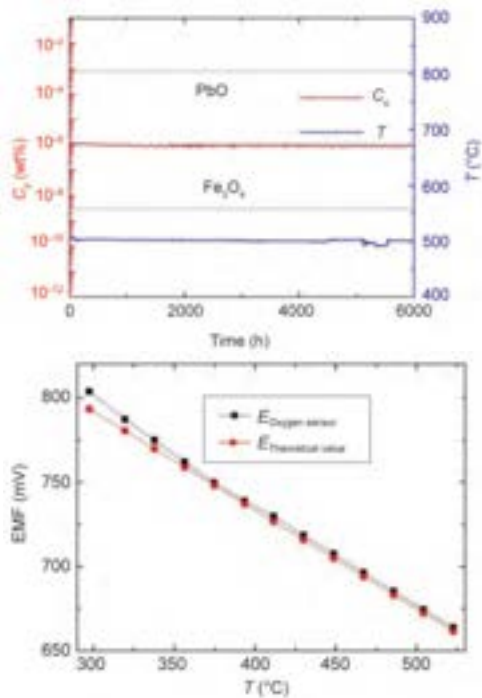
R&D of Key Technologies

Heavy liquid metal coolant technology R&D activities were mainly focused on key components, structural material and fuel, reactor operation and control. Key components including the main pump, heat exchanger, Control Rod Drive Mechanism, and refueling system for principle verification have been fabricated and tested to comprehensively validate and test the key component prototypes and the integrated operating technology of the lead-based reactor [13].

LBE process technology

LBE smelting & online purification, oxygen measurement & control, and ^{210}Po purification LBE process technologies were developed. A cold trap and a magnetic trap were developed for LBE online purification. Different type of oxygen sensors (Pt/air, Bi/Bi₂O₃, Cu/CuO) and. Gas phase & solid phase oxygen control systems were successfully developed and maintained in stable conditions, running for more than 6000 h (shown in Fig. 6). Common stainless steel and a new graphene-based composite were used as a filter to purify the radioactive isotopes ^{210}Po .

Figure 6. (a) Oxygen steadily controlled in the LBE loop; (b) test of oxygen sensor



Structural and cladding materials

A series of facilities for corrosion and mechanical property testing have been built and experiments are ongoing. Corrosion tests with different oxygen concentrations were carried out to identify the optimal range of oxygen concentration in LBE. A long-term corrosion test simulating operating condition with 1×10^{-6} wt% to 3×10^{-6} wt% dissolved oxygen was carried out. The accumulated time is more than 30,000 hours. In addition, mechanical testing facilities (e.g., for tensile, creep and fatigue testing) have been developed in LBE with the function of oxygen control, and the corresponding experiments are ongoing.

Fuel assembly technology

Fuel cladding material for lead-based reactor is developed and the manufacturing method for fuel cladding tubes and hexagonal wrapper tubes is already mature. The key technologies of fuel assembly fabrication have been tested and verified including the integrated assembling technologies for small modular reactor, such as welding and 3D printing technologies. A series of simulated assemblies were fabricated to investigate the flow, heat transfer, and structural stability features.

Figure 7. (a) Flowing test assembly; (b) heat transfer test assembly; (c) structural stability test assembly



Reactor key components

Horizontal and vertical pumps have been developed for LBE technology validation, and their performance had been tested. In addition a prototype pump has been designed and manufactured to provide higher flow rate for a pool type platform. Meanwhile, to improve the operation lifetime of pump, research of ceramic materials and coating technology has also been conducted in our laboratory.

A bayonet-type heat exchanger (HX) with double wall tubes was designed and developed to avoid direct contact between media on both sides of the tube. A full-size heat exchanger prototype has been fabricated and was successfully operated in LBE condition. The processing technology of Double Wall Bayonet Tubes (DWBT) was verified and the heat transfer performance was tested.

A GRDM testing facility has been accomplished, in which counterweight and vapor sealing were designed to attain the rod drop in LBE and to avoid the probable hang up issue caused by lead vapor. Tests in LBE were carried out on the rod position and velocity control, rod drop, driving motor, and grippers' applicability.

Test Facilities and Experiments

Based on the single engineering technology test and the equipment principle prototype development described above, the Multi-functional lead-bismuth loop KYLIN-II and three integrated test facilities are being constructed, including the lead alloy-cooled integrated non-nuclear pool type facility CLEAR-S, the lead-based zero-power nuclear reactor CLEAR-0, and the lead-based virtual reactor CLEAR-V. These test facilities are aimed to satisfy the integrated testing requirements of the key components and technologies for CLEAR.

KYLIN-II

KYLIN-II is a large multi-functional LBE integrated experimental loop, shown in Fig. 8. To carry out the LBE process technology test, structural materials corrosion experiment, LBE thermal-hydraulic experiment, components prototype proof test, and heat exchanger tube rupture accident investigation. Key components including the main pump, heat exchanger, CRDM, and refueling system for principle verification have been fabricated and tested under LBE environment.

Figure 8. Multi-functional lead-bismuth loop KYLIN-II



CLEAR-S

In support of the CLEAR series reactor, a 2.5MW mock-up pool type facility named CLEAR-S [14] has been constructed. CLEAR-S has the main vessel of 2m diameter and 6.5m height and >200t LBE inventory. There are seven fuel pin simulators (FPSs). The pool thermal-hydraulic features will be experimented to feedback the design and validations, especially core heat transfer and flow distribution. Moreover, the 1:1 prototype components for CLEAR-I have been fabricated. Up to now, the first stage commissions and steady condition tests, including the forced circulation test, pump hydraulic performance test, heat exchanger performance test and turbine power generation test have been conducted.

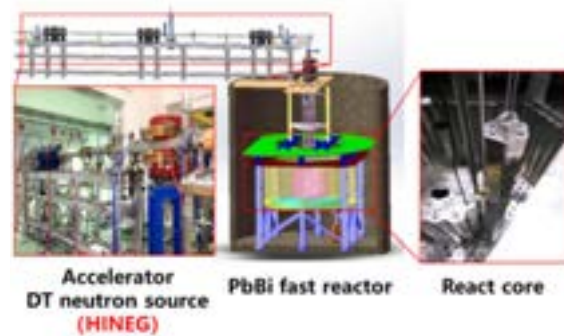
Figure 9. Lead-based Engineering Validation Platform CLEAR-S



CLEAR-0

A Lead-based Zero Power Critical/Subcritical Reactor CLEAR-0 is constructed, which consists of Lead-based zero power core and High Intensity D-T Fusion Neutron Generator (HINEG-I) [15] which serves as neutron source which produces fusion neutrons to drive the CLEAR-0 reactor in subcritical model. (shown in Fig. 10). CLEAR-0 is a multi-functional zero-power reactor which can be operated at both critical and subcritical model. HINEG-I has been constructed and successfully produced a D-T fusion neutron yield of up to 6.4×10^{12} n/s.

Figure 10. Lead-based Zero Power Critical/Subcritical Reactor CLEAR-0



CLEAR-V

To assist with the requirements for the activities of CLEAR-I design, optimisation, construction, and operation, CLEAR-V has been developed based on the virtual nuclear power plant for digital society (Virtual4DS) system (shown in Fig.11). Analysis models and modules of neutron physics, radiation shielding, thermal hydraulics, structural mechanics, safety, and environmental impact are included in CLEAR-V. This virtual reactor can be used for lead-based reactor design and safety assessment and can be used as a full-scope training simulator for operator training.

Figure 11. Lead-based virtual reactor CLEAR-V



Summary

Lead-based reactor is one of the most promising nuclear energy systems for Generation-IV reactor and ADS. INEST/FDS Team placed more emphases on CLEAR design and R&D for more than 30 years.

The concepts of mini-reactor CLEAR-M for energy production and external neutron source driven system CLEAR-A for multi-purpose as well as three experimental reactors have been presented. The technologies for CLEAR reactor licensing and construction are under development. The key component prototypes

including the main pump, heat exchanger, CRDM, refueling system, and FA have been fabricated and tested under LBE conditions. Several experiment platforms are constructed and under commissioning, KYLIN series LBE experimental loops were constructed to perform structural material corrosion experiments, thermal-hydraulic tests, and safety experiments. In order to validate and test the key components and the integrated operating technology lead alloy integrated non-nuclear test facility CLEAR-S, the lead-based zero power critical/subcritical reactor CLEAR-0, the lead-based virtual reactor CLEAR-V have been constructed.

References

- [1] Alemberti A, Smirnov V, et al. Overview of lead-cooled fast reactor activities. *Journal Progress in Nuclear Energy* 2014; 77:300–307.
- [2] Zhan WL, Xu HS. Advanced fission energy program-ADS transmutation system. *Journal Bulletin of Chinese Academy of Sciences* 2012; 27(3):375–381.
- [3] Y. Wu, Y. Bai, Y. Song, et al, “Development strategy and conceptual design of China Lead-based Research Reactor”, *Annals of Nuclear Energy*, 87(2): 511-516, 2016
- [4] Y. Wu, “Design and R&D Progress of China Lead-Based Reactor for ADS Research Facility”, *Engineering*, 2(1): 124-131, 2016
- [5] Wu YC, Bai YQ, et al. Conceptual design of China lead-based research reactor CLEAR-I. *Journal Chinese Journal of Nuclear Science and Engineering* 2014; 2:201–208.
- [6] Wu YC, Bai YQ, Song Y, et al. Development strategy and design options of china lead-based research reactor for ADS transmutation system. *Journal Annals of Nuclear Energy* 2016; 87:511–516.
- [7] Huang QY, Baluc N, Dai YQ, et al. Recent progress of R&D activities on reduced activation ferritic/martensitic steels. *Journal of Nuclear Materials* 2013; 442 (1-3):S2–S8.
- [8] Huang QY, Gao S, Zhu ZQ, et al. Progress in compatibility experiments on lithium-lead with candidate structural materials for fusion in China. *Journal Fusion Engineering and Design* 2009; 84:242–246.
- [9] Wu YC, the FDS Team. Design status and development strategy of China liquid lithium-lead blankets and related material technology. *Journal of Nuclear Materials* 2007; 367–370:1410–1415.
- [10] Wu YC, Team FDS. Design analysis of the China dual-functional lithium lead (DFLL) test blanket module in ITER. *Journal Fusion Engineering and Design* 2007; 82:1893–1903.
- [11] Wu YC, Huang QY, Zhu ZQ, et al. R&D of dragon series lithium lead loops for material and blanket technology testing. *Journal Fusion Science and Technology* 2012; 62-1:272–275.
- [12] Song J, Sun GY, Chen ZP, et al. Benchmarking of CAD-based SuperMC with ITER benchmark model. *Fusion Engineering and Design* 2014; 89:2499–2503
- [13] Wu YC, Wang MH, Huang QY, Zhao ZM, Hu LQ, Song Y, et al. Development status and prospects of lead-based reactors. *Nucl Sci Eng* 2015;35(2):213–21. Chinese.
- [14] WU YC, FDS Team. CLEAR-S: An Integrated Non-nuclear Test Facility for China Lead-based Research Reactor. *International Journal of Energy Research*, 2016, 40(14):1951-1956.
- [15] WU YC, FDS Team. Development of High Intensity D-T Fusion Neutron Generator HINEG, *International Journal of Energy Research*, doi:10.1002/er.3572.

MOLTEN-SALT REACTOR AS NECESSARY ELEMENT FOR THE CLOSURE OF THE NUCLEAR FUEL CYCLE FOR ALL ACTINIDES (V. IGNATIEV ET AL)

Victor Ignatiev⁽¹⁾, Olga Feinberg⁽¹⁾, Angelika Khaperskaya⁽²⁾, Oleg Kryukov⁽²⁾

(1) NRC "Kurchatov Institute", Russian Federation.

(2) ROSATOM, Russian Federation.

Abstract

The Molten Salt Reactor designs, where fissile and fertile materials are dissolved in the liquid salt fluorides /chlorides, under consideration in the framework of the Generation IV International Forum, are briefly described, including MSR activity in the Russian Federation focused mainly on liquid fuel fluoride based systems with homogeneous core. This paper mainly considers the Molten Salt Actinide Recycler & Transmuter system without and with U-Th support fueled with different compositions of transuranic elements from spent VVER fuel. New design options for fuel salts with high enough solubility of transuranic elements trifluorides are being examined because of new goals. Last developments concerned single fluid MOSART design addresses advanced large power unit with main design objectives to close nuclear fuel cycle for all actinides, including Np, Pu, Am and Cm. The optimum spectrum for Li,Be/F MOSART is fast spectrum of homogeneous core without graphite moderator. The effective flux of such system is near $1 \times 10^{15} \text{ n cm}^{-2} \text{ s}^{-1}$. Single fluid 2.4 GWt MOSART unit can utilise up to 250 kg of minor actinides per year from spent VVER fuel. The main attractive features of MOSART system deals with the use of (1) simple configuration of the homogeneous core (no solid moderator or construction materials under high flux irradiation); (2) proliferation resistant multiple recycling of actinides (separation coefficients between TRU and lanthanide groups are very high, but within the TRU group are very low); (3) the proven container materials (high nickel alloys) and system components (pump, heat exchanger etc.) operating in the fuel circuit at temperatures below 1023K, (4) core inherent safety due to large negative temperature reactivity coefficient (-3.7 pcm/K), (5) long periods for soluble fission products removal (1-3 yrs). The fuel salt clean up flowsheet for the Li,Be/F MOSART system is based on reductive extraction in to liquid bismuth. The paper has the main objective of presenting the transmutation advantages and fuel cycle flexibility of the large power Li,Be/F MOSART system while accounting technical constrains and experimental data received in this study. The main design choices and characteristics for MOSART concept are explained and discussed, including fuel maintenance and engineering safety features. Particularly, the need for the experimental small power Demo MOSART unit to demonstrate the control of the reactor and fuel salt management with different TRU loadings for start up, transition to equilibrium, drain-out, shut down etc. with its volatile and fission products.

I. Introduction

Facilities of Experimental Demonstration Centre being built at the site of the Mining and Chemical Combine after 2020 will begin reprocessing of SNF from VVER-1000 reactors on the basis of innovative technology, providing a recovered nuclear material (refined products) for recycling in thermal and fast solid fuel reactors [1] After adjustment of all

technological processes EDC will become the reference basis for a large-scale RT-2 plant, which will provide an environmentally and economically acceptable system of SNF VVER-1000/1200 recycling both in Russia and abroad. In accordance with the EDC flowsheet, the highly active raffinate, containing long-lived actinides (^{243}Am , ^{245}Cm , ^{247}Cm , ^{248}Cm), is sent for conditioning. The obtained vitrified HLW belong to the 1st class of radwaste. Use of dedicated reactor unit as a TRU burner,

remaining after the main part of uranium and plutonium recycling to solid fuel thermal and fast reactors, may reduce the volume and radiotoxicity of HLW.

It is obvious that for operation with TRU loadings, which cannot be claimed by conventional solid-reactors, suitable reactor systems must allow: 1) widely vary the composition of fuel loading without changing the core structure, 2) maintain the inherent safety features of the reactor when changing the fuel composition, 3) abandon the manufacture of fuel pellets, 4) ensure the minimum possible actinides losses in multiple recycling. Finally, technologically such a reactor must be prepared for implementation, i.e. should rely on scientifically sound and feasible in the nearest future technological basis, equipment and materials.

Solid-fuel reactor systems with a fast neutron spectrum are theoretically able to burn TRU successfully. However, the introduction of minor actinides into traditional fast neutron reactors will complicate the design of these reactors, will require the development of new fuels, will complicate and lead to an increase in the cost of its fabrication. The scientific and engineering issues of manufacturing a fuel pellet with significant additions of minor actinides, as well as issues of justifying the safety of a fast reactor with such fuel, are not solved nowhere in the world. In addition, for solid fuel reactors with a limited burnup, the loss of TRU to waste stream in multiple recycling will be comparable to the amount of MA burned during the same time.

From the outset molten salt reactors were thermal-neutron-spectrum graphite-moderated designs. The first experimental studies and design developments of MSR were performed in the 60-70s of the last century in the US ORNL [2-5]. The 8 MWt MSRE reactor was built and successfully operated from 1964 to 1969. The success of MSRE stimulated the development of a thorium-uranium 1 GWe MSBR design with thermal neutron spectrum. In the Russian Federation, the MSR studies began at the NRC "Kurchatov Institute" in the second half of the 1970s [6].

Within GIF, MSR R&D has mainly focused on fast-spectrum MSR options combining the generic advantages of fast neutron reactors (extended resource utilisation, waste minimisation) with those related to molten salt fluorides as both fluid fuel and coolant (low pressure; high boiling temperature; good compatibility with high Ni-alloys, SiC ceramics

and graphite; no exothermic reactions with water, air and, optical transparency) [7]. The main attractive features of advanced MSR designs under consideration are as follows:

- minimum number of parasitic absorbers and as a consequence less number of fissile materials in the core;
- non limited fuel burn-up with minimal losses of actinides to waste in multiple recycling;
- flexibility of the fuel cycle - the ability to work with fuels of various nuclide composition without reactor shutdown and special modifications of the core;
- on-site fuel processing - no temporary storage is required to hold SNF, transportation of SNF and fuel loading for the next transmutation cycle;
- high thermal efficiency, due to the high temperature of the fuel salt (>700C);
- operation in load follow mode.

Chloride salts have been also considered as an alternative fluid fuel to obtain a fast neutron spectrum due to high solubility of TRU in the melt. Severe problems related to structural material corrosion (particularly at the high end of the temperature range), chemical stability of such systems and poor separation ability between some representatives of actinides and lanthanide's groups have been pointed out. Also, during irradiation ^{35}Cl transmuted to ^{36}Cl with $T_{1/2}=300\ 000\text{yr}$. Binary and ternary systems of fluorides fuels still remain an interesting way out.

GIF MSR developments in the Russian Federation on the 2.4 GWt MOSART design address the concept of large power units with a fast neutron spectrum in the core without graphite moderator. The main characteristics of the MOSART design are given in Table 1.

Table 1. Main characteristics of the MOSART design

Fuel circuit	MOSART
Fuel salt, mole%	$\text{LiF}\cdot\text{BeF}_2+1\text{TRUF}_3$ $\text{LiF}\cdot\text{BeF}_2+5\text{ThF}_4+1\text{UF}_4$
Temperature, °C	620-720
Core radius/height, m	1.4/2.8
Core specific power, W/cm ³	130
Container material	KHN80MTY alloy
Removal time for soluble FPs, yrs	1-3

Since year 2000, the NRC “Kurchatov Institute” carried out complex studies on the MOSART project, which included for configurations selected: neutronic, thermal hydraulic and safety analysis; experiments concerned the main physical and chemical properties of fuel / coolant salts; compatibility of structural materials and fuel/coolant salts with its chemistry control [8-10]. The accumulated experience now allows us to move from studying the calculated and experimental capabilities of MOSART concept to obtaining specific technical and technological solutions. The MOSART feasibility at present is beyond doubt. In this paper focus is placed on MOSART system without Th support with main design objective to close nuclear fuel cycle for all actinides, including Np, Pu, Am and Cm.

The effective flux of such system is near 1×10^{15} n cm⁻² s⁻¹. The possibility of creating a high neutron flux and the lack of structural materials in the liquid homogeneous core, leads to optimisation of the neutron balance, as well as the possibility to change the fuel salt composition without core modification and reactor shutdown, creates favorable conditions for the TRU utilisation. The MA burning rate is directly proportional to the core specific power. When choosing this parameter, it is advisable to be within technical limits.

Summary times and possible methods for fission product removal and actinides recycling in MOSART system are presented in the Table 2.

Even in the homogeneous core, where removal times for soluble fission products are long enough, taking away of neutronic poisons is, of course, the primary purpose of fuel processing. All actinides are immediately returned to fuel circuit. The consideration done demonstrated the potential of the MOSART as systems with flexible configurations and fuel cycle scenarios which can operate within technical limits with different loadings and make up based on TRUs (from spent VVER fuel with MA/TRU ratio up to 0.45) as dedicated actinide transmuter, as self-sustainable system (CR=1) or even as a breeder (CR>1).

The main advantages of MOSART are the ability to vary widely the MA content in fuel salt without losing the inherent safety and the absence of stages related to the fuel fabrication and re-fabrication in multiple actinides recycling. The molten salt fluoride mixtures, due to the high separation coefficients between actinides and lanthanides, make it possible to organise an effective removal of soluble fission products, based on the reductive extraction, to

substantially reduce the time of the external fuel cycle for actinides and its losses in waste stream in multiple recycling in comparison with solid fuel reactors.

Table 2. Summary times for fission product removal and actinides recycling for MOSART

Element	Time
Kr, Xe	50 s
Zn, Ga, Ge, As, Se, Nb, Mo, Ru, Rh, Pd, Ag, Tc, Cd, In, Sn, Sb, Te	2-4 hrs
Zr	1-3 yrs
Ni, Fe, Cr	1-3 yrs
Pu, Am, Cm, Np, U	1-3 yrs
Y, La, Ce, Pr, Nd, Pm, Gd, Tb, Dy, Ho, Er	1-3 yrs
Sm, Eu	1-3 yrs
Sr, Ba, Rb, Cs	5-10 yrs
Li, Be, Th	30 yrs

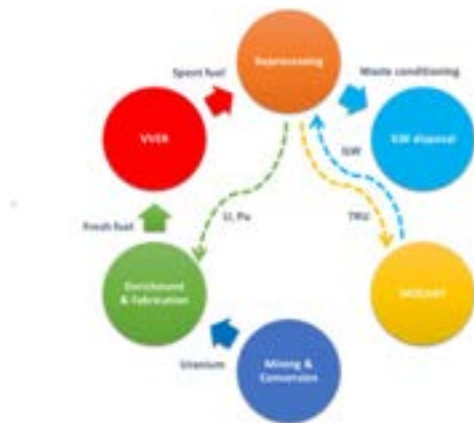
Thus, the MOSART concept, using the advantages associated with the liquid fuel structure, opens the prospect of a significant improvement in nuclear power technology with regard to the closure of the fuel cycle for all actinides. It is proposed to use the technical and technological capabilities of the MCC site to place MOSART in the immediate vicinity of SNF reprocessing facilities, linking it to the EDC infrastructure. It is assumed that the fuel cycle of this complex will be organised as follows (see Figure 1): the bulk of the removed uranium and plutonium return to thermal and fast solid fuel reactors, and the remaining TRU are transferred for utilisation in the MOSART system. The collocation of MOSART and SNF reprocessing plants, will provide the complex and the surrounding by electricity, facilitates the problems of nuclear materials transport and radwaste management.

The creation of a full-scale MOSART is proposed to be preceded by the construction of an experimental small power Demo unit demonstrate the joint operation of the reactor loaded by different TRU compositions with fuel salt processing unit. The configuration, materials and characteristics of the MOSART fuel circuit were chosen primarily for reasons of technological validity.

In the MOSART, a well-established molten LiF-BeF₂ salt mixture, is chosen as a solvent for TRU trifluorides fuel addition. The molten fluoride chemistry (solubility, redox chemistry, chemical activity etc) for the LiF-BeF₂ system is

well established and can be applied with great confidence, if TRU based fuels are to be used in the LiF-BeF₂ solvent. The solubility of TRU trifluorides in molten 73LiF-27BeF₂ (in mole%) salt mixture with decreased beryllium difluoride fraction of 0.27 and the minimum temperature in the fuel circuit of 600°C is more than 2 mole%. The structural material selected for the MOSART container is the special Ni-Mo alloy kH80MTY with a low concentration of Cr alloyed by 1% of Al [6]. The composition of the alloy was optimised by Kurchatov Institute researchers for corrosion resistance (both in a low oxygen gas atmosphere and in molten fluorides), irradiation resistance and high temperature mechanical properties [8-10].

Figure 1. Nuclear fuel cycle with MOSART



The performed calculations show that the Li,Be/F MOSART, starting at TRU from SNF of VVER with the ratio of MA to (Pu + MA) equal 0.1, without core modification and changing temperature in the fuel circuit, can use any TRU make up with the MA to (Pu + MA) ratio up to 0.33. At equilibrium ²⁴⁵Cm fission contribute 28% to the core reactivity. This allows 2.4 GWt MOSART with a fuel salt of the selected composition to utilise up to 250 kg of MA per year [3].

For core reflectors located inside the reactor vessel, it is proposed to use graphite or Ni-based alloy. The radiation resistance of these materials determines the upper limit core specific power in the MOSART design. If the damage caused by fast neutrons is critical for graphite, then for high-nickel alloys, the reduction in plasticity at a temperature above 500°C, associated with the formation of helium along the grain boundaries, is the most important process, caused by both fast and thermal neutrons. To obtain an acceptable

service life for reflectors (> 5 years), the core specific power should not exceed 130-150 W/cm³. Otherwise, frequent stops to replace the reflector will result in a reduction in the reactor load factor and an unjustified increase in operating costs. In addition, with this limitation for the core specific power, there is no problem of heat removal from the fuel circuit. In this case the service life for the reactor vessel, made of the kHN80MTY alloy, will be about 50 yrs.

For 2.4 GWt MOSART, taking into account the adopted limits, the primary circuit will contain 50 m³ of fuel salt, of which only half is in the core. It is obvious that the demonstration reactor should have significantly less specific power and thermal capacity to test the MSR.

II. Fuel Maintenance

In general, to achieve fuel maintenance, (1) the fuel must be delivered to and into the reactor in a proper state of purity and homogeneity, (2) the fuel must be sufficiently protected from extraneous impurities, and (3) sound procedures must exist for addition and recycling of the actinides required and (4) provision of the required redox potential in the system.

For MOSART that propose chemical reprocessing to remove fission products (see Table 2), the required fuel maintenance operations also include (1) continuous removal (by the sparging and stripping section of the reactor) of fission-product krypton and xenon, (2) addition of U and TRUs to replace those lost by burnup, (3) in situ production of UF₃ to keep the redox potential of the fuel at the desired level, (4) recycling of all actinides, (5) removal of soluble fission products (principally rare earths); they probably also include (6) removal of inadvertent oxide contaminants from the fuel; in addition, they may include (7) addition of ThF₄ to replace that lost by transmutation or stored with fuel removed from the operating circuit and (9) removal of a portion of the insoluble noble and semi noble fission products. Each of these is discussed briefly below.

Preparation of initial fuel. Initial purification procedures for the MSR present no formidable problems. Nuclear poisons (e.g., boron, cadmium, or lanthanides) are not common contaminants of the constituent raw materials. All the pertinent compounds contain at least small amounts of water, and all are readily hydrolysed to oxides and oxyfluorides at elevated temperatures. The compounds LiF and

BeF₂ generally contain a small quantity of sulfur as sulfate ion. Uranium tetrafluoride commonly contains small amounts of UO₂, UF₅, and UO₂F₂.

Purification procedures used to prepare materials in many laboratories and engineering experiments have treated the mixed materials at high temperature (usually at 600°C) with gaseous H₂-HF mixtures and then with pure H₂ in equipment of nickel or copper. The HF-H₂ treatment serves to (1) reduce the U⁵⁺ and U⁶⁺ to U⁴⁺, (2) reduce sulfate to sulfide and remove it as H₂S, (3) remove Cl⁻ as HCl, and (4) convert the oxides and oxyfluorides to fluorides. Final treatment with H₂ serves to reduce FeF₃ and FeF₂ to insoluble iron and to remove NiF₂ that may have been produced during hydrofluorination. To date, all preparations have been performed in batch equipment, but continuous equipment has been partially developed. Such a purification procedure can provide a sufficiently pure and completely homogeneous fuel material for initial operation of the reactor.

Addition of actinides. It will apparently be necessary, assuming the fuel volume changes from these additions or other causes do not require removal of any fuel to storage. These will be inherently more complex (and radioactively dirty), and stating which of the options would be preferred is not presently possible. If making a few additions of plutonium and minor actinides to the reactor fuel during its lifetime is necessary, then adding it e.g. as a liquid containing ⁷LiF -PuF₃ mixture should be possible. A possibility would be a melts containing about 80LiF-20PuF₃ (in mole%) melting near 740 °C. Alternatively, a procedures presumably could be developed for addition of solid TRUF₃.

Maintaining the desired UF₃/UF₄ ratio. Operation of the MSRE demonstrated that in situ production of UF₃ could be accomplished readily and conveniently by permitting the circulating fuel to react in the pump bowl with a rod of metallic beryllium suspended in a cage of HN80MTY. This technique could be adapted for use in other MSR designs; beryllium reduction would be desirable if the fissionable and fertile uranium additions are to be made as Li₃UF₇

Removal of fission-product krypton and xenon. Stripping of krypton and xenon makes possible their continuous removal from the reactor circuit by the purely physical means of stripping with helium. Such a stripping circuit would remove an appreciable (but not a major) fraction of the tritium and a small (perhaps very

small) fraction of the noble and semi noble fission products as gas-borne particulates. In addition, the stripper would remove BF₃ if leaks of secondary coolant into the fuel were to occur. None of these removals (except possibly the last) appreciably affects the chemical behavior of the fuel system.

Partial removal of noble and seminoble metals.

The behavior of these insoluble fission-product species, as indicated previously, is not understood in detail. If they precipitate as adherent deposits on the MOSART heat exchanger, they would cause no particularly difficult problems. However, should they form only loosely adherent deposits that break away and circulate with the fuel, they would be responsible for appreciable parasitic neutron captures. To the extent that they circulate as particulate material in the fuel, insoluble fission-product species could probably be usefully removed by a small bypass flow through a relatively simple Ni based-wool filter system. Presumably, such a system would need to have a reasonably low pressure drop and probably would need to consist of sections in parallel so that units whose capacity was exhausted could be reasonably replaced.

Fuel chemical processing. In MSRs, from which xenon and krypton are effectively removed, the most important fission products poisons are among lanthanides which are soluble in the fuel. Also, the trifluoride species of actinides and the rare earth's are known to form solid solutions so, that in effect, all the LnF₃ and AnF₃ act essentially as a single element. In combination of all trifluorides, actinides solubility in the melt is decreased by lanthanides accumulation. Since actinides must be removed from the fuel solvent before rare earth's fission products the MSR must contain a system that provides for removal of all actinides from the fuel salt and their reintroduction to the fresh or purified solvent. This fuel processing system can be based principally on three types of operations: removal of actinides, rare earths, and other fission products from the salt by extraction into molten bismuth. The chemical basis on which the processing system is founded is well established (the coefficients of the distribution of actinides and lanthanides in the Li,Be/F - liquid bismuth system with respect to plutonium at T = 873 K are respectively 6 for curium, 3.000 for neodymium and 25.000 for lanthanum); however, only small engineering experiments have been carried out to date, and a considerable engineering effort remains.

In fuel salt, approximately 10% of the initial amount of lanthanides remains (mainly cerium). The purified salt is then transferred to the actinide recycling. The lanthanide precipitate with salt residues is sent for vacuum distillation of the salt components. The lanthanide salts remaining after the distillation are sent to the EDC for conditioning and subsequent near-surface disposal.

III. Engineered Safety Features

The main feature of the MSR which sets it apart from the solid fuel reactors is that the nuclear fuel is in fluid form (molten fluoride salt) and is circulated throughout the primary coolant system, becoming critical only in the core. Thus, for an MSR to have equivalent overall containment, greater requirements must be placed on the containment barriers from the fuel salt outward.

The possible problems and engineered safety features associated with this type of reactor will be quite different from those of the present day solid fuel designs. In the MSR, the primary system coolant serves the dual role of being the medium in which heat is generated within the reactor core and the medium which transfers heat from the core to the primary heat exchangers. Thus the entire primary system will be subjected to both high temperatures (>700°C at core outlet) and high levels of radiation by a fluid containing most of the daughter products of the fission process. On the other hand, the fuel-coolant barrier in a solid-fuel reactor, interposed between the heat source and the cooling fluid, is the barrier most vulnerable to damage in a nuclear excursion so that its protection and the consequences of its failure tend to impose more restrictive nuclear safety requirements on a solid-fuel reactor. Because of the low fuel salt vapor pressure, however, the primary system design pressure will be low, as in an liquid metal cooled designs. The entire primary coolant system as analogous, in terms of level of confinement, to the cladding in a solid fuel reactor. Although much larger, it will not be subjected to the rapid thermal transients with melting associated with accident scenarios for VVER and liquid metal cooled designs. Two additional levels of confinement will be provided in the MSR in accordance with present practice. The problem of developing a primary coolant system which will be reliable, maintainable (under remote conditions), inspectable, and structurally sound over the plant's lifetime will probably be the key factor in demonstrating ultimate safety and licenceability.

It is the breach of the primary coolant system boundary, resulting in a large spill of radioactive salt into the primary containment, which will provide the design basis accident. The analogues level of occurrence in a solid fuel reactor would be from major cladding failure (min) to core meltdown (max). Possible initiators of this accident include pipe failure missiles, and pressure or temperature transients in the primary coolant system, failure of the boundary between the primary and secondary salt in the intermediate heat exchanger could be especially damaging. In the event of a salt spill, a possibly redundant system of drains would be activated to channel the salt to the cooled drain tank. The primary system containment, defined as the set of vertically sealed, concrete-shielded equipment cell, would probably not be threatened by such a spill, but cleanup operations would be difficult.

A unique safety feature of the MSR is that, under accident shutdown conditions, the fuel material would be led to the emergency core cooling system (represented by drain tank cooling), rather than vice versa. The reactor and containment must be designed so that the decay heated fuel salt reaches the drain tank under any credible accident conditions. In any case, the decay heat is associated with a very large mass of fuel salt, so that melt through does not appear to be a problem.

The safety philosophy for accidents involving the reactor core is very different for fluid-fueled reactors and for solid-fueled ones because the heat source is (mainly) in the liquid and not in a solid, which requires continuous cooling to avoid melting. An LMR, for example, has a tremendous amount of stored energy in the fuel pins which must be removed under any accident conditions. Dry out, which leads to almost immediate meltdown in an LMR, would not be nearly as severe in the MSR because the heat source would be removed along with the heat sink capability.

For 2.4 GWt MOSART severe accident with the rupture of the primary circuit and fuel discharged on the reactor box bottom was estimated. The model based on mass transfer theory describing main radionuclides distribution between the fuel salt, metallic surfaces of the primary circuit, graphite and the gas purging system was applied for calculation releases to the containment atmosphere. A great deal of practical information on the disposition of these different fission products groups was provided by operation of the MSRE.

As a criteria characterising an isotope yield from the fuel salt is accepted the ratio of this isotope activity changed into a gas phase of a containment (A_g) to its full activity built up in a reactor by the moment of the accident (A_o). For a molten salt fuel there are three broad classes of fission products: whose fluorides are stable in the salt at its redox potential (soluble fission products), the noble gases and the noble metals. The major soluble fission products are rare earths (including Y), Zr, Ba and Sr, Rb and Cs, I and Br. The noble gases have very low solubility in molten salt and take first opportunity to migrate to any gas phase in contact with fuel. The competitive sinks for noble gases are the pore spaces in the graphite and the circulating bubbles of the cover gas. Another major group of fission products, consisting largely of Nb, Mo, Tc, Ru and Te, does not form fluorides that stable at the redox potential of the fuel salt and is therefore called noble. They are not wet by the salt and also tend to migrate to the salt surfaces. For noble metals it was estimated that about 50% on the metal surfaces and 50% would go into the off-gas system with the bubbles.

After accident considered all noble gases and metals available should move to the gas phase ($A_g / A_s = 1$, where A_g / A_s - the ratio of isotope activity in the gas phase of the containment after an accident to its activity concentrated in the fuel salt by the moment of the accident). However, already as it noted before during the normal operation these nuclides are almost completely leave the fuel salt. As can see from the Table 3 only from 0,1 to 3,4% of them is remained in the fuel. Therefore, the release for the noble metals is not so big. Only for Te129 it amounts to 25%. This isotope has a sufficiently small half - life period ($T_{1/2}=69$ min) to leave the fuel salt completely, for example in comparison with Te132 ($T_{1/2}=78$ h).

Alkaline and alkaline earth metals and rare earth form in the fuel salt stable and well soluble fluorides which have enough high temperature of melting (above 1200 oC). For this group in normal operation A_s / A_o ratio is about 0,95. As a result for isotopes of these group the relative activity yield A_g / A_o comes up 0,1 to 2,5%. Note, that such isotopes as Sr89 and Cs137 have gas precursors Kr89 and Xe137 with a low half-life. But because of low concentration of noble gases in the fuel salt an escape of Sr89 and Cs137 into the gas phase due to gas precursors is insignificant and relative activity yield for these isotopes is not different for others.

Table 3. Activity releases into the MOSART containment for the accident with the fuel circuit failure

Isotope	A_s / A_o	A_g / A_s	A_g / A_o
Te129	0,25	1	0,25
Te132	0,005	1	0,005
Ru103	0,01	1	0,01
Ru106	0,001	1	0,001
Nb95	0,034	1	0,034
Zr95	0,99	0,0011	0,0011
Sr89	0,99	0,00046	0,00046
Sr90	0,98	0,00046	0,00046
Ba140	0,97	0,006	0,006
La140	0,98	0,026	0,025
Ce141	0,99	0,0024	0,023
Ce144	0,96	0,0024	0,023
I131	0,62	0,43	0,27
I133	0,94	0,43	0,43
Cs137	0,7	0,016	0,011

IV. Conclusion

It is obvious from the discussion above that use of molten fluorides as fuel and coolant for a reactor system of energy production and incinerator type faces a large number of formidable problems. Several of these have been solved, and some seem to be well on the way to solution. But it is also clear that some still remain to be solved. The molten salts have many desirable properties for such applications, and it seems likely that - given sufficient development time and money - a successful burner system could be developed.

Extraction of long-lived actinides from high-level radwaste with their further utilisation in a dedicated reactor system will allow to reduce the volume of high-level waste and radiotoxicity of reprocessing for spent nuclear fuel and exclude the costs of long-term storage and subsequent disposal of selected minor actinides, thereby increasing the public acceptability and commercial attractiveness of SNF reprocessing.

The advantages of MOSART as a TRU burner from SNF reprocessing before solid-fuel reactor systems are primarily due to the lack of the need to manufacture a fuel pellet and the possibility of widely varying the content of long-lived actinides in fuel salt.

MOSART will allow to burn all the produced MA and approximately 500 kg / year of recycled reactor grade plutonium, while producing 1 GWe of electricity consumed by the EDC and surrounding companies. The construction of a

large power MOSART is proposed to be preceded by the construction of experimental 5-10 MWt Demo MOSART unit to demonstrate the control of the reactor and fuel salt management with different TRU loadings for start up, transition to equilibrium, drain-out, shut down etc. with its volatile and fission products. There are opportunities to further improve the efficiency of burning minor actinides in MOSART, which will be justified by the results of the experimental setup.

The industrial site of the MCC has all the necessary engineering communications, automobile and railway access roads, areas for the expansion of storage facilities, heat and power supply systems, water supply, electric networks. MOSART plants can use the existing radiochemical infrastructure of the MCC, which should somewhat reduce investment costs through the use of existing mine workings, the absence of long arms to transport SNF and processed products, and the availability of qualified personnel.

Introduction of MOSART into the Russian nuclear power system as an integral element will allow solving the problem of utilisation of long-lived actinides from SNF reprocessing. The development of the proposed technology on an

industrial scale will certainly require solving of a number of technical tasks, however, there are no deadlock problems on this path.

Nomenclature

EDC	Experimental demonstration centre
HLW	High level waste
HN80MTY	Advanced high nickel alloy developed for MSR in Russia
MA	Minor actinides
MCC	Mining and Chemical Combine
MOSART	Molten salt actinide recycler & transmuter
MSBR	Molten salt breeder reactor
MSR	Molten salt reactor
MSRE	Molten salt reactor experiment
RT-2	Reprocessing plant of Russian design
SNF	Spent nuclear fuel
TRU	Transuranic elements
VVER	Pressurised water reactor of Russian design

References

- [1] Gavrilov P., Merkulov I., Kryukov O., et al. Experimental-Demonstration Center as a Key Element of Creation of an Integrated Center for NPP Spent Fuel Reprocessing at MCC // Proc. Intern. Conference "Global 2015. Nuclear Fuel Cycle for a Low-carbon Future", September 21-24 2015, Paris, France. - 2015, Paper 5078
- [2] Rosenthal M. W. et al. Molten salt reactors - history, status, and potential. Oak Ridge National Laboratory, Oak Ridge, 1969
- [3] Rosenthal W., The Development Status of Molten-Salt Breeder Reactors, ORNL-4812 August, 1972
- [4] McNeese L.E. et al. The Program Plan for Development of Molten Salt Breeder Reactors. Report # ORNL-5018 Oak Ridge National Laboratory, 1974
- [5] Engel J.R., e.a. Development status and potential program for development of proliferation-resistant molten salt reactors, ORNL/TM-6415, March, 1979
- [6] Novikov V, e.a., Molten salt reactors: perspectives and problems, M., Energoatomizdat, 1984
- [7] Serp J. e.a., The molten salt reactor (MSR) in generation IV: Overview and perspectives, Progress in Nuclear Energy, Volume 77, November 2014, Pages 308-319
- [8] Ignatiev V.,e.a., Molten salt reactors - new challenges and solutions - Atomic energy, 2012, Vol.112, issue 3, pp.157-165
- [9] Ignatiev V. et al., 2014, Molten salt actinide recycler & transforming system without and with Th-U support: fuel cycle flexibility and Key material properties, Annals of Nucl. Energy, 64, 408-420
- [10] Ignatiev V., e.a., Key Experimental Results of the PYROSMANI Project, Procedia Chemistry, 2016, V. 21, p. 417

THREE DIMENSIONAL TRANSIENT ANALYSIS FOR CONTROL RODS DROP INTO CSR1000 CORE (W. LIANJIE ET AL)

Wang Lianjie, Lu Di, Zhao Wenbo, Xia Bangyang, Li Xiang, Li Qing

Nuclear Power Institute of China, China.

Abstract

Transient performance of CSR1000 core during the control rods (CR) drop into the core is analysed and evaluated with the coupled three dimensional neutronics and thermal-hydraulics SCWR transient analysis method. The 3-D CR drop transient analysis shows that while the high worth CR drop into the core, the core power in the initial stage of the CR drop process decreases rapidly. The core power descent rate exceeds the shutdown setting value, which will trigger the protection shutdown. While the low worth CR drop into the core, due to the reactivity feedback of the water density, the core power decreases slowly, and the core power descent rate cannot reach the shutdown setting value, which will not trigger the protection shutdown. The CR drop into the core has little influence on the axial power distribution. The power decrease of fuel assembly (FA) in the CR drop area is more obvious than the low worth CR drop caused by the high worth CR drop. In the transient process, the peak value of maximum cladding surface temperature (MCST) remains lower than the transient safety limit of 850°C, whether it is a high worth CR drop or a low worth CR drop. The safety performance of CSR1000 core can be ensured in the process of CR drop into the core under the salient reactivity feedback of water density and the essential reactor protection system.

I. Introduction

The core coolant of Supercritical water-cooled reactor (SCWR) has high temperature and low density. The core reactivity cannot be controlled by adding boric acid in the coolant. Therefore, a large number of control rods are needed to suppress the excess reactivity of the core and compensate a variety of reactivity losses. The impact of abnormal control rod (CR) action is the main reason for the abnormal SCWR reactive events. Taking the CR drop into the core as an example, the radial power distribution of the core will be abnormal, and then the maximum cladding surface temperature (MCST) of the SCWR fuel will be affected. The traditional method of transient analysis using point Kinetics or one dimensional neutron dynamic mode does not have the ability to calculate the three dimensional power of the core, and cannot accurately describe the radial distribution of the core power, so it cannot be used for the

transient analysis of the SCWR CR drop into the core event.

In this paper, in view of the characteristics of the SCWR CR drop into the core event, the coupled three dimensional neutronics and thermal-hydraulics analysis method is adopted to establish the core 3-D transient calculation model and analysis the process of the SCWR core control rods drop transient. The core performance of the China supercritical water-cooled reactor with the rated electric power of 1000MWe (CSR1000) [1] during the transient process of CR drop into the core is analysed and evaluated.

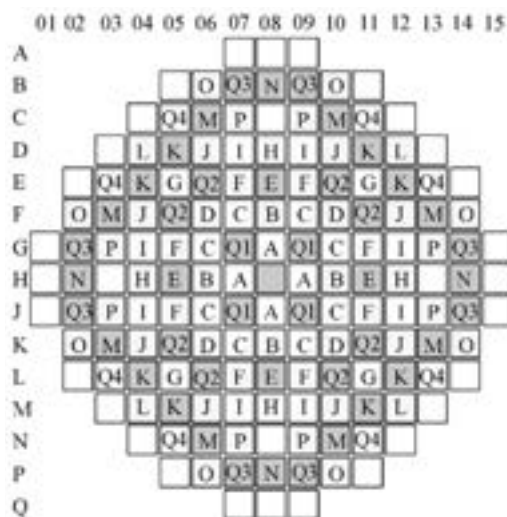
II. Description of Core and CR Drop Event

II.A CSR1000 core

The CSR1000 core with thermal power of 2300 MWt consists of 157 combined square fuel assemblies with stainless steel fuel cladding

and structure material. The improved CSR1000 core with the refuelling cycle of 580 effective full power days (EFPD) adopts a two-pass flow scheme, three-batch fuel management with low-leakage fuel loading patterns, and a reactivity control method via 124 control rods and burnable poison Er_2O_3 . Underrated conditions, the MCST shall not exceed 650°C . Figure 1 shows the layout of CSR1000 core control rods. The 124 control rods arranges in the core, which are divided into 17 groups [1]. The group Q is the safety group, with a total of 28 bundles.

Figure 1. CSR1000 Control Rods Layout



II.B CR drop event

By analogy analysis with PWR and BWR, among the abnormal events of reactivity and power distribution in SCWR, the CR drop into core event is classified as transient [2]. Under transient conditions, safety criteria require that there should be no systematic fuel rod damage, fuel pellets damage or pressure boundary damage. The analysis of CR drop into core transient process in this paper is limited to the core, so the pressure boundary problem is not considered at this time. For stainless steel 310s cladding used for CSR1000 core fuel, in order to ensure the integrity of fuel rods, the transient safety criterion is set as MCST not exceeding 850°C [3].

The event of CR drop into core may result from the mechanical failure of the reactor CR system, which will reduce the core power and reactivity. CR drop events include two Kinds of situations:

high worth CR drop into the core and low worth CR drop into the core. When the high worth CR drop into the core and the negative reactivity introduced is large enough, the negative neutron flux change rate (absolute value) high shutdown signal will be triggered, and the power of the reactor decreases. When the low worth CR drop into the core and the negative reactivity insertion rate cannot trigger protection system action, the feedback effect caused by the increase of water density may cause the nuclear power to rise to a new balance. If CR drop events cannot be put into protection in time, it may lead to high local power level and the deterioration of radial power distribution in the core. It is possible that the MCST may exceed the transient limit. Corresponding to the above two situations, this paper analyses the problems of high worth CR drop and low worth CR drop respectively under the hot full power (HFP) condition. In the calculation and analysis of the CR drop problem, it is assumed that the CR drops into the core at a constant speed within 2.0 s, and the CR dropping speed is 210 cm/s.

III. 3-D Transient analysis method

Due to the traditional point kinetics or one dimensional neutron dynamic mode cannot describe core radial power distribution change with time, the transient analysis of CSR1000 CR dropping into core is carried out by using 3-D transient analysis method. The SCWR core 3-D transient analysis code STTA is used to establish the CSR1000 core 3-D transient calculation model, and to analyse the transient performance of the core in CR dropping into core transient processes, and to evaluate the safety performance of the core under CR drop transient conditions. STTA is developed by coupling 3-D neutron spatial kinetics code NGFMN_K and sub-channel thermal-hydraulics code ATHAS. Nodal Green's Function Method based on the second boundary condition is used for solving transient neutron diffusion equation. The Dynamic Link Libraries method is adopted for coupling computation for SCWR multi-flow core transient analysis. The reliability and applicability of STTA are preliminarily validated by the NEACRP-L-335 PWR benchmark problem and SCWR rod ejection problems. The numerical results show that STTA meets the requisition of code for SCWR core 3-D transient preliminary analysis [4].

IV. CR DRop Transient Analysis

IV.A High worth CR drop

The initial power of CSR1000 core under HFP condition is 2300 MWt (normal power, NP), and the time when the CR drop problem occurs is selected as the beginning of life with equilibrium xenon (BLX, 2 EFPD). At this time, the control rod positions of each group in the core are shown in Figure 2, and the core radial power distribution is shown in Figure 3. The core radial power peak factor (PPF) is 1.414, which appears at the E12 position.

Figure 2. Control Rods Initial Position (HFP, BLX)

N 368	Q3 420	O 420					
	P 18	M 368	Q4 420				
H 0	I 420	J 138	K 358	L 338			
E 420	F 28	Q2 420	G 53	K 358	Q4 420		
B 23	C 338	D 0	Q2 420	J 138	M 368	O 420	
A 58	Q1 420	C 338	F 28	I 420	P 18	Q3 420	
	A 58	B 23	E 420	H 0		N 368	

* --- CR group number
** --- Rod position (cm)

Figure 3. Core radial power distribution (HFP, BLX)

	8	9	10	11	12	13	14	15
A	0.500	0.428						
B	1.010	1.073	1.016	0.565				
C	0.943	0.960	1.343	1.272	0.613			
D	0.951	1.192	1.198	1.414	1.228	0.613		
E	1.087	1.012	1.306	1.101	1.414	1.272	0.565	
F	0.832	1.043	0.981	1.306	1.198	1.343	1.016	
G	0.752	0.833	1.043	1.012	1.192	0.960	1.073	0.428
H	0.647	0.752	0.832	1.087	0.951	0.943	1.010	0.500

The value of each CR cluster in CSR1000 core at BLX time under HFP condition is compared. The results show that rod K (with higher initial rod position and larger power share of the fuel assembly (FA) where the CR located) has the larger reactivity worth. Therefore, in high worth CR drop analysis, rod K (D11 position) is assumed as the dropped CR cluster. The starting position of rod K is 358 cm from the bottom of the core, and it drops with a uniform velocity at a speed of 210 cm/s to the ending position of 0 cm. The reactivity worth of rod K is 233 pcm.

The code STTA is used to establish a 3-D core model and calculate the core performance in the process of CR drop transient. At the early stage of the high worth CR drop into the core, the core power is reduced to about 0.9NP at a relatively rapid rate. Later, due to the reactivity feedback of water density, the core power slowly recovers to a new balance.

Figure 4 and Figure 5 show the variation of core power and its variation rate with time in high worth CR drop process without the intervention of protection shutdown, respectively. The core power rapidly decreases to the lowest value of 0.894 NP in 1.5 s, and then slowly recovers to 0.935 NP. During this period, the density of outlet coolant increases from 0.195 g/cm³ to 0.215 g/cm³. The maximum cladding surface temperature (MCST) and maximum central fuel temperature (MCFT) remain basically unchanged. The maximum value of MCST is 680°C, which is lower than the transient safety limit of 850°C. It can be seen that the safety criterion of high worth CR drop into core transient can be satisfied.

In the actual operation of CSR1000, within 1.5 s of the high worth CR drop into the core, the average rate of core power decline is -7.1% NP/s, which exceeds the negative neutron flux change rate (absolute value) high shutdown signal of -5% NP/s (referring to PWR), and will trigger the protection shutdown.

Figure 6 and Figure 7 show the variation of core axial power distribution and FA power with time in high worth CR drop process, respectively. The influence of high worth CR drop into the core has little effect on the core axial power distribution, but the power level of fuel assemblies in the CR dropping area has obviously decreased. At the end of CR drop transient (t=10 s), the core radial PPF is 1.613, which appears in FA M05 at the rotating symmetric position of the dropping rod position D11.

Figure 4. Core power variation with time (high worth CR drop)

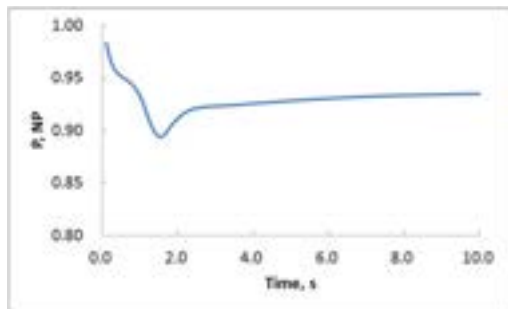


Figure 5. Core power variation rate with time (high worth CR drop)

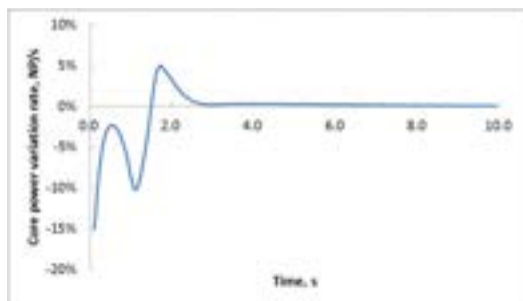


Figure 6. Core axial power distribution (high worth CR drop)

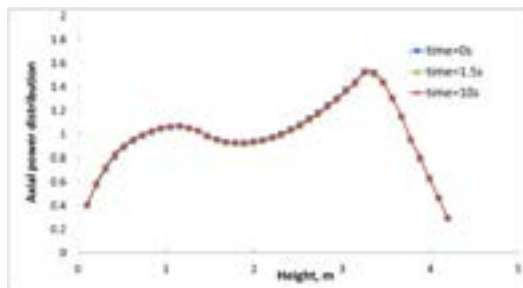
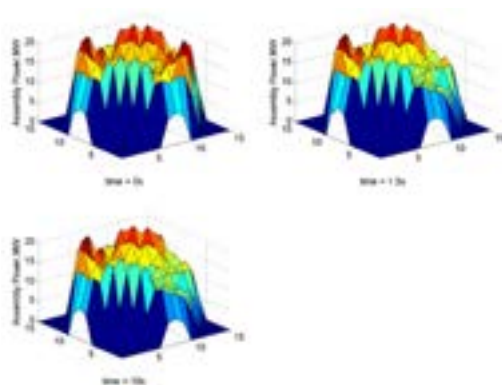


Figure 7. FA power variation with time (high worth CR drop)



IV.B Low worth CR drop

The value of each CR cluster in CSR1000 core at BLX time under HFP condition is compared. The results show that rod O has the smaller reactivity worth. Therefore, in low worth CR drop analysis, rod O (F14 position) is assumed as the dropped CR cluster. The starting position of rod O is 420 cm from the bottom of the core, and it drops with a uniform velocity at a speed of 210 cm/s to the ending position of 0 cm. The reactivity worth of rod K is 116 pcm.

The code STTA is used to establish a 3-D core model and calculate the core performance in the process of CR drop transient. In the process of low worth CR drop into the core, the core power decreases slowly due to the reactivity feedback of water density. Figure 8 and Figure 9 show the variation of core power and its variation rate with time in low worth CR drop process without the intervention of protection shutdown, respectively. The core power decreases slowly in the process of low worth CR drop. At 3.5 s, the core power drop rate reaches the maximum value, which is only -1% NP/s, failing to reach the negative neutron flux change rate (absolute value) high shutdown signal of -5% NP/s, and cannot trigger the protection shutdown signal.

Even without the protection shutdown intervention, due to the reactivity feedback of water density, the core power decreases slowly, and only drops to 0.967 NP at 10 s after rod dropping. During this period, the density of outlet coolant increases from 0.195 g/cm³ to 0.203 g/cm³. The MCST and MCFT remain basically unchanged. The maximum value of MCST is 680°C, which is lower than the transient safety limit of 850°C. It can be seen that the safety criterion of low worth CR drop into core transient can be satisfied.

Figure 8. Core power variation with time (low worth CR drop)

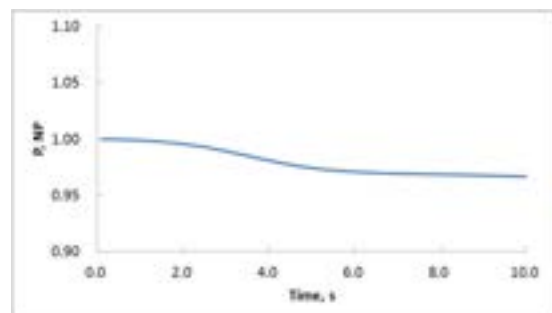


Figure 9. Core power variation rate with time (low worth CR drop)

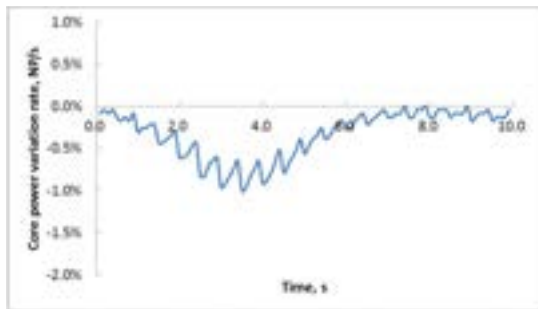


Figure 10. Core axial power distribution (low worth CR drop)

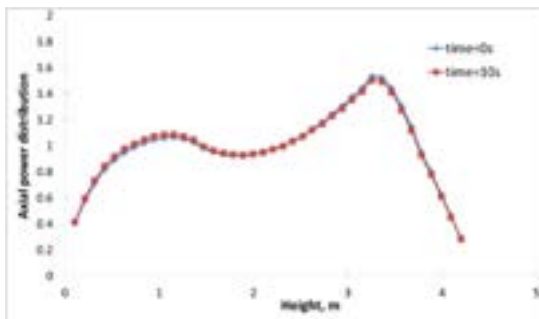


Figure 11. FA power variation with time (low worth CR drop)

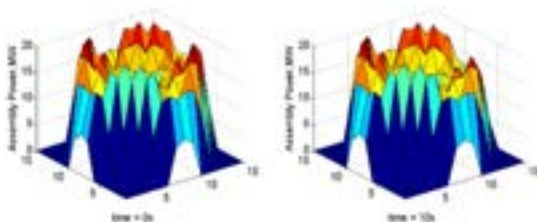


Figure 10 and Figure 11 show the variation of core axial power distribution and FA power with time in low worth CR drop process, respectively. The influence of low worth CR drop into the core has little effect on the core axial power distribution, and the power level of the FA in the rod dropping area collapses, but it is not as obvious as the high worth rod drop. At the end of CR drop transient ($t=10$ s), the core radial PPF is 1.535, which appears in FA L04. Due to the smaller worth of rod O, the radial power peak does not appear in the rotating symmetric position of the dropping rod position F14, but appears in the position of the high power FA with the symmetry quadrant of the dropping rod.

V. Conclusion

In this paper, the SCWR core three dimensional transient analysis method is firstly adopted to study and analyse the CSR1000 core performance during the transient process of CR drop into the core. The safety performance of CSR1000 core is studied for the unprotected CR drop in both high and low CR reactivity cases. While the high worth CR drop into the core, the core power decreases rapidly in the early stage of the CR drop process. After that, due to the reactivity feedback of water density, the core power slowly recovers to a new balance. The core power descent rate exceeds the negative neutron flux change rate (absolute value) high shutdown setting value, which, under normal operating conditions will trigger the protection shutdown. While the low worth CR drop into the core, due to the reactivity feedback of the water density, the core power decreases slowly, and the core power descent rate cannot reach the shutdown setting value, which will not trigger the protection shutdown under normal operation conditions. The CR drop into the core has little influence on the axial power distribution. The power collapse of FA in the CR drop area is more obvious than the low worth CR drop caused by the high worth CR drop. In the CR drop transient process, the peak value of MCST retains lower than the transient safety limit of 850°C , whether it is a high worth CR drop or a low worth CR drop. The 3-D CR drop transient analysis shows that the safety performance of CSR1000 core can be ensured in the process of CR drop into the core under the salient reactivity feedback of water density and the essential reactor protection system.

Nomenclature

ATHAS	Advanced Thermal-Hydraulics Analysis Sub-channel
BLX	Beginning of Life with equilibrium Xenon
BWR	Boiling Water Reactor
CR	Control Rod
CSR1000	China Supercritical Water-cooled Reactor with the rated electric power of 1000MWe
EFPD	Effective Full Power Days
FA	Fuel Assembly
HFP	Hot Full Power
MCFT	Maximum Central Fuel Temperature
MCST	Maximum Cladding Surface Temperature

NGFMN_K	Nodal Green's Function Method based on Neumann boundary condition for kinetics	PWR	Pressurised Water Reactor
NP	Normal Power	SCWR	Supercritical Water-cooled Reactor
PPF	Power Peak Factor	STTA	SCWR Three dimensional Transient Analysis code

References

- [1] Wang, L., Yang, P., Lu, D., et al. Study on Optimization Design for CSR1000 Core [J]. Journal of Nuclear Engineering and Radiation Science, 2018, 4(1), p. 011013.
- [2] Ishiwatari Y, Oka Y, Koshizuka S., et al. Safety of Super LWR, (I) Safety System Design [J]. Journal of Nuclear Science and Technology, 2005, 42(11): 927-934.
- [3] Oka Y, Koshizuka S , Ishiwatari Y, et al .Super Light Water Reactors and Super Fast Reactors [M]. Springer New York Dordrecht Heidelberg London, 2010:210-217.
- [4] Wang L., Zhao W., Chen B., et al. Development of three dimensional transient analysis code STTA for SCWR core [J]. Journal of Annals of Nuclear Energy, 2015, 78: 26–32.

PROGRESS IN GFR TECHNOLOGY (B. HATALA ET AL)

Branislav Hatala⁽¹⁾, Boris Kvizda⁽¹⁾, Alfredo Vasile⁽²⁾, Janos Gado⁽³⁾, Ladislav Belovsky⁽⁴⁾

(1) VUJE , a.s., Slovak Republic.

(2) CEA, France.

(3) 2 MTA EK, Budapest, Hungary.

(4) ÚJV řež, a. s., Czech Republic.

Abstract

The Gas-cooled Fast Reactor (GFR) system features a high temperature helium cooled fast spectrum reactor that can be part of a closed fuel cycle. The GFR cooled by helium is proposed as a longer-term alternative to liquid-metal cooled fast reactors. This type of innovative nuclear system has several attractive features: The helium is a single phase, chemically inert, and transparent coolant. The high core outlet temperature above 750°C (typically 800-850°C) is an added value of GFR technology.

The reference GIF concept for GFR is a 2400 MWth plant operating with a core outlet temperature of 850°C enabling an indirect combined gas-steam cycle to be driven via three intermediate heat exchangers. The high core outlet temperature places onerous demands on the capability of the fuel to operate continuously with the high power density necessary for good neutron economy in a fast reactor core. This represents the biggest challenge in the development of the GFR system. The second significant challenge for GFR is ensuring decay heat removal in all anticipated operational and fault conditions. A necessary step in the development of a commercial GFR is the establishment of an experimental demonstration reactor for qualification of the refractory fuel elements and for a full-scale demonstration of the GFR-specific safety systems. The proposed demonstration reactor for the reference GIF GFR concept will be ALLEGRO.

I. Introduction

In order to make nuclear energy production sustainable, the development and deployment of fast reactors is inevitable. Therefore a worldwide cooperation in research and development of fast reactors has been restarted with the participation of the most significant countries applying nuclear energy. Three of the six Generation IV systems proposed in the original roadmap were fast reactors. All of the fast reactors are required to operate in closed fuel cycle burning plutonium and converting uranium-238 into plutonium through a breeding reaction which occurs in their cores.

The main advantages of Gas-cooled Fast Reactors (GFRs) beside the closed fuel cycle are:

- High operating temperature, allowing increased thermal efficiency and high

temperature heat for industrial applications

- Low value of the void coefficient
- Helium is a chemically inert and a non-corrosive coolant
- Helium is transparent, facilitating in service inspection and repair.

The main drawbacks are related to:

- The need to operate under pressurised conditions
- The low cooling efficiency of Helium, in particular in natural convection.

This paper illustrates the technical progress achieved in the countries participating to the GIF effort on the GFR system.

I. GFR Reference Concept

The reference concept for GFR is a 2400 MW_{th} plant having a core, operating with a core outlet temperature of 850°C [1]. It is proposed as an indirect combined gas-steam cycle to be driven via three intermediate heat exchangers. The high core outlet temperature places onerous demands on the capability of the fuel to operate continuously with the high power density necessary for good neutron economics in a fast reactor core. The core consists of an assembly of hexagonal fuel elements, each consisting of ceramic-clad, mixed-carbide-fuelled pins contained within a ceramic hex-tube. The favoured material at the moment for the pin clad and hextubes is silicon carbide fibre reinforced by amorphous silicon carbide (SiCf/SiC). The whole primary circuit with three loops is contained within an additional pressure boundary, the guard containment. The produced heat is converted into electricity in the indirect combined cycle with three gas turbines and one steam turbine. The cycle efficiency is approximately 48%. A heat exchanger transfers the heat from the primary helium coolant to a secondary gas cycle containing a helium-nitrogen mixture. The waste heat from the gas turbine exhaust is used to raise steam in a steam generator, which is then used to drive a steam turbine. Such a combined cycle is common practice in natural gas-fired power plants so represents an established technology, with the only difference in the GFR case being the use of a closed cycle gas turbine.

The main characteristics of the reference concept for GFR are summarised in the table 1.

The viability of the GFR technology shall be demonstrated by constructing and operating the ALLEGRO reactor. ALLEGRO shall be used not only for technology demonstration but also for the development and qualification of innovative components & systems, first of all the refractory fuel (UPuC pellets in SiC-SiCf cladding).

Table 1. Reference design characteristics of the GFR

GFR Reference main characteristics	
Nominal Power - Thermal	2400 MW _{th}
Nominal Power - Electrical	1150 MWe
Fuel / Cladding	UPuC / SiC-SiCf
Power density	100 MW/m ³
Pu content	16,3%
Breeding gain	0
Number of primary loops	3
Primary coolant	Helium
Primary pressure	7 MPa
Core inlet / outlet temperature	400°C / 850°C
Number of secondary loops	3
Secondary coolant	Helium-Nitrogen
Secondary pressure	6,5 MPa
Power Conversion system	Closed cycle gas turbine and Steam Generator

II. V4G4 Centre of Excellence

Central European members of the European Union, the Czech Republic, Hungary and Slovakia are traditionally prominent users of nuclear energy. They intend to use nuclear energy on the long run and besides the lifetime extension of their nuclear units, each country decided to build new units in the coming years.

Four nuclear research institutes and companies of the Visegrad-4 region (ÚJV Rež, a.s. - Czech Republic, MTA EK - Hungary, NCBJ - Poland, VUJE, a.s. - Slovak Republic) decided to start joint preparations aiming at the construction and operation of the demonstrator (ALLEGRO) of the concept of Generation IV gas-cooled fast reactor (GFR) based on a Memorandum of Understanding signed in 2010. CEA, France, as promoter of the GFR concept since 2000, supports the joint preparations, bringing its Knowledge and its experience in building and operating experimental reactors in particular fast reactors.

In order to study safety and design issues and also the medium and long-term governance and financial issues, the four aforementioned organisations created in July 2013 a legal entity, the V4G4 Centre of Excellence, which performed the preparatory works needed to launch the ALLEGRO Project. V4G4 Centre of Excellence is also in charge of the international representation of the project.

As a result of the preparatory works it turned out that during the earlier works certain safety and design issues remain unsolved and in several aspects a new ALLEGRO design has to be elaborated. Therefore in 2015, when the ALLEGRO Project was launched, a detailed technical program was established with a new time schedule.

In 2015 the Design and Safety Roadmap of the Preparatory Phase was approved. It consists of 47 tasks (most of them divided into sub-tasks). The task leading organisation and the contributing organisations are given. The objective of the (sub-) tasks is defined. The level to be reached at the various stages of the design is determined and some further information is also provided.

During the Definition of the basic safety and performance goals the documents ALLEGRO Design Specification as well as the ALLEGRO Safety Requirements were approved. The basic system data were specified in ALLEGRO V4G4 Concept Database.

During the Pre-conceptual design phase the options of the new design will be preliminarily chosen and finally the Introductory Safety Analysis Report will be prepared.

During the Conceptual design phase the main design options will be decided and justified and the Preliminary Safety Analysis Report will be elaborated. The needs for system qualification will be fixed.

During the Preparatory Phase national nuclear R&D projects and EURATOM projects will provide the main source of funding of Design/Safety activities. The positive example is Hungary, where a national nuclear R&D project covers the Hungarian contribution for 2015-2018, and Slovakia, where a national nuclear R&D project covered the first stage of activities. In Slovakia and the Czech Republic similar projects are under preparation. In the Czech Republic the SUSEN project financed by the EU Structural Funds is already running. In Poland, government recently announced the programme to deploy thermal High Temperature Gas-cooled Reactors (HTGR) to provide industrial heat. This will create additional possibilities for development of nuclear helium cooled systems.

The ALLEGRO Project is controlled by the V4G4 Steering Committee. In order to organise the joint activities a Project Coordination Team is established. It is the forum of harmonising activities of the various national and international projects with the tasks of the

Design and Safety Roadmap. In order to prepare solutions for legal issues a Working Group on Governance and Financing was also established.

III. ALLEGRO Objective and Mission

The ALLEGRO demonstrator is an essential step to establish confidence in the innovative Gas Cooled Fast Reactor (GFR) technology. The development of ALLEGRO is supported by the European Sustainable Nuclear Energy Technology Platform (SNETP) [2]. The European Sustainable Nuclear Industrial Initiative (ESNII) as a one pillar of SNETP addresses the need for demonstration of Generation IV Fast Neutron Reactor technologies.

The proposed demonstrator, would be the first ever gas cooled fast reactor to be constructed. The ALLEGRO was originally designed by the French Alternative Energies and Atomic Energy Commission (CEA) [3], [4], [5] among others under EU financed GOFASTR project and it is successor of ETDR 50 MW concept [6].

The objectives of ALLEGRO are to demonstrate the viability and to qualify specific GFR technologies such as fuel, the fuel elements, helium-related technologies and specific safety systems, in particular, the decay heat removal function, together with demonstration that these features can be integrated successfully into a representative system. The demonstration of the GFR technology assumes that the basic features of the GFR commercial reactor can be tested in the 75 MWth ALLEGRO and it will not produce any electricity.

The original design of the ALLEGRO consists of two He primary circuits, three decay heat removal (DHR) loops integrated in a pressurised cylindrical guard vessel (Figure 1). The two secondary gas circuits are connected to gas-air heat exchangers. The ALLEGRO reactor would function not only as a demonstration reactor hosting GFR technological experiments, but also as a test pad of using the high temperature coolant of the reactor in a heat exchanger for generating process heat for industrial applications and a research facility which, thanks to the fast neutron spectrum, makes it attractive for fuel and material development and testing of some special devices or other research works.

The 75 MWth reactor shall be operated with two different cores (Figure 2). The starting core with UOX or MOX fuel in stainless steel claddings will serve as a driving core for six experimental fuel assemblies containing the advanced

carbide (ceramic) fuel. The second core will consist solely of the ceramic fuel and will enable to operate ALLEGRO at the high target temperature.

Fuel development to satisfy the needs of a GFR is one of the basic goals of the ALLEGRO project. Safety considerations may strongly influence the fuel development.

Figure 1. ALLEGRO Systems

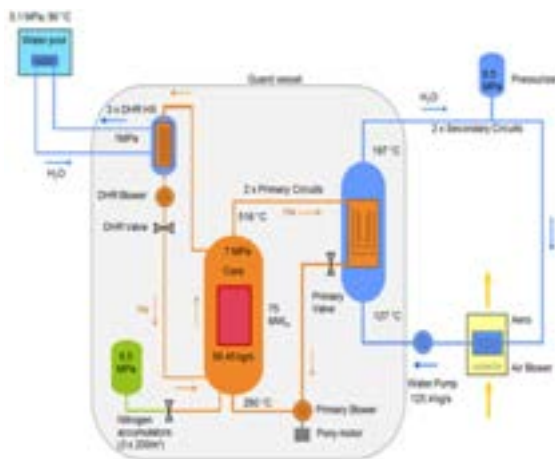


Figure 2. First ALLEGRO reactor core

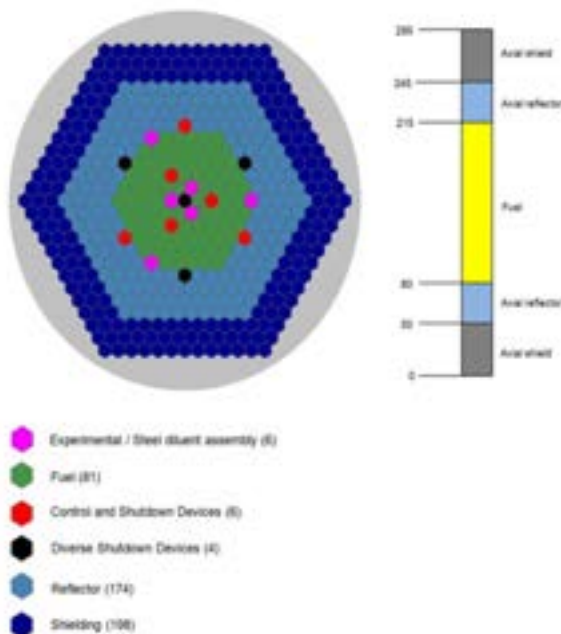


Table 2. ALLEGRO main design characteristics

ALLEGRO main design characteristics		
Nominal Power - Thermal	75 MW _{th}	Reduced power is being considered in the range 30 – 75 MW.
Nominal Power - Electrical	0 MWe	
Fuel / Cladding	UPuC / SiC-SiCf	
Power density	100 MW/m ³	Reduced power density is being considered in the range 50 – 75 MW/m ³ .
Fuel	MOX/SS cladding	Start-up core. Feasibility of LEU UOX for the start-up core is being investigated.
	UPuC/ SiC/SiCf cladding	Long term core
Number of primary loops	2	
Primary coolant	Helium	
Primary pressure	7 MPa	
Number of secondary loops	2	
Secondary coolant	Water	
Secondary pressure	6,5 MPa	

Fuel and core design issues

Gas-cooled Fast Reactors will be fuelled with so called refractory fuel. ALLEGRO cannot use this type of fuel from the very beginning since this fuel is not developed and cannot be qualified without irradiations in GFR conditions and the subsequent post irradiation examinations. Therefore, according to previous considerations the first cores will be built up from stainless steel clad fast reactor oxide fuel. Some core positions will be reserved for the development of the refractory fuels through the irradiation of fragments, rods and sub-assemblies. In these positions an elevated helium outlet temperature (800-850°C) is created by reducing the coolant flow rate.

A serious problem may emerge if ALLEGRO (or any other Generation IV reactor) is built in V4 countries. This is because qualification and use of MOX fuel involves several legal and proliferation issues. In order to overcome these potential difficulties, now it is investigated whether using low enriched UOX pellets a can be feasible for ALLEGRO core. It has to be added that the use of low enriched UOX does not solve in itself the future problem of investigating and using refractory Pu-containing fuel.

In the existing design of the ALLEGRO core, safety and control rods of identical type are grouped into two independent groups of absorbers. In order to increase the safety of core design a completely diverse type of absorber has to be developed which would be activated purely by physical principles in a completely passive manner.

Decay heat removal issues

Decay heat removal in accident conditions is one of the crucial challenges in design of a GFR reactor because of low thermal inertia of the reactor system and relatively high volumetric power density, one order of magnitude higher in comparison with Very-High-Temperature Reactor (VHTR). The situation in ALLEGRO is further complicated by the wide use of stainless steel in the driver (start-up) core, because e.g. the 15-15Ti (AIM1) stainless steel claddings start to melt already at $\sim 1320^{\circ}\text{C}$. The acceptance criterion (temperature) for fuel rod failure is even lower.

Specific loops for decay heat removal in case of emergency are directly connected to the primary circuit using a cross duct piping, in extension of the pressure vessel, and are equipped with heat exchangers and forced convection devices. This system arrangement allows the residual power to be extracted safely in many accidental situations. In addition, thanks to the low pressure drop of the core design, a passive gas natural circulation can be used in most of the situations.

The original concept of decay heat removal in the 75 MW_{th} ALLEGRO CEA 2009 ($\sim 100 \text{ MWt/m}^3$ power density) was mainly based on active elements in the decay heat removal (DHR) system, and its malfunction in some cases can easily result in core melting. As the increased use of passive features in safety systems is a pre-requisite of licensing a Generation IV reactor after the Fukushima accident [7], a new concept of combined active-passive DHR system has to be developed. This is why there are several potential elements of the new DHR system under development.

IV. ALLEGRO Needs for Development

Starting from a reference design studied at CEA prior to 2009, the project explored a new target of nominal power (in the range of 30 – 75 MW thermal) and power density (in the range 50 – 100 MW/m³) compatible with the safety limits and the design requirements. At the same time, the feasibility of a low enriched UOX start-up

core as alternative to a standard MOX core is being considered. This start-up core, to be used in the first period of the reactor operation, will include experimental positions dedicated to the refractory fuel development. The development of an acceptable fuel system that meets the target criteria (1000°C normal operation cladding temperature, no fission product release at 1600°C cladding temperature during a few hours, and maintaining the core-cooling capability up to 2000°C clad temperature) is a Key viability issue for the GFR system. It is necessary to develop an initial cladding material that meets the core specifications in terms of length, diameter, surface roughness, apparent ductility, level of leak tightness (including the potential need of a metallic liner on the cladding), compatibility with helium coolant (plus impurities), and the anticipated irradiation conditions. The needs include fabrication capacities and material characterisation under normal and accidental conditions for fresh and irradiated fuel.

The GFR also requires a specific dense fuel element that can withstand very high temperature transients, due to the lack of thermal inertia of the system. UPuC pins fabrication methods, as well as their behaviour under irradiation must be studied. Ceramic or refractory metal clad should be selected, developed and qualified. Such a programme requires material properties measurements, selection of different materials, their arrangement and their interaction, out-of pile and in-pile tests up to qualification, as well as demonstration tests.

The specific operating conditions of the ALLEGRO oxide fuel pins (viz. maximum fuel temperature below 1000°C, linear pin power below 100 W/cm) are not covered by fuel pin behaviour codes. The results of such codes, appeared to be very sensitive to fission gas release predictions. In this context, a programme of post-irradiation examinations on selected pins of the in PHENIX Sodium Fast Reactor irradiated CPed6106 standard fuel subassembly is suitable for obtaining experimental data on fission gas release for operating conditions similar to those foreseen for the ALLEGRO oxide core fuel pins. Alternatively, a specific irradiation program in other potentially available fast reactors (e.g. JOYO, BOR60, or MBIR) could be envisaged.

In addition to the qualification of the oxide fuel, the reference GFR fuel (i.e. carbide fuel with composite SiC and fiber reinforced SiC clad) development efforts must continue. In

particular, it is necessary to develop a ceramic clad that meets the specifications in terms of length, diameter, surface roughness, apparent ductility, level of leak tightness (including the potential need of a metallic liner on the clad), compatibility with polluted helium, and with the irradiation conditions. The needs include fabrication capacities and material characterisation under normal and accidental conditions for fresh and irradiated fuel.

In the area of neutronics, existing calculation tools and nuclear data libraries have to be validated for gas-cooled fast reactor designs. The wide range of validation studies on sodium-cooled fast reactors must be complemented by specific experiments that incorporate the unique aspects of gas-cooled designs: slightly different spectral conditions, innovative materials and various ceramic materials (UC, PuC, SiC, ZrC, Zr₃Si₂). In addition some unique abnormal conditions (e.g. depressurisation, steam ingress, etc.) must be considered.

Given the high temperature environment of the ALLEGRO ceramic core, the design margins considered in terms of material characteristics, as well as in the applied thermal hydraulics correlations must be as low as possible. Therefore, air, followed by helium tests on subassembly mock-ups under representative temperature and pressure conditions are necessary to assess the heat transfer and pressure drop uncertainties for the specific GFR design.

Moreover, large-scale air and helium tests to demonstrate the passive decay heat removal function will be required for the licensing process of ALLEGRO.

V. Conclusion

Fast reactors will play a significant role in developing of the sustainable use of nuclear energy. Nuclear energy remains a decisive component of electricity production in the 21st century. With the Central European Consortium project ALLEGRO is now becoming a wider European project and it is our hope, that ALLEGRO can fulfil the role as a European GFR technology demonstrator and fast neutron irradiation facility as well. In the framework of the Visegrád cooperation the relevant European governments (of the Czech Republic, Hungary, Slovak Republic and Poland) have already started to discuss hosting the GFR ALLEGRO in the region.

Acknowledgements

Project Allegro has been done by V4G4 Centre of Excellence with the aim to involve scientists, researchers and technicians from this region into research activities.

Nomenclature

DHR	Decay Heat Removal
GFR	Gas-cooled Fast Reactor
GIF	Generation IV International Forum
MOX	Mix Oxide
VHTR	Very-High-Temperature Reactor
UOX	Uranium Oxide

References

- [1] C. Poette et al., Gas Cooled Fast Reactors: recent advances and prospect, FR13, Paris, 4-7 March 2013.
- [2] Strategic Research and Innovation Agenda, SNEPT, February 2013.
- [3] C. Poette: ALLEGRO Preliminary Viability Report. CEA/DEN/CAD/DER/SESI/LCSI NT-DO12, December 2009.
- [4] C. Poette, F. Morin: Contribution to ALLEGRO Viability Report. FP7 GoFastR Project, Deliverable D1.2-10, 2012.
- [5] C. Poette, R. Stainby: ALLEGRO 75 MW system definition at start of GOFASTR, November 2010.
- [6] C. Poette, J.C. Garnier, J.C. Klein, F. Morin, A. Tosello, I. Dor, F. Bertrand, C. Mitchell, D. Every, P. Coddington, 2007. Status of the ETDR desing. In: Proceedings of the 2007 International Congress on Advanced in Nuclear Power Plants – ICAPP'07, May 13-18. Nice Acropolis, France.
- [7] Technology Roadmap Update for Generation IV Nuclear Energy Systems. OECD NEA for the Generation IV International Forum, January 2014.

PAST, PRESENT AND FUTURE OF SCWR DEVELOPMENT IN CANADA (L. K. H. LEUNG ET AL)

L. K. H. Leung⁽¹⁾, D. Brady⁽²⁾ and K. Huynh⁽³⁾

(1) Canadian Nuclear Laboratories, Canada.

(2) Natural Resources Canada, Canada.

(3) Atomic Energy of Canada Limited, Canada.

Abstract

Canada initiated the Generation-IV National Program in 2005 to support the research and development (R&D) at federal laboratories and agencies, and Canadian academia. Significant achievements were accomplished over the past decade. These achievements include the success in developing a conceptual Super-Critical Water-cooled Reactor (SCWR) design, establishing new infrastructures for nuclear R&D and training of Highly Qualified Personnel for nuclear and non-nuclear industries. The current program, supported by AECL's Federal Nuclear Science and Technology (FNST) Work Plan, focuses on the associated R&D of SCWR and its application to other advanced reactors, including Small Modular Reactors, in support of Canada's priorities and continued collaboration with SCWR partners. A number of joint projects with SCWR partners have been identified for the next decade. These projects include the in-reactor materials and fuel testing, and the integral safety testing, which could be used to support the development of a SCWR prototype. A summary of past achievements, current activities and the future interests of Canada's SCWR program is presented.

I. Introduction

Canada is one of the founding members of the Generation-IV International Forum (GIF) to support the development of the next generation nuclear reactor systems. Canada signed the Charter in 2001 with nine other members and the Framework Agreement in 2005 with five other members. Both the Charter and the Framework Agreement have been renewed in 2011 and 2015, respectively [1].

Canada's participation in the GIF aims to achieve strategic goals in energy and resource prosperity, enhanced security, safety, and environmental sustainability [2]. Canada has been an active partner within the GIF with representatives in the Policy Group, Experts Group, three cross-cutting working groups and various task forces.

The GIF selected six advanced nuclear systems for joint R&D collaboration [1]. Canada's participation focuses mainly on the Super-Critical Water-cooled Reactor (SCWR) and signed the System Arrangement in 2006 with

Japan and European Union. The System Arrangement was renewed in 2016 with four partners (i.e., China, Euratom, Japan and the Russian Federation). Two projects have been initiated within the SCWR System: 1) thermal-hydraulics and safety project, and 2) materials and chemistry project. Their respective Project Arrangements were signed in 2007 and renewed in 2017.

In addition to the SCWR, Canada participated in the Very High Temperature Reactor (VHTR) System through the Materials and the Hydrogen Production Projects. These projects were synergistic to the development of the SCWR. In 2012, Canada decided to focus its R&D effort on the SCWR and withdrew from the VHTR System and the Materials Project but remains an active participant in the Hydrogen Production Project.

Over the past decade, significant achievements were accomplished in the development of the SCWR concept and supporting research. The objective of this paper is to present the past

achievements, current activities and future interests of Canada's SCWR program.

II. Canada's Generation-IV National Program

A national program (referred to as the Generation-IV National Program) was initiated in 2005 to support the R&D for Gen-IV nuclear systems at federal laboratories and agencies, and Canadian academia [2]. It was separated into two phases and was managed by Natural Resources Canada (NRCAN). The first phase (Phase I) focused on the basic research over three years from 2008 April to 2011 March. Participants in this phase built their capability, developed new analytical tools and enhanced their Knowledge bases to support the development of SCWR concept (e.g., thermal-hydraulics and safety R&D [3]). Several preliminary concepts were reviewed before deciding on a reference concept, the Canadian SCWR, for pursuing [4]. The second phase (Phase II) focused on applied research covering four years from 2011 April to 2015 March. R&D in this phase covered all relevant technology areas that were directly applicable to the development of the Canadian SCWR concept (e.g., thermal-hydraulics and safety R&D [5]).

NRCAN recognised the training aspect of the Generation-IV National program and engaged the Natural Science and Engineering Research Council (NSERC) in establishing a Gen-IV University program to support the SCWR development [5]. Atomic Energy of Canada

Limited (AECL) participated in the program to provide technical support to university researchers. Similar to the national program, the university program was held in two phases; the first phase from 2009 March to 2012 February and the second phase from 2012 March to 2016 February. The interest was overwhelming with over twenty universities participating in the program. Figure 1 shows the participating universities in the Gen-IV University Program. Some of these universities had not been participating in nuclear research before joining the program and provided an opportunity for universities to expand their capability to support the nuclear industry.

After completing the Phase-II Program, the development of the SCWR concept is continuing with the confirmatory R&D phase through AECL's Federal Nuclear Science and Technology Program. R&D findings are contributed to GIF SCWR System in support of Canada's participation.

III. Achievements of Canada's National Program

Studies of Canada's National Program focused on the development of the Canadian SCWR concept and associated research in various technology areas. A number of technical advancements have been achieved. Selected achievements are described in the following sections.

Figure 1. Canadian Universities that Participated in the Gen-IV University Program



III.1 Canadian SCWR concept

One of the significant achievements of Canada's National Program is the development of the Canadian SCWR concept, which evolved from the CANDU¹ and Boiling Water Reactors. The core concept is based on the pressure-tube configuration that separates the coolant from the moderator [4]. Figure 2 illustrates the Canadian SCWR core concept.

Figure 2. Canadian SCWR Core Concept



The core consists of 336 fuel channels, which are submerged inside the low-pressure heavy-water moderator in the calandria vessel. Each fuel channel is welded to the tubesheet of the inlet plenum and is connected to the outlet header, which is installed inside the inlet plenum to minimise the temperature and pressure gradients over the header wall. The configuration of the inlet plenum is similar to that of a pressure vessel. However, the inlet plenum is not located in the active zone to avoid any potential damage to the material due to radiation. The coolant enters the core at the temperature of 350°C and discharges directly to the high-pressure turbine at the temperature of 625°C (direct cycle). This high outlet temperature has led to an increase in efficiency

to 48% (compared to 35% of the current nuclear reactor system). The increase in efficiency would reduce the use of fuel and hence the generation of spent fuel (enhanced sustainability) and the number of plants required for the same power (enhanced economics).

The fuel concept for the Canadian SCWR consists of a “flask”-like structure that contains the fuel assembly [7]. Several nozzles are introduced for the coolant entering into the structure. These nozzles also serve as orifices to control the flow rate matching the power generation in the channel (another set of openings are also installed at the top of the pressure tube). The fuel assembly consists of two rings of 32 fuel rods and an active length of 5 metres. Spacing between fuel rods is maintained with a wire-wrapped spacer. A central flow tube is installed for the coolant to travel down from the nozzles to the bottom of the fuel channel. Furthermore, it improves the moderation for the inner-ring rods resulting in a balanced radial power profile. The coolant travels upward through the fuel assembly to the outlet header, and is discharged to the high-pressure turbine.

A mixture of thorium and plutonium (on 15 wt% on average) is selected as the reference fuel for the pellets of the Canadian SCWR [8]. However, other fuel types (such as enriched uranium, thorium with enriched uranium, thorium with U-233 and mixed oxide) can also be adopted [9]. The use of thorium fuel would enhance the economics, safety, sustainability and proliferation resistance characteristics of the Canadian SCWR concept [10].

The development of the Canadian SCWR plant concept was based on the Advanced Boiling Water Reactor [11]. As indicated above, a direct thermal cycle has been adopted eliminating the need of steam generators, as in pressurised water reactors, or recirculation pumps and moisture separator reheaters, as in boiling water reactors. This has led to more compact containment and reactor building.

Figure 3 illustrates the Canadian SCWR plant concept. Passive heat-removal systems have been introduced to the plant configuration. In particular, the passive moderator-cooling system could continuously remove heat from fuel and clad during large-break loss-of-coolant

¹ CANDU – Canada Deuterium Uranium (a registered trademark of Atomic Energy of Canada Limited)

accidents or station blackout events. It facilitates achieving potentially the “no-core-melt” safety design goal for the Canadian SCWR. Heat is transferred to the reserved water pool, which is connected to heat exchangers installed externally near the top of the reactor building. Ambient air is the ultimate heat sink to these heat exchangers.

The Canadian SCWR concept was reviewed by peers in the Canadian nuclear industry in 2015 and in the international SCWR community in 2017. It has been identified as a viable option for continuing the development. Several improvements were suggested.

Figure 3. Canadian SCWR Plant Concept



III.2 Technological advancements

Canada’s National Program supported the advancement in technology areas relevant to the development of the Canadian SCWR concept. The main interest is focused on materials, chemistry, thermal-hydraulics and

safety, where two Project Arrangements have been signed with GIF SCWR partners. Other studies related to reactor physics, fuel and fuel channel were also performed.

An extensive database on materials was compiled and used in selecting the reference materials for various components of the Canadian SCWR (i.e., in-core and out-of-core components). The major challenge is related to the selection of the cladding material, which encounters the highest temperature in the core. Technical information on material properties has been compiled for five potential candidates for cladding material [12]. Table 1 lists ranking of these candidates based on material properties.

The density of the water reduces drastically through the pseudo-critical temperature point at supercritical pressures. This has led to a significant change in chemical properties of the coolant. Furthermore, the in-core radiolysis behaviours in the SCWR are different from those of conventional water-cooled reactors [13]. This would have an impact on corrosion and stress corrosion cracking. A chemistry strategy has been developed to minimise corrosion rates, stress corrosion cracking and deposition on fuel cladding and turbine blades.

An extensive heat transfer database has been compiled for water and surrogate fluid in tubes, annuli and bundles at supercritical pressures [14]. These data were applied in verification and development of prediction methods for subchannel codes and system codes, as well as in validation of computational fluid dynamics tools.

Table 1. Ranking of Candidate Cladding Materials for SCWRs

Alloy	Property							
	Corrosion	Oxide Thickness	SCC (un-irradiated)	IASCC	Creep	Void Swelling	Ductility (4% elongation)	Strength
800H	GREEN	YELLOW	YELLOW	YELLOW	GREEN	GREEN	GREY	YELLOW
310S	GREEN	GREEN	YELLOW	GREY	GREEN	YELLOW	GREY	YELLOW
625	GREEN	GREEN	YELLOW	YELLOW	GREEN	GREEN	GREY	GREEN
347	GREEN	YELLOW	YELLOW	YELLOW	GREEN	RED	GREY	GREEN
214	GREEN	GREEN	GREY	GREY	GREY	YELLOW	GREY	RED

- GREEN – Available data suggest that this alloy meets the performance criteria under all conditions expected in the core
- YELLOW – Some (or all) available data suggest that this alloy may not meet the performance criteria under some conditions expected in the core
- RED - Some (or all) available data suggest that this alloy will not meet the performance criteria under some conditions expected in the core
- GREY – There are insufficient data to make even an informed guess as to the behavior in an SCWR core

IV. Achievements of Canada's University Program

The University Program was part of Canada's National Program and involved twenty Canadian universities in eight provinces [6]. Experimental and analytical studies were carried out to advance the technology and training of highly qualified personnel for nuclear and non-nuclear industries.

In the first phase of the program, a number of new infrastructures were constructed to support R&D activities on materials, chemistry, thermal-hydraulics and safety.

illustrates the new infrastructures constructed in support of materials and chemistry R&D.

These facilities were used to obtain experimental data on corrosion, stress corrosion cracking, and the fluid structure of water at supercritical pressures.

Figure 5 illustrates the new infrastructures for thermal-hydraulics and safety related experiments. Data on heat transfer, and hydraulics resistance for tubes, annuli or bundles with refrigerant and carbon dioxide flows at supercritical pressures were obtained. In addition, stability characteristics in single and parallel channels were examined with carbon dioxide flow and critical flow phenomena was studied with water through different types of nozzle.

Figure 4. Infrastructure Constructed for SCWR Materials and Chemistry R&D

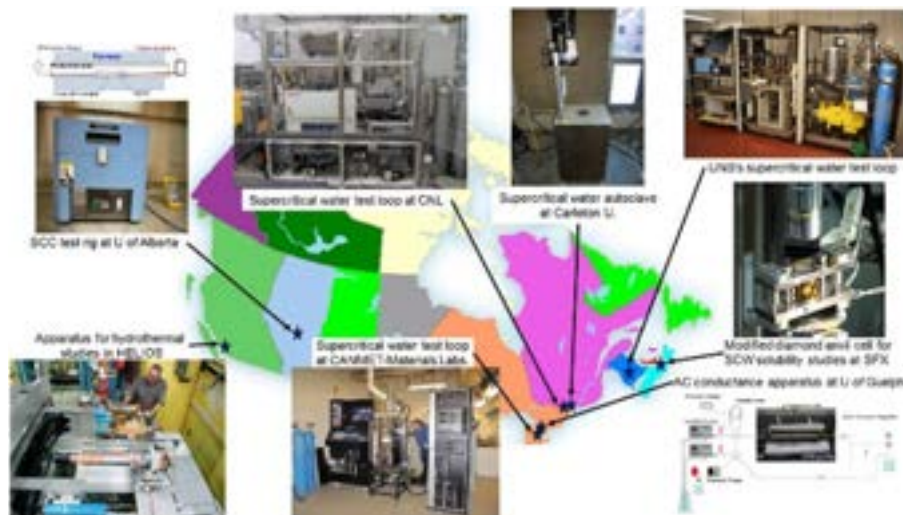
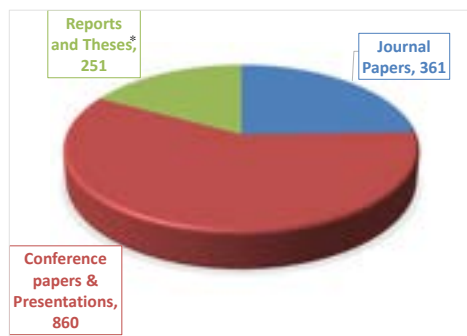


Figure 5. Infrastructure Constructed for SCWR Thermal-Hydraulics and Safety R&D



In addition to providing experimental data, the university program also performed analyses and developed models. Results have been disseminated through journal and conference publications as well as technical reports. Figure 6 shows the number of publications and reports that were generated from the university program.

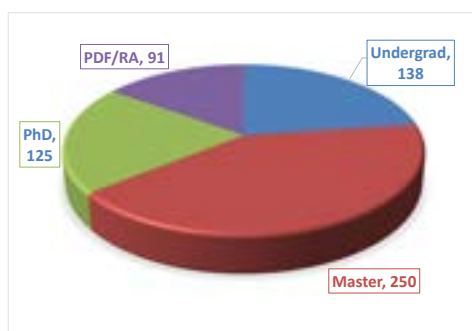
Figure 6. Publications Generated from Canada's Gen-IV University Program



*Number of theses were under-reported

One of the most significant contributions of the university program is the training of highly qualified personnel (which includes undergraduate, Master and Ph.D. students as well as Post-Doctoral Fellows (or PDFs)). Most of these students had not been involved in nuclear research previously. The program provided them the opportunity to get familiar with the technology and understand the benefit of nuclear power generation. Figure 7 illustrates the number of highly qualified personnel trained from the university program. After completing the training, these personnel were employed at nuclear or non-nuclear industries.

Figure 7. Training of Highly Qualified Personnel in Canada's Gen-IV University Program



V. Current Progress

The Canadian SCWR concept is an advanced innovative nuclear system, which has been designed for operating conditions beyond the current fleet of nuclear reactors. A number of simplifying assumptions and extensions of the current experimental databases were applied in various technology areas. The current program focuses on the verification and validation of Key components to strengthen the Canadian SCWR concept. These components include mechanical devices (such as cladding material and insulator of the fuel assembly), manufacturing techniques (such as co-extrusion of stainless-steel and zirconium) and technology areas (such as reactor physics and thermal-hydraulics).

In most cases, the selected components are considered critical in meeting the GIF technology goals (i.e., economics, safety, sustainability, and proliferation resistance). Understandably, it is challenging to verify or validate some components due to availability of experimental set up and/or testing duration (such as reactor physics parameters and fuel burnup). A roadmap has been developed to lay out the strategy, plan and schedule for verification and validation of selected components. It specifies the verification or validation approach (such as experimental, analytical or a combination) to be applied in various technology areas.

Some of the recent achievements include the confirmation of using superheated steam as the surrogate for supercritical water in corrosion testing. This facilitates testing at reduced pressures minimising the facility requirement and expediting the test duration.

Corrosion tests were performed for two different materials in support of the second Round-Robin corrosion testing organised by the GIF SCWR Materials and Chemistry Project Management Board. Test results were submitted to the organiser for comparison against those of other participants.

Canadian researchers participated in several benchmarking exercises of analytical tools for heat transfer in bundles. The results were shared among participants of the benchmarking exercises to understand the tool deficiencies and discuss mitigation strategy.

VI. Future Developments

The development of the Canadian SCWR concept and Canada's participation in GIF are continuing through AECL's Federal Nuclear Science and Technology Program. R&D focus on confirming the advanced components and analytical tools to strengthen the SCWR concept jointly with signatories of the GIF SCWR System. In addition, the feasibility of expanding applications of the SCWR concept is explored.

The Canadian SCWR concept has been developed for large base load power generation of 1200 MWe, which is considered too large for replacing coal-fire stations in Canada and excessive for industrial applications, remote communities, mining operations and oil sands production. The modular configuration of the SCWR concept can be scaled down to generate 150-300 MWe power for meeting requirements of local deployment [15].

A development strategy for small and very small SCWR concepts has been established. It provides the specific requirements for the proposed concepts, such as enhanced safety and reliability, extended refuelling duration and modular construction. Several potential core options were explored. Scaled-down versions of the Canadian SCWR concept appear to be the most prudent approach to proceed. However, several changes have been proposed to enhance reliability and operating efficiency. The scaled-down SCWR concepts would facilitate co-generation for hydrogen and steam/heat production. Figure 8 illustrates a proposed scaled down version of the SCWR core concept.

Development and/or optimisation of the reference and scaled-down versions of Canadian SCWR would require continuous R&D support in various technology areas. One of the major concerns is the irradiation effect on cladding materials. Experimental data are required to quantify the extent of irradiation damage to materials at supercritical pressures. An in-reactor test facility, capable to withstand pressures up to 32 MPa, has recently been constructed at Rež Research Centre. It facilitates testing of materials over a range of temperatures at supercritical pressures. Figure 9 shows the in-reactor test facility and the material test section for supercritical pressure testing at Rež Research Centre. The test section is undergoing out-reactor commissioning and will be installed into the test loop for in-reactor commissioning and testing. Canada is working closely with Rež Research Centre in testing various cladding and pressure-tube materials.

Figure 8. A Proposed Scaled-Down SCWR Core



Another strong interest among the SCWR community is the fuel irradiation at supercritical pressures, as there is a lack of in-reactor fuel data at relevant conditions. The test facility at Rež Research Centre can accommodate fuel testing. Approval from the regulator for fuel testing will be sought once the material testing are completed. Canada plans to continue the collaboration with Rež Research Centre in support of the licensing and testing effort.

The GIF SCWR System Research Plan has identified a separate phase for the design and construction of an integral testing facility (mainly for safety confirmation), which requires a strong collaboration among the SCWR community. Constructing a full-scale integral (safety) test facility for supercritical pressures is costly and time consuming. A scaled-down version of the test facility is capable to simulate the phenomena of interest to confirm the safety system effectiveness. Canada has initiated the effort in designing a scaled-down version of the integral test facility. Components in the Canadian SCWR safety system were examined and confirmed feasibility for scaling down. Scaling analyses of the safety system will be performed using the safety analysis tool. A scaled safety system will be proposed for discussion.

Figure 9. In-Reactor Test Facility and Material Test Section for Supercritical Pressure Testing



The ultimate goal of the GIF SCWR System is to construct a prototype reactor. Nuclear Power Institute of China has proposed the construction of a prototype SCWR in China. The core configuration will simulate China's pressure-vessel type SCWR, but in much smaller size and lower power. Canada considers the small SCWR demonstration relevant to the development of the Canadian SCWR and would consider exploring how a collaborative effort could be undertaken in GIF to support the development of a prototype SCWR.

VII. Conclusion

- Significant achievements have been accomplished through Canada's Generation-IV National Program in the past decade.
- The Canadian SCWR concept has been developed and has successfully undergone Canadian and international peer reviews for its viability.

- The modular configuration of the Canadian SCWR concept facilitates size scaling to meet local deployment needs.
- Canada continues to collaborate with GIF SCWR partners on future joint projects.

Acknowledgements

The authors would like to thank Natural Resources Canada (NRCan), Atomic Energy of Canada Limited (AECL) and Natural Science and Engineering Research Council (NSERC) for their financial support. Efforts of G. Harrison of NRCan as well as researchers and students of Canadian universities participating in the NSERC/NRCan/AECL Generation-IV Energy Technology Program are much appreciated.

Nomenclature

AECL	Atomic Energy of Canada Limited
CANDU	Canada Deuterium Uranium (a registered trademark of Atomic Energy of Canada Limited)
Gen-IV	Generation-IV
GIF	Generation IV International Forum
HQPs	Highly Qualified Personnel
NSERC	Natural Science and Engineering Research Council
NRCan	Natural Resources Canada
PDF	Post-Doctoral Fellows
R&D	Research and Development
SCWR	Super-Critical Water-cooled Reactor
U	Uranium
VHTR	Very High Temperature Reactor
wt	Weight

References

- [1] OECD Nuclear Energy Agency, "Technology Roadmap Update for Generation IV Nuclear Energy Systems", January 2014.
- [2] Pynn, G., Brady, D., Zheng, W., Leung, L. and C.-A. MacKinlay, "Canada's Generation IV National Program", CNL Nuclear Review, Vol. 5, No. 2, pp. 173-179, 2016.
- [3] Leung, L.K.H., "Achievements of Phase-I Thermalhydraulics and Safety Program in Support of Canadian SCWR Concept Development", Proc. 6th International Symposium on Supercritical Water-Cooled Reactors (ISSCWR-6), Shenzhen, Guangdong, China, March 03-07, 2013.
- [4] Yetisir, M., Gaudet, M., Pencer, J., McDonald, M., Rhodes, D., Hamilton, H. and Leung, L., "Canadian Supercritical Water-Cooled Reactor Core Concept and Safety Features", CNL Nuclear Review, Vol. 5, Number 2, pp. 189-202, December 2016.
- [5] Leung, L.K.H., "Thermalhydraulics and Safety Research in Support of Phase-II of the Canadian Generation-IV National Program", Proc. 19th Pacific Basin Nuclear Conference (PBNC 2014), Vancouver, British Columbia, Canada, August 24-28, 2014.
- [6] Anderson, T., Leung, L.K.H., Guzonas, D., Brady, D., Poupore, J. and Zheng, W., "Building Generation Four: Results of Canadian Research Program on Generation IV Energy Technologies", Proc. 19th Pacific Basin Nuclear Conference (PBNC 2014), Vancouver, British Columbia, Canada, August 24-28, 2014.
- [7] Schulenberg, T. and Leung, L., "Supercritical water-cooled reactors", Handbook of Generation IV Nuclear Reactors, Editor: I.L. Pioro, Woodhead Publishing Series in Energy: 103, 2016.
- [8] Pencer, J. and Colton, J., "Progression of the Physics Conceptual Design for the Canadian Supercritical Water Reactor", Proc. 34th Annual Conference of the Canadian Nuclear Society, June 09-12, 2013.
- [9] Wojtazek, D., "Future Nuclear Power Generation in Canada: Transition to Thorium Fuelled SCWRs", Proc. 7th International Conference on Modeling and Simulation in Nuclear Science and Engineering (7ICMSNSE), Ottawa, October 18-21, 2015.
- [10] Leung, L.K.H., Yetisir, M., Pencer, J., and Hamilton, H., "Improving Safety, Economic, Sustainability, and Security of Nuclear Energy with Canadian Super-Critical Water-Cooled Reactor Concept", Proc. 18th Pacific Basin Nuclear Conference (PBNC 2012), Busan, Korea, March 18-23, 2012.
- [11] Yetisir, M., Gaudet, M., Bailey, J., Rhodes, D., Guzonas, D., Hamilton, H., Haque, Z., Pencer, J. and Sartipi, A., "Reactor Core and Plant Design Concepts of the Canadian Supercritical Water-cooled Reactor", Proc. 2014 Canada-China Conference on Advanced Reactor Development (CCARD-2014), Niagara Falls Marriott Fallsview Hotel & Spa, Niagara Falls, Ontario Canada, April 27-30, 2014.
- [12] Guzonas, D., Edwards, M. and Zheng, W., "Assessment of Candidate Fuel Cladding Alloys for the Canadian Supercritical Water-cooled Reactor Concept", Proc. 7th Int. Sym. on SCWRs (ISSCWR-7), Helsinki, Finland, 15-18 March 2015.
- [13] Guzonas, D. and Cook, W., "Water Chemistry Specifications for the Canadian Supercritical Water-Cooled Reactor Concept", Proc. 7th Int. Sym. on SCWRs (ISSCWR-7), Helsinki, Finland, 15-18 March 2015.
- [14] Leung, L.K.H. and Yamada, K., "International Contributions to IAEA-NEA Heat Transfer Databases for Supercritical Fluids", Proc. 2012 Int. Congress on Advances in Nuclear Power Plants (ICAPP'12), Chicago, USA, June 24-28, 2012.
- [15] Yetisir, M., Pencer, J., McDonald, M., Gaudet, M., Licht, J. and Duffey, R., "The Supersafe® Reactor: a Small Modular Pressure Tube SCWR", AECL Nuclear Review, Vol. 1, Number 2, December 2012.

CURRENT PROGRESS IN EXPERIMENTAL DEVELOPMENT OF MSR AND FHR TECHNOLOGIES (J. UHLIR ET AL)

Jan Uhlíř⁽¹⁾, Martin Mareček⁽¹⁾, Evžen Losa⁽¹⁾, Martin Straka⁽²⁾, Martina Koukolíková⁽³⁾,
Petr Toman⁽⁴⁾ and Tomáš Trojan⁽⁵⁾

- (1) Research Centre Řež, Czech Republic.
 (2) ÚJV Řež, Czech Republic.
 (3) COMTES FHT, Czech Republic.
 (4) MICO, Czech Republic.
 (5) ŠKODA JS, Czech Republic.

Abstract

A technology of Molten Salt Reactor (MSR) system with liquid fluoride salt fuel has been investigated in the Czech Republic since 1999. Since 2005, the studies cover also the areas of thorium – uranium fuel cycle technology and material research, since 2013 the original MSR activities were broaden also to the selected areas of Fluoride-salt-cooled High-temperature Reactor (FHR) system with prismatic TRISO fuel.

Present activities in the development of MSR/FHR technology are solved by the consortium Czech research institutions and industrial companies. The R&D program covers both theoretical and experimental research and development in MSR/FHR physics, fluoride salt neutronics, experimental verification of selected steps of MSR fuel cycle including the liquid fuel processing and on-line pyrochemical reprocessing, development of main MSR/FHR structural material – nickel alloys and the design, manufacture and experimental tests of selected components of salt reactor technology like pumps, valves and gaskets.

The paper describes the recent results achieved within the running Czech MSR project in these areas and the outline of near-future activities.

I. Introduction

The experimental development of molten salt technologies devoted to Molten Salt Reactor (MSR) and Fluoride-salt-cooled High-temperature Reactor (FHR) have been an invisible part of Czech MSR research and development program. A technology of nuclear reactor systems with liquid molten salt fuel has been investigated in the Czech Republic since 1999. The original effort came from the national Partitioning and Transmutation concept based on the subcritical Accelerator Driven System for incineration of transuranium elements with liquid fluoride fuel and pyrochemical partitioning fuel cycle technology. After 2005, the original R&D intentions were gradually converted to classical MSR technology and to thorium – uranium fuel cycle. The aim of this

choice was to contribute to the development of an advanced nuclear technology, which can minimise environmental impact of nuclear power, save the natural resources and which has some potential to be deployed also in a non-superpower country.

The basic technological development of selected areas of MSR and Th – U fuel cycle technology was realised in the frame of the SPHINX project solved in 2005 – 2012. [1,2] In addition to the domestic activities of the MSR technology development, in 2012 the Czech Ministry of Industry and Trade and the US – Department of Energy concluded an agreement (Memorandum of Understanding) about the collaborative R&D on Molten Salt Reactor and Fluoride-salt-cooled High-temperature Reactor technologies. These facts and results created

the principal background for the present national program on the MSR/FHR technology development which was approved by the Ministry of Industry and Trade in 2016 and is granted by the Technological Agency of the Czech Republic.

II. Present Development of MSR/FHR Technology

In 2017 a new four year project of MSR/FHR technology development was launched as the Key component of the Czech R&D program on the fluoride salt-cooled nuclear reactor systems. [3] The project is a follow-up and broadening of previous Czech activities in MSR. The aim of the project is to contribute to the development of MSR and FHR reactor technology in the area of reactor physics, nuclear – chemical engineering and material research.

One of the main objectives of the project is the experimental determination of main neutronic properties and characteristics of MSR and FHR reactors cooled by ${}^7\text{LiF} - \text{BeF}_2$ salt (FLIBE salt). The other objectives of the project are focused on the MSR fuel cycle technology and MSR reactor core chemistry, further development of MSR/FHR structural material – Ni-based alloys and subsequent design and manufacture of selected components of the MSR/FHR technology. The project creates a platform for running Czech – US cooperation in MSR/FHR development.

The project is solved by a consortium of Czech research institutions and industrial companies led by the Research Centre Řež. The other members of the consortium are ÚJV Řež – Nuclear Research Institute, COMTES FHT, MICO Ltd and ŠKODA JS – Nuclear Machinery.

The work-packages of the project are:

- Theoretical and experimental physics of MSR/FHR system
- Chemistry and chemical technology of MSR
- Structural materials and components of MSR/FHR technology

These main work-packages are complemented by system studies covering also the non-proliferation and physical protection issues of thorium – uranium fuel cycle and MSR mock-up design.

III. Theoretical and Experimental Physics of MSR/FHR System

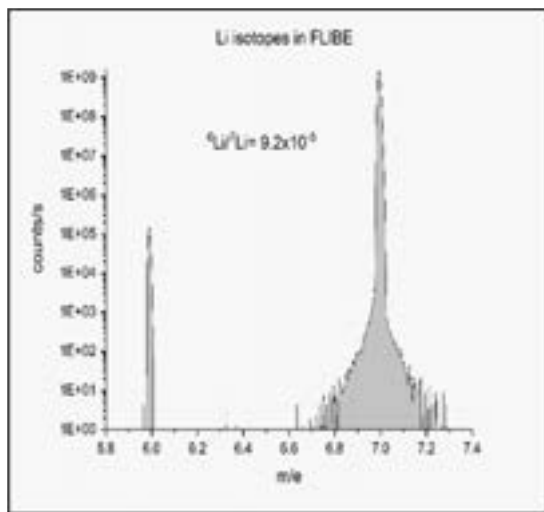
The effort, which is the follow-up of previous activities is focused mainly to the interconnection of theoretical and experimental studies of thermal spectrum MSR reactor physics and MSR/FHR neutronic studies. [4] The main part of experimental work concerning the pure FLIBE salt neutronics and FLIBE with thorium and uranium fluorides neutronics has been carried out at LR-0 experimental reactor of Research Centre Řež. The LR-0 core consists of six pin-type fuel assemblies (VVER-1000 design) with nominal enrichment of 3.3% and empty experimental channel, forming driven zone in the core center. Material insertions are put into the driven zone, occupying one position in the lattice. [5] The tests with FLIBE were performed with real MSR/FHR reactor (66-33 mol%) LiF-BeF₂ coolant salt containing Li-7 isotope (99.994 mol%), which was provided by Oak Ridge National Laboratory and were aimed at studies of neutron spectrum shape to confirm previous results with LiF-NaF salt. Neutron spectra in the 0.8–10 MeV energy range were measured with a Stilbene scintillator (10 × 10 mm) with neutron and gamma pulse shape discrimination. The inserted zone with the FLIBE salt is shown in Figure 1.

Figure 1. Loading of FLIBE zone into LR-0 reactor



The analysis of isotopic composition of Li in FLIBE was determined by SIMS method, the result of the Li-6 and Li-7 isotope rate is evident from Figure 2.

Figure 2. Evaluation of Li isotopes by SIMS method



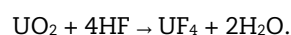
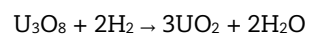
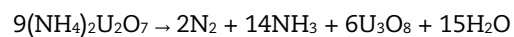
For criticality and neutron spectrum calculations, an LR-0 model has been analysed using MCNP6.1 with data from various nuclear libraries (ENDF/B-VII.1, ENDF/B-VII.0, JEFF-3.2, JEFF-3.1, JENDL-3.3, JENDL-4, RUSFOND-2010, JENDL-3.1). The older versions of libraries (ENDF/B VII.0 and JEFF-3.1) were used for comparison with older data and data from benchmarks. Different data libraries were used only for definition of the material insertion; the definition of fuel, moderator, and structural materials is fixed in ENDF/B-VII.0 to suppress the other possible effects to criticality (e.g. from fuel) that are not being investigated in this study. ENDF/B-VII.0 is approved by the national regulator for use in performing licensing calculations at LR-0. The free gas model was used for thermal neutron scattering treatment in case of FLIBE, Teflon, and stainless steel canister description, and the photo-neutron production is switched off in the physical model.

Existing measurement with FLIBE was done in room temperature, neutronic tests planned within the new project will be performed in special heated inserted zone put into LR-0 at the temperature range of 500 – 750°C. The main objectives of the tests will be determination of reactivity coefficients. Continuation of a close collaboration between Research Centre Řež and Oak Ridge National Laboratory is achieved in this area. mock-up design.

IV. Chemistry and Chemical Technology of MSR

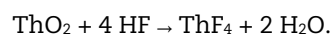
Existing research and development studies in chemistry and chemical technology were focused on the verification of liquid MSR fuel processing – experimental production of UF_4 and ThF_4 , basic electrochemical studies of actinide / fission product separation from fluoride molten salt media and the flow-sheet studies of the single-fluid and double-fluid on-line pyrochemical reprocessing of MSR thorium-breeder. The present effort and future directions cover also the development and experimental verification of fused salt volatilisation technique proposed for the extraction of uranium (in the chemical form of UF_6) from the MSR fuel salt.

Experimental fresh MSR fuel processing was at first studied in ÚJV Řež and later on verified in higher laboratory conditions in Research Centre Řež. Typical MSR liquid fuel consists from the ${}^7\text{LiF} - \text{BeF}_2$ carrier (acronym FLIBE) in which uranium tetrafluoride UF_4 and thorium tetrafluoride ThF_4 are dissolved. UF_4 and ThF_4 were prepared by the hydrofluorination of uranium and thorium dioxides. Processing of both tetrafluorides was verified in the typical amounts of several hundred grams of the product per batch. [2] It was verified that the highest purity of UF_4 (lower amount of residual oxygen) can be reached if the uranium dioxide is freshly prepared from ammonium diuranate according to the reactions:



Calcination of uranium diuranate and reduction of U_3O_8 were done at 600°C, subsequent hydrofluorination by anhydrous hydrogen fluoride was done at 400°C.

The experimental preparation of the ThF_4 was performed at the temperature range from 250 to 550°C by the reaction



The final experimental fresh MSR fuels were prepared by melting of FLIBE salt with uranium and thorium tetrafluorides. The produced MSR fuel was later on used for neutronic experiments done in the LR-0 reactor of the Research Centre Řež. The frozen samples of FLIBE salt containing uranium tetrafluoride are shown in Figure 3.

Figure 3. Frozen samples of UF₄ in FLIBE

The previous program in electrochemistry, realised by ÚJV Řež, was focused on the development of experimental set-up for molten fluoride salt media – including the development of reference electrode based on the Ni⁰/Ni²⁺ red-ox couple and the evaluation of red-ox potentials for uranium, thorium and selected fission products in individual selected molten fluoride salts (LiF-NaF-KF – FLINAK, LiF-BeF₂ – FLIBE and LiF-CaF₂). [6]

Results obtained from the measurements can be interpreted in following way:

- In FLIBE melt, there is a good possibility for electrochemical removal of uranium.
- In FLINAK melt, only uranium can be directly separated.
- In LiF-CaF₂ melt, uranium, thorium and most of fission products (mainly lanthanides) can be separated. [7]

The present effort is focused on the development and verification of quantitative electrochemical extraction of uranium and thorium and on removal of main neutron poisons (fission products) from the MSR carrier salt (FLIBE). A special attention will be paid to the electrochemical studies of protactinium. These studies are planned to be realised in collaboration between the Research Centre Řež, ÚJV Řež and the European JRC – Institute for Transuranium Elements Karlsruhe.

V. Structural Materials and Components of MSR/FHR Technology

Material research for molten fluoride technologies played an important role in existing R&D activities focused on MSR development. The most important was the development of nickel-based superalloy MONICR. MONICR was designed and developed by COMTES FHT

company as the Czech structural material for MSR and FHR technology. [8]

The basic corrosion and irradiation tests of MONICR were realised in previous projects, a further development of the semi-pilot production and further tests of high/temperature microstructure stability, high-temperature mechanical stability and radiation embrittlement are studied in the new project. Another studies concerning to MSR/FHR component development concern of the continuation of special graphite gasket seals development and of the design and development of pumps (impellers) and valves for fluoride salt media. This activities are realised by MICO Ltd and by ŠKODA JS company. In relation to the development of materials and components, a molten fluoride salt loop program was initiated.

A new forced FLIBE loop was built and put in operation in the first half of 2017. The loop is intended to material research and testing of components of the MSR and FHR technologies. The loop is electrically heated and thermally insulated and consists from impeller, two experimental channels for samples, freeze valve and a storage tank. The structural material of the loop is Inconel 718. The working temperature range is from 550°C to 750°C. The loop program covers the material corrosion tests, development and verification of special graphite gasket seals and further development of pumps and valves for fluoride salt media. A picture of the loop is shown in Figure 4.

Figure 4. FLIBE loop in the Research Centre Řež

The out of pile loop program will contribute to the preparation of the MSR mock-up design, which should be a final stage of the new project.

VI. Conclusion

Future deployment of MSR and FHR technology still requires a broad and intensive technical and technological development. The new project focused on several areas of MSR/FHR technology represents a significant contribution of the Czech Republic to the development of advanced safe and sustainable nuclear power. The intention of the project is to contribute to the international development of MSR and FHR systems.

Acknowledgements

Existing research and development on MSR and FHR technology has been realised under the financial support of the Ministry of Industry

and Trade, the Ministry of Education within the project CZ.1.05/2.1.00/03.0108 and of the Technological Agency of the Czech Republic within the project TA03021147.

Nomenclature

FHR	Fluoride-salt-cooled High-temperature Reactor
FLIBE	Eutectic mixture of lithium and beryllium fluorides
MONICR	Commercial name (trademark) of Ni alloy produced by COMTES FHT
MSR	Molten Salt Reactor
SIMS	Secondary-ion mass spectrometry
SPHINX	Spent Hot fuel Incineration by Neutron flux - Czech project devoted to MSR technology

References

- [1] M. HRON, M. MIKISEK, "Experimental verification of the SPHINX concept of MSR", *Prog. Nucl. Energy*, 50 (2-6), pp. 230-235 (2008).
- [2] J. UHLÍŘ et al., Report MPO No. 2A-1TP1/30, ÚJV Řež, March 2013, 2012 (in Czech).
- [3] Program Epsilon 2, Project No. TH02020113, Technological Agency of the Czech Republic, 2016, www.tacr.cz
- [4] J. FRÝBORT and R. VOČKA, "Neutronic Analysis of Two-Fluid Thorium Molten Salt Reactor", *Proc. of ICAPP '09*, Tokyo, Japan, May 10-14, 2009
- [5] M. KOŠŤÁL et al., "Comparison of fast neutron spectra in graphite and FLINA salt inserted in well-defined core assembled in LR-0 reactor," *Ann. of Nucl. En.*, 83, pp.216-225 (2015).
- [6] M. STRAKA, M. KORENKO, F.LISY, "Electrochemistry of uranium in LiF-BeF2 melt", *J Radioanal Nucl Chem*, 284, 1, 245-252 (2010).
- [7] M. STRAKA, L. SZATMÁRY, "Separation of actinides from lanthanides in molten fluorides by the modulated-current electrolysis", *ANS Transactions*, Vol. 116, p. 171, San Francisco, 2017.
- [8] Z. NOVY, J. DZUGAN, P. MOTYCKA, P. PODANY, J. DLOUHY, "On Formability of MoNiCr Alloy", *Advanced Materials Research*, 295-297, 1731-1737. www.scientific.net / AMR.295-297.1731. (2011).

SUBCHANNEL ANALYSIS OF A LBE-COOLED FAST REACTOR BLESS (C. SUN ET AL)

Cunhui Sun, Linsen Li, Ziguan Wang, Yaodong Chen, Yuquan Li

State Power Investment Corporation Research Institute, China.

Abstract

A project of a LBE (Lead-Bismuth Eutectic alloy)-cooled Fast Reactor BLESS (Breeding Lead-based Economical and Safe System) has been proposed by China State Power Investment Corporation Research Institute and designed to meet the public demands of a safer, more economical and more environmental-friendly nuclear system. In the roadmap among several proposed BLESS reactor, BLESS-D (BLESS-Demonstration) is a pool-type reactor cooled by LBE. The thermal power is 300MW while the electric power is set at about 120 MW. The thermal-hydraulic behavior analysis is necessary for the safety and economic performance of the design. Subchannel analysis is the basic thermal-hydraulic analysis method used to predict the coolant enthalpy, density, mass velocity rate, liquid temperature, and pressure distribution. In the subchannel analysis, the core or section of symmetry is defined as an array of parallel flow channels with lateral connections between adjacent channels. In this study, the analysis of thermal-hydraulic behavior for BLESS-D was completed. LBE Property and some models in the sub-channel code are discussed and adapted for LBE-cooled fast reactor. Preliminary subchannel analysis results of the BLESS-D core design are obtained. According to the calculation results in this study, it is indicated that the analysis method could be used in the preliminary evaluation and analysis for LBE-cooled reactor.

Key Words: LBE-cooled fast reactor, Subchannel analysis, BLESS-D

I. Introduction

Lead-cooled Fast Reactor (LFR), as one of the six nuclear reactor technologies selected by the Generation IV International Forum (GIF), has become one of the most promising concepts and attracted more attention from the industry.

In recent years, many types of design of Lead-cooled fast reactor are proposed by research organisations, for example, SVBR-100 and BREST-300 in Russia, ALFRED and ELSY in Europe, and SSTAR in the USA.

A project of a Lead-Bismuth Eutectic (LBE) cooled Fast Reactor named BLESS (Breeding Lead-based Economical and Safe System, BLESS) has been proposed by China State Power Investment Corporation Research Institute and designed to meet the public demands of a safer, more economical and more environmental-friendly nuclear system.

In this project, the basic reactor design is named BLESS-D (BLESS-Demonstration) devoted to demonstrating the technology of China LBE-cooled fast reactor. In the roadmap of several proposed BLESS reactors, BLESS-D is a pool-type reactor cooled by LBE. The thermal power is 300 MW while the electric power is set at about 120 MW. UO₂ fuel rod was chosen as fuel in order to take the advantages of mature fuel-fabrication industry.

It is expected that the design of BLESS-D can validate and demonstrate crucial technical problem solutions and be expended to an industrial scale (about 1000 MWe) or be converted to modular design in order to meet different requirements. The preliminary subchannel analysis of BLESS-D is presented in this paper.

II. Brief Introduction of BLESS

BLESS-D is a pool-type reactor cooled by LBE. The thermal power is 300MW while the electric power is set at about 120 MW. BLESS-D has four loops. The main components including eight steam generators, four main pumps, reactor vessel, internal components, and control rod drive mechanism. Table 1 lists the main design parameters of BLESS-D.

Table 1. The main design parameters of BLESS-D

Parameters	Value
Thermal Power	300 MW
Coolant	LBE
Fuel	UO ₂
Average linear power density	185 W/cm
Core diameter	2422 mm
Core height	700 mm
Primary cooling system	Pool-type
Primary coolant circulation	Forced
Inlet/outlet temperature	340°C/490 °C
Number of FAs	252
Number of fuel rods per FA	127
Number of reactor control system (CS) assemblies	9
Number of reactor safety system (SS) assemblies	9
Steam generators	8
Main pumps	4

Figure 1. Fuel assembly layout

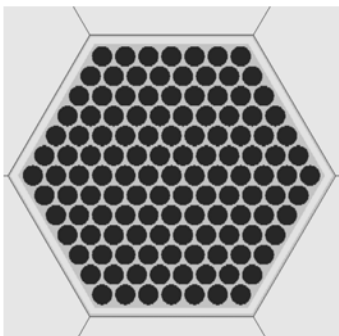


Fig. 1 shows fuel assembly of BLESS-D. Each fuel assembly includes 127 fuel pins. The active region height is 70 cm.

Figure 2. Core Arrangement of BLESS-D.

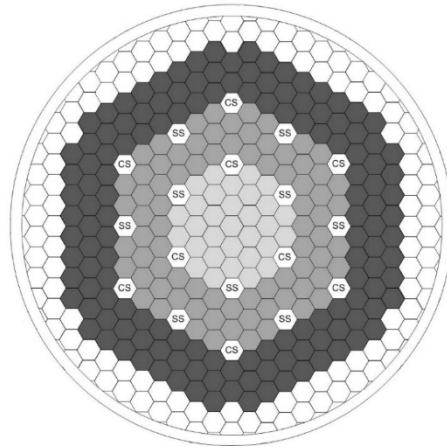


Fig. 2 shows the core arrangement of BLESS-D. The core consists of 252 fuel assemblies arranged in 3 regions. The 252 fuel assemblies are surrounded by two rings of stainless shielding assemblies, which have been filled with stainless steel reflector block.

III. Validation of Subchannel Code

Subchannel analysis is the basic thermal-hydraulic analysis method used to predict the coolant enthalpy, density, mass velocity, liquid temperature, and static pressure distribution. In the subchannel analysis the reactor core is defined as an array of parallel flow channels with lateral connections between adjacent channels. A channel represents true subchannel within a rod array, closed tube or larger flow area representing several subchannels or rod bundles. Core thermal-hydraulic analysis code used to predict the local fluid conditions of hot subchannel.

In order to analyse BLESS-D thermal-hydraulic performance, a subchannel code for LBE-cooled reactor was developed. A preliminary validation for this code was completed using hexagonal 19-rod bundle LBE experiment by KIT.

This experiment was installed in a vertical test port of the THEADES loop at KIT-KALLA. The test section consists of a bundle of 19 electrically-heated rods, embedded in a hexagonal channel. Fig. 3 shows the side view of this arrangement.

In addition to the information required for operating and controlling the loop, four types of variables are measured in this experimental campaign: flow rate, differential pressure,

temperature and thermal power. In total 80 thermocouples (TCs, type K with a steel jacket) were used. Seven TCs were used for monitoring the temperature of the pressure-sensing probes. One TCs was placed at the inlet and three at the outlet. In the heated region three measuring levels (MLs) are defined as shown in Fig. 4.

Figure 3. The side view of the test section

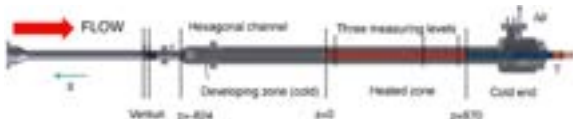
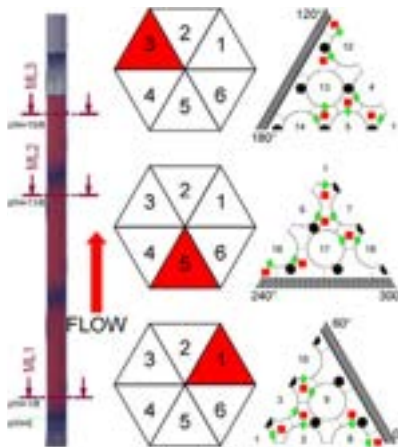


Figure 4. Three measuring levels



A reference case was used for the preliminary validation of the subchannel code. Table 2 shows the input parameters.

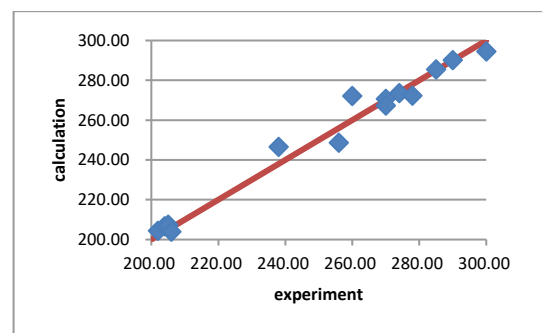
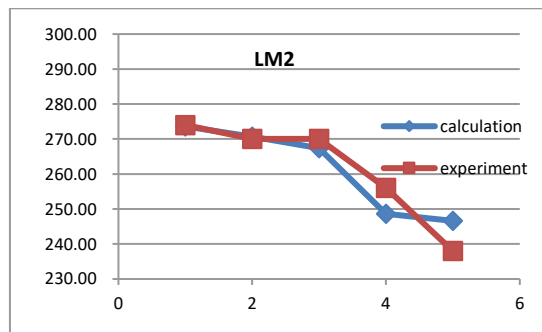
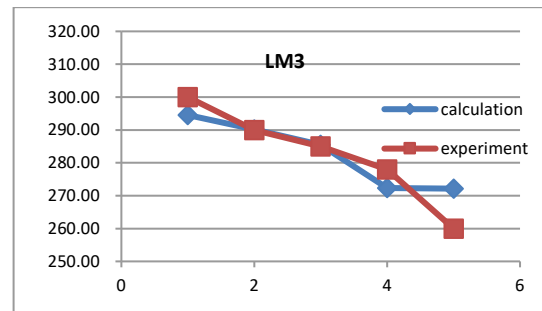
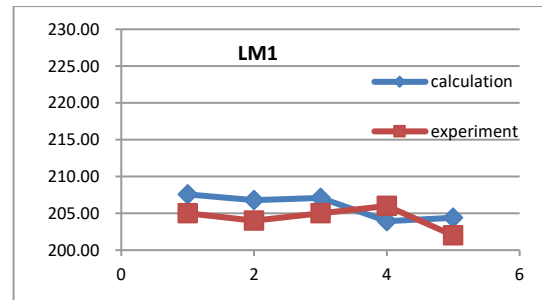
Table 2. Input parameters

Parameter	Value
T_{in}	200.00 ± 0.10 C
m	15.99 ± 0.14 kg/s
Q	197.01 ± 1.97 kW

A subchannel analysis was completed for the reference case. Fig. 5 shows the comparison of calculation results and experiment results.

According to Figure 5, the comparison of the calculation results and the experiment results is consistent. Therefore, the subchannel code could be preliminarily used for the conceptual analysis of BLESS-D.

Figure 5. Comparison of calculation results and experiment results



III. Subchannel Analysis

For subchannel analysis, the 1/12 fuel assembly of BLESS-D was divided into 25 subchannels and 16 rods. Fig. 6 shows the channel number and rod number.

Figure 6. The channel number and rod number

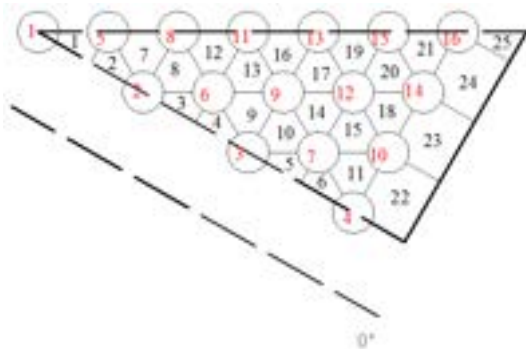


Table 3 shows the main boundary parameters. Table 4 shows the radial power distribution.

Table 3. The boundary parameters

Parameter	Value
Inlet temperature	340°C
Mass flux	11702.6 kg/s-m ²
Power density	372.99 KW/m ²
Pressure	101.3 KPa

Table 4. The radial power distribution

Rod number	Radial power distribution
1	0.90653
2	0.94528
3	0.99033
4	1.00205
5	0.92906
6	0.98222
7	0.99484
8	0.96059
9	0.99574
10	1.00385
11	0.97952
12	1.01556
13	1.00024
14	1.02908
15	1.02818
16	1.16300

Fig. 7 shows the results of subchannel analysis.

Figure 7. The results of subchannel analysis

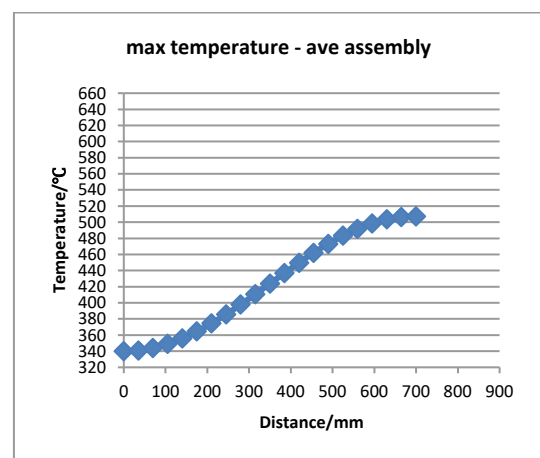
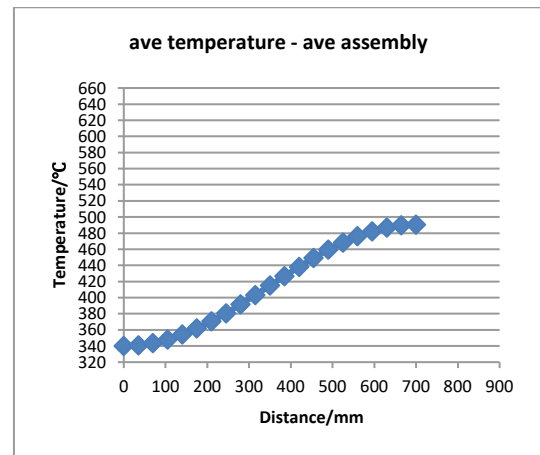
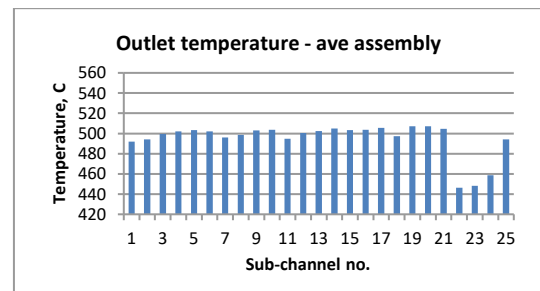
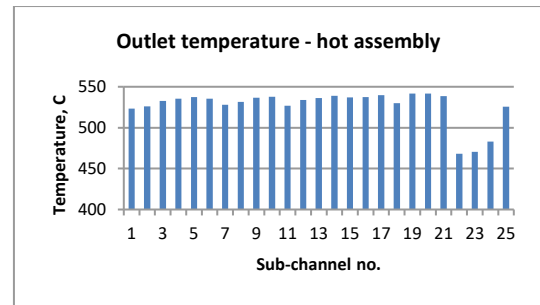
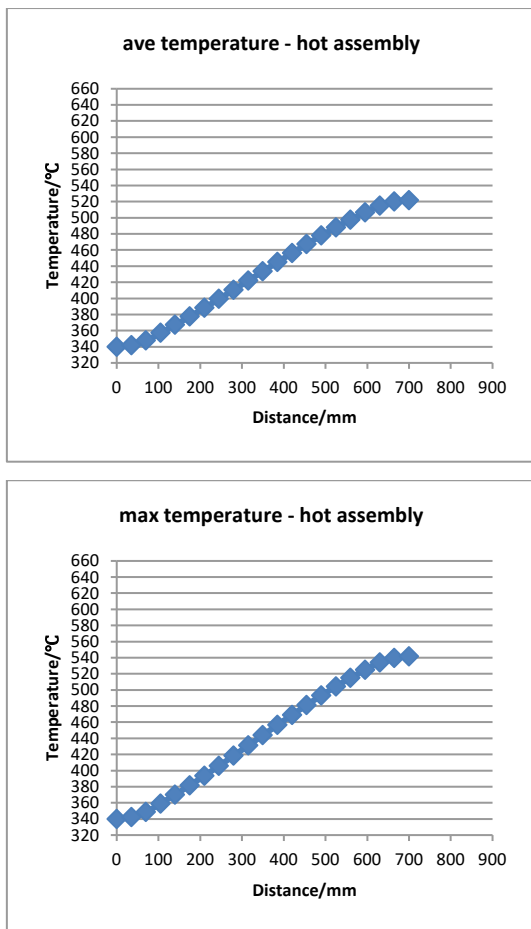


Figure 7. The results of subchannel analysis (cont'd)



IV. Conclusion

According to the subchannel analysis of BLESS-D, the maximum outlet temperature is 541.6 C, the maximum cladding temperature is 545.4 C, the maximum fuel center temperature is 1055.9 C, and the maximum coolant velocity is 1.2 m /s. All the results of the subchannel analysis meet the design criteria.

References

- [1.] Abram T, Ion S. Generation-IV nuclear power: A review of the state of the science[J]. Energy Policy, 2008.
- [2.] Zrodnikov A V, Toshinsky G I, Komlev O G, et al. SVBR-100 module-type fast reactor of the IV generation for regional power industry[J]. Journal of Nuclear Materials, 2011.
- [3.] Adamov E O, Orlov V V, Filin A I, et al. Conceptual design of BREST-300 lead-cooled fast reactor[C] //Proceedings, International Topical Meeting on Advanced Reactor Safety, ARS '94, Pittsburgh, USA. 1994.
- [4.] Alemberti A, Frogheri M, Mansani L. The lead fast reactor: demonstrator (ALFRED) and ELFR design[J]. 2013.
- [5.] Pacio, M. Daubner, F. Fellmoser, K. Litfin, Th. Wetzel. Experimental study of heavy-liquid metal (LBE) flow and heat transfer along a hexagonal 19-rod bundle with wire spacers[J]. Nuclear Engineering and Design, 2016.
- [6.] X.J. Liu, N. Scarpelli. Development of a sub-channel code for liquid metal cooled fuel assembly[J]. Annals of Nuclear Energy, 2015

NUMERICAL AND EXPERIMENTAL THERMAL HYDRAULICS STUDIES OF HIGH TEMPERATURE MOLTEN SALTS FOR GENERATION IV NUCLEAR REACTORS (P. RUBIOLO ET AL)

Pablo Rubiolo, Mauricio Tano Retamales, Julien Giraud, Véronique Ghetta, Juan Blanco

Univ. Grenoble Alpes, Institute of Engineering (INP), CNRS, France.

Abstract

Molten salts are being considered as candidate for coolant in various Generation IV reactors concepts such as the Fluoride salt-cooled High-temperature Reactor (FHR) and the Molten Salt Fast Reactor (MSFR). Numerical models for these new reactor concepts possess unique challenges because some of the intrinsic molten salts phenomena are not found in other coolants. For example, in the case of the salt fuel-cooled MSR the transport of the delayed neutron precursors in the liquid fuel causes a reduction of the effective fraction of the delayed neutrons and therefore a coupling between the reactor thermal-hydraulics and neutronics behaviours not found in other types of reactor. Moreover, the reactivity feedback coefficients in this type of MSR can also be affected by the fuel salt compressibility, the presence of bubbles and the overall flow characteristics. Some other more convective phenomena such as thermal heat radiation transfer or flow phase change have to be taken into account in the models and are relatively different with respect to those encountered in coolants such as water and liquid metals. Due to their complexity, most of these phenomena require the use of multi-scale and multidisciplinary approaches that allow taking into account the coupling existing between neutronics, thermal hydraulics and thermo-mechanics reactor aspects. While significant progress has been made on model developments, further work is still required for the modelling of the thermal-hydraulics phenomena and also for the coupling with the thermo-mechanics and chemistry phenomena. In the frame of the European Project SAMOFAR an experimental facility named SWATH (Salt at Wall: Thermal exCHanges) has been built at the CNRS (LPSC, Grenoble) to study some of these thermal-hydraulics challenges and thus to contribute to the improvement of the molten salt numerical models, in particular those implemented in Computational Fluid Dynamics (CFD) codes. This paper presents the progress made on the experimental and numerical studies of high temperature molten salt carried-out in the SWATH facility.

I. Introduction

Molten salts are being considered as candidate for coolant in various Generation IV reactors concepts. In salt-cooled MSR such as the Fluoride salt-cooled High-temperature Reactor (FHR), a molten salt is used as coolant while the core contains a solid fuel based on a TRISO coated particles [1]. The use of a molten salt as a coolant allows the FHR to work at high temperature while keeping the coolant pressure low. In salt fuel-cooled MSR concepts such as the Molten Salt Fast reactor (MSFR), a molten salt is used both as a coolant and fuel

carrier. In this reactor the molten fuel salt is heated by the nuclear fission reactions in the core (where the fuel salt reaches the criticality condition) and then circulated by pumps toward the heat exchangers where it is cooled down before returning to the core [2-3]. The use of a molten salt as fuel carrier opens new possibilities in terms of reactor design and safety options. Some of the advantages of the MSFR are the possibility for actinide burning and extending fuel resources, on-line fuel loading and reprocessing and the use of novel passive safety systems such as the fuel salt draining system. Moreover, reprocessing requirements

in the MSR design are reduced because of the fast spectrum.

As the design and safety studies of these new MSRs designs go in higher detail, more accurate molten salt numerical models are needed. Nevertheless numerical modelling of a high temperature molten salt coolant poses unique challenges because some of the intrinsic molten salts phenomena are not found in other coolants. Significant progress has been made concerning the neutronics modeling of the MSRs, in particular for the strong neutronics and thermal-hydraulics coupling due to the delayed neutron precursors transport by the liquid fuel and the neutronics feedback effects [4]. While some thermal-hydraulics properties of molten salts are not very different from water, there are a number of phenomena that require particular attention [5]. To mention a few of them: salt solidification and melting, complex heat transfer mechanisms including radiative heat transfer (some molten salts can be considered as semi-transparent participating medium), internal heat generation, strong 3D flow patterns in some reactor components. Development of suitable thermal-hydraulics numerical models requires validation of these models against experimental data. The Salt at WALL: Thermal Exchange (SWATH) experiment is one of the research activities of the European H2020 SAMOFAR project (Safety Assessment of the Molten Salt Fast Reactor - MSFR). The aim of the SWATH experiment is to improve molten salt numerical models, in particular those needed for the MSFR.

The MSFR is a fast-spectrum breeder reactor with a large negative power coefficient that can be operated in a Thorium fuel cycle. A lithium fluoride salt is currently being considered as the fuel matrix of the MSFR. The initial composition (non-irradiated) of the MSFR fuel salt is a mixture of a lithium fluoride, thorium fluoride salts and actinides fluoride ($\text{LiF-ThF}_4\text{-}^{233}\text{UF}_4$ or $\text{LiF-ThF}_4\text{-}^{\text{enr}}\text{UF}_4\text{-(Pu-MA)F}_3$), with the proportion of LiF fixed at about 77.5%. Since the accidental configurations of the MSFR are currently being studied and thus not completely well determined, SWATH experiment is focused on understanding the underlying physical principles of molten salt flows rather than developing experimental correlations.

Accordingly, simple geometries are investigated in SWATH in order to study the validity of the CFD heat transfer models. Most of the thermal hydraulics models developed in this work were implemented in the OpenFOAM software package. This paper presents some of the progress made on the experimental and

numerical studies carried-out in the SWATH facility.

II. Experimental Strategy

The first step before designing the SWATH facility was to identify the Key phenomena that are relevant to the MSR concept and require experimental data to assess the accuracy of the thermal models. This task was somehow subjective and required carrying-out a qualitative review of the different thermal hydraulic phenomena that are believed to occur in the reactor. The following qualitatively criteria were adopted in the analysis:

- a) Importance of the phenomenon for the MSFR design and safety studies,
- b) Knowledge level and/or accuracy that could be achieved on the numeric modelling of the phenomenon,
- c) Feasibility for designing an experiment with sufficient precision to investigate the phenomenon.

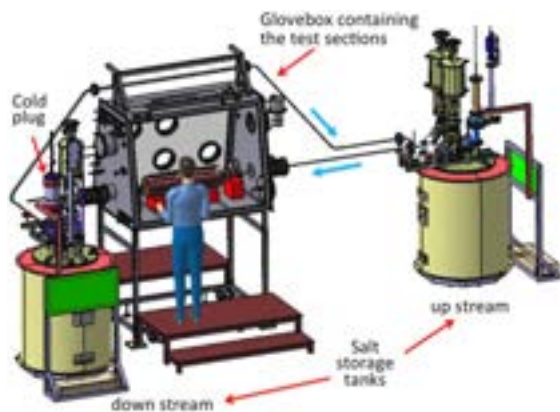
A Phenomena Identification and Ranking Table (PIRT) was therefore developed based on the MSFR phenomena that are expected to happen and these three criteria. Particular attention was given to some critical reactor processes, such as the fuel draining process. The PIRT analysis led to identify the following priority phenomena for SWATH:

- Heat transfer in very simple geometries,
- Evolution of the salt solidification interface with and without forced convection,
- Solidification along a cold wall after successive molten salt flows (lava flow like),
- Flow structure characteristics (flow rate, film thickness, etc.) in an open channel,
- Turbulence effects on the flow velocity field,
- Radiative heat transfer in the salt.

Performing experiments with a molten salt involves in general high temperatures and the risk of chemical reactions. These particular conditions make hydraulics measurements such as flow rate, liquid level, pressure or flow visualisation quite challenging. To overcome some of these challenges a strategy using two separate facilities was adopted. The first facility called SWATH-W uses water as working fluid to

study hydraulics aspects while the second one called SWATH-S uses a molten fluoride salt to study heat transfer. The operation of both SWATH facilities is based on a discontinuous working principle in which the flow is established in a channel section (for example a circular close channel) by regulating the pressure difference between two tanks. This solution was better suitable for the project constraints (time and cost) than the alternative one that would be developing a pump for the experiment. The pressure control system is designed to maintain a stable flow during the operation of the loop by regulating opening and closing of a set of tanks valves connected to a pressurised argon tank and the atmosphere. This control system uses information related to the flow rate such as the salt level in the tanks or the pressure drop at a specific component of the circuit. During the experiment, the salt mass flow rate is calculated from the variation of the tank levels measured by two independent methods: a laser beam system and electrical contactors system. Figure 1 shows a layout of the SWATH-S facility which is composed by the two salt storage tanks, the circuit pipes with the heating system and the thermal insulation (not shown in the figure), automatic valves, cold plug, glovebox, pressure control system and instrumentation. The glovebox is required to host the test section and allows for manipulation in a chemically inert argon atmosphere.

Figure 1. Layout of the SWATH facility



Close, open channels and other type of simple geometries were selected for study in SWATH. In order to reduce as much as possible the experimental uncertainties a multiple stages experimental approach was adopted. Then, some of these geometries are studied in both water and salt facilities. The room temperature and pressure working conditions of SWATH-W

make possible to build the test sections on Plexiglas. This allows performing PIV measurements (Particle Image Visualisation) to precisely determine the flow conditions inside the test section (on the contrary of SWATH-S where the utilisation of the PIV technique is not practical) and thus compare it to the CFD predictions for an isothermal flow. This approach is justified since the Kinematic viscosity is very similar between LiF-ThF₄ and water. The five general types of geometries reported in the Table 1 are used for building the test sections that are currently being investigated in SWATH.

Table 1. Geometries investigated in SWATH

Geometry	Facility	Measurements
Backward Facing Step (BFS)	SWATH-W	<ul style="list-style-type: none"> Flow rate Velocity profile
Circular and rectangular close channels	SWATH-W SWATH-S	<ul style="list-style-type: none"> Flow rate Velocity profile Temperature
Rectangular open channel	SWATH-W SWATH-S	<ul style="list-style-type: none"> Flow rate Temperature Solid phase thickness
Molten cavity	SWATH-S	<ul style="list-style-type: none"> Temperature Solidification thickness Structure
Cold plug	SWATH-S	<ul style="list-style-type: none"> Electrical and cooling power Melting time Molten salt level in the cavity

The Table 1 summarises the facility where the geometry is tested and the expected measurements. Velocity profiles are measured only in SWATH-W while temperatures are only measured in SWATH-S. Next sections provide the main characteristics of each facility and discuss some of the experiments.

II.1 SWATH-W (Water) experiments

The SWATH-W facility uses water at nearly room temperature conditions. The main purposes of SWATH-W are: (1) Perform purely hydraulic measurements, (2) Aide for the experiment design of SWATH-S and the test sections (e.g. confirm adequate flow stability is obtained or verify the accuracy of the flow rate measurement instruments) and (3) Aide to the definition of the experiment procedures implemented in SWATH-S. Following the same working principle as shown in Figure 1 the

SWATH-W set-up is composed of two tanks, the mechanical valves, the flow instrumentation (pressure and flow rate measurements) and can host different test sections to be studied. Main characteristics of SWATH-W are listed in Table 2. Different flow measurements can be made: volumetric rate, pressure at selected locations, water level in the tanks and the detailed velocity flow field in the experimental section. The latter is performed using a Particle Image Velocimetry method (PIV), which is well adapted to this facility. The PIV is a nonintrusive measurement technique based in the diffusion of light by tracer particles in a fluid. The PIV technique allows measuring the two components of the velocity field in a flow over a plane. The laser sheet was generated from the bottom of the test section. A double frame high-speed camera was placed in front of the test section and calibrated with a rectangular grid printed in a steel plate placed at its mid-plane on top of the section as seen in Figure 2 in the case of the Backward Facing Step (BFS) test section.

Table 2. Main characteristics of SWATH-W

Fluid	Water at room temperature and pressure
Tank material	Plexiglas
Tank dimension	Inner/Outer diameters : 480 mm/500 mm Inner height : 810 mm
Fluid volume	60 liters
Piping	Inner/Outer diameters : 11 mm/16 mm
Flow rate measurements	Compact Ultrasonic Flowmeter
Water level	Laser measurements and electronic contactors
Min-Max flow	By pressure control: 0.5 l/min to 7 l/min By pump : 0.5 l/min to 10 l/min

Figure 2. System used for calibration of the BFS section PIV experiments

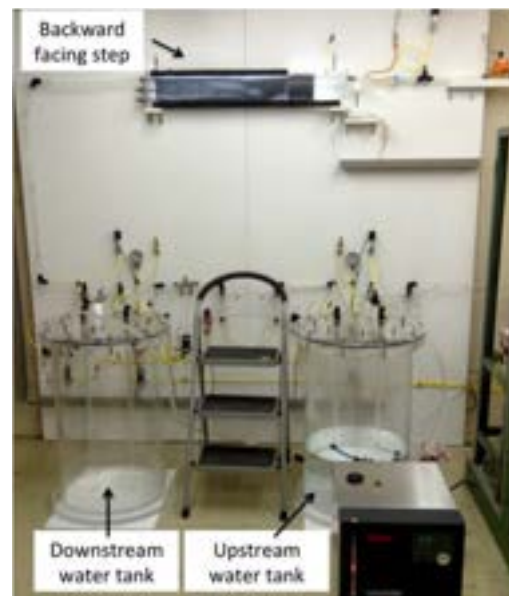


The Figure 3 shows SWATH-W hosting this BFS test section, which was studied to:

- Improve the accuracy of the turbulence models
- Study the stability of the flow rate obtained in the facility using the pressure control system in comparison with using the pump (black box in the right down side of the Figure 3).

The BFS geometry was not intended for investigating heat transfer and thus it was not implemented in SWATH-S. However other geometries studied in SWATH-S will be also investigated in SWATH-W.

Figure 3. SWATH water facility with the BFS section



II.2 SWATH-S (Salt) experiments

The second facility, was designed to perform the high temperature thermal-hydraulics experiments with molten salt and to investigate the accuracy of the salt models regarding heat transfers and phase change. These phenomena cannot be studied in SWATH-W. One critical point in the design of SWATH-S was the selection of coolant. Molten salts have excellent heat storage capacities but less good thermal conductivity. This means that in molten salts convective heat transfer mechanism is more efficient than conduction in comparison to other coolants. In the experiment, a reasonable similitude with the lithium fluoride fuel salt of

the MSFR requires considering at least the Reynolds, Prandtl and Grashof dimensionless numbers. The use of a molten salt with a relative low temperature melting point in SWATH-S was initially considered but finally abandoned because it would have prevented to study the effect of radiative heat transfer which is expected to play a significant role in some extreme conditions. The use of a lithium fluoride salt (melting point is at about 850°C) was neither retained since it would impose too high working temperature. Practical considerations (facility licensing for example) excluded also the possibility of employing a salt containing Thorium (i.e. LiF-ThF₄) which has a lower melting point (about 585°C). A FLiNaK salt was finally selected a good compromise since it allows obtaining a very good similitude with respect to the phenomena encountered in a Molten Salt Reactor. In addition FLiNaK has a relatively high (but not too high) melting point (at about 450°C), which allows investigating the effect of radiative heat transfer in some of the process. Reynolds and Grashof numbers can be adjusted in SWATH-S to obtain reasonable similitude by changing the experimental setup characteristic length and the flow velocity and the temperature. Reynolds numbers up to 15,000-20,000 can be obtained in the experimental section. These Reynolds numbers are not expected to cover all possible values existing in the MSFR but would allow for studying laminar flow and some turbulent flow configurations. On the other hand adequate Prandtl Number range covering most likely normal and accidental conditions can be obtained by changing the FLiNaK temperature between 500°C and 700°C.

After SWATH-S facility completion, the thermal insulation covers all the components of containing molten salt (in particular the pipes). This can be observed in the photograph presented in Figure 4. Molten salt flows from the “Upstream” tank situated in the right to the “Downstream” tank on the left, in the photo behind the control valves panel. Most of the components of SWATH-S are made on stainless-steel (SS 304L). The operating experience on a similar molten salt loop shows that this material provides adequate performance for the project requirements. The main characteristics of the facility are summarised in Table 3.

The next paragraphs describe two examples of numerical and experimental studies carried-out in SWATH.

Figure 4. SWATH-S facility after completion



Table 3. Main characteristics of SWATH-S

Fluid	FLiNaK Service temperature: 500°C to 700°C
Tank volume	60 liters
Tank material	304 L Stainless Steel
Tank dimension	Inner/Outer diameters: 440 mm/456 mm Inner height: 938 mm
Design Pressure	1 bar at 600°C
Piping	Inner/Outer diameter : 20 mm/25 mm Material : SS 304L (seamless tube)
Flow rate	1 l/min to 8 l/min

III. Flow Studies With the Backward Facing Step (BFS)

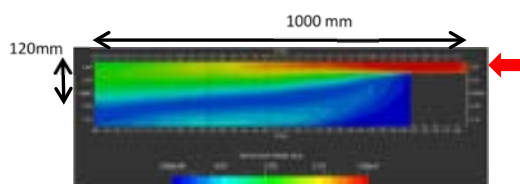
Performing multiphysics steady or transient studies at the scale of the MSR system requires the coupling of the thermalhydraulics with neutronics models. For most reactors geometries and sizes and given the complexity of the phenomena being modelled, the Reynolds Average Navier Stokes (RANS) approach provides usually a good compromise between computational cost and accuracy among the different Computational Fluid Dynamics (CFD) techniques. Other techniques such as Large Eddy Simulations (LES) techniques can be used for smaller systems or for selected components of the reactor. More accurate techniques such as Direct Numerical Simulation (DNS) are still limited to very simple geometries because of their computational cost. For the present studies, the modelling effort was then focused on the improvement of the RANS models for molten salts since these models are more suitable to be implemented in the reactor multi-physics code.

RANS models are computationally less demanding than other CFD techniques (such as LES or DNS) but have an important drawback: the choice of the RANS model to be used in the simulations among the various existing is not always straightforward. Indeed differences on the predicted velocity flow fields from similar RANS model can become relatively important (more than 10-20%) in some cases. In order to improve the accuracy of the RANS turbulence models a Backward Facing Step (BFS) test section has been used. The BFS geometry is particularly interesting in our applications since the flow phenomena in this geometry is representative of conditions that exist in various key reactor components such as the entrance region of the MSFR core cavity. The BFS geometry is particularly challenging for standard RANS models since they usually cannot fully predict the richness of the turbulent structures generated past the BFS. As an example of such difficulties Table 4 presents the relative error and the computational cost of three standard turbulence models: $k-\epsilon$, $k-\omega$ and RSS model when used to predict the flow field in the BFS. The relative error reported in Table 4 was calculated as the average weighted quadratic error between the model prediction and the experimentally measured velocity by using a PIV method (Particle Image Velocimetry). Example of a flow field in the BFS is shown in Figure 5.

Table 4. Relative errors and computational cost for the BFS

Model	Relative error	CPU Time (16 core x1.2GHz)
$k-\epsilon$	13.2%	721 sec
$k-\omega$	7.2%	785 sec
RSS model	6.4%	1921 sec
Non-linear Cubic	5.1%	1372 sec
LES	0.7%	115869 sec

Figure 5. PIV averaged velocity field in the BFS at Reynolds equal 3900



As can be seen in Table 4, it is difficult to decrease the relative error below 5-10% and in some cases such as for the $k-\epsilon$ model, the error is well above 10%. This is problematic because some of the phenomena investigated in SWATH have a relatively small impact in the experiments. It was therefore necessary to develop a methodology and a tool that allows improving the accuracy of the RANS model velocity field predictions for the SWATH test sections. This tool is called the Genetic Evolutionary Algorithms for Turbulence modelling tool (GEATFOAM) [6]. GEATFOAM allows constructing a mathematical expression that is used to calculate a Reynolds Shear Stress (RSS) tensor that minimises the relative error between the model predictions and the experimental flow data. GEATFOAM is a library developed in C++ that can be compiled with the OpenFOAM code, which is an open source Computational Fluid Dynamics (CFD) Toolbox. A genetic algorithms is used in the tool to perform the optimisation process since it provides good robustness and decreases the computational time. GEATFOAM was applied to improve the numerical predictions for the BFS results by optimising the parameters of a standard $k-\epsilon$ model and a non-linear cubic model. The non-linear cubic model uses a third order tensor expression to describe the non-isotropic part of the RSS tensor and allows to take into account the upstream flow or fluid history dependency of the turbulence in the BFS. The optimisation of the parameters of this model by GEATFOAM allow decreasing the relative error to about 5% without further computation cost. This level of accuracy was judged adequate for the purpose of the analyses performed in SWATH. Accuracy of hydraulics RANS models is therefore improved from SWATH-W data and before use them to study thermal-hydraulics effects in SWATH-S. More details on GEATFOAM can be found in [6].

A second key point investigated with the Backward Facing Step was the flow field stability obtained in the test sections with the pressure control system. To estimate the uncertainty of the flow rate, the flow field in the BFS section was measured with PIV technique using two different manners to establish the flow. In the first one the SWATH-W facility used a convective centrifugal pump to establish the flow circulation. This is supposed to provide a more stable flow rate. In the second condition, the flow circulation was established with the pressure control system. The PIV measured flow profiles in both conditions were then compared at three different regimes ($Re=200$,

1100 and 3900). The PIV results showed that pressure control system allows good stability for flows greater than 0.5 l/min.

IV. Salt Phase Change Modeling

The main objective of the phase change experiments in SWATH was to validate the two numerical models developed for the solidification of the FLiNaK (ternary system LiF-KF-NaF): MASOFOAM and MUSOFOAM [7]. Both models are currently implemented in the code OpenFOAM. The MASOFOAM (MAcro-scale SOLidification Foam) solver implements a solidification-convection coupled solver based on a standard mixture model. In this mixture model the system is divided in three regions: the liquid phase, the solid phase and the mushy zone. MASOFOAM solves the mass, linear momentum and energy conservation equations in each of these regions. In the liquid phase the fluid is considered as incompressible and the buoyancy effects are modelled in the momentum conservation equation using a Boussinesq's approximation [8]. In the solid phase the Duhamel-Neumann constitutive equations are used [9] with the expansion work being neglected in the energy equation. In the mushy zone a porous medium approach is used with approximate closure equations for the stress tensor and the mixture enthalpy [10]. MUSOFOAM (MUlti-scale SOLidification Foam) solver is complementary to MASOFOAM and allows improving the accuracy of MASOFOAM by providing more accurate estimate of the macroscopic properties of the solid phase (for example the thermal conductivity tensor). To obtain these properties MUSOFOAM solves the species diffusion equation with a length adaptable phase field model and then calculate the volume average values of the properties. More details on both models are given in [7].

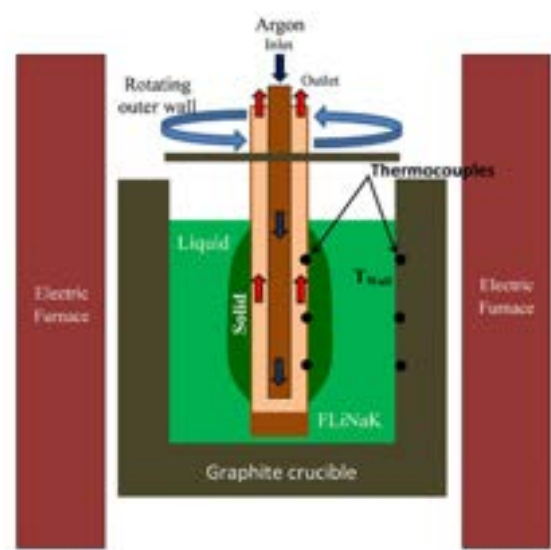
It is expected that during normal and accidental conditions the solidification (or melting) can occur in presence of flow convection and since this condition will have a noticeable effect on the shape of the solidification front, SWATH experiments consider two conditions: (a) Natural convection and (b) forced convection. Moreover to decrease the uncertainties associated with the numerical modelling of flow velocity field conditions, a relatively simple geometry has been adopted in the experiment. As can be seen in Figure 6 the solidification experiment employs a rotating tube inside an annular cavity filled with molten salt. The rotating tube contains an inner tube that allows for the circulation of a gas coolant

(argon) to decrease the temperature of the external wall of the outer tube below the FLiNaK melting point and thus initiating the solidification process. The tube rotation generates a relative simple forced convection velocity field in the fluid. The inner wall temperature of the graphite crucible is maintained at a constant temperature (above the melting point) by regulating the electric furnace power. The rotating tube and the crucible walls are instrumented with thermocouples.

The setup presented in Figure 5 has several advantages:

- The solidification front profile can be measured at any time by extracting the rotating tube from the molten salt bath;
- Flow field established in the cavity is relatively simple although flow instabilities may appear (Taylor-Couette instability);
- Heat extracted from the tube can be estimated by performing the enthalpy balance on the argon flow;
- Boundaries conditions on the molten salt cavity can be controlled or at least measured;
- Instrumentation using thermocouple is relatively simple.

Figure 6. Simplified layout of the SWATH-S solidification experiment

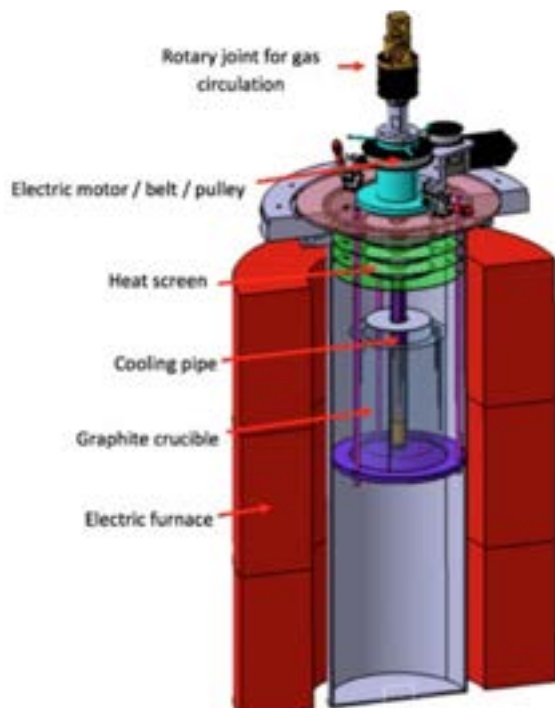


The experiment design is still relatively complex and requires to be installed inside a glovebox with an inert atmosphere. Special attention has to be given to the design of the thermal radiation shielding (heat screen) above the molten salt cavity to avoid excessive heating on the upper structure. In addition, a rotary tightness joint to allow for the argon gas circulation inside the tube is required on the upper part of the rotating shaft. The main mechanical parameters of the solidification experiment in SWATH-S are provided in Table 5. A more detailed layout of the SWATH-S solidification experiment is shown in Figure 7.

Table 5. Main characteristics of the SWATH-S solidification experiment.

Salt	FLINAK
Graphite crucible	Outer/Inner diameters: 160 mm/120 mm Height : 220 mm
Cooling tube (outer tube)	Outer/Inner diameters: 25 mm/ 20 mm Material : SS 304 L Maximum RPM : 20
Cooling gas	Argon Flow rate : 15 NI/min to 60 NI/min

Figure 7. Simplified layout of the SWATH-S solidification experiment.



Experiments were carried-out by starting the tube cooling after temperatures were stabilised in the molten salt bath. More than twenty different solidification transient conditions were investigated by changing the argon rate, the rotation speed and the salt temperature at the external wall. Re-melting transients were also investigated.

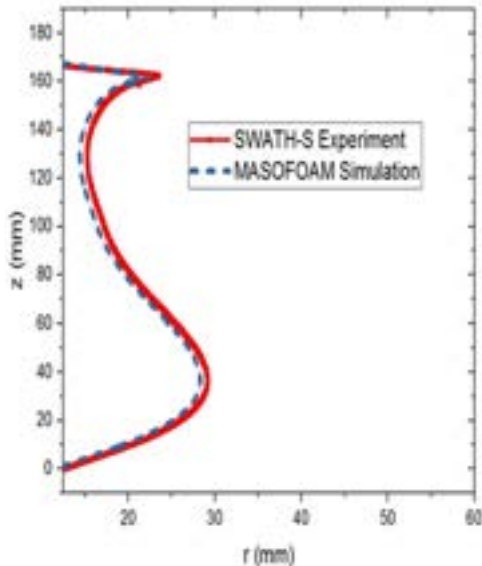
Once the experiment was stopped, the tube was withdrawn from the molten salt bath and the shape of the solidified salt over the tube was picture recorded and measured after cooling. Typical profiles of the solidified salt ingot are show on Figure 8. On the left side of the figure, the solid ingot was obtained after four hours of experiment without rotation of the cooling tube. On the left side the solid ingot was obtained after eight hours of experiment and using a rotation speed of the cooling tube of 9 RPM.

The solidification profiles obtained from these experiments were compared against the predictions from MasoFOAM (with solid phase properties calculated with MusoFOAM). An example of these comparisons is shown in Figure 9. As can be see a good agreement was found between the experimental data and the solidification model predictions.

Figure 8. Flinak ingots obtained in the solidification experiments.



Figure 9. Comparison of MASOFOAM solidification front profiles against SWATH-S experimental results



Other solidification experiments were also performed concerning the cold plug but are not reported here. More details can be found in [11].

V. Conclusion

A high temperature molten salt (Flnak) facility called SWATH-S (Salt) has been built in the framework of the European project SAMOFAR. The purpose of this facility is to collect experimental data on molten salt thermal hydraulics phenomena to help improving the current CFD models used for the design and safety studies of MSRs. To overcome some of the challenges caused by working with high temperature molten salts a second experiment called SWATH-W (Water) was also used. SWATH-W has a similar geometry but uses water as coolant and thus allows implementing PIV measurements in a straightforward manner. The experimental strategy is therefore to use SWATH-W to study only hydraulics aspects while SWATH-S is used to study heat transfer phenomena. SWATH experiments have started at the end of 2016 and are expected to continue at least until mid-2019. Data from these experiments have showed that the pressure

control system used in SWATH to setup the flow rate is providing a stable flow rate and thus adequate experimental conditions. PIV measurements obtained in SWATH-W have been used to improve the accuracy RANS models employed to study the heat transfer phenomena in SWATH-S. Other experiments such as those involving the solidification or the molten salt flow in close channels are providing useful data that is being against the molten salt CFD models. Results from these developments will provide useful recommendations for improvements of the numerical models for the fuel salt flow and also the feasibility of the principles used by the passive reactor draining system.

Acknowledgements

This project has received funding from the Euratom research and training program 2014-2018 under grant agreement No 661891. The content of this article does not reflect the official opinion of the European Union. Responsibility for the information and/or views expressed in the article lies entirely with the authors.

Nomenclature

BFS	Backward Facing Step
CFD	Computational Fluid Dynamics
DNS	Direct Numerical Simulation
FHR	Fluoride salt-cooled High-temperature Reactor
LES	Large Eddy Simulations
MSFR	Molten Salt Fast Reactor
MSR	Molten Salt Reactor
PIV	Particle Image Visualisation
PIRT	Phenomena Identification and Ranking Table
RANS	Reynolds Average Navier Stokes
RSS	Reynolds Shear Stress
SAMOFAR	Safety Assessment of the Molten Salt Fast Reactor – MSFR
SWATH	Salt at WALL: Thermal exChanges

References

- [1] C. Forsberg, P.F. Peterson. Basis for Fluoride Salt-Cooled High-Temperature Reactors with Nuclear Air-Brayton Combined Cycles and Firebrick Resistance-Heated Energy Storage, *Nuclear Technology*, 196(1), 13-33 (2016).
- [2] L. Mathieu, D. Heuer, E. Merle-Lucotte, R. Brissot, C. Le-Brun, E. Liatard, J.-M. Loiseaux, O. Meplan, A. Nuttin and D. Lecarpentier. "Possible configurations for the thorium molten salt reactor and advantages of the fast non-moderated version", *Nuclear Science and Engineering*, 161(1), 78-89, (2009).
- [3] D. Heuer, E. Merle-Lucotte, M. Allibert, M. Brovchenko, V. Ghetta and P. Rubiolo, "Towards the thorium fuel cycle with molten salt fast reactors", *Ann. Nucl. Energy*, 64, 421-429 (2014).
- [4] M. Auffero, Development of advanced simulation tools for circulating fuel nuclear reactors. PhD thesis, Politecnico di Milano (2014).
- [5] P.R. Rubiolo, M. Tano Retamales, V. Ghetta and J. Giraud, "High temperature thermal hydraulics modeling of a molten salt: application to a molten salt fast reactor (MSFR)", *ESAIM: Proceedings and surveys*, 58, 98-117 (2017).
- [6] M. Tano-Retamales, P. Rubiolo and O. Doche, "Development of Data-Driven Turbulence Models in OpenFOAM Application to Liquid Fuel Nuclear Reactors", *OpenFOAM*, Springer (2018).
- [7] M. Tano-Retamales, P. Rubiolo and O. Doche, "Progress in modeling solidification in molten salt coolants ", *Modelling and Simulation in Materials Science and Engineering*, 25.7 (2017).
- [8] K. Fezi, A. Plotkowski, M. J. M. Krane, "Macro-segregation modeling during direct-chill casting of aluminium alloy 7050". *Numerical Heat Transfer, Part A: Applications*, 70(9), 939-963, (2016).
- [9] S. H. Kang, Y. T. Im, "Thermo-elasto-plastic finite element analysis of quenching process of carbon steel", *Journal of Materials Processing Technology*, 192, 381-390 (2007).
- [10] A. Vakhrushev, A. Ludwig, M. Wu, Y. Tang, G. Hackl and G. Nitzl, "Advanced multiphase modelling of solidification with Openfoam®", In *7th OpenFOAM® Workshop*, 29-30, (2012).
- [11] J. Giraud, V. Ghetta, P. Rubiolo and M. Tano-Retamales, "Development and Test of a Cold Plug Valve with Fluoride Salt", *12th International Topical Meeting on Reactor Thermal-Hydraulics, Operation, and Safety (NUTHOS-12)* will take place in Qingdao City, Shandong Province, China, on October 14-18 (2018).

TRACK 3: HUMAN CAPITAL DEVELOPMENT

GIF WEBINARS: AN ONLINE EDUCATIONAL RESOURCE (P. PAVIET ET AL)

Patricia Paviet⁽¹⁾, P. Alekseev⁽²⁾, C. Fazio⁽³⁾, M. Fratoni⁽⁴⁾, G. Harisson⁽⁵⁾, I. S. Hwang⁽⁶⁾, X. Liu⁽⁷⁾, T. Mihara⁽⁸⁾, K. Mikityuk⁽⁹⁾, N. Mpoza⁽¹⁰⁾, Y. Nam⁽¹¹⁾, C. Renault⁽¹²⁾, J. Sun⁽¹³⁾

- (1) US Department of Energy, United States.
- (2) Russian Research Center Kurchatov Institute, Russian Federation.
- (3) Joint Research Center, Germany.
- (4) University of California Berkeley, United States.
- (5) Canadian Nuclear Laboratories Limited, Canada.
- (6) Seoul National University, Republic of Korea.
- (7) Shanghai Jiao Tong University, China.
- (8) Japan Atomic Energy Agency, Japan.
- (9) Paul Scherrer Institute, Switzerland.
- (10) Department of Energy, South Africa.
- (11) Korea Atomic Energy Research Institute, Republic of Korea.
- (12) Commissariat à l'Energie Atomique et aux Energies Alternatives, France.
- (13) Tsinghua University, China.

Abstract

Disseminating information on the research and development on advanced reactor systems, the associated training for the Generation IV workforce, and the retaining of qualified engineers, are all vital for fulfilling the mission of the Generation IV International Forum (GIF) Education and Training Task Force (ETTF). The task force's objectives are to support GIF by serving as a platform to enhance open education and training, communication, and networking. Supporting the GIF intellectual capital in Gen IV reactor systems and cross-cutting subjects is realised via free webinar presentations using internet technologies to communicate the know-how in this field, to increase the knowledge in new advanced concepts, and to avoid the loss of the knowledge and competences that could seriously and adversely affect the future of nuclear energy. The ETTF has launched a webinar series on Gen IV systems in September 2016, which is accessible to a broad audience and is educating and strengthening the knowledge of participants in applications of advanced reactors. This achievement is the direct result of partnering with university professors and subject matter experts who conduct live webinars on a monthly basis. The live webinars are recorded and archived as an online educational resource on the public GIF website (www.gen-4.org). In addition, the webinars offer unprecedented opportunities for interdisciplinary crosslinking and collaboration in education and research. The GIF webinars, with their expansion of topics, target a large spectrum of those that do not know, but are desiring to learn about the many aspects of advanced reactor systems. The details and examples of the GIF webinar modules will be presented in our paper.

I. Introduction

Nuclear power is an economic source of electricity generation combining the advantages of security, reliability cost, competitiveness, safety, and environmental benefits. Future power generation will certainly increase worldwide. Specifically, the amount of nuclear energy used in the world could increase

by a factor of 3 according to the World Nuclear Association program, called Harmony, to a total nuclear capacity by 2050 of 1250 GWe (compared with 301.6 GWe in 2016) [1-2]. With the projected growth of renewable energy and nuclear energy, the potential creation of jobs will emerge and for this reason, a skilled workforce will be needed. The Generation IV Education and Training Task Force (ETTF) was

created in 2015 with an objective to develop and provide quality nuclear education and services on Gen IV nuclear reactors and associated fuel cycles in a manner that fosters international engagement and opportunities[3]. Essential to the success of GIF, considering the long time needed to achieve the challenging goals of Gen IV reactor systems, is education and training of not only the nuclear workforce, but also the general public, policy makers, and students. Considering the increase in nuclear activities around the world and the associated request from most interested countries to obtain up-to-date information on the present status of the ongoing research, the ETTF launched, in September 2016, a series of webinars to widely spread educational information on Generation IV systems and associated cross-cutting subjects. The webinars are promoting the main Gen IV concepts and should stimulate worldwide interest.

II. Education and Training on the GIF Systems

Bolstered by the need for carbon-free energy, the nuclear industry is doing its part with about 60 power reactors currently being constructed in 13 countries notably China, India, the United Arab Emirates, the United States, France, Finland, Belarus, and Russia, which are equivalent to 16% of existing capacity, while an additional 150-160 are planned, equivalent to nearly half of existing capacity [1]. Recognising the need for a talented workforce and the world demand for dedicated nuclear engineers, and considering the long time needed to achieve the challenging goals of Gen IV reactor systems, the GIF ETTF chose the webinar platform to offer a once a month webinar on advanced reactor systems to educate and train not only students currently pursuing their formal education in universities, but also the workforce who may need a refresher course or a better understanding of a specific topic, and most importantly a broader audience. Training can require complicated logistics and planning, extensive travel, and the ability to convince trainees, over and over again, that their time will not be wasted. For the past two decades, webinars (i.e. seminars on the web), have been used exponentially to deliver focused contents on multiple subjects. For this reason, the GIF ETTF is using this modern internet technology to promote training on Gen IV systems and to ensure a knowledgeable workforce exists. In addition, the ETTF is developing world-class webinars that will also be useful to technicians,

managers, regulators, and others who may benefit from an enhanced understanding of advanced reactor concepts in their work.

Member countries proposed more than a hundred nuclear reactor systems [4], of which GIF selected six, that were considered to be the most promising in light of various criteria based on the following objectives:

1. continuation of the progress made by Generation III water reactors in terms of competitiveness and safety;
2. more effective use of uranium resources;
3. less radioactive waste, especially high-level, long-lived waste;
4. greater protection against malicious acts and the diversion or theft of nuclear materials.

The six systems selected by GIF are:

Sodium-cooled Fast Reactors (SFR); Very High Temperature Reactors (VHTR); Gas-cooled Fast Reactors (GFR); Lead-cooled or Lead-Bismuth Eutectic (LBE) cooled Fast Reactors (LFR); Molten Salt Reactors (MSR); and Super-Critical Water Reactors (SCWR) (Fig 1), and these are the ones presented in the GIF webinar series.

Figure 1. GIF members' involvement in Gen IV systems R&D

	Australia	Canada	China	France	India	Japan	Korea	Russia	South Korea	Switzerland	USA
SFR			*	*	*	*	*	*			*
VHTR	*	*	*	*	*	*	*	*			*
LFR				*	*	*	*	*			*
SCWR		*	*	*	*	*	*	*			*
GFR				*	*	*	*	*			*
MSR	*			*	*	*	*	*	*	*	*

★ signatory of System Arrangement
★ signatory of Project Arrangement

The GIF-ETTF has established collaborative associations with universities and nuclear organisations (Table 1) actively involved in Gen IV systems to foster the exchange of scientific and technical information for the development of these webinars.

Table 1. Organisations involved with the Development of GIF webinars

	Country
U.S. Department of Energy – Office of Nuclear Energy	U.S.A.
Institute of Energy and Environment, Youngsan University	Republic of Korea
Commissariat à l’Energie Atomique et aux Energies Alternatives	France
Argonne National Laboratory	U.S.A.
Canadian Nuclear Laboratories	Canada
University of California, Berkeley	U.S.A.
US Naval Postgraduate School	U.S.A.
Nuclear Energy Agency	NEA/OECD
Idaho National Laboratory	U.S.A.
Nuclear National Laboratory	U.K.
INET, Tsinghua University	China
Los Alamos National Laboratory	USA
SCK.CEN	Belgium
Brookhaven National Laboratory	USA
NRC “Kurchatov Institute”	Russia
Institute of Physics and Power Engineering	Russia
Ansaldo Nucleare	Italy
European Commission	Belgium
UJV Rez, A.s	Czech Republic

III. Development of the GIF Webinar Series

The GIF webinars are organised in a series of topics related to Gen IV systems and cross-cutting. As of June 2018, the series consists of 20 monthly lectures covering the Gen IV systems (Table 2). The webinars are currently underway and an additional six webinars are planned until December 2018 (Table 3). These webinars, posted by the Department of Homeland Security to the Interagency Network and the GIF website, consist of a one-hour online lecture (on specific Gen IV systems or cross-cutting topics) by top-level international experts, with free attendance registration at gen-4.org. These webinars also provide an opportunity for the audience to comment or ask questions at the end of each presentation. The system is designed for web conferencing and includes many features such as:

- Attendee registration.
- Attendee questionnaires about the webinar they followed.
- Scheduled reminders for the registered participants and follow up questionnaires, if desired.

- Conferencing capabilities for 200 attendees at one time.
- And a certificate of attendance sent automatically for those who followed the live webinar presentation.

Table 2. List of Webinars presented and archived from September 2016 to June 2018

Webinars presented and archived as of June 2018	
Atoms for Peace - the next generation Dr. John Kelly, Department of Energy, USA	Nuclear Fuels Dr. Steven Hayes, Idaho National Laboratory, USA
Closing the Fuel Cycle Dr. Myung Seung Yang, Institute of Energy and Environment, Youngsan University, Republic of Korea	Energy Conversion Dr. Richard Stainsby, Nuclear National Laboratory, United Kingdom
Introduction to Nuclear Reactor Design Dr. Claude Renault, CEA, France	Feedback Phenix and Superphenix Dr. Joel Guidez, CEA, France
Sodium Cooled Fast Reactors (SFR) Dr. Robert Hill, Argonne National Laboratory, USA	The Sustainability, a relevant Framework for addressing GEN IV Nuclear Fuel Cycles Dr. Christophe Poinssot, CEA, France
Gas Cooled Fast Reactors (GFR) Dr. Alfredo Vasile, CEA, France	Design, Safety Features and Progress of the HTR-PM Prof. Dr. Yujie Dong, INET, Tsinghua University, China
Thorium Fuel Cycle Dr. Franco Michel-Sendis, OECD/NEA, France	GEN IV Materials and their Challenges Dr. Stu Maloy LANL, USA
Supercritical Water Reactors Dr. Laurence Leung, Canada National Laboratory, Canada	Very High Temperature Reactors Mr. Carl Sink, Department of Energy, USA
Fluoride Cooled High Temperature Reactors Dr. Per Peterson, UC Berkeley, USA	SCK.CEN’s R & D on MYRRHA Prof. Dr. Hamid Ait Abderrahim, SCK.CEN, Belgium
Molten Salt Reactors (MSR) Dr. Elsa Merle, CNRS, France	Lead Fast Reactor (LFR) Dr. Craig Smith, US Naval Graduate School

In connection with this activity, flyers are developed to advertise the webinars on the Gen IV website and on LinkedIn as well, and are sent via email or posted on the LinkedIn Gen IV site. Outreach and informational meetings are organised by NEA/OECD. Brochures to advertise

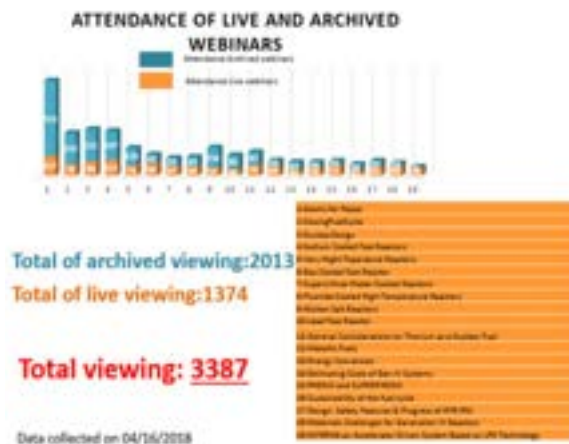
the GIF-ETTF webinars activities are being developed and distributed at various national and international conferences where the presentation of the GIF ETTF’s activities are planned. Information is accessible without restrictions via the Gen IV website. Since the first webinar presented by Dr. John Kelly in 2016, the GIF ETTF has coordinated 20 free, live, interactive webinars. As of April 2018, attendance during the live webcasts totals 1,374 and the number of viewings of recorded webinars in the online archive is 2,013 for a total of webinar viewing of 3,387 (Figure 2).

The Task Force is tracking statistics associated with the viewing of these webinars (numbers), as well as identifying the sites associated with these views (country, organisation) which are displayed in Figures 2-4.

Table 3: List of Webinars planned until December 2018

Title of Webinar	Tentative date for Webinar presentation
Astrid – Lessons Learned	July 2018
BREST-300 Lead Cooled Fast Reactor	August 2018
Advanced Lead Fast Reactor European Demonstrator – ALFRED project	September 2016
Safety of Gen IV Reactors	October 2018
The ALLEGRO Experimental Gas Cooled Fast Reactor Project	November 2018
Russia BN 600 and BN 800	December 2018

Figure 2. Webinar Attendance and Number of Archived Viewings



The participants in the GIF webinars include representatives from multiple organisations including federal agencies, national laboratories, various state agencies, universities, international organisations, contractors, and commercial organisations. As shown in Figure 3, 31% of webinar participants are from international organisations. Representatives from state agencies comprise the next largest single organisation type.

Figure 3. Participants by organisation types (Data collected in April 2018)



Figure 4. Example of a GIF Webinar Attendance Distribution



There are no fees associated with these webinars, which make the webinars very attractive. The success of these webinars relies on the presenters who are internationally recognised experts. The GIF webinar attendance distribution for the webinar on “Design, Safety Features & Progress of HTR-PM” presented in January 24, 2018, is displayed in Figure 4, and shows attendees from diverse organisations, federal agencies, state agencies, universities and national laboratories.

The attendees thus far have been extremely positive about the quality and content of these webinars as reflected by the following statements:

“I thought it was very interesting. The material is not often presented in other than a graduate school setting so many of us don't have access to it; other than from books. Thank you for making it possible.”

“Excellent introduction. I look forward to the ongoing program.”

“These webinars will benefit a vast audience, keep up the great work!!”

“Very good format. Great outreach. Please continue.”

“Excellent, clear and well organised presentation that covered central issues on the topic.”

“The technical content of the slides for this webinar were EXCELLENT.”

“I like the link to the GIF webinars on the Gen-4 webpage. This makes it very convenient to watch the webcasts and/or download the presentations.”

IV. Conclusion

Since September 2016, the GIF ETTF has been offering short (60 to 90 minutes) webinar presentations on specific advanced reactor topics which have been developed and are offered as interactive on-line conferences. The webinars are recorded and archived to become a library or collection of seminars for on-line access from the Gen IV website (www.gen-4.org). The GIF webinars have successfully reached a broad audience and continue to gain interest. The momentum and overwhelmingly positive feedback from participants affirm the benefits in these unique educational opportunities and validate the need for additional resources to maintain a high level of expertise in Gen IV systems. GIF webinars will continue to be a useful education resource for current and future workforce.

Acknowledgements

The authors would like to thank Berta Oates from Portage Inc., Bonnie Hong and Alexander Stanculescu from the Idaho National Laboratory, Henri Paillère and Gisela Grosch from OECD/NEA, and John Kelly from the American Nuclear Society for their valuable support.

References

- [1] Nuclear Power in the World Today, April 2018, <http://world-nuclear.org/information-library/current-and-future-generation/nuclear-power-in-the-world-today.aspx>
- [2] Worldwide nuclear capacity continues to grow in 2016, January 2017, <http://www.world-nuclear-news.org/NP-Worldwide-nuclear-capacity-continues-to-grow-in-2016-0301175.html>
- [3] P. Paviet, P. Alekseev, C. Fazio, M. Fratoni, I. S. Hwang, J. Kelly, X. Liu, T. Mihara, K. Mikityuk, N. Mpoza, Y. Nam, G. Pynn, C. Renault, J. Sun, “GEN IV Education and Training Initiative via Public Webinars”, Proc. of International Conference on Fast Reactors and Related Fuel Cycles: Next Generation Nuclear Systems for Sustainable Development (FR17), Yekaterinburg, Russia, IAEA-CN-245-13, International Atomic Energy Agency, June 2017.
- [4] Review of Generation IV Nuclear Energy Systems, Institut de radioprotection et de sûreté nucléaire (IRSN) 2015, http://www.irsn.fr/EN/newsroom/News/Documents/IRSN_Report-GenIV_04-2015.pdf
- S. Bortot, J. Wallenius, K. Mikityuk, “GEN-IV FAST SPECTRUM REACTORS: E-LEARNING TEXTBOOK AND COURSE DEVELOPMENT AT KTH”, In: Proceedings of Atoms for the Future 2018 & 4th GIF Symposium, Paris, France, October 16-17, 2018
- S. Bortot, K. Mikityuk, J. Wallenius, “GEN-IV FAST SPECTRUM REACTORS: PILOT MOOC DEVELOPMENT AT EPFL”, In: Proceedings of Atoms for the Future 2018 & 4th GIF Symposium, Paris, France, October 16-17, 2018

TEACHING SODIUM FAST REACTORS IN CEA (C. LATGE ET AL)

Christian Latge⁽¹⁾, François Beauchamp⁽¹⁾, Leïla Gicquel⁽²⁾

(1) CEA Cadarache, Nuclear Energy Directorate, Nuclear Technology Department, France.

(2) CEA Cadarache, INSTN, France.

Abstract

Among the Fast Neutron Reactor Systems, the SFR has the most comprehensive technological basis as result of the experience gained from worldwide operation of several experimental, prototype, and commercial size reactors since the 1940s. This experience corresponds to about 402 years of operation by end of 2010. Six reactors are in operation: BOR60, BN600 and BN800 in Russia, Joyo in Japan, FBTR in India and CEFR in China. One reactor is being commissioned: PFBR (500MWe) in India and several projects are currently developed: FBR1 and 2 in India, BN1200 in Russia, JSFR in Japan, PGSFR in Korea, CFR-600 in China and ASTRID in France. In order to support operation of existing reactors, design activities for new projects and decommissioning of old reactors, it is mandatory to develop skills, more particularly among the young generation, who will operate these new reactors. In addition, education and training is also essential to share the knowledge among the teams involved in Research and Development. Several strategies are developed at the national level, or within multilateral framework, like EU or IAEA to support development of Fast Reactors.

In France, to answer to this increasing demand of Education & Training, four sessions are proposed, within the frame of INSTN (French National Institute for Nuclear Science and Technology):

- SFR: History, main options, design and operational feedback
- SFR: Functional analysis and design
- SFR: Safety and operation
- SFR: Sodium structures interactions

The French Na School (ESML) provides since 1975 also several sessions dedicated to Na facilities design, safe operation, handling, and also decommissioning and sodium treatment. Beside courses, practical exercises are organised during each session. 10 different modules are available, ranging in length from 1 to 5 days.

CEA contributes also to the organisation of European Sessions dedicated to Sodium Fast Reactors, organised within the frame of the European Commission (CP-ESFR, ESNII+ , ESFR-SMART).

This Education and Training strategy is a key element for the future of the development of Sodium Fast Reactors, and more particularly ASTRID project. CEA is ready to share training experience and to collaborate with other foreign Education and Training Entities.

I. Introduction

Among the Fast Neutron Reactor Systems, the Sodium Fast Reactor (SFR) has the most comprehensive technological basis as result of

the experience gained from worldwide operation of several experimental, prototype, and commercial size reactors since the 1950s. This experience corresponds to around 420 years of operation by end of 2017. Six reactors are in operation: BOR60, BN600 and BN800 in

Russia, Joyo in Japan, FBTR in India and CEFR in China. One reactor is being commissioned: PFBR (500MWe) in India and several projects are currently developed: FBR1 and 2 in India, BN1200 in Russia, JSFR in Japan, PGSFR in Korea, CFR-600 in China and ASTRID in France, in partnership with Japan. In order to support operation of existing reactors, design activities for new projects and decommissioning of old reactors, it is mandatory to develop skills, more particularly among the young generation, who will operate these new reactors. In addition, education and training is also essential to share the knowledge among the teams involved in Research and Development. Several strategies are developed at the national level, or within multilateral framework, like EU or IAEA to support development of Fast Reactors [1]

In France, the new objective is to build a GENERATION IV reactor prototype so-called ASTRID. This decision has motivated an important and rapid increase of R&D work, oriented towards the design and conceptual evaluations. Two reactors are currently being dismantled, Phenix and Superphénix. It was therefore necessary to support these activities and promote Education and Training Initiatives. To support this requirement, ESML (Ecole du Sodium et des Métaux Liquides), EC (Ecole des Combustibles), both located in CEA-Cadarache and INSTN (Institut des Sciences et Techniques Nucléaires) are the key schools to support the development of Sodium Fast Reactors.

II. Education and Training at ESML

The objectives of the Sodium School (ESML) are to synthesise knowledge, to share it between CEA experimental facilities operators and consequently to support R&D activities, to train operators able to work on Sodium Fast Reactors, to train design engineers involved in SFR projects and to train fire brigades. Its role has always been to adapt its offer and its training content to the changing needs for reactor operation, experimentation and for design activities. Trainees usually belonged to French companies such as CEA, EDF, AREVA and IRSN, or any companies involved in sodium activities belonging or not to the nuclear industry. At the early stage of its creation, ESML intended to be opened to foreign countries. Specific training sessions were provided for German operators for SNR300 (1983), Japanese operators for the first start-up of Monju reactor (90's) or in support to the PFR and DFR decommissioning projects (UK). More recently, ESML in association with PHENIX plant operator has

extensively increased its opening to foreign institutes, such as trainees from CIAE in China, ROSATOM in Russia on Reactor technologies, safety and operation, or IGCAR in India dedicated to Safety. ESML provided also specific sessions to Chemical industry, such as UOP (USA).

The pedagogical approach consists in a combination of various educational means: lectures, discussions and Training on a Sodium loop. Since 1975, more than 6000 trainees have received a training at the Sodium School. The following items are currently addressed: physico-chemistry of sodium coolant (physical and chemical properties), purification, corrosion, contamination, cleaning and decontamination...

Sodium technology, description and operation of components, instrumentation, visualisation, inspection and repair, are also presented in dedicated sessions; during these sessions, exercises involving operation and intervention procedures on the sodium loop are organised. Sodium safety is always a key part of the sessions. Specific hazards induced by the chemical properties of sodium are described: sodium-water reaction and hydrogen risk assessment, sodium fires, safety rules, prevention, intervention, exercise on a real sodium fire... In support to the processes used for decommissioning SFRs, ESML lecturers present and address the following items: some specific risks, dismantling techniques, sodium treatment, sodium waste storage, decommissioning of Na-K facilities....

Currently, nine theoretical and practical modules are proposed (the duration of each module depends on the topic):

- Na risk management and safety (1 day)
- Na hazard basics validation (0,5 day)
- Na circuit operation & maintenance (5 days)
- Na facilities decommissioning (5 days)
- Practice of component cleaning and decontamination (3 days)
- Management of Na-K (sodium-potassium) and associated hazards (3 days)
- Intervention on Na facilities (2 days)
- Practice of Na circuit operation (3 days)
- Practice of sodium purification (3 days).

Every year, ESML organises about 15 sessions, which represent about one hundred trainees.

Devices and facilities are available to conduct practical exercises or experiments:

- Na facility designed for training participants in sodium circuit operation (SUPERFENEC loop). (Fig.1)
- Cleaning pits for the treatment of components containing sodium (MININANET, PEELA facilities). (Fig.2)
- Observation of a sodium fire, hydrolysis of sodium by spraying water in shielded cell (VAUTOUR facility). (Fig.3)
- Cutting operations of sodium components, ...

Figure 1. Superfennec Na loop



Figure 2. MININANET facility



Figure 3. Na fire extinguishing exercise



New pedagogical tools for the Na School:

New pedagogical tools for the Na School are currently set-up. To improve our pedagogical means, four new educational tools are presently developed and are dedicated to the following main phenomena involved in Na technology:

- US transmission
- Magneto-hydrodynamics
- Na-Water reaction
- Na fire

Four benches will allow the Sodium School to up-date the pedagogy and contribute to improve the offer of training sessions and the skills acquired by the trainees. These educational tools will be dedicated to training but also used for communication purpose to improve the public acceptance.

Bench N°1: Ultrasound imaging technology

In-service inspection and repair (ISI&R) is considered as a challenge for Generation IV sodium-cooled fast reactors, due to sodium coolant opacity, chemical reactivity. ISIR mainly focus on the inspection of reactor block structures, immersed in sodium at about 200°C: telemetry, under-sodium viewing, crack detection....In order to illustrate the potentialities of Ultra-Sounds (US) technologies, telemetric measurements, creation of images from simple shapes, use of Transducers Ultra-Sound able to be operated at High Temperature (TUSHT®), some dedicated laboratory devices will be implemented, at ESML

Bench N°2: Magneto-hydrodynamics (MHD)

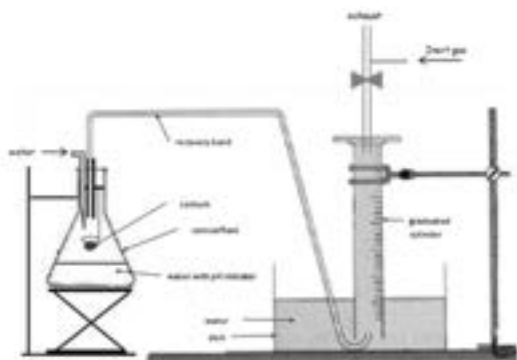
Due to their high electrical conductivity, liquid metals, and in particular sodium and its alloys like NaK, allow the use of magneto-hydrodynamic devices as actuators and sensors. Electro-Magnetic Pumps (EMP), Eddy Currents Flow Meter (ECFM) are one of the most widely used devices in liquid sodium circuit. In both cases, working principle is based on the interaction of an electrical current density, a magnetic flux density and the velocity field of the liquid metal. Understanding, implementing and using of such devices in liquid metal facility needs specific Knowledge on applied electrotechnics and magneto-hydrodynamics (MHD). Dedicated benches will be proposed to support dispensed courses based on more theoretical notions.

Bench N°3: Na-water interaction

Hazard induced by the potential large interaction of Na and water in a Steam Generation Unit or a cleaning pit is often underlined: there is one discontinuous source of hydrogen and sodium hydroxide, inducing related hazards.

Nevertheless, this reactivity with water is commonly used for the development of cleaning processes for structural material wetted with sodium, during handling operations and moreover for the conversion of the large amounts of sodium into sodium hydroxide, at the end of the reactor operation, during the decommissioning phase. A process, called NOAH, has been developed in CEA Cadarache and applied successfully to convert the primary sodium from Rapsodie, PFR, KNK-2 and Superphenix. It will be used also to process the sodium from Phenix. Thus, it has been decided to design and set-up two Sodium Water Reaction benches: a device for educative practical works (Figure 5) and another one for a demonstration of sodium treatment by hydrolysis with water.

Figure 4. Bench dedicated to the characterisation of Na-water interaction



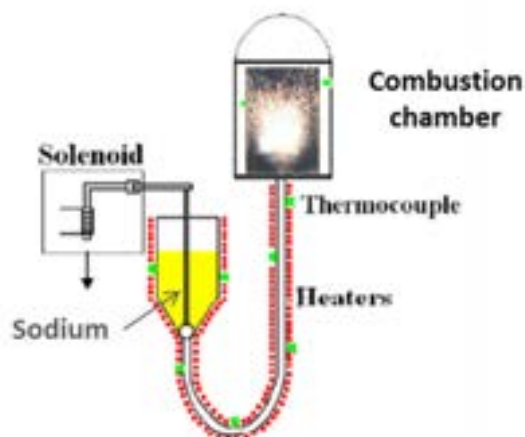
This first educational facility (geometries and volumes of the glass equipment) will be optimised with regards safety standards and designed for a pressure resistance of about 1.5 bar. abs.

Bench N°4: Sodium fire

A dedicated bench will be devoted to the design of a spray fire device to carry out small-scale sodium fire experiments (Figure 5). It will be limited to a few grams of Na of sodium (10 g max). Thermocouples are located inside the combustion chamber for measuring the spray

temperature. High-speed camera and thermal imaging can be used to visualise the sodium fire combustion, in particular the distribution of the particles sizes in the jet during combustion, the temperature distribution, effects of sodium temperature and oxygen concentration.

Figure 5. Basic principle of spray fire demonstrative facility



III. Education and Training at INSTN

Within the frame of INSTN (Institut National des Sciences et Techniques Nucléaires) (www-instn.cea.fr), several sessions are currently provided:

- SFR history, main options, design and operational feedback;
- SFR functional analysis and design
- SFR safety and operation;
- SFR: interaction between Na and structures;
- SFR: Core physics ;
- SFR: ERANOS code.

In addition, the INSTN (Institut National des Sciences et Technologies Nucléaires), develops its own Nuclear Engineering Master level (or specialisation) degree and a catalogue of more than 200 vocational training courses.

INSTN is partner of ENEN (European Nuclear Energy Network). (www.enen-assoc.org).

To address more particularly SFR training needs related to the operation of SFR, it was intended to develop a SFR simulator, including the Energy Conversion System. The SIRENa simulator, developed by Reactor Studies

Department, in Cadarache Research Center (France) (Figure 6) is used in engineering courses as an adjunct to lectures on safety and operation and can be used for human factor studies and human machine interface design. Training on such a simulator permits to perceive the effects of constraints governing the operation of a reactor (inertia, cons-reactions, regulations ...) or to apply theoretical knowledge (eg sub-critical approach). Within this project, the main functional specifications of the simulator and the needs of development of dynamic models, have been defined. This simulator represents a "Pool type" SFR, the most common concept selected for large SFRs. The design consists of a safety vessel, which contains the primary vessel, reactor core, intermediate heat exchanger (IHX), secondary heat exchange, control rods, balance-of-plant and intermediate circuit pipework. Core cooling in SFR may be achieved by forced or natural circulation. The user can modify plant parameters, to adjust various aspects of the plant configuration and to accommodate differences between specific designs. An example of one such variation could be in the number of intermediate heat exchangers that are contained within the pressure vessel, the inclusion of coolant pumps onto the pressure vessel, In pool-type SFRs, the sodium in the primary circuit does not directly exchange its heat with the coolant of the Energy Conversion System (ECS): water if the Rankine cycle is selected, gas if the Brayton cycle is selected. The main components with their associated models are included in the simulator: pumps, heat exchangers, Plant control and protection systems, Purification Systems and their cold traps, Decay Heat Removal Systems....

The simulator is capable of simulating the following standard operational events:

- Power Increase and Decrease, in this mode user can change power with ramp in range among 0% to 100% by control rod
- Reactor Scram and Restart
- Reactor Start-up and Heat up
- Reactor Shutdown and Cooling

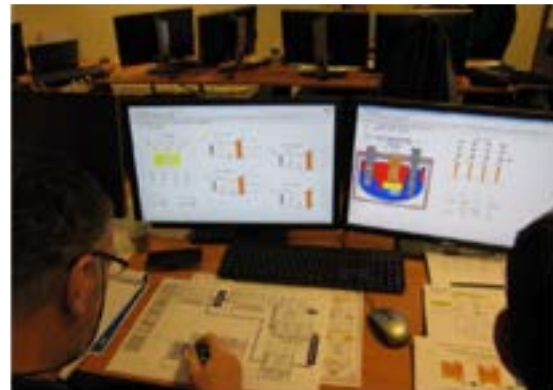
Moreover, the user can change the speed of pumps; accordingly, simulator shows its effect on Primary heat transport, intermediate heat transport system and steam/ gas system.

Simulator allows also the user to change the material of fuel, cladding and shows it affects

(through thermal properties and reactivity coefficients).

Simulator is able of generating malfunction like pump shutdowns, valve failures, and regulation system failures...

Figure 6. SIRENa simulator for SFRs



IV. Education and Training at I2EN

France has an important nuclear teaching platform organised around engineering schools, universities, involving also research laboratories, technical schools and also nuclear companies or dedicated entities, for professional training. In this context, I2EN, the *International Institute for Nuclear Energy* set up in 2010, is federating French entities delivering high level curricula in nuclear engineering and science related to the main following items:

- Nuclear safety and radiation protection
- Reactor physics & nuclear engineering
- Waste management, disposal, nuclear decommissioning & safety
- Materials science for nuclear energy
- Chemistry for nuclear energy & environment
- Instrumentation for nuclear industry ...

Even if I2EN provides mostly initiatives tailored to the needs of industry (mostly PWRs in France), several masters address Fast Neutron Reactors (essentially SFRs) and more particularly the main fields underlined previously. The list of initiatives is provided in the I2EN web-site: <http://www.i2en.fr>.

V. Conclusion

To support the development of SFRs, an efficient Education and Training strategy is essential for the future of the development of Sodium Fast Reactors. Sodium School (ESML) and INSTN are key actors in France to develop new skills in support to SFR studies. A general consensus is to apply modern approaches to course design ie the application of the intended learning outcome (ILO) approach and the implementation of interactive methodologies.

CEA is ready to share training experience and to collaborate with other foreign Education and Training Entities.

Nomenclature

DHRS	Decay Heat Removal System
GIF	Generation IV International Forum
IHX	Intermediate Heat Exchanger
INSTN	National Institute for Nuclear Science and Technology
MHD	Magneto-hydrodynamics
SFR	Sodium Fast Reactor
SGU	Steam Generator Unit

References

- [1] C. Latgé, M. Soucille, C. Grandy, Xu Mi, R.Garbil, M. Sai Baba, P. Chellapandi, T. Kitabata, Y-G Kim, S. Monti "Education & Training in support to Sodium Fast Reactors around the world", IAEA International Conference on Fast Reactors and Related Fuel Cycles – FR13 Paris (France) Mars 2013

TRACK 4: RESEARCH INFRASTRUCTURES

THE DEVELOPMENT AND COMMISSIONING OF THE LIQUID LEAD LABORATORY (LILLA) FOR MECHANICAL TESTING IN LIQUID LEAD (Z. SZARAZ ET AL)

Zoltán Száraz⁽¹⁾, Kamil Tuček⁽¹⁾, Radek Novotný⁽¹⁾, Theo Timke⁽¹⁾, Theo Heftrich⁽¹⁾, Karl-Fredrik Nilsson⁽¹⁾, Michael Fütterer⁽¹⁾, Pekka Moilanen⁽²⁾

(1) European Commission, Joint Research Centre, Directorate G – Nuclear Safety & Security, the Netherlands.
(2) Pneumatic Solutions & Innovations, Finland.

Abstract

The paper presents development of heavy liquid metal experimental facility for conducting pre-normative, separate effect tests of candidate structural materials for lead cooled fast reactors (LFRs) inside realistic environmental conditions of liquid lead in temperatures up to 650°C. The facility is a part of the JRC's Liquid Lead Laboratory (LILLA), developed in the joint programming with EU Member States, in support to the European heavy liquid metal cooled reactor concepts, MYRRHA and ALFRED, and related activities ongoing within the Generation IV International Forum.

The facility allows studying stress corrosion cracking / liquid metal embrittlement phenomena under tensile and compressive stress, as well as performing tensile, fatigue, creep, small punch, cone mandrel, and fracture toughness tests with well-controllable parameters of temperature, oxygen content in liquid lead, mechanical load, and lead flow. Tests of the reliability of lead chemistry control systems as well as related components, including instrumentation, are also possible.

The paper reports on the design of the facility and test sections with unique, pneumatic bellows-based loading devices, as well as on outcomes of the facility commissioning and the first mechanical tests performed in liquid lead.

I. Introduction

As an in-house science service of the European Commission, Joint Research Centre (JRC) provides an independent, evidence-based scientific and technical support to the development of the European Union policies. JRC tackles key societal challenges, such as energy, climate, and nuclear safety. JRC also stimulates innovation through developing new methods, tools and standards. To this end, JRC hosts a number of unique facilities, including the High Flux Reactor (HFR) in Petten.

Together with international partners, JRC also conducts feasibility studies of innovative, sustainable reactor concepts aiming at improved safety performance, waste management, and economy. These advanced reactor concepts are being developed in a

multilateral collaboration of 14 countries, members of the Generation IV International Forum (GIF), including European Union (EURATOM) [1-2].

One of these innovative concepts is the Lead cooled Fast Reactor (LFR). Use of liquid lead as a coolant provides several important inherent safety advantages. It allows operating the reactor at close to atmospheric pressure and provides high thermal inertia and natural convection characteristics leading to robust passive safety behaviour. Lead is also chemically relatively inert in contact with air and water, which allows improving both safety and economic performance [3].

The paper presents the development of heavy liquid metal experimental facility for conducting pre-normative, separate effect tests of candidate structural materials for LFRs inside

realistic environmental conditions of liquid lead at temperatures up to 650°C. The facility is part of the JRC's LIquid Lead LABoratory (LILLA), developed in the joint programming with EU Member States, in support to the European heavy liquid metal cooled reactor concepts, MYRRHA [4] and ALFRED [5], as well as related activities ongoing within GIF [6].

The facility allows studying stress corrosion cracking/liquid metal embrittlement phenomena under tensile and compressive stress, as well as performing tensile, fatigue, creep, small punch, cone mandre², and fracture toughness tests with well-controllable parameters of temperature, oxygen content in liquid lead, mechanical load, and lead flow. Tests of the reliability of lead chemistry control systems as well as related components, including instrumentation, are also possible.

The paper reports on the design of the LILLA facility and test sections, the latter with unique, pneumatic bellows-based loading devices, as well as on outcomes of the laboratory commissioning and first mechanical tests performed in liquid lead.

II. Description of the LILLA Facility

The LILLA facility consists of two cylindrical tanks, measuring tank and dump tank, and connecting piping to transport molten lead between the tanks as well as to deliver and extract gases to and from the facility, respectively. A 3D drawing and view of the facility are displayed in Figures 1-2.

The main characteristics of the facility are:

- Working temperatures in lead: up to 650°C;
- Working range of oxygen concentrations in lead: from saturation (at 400°C) down to 10-10 weight%;
- Design pressure: 0.4 MPa;
- Operating pressure: 0.2 MPa;
- Lead inventory: ca. 35 l;
- Structural material: AISI 316 Ti;
- Surfaces in contact with molten lead are protected by aluminium coating using the pack cementation technology;

- Active control of gas / oxygen injected to cover gas space and to molten lead (below surface);
- Two reserve ports (diameter 35 mm) with possibility for multiple feed-throughs;
- Online sampling of lead during operation of the facility; and
- Gas and lead filtering capability.

Figure 1. The 3D drawing of the LILLA experimental facility for mechanical testing in liquid lead with the main systems and components indicated

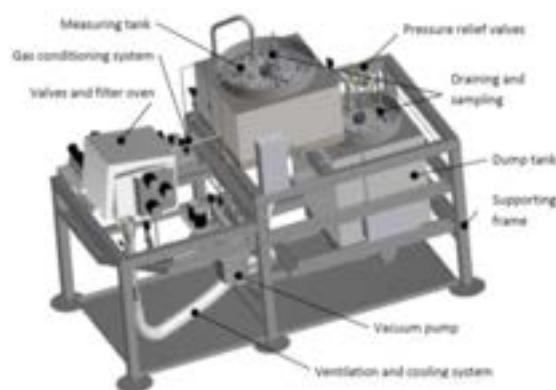


Figure 2. View of the LILLA experimental facility for mechanical testing in liquid lead



Pressurised inert gas – Ar – is used to flush the facility and to transport molten lead there. Argon also acts as a cover gas in the tanks. The oxygen control in molten lead is achieved by an

² To determine hoop tensile properties of thin-walled cladding tubes.

appropriate admixture and delivery of Ar, Ar-H₂, and air to the facility.

Heaters are placed in sections around the tanks and pipes, each with its own power regulator. The heaters are operated automatically as well as manually, allowing melting, heat-up, maintenance of temperatures, shutdown of the facility, and passive drainage of lead to the dump tank. The degree of the lead natural convection flow in the measuring tank is possible to regulate through variation of the power of external heaters and heat losses to an internal cooling channel. This feature facilitates a time-efficient control and adjustment of oxygen content in lead, in addition to an oxygen diffusion process from the cover gas space. Due to low dissolution kinetics of oxygen in molten lead, the diffusion process is relatively slow, especially at temperatures below 500°C.

Alternatively, gases can also be injected directly to lead in both measuring and dump tanks.

The installed components and instrumentation include:

- Oxygen sensors in gas and in lead to control the amount of oxygen dissolved in molten lead;
- Hydrogen and humidity sensors in gas to control the gas chemistry;
- Thermocouples in gas and lead;
- Lead weighing tensometric sensors to measure lead level in the tanks;
- Pressure transducers;
- Overpressure protection through gas relief valves; and
- Windows on the tank lids to control the surface of lead and state of the cold traps.

All experimental and measured values are also automatically recorded by the digital data acquisition system and are archived on a dedicated data drive for quality assurance and further evaluations.

III. Description of Test Sections

Material testing can be done on a wide variety of test specimens. The material testing standards, such as ANSI, ASTM, DIN, and ISO define the test specimen type and size to be used for a specific material test. In many cases the specimen size determined by the standards cannot be implemented and, typically, material

testing under very difficult conditions require a small specimen size. These harsh testing environments include irradiation, high-temperature liquid or gas conditions, corrosive environments, and high-pressure conditions.

Naturally, the testing of nuclear power plant materials in representative conditions is difficult due to challenges posed by the testing environment. The lifetime management of the current-generation nuclear power plants is a good example of such difficult circumstances. Surveillance programs are typically based on the testing of materials already irradiated, thereby reducing further the availability of these materials for subsequent examinations. One solution to this challenge is the use of small test specimens to conduct the required surveillance as well as material qualification programs.

The qualification of the existing and/or newly-developed materials for the future Generation IV reactor concepts is equally challenging. These advanced reactor concepts often seek increasing operating temperatures for higher efficiency and/or product flexibility as well as envisage the use of innovative coolants. New materials and/or testing environments hence require the development of a new testing equipment which can be used reliably and safely with the small-size (i.e., sub-size) specimens in such demanding testing conditions.

For the use in the LILLA facility, a new, innovative test equipment was developed, assembled and calibrated to conduct mechanical tests on small specimens in high temperature liquid lead up to 650°C. Benefitting from the flexibility of the developed design solution, a wide variety of test specimens can be used, including the disk-shaped compact tension DC(T), round bar and flat tensile, cone mandrel and small punch types of the specimens.

The load in the test sections is generated by a new type of the pneumatically-powered double bellows loading apparatus (D2B loading device), cf. Figure 3. This device allows generating both tensile and compressive loads, which are measured by a commercial load sensor in a continuous way.

The LILLA facility currently features four independent test sections integrated into the measuring tank with the following characteristics, cf. also Figure 4:

- Maximum pressure in the test sections: 15 MPa of air for pneumatic bellows-based loading system;
- Maximum load: 12 kN, push/pull;
- Displacement rates: 10⁻⁸ to 10⁻² mm/s;
- Strain rates: 10⁻⁷ to 10⁻² s⁻¹;
- Fatigue: maximum 0.1 Hz;
- Range of amplitudes: 0.1 to 0.0005 Hz;
- Test / hold times: at least 100 s up to 5,000 h;
- Each test section is equipped with its own Pt-air reference electrode oxygen sensor and thermocouple.

Figure 3. The double bellows loading device

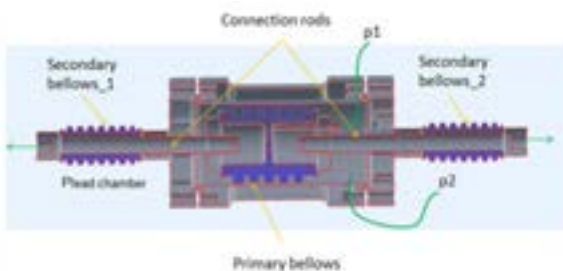
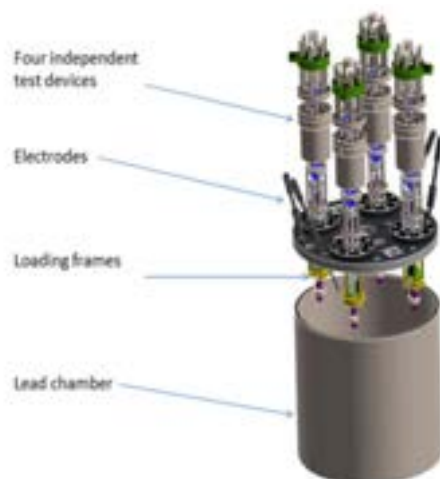


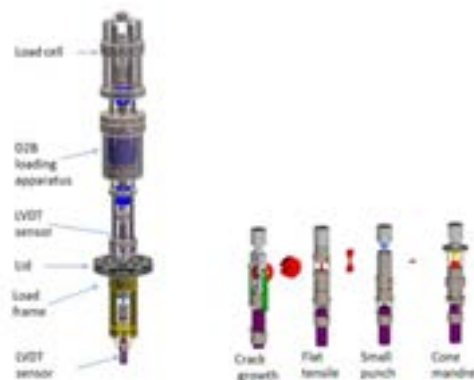
Figure 4. The D2B loading devices with the test sections integrated in the LILLA measuring tank



The test sections of the LILLA facility consequently allow a variety of tests, including:

- Constant strain rate tensile tests, incl. Slow Strain Rate Tensile (SSRT) tests;
- Fracture Toughness tests;
- Crack Growth Rate tests; and
- Small Punch as well as Segmented Cone Mandrel Tests.

Figure 5. Main parts of the test section together with the fittings for the crack growth, tensile, small punch, and cone mandrel tests



Every test section is equipped with a detachable fixing system for the various test specimen types, cf. Figure 5. Each test section is also independently controlled by a pneumatic servo-controlled pressure control circuit using the PLC (Programmable Logic Control). The required PLC programs for the controlling system (using the MACS software) have also been developed and thoroughly tested.

IV. Commissioning Tests

IV.1 The LILLA facility

A series of commissioning and acceptance tests of the LILLA facility was conducted according to a pre-defined programme to demonstrate that the facility operates in accordance with the technical requirements. The LILLA facility has been placed in a dedicated laboratory space equipped by a forced ventilation system with high-efficiency particulate air (HEPA) filters. The ventilation system allows exchanging volume of ambient air in the laboratory up to 10x per hour while constantly maintaining a slight under-pressure (5-10 Pa) in the facility room.

The commissioning tests included heat-up of the LILLA facility from cold to hot state (the target temperatures were 430°C for the dump tank and 550°C for the measuring tank, respectively). All operating modes of the facility were thoroughly tested, including:

- Heating mode, incl. vacuuming, facility flushing with Ar, lead melting in the dump tank, heating, gas / oxygen conditioning, and filling of the measuring tank with the conditioned molten lead;
- Nominal operating mode, incl. maintenance of temperature, gas / oxygen conditions, as well as lead in the measuring tank;
- Cooling mode, incl. cooling, draining and lead freezing in the dump tank;
- Stand-by mode, incl. Ar injection and control in the tanks;
- Purification mode, incl. Ar/H₂ gas injection and H₂, O₂, and humidity control; and
- Lead filtration.

The outcomes of these commissioning tests are illustrated in Figures 6-9.

The oxygen sensors were further calibrated and qualified to measure the amount of oxygen dissolved in liquid lead with an accuracy better than $\pm 10\%$.

Figure 6. Temperature of molten lead in the measuring tank during the heating mode

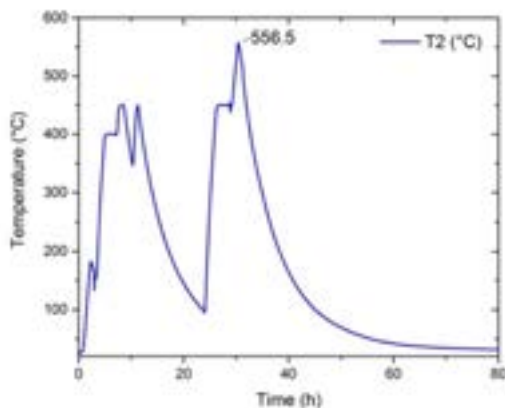


Figure 7. Temperature of molten lead in the dump tank during the heating mode.

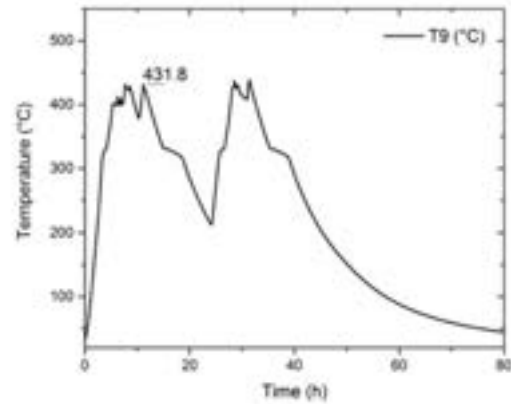


Figure 8. Weight of molten lead in the measuring (blue) and dump (black) tanks during the lead transfer operation.

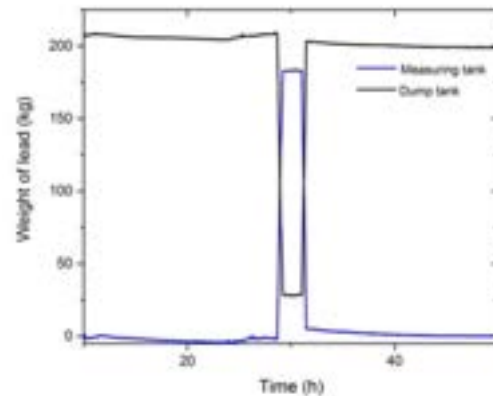
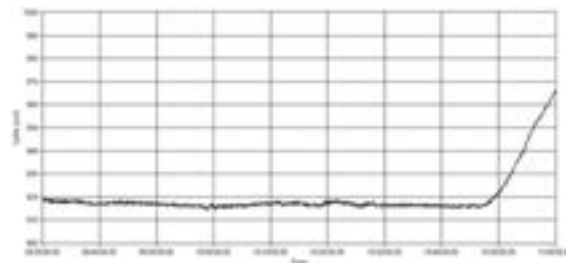


Figure 9. Response of the Pt-air reference electrode oxygen sensor measuring the amount of oxygen dissolved in molten lead in the measuring tank.



Additionally, in the asymptotic mode, main heaters' performance was evaluated using the proportional-integral-derivative (PID) controller

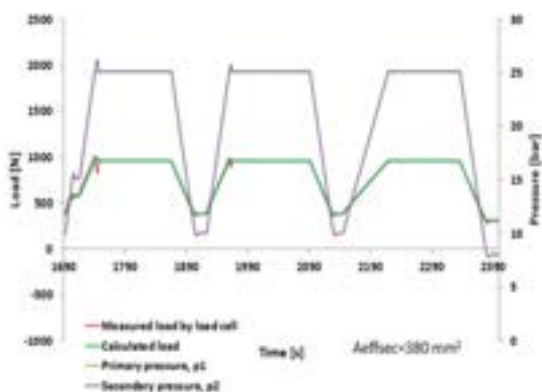
regulation to ascertain their operation at temperatures up to 650°C and 550°C in the measuring and dump tanks, respectively.

IV.2 The test sections

Before its first use, the D2B loading apparatus of each test section must be calibrated and its load symmetry verified. To this end, load cells and displacement sensors were therefore installed at both ends of each test section.

The calibration entailed comparing readings given by both load cells as a function of different primary and secondary pressures, and comparing these readings with calculated theoretical values. The first calibration step was performed under the condition of the primary (p1) and secondary pressures (p2) being the same up to the pressure of 25 bar (i.e., their ratio equal to 1). Figure 10 displays the very good agreement achieved between measured and calculated loads as a function of time.

Figure 10. Primary and secondary pressures, $p_1 = p_2$ as a function of calculated and measured load values.

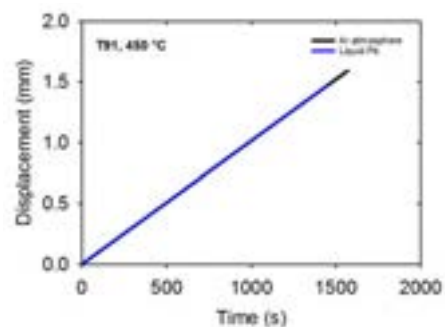


In subsequent steps, the test sections were further calibrated under the conditions of decreasing primary pressure (while the secondary pressure was kept constant) as well as under representative conditions of the control of a displacement-strain. In the latter case, the primary bellows' pressure was controlled by the strain value while the secondary pressure was kept constant (or vice versa).

As a part of the commissioning tests, several tensile tests of T91 material were also performed in air at room temperature as well as in high temperature argon at 420°C and 450°C. Furthermore, one test was performed under

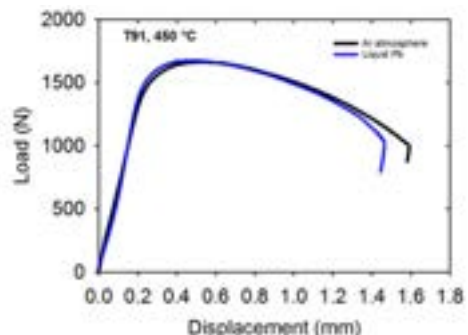
liquid lead at 450°C with the oxygen content in liquid lead actively controlled at $\sim 10^{-5}$ wt.%. The set displacement rate for all tests was 0.001 mm/s, which was accomplished with better than ± 0.2 μm accuracy. Load as a function of the displacement was measured continuously during these tests and the full displacement curves for the tested material were achieved. The accuracy of load generated during the tests was better than ± 2 N, achieving thus a very good linearity of the displacement response, cf. Figure 11.

Figure 11. Displacement as a function of time during the tensile tests of T91 in argon and liquid lead at 450°C.



Load-displacement curves of the mechanical tests of T91 conducted in argon and liquid lead at 450°C are shown in Figure 12.

Figure 12. Load-displacement curves of T91 from tensile tests conducted in argon and liquid lead at 450°C.



In further subsequent tests, the very good leak-tightness of the LILLA facility and its capability to reach and control oxygen concentrations in liquid lead below 10^{-10} wt.% was also demonstrated.

V. Conclusions

The paper presented the development, calibration and commissioning of heavy liquid metal experimental facility for conducting pre-normative, separate effect tests of candidate structural materials for LFRs inside realistic environmental conditions of liquid lead in temperatures up to 650°C. To this end, unique, pneumatic bellow-based loading devices were developed, assembled, and successfully qualified. The developed test sections provide great flexibility with respect to the type of a mechanical test and specimen that can be used. The capability to achieve the targeted test temperatures and oxygen concentrations in liquid lead (the latter being well below 10⁻⁸ wt.%) was also demonstrated.

Tensile (incl. SSRT), fracture toughness, and creep tests in molten lead will further be conducted with the objective to contribute to joint international and European efforts to establish representative test and assessment procedures, complement the related databases, and subsequently contribute to the development of Design Rules specifically for welded components of LFRs.

The focus of the work is on reference structural materials considered for the reference GIF concepts and for European heavy liquid metal cooled reactor concepts, MYRRHA and ALFRED, i.e. relatively thick-walled welded components of 316L.

Since AFCEN's RCC-MRx Design Code has been chosen for the design of both MYRRHA and ALFRED, the primary goal is to support the development of Design Rules into RCC-MRx. This contributes towards the objective of EERA JPNM as well as CEN/WS-64 to develop RCC-MRx into a joint European code for all future European innovative nuclear installations.

The LILLA facility also supports an open access policy to the EURATOM research infrastructures.

Acknowledgements

The authors wish to acknowledge the continuous support of the European and international collaborative partners provided to the R&D activities carried out in this field, forming also as a part of the EURATOM contribution to the Generation IV International Forum, European Sustainable Nuclear Energy Technology Platform (SNETP) and its ESNII pillar.

Nomenclature

AFCEN	Association Française pour les règles de Conception, de construction et de surveillance en exploitation des matériels des Chaudières Électro Nucléaires
AISI	American Iron and Steel Institute
ALFRED	Advanced Lead Fast Reactor European Demonstrator
ANSI	American National Standards Institute
ASTM	American Society for Testing and Materials
CEN	Comité Européen de Normalisation
D2B	Double2Bellows
DC(T)	Disk-shaped Compact Tension
DIN	Deutsches Institut für Normung
EERA	European Energy Research Alliance
ESNII	European Sustainable Nuclear Industrial Initiative
EURATOM	EUROpean ATOMic Energy Community
GIF	Generation IV International Forum
HEPA	High-efficiency Particulate Air
HFR	High Flux Reactor
ISO	International Organisation for Standardisation
JPNM	Joint Programme on Nuclear Materials of EERA
JRC	Joint Research Centre of the European Commission
LFR	Lead cooled Fast Reactor
LILLA	Liquid Lead Laboratory
MYRRHA	Multipurpose hYbrid Research Reactor for High-tech Applications
PID	Proportional-Integral-Derivative
PLC	Programmable Logic Control
R&D	Research & Development
RCC-MRx	Règles de Conception et de Construction pour les Matériels mécaniques des structures à hautes températures et des Réacteurs expérimentaux et à fusion
SNETP	Sustainable Nuclear Energy Technology Platform
SSRT	Slow Strain Rate Tensile
WS	Workshop

References

- [1] A Technology Roadmap for Generation IV Nuclear Energy Systems, Generation IV International Forum, GIF-002-00, December 2002.
- [2] Technology Roadmap Update for Generation IV Nuclear Energy Systems, Generation IV International Forum, January 2014.
- [3] Handbook on Lead-bismuth Eutectic Alloy and Lead Properties, Materials Compatibility, Thermal-hydraulics and Technologies, 2015 Edition, NEA. No. 7268, OECD, 2015.
- [4] H. Ait Abderrahim et al., MYRRHA: A Multipurpose Accelerator Driven System for Research & Development, Nuclear Instruments & Methods in Physics Research, A 463, 2001.
- [5] M. Frignani et al., FALCON Advancements towards the Implementation of the ALFRED Project, International Conference on Fast Reactors and Related Fuel Cycles: Next Generation Nuclear Systems for Sustainable Development (FR17), IAEA-CN245-485, Yekaterinburg, Russian Federation, 26–29 June 2017.
- [6] A. Alemberti et al., Status of Generation-IV Lead Fast Reactor Activities, International Conference on Fast Reactors and Related Fuel Cycles: Next Generation Nuclear Systems for Sustainable Development (FR17), IAEA-CN245-65, Yekaterinburg, Russian Federation, 26–29 June 2017.

R&D EXPERIMENTAL CAPABILITIES FOR ADVANCING GIF SCWR SYSTEM IN THE NEXT DECADE (L. K. H. LEUNG ET AL)

L.K.H. Leung⁽¹⁾, Y.-P. Huang⁽²⁾, R. Novotny⁽³⁾, S. Penttilä⁽⁴⁾, A. Sáez-Maderuelo⁽⁵⁾ and M. Krykova⁽⁶⁾

- (1) Canadian Nuclear Laboratories, Canada
- (2) Nuclear Power Institute of China, China
- (3) Joint Research Centre, the Netherlands
- (4) VTT Technical Research Centre of Finland Ltd., Finland
- (5) CIEMAT, Spain
- (6) Centrum vyzkumu Rez, s.r.o., Czech Republic

Abstract

The Super-Critical Water-cooled Reactor (SCWR) is a high-temperature, high-pressure water-cooled reactor that operates above the thermodynamic critical point of water (374°C, 22.1 MPa). Experimental studies for the SCWR R&D have been performed using existing facilities supporting light-water reactors and supercritical fossil-fuel power plants. However, due to the high operating temperatures and pressures for the SCWRs, new facilities have been established for materials, chemistry, thermal-hydraulics, and safety-related testing to enhance the knowledge base of technology areas and provided data for developing, verifying and validating analytical toolsets. Continuing the path forward as identified in the SCWR System Research Plan, additional infrastructures will be needed to support the design and operation of a prototype-of-a-kind (POAK) SCWR. Experimental facilities and identified infrastructure are summarized for developing the POAK SCWR in the next decade.

I. Introduction

The Super-Critical Water-cooled Reactor (SCWR) is a high-temperature, high-pressure water-cooled reactor that operates above the thermodynamic critical point of water (374°C, 22.1 MPa) [16]. Two types of SCWR core configuration are being pursued: pressure vessel and pressure tube. These core configurations have been evolved from the light-water-cooled reactors and heavy-water-cooled reactors. The balance-of-plant configuration is based on that of the fossil-fired power plant.

In general, four critical technology areas have been identified for the development of the SCWRs (i.e., materials, chemistry, thermal-hydraulics and safety). Identification of material candidates for cladding has been the main focus for R&D since materials of light-

water reactors and fossil-fired power plants can be adopted for in-core and out-of-core components. Material properties (such as strength), corrosion behaviour, and irradiation damage are the key areas for investigation. Reactor chemistry (especially radiolysis) has a strong impact on the corrosion characteristics of cladding materials. The study on activity transport would help minimising dosage to workers during inspection and maintenance. Thermal-hydraulics studies have been focusing on the deteriorated heat transfer phenomena, which could lead to a sharp rise in cladding temperature affecting its integrity. Furthermore, there are insufficient experimental data on separate effects (such as axial and radial power profiles, spacer, etc.) on thermal-hydraulics parameters at supercritical pressures to support design and safety analyses. Safety-related R&D focus on specific components and the qualification of the safety-analysis tools.

One of the key components is the critical-flow behaviour, which is required for the safety analysis of the postulated large-break loss-of-coolant accidents and the design of the pressure-relieve valve.

Experimental studies for the SCWR R&D were performed using existing facilities supporting light-water reactors and fossil-fired power plants. However, due to the high operating temperatures (up to 625°C at the core outlet) and pressures (nominal 25 MPa) for the SCWRs, new facilities have been established for materials, chemistry, thermal-hydraulics and safety-related testing in Canada, China, Europe, Japan and the Russian Federation. Experiments performed using these facilities have enhanced the understanding of various technology areas and provided data for developing prediction methods, as well as verifying and validating analytical toolsets. This facilitates the completion of the Canadian SCWR concept in Canada, the High Performance Light Water Reactor (HPLWR) in Europe and the JSCWR in Japan [17]. The CSR-1000 SCWR concept is also close to completion in China [18].

With the completion of the concept development, the SCWR System Research Plan identifies the path to focus on the prototype-of-a-kind (POAK) SCWR development [16]. Additional infrastructures are needed to be established for achieving that goal. This paper describes experimental facilities currently available in support of the SCWR development and the identified infrastructure for developing the POAK SCWR in the next decade. In view of the large number of facilities available world wide, only selected facilities are introduced.

II. Materials and Chemistry R&D Infrastructures

Material candidates for in-core and out-of-core components, except for the fuel cladding, have been selected from materials established for light-water reactors and supercritical fossil-fired power plants. Infrastructures available in support of these reactors and plants are applicable for development and qualification of material candidates. The main issue for the identification of cladding material candidates is attributed to high-pressure and high-temperature operating conditions, which are well beyond the operating range of current fleet of reactors. Specific R&D infrastructure applicable for materials and chemistry testing at those conditions are required.

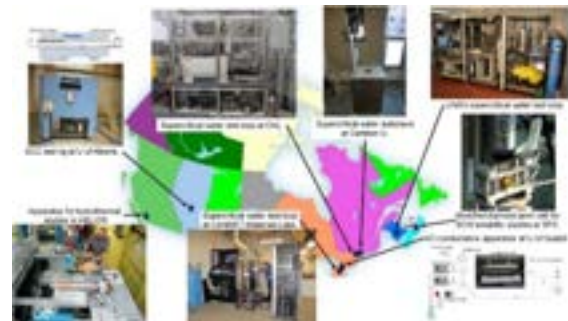
Major concerns on cladding material are creep behaviour, high temperature strength, corrosion characteristics, and stress corrosion cracking (SCC) behaviour. In addition, the adverse impact of irradiation to these behaviours and material properties is required to quantify at relevant conditions.

Canada, China and Euratom are signatories of the Materials and Chemistry Project Arrangement under the GIF SCWR System. Each signatory has established specific infrastructures to support SCWR materials and chemistry R&D. These infrastructures are summarised below. A number of SCW facilities were also established for materials and chemistry R&D in other countries (e.g., Japan, the Russian Federation, United States of America and South Korea). These facilities are not covered here.

II.1 Canada's infrastructure

Canada established a national program to support R&D for Gen-IV nuclear systems (referred to as the Generation-IV National Program) [19]. It was separated in two phases and was managed by Natural Resources Canada (NRCan). The first phase (Phase I) focused on basic research, including establishment of infrastructures, to support the development of the SCWR concept. Figure 10 shows selected facilities constructed for SCWR materials and chemistry R&D in Canada. Several static autoclaves have been constructed for corrosion testing at supercritical pressures and temperatures (the one installed at the Carleton University is illustrated). These autoclaves are applicable for studying the effectiveness of coating materials to mitigate corrosion issues.

Figure 10. Infrastructures for SCWR Materials and Chemistry R&D in Canada



The effect of coolant flow velocity on corrosion has been studied in flow loops with water at supercritical temperatures and pressures. These flow loops have been constructed at University of New Brunswick, NRCan Canmet-Materials Laboratories and recently at the Canadian Nuclear Laboratories.

Static autoclave systems have also been used to study material behaviours of stress-corrosion cracking (the one installed at the University of Alberta is illustrated in Figure 10). Test pieces included C-rings and pressurised capsules [20]. These facilities had generated key SCC data for candidate fuel cladding materials.

A suite of high-temperature mechanical testing equipment has been installed at NRCan Canmet-Materials laboratories to provide creep and other mechanical property data for candidate alloys. The creep testing systems have the capacity to measure on-line creep rate, up to 1000°C. Special test setup also allowed measurements under compression loading. The new vacuum furnace, new rolling facility, and extrusion press have also been used in making modified stainless-steels and ferritic alloys for SCWR research.

Two main issues in water chemistry are corrosion product transport and radiolysis. Diamond-anvil cells coupled with X-ray absorption fine structure spectroscopy were constructed at the St. Francis Xavier University to characterise solubility of metal oxides in supercritical water [21]. A state-of-the-art high pressure flow alternating current conductance apparatus was established at the University of Guelph to determine the association constants of model fission products at temperatures up to 350°C [22]. A unique bench-scale flow loop was built at the Trent University to study the effects of pH control additives and the slow release of metallic ions in SCW as well as corrosion of alloys in SCW [23].

The synchrotron operated by TRIUMF at Canada's National Laboratory for Particle and Nuclear Physics has been used to understand the behaviours of water radiolysis in SCW. An advanced proton accelerator at Queen's University was used to introduce irradiation damage (by protons) into materials for studying materials behaviour under neutron bombardment.

II.2 China's infrastructure

Material and chemistry R&D for SCWR are being performed at Nuclear Power Institute of China (NPIC), Shanghai Jiao Tong University (SJTU)

and the University of Science and Technology in Beijing (USTB) in China. Figure 11 shows infrastructures for material and chemistry R&D at these organisations.

Figure 11. Infrastructures for SCWR Materials and Chemistry R&D in China



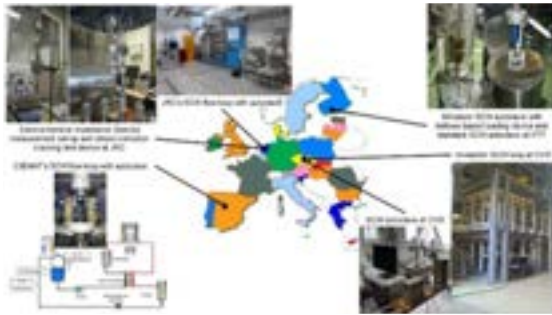
A general corrosion test facility was developed jointly by China and Japan and has been installed at NPIC for material testing. It consists of an autoclave and a flow loop designed for high pressure and high temperature operations. A separate test facility for stress corrosion cracking behaviours of materials has also been constructed at NPIC. These facilities support the establishment of cladding-material candidates for the Chinese SCWR concept (CSR-1000).

A SCW stress corrosion cracking testing facility has also been installed at SJTU in support of the cladding-material selection [24]. Different types of material were examined. A slow strain rate testing facility was constructed to study the growth behaviours of cracks in materials.

II.3 EU's infrastructure

Figure 12 shows infrastructures for material and chemistry R&D at various countries within the European Union. Several SCW autoclaves for corrosion and stress corrosion cracking tests have been constructed for material testing at Centrum výzkumu Řež (CVR) in Czech Republic, Joint Research Centre (JRC) in the Netherlands [25], Centro de Investigaciones Energéticas, Medioambientales y Tecnológicas (CIEMAT) in Spain and VTT in Finland [26]. VTT developed also a miniature SCW autoclave with bellows-based loading device for stress-corrosion cracking tests [27]. JRC-Petten developed a new measurement facility using the electrochemical impedance spectra (EIS) technique to study radiolysis in supercritical water.

Figure 12. Infrastructures for SCWR Materials and Chemistry R&D in EU



An in-reactor SCW loop has recently been constructed and installed into the LVR-15 reactor of CVR in Czech Republic for material corrosion testing. This facilitates the study of the irradiation effect on material characteristics. The test section is installed at one of the sites in the reactor, but most components of the facility are located out-of-core. The photo in the figure illustrates the out-of-core components.

III. Thermal-Hydraulics and Safety R&D Infrastructures

Experimental data on heat transfer in supercritical flow are required for the development and optimisation of the fuel assembly concept. Performing heat-transfer experiments with SCW flow is complex and expensive due primarily to the harsh operating environment. Surrogate fluids (such as carbon dioxide and refrigerants) have been used for modelling water in heat transfer studies. This approach is valid for improving the understanding of heat-transfer phenomena and examining separate effects.

Infrastructures established by signatories of the Thermal-Hydraulics and Safety Project Arrangement in the GIF SCWR System (i.e., Canada, China and EU) are described below. Other facilities applicable for thermal-hydraulics and safety experiments at supercritical pressures are available in Japan, the Russian Federation, United States of America, South Korea and India.

III.1 Canada's infrastructure

Several facilities for thermal-hydraulics and safety-related tests at supercritical pressures have been established in Canada to support the Phase-I Generation-IV National Program [19]. Figure 13 shows the facilities with water, carbon dioxide or refrigerant as working fluids.

Figure 13. Infrastructures for SCWR Thermal-Hydraulics and Safety R&D in Canada



A supercritical water loop has recently been constructed at the Carleton University. It is applicable for thermal-hydraulics tests with tubes, annuli and small bundle assemblies. A complementary test facility was also constructed for experiments with Refrigerant-134a as coolant through a tube, an annular channel, and a 7-element bundle at supercritical pressures [28]. It has been used to study experimentally the effect of spacer configuration and size on supercritical heat transfer in support of the development of fuel assembly concept for the SCWR.

A test loop was constructed at the University of Ottawa to investigate heat transfer in tubes and a 3-rod bundle with carbon-dioxide flow [29]. Its design pressure is up to 11 MPa, which can accommodate other fluids (such as refrigerants) at supercritical pressures and even water at sub-critical pressures. Experimental data from these tests have been used in assessment of prediction methods for heat transfer, subchannel codes (such as ASSERT), and computational fluid dynamics tools (such as STAR CCM+).

A natural-circulation test facility with carbon dioxide as the working fluid was established at the University of Manitoba [30]. It facilitates testing with single and parallel tubes in vertical or horizontal orientation. Experimental data from these tests have been applied in establishing the stability boundaries over a range of flow conditions and assessing the analytical model and system codes (such as CATHENA).

A water test facility was constructed at École Polytechnique de Montréal to study critical-flow behaviours [31]. It consists of a nozzle section with a small opening. Water at supercritical pressures is discharged through the nozzle to a medium pressure test facility

(which facilitates the control of discharged pressures other than atmospheric). Experimental results obtained with 2 sharp-edge nozzles of different sizes of opening have been used to assess the critical-flow models implemented in the system codes, which are being applied in the postulated large-break loss-of-coolant accident.

III.2 China's infrastructure

Figure 14 shows thermal-hydraulics facilities available in China. Several test loops were constructed at the Nuclear Power Institute of China to support the development of the CSR-1000. A small-scale SCW test loop was designed for thermal-hydraulics testing using tubes and annuli. Testing with bundle subassemblies has been performed with the large-scale SCW test loop, which provides higher power and flow than the small-scale test loop. Experimental data have been applied in developing heat-transfer correlations for the CSR-1000 fuel assembly and validating analytical tools (such as SC-TRAN). In addition, a natural-circulation test loop was constructed to investigate heat transfer and stability [32], [33]. It was designed for experiments with water flow but has also been adopted for experiments using carbon dioxide as working medium. Experimental data are available to define the stability boundaries of supercritical flow and fluid-to-fluid modelling criteria.

Figure 14. Infrastructures for SCWR Thermal-Hydraulics and Safety R&D in China



A SCW heat-transfer test loop has also been constructed for testing with tubes, annuli and 4-rod bundles at the Shanghai Jiao Tong University [34], [35]. The 4-rod bundle design simulated the proposed fuel for the GIF collaboration on fuel qualification testing at CVR. Two different types of spacing devices (i.e., grids and wrapped wires) were tested to

examine their impact on heat transfer. Transient experiments were also performed to quantify the impact of power, flow and pressure variations on heat transfer.

The SCW heat-transfer test loop at Xi'an Jiaotong University was constructed mainly for supporting the SC fossil-fired power plant. It has been applied for heat-transfer experiments with tubes, annuli and a 4-rod bundle (which also simulated the fuel design for the Czech Republic fuel qualification testing) in support of SCWR development [36], [37]. Effects of flow area and spacer on heat transfer were examined in the annuli tests. Detailed temperature distributions along heated surfaces of the 4-rod bundle were obtained to quantify variations in subchannels and gaps.

III.3 EU's infrastructure

Supercritical heat transfer facilities were constructed at the Karlsruhe Institute of Technology (KIT) in Germany and the Hungarian Academy of Sciences (HAS) in Hungary within the EU. Figure 15 shows EU's facilities in support of SCWR development.

Figure 15. Infrastructures for SCWR Thermal-Hydraulics R&D in EU



The model-fluid test loop at KIT was designed to use refrigerants as the working fluid. Experiments with Refrigerant-134a in tubes were performed to provide data for validating heat-transfer correlations and fluid-to-fluid modelling parameters.

A test loop has been installed at HAS to study natural circulation behaviours with water at supercritical pressures [38]. It was also used to examine the flow structure of supercritical water using the neutron radiography technique [39].

IV. Future Infrastructure Needs

The GIF SCWR System Research Plan identifies several key components in each project before proceeding to the deployment phase. Required infrastructures are described below for selected components only. A detailed review is ongoing for establishing future needs to support design and deployment of SCWRs.

IV.1 System integration and assessment

A prototype fuelled loop and a prototype-of-a-kind demonstration SCWR are required for the System Integration and Assessment Project. The fuel loop is needed to qualify the SCWR fuel and demonstrate the capability to design and operation of an in-reactor supercritical-pressure fuel facility (which is a pre-requisite for the demonstration plant). While the supercritical water material test loop recently constructed at CVR in Czech Republic has provided ample experience on design, construction, installation, licensing and operation, further complexity is anticipated for the design and construction of an in-reactor fuel loop. Figure 16 illustrates the SCW loop and test section installed at CVR in Czech Republic. A similar test section can be designed for fuel test in the same loop to obtain operating experience and much needed fuel information.

Figure 16. In-Reactor SCW Loop and Test Section at CVR in Czech Republic



Another potential site for SCWR fuel irradiation is the proposed facilities to be constructed at the new research reactor of NPIC in China (see Figure 17). A design of the fuel assembly for testing has to be proposed. International collaborations are required for achieving the test.

Reactor physics analyses have been performed using analytical tools developed for light-water and heavy-water reactors. Nuclear data are available for high-temperature conditions but not at relevant pressures. Previous analyses considered the effect of pressure on reactor physics parameters is small. However, nuclear data would be required for the construction of the demonstration SCWR plant.

Figure 17. Proposed Fuel Irradiation Facilities at NPIC in China



A test facility has been proposed to obtain reactor physics data in the Zero Energy Deuterium (ZED-II) research reactor at Canadian Nuclear Laboratories (see Figure 18). It consists of a channel housing the fuel assembly, which will be inserted into the reactor. Two phases at high temperatures are being considered: low-pressure tests and high-pressure tests. A feasibility study for the design and installation is being carried out.

A separate test facility is needed to understand the structure of the water at supercritical pressures. It has been designed to observe the change in fluid structure using the neutron scattering technique. Construction will be initiated once a collaboration is established with the neutron beam facility.

A demonstration SCWR plant is required before deployment. NPIC has proposed to design and construct a prototype SCWR, which simulates their CSR-1000 design. The power rating would be 150 MWe matching the requirement for the super-critical pressure turbine. This small size prototype is representative to Euratom's High Performance Light Water Reactor, Japan's SCWR and a fuel channel of Canada's pressure-tube type SCWR. Therefore, a strong collaborative effort can be established in its design and construction.

Figure 18. ZED-II Reactor for Physics Experiments in Canada



IV.2 Materials and chemistry

Future development on materials and chemistry remains focusing on the cladding, which would operate at high pressure and high temperature conditions. A significant number of corrosion and stress-corrosion-cracking testing have been performed for cladding material candidates in out-reactor facilities. An irradiation facility is required to examine the effect on material properties and characteristics.

Autoclaves currently used in corrosion and stress-corrosion-cracking tests are limited to supercritical water temperatures at about 650°C, which is lower than anticipated cladding temperatures of 700-800°C during normal operations and 1200°C during postulated accidents. High-temperature autoclaves are required to extend testing to relevant conditions of interest.

Mechanical properties for cladding materials are generally available at temperatures up to about 800°C. High-temperature test facilities are required to obtain mechanical properties at relevant conditions of interest.

IV.3 Thermal-hydraulics and safety

The SCWR System Research Plan identifies the "Integral Facility Tests" as the major component for licensing of the demonstration SCWR plant and deployment. Performing these tests would require an integral test facility to

demonstrate the effectiveness of the safety system design. While several SCWR core concepts have been proposed, their safety systems have been evolved mainly from the advanced boiling water reactor (in particular the thermal-spectrum SCWRs) and their operating conditions are similar. This could lead to joint design and construction of the facility.

Design and construction of a full-scale integral facility are time consuming and costly. A scaled system could be applicable to examine the phenomena and minimise the time and cost. Scaling analyses have been performed for major components in the safety system to confirm feasibility. An integral analysis is being carried out to quantify the appropriate scaling factor using a safety analytical tool.

Thermal-hydraulics experiments were performed using simple channels (such as tubes and annuli) and bundle subassemblies with three, four or seven rods. Licensing of the demonstration unit and full-scale SCWR plant would require thermal-hydraulics data for full-scale fuel assemblies. Power supplies and pumps installed at test facilities described in Section III are insufficient for performing full-scale bundle tests. Significant expansion of current facilities is required for licensing purposes.

V. Conclusion

- A large number of experimental facilities are available to support the development of SCWRs.
- Fundamental R&D studies have been performed to provide experimental data for improving the understanding of the technologies, developing prediction methods and validating models/codes.
- Irradiation facilities are available but design and installation of in-reactor supercritical water loops are challenging.
- Large-scale facilities capable of operating at relevant pressures and temperatures are required.
- Completing the installation of these infrastructures would expedite the demonstration and deployment of SCWR plants.

Acknowledgements

The authors would like to thank X. Cheng (KIT) and L.-F. Zhang (SJTU) for providing information on their facilities.

L.K.H. Leung expresses his sincere appreciation of the financial support of the Natural Resources Canada (NRCan), Atomic Energy of Canada Limited (AECL) and Natural Science and Engineering Research Council (NSERC).

Nomenclature

BME	Budapest University of Technology and Economics
CIEMAT	Centro de Investigaciones Energéticas, Medioambientales y Tecnológicas
CVR	Centrum výzkumu řež
EIS	Electrochemical Impedance Spectra
EU	European Union
Gen-IV	Generation-IV
GIF	Generation IV International Forum

HAS	Hungarian Academy of Sciences
HPLWR	High Performance Light Water Reactor
JRC	Joint Research Centre
JSCWR	Japan SCWR
KIT	Karlsruhe Institute of Technology
NPIC	Nuclear Power Institute of China
NRCan	Natural Resources Canada
POAK	Prototype Of A Kind
R&D	Research and Development
SC	Super-Critical
SCC	Stress Corrosion Cracking
SCW	Super-Critical Water
SCWR	Super-Critical Water-cooled Reactor
SJTU	Shanghai Jiao Tong University
USTB	University of Science and Technology in Beijing
XJTU	Xi'an Jiaotong University
ZED	Zero Energy Deuterium

References

- [16] OECD Nuclear Energy Agency, "Technology Roadmap Update for Generation IV Nuclear Energy Systems", January 2014.
- [17] Schulenberg, T. and Leung, L. "Super-critical water-cooled reactors", Handbook of Generation IV Nuclear Reactors, Editor: I.L. Pioro, Woodhead Publishing Series in Energy: 103, 2016.
- [18] IAEA, "Status Report - Chinese Supercritical Water-Cooled Reactor (CSR1000)", IAEA Advanced Reactors Information System (ARIS) Database, December, 2015.
- [19] Pynn, G., Brady, D., Zheng, W., Leung, L. and C.-A. MacKinlay, (2016), "Canada's Generation IV National Program", CNL Nuclear Review, Vol. 5, No. 2, pp. 173-179.
- [20] Swift, R., Cook, W., Bradley, C. and Newman, R.C., "Validation of Constant Load C-Ring Apex Stresses for SCC Testing in Supercritical Water," Journal of Nuclear Engineering and Radiation Science, Vol. 3, No. 2, pp. 021004-021004-7, 2017.
- [21] Mayanovic, R.A., Anderson, A.J., Dharmagunawardhane, H.A.N., Pascarelli, S. and Aquilanti, G., "Monitoring Synchrotron X-ray-Induced Radiolysis Effects on Metal (Fe, W) Ions in High-Temperature Aqueous Fluids", Journal Synchrotron Radiation, Vol. 19, pp. 797-805, 2012.
- [22] Zimmerman, G.H., Arcis, H. and Tremaine, P., "Ion-pair formation in strontium chloride and strontium hydroxide solutions under supercritical water reactor operating conditions," Proceeding of the 5th International Symposium on Supercritical Water-Cooled Reactors (ISSCWR-5), Vancouver, BC, Canada, 13-16 March 2011.
- [23] Carvajal-Ortiz, R.A., Plugatyr, A. and Svishchev, I.M., "On the pH Control at Supercritical Water-Cooled Reactor

- Operating Conditions”, Nuclear Engineering and Design, Vol. 248, pp. 340–342, 2012.
- [24] Guo, X.-L., Chen, K., Gao, W.-H., Shen, Z., Lai, P. and Zhang, L.-F., “A research on the corrosion and stress corrosion cracking susceptibility of 316L stainless steel exposed to supercritical water”, Journal of Corrosion Science, Vol. 127, pp. 157-167, 2017.
- [25] Novotny, R., Janík, P., Penttilä, S., Hähnera, P., Macák, J., Siegl, J. and Haušil, P., “High Cr ODS steels performance under supercritical water environment”, Journal of Supercritical Fluids, Vol. 81, pp. 147-156, 2013.
- [26] Penttilä, S., Toivonen, A., Li, J., Zheng, W. and Novotny, R., “Effect of surface modification on the corrosion resistance of austenitic stainless steel 316L in supercritical water conditions”, Journal of Supercritical Fluids, Vol. 81, pp. 157-163, 2013.
- [27] Penttilä, S., Moilanen, P., Karlsen, W. and Toivonen, A., “Miniature autoclave and double bellows loading device for material testing in future reactor concept conditions - Case supercritical water”, Journal of Nuclear Engineering and Radiation Science, Vol. 4, No. 1, pp. 011016-011016-7, 2017.
- [28] Balouch, M. and Yaras, M.I., “Design of an R-134a Loop for Subcritical and Supercritical Forced-Convection Heat Transfer Studies”, Proceeding of the International Conference on Future of Heavy Water Reactors, Ottawa, ON, Canada, 02–05 October 2011.
- [29] Jeddi, L., Jiang, K., Tavoularis, S. and Groeneveld, D.C., “Preliminary Tests at the University of Ottawa Supercritical CO₂ Heat Transfer Facility,” Proceeding of the 5th International Symposium on Supercritical Water-Cooled Reactors (ISSCWR-5), Vancouver, BC, Canada, 13–16 March 2011.
- [30] Mahmoudi, J., Chatoorgoon, V. and Leung, L., “Experimental Thermal-Hydraulic Analysis of Supercritical CO₂ Natural Circulation Loop”, Proceeding of the 33rd CNS Annual Conf./36th Annual CNS/CNA Student Conference, Saskatoon, SK, Canada, 10–13 June 2012.
- [31] Muftuoglu, A. and Teysseidou, A., “Experimental Study of Abrupt Discharge of Water at Supercritical Conditions”, Experimental Thermal Fluid Science, Vol. 55, pp. 12–20, 2014.
- [32] Xiong, T., Yan, X., Xiao, Z.-J., Li, Y.-L., Huang, Y.-P. and Yu, J.-C., “Experimental study on flow instability in parallel channels with supercritical water”, Annals of Nuclear Energy, Vol. 48, pp. 60–67, 2012.
- [33] Liu, G.-X., Huang, Y.-P., Wang, J.-F., Lv, F. and Leung, L.K.H., “Experiments on the basic behavior of supercritical CO₂ natural circulation”, Nuclear Engineering and Design Vol. 300, pp. 376–383, 2016.
- [34] Hu, Z.-X. and Gu, H.-Y., “Heat transfer of supercritical water in annuli with spacers”, International Journal of Heat and Mass Transfer, Vol. 120, pp. 411-421, May 2018.
- [35] Gu, H.Y., Hu, Z.X., Liu, D., Xiao, Y. and Cheng, X., “Experimental studies on heat transfer to supercritical water in 2 × 2 rod bundle with two channels”, Nuclear Engineering and Design, Vol. 291, pp. 212–223, 2015.
- [36] Wu, G., Bi, Q., Yang, Z., Wang, H., Zhu, X., Hao, H. and Leung, L.K.H., “Experimental Investigation of Heat Transfer for Supercritical Pressure Water Flowing in Vertical Annular Channels”, Nuclear Engineering Design, Vol. 241, Issue 9, pp. 4045-4054, 2011.
- [37] Wang, H., Bi, Q., and Leung, L.K.H., “Heat Transfer from a 2x2 Wire-Wrapped Rod Bundle to Supercritical Pressure Water”, Int. J. of Heat and Mass Transfer, Vol. 97, pp. 486–501, 2016.
- [38] Kiss, A., Balaskó, M., Horváth, L., Kis, Z. and Aszódi, A., “Experimental investigation of the thermal hydraulics of supercritical water under natural circulation in a closed loop”, Annals of Nuclear Energy, Vol. 100, pp. 178–203, 2017.
- [39] Balaskó, M., Horváth, L., Horváth, A., Kiss, A. and Aszódi, A., “Study on the properties of supercritical water flowing in a closed loop using dynamic neutron radiography”, Physics Procedia, Vol. 43, pp. 254 – 263, 2013.

INTRODUCTION ON SOME EXPERIMENTAL FACILITIES FOR VHTR SYSTEM (Y. ZHENG)

Zheng Yanhua⁽¹⁾

(1) Institute of Nuclear and New Energy Technology, Collaborative Innovation Center of Advanced Nuclear Energy Technology, Key Laboratory of Advanced Reactor Engineering and Safety of Ministry of Education, Tsinghua University, China

I. Introduction

Very High Temperature Reactor (VHTR) is one of the candidates for the Generation IV Nuclear Energy Systems, so it is important to identify some key phenomena via experimental research, and it is also a major challenge to validate specified computational tools and methods used in the design and analysis of the VHTR.

To further understand the phenomena of VHTR, as well to support the design, safety analysis and licensing of the Chinese 200 MWe High Temperature gas-cooled Reactor Pebble-bed Module (HTR-PM), several experimental facilities were designed in the Institute of Nuclear and new Energy Technology (INET), Tsinghua University. Besides, experimental data from the 10 MW High Temperature gas-cooled test Reactor (HTR-10) also can play an important role for the study of the phenomena and for the code validation.

The Computational Methods Validation and Benchmark (CMVB) Project under the Generation IV International Forum (GIF) VHTR system is now planned and will focus on ensuring the numerical models used for reactor system analysis are capable of calculating the reactor system behaviour at normal operational conditions and for operational transients and accident scenarios. Experimental data from different members will be shared and the validation studies will be performed.

In this paper, some experimental facilities in INET, as well as some experiments selected to be used for validation studies in cmVB project, are introduced.

II. Experimental Facilities in INET

The HTR-PM, which plays an important role in the world-wide development of Generation-IV nuclear energy technology, has been designed and is now under construction in China [1, 2]. The first concrete for the HTR-PM reactor building was poured in December 2012, and the test run is expected at the end of this year.

To study the key phenomena and solve engineering problems for HTR-PM, an engineering laboratory (as shown in Fig. 1) was built in INET and many test facilities were designed (listed in Tab. 1).

Figure 1. Overview of the engineering laboratory in INET



Table 1. Engineering test facilities in INET

Name	Parameter	Function
ETR-HT (Engineering Test Facility – Helium Technology)	10MW _{th} , 7.0 MPa, 250-750°C, helium	Heat source to verify steam generator
ETF-SG (Engineering Test Facility – Steam Generator)	10MW _{th} test power, 13.25 MPa, 205-570°C, water	Secondary loop and third loop to verify steam generator
ETF-HC (Engineering Test Facility – Helium Circulator)	4.5MW _{th} test power, 7.0 MPa, 250°C, helium	Full scale verification of helium circulator
ETF-FHS (Engineering Test Facility – Fuel Handling System)	7.0 MPa, 100-250°C, helium, two chain	Full scale verification of fuel handling system
TF-FHS (Test Facility – Fuel Handling System)	Full geometry size, air, 0.1 MPa	Verification of the fuel movement in the FHS System
ETF-CRDM (Engineering Test Facility – Control Rods Driving Mechanism)	1 MPa, 100-250°C, helium	Full Scale verification of control rods driving mechanism
ETF-SAS (Engineering Test Facility – Small Absorber Sphere System)	7.0 MPa, 100-250°C, helium	Full scale verification of small absorber sphere system
ETF-SFS (Engineering Test Facility – Spent Fuel Storage)	Full geometry size, air, 0.1 MPa	Full scale verification of major components of spent fuel storage system
TF-SFCD (Test Facility – Spent Fuel Canister Drop)	Full geometry size, full height (30m), full weight (17t)	Full scale drop verification of spent fuel canister
ETF-HPS (Engineering Test Facility – Helium Purification System)	7.0 MPa, 25-250°C, helium purification flow rate: 40kg/h	Verification of purification efficiency (greater than 95% and system resistance less than 200kPa)
ETF-DCS (Engineering Test Facility – Distributed Control System)	Reactor power control system, fuel cycle control system, VDU-based man-machine interface	Verification of DCS architecture and major control systems
ETF-RPS (Engineering Test Facility – Reactor Protect System)	Prototype of reactor protect system with 4 channels	Full scale verification of reactor protect system
ETF-MCR (Engineering Test Facility – Main Control Room)	1:1 MCR control consoles, mimic panels, layouts and inner environments	Full scale verification of man-machine interface
TF-PBEC (Test Facility – Pebble Bed Equivalent Conductivity)	1600°C, helium/vacuum	Measurement of pebble bed equivalent conductivity
TF-PBF3D (Test Facility – Pebble Bed Flow 3D)	atm, room temperature, air	Three-dimensional simulation test of pebble bed flow (1:5 scale)
TF-HGM (Test Facility – Hot Gas Mixing)	atm, 20-150°C, air	Reduced scale (1:2.5) verification of hot gas mixing at reactor core outlet

Several experiments are selected to be introduced in this paper.

II.1 Pebble bed flow 3D test facility

The on-line charge and discharge of the fuel elements were realised in the HTR-10 and are now also adopted in the HTR-PM, thus the reactor can keep lower excess reactivity and flatter power density distribution. In the equilibrium state, each fuel element may pass through the core 15 times (stay in the core for more than 1000 days) before reaching the target burn-up.

For a pebble bed core consisting of about 420,000 fuel elements, the pebble flow of the HTR-PM might be a very complicate phenomenon. It is potential for pebbles to be entrained, recirculated or held-up unexpectedly, affecting core maximum temperatures and pebble burn-up [3].

Figures 2 a & b. Pebble bed flow 3D test facility

Figure 2a. Solid diagram of the test facility

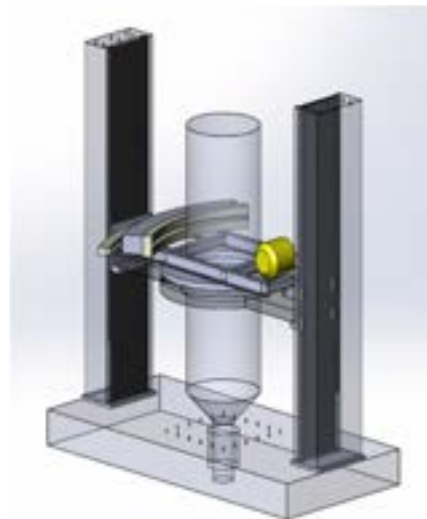


Figure 2b. Experimental spheres (left) and identification spheres (right)



Fig. 2a) shows the solid diagram of the pebble bed flow 3D test facility, with a scale of 1:5 compared to the HTR-PM. Two kinds of spheres (as shown in Fig. 2b), including 500,000 experimental spheres of polyformaldehyde and 200 identification spheres of iron/aluminium packed with ABS (Acrylonitrile Butadiene Styrene) plastic, are manufactured. The CT (Computerised Tomography) detecting system is designed to locking the location of the identification spheres, so as to study the pebble flow track in the core. The space distribution of the velocity vector, the space distribution of the sphere's detention time, the mixture of the spheres from different areas, and so on also can be acquired to further understand the porosity of the pebble bed and the detention area of the spheres.

Some 2D experiments and pre-experiments have been carried out. This 3D experiment is planned to be carried out in August and expected to be finished at the end of this year.

II.2 Pebble bed equivalent conductivity test facility

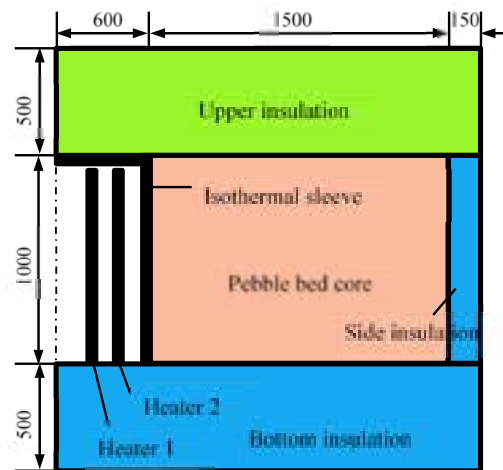
Pebble bed equivalent conductivity is an important parameter which describe the heat transfer property in the pebble bed core includes heat conductivity, convection and radiation. It has been assigned an importance rank of 'High' and knowledge level of 'Medium' [3]. Especially in the Depressurised Loss Of Forced Cooling (DLOFC) accident, it will affect the maximum fuel temperature, which is the important design limitation for the HTGR.

Many theoretical and experimental studies have been carried out for the pebble bed equivalent conductivity [4-8]. The test facility SANA was installed at the Research Centre Jülich to research on the heat transport mechanisms inside the core of a HTGR. In SANA, approximately 9500 graphite pebbles with a diameter of 6 cm accumulated in irregular arrangement to form pebble bed core, and the maximum temperatures during the experiment were less than 1200°C.

Taking example for the HTR-PM, the temperature limitation for the fuel elements in design basis accident (DBA) is 1620°C. According to the safety analysis, during the DLOFC accident scenarios, the maximum fuel temperature may reach 1500°C, which means the pebble bed equivalent conductivity at higher temperature will play an important role for the design and safety analysis of the HTGR.

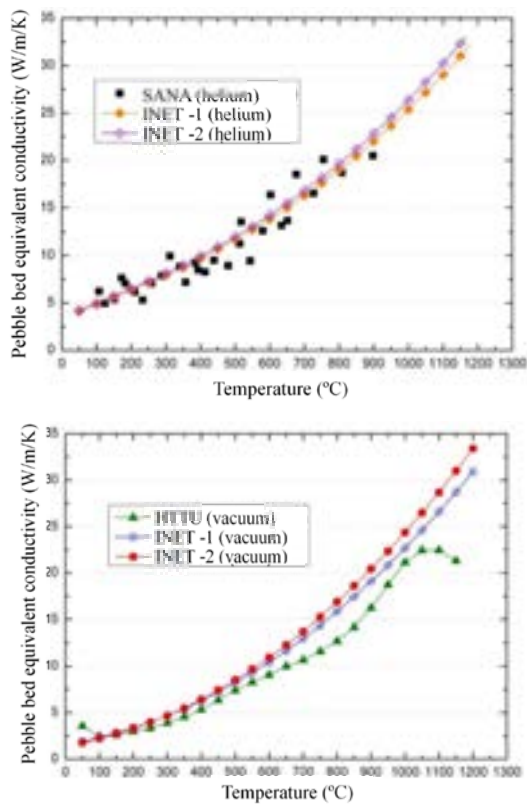
To further understand the heat transport mechanisms inside the pebble bed core, and get more data especially the data under high temperature conditions, the pebble bed equivalent conductivity test facility [9] was designed in INET, as shown in Fig. 3. The annular pebble bed core, with the inner diameter of 0.6 m and the outer diameter of 2.1 m, as well the height of 1 m, includes nearly 70,000 graphite spheres with the diameter of 6 cm. The experimental temperature can reach 1600°C.

Figure 3. Pebble bed equivalent conductivity test facility



A series of experiments were performed under both vacuum condition and helium atmosphere. Fig. 4 shows some experimental results compared with German SANA experimental results and South Africa HTTU experimental results [9].

Figure 4. Experimental results of pebble bed equivalent conductivity



- Emission behaviour of graphite dust at accident
- Radioactive behaviour of graphite dust

Figures 5 a & b. Study of abrasion behaviour of graphite pebble in the lifting pipe

Figure 5a. Schematic of experimental platform for lifting of graphite pebble

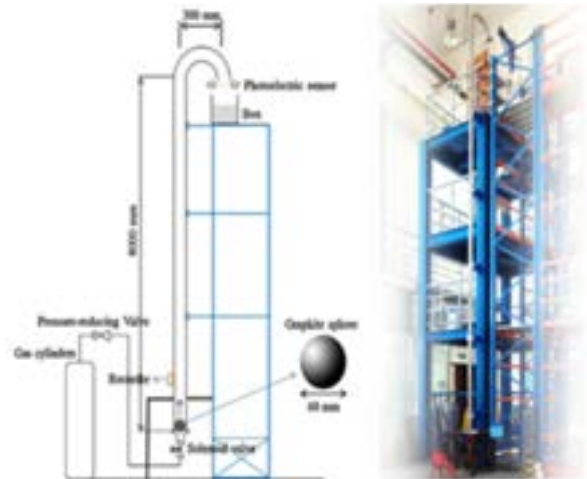


Figure 5b. Surface of worn graphite pebble

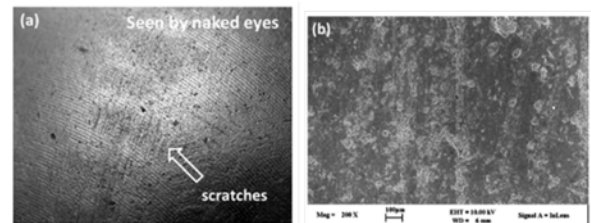


Fig. 5 and Fig. 6 show parts of the experimental facilities and some experimental results [10, 11]. Tab. 2 lists the experiment conditions of the resuspension behaviour of graphite dust.

II.3 Experimental facilities studying the graphite dust behaviour

Graphite dust will be produced mainly due to the mechanical abrasion of the fuel elements while they multi-pass through the core, the fuel charging tube and the discharging tube. Graphite dust could adsorb fission products, and the radioactive dust could be transported by the coolant and deposited on the surface of the primary loop. Besides, in DLOFC accident, the deposited dust will re-suspend due to the high fluid speed, resulting in release of radioactive graphite dust into the environment. So graphite dust is an important safety concern of the HTGR.

Experiments were designed in INET to study the below behaviour of the graphite dust:

- Abrasion behaviour of graphite pebble
- Deposition behaviour of graphite dust
- Resuspension behaviour of graphite dust

Figure 6. Schematic of experimental platform for deposition behaviour of graphite dust



Table 2. Experiment conditions of the resuspension behaviour of graphite dust

	Unit	Value
Gas		Air
Particles		Graphite dust (IG110, NBG18, MCMB)
Diameter of dust	mm	0.1-30
Surface material		Mica, Graphite, Inconel 800H
Surface roughness	μm	1.66-5.56
Pressure	MPa	normal

III. Experimental Facilities Involved In CmVB Project

After several years' discussion, the cmVB project is expected to be started up soon, and the participants include INET from China, Korea Atomic Energy Research Institute (KAERI) from the Republic of Korea, Department Of Energy (DOE) for the USA, Joint Research Centre (JRC) for EURATOM and Japan Atomic Energy Agency (JAEA) for Japan. This project is organised into work packages and tasks, and experimental data from different countries will be contributed as basis to perform systems analysis code validation calculations.

The selected experiments include:

- Reactor Cavity Cooling System (RCCS) experiment in Texas A&M University
- Oregon State University (OSU) High Temperature Test Facility (HTTF)

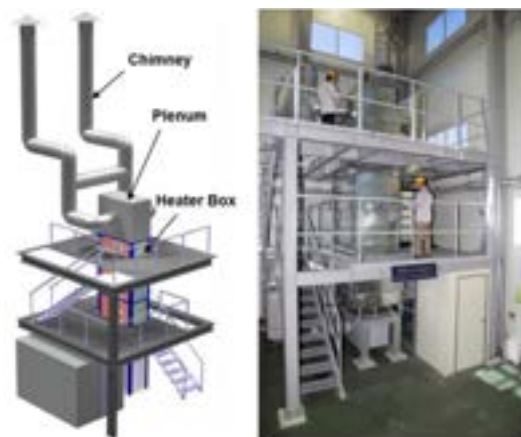
- Argonne National Laboratory (ANL) air-cooled RCCS and water-cooled RCCS experiments
- HTR-10 RCCS experiments in INET
- Korea hybrid RCCS experiment
- German (NAturzug im COre mit Korrosion (NACOK) II experiments

Below two experiment facilities are selected to be simply introduced in this paper.

III.1 Korea RCCS facilities

In order to verify the capability of the RCCS of Korea PMR 200MWth Prototype Reactor, a 1/4 – scale mockup of the RCCS, the NATural Cooling Experimental Facility (NACEF) was designed at KAERI. The 3D view of NACEF is shown in Fig. 7 [12].

Figure 7. Schematic of NACEF



The hot panels, a mockup of the reactor vessel, were constructed to be 4 m in height, and two chimneys are 8 m in height. Twenty ceramic mold heaters of 2.6 kW (with the maximum heat flux of 20 KW/m²), with total capacity of 52 kW, were equipped on the hot panels in two rows. The hot panels were oxidised and blackened to provide a high emissivity of about 0.8 at 350°C.

Steady-state tests with uniform heat flux conditions were performed to demonstrate the passive safety concept of the air-cooled RCCS. KAERI and ANL performed the bi-lateral collaboration study to develop and confirm the scaling analysis methodology through a comparative study between two reduced scale-down tests for RCCS at KAERI and ANL during 2015-2017 [13].

Furthermore, KAERI developed the hybrid RCCS concept for the passive safety at no natural circulation condition by the chimney blockage. The NACEF facility was modified to demonstrate the hybrid RCCS design concept in 2016. KAERI is producing the experimental data to validate the system analysis code. The data will also be provided for GIF VHTR cmVB.

III.2 OSU HTTF

The HTTF is an integral test facility, which has been designed to model the behaviour of interest for the Modular High Temperature Gas Reactor (MHTGR) during the depressurised conduction cooldown (DCC) event [14]. It also has the potential to conduct limited explorations into the progression of the Pressurised conduction cooldown (PCC) event and phenomena during normal operations. The facility is scaled 1:4 by height and 1:64 by volume. The maximum core power for the facility is approximately 2.2 MW.

The HTTF consists of the following systems:

- A primary system consisting of the reactor pressure vessel (RPV), the circulator, cross over ducts and primary piping. The core internals sit inside the RPV and provide support for the core and core heaters.
- A secondary system consisting of a steam generator, feed water system and main steam system.
- A reactor cavity simulation system consisting of a cavity tank, gas conditioning system and a series of break valves. At the HTTF, the cavity is modelled as a separate tank, the reactor cavity simulation tank (RCST) and is connected to the RPV through break valves – hot leg, cold leg, upper break, and lower break.
- A RCCS consisting of a series of water cooled panels and the water supply system for these panels. The HTTF RCCS is not a scaled prototypical RCCS system for the MHTGR. It is provided in the HTTF in order to set the boundary condition for radiation heat transfer from the RPV.
- Various auxiliary systems including the city water supply system, the electrical power supply and distribution system, the chilled water system and the instrument air system.

Figure 8 shows the location of the main core components. The core consists of four major sections: (1) the ceramic core blocks which model the inner reflector region, the heated region and the outer reflector region, (2) the side reflectors which model the permanent side reflectors, (3) the lower plenum structure including the lower plenum support posts, and (4) the heaters. With the ceramic core blocks are flow channels through which the coolant can flow.

Figure 8. HTTF core components

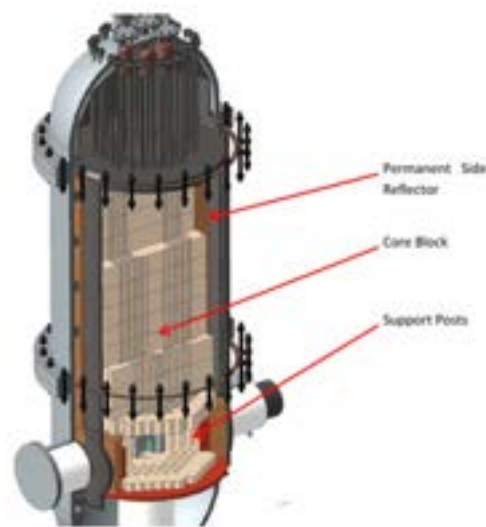
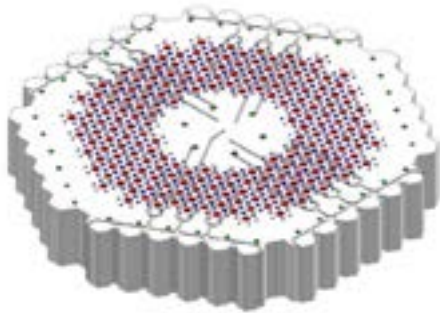


Figure 9 shows a rendering of one of the ceramic core blocks. Nine core blocks are stacked upon one another in order to model the graphite core of the MHTGR. Each of the ceramic core blocks is 19.8 cm tall. There are 210 channels with diameter of 2.5 cm cast in each ceramic core blocks to accommodate the heater rods. In addition, there are 516 coolant flow channels cast into each ceramic core block. 6 inner and 36 outer flow channels are also cast into each ceramic core block beyond the annular heater regions, allowing the facility to model bypass flow through the inner and outer reflector regions of the prototypical plant. The height from the bottom of lower reflector to the top of the upper plenum floor plate is 268.0 cm. The tests could be performed in different power levels, including 700 kW, 1500 kW and 2200 kW.

Figure 9. Core block #1 through #9

Various types of tests are planned, including:

- Depressurised conduction cooldown tests
- Pressurised conduction cooldown tests
- Inlet plenum mixing tests
- Outlet plenum mixing tests

For example, the purpose of the DCC tests is to collect data for the air ingress and natural convection phases of the DCC event, including double ended inlet-outlet crossover duct break, control rod drive nozzle break, instrumentation port break, inlet crossover duct break, DCC with a typical RCCS and DCC with increased decay heat.

The data collected would be to support code validation efforts but the data collected should be of sufficient quality and quantity to support the phenomenological analysis of each event.

IV. Conclusion

VHTR is one of the candidates for the Generation IV Nuclear Energy Systems. Some experimental facilities which were designed to study the Key phenomena of VHTR, as well to support the safety analysis and licensing of the HTR-PM, are introduced in this paper.

Besides, to collect a full set of useful data and to perform an effective system code validation, cmVB project is being planned under the GIF VHTR system. The experimental data from different countries are selected as the benchmark and participants will use their own codes to do the validation calculation respectively.

To further understand the phenomena of the VHTR, more experiments need to be designed and the system code validation need to be

carried out. Besides, the international cooperation is very important and expected.

Acknowledgements

I would like to express my sincere gratitude to Dr. Hans Gougar (INL), Dr. Chang Keun Jo (KAERI), Dr. Shi Lei (INET), Dr. Peng Wei (INET), Dr. Fang Xiang (INET) and Dr. Ren Cheng (INET), who help me finish this paper by offering valuable and import data.

Nomenclature

GIF	Generation IV International Forum
VHTR	Very High Temperature Reactor
CMVB	Computational Methods Validation and Benchmark
HTR-PM	High Temperature gas-cooled Reactor Pebble-bed Module
HTR-10	10 MW High Temperature gas-cooled test Reactor
MHTGR	Modular High Temperature Gas Reactor
INET	Institute of Nuclear and new Energy Technology
KAERI	Korea Atomic Energy Research Institute
DOE	Department of Energy
JRC	Joint Research Centre
JAEA	Japan Atomic Energy Agency
OSU	Oregon State University
ANL	Argonne National Laboratory
RPV	Reactor Pressure Vessel
RCST	Reactor Cavity Simulation Tank
HTTF	High Temperature Test Facility
NACOK	NAturzug im COre mit Korrosion
NACEF	NAtural Cooling Experimental Facility
DLOFC	Depressurised Loss Of Forced Cooling
DCC	Depressurised Conduction Cooldown
PCC	Pressurised Conduction Cooldown
DBA	Design Basis Accident
ABS	Acrylonitrile Butadiene Styrene
CT	Computerised Tomography

References

- [1] Zhang, Z., et al., Economic potential of modular reactor nuclear power plants based on the Chinese HTR-PM project. Nuclear Engineering and Design, vol 237, 2265-2274, 2007.
- [2] Z.Y. Zhang, Z.X. Wu, D.Z. Wang, Y.H. Xu, Y.L. Sun, F. Li, Y.J. Dong, Current Status and Technical Description of the Chinese 2×250MWth HTR-PM Demonstration Plant. Nuclear Engineering and Design, v239, p.1212, 2009.
- [3] United States Nuclear Regulatory Commission (U.S.NRC), Next Generation Nuclear Plant Phenomena Identification and Ranking Tables (PIRTs) Volume 2: Accident and Thermal Fluids Analysis PIRTs. NUREG/CR-6944, Vol. 2, 2007.
- [4] Robold, K., Wärmetransport im inneren und in der randzone von Kugelschüttungen. Jül-1796-RW, Juli, 1982.
- [5] Zehner, P., Schlünder, E.U., Einfluss der wärmestrahlung und des druckes auf den wärmetransport in nichtdurchströmten schüttungen. Chem.-Ing. Techn., 4 Jahrg. 1972/Nr.23.
- [6] Schürenkrämer, M., Barthels, H., Experimentelle untersuchungen zur thermohydraulik in Kugelschüttungen im vergleich mit dem rechenprogramm Thermix-2D. Die untersuchung des dispersiven wärmetransportes am beispiel einer Kaltgassträhne. Jül-1839-RW, 1983.
- [7] Barthels, H., Schürenkrämer, M., Die effective wärmeleitfähigkeit in Kugelschüttungen unter besonderer berücksichtigung des hochtemperaturreaktors. Jül-1893-RW, Februar, 1984.
- [8] Bernd Stöcker, Hans-Ferdinand Nie en, Data sets of the SANA experiment 1994-1996. Jül-3409, July, 1997.
- [9] Final report of HTGR pebble bed equivalent conductivity experiment. Institute of nuclear and new energy technology, ZX06901-00102EP18001, 2018.
- [10] Ke Shen, Wei Peng, et al., Characterization of graphite dust produced by pneumatic lift. Nuclear Engineering and Design, v305, 104-109, 2016.
- [11] Ke Shen, Jiageng Su, et al., Abrasion behaviour of graphite pebble in lifting pipe of pebble-bed HTR. Nuclear Engineering and Design, v293, 395-402, 2015.
- [12] J. H. Kim, Y. Y. Bae, et al., The test results of the NACEF RCCS test facility. Transactions of the Korean Nuclear Society Spring Meeting, Jeju, Korea, May 7-8, 2015.
- [13] C. S. Kim, D. Lisowski, G. C. Park, Comparative study between two reduced-scale test results for air-cooled RCCS scaling law, Transactions of the Korean Nuclear Society Spring Meeting, Jeju, Korea, May 17-18, 2018.
- [14] Brian G. Woods, et al., Basic research on high temperature gas reactor thermal hydraulics and reactor physics, Final report, NRC-04-08-138, March, 2015.

DEVELOPMENT AND LICENSING OF A MOLTEN SALT TEST REACTOR, TMSR-LF1 (K. CHEN)

Kun Chen

Shanghai Institute of Applied Physics, China

Abstract

The Shanghai Institute of Applied Physics, Chinese Academy of Sciences is designing and constructing a 2 MW thermal power molten salt test reactor, TMSR-LF1, in China. The reactor uses molten LiF-BeF₂-ZrF₄-UF₄ salt fuel and graphite moderator. The nuclear fuel and the moderator are contained in a reactor vessel made of a nickel-based alloy. The reactor has a secondary loop filled with molten LiF-BeF₂ salt coolant to remove the nuclear heat from the fuel salt and dissipate the heat into the air. The test reactor has experimental channels that allow samples and instruments to be inserted into the reactor core. Thorium fuel samples will be irradiated and studied on the test reactor. The candidate site of the test reactor is in Minqin County of Gansu Province. The Shanghai Institute of Applied Physics has submitted the environmental impact assessment report and the site safety analysis report to the National Nuclear Safety Administration of the Ministry of Ecology and Environment of China. The institute has completed the preliminary engineering design of the test reactor and started to procure materials and major components. Site preparedness is scheduled to begin in 2018 and the test reactor is scheduled to reach criticality by the end of 2020. Once in operation, TMSR-LF1 may become a major experimental infrastructure for international molten salt reactor research.

I. Introduction

Molten Salt Reactor (MSR) is one of the six kinds of Generation IV reactors. Unlike other five kinds of Generation IV reactors, MSR uses molten salts as both the nuclear fuel and the coolant. Potential advantages of MSR are improved safety, lowered cost, and convenience for fuel management, which may enable the use of alternative nuclear fuel such as thorium [1][2].

Based on previous experience, Oak Ridge National Laboratory (ORNL) conducted the Molten Salt Reactor Experiment (MSRE) in the 1960s. The MSRE demonstrated the viability of the MSR concept [3]. China started her MSR research in the 1960s. In 1971, a zero-power MSR reached criticality in Shanghai.

After several decades, Chinese Academy of Sciences (CAS) restarted China's MSR research program in 2011 [4]. The program intended to

use MSR to explore the possibility of adopting thorium as an alternative nuclear fuel since thorium is considered to be an abundant potential energy source in China. The program was, therefore, named as Thorium Molten Salt Reactor Energy System program, or TMSR program. And Shanghai Institute of Applied Physics (SINAP) was designated by the CAS to lead the TMSR program. The main objective of the program is to design and construct a 2 MW thermal power molten salt test reactor, TMSR-LF1. The reactor will be used to conduct experiments such as uranium and thorium fluorides fuel tests, molten salts thermal hydraulics tests, components tests, and operation and maintenance practice. Once built, TMSR-LF1 may become a major experimental facility for the molten salt reactor research and development.

II. Design

TMSR-LF1 uses molten fluoride salts as the fuel and the coolant. The composition of the initial fuel salt is LiF (65.34%) - BeF₂ (28.54%) - ZrF₄ (4.76%) - UF₄ (1.36%). The enrichment of the uranium is 19.75% or lower. Lithium-7 in the salt is also enriched to 99.95% or higher in order to reduce the production of tritium and improve the neutron economy. Thorium fluoride will be added to the fuel as an experiment at a later time.

TMSR-LF1 is a thermal spectrum reactor that uses fine grain isotropic nuclear graphite as the moderator and the reflector. The graphite is designed to minimise the infiltration of the fuel salt. The components that are in contact with the salts are all made of the UNS N10003 nickel alloy. This type of material provides excellent corrosion resistance against fluoride salts and good mechanical properties at high temperatures.

The reactor core is composed of graphite blocks. Large quantities of vertical channels penetrate the graphite core. During the operation, the fuel salt flows through these channels from the bottom to the top driven by a salt pump at the top of the core. After leaving the pump, the fuel salt then flows through the shell side of a heat exchanger at one side of the core, and eventually flows back to the bottom of the core. The fuel salt, the graphite blocks, the pump bow and the heat exchanger are contained in a reactor vessel. The vessel has multiple welded thimbles that extend from the top of the vessel into the channels in the graphite core. This configuration allows control rods and instruments to be inserted through the thimbles into the core without contacting the fuel salt. Figure 1 shows the section view of the internals of the reactor vessel.

The coolant salt flows through the U-shape tubes of the heat exchanger and removes the nuclear heat from the fuel salt. The composition of the coolant salt is LiF - BeF₂ and the lithium-7 in the coolant salt is also enriched to 99.95% or higher. The coolant salt is pumped to a salt-air heat exchanger and the heat is discharged into the air.

During the operation, argon gas is blown through the pump shaft seal into the upper space of the reactor vessel. The argon gas above the fuel salt serves as the cover gas of the fuel salt. The cover gas continuously flows out of the reactor vessel into the cover gas cleanup system, which uses charcoal bed, decay tank and filters to remove most radioactive noble

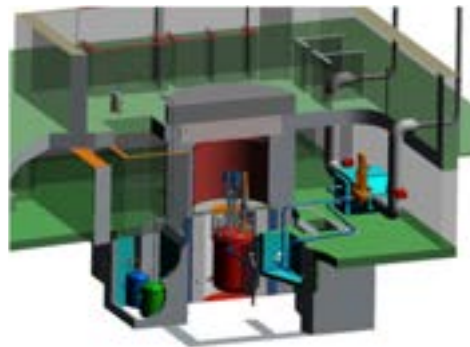
gases, halogens and particles from the reactor. This design significantly reduces the amount of radioactive isotopes that may be released into the environment during accidents.

Figure 1. Internals of the Reactor Vessel



TMSR-LF1 has two engineered safety features, the decay heat removal system and the reactor containment vessel. The heat exchangers of the decay heat removal system sit close to the outer surface of the reactor vessel. The system cools the reactor vessel using the natural circulation of the air and the designed cooling power is 40 kW. The cooling of the reactor vessel requires no electric power and operator intervention. The containment vessel is the second physical barrier against the release of the radioactive isotopes. The design leak rate of the containment vessel is less than 5% volume per day under all accidents. Figure 2 shows the layout of the systems of TMSR-LF1.

Figure 2. Layout of TMSR-LF1



III. Schedule

Table 1 shows the schedule of the design and construction of TMSR-LF1. During the initial critical experiment, the reactor will not contain thorium. Thorium experiments will be conducted later. A comprehensive experimental plan is under development in the hope of supporting domestic and international thorium fuel and MSR research.

Table 1. Schedule of Design and Construction

Conceptual Design	Nov. 2017
Preliminary Design	May 2018
Construction Design	Sep. 2018
First Concrete Date	June 2019
Fuel Loading	July 2020
Criticality	Dec. 2020

IV. Licensing

The construction of TMSR-LF1 is required to follow three licensing steps defined by the laws and regulations in China. Before using a site for the construction of TMSR-LF1, SINAP shall obtain the nuclear facility site selection review opinions from the National Nuclear Safety Administration (NNSA) under the Ministry of Environment and Ecology after the review finds the site conform to the requirements for nuclear safety. The candidate site of TMSR-LF1 is in Minqin County in a western province of Gansu in China. SINAP has submitted a site safety analysis report and an environment impact assessment report to the NNSA for review. At the time when this paper is prepared, the review is still in progress. Figure 3 shows the area where TMSR-LF1 is going to be constructed.

Figure 3. Area of the Candidate Site



After NNSA permits the using of the site, SINAP will apply for the construction license before the first concrete of the reactor building can be poured. SINAP is in the process to prepare the necessary documents such as the preliminary safety analysis report and the quality assurance plan and etc., which support the application.

After the construction license is granted, SINAP will apply for the operation license before the nuclear fuel can be loaded into the test reactor. Once licensed, TMSR-LF1 shall reach criticality and operate strictly following the specifications in the operation license.

V. Accident Analysis

One of the major challenges of licensing TMSR-LF1 is to identify the maximum hypothetical accident (MHA). Considering the pilot nature of TMSR-LF1 and its low power level, even though comprehensive safety analyses are desired, the reviewers will find the design to be acceptable if an MHA can be defined. The radiological consequence of the MHA may be used as a basis to set some principle rules, for example, the size of the emergency response zone, the safety classification of the components and etc., especially in the early stage of the licensing process. Defining the MHA and obtaining its radiological consequence allow the project to proceed in the early stage without requiring detailed engineering design and safety analyses.

In a typical MSR such as TMSR-LF1, the fuel salt has the capability of containing most of the fission products, for example, cesium and strontium. If the fuel salt is in a right reduction-oxidation reaction (Redox) status, only noble gases and part of the halogens shall be released from the fuel salt. This is proved to be one of the safety features of the MSR [5][6].

TMSR-LF1 has a cover gas space above the fuel salt. Once fission products are released from

the fuel salt and enter the cover gas, the cover gas cleanup system will continuously remove them so that the accumulation of the fission products is minimised. The fuel salt pump used in TMSR-LF1 is designed such that minimal salt mist shall be generated during the operation. Therefore, we conservatively assumed that all noble gases and 10% of iodine are released into the cover gas during the operation.

TMSR-LF1 has two physical barriers against the release of radioactive materials. The first barrier is the fuel salt and its cover gas boundary. The second barrier is the reactor containment vessel. Considering the reactor shutdown system and the decay heat removal system are all passive systems requiring no power and operator action, based on preliminary accident analysis, we found that the complete release of the fuel salt cover gas is the MHA. During the MHA, the first barrier is breached and the cover gas is completely and instantaneously released to the containment vessel. The containment vessel has a leak rate of 5% volume per day in the MHA.

Using the local meteorology information, we calculated the total effective dose equivalent (TEDE) at the exclusive area boundary (EAB) or site boundary to be significantly smaller than 3.75 mSv during the MHA. Because the MHA bounds all other accidents, this result shows that TMSR-LF1 has very limited radiological consequences in any accident and requires no

off-site emergency preparedness. As the engineering design evolves, detailed accident analyses will provide more information about the behavior of the reactor in an accident, but the radiological consequence shall not exceed the limits set by the MHA.

Acknowledgements

This work is supported by the Thorium Molten Salt Reactor Nuclear Energy System program under the Strategic Pioneer Science and Technology Project of the Chinese Academy of Sciences under the contract No. XDA02000000. The author appreciates the valuable design information provided by many individuals from the TMSR team.

Nomenclature

MSR	Molten Salt Reactor
SINAP	Shanghai Institute of Applied Physics
CAS	Chinese Academy of Sciences
ORNL	Oak Ridge National Laboratory
NNSA	National Nuclear Safety Administration
MHA	Maximum Hypothetical Accident
Redox	Reduction–Oxidation Reaction

References

- [1] V. Ignatiev et al, Molten salt reactor: new possibilities, problems and solutions, *Atomnaya energia*, 112: 3, p.135 (2012)
- [2] C.W. Forsberg et al, Liquid Salt Applications and Molten Salt Reactors, *Revue Générale du Nucléaire* N° 4/2007, 63 (2007)
- [3] P.N. Haubenreich and J.R. Engel, Experience with the Molten-Salt Reactor Experiment, *Nuclear Applications and Technology*, 8: 118–136 (1970)
- [4] M. Jiang et al, Advanced Fission Energy Program - TMSR Nuclear Energy System, *Bulletin of Chinese Academy of Sciences*, Vol. 27-3, p.366 (2012)
- [5] S.E. Beall et al, MSRE Design and Operation Report, Part V, Reactor Safety Analysis Report, ORNL-TM-732, (1964)
- [6] E. L. Compere et al, Fission Product Behavior in the Molten Salt Reactor Experiment, ORNL-4865, (1975)

GENERATION-IV SYSTEMS' EXPERIMENTAL INFRASTRUCTURE NEEDS (R. GARBIL ET AL)

Roger Garbil⁽¹⁾, Alfredo Vasile⁽²⁾, Sang Ji Kim⁽³⁾, Alexander Stanculescu⁽⁴⁾, Alessandro Alemberti⁽⁵⁾, Iurii Ashurko⁽⁶⁾, Michel Bertelemey⁽²⁾, Olivier Gastaldi⁽²⁾, Marc Deffrennes⁽⁷⁾, Lyndon Edwards⁽⁸⁾, Mmeli Fipaza⁽⁹⁾, Petr Fomichenko⁽¹⁰⁾, Michael Futterer⁽¹⁾, Jean-Paul Glatz⁽¹⁾, Gisela Grosch⁽⁷⁾, Robert Hill⁽¹¹⁾, Bonnie Hong⁽⁴⁾, Victor Ignatiev⁽¹⁰⁾, Tatiana Ivanova⁽⁷⁾, Laurence Leung⁽¹²⁾, Stefano Monti⁽¹³⁾, François Storrer⁽²⁾, Tomas Sowinski⁽¹⁴⁾, Henri Paillère⁽⁷⁾, Zukile Zibi⁽¹⁵⁾

- (1) European Commission, Euratom, Belgium
- (2) Commissariat à l'énergie atomique et aux énergies alternatives, France
- (3) Korea Atomic Energy Research Institute, Republic of Korea
- (4) Idaho National Laboratory, United States of America
- (5) Ansaldo S.p.A, Italy
- (6) Institute for Physics & Power Engineering, the Russian Federation
- (7) OECD Nuclear Energy Agency, France
- (8) Australian Nuclear Science and Technology Organisation, Australia
- (9) Eskom, South Africa
- (10) National Research Centre Kurchatov Institute, the Russian Federation
- (11) Argonne National Laboratory United States of America
- (12) Canadian National Laboratories, Canada
- (13) International Atomic Energy Agency, Austria
- (14) Department of Energy, United States of America
- (15) Department of Energy, South Africa

I. Introduction

The Generation IV International Forum (GIF) is a co-operative international endeavour coordinating the research and development (R&D) needed to establish the feasibility and performance of the next generation (GEN IV) nuclear energy systems. This paper summarises the first results of the GIF R&D Infrastructure Task Force (GIF RDTF).

The GIF-RDTF was established early 2018, for a period of up to two years, as approved by the 44th GIF Policy Group in Cape Town (ZA), in October 2017. A brief introduction of the Terms of Reference (ToR) and objectives is provided.

First steps of actions taken to meet the first objective was to 'Identify essential R&D experimental facilities needed for development, demonstration and qualification of GEN IV components and systems, including activities to meet safety and security objectives'.

Generation-IV systems (SFR, LFR, GFR, VHTR, SCWR and MSR) major (or critical) experimental infrastructure (or facilities) needs in function of the respective R&D objectives for the next decade (i.e. viability, performance, or demonstration – depending on the respective system TRL) are presented, based upon national R&D programmes and considering industrial needs.

Identification of existing experimental facilities in response to the aforementioned needs highlighted some gaps. Planned experimental infrastructure constructions, availability of experimental infrastructures outside the GIF countries are briefly discussed.

Forward looking and planned activities of GIF RDTF in view of meeting its second objective are discussed, the latest being to 'Promote the utilisation of the experimental facilities for collaborative R&D activities among the GIF partners'. To this end, identify existing mechanisms and approaches, including

organisational points of contact, for obtaining access to relevant R&D facilities in the GIF member countries is needed. This information should then be made accessible to GIF participants, e.g. on the GIF website, including closer OECD/NEA, GIF and IAEA international cooperation initiatives, to stimulate joint funding from Member States and/or enterprises, and benefits to be capitalised. [1]

First conclusions and outlook of the GIF RDTF to ensure a successful implementation of the Generation-IV Systems' Experimental Infrastructure Needs are provided.

II. Approach

At the 43rd GIF Policy Group (PG) meeting held on 13-14 April 2017 in Paris, France, it was decided to establish a new Task Force (TF) on R&D Infrastructure. The PG tasked the Technical Director (TD) to develop, in collaboration with the PG vice chair in charge of external collaboration and with the Technical Secretariat (TS), the Terms of Reference (ToR) for the GIF R&D Infrastructure Task Force.

The task Force was initiated around each GEN IV System Steering and provisional System Steering Committee (SSC and pSSC) and Expert Group (EG) designated representatives. It reports to the PG vice-chair in charge of external collaboration. Members meet as needed, taking advantage of audio- and teleconferences when practical. At its kick-off meeting on 19 February 2018, it determined its chair and vice chairpersons, agreed upon a two-year work plan, deliverables and milestones, taking advantage of relevant work of IAEA and NEA in the area of infrastructures. With the approval of the PG in Sun Valley, USA, on 17-18 May 2018, a goal has been set to complete its first objective in due time, for presentation at the October 2018 GIF Symposium, and its second objective by the spring of 2019 at the EG/PG meetings. It also foresees the organisation of an international workshop on the 'Needs for dedicated experimental facilities, and R&D infrastructure needs from industry and private start-ups' initiatives'. The TD supervises all activities of GIF RDTF and will make use of the EG to review for quality and completeness all key outputs.

GIF RDTF takes advantage of GIF Member State's, IAEA's and NEA's relevant work, among others: a) R&D needs Outlook(s) along with; b) R&D infrastructures, databases, reports, compendium, International Cooperation initiatives and collaborative projects (e.g. IAEA

CRPs, ICERR, NEA joint projects, NEST, NI2050, and EU/EURATOM projects). [2]

The Task Force benefits from GIF Member State's latest relevant updates together with: a) IAEA database of Facilities in Support of Liquid Metal-cooled Fast Neutron Systems Facilities and its latest compendium; b) The Advanced Reactor Information System (ARIS); c) The Research Reactor database (RRDB); c) OECD/NEA Research and test facilities database (RTFDB); d) OECD/NEA Task Group on Advanced Experimental Facilities (TAREF) on SFR and GFR but also the Support Facilities for Existing and Advanced Reactors (SFEAR); and e) EU/EURATOM projects' roadmap proposal for building knowledge and facilities needed for the development of nuclear energy systems such as ADRIANA (ADvanced Reactor Initiative And Network Arrangement). [3]

An opportunity is also taken to propose any update of existing IAEA and NEA databases (including any new infrastructures or facilities launched) with the close support of GIF SSC (or pSSC) and EG groups. Upon completion of the two objectives of the GIF-RDTF, SSCs and pSSCs will be expected to maintain cognisance of infrastructure needs and approaches for their access as work evolves.

GIF RDTF identified the following technical areas to be addressed: a) Thermal-hydraulics; b) Fuel safety; c) reactor physics; d) Severe accidents; e) Structural integrity, system components and validation; f) Coolant chemistry; g) Cross-cutting areas (instrumentation, ISI&R, E&T,...); and h) Any other issues.

With the benefit of TAREF and latest reports, elaboration of a PIRT-like (PIRT exercise = Phenomena Identification and Ranking Tables) was confirmed to be already available within GIF SSC's documentation. In general, the ranking tables of experimental facilities provide: a) A ranking of the issues to be investigated; b) A ranking of the facilities in connection with their capability to address each topic; and c) A ranking of the needed experimental infrastructures to be upgrade and/or constructed.

Safety (and security) NEEDS (or challenges) requiring key research were based upon the following criteria: a) Status of knowledge, Low (L), Medium (M), High (H); b) Design relevance (contribution of dedicated facilities to solve a design issue, L, M, H); c) Safety relevance (contribution of dedicated facilities to solve a safety issue, L, M, H); d) Operational relevance

(contribution of dedicated facilities to solve an operational issue L, M, H); e) Implement a scheduling of the needs to iterate within the projects (Short term 0–2 years (H), medium term 2–5 years (M), long term > 5 years (L)).

Based on the information assembled on both safety (and security) challenges and related facilities, Task Force members assessed prospects and priorities for safety research and recommendations as priorities regarding facility utilisation through multi-lateral and GIF cooperative programmes.

The main CRITERIA FOR RANKING were: a) Technical relevance (relevance of the facility to cover a specific issue); b) Uniqueness (No alternative facility for the same goal, e.g. one of a kind for in-pile testing); c) Availability (Availability for a given identified programme addressing the issue); d) Readiness (Facility or test section for the specific issue is available; staff available to run it); e) Construction (or refurbishment) costs (N/A, L: < 1, M: 1–5, H: > 5 MUSD); f) Operating costs (actual or estimated) (L: < 0.3, M: 0.3–1, H: > 1 MUSD); g) Experimental device costs (N/A, L: < 1, M: 1–3, H: > 3 MUSD); h) Flexibility (Capacity to be adapted to various technical areas thus ensuring good return of investment); i) Time for availability (Short term 0–2 years (H), medium term 2–5 years (M), long term > 5 years (L)); j) Existence of preliminary schedule and refurbishment of the facility (Level of financial and scheduling elements related to the facility for the specific issue considered. (H) means that funding for refurbishment and scheduling are available).

Based on the above characteristics, Generation-IV systems (SFR, LFR, GFR, VHTR, SCWR and MSR) major (or critical) experimental infrastructure (or facilities) needs in function of the respective R&D objectives for the next decade (i.e. viability, performance, or demonstration – depending on the respective system TRL) are presented, based upon national R&D programmes and considering industrial needs.

III. SFR R&D Infrastructures

The Sodium-cooled Fast Reactor (SFR) uses liquid sodium as the reactor coolant enabling high power density, a fast neutron spectrum enabling fissile fuel regeneration and minor actinide management, and enhanced inherent and passive safety operating regimes. Moreover, the high boiling point of metallic sodium (894°C at atmosphere pressure) allows operating the reactor at a pressure close to atmospheric

pressure and offers a large range of liquid state. Sodium density and viscosity in the same range as of water give advantages in term of fluid transport. High outlet temperatures (500–550°C) and innovative capital cost-reducing R&D can provide an economically competitive case for SFRs in future electricity markets. Current plant options under consideration include pool and loop type primary systems and range from small modular reactors (50 to 300 MWe) to larger plants (up to 1500 MWe). Over 60 years of international SFR demonstration and operation programs (e.g., PHENIX, Joyo, EBR-II, BN-600, etc.) have established much of the base SFR technology making it one of the nearest-term deployable Generation IV systems.

Current international programs look to address remaining R&D challenges associated with SFR cost reduction, safety and reliability enhancement, in-service inspection, energy conversion systems, and advanced fuel development. The GIF SFR SSC maintains a list of key R&D areas necessary to drive SFRs to commercialisation. Priority SFR R&D areas on the list include: inherent safety, severe accident mitigation, safety analysis tools, decommissioning experience, evaluation of advanced fuel options, high burn up fuels, fabrication of minor actinide fuels, demonstration of minor actinide recycle, monitoring instrumentation, in service inspection and repair, high temperature leak before break and defect inspection, fuel handling technology and strategy, energy conversion technology, advanced materials, nuclear data, advanced modelling and simulation, benchmarks, codes and standards, long term behaviour of structural material and advanced core design.

SFR SSC members currently maintain various experimental capabilities supporting key SFR R&D areas. France capabilities include a short to long term material corrosion in-sodium testing facility, sodium to gas heat exchanger testing facility, under-sodium instrumentation and SFR component in-sodium testing facility, sodium handling training facilities, and sodium versatile medium scale loops able to support fuel, heat exchanger, and other SFR instrumentations or components development. Other facilities allow studying interaction between sodium and other compounds such as water or CO₂ at different scales. Some other facilities, available in France, are able to simulate sodium behaviour by water in particular for hydraulic tests of fuel sub-assemblies or specific primary circuits design. South Korea capabilities include large scale

sodium loops and facilities for sodium to sodium and sodium to air heat exchanger development supporting passive SFR safety systems, facilities for SFR fuel prototypic assembly pressure and flow rate distribution testing, a control rod drive testing facility, and under-sodium viewing testing experiment supporting in-service inspection development.

United States capabilities include prototypic sodium environment loops for intermediate-scale SFR component and material testing, sodium-SCO₂ interaction loop based on Brayton cycle supporting energy conversion systems, test reactor supporting thermal spectrum irradiations, hot fuel examination facilities supporting post irradiation examination, SFR passive safety system performance testing facility, and advanced fast reactor modelling and simulation. Euratom capabilities include several loops and facilities to investigate liquid sodium flow, thermal hydraulic phenomena, high temperature SFR candidate materials and components performance, and instrumentation development in prototypic sodium environments.

China capabilities include sodium test loops supporting SFR safety analysis and high temperature material and component testing, the China Experimental Fast Reactor (CEFR) that will provide SFR oxide fuel performance, inherent safety, passive decay heat removal, instrumentation, and operational benchmark data, SFR natural circulation testing facility, and SCO₂ thermal-hydraulic performance and sodium-SCO₂ heat exchanger performance testing experiments. Japan capabilities include AtheNa facility for large scale component and system sodium test with 60MW heat capacity, PLANDTL for thermal-hydraulic transient sodium test, CCTL for subassembly and component sodium test, SWAT for sodium water reaction, Sodium fatigue test loop, FRAT for sodium fire test, MELT for molten fuel behaviour, SERT for ISIR development, and Experimental Fast Reactor Joyo for fast flux irradiation.

While current global experimental infrastructure exists to address some SFR R&D needs, the SFR SSC has identified key experimental and analytical infrastructure gaps. For SFR advanced fuel and material qualification, worldwide fast neutron irradiation capability is largely lacking. Light water-cooled test reactors lack the high fast to thermal neutron flux ratio needed to develop fast spectrum systems and to accelerate

materials irradiations needed for fast reactors. For inherent safety testing, SFR SSC members identified the need for integral effects experimental facilities supporting comprehensive SFR system transient behaviour and safety analysis. Members also identified the need for benchmark data on natural circulation transient behaviour.

For advanced energy conversion, SFR SSC members identified the need for increased sodium – SCO₂ interaction and heat exchanger testing capabilities. For SFR component testing, SFR SSC members identified the need for large scale component (e.g., full fuel assembly and control rod drive mechanism mock-ups) in-sodium testing capability. For safety analysis, SFR SSC members identified the need for particle/aerosol tracing facilities to support SFR mechanistic source term activities. Members also identified the need for an in-sodium seismic performance test loop/facility. For in-service inspection, SFR SSC members identified the need for larger test sections to accommodate under-sodium ultrasonic sensor performance tests. For severe accidents studies, it is likely identified that some facilities are needed for sodium/corium interaction and for qualification of associated mitigation technical solutions.

SFR SSC member nations look to address some of these infrastructure gaps through a combination of modified and new facilities and potential facility sharing among members. The GIF R&D Infrastructure Task Force currently aims to assist member nations in identifying access pathways to international capabilities and potentially developing international facility use access mechanisms within GIF.

IV. LFR R&D Infrastructures

The Lead Fast Reactor (LFR) features a fast-neutron spectrum and a closed fuel cycle for efficient utilisation of the energy value of fertile uranium and consumption of accumulated transuranic elements, thus minimising the volume and radiotoxicity of long-lived, high-level waste. One of the most important features of the LFR is the enhanced safety that results from favourable basic and intrinsic characteristics of lead as primary coolant. Lead features high boiling point (1749°C), which provides the ability to operate the reactor at close to atmospheric pressure. Lead is at the same time relatively inert in contact with air and water, featuring also high thermal inertia and natural convection capability for enhanced passive safety. LFRs have the potential to be

deployed for large grid-connected power stations as well as to meet the electricity needs of remote sites as small modular reactors.

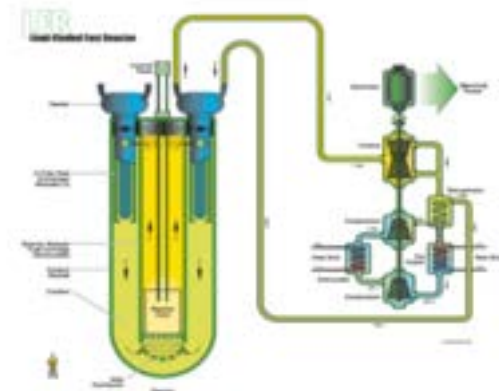
LFR is a very promising Generation IV reactor since it is expected to naturally comply with and fulfil all GIF goals: (i) sustainability, through the use of a closed fuel cycle; (ii) robust and improved safety performance; (iii) favourable economics, in particular due to design simplifications; and (iv) bringing substantial advantages in term of proliferation resistance and physical protection.

LFRs require on the other hand additional development in a number of technical areas before reaching full industrial maturity. The main R&D objectives for the development of the LFR were identified in the 2014 GIF Roadmap Update and are further addressed in the LFR System Research Plan:

- materials corrosion-erosion and lead chemistry;
- core instrumentation;
- fuel handling technology and operation;
- fuel development (MOX and Nitrides);
- actinide management;
- fuel reprocessing and manufacturing;
- in-service inspections and repair (ISI&R);
- seismic impact mitigation;
- phenomenology of lead-water/steam interactions;
- fuel-coolant thermodynamic and chemical interactions, incl. retention of radioactive products in lead; and
- development of design codes and standards.

Most of the present activities related to LFRs are centred on material science and material compatibility with the coolant as well as other aspects specific to the LFR technology. Such needs are well described in the GIF-LFR System Research Plan that has been developed taking into account the needs of the different Countries participating in the provisional System Steering Committee (pSSC) activities.

Figure 1. Sketch of LFR



In terms of availability of R&D infrastructures and facilities the LFR presents a rather well-developed situation. Benefitting from the efforts made since the beginning of GIF activities, a number of facilities, infrastructures, equipment and experimental set-ups are available and are presently generating data dedicated to the technology development and qualification. The main information on such facilities is efficiently collected in the IAEA liquid metal data base, the so called LMFNS Catalogue (Catalogue of Facilities in Support of Liquid Metal-cooled Fast Neutron Systems), collecting also the information related to facilities supporting the development of SFRs.

The review of the database data reveals that, at least in terms of the number of facilities, the situation for LFRs is comparable to that for SFRs, traditionally considered a very well-developed technology.

Coherently with the scope of the Task Force on R&D Infrastructure the LFR-pSSC decided to ask the member Countries to keep updated as much as possible the IAEA database and also to ask laboratories hosting infrastructures and facilities to add information about the present status of the installation including the availability to perform additional tests on specific requests, and share their results.

Although a detailed review of the needs of LFR system is on-going, one may anticipate that most of the needs will be related to the testing and qualification of full scale components and to experiments allowing the simultaneous reproduction of synergetic effects of thermal-mechanical load, irradiation and coolant environmental conditions on material behaviour.

For what the status of the LFR development is concerned, it has to be cited that the BREST-OD-300 project carried out in the Russian Federation is undoubtedly the most advanced demonstration/prototype reactor presently under licensing review. Other countries are also considering the realisation of the so-called “demonstrators” in order to gain the necessary confidence and operational experience feedback allowing further improvement of the performance characteristics necessary as prerequisite of an industrial deployment of the LFR technology.

It has to be finally noted that the LFR system exploits a very high synergy with the development of the Accelerator Driven System that, although not included in GIF activities, are being developed in several countries around the world and are based on the same coolant technology development.

V. GFR R&D Infrastructures

The GFR is a promising and attractive GEN IV concept, combining the benefits of a fast spectrum and of a high temperature ($\sim 850^{\circ}\text{C}$ at the core outlet). The reference design is a pressurised (7 MPa) helium cooled reactor. The concept is clearly innovative compared to other reactor concepts and no demonstrator has ever been built. The project of an industrial GFR has to address Key R&D challenges, especially regarding, the fuel technology, core performance and safety, in particular the decay heat removal (DHR) issue.

The viability of the GFR technology shall be demonstrated by designing, constructing and operating the 75 MW ALLEGRO experimental reactor (Table 1). ALLEGRO shall be used not only for technology demonstration but also for the qualification of innovative components, first of all the ceramic fuel (UPuC pellets in SiC-SiCf cladding). The DHR systems are being designed to operate at least partially under passive mode (natural convection) in depressurised conditions.

In support to the design and the corresponding safety assessment, experimental data from helium facilities are needed for the validation of thermal hydraulic system codes. In addition, experimental programs are needed for the development of the GFR related instrumentation, gas purification and tightness, tribology, high temperature materials and thermal isolations as well as specific components.

Table 1. ALLEGRO main characteristics

Nominal thermal power	75 MW
Nominal electric power	0 MW
Start-up core fuel	Oxide
Experimental positions in the core	6
Long term fuel	Carbide
Primary coolant	Helium
Number of primary loops	2
Core inlet temperature	260°C
Core outlet temperature	530°C
Primary pressure	7 MPa
Secondary coolant	Water
Number of secondary loops	2
DHR systems coolant	Helium
Number of DHR systems (connected to the primary vessel)	3
Number of safety injection accumulators	3

As mentioned before, the DHR is a key issue to demonstrate the feasibility of the GFR and its experimental first step ALLEGRO. Two facilities were built recently and will be used in support to such demonstration, the S-ALLEGRO loop (Figure 2), in Czech Republic owned and operated by the Research Centre Řež and the STU Helium loop (Figure 3), located in Trnava, Slovakia, operated by the Slovak University of Technology in Bratislava Faculty of Mechanical Engineering.

Figure 2. S-ALLEGRO loop



Figure 3. STU Helium loop

Coaxial pipes where hot Helium circulates in the inner pipe and the cold in the outer is one specific design feature of GFRs. Consequently, transients where the coolant bypasses the core due to the inner pipe rupture, plays a pivotal role in the design process. Further experiments are proposed in the near future to select the worst-case bypass configuration. In order to achieve this goal, first a small experimental mock-up is proposed using air working fluid. If the results of this mock-up reveal the need of further investigations, a larger experimental test facility is envisaged using helium working fluid.

The development and qualification of fuel for ALLEGRO reactor will require irradiation capabilities and post-irradiation examination laboratories. The first core with UOX/MOX pellets with 15-15Ti stainless steel cladding will need qualification procedures similar to that of SFRs. The refractory core with carbide pellets and SiCf/SiC cladding will have to be tested in up to high doses in high temperature reactors. Today the only material testing research reactor with fast spectrum is the BOR-60 in Russia. The planned MYRRHA and MBIR reactors could be used for irradiation purposes in the future. In order to carry out fuel examination of irradiated ALLEGRO fuel new hot cell facilities are proposed to be built in Hungary at the Paks NPP.

UJV Rez together with its daughter company Research Center Rez (CVR) will in 2020 commission an integral experimental facility aimed at demonstrating the technical and economic feasibility of recovery of leaked

helium from the guard vessel nitrogen (and helium) atmosphere.

UJV & CVR together with other academical and research partners will also experimentally assess between 2019 and 2024 the compatibility of selected heat transport systems-related structural materials with nitrogen at elevated temperatures up to 800-850°C, the coolant expected for the secondary circuit of GFRs. In addition, experimental experience was reached in the domain of: 1) gas coolant purification including gaseous FP noble gases as Xe and Kr; and 2) helium sealing.

CVR & UJV will also analytically and experimentally assess between 2019 and 2024 the performance of disc check valves proposed by CEA for isolating the gas flow through the DHR system in reactor start-up conditions.

In support of technological developments and R&D in the fields of helium purification and tightness, tribology, high temperature materials and thermal insulation but also components development, France constructed an experimental platform the first decade of the years 2000. This helium platform is composed of several circuits or benches (HETIQ, HPC, HEDYT ...) responding to the needs in these fields. They are currently under cocoon for around 10 years. However, they could eventually cover some needs expressed by the international community after refurbishment and restart (if any dedicated funding is obtained).

VI. VHTR R&D Infrastructures

The GIF VHTR system is a helium-cooled graphite moderated reactor using fully ceramic coated particle fuel. All modern designs feature passive decay heat removal, a robust coated particle fuel form, and a large graphite thermal buffer the combination of which yields an unprecedented level of inherent safety. The unique coated particle fuel and the high temperatures to which primary coolant circuit materials are exposed have meant that much of the focus of R&D has been on fuel and material qualification in support of near-term demonstration of concepts. These and other focus areas that will require experimental facilities are listed here.

- Completion of fuel testing and qualification capability (including fabrication, QA, irradiation, safety testing and Post-Irradiation Examination [PIE]), to be completed in

some countries. Waste reduction and fuel recycling.

- Qualification of graphite, hardening of graphite against air/water ingress, e.g. by SiC infiltration, management of graphite waste.
- Coupling technology and related components (e.g. isolation valves, intermediate heat exchangers).
- Establishment of Design Codes & Standards for new materials and components, including C-C and SiC-SiC composites.
- Advanced manufacturing methods (cooperation with the GIF Cross-cutting Interim Task Force).
- Cost cutting R&D and interaction with EMWG and industry to optimise VHTR design.
- Development, experimental validation, and uncertainty characterisation of modern core analysis methods.
- Licensing and Siting: V&V of computer codes for design and licensing.
- Integration with other energy carriers in Hybrid Energy Systems.
- Analysis of HTR-PM startup physics and demonstration tests.
- HTTR: safety demonstration tests and coupling to H₂ production plant (subject to regulatory approval for restart).
- Enhanced information exchange among vendors, private investors, new national programs, multinational organisations, and regulators.

A specific report produced by the Euratom NC2I-R project has compiled the needs for Industrial Infrastructures including computer tools required for the licensing and demonstration of Nuclear Cogeneration technology using High Temperature Gas-cooled Reactors [4].

The methodology used consisted in confronting a bottom-up with a top-down approach. In the bottom-up phase, information was collected on existing or former infrastructures. Examples for

that are known subjects from different sources such as reports from commercial companies, research centres, and the OECD TAREF database. In a parallel top-down approach, the authors have produced a priority table of critical infrastructure items and have filled in the missing information using a variety of sources including scientific literature, conference proceedings (in particular the HTR conference series), networking, information from the Generation IV International Forum, web-browsing, expert opinion, personal communication and databases. The collected information enabled the preparation of a gap analysis to identify those R&D and Industrial Infrastructures which are not available and which would need to be built [5].

The analysis identified the gaps in industrial infrastructure and competencies for R&D which need to be bridged prior to licensing, construction and operation of an HTR demonstrator. Emphasis is given to existing industrial infrastructure and R&D competences. Based on the valuable results of the German HTR development program up to the late 1980s, significant progress has been made by several GIF signatories. The most outstanding examples are in the areas of fuel production, its quality control and qualification under irradiation, the qualification and coding of high temperature structural materials and new graphite grades (incl. through irradiation testing), component development (e.g. turbomachines, heat exchangers), helium technologies and licensing-relevant modelling (e.g. reactor physics, thermo-fluid dynamics, mechanics, tritium transport, source term calculations, system code integration).

In addition, significant improvement was achieved in understanding the market and end-user needs so as to design a power plant accordingly. Several industrial designs worldwide reflect this development.

Due to the time gap between the last running HTR and the HTR "revival" in the 1990s, some facilities had been shut down, mothballed or refurbished to support other projects and developments. A number of them could be recovered and have produced significant results. The situation is similar for graphite qualification.

Table 2. Gaps for short and long term VHTR deployment

R&D Area	Gaps for demonstrator	Gaps for future VHTR development
Computer codes	-Validation of updated codes in support of licensing -Modelling of source-term (dust formation and transport)	-Validation of updated codes -Modelling of source-term (dust formation and transport)
Components	-Component qualification in large scale facilities	-Development and qualification of IHX -High temperature ceramics (SiC-SiC, C-C)
Tribology and corrosion	-None	-Large scale facilities to measure wear and friction may be required for better estimates of dust-related source term releases
Fuel	-Fuel is available, but needs qualification	-Development and qualification of high temperature fuel
Material R&D	-Graphite qualification Some focussed R&D on oxidation under accident conditions	-Additional effort will be required for high temperature materials such as ceramics and composites, but also graphite properties at high temperature
Safety analysis and demonstration	-Large scale loop for component testing Compliance of plant design with Safety Regulation	-Effect of very high temperatures on safety margins
Coupling	-Demonstration and licensing	
Design and system integration	-Demonstrator design and test program	
Development of a licensing framework	-Assess existing licensing framework for suitability to license HTR demonstrator for cogeneration	
Fuel/Graphite waste minimization and recycling	-Qualify decontamination and recycling of irradiated graphite -Compliance with new Nuclear Waste Directive	-Evaluate direct disposal vs. reprocessing for symbiotic fuel cycles

New or repurposed test facilities have been constructed in support of China's HTR-PM demonstration, the US NNGP project, and the HTR programs in Korea and Japan, often with the support and investment of industrial partners. Universities have also constructed some smaller research facilities, particularly for materials testing and experimental thermal-fluid model validation.

What should not be underestimated is the time and effort required for qualification. Assuming that the currently ongoing international collaboration towards fuel and materials (metals, graphite, composites) qualification are confirmed successful, there is still work ahead in view of licensing related to computer codes and to large-scale test facilities for the qualification of components and subsystems. These include steam generators, heat exchangers, the Reactor Cavity Cooling System, circulators with magnetic bearings, isolation valves, control rod mechanisms, instrumentation and others. Specific qualification test rigs will be needed.

VII. SCWR R&D infrastructures

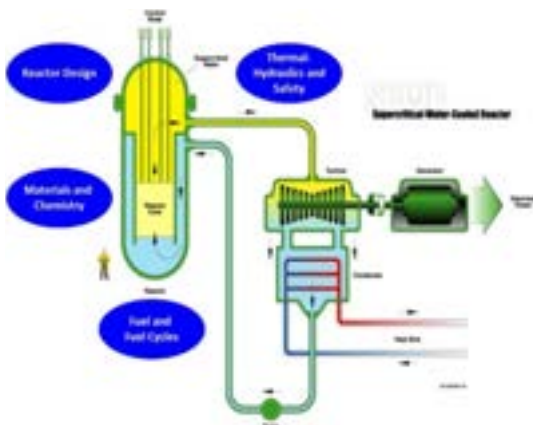
The Super-Critical Water-cooled Reactor (SCWR) is a high-temperature, high-pressure water-cooled reactor that operates above the thermodynamic critical point of water (374°C, 22.1 MPa). Its main mission is to generate electricity efficiently, economically and safely. In addition, the high core outlet temperature of SCWRs (up to 625°C) facilitates co-generation, such as hydrogen production, space heating and steam production.

Development of SCWR concepts has been based on over 50 years of design and operation experience of light-water reactors and super-critical fossil-fuel fired power plants. Existing infrastructures of these industries are applicable in support of the SCWR development. However, due to the high operating temperatures (up to 625°C at the core outlet) and pressures (nominal 25 MPa), new facilities have been established for key technology areas among signatories of the SCWR System

Arrangement [6]. Experiments performed using these facilities have enhanced the understanding of various technology areas and provided data for developing prediction methods, as well as verifying and validating analytical toolsets.

The SCWR System Research Plan identifies key technology areas for designing SCWR (see Figure 4). Establishment of mechanical components and system configurations in the design of the core and plant facilitates meeting GIF technology goals of enhanced economics and safety. Implementation of advanced fuel and fuel cycle would enhance sustainability and proliferation resistance of SCWRs. Material candidates for in-core and out-of-core components, except for the fuel cladding, have been selected from materials established for light-water reactors and supercritical fossil-fired power plants. Identification of cladding material candidates is critical due to high pressure and high temperature operating conditions, which are well beyond the operating range of current fleet of reactors. Similarly, a chemistry strategy is needed to minimise corrosion and activity transport. An accurate prediction of cladding temperature is the key to achieving the enhanced safety technology goal since the traditional critical heat flux criteria is no longer applicable for SCWR where phase change of coolant is not present at supercritical pressures.

Figure 4. Technology Areas supporting SCWR development



The development of SCWR concepts in Canada, EU and Japan are complete and have been reviewed by international peers for their viability. Other concepts being developed in China, Japan (fast spectrum) and the Russian Federation (fast spectrum) are also close to

completion. Furthermore, the development is being expanded to the SCW small modular reactor for deployment in small remote communities.

The GIF SCWR System Research Plan specifies key infrastructures before proceeding to the deployment phase. A prototype fuelled loop for fuel qualification and a prototype-of-a-kind demonstration SCWR are required. Future development on materials (such as corrosion and stress corrosion cracking) and chemistry (such as radiolysis and activity transport) remains focusing on the cladding, which would operate at high pressure and high temperature conditions. An irradiation facility is required to examine the effect of irradiation on material properties and characteristics. The integral safety test facility is needed to demonstrate effectiveness of the safety system, which is a requirement for licensing of the demonstration SCWR plant and deployment. Thermal-hydraulics facilities capable to accommodate full-scale fuel assemblies are also envisioned for obtaining qualification data in support of licensing of the demonstration unit and full-scale SCWR plant. A detailed review is ongoing for establishing future needs to support design and deployment of SCWRs.

VIII. MSR R&D infrastructures

From the 1940s up to now, many liquid fueled MSR concepts have been proposed all over the world using different salt compositions (chlorides, fluorides...) basing on governmental or private support [7, 8]. Proposed neutron spectra range from very thermal to very fast and also include time varying spectra. Almost every known form of fissile / fertile material or fuel cycle is under consideration as a fuel source. Most of the designs remain at the concept study or lab scale development phase. Even for the concepts driven by private companies, proprietary restrictions on design information limits the accuracy of any evaluation using only public data.

8 MWt Molten-Salt Reactor Experiment (MSRE) test reactor at US ORNL went critical in 1965 and operated with great success in a thermal neutron spectrum for 4.5 years until its shutdown in Dec. 1969. The fuel salt for the MSRE was $\text{LiF-BeF}_2\text{-ZrF}_4\text{-UF}_4$ (65-29-5-1 mol.%), moderated by pyrolytic graphite, its secondary coolant was molten 2LiF-BeF_2 salt mixture. The MSRE operated with three different fissile fuels: ^{233}U , ^{235}U , and ^{239}Pu . All metallic parts of the system in contact with the salt were made from the nickel-based Hastelloy-N alloy.

Main mission of the MSR pSSC is to support development of new concepts that have the potential to provide significant safety and economic improvements over existing reactors [7]. Within the MSR pSSC, R&D is performed under an MOU signed by Euratom, France, Russia, Switzerland, the United States and Australia, with Canada, China and Japan as observers.

Canada, China, Japan, and South Korea are focused on the development of the small and medium power liquid fuel units with thermal spectrum graphite moderated cores. In China, the Thorium Molten Salt Reactor (TMSR) Program was initiated by the Chinese Academy of Sciences (CAS) in 2011, which involves a closed U-Th fuel cycle for MSR.

Developments in Russia on the 1.0 GWe molten-salt actinide recycler and transmuter (MOSART) [9] and in France, Euratom and Switzerland on the 1.4 GWe non-moderated thorium molten-salt reactor (MSFR) [10] address the concept of large power units with a fast neutron spectrum in the core. In both designs fuel salt based on fluorides heats up in the core above 700°C before being cooled down in the heat exchangers. Third concept has been under development by TerraPower Inc: the “molten chloride fast spectrum reactor” (MCFR). It represents the first US Government funding for a liquid-fueled MSR in 40 years. The MCFR is intended to have a very hard neutron spectrum to avoid requiring fissile material input after its initial core load or separation of fissile materials from the remainder of the fuel salt.

Fast MSRs have large negative reactivity coefficients, a unique safety characteristic not found in solid-fuel fast reactors. Compared with solid-fuelled reactors, these systems have lower fissile inventories, no radiation damage constraints on attainable fuel burnup, no used nuclear fuel, no requirement to fabricate and handle solid fuel, and a homogeneous isotopic composition of fuel in the reactor.

Although the different MSRs concepts interests are focused on different baseline concepts, large commonalities in basic R&D areas exist and the GIF framework is useful to optimise the R&D efforts and infrastructures. The main MSR R&D challenges as identified in the 2014 Roadmap Update were:

- Compatibility of salts with structural materials for fuel and coolant circuits, as well as for fuel processing components. This challenge is addressed through academic lab-scale studies aiming to

improve the basic knowledge on available high nickel alloys and other advanced materials, as well as through integrated corrosion studies in loops or demonstrator facilities aiming at testing the same materials under realistic conditions and for long exposure times.

- Instrumentation and control of liquid salts. This challenge requires the development of in-situ measurement methods and tools to monitor the redox potential that impacts the corrosion of the structure materials in both the fuel and coolant salts.
- Comprehensive understanding of the Key physical and chemical properties of the salts impacting the behavior of the fuel and coolant salts and, notably, the coupling mechanisms between neutronics, thermal hydraulic and chemistry. This understanding is of paramount importance for the development and qualification of appropriate simulation tools to study normal and accidental MSR behavior.
- Development and demonstration of on-site fuel processing concepts.
- Availability of inactive-salt testing loops. Such facilities are needed to support salt preparation and handling studies, chemical control, accidental leak and freezing management, validation of thermal hydraulics models, process instrumentation, components testing (including heat exchanger, pump, valves etc.), gaseous and volatile fission product and particle behavior and separation. Both forced and natural convection loops have to be considered to better understand heat and mass transfer and material long time exposure to fuel and coolant salts.
- Design, construction and operation of a mock-up demonstrator without induced fission capable of full-scale prototypic reactor components testing.
- Availability of a demonstrator with induced fission for in-pile and on-line chemical potential control, monitoring of the evolution of the salt composition, measurement of corrosion in a neutron field, fission product removal through helium bubbling in a fuel salt environment, as well as testing of maintenance techniques.

When reviewing the major achievements in response to these challenges, it must be noted that in spite of an increase in private initiatives, MSR suffered from a lack of public funding that curtailed the volume of R&D work within the GIF framework and slowed down its pace. Therefore, the aforementioned challenges could be tackled only partly. Progress achieved on the last three challenges described above is summarised in the following.

In CNRS, France the SWATH-W and SWATH-S facilities were designed and commissioned to investigate salt heat transfer and phase change phenomena. Helium bubbling and liquid – gas separation tests have been performed in the Forced Fluoride Flow for Experimental Research (FFFER) facility. The data will be used to improve numerical models used for molten salt design and safety studies [10] An electrically heated and thermally insulated, forced convection FLIBE loop was built and commissioned in the Research Centre Řež [11]. The loop is intended for MSR and FHR material research and components testing. The liquid salt test loop (LSTL) was created at the ORNL [12]. It is a versatile facility in support of the development and demonstration support development and demonstration FHR components. Finally, existing test loops and loops being constructed within the framework of the TMSR programme in SINAP, China are establishing an important experimental complex in support of future R&D on MSR.

The mock-up facility TMSR-SF0 was designed (and is currently under construction in SINAP, China) within the framework of the TMSR programme. It will provide data for the validation of thermal hydraulics and safety analysis codes. The conceptual design of the TMSR-LF1 test reactor (LiF-BeF₂-ThF₄-UF₄ fuel, thermal neutron spectrum) is ongoing [13]. The reactor is scheduled to reach criticality in December 2020 using existing TMSR funds.

As applied to MSFR the irradiation experiment SALIENT-01 (SALt Irradiation Experiment) of small ⁷⁸LiF-²²ThF₄ salt samples in graphite crucibles was planned and is being currently conducted at HFR Petten. In parallel, a concept design was developed for a 125 kW (fissile) molten salt loop driven by neutrons from the HFR Petten as a demonstrator for in-pile performance of an integrated system.

The MSR development needs for the 2018 + 10 years period can be expressed in terms of the following grand challenges:

- Identifying, characterising, and qualifying successful salt and materials combinations for MSRs.
- Developing integrated reactor performance modeling and safety assessment capabilities that capture the appropriate physics and fuel chemistry needed to evaluate the plant performance over all appropriate timescales and to license MSR designs.
- Demonstrating the safety characteristics of the MSR at laboratory and test reactor levels.
- Establishing a salt reactor infrastructure and economy that includes affordable and practical systems for the production, processing, transportation, and storage of radioactive salt constituents for use throughout the lifetime of MSR fleets.
- Licensing and safeguards framework development to guide research, development and demonstration.

IX. Cross-cutting R&D Infrastructures

In support to the development of Generation-IV systems, capabilities include several cross-cutting R&D infrastructures, such as, in France, material testing reactor (CABRI) or irradiation means (JANNUS) and in the future Jules Horowitz Reactor, such as hot laboratories for materials and fuel (LECI, LECA and MOSAIC in the future), such as technological platforms in the fields of thermal hydraulics, hydro-mechanics, materials, corrosion and structural integrity, mechanics with large shaking tables and severe accidents (hydrogen risk, corium studies...). Some generic technologies and know-how can likely be proposed in the decommissioning field of activity with a potential impact on different design choices. Further assessment will be provided within the GIF RDTF report.

X. Forward Looking and Planned Activities

Forward looking and planned activities of GIF RDTF in view of meeting its second objective will be discussed, the latest being to 'Promote the utilisation of the experimental facilities for collaborative R&D activities among the GIF partners'. Collaboration and synergies between GIF Member States and together with other international organisations is needed to promote R&D on Gen-IV systems efficiently and

effectively. It will also help to achieve GIF's four goals namely Sustainability, Economics, Safety & Reliability, and Proliferation Resistance and Physical Protection.

An optimal use of GIF Member States' infrastructures should be vigorously pursued. It is essential to minimise large investment and/or upgrade capital costs, to further improve any cooperation between research facilities, to facilitate trans-national access wherever possible, and to maintain competences in all fields of nuclear sciences. To this end, GIF RDTF will try to identify the main existing legal and financial mechanisms, and organisational approaches, to foster any further collaborative access to relevant GIF MS's R&D facilities identified by the task force. In addition, it should benefit from closer OECD Nuclear Energy Agency (NEA), GIF and the International Atomic Energy Agency (IAEA) international cooperation initiatives. Further coordination support to partnerships between public/private industries, research and academic organisations, taking care of potential challenging intellectual property rights, to stimulate joint funding from Member States and/or enterprises, can only enhance scientific international cooperation.

GIF has collaborations with the IAEA. Annual meetings are organised between GIF and IAEA International Project on Innovative Nuclear Reactors and Fuel Cycles (INPRO), interactions with the Departments of Nuclear Energy, Nuclear Safety and Security, as well as Safeguards and Technical Working Groups within the Department of Nuclear Energy. Evaluation methodologies, specific topical areas, LMFR (SFR and LFR), VHTR, MSR, SCWR, non-electrical applications, education and training, R&D infrastructures, modelling and simulation are significant possible areas for a broadened and strengthened cooperation between GIF and the IAEA. Till now, the main focus has been on information exchange, methodology development, development of safety design criteria, and establishing guidelines e.g. guidance for Proliferation Resistance and Physical Protection (PRPP), SFR Safety Design Criteria / Guidelines (SDC/SDG), licensing framework for advanced reactors, and implementation of SDC/SDG by designers of innovative SFR concepts.

GIF RDTF should benefit from IAEA's key initiative on International Centres based on Research Reactors (ICERR) which is intended to help Member States gain timely access to relevant infrastructure based on Research

Reactor (RR) facilities, to achieve the nuclear R&D and capacity building objectives relevant to their identified national priorities. ICERRs are organisations which make their RRs, ancillary facilities, and resources available to organisations and institutions of IAEA Member States through bilateral arrangements, facilitated by the IAEA. Excellence is gathered today around the French Alternative Energies and Atomic Energy Commission (CEA, Research Centres of Saclay and Cadarache), the Russian Research Institute of Atomic Reactors State Scientific Centre (RIAR), the Belgian Nuclear Research Centre (SCK•CEN), United State Department of Energy (US DOE) Idaho National Laboratory (INL) and Oak Ridge National Laboratory (ORNL).

The Task Force will benefit from (and will provide any) relevant updates of IAEA databases such as: a) Facilities in Support of Liquid Metal-cooled Fast Neutron Systems Facilities and its latest compendium (LMFNS); b) The Advanced Reactor Information System (ARIS); c) The Research Reactor database (RRDB); and IAEA Cyber Learning Platform for Network Education and Training (CLP4NET), an online platform that allows users to find educational resources easily.

OECD Nuclear Energy Agency (NEA) addresses scientific and safety issues for both current and advanced concepts of nuclear energy systems and helps to maintain the necessary R&D infrastructure through international co-operation. A winning strategy for both GIF and NEA organisations is a more systematic involvement of GIF SSCs and PMBs representatives in relevant NEA activities and future programmes together with NEA's participation at GIF PG meetings to present a broader view of its activities relevant to GIF.

OECD/NEA Research and test facilities database (RTFDB), OECD/NEA Task Group on Advanced Experimental Facilities (TAREF) on SFR and GFR but also the Support Facilities for Existing and Advanced Reactors (SFEAR) will benefit the assessment of the task force.

OECD/NEA Nuclear Innovation 2050 Roadmap Initiative (NI2050) has been launched in July 2015. Its objectives are fully complementary to the ones of GIF RDTF and synergies should emerge in due time: a) to map existing nuclear fission R&D programmes and infrastructures; b) to define R&D priorities enabling innovation and to foster the longer term role of nuclear fission in a sustainable low carbon energy future; and c) to evaluate the potential for international cooperation (EU, JP, KR, CA, RU,

US, further NEA participant countries) which could enable the implementation of some of these priorities, in particular when gaps have been identified.

Similarly, one has to assess how the GIF RDTF could benefit from the Department of Energy Office of Nuclear Energy (DOE-NE) latest initiative. It has established the Gateway for Accelerated Innovation in Nuclear (GAIN) to provide the nuclear community with access to the technical, regulatory, and financial support necessary to move innovative nuclear energy technologies toward commercialisation while ensuring the continued safe, reliable, and economic operation of the existing nuclear fleet.

A 2-days' workshop will be organised around March 2019, benefitting from the GAIN experience within the US, and last year's OECD/NEA workshop on market issues which included some identification of private needs for research facilities. In addition, GIF Senior Industry Advisory Panel (SIAP) guidance and engagement could further benefit from R&D cooperation and future deployment of technologies.

OECD/NEA Nuclear Education Skills and Technology's (NEST) Framework launched in May 2017 should help address important gaps in nuclear skills capacity building, knowledge transfer and technical innovation in an international context. It is a multinational approach inherently attractive to young people and of large interest for GIF RDTF.

GIF Member States, OECD/NEA or IAEA, all have a long-standing experience in co-founding collaborative research programmes with the participation of public/private consortia, following competitive call for proposals or on an ad hoc basis. GIF MS provide to support researchers, by integrating activities combined in a closely co-ordinated manner: a) Networking activities, to foster a culture of co-operation between research infrastructures, scientific communities, industries and other stakeholders as appropriate, and to help develop a more efficient and attractive framework; b) Transnational access or virtual access activities, to support scientific communities in their access to identified key research infrastructures; and c) Joint research activities, to improve, in quality and/or quantity, the integrated services provided international level by these infrastructures.

As the refurbishment and/or construction of the next generation of large-scale facilities is increasingly complex and costly, innovative

'financial and legal frameworks and/or mechanisms' are needed and the GIF RDTF will further assess the most promising ones. Recommendations by Member State's ministry representatives, research programme owners and programme managers, research and technical organisations, industrial representatives and relevant international for a included support through: a) loans for research infrastructures; b) tax exemptions e.g. thanks to a dedicated Joint Undertaking legal entity; c) incentives (or grants) dedicated to the construction of research infrastructures; d) attracting private investors, energy providers or research organisations; e) capitalising any access to national public research organisations; f) sharing investments from the hosting country to support infrastructures as a host of any new facility.

Another successful contribution should be from EU/Euratom Education and Training (E&T) initiatives which are increasingly being organised with the support of the EU/Euratom to the European Nuclear Education Network (ENEN), and within the frame of projects co-funded through the Euratom Framework Programmes. ENEN was established in 2003 as a French non-profit association to preserve and further develop expertise in the nuclear fields through Higher Education and Training. ENEN has currently over 60 members, mainly in Europe but also from Japan, Russia, South Africa, Canada, Ukraine including strengthen cooperation with IAEA. This objective is realised through the cooperation between universities, research organisations, regulatory bodies, industry and any other organisations involved in the application of nuclear science, and supporting international mobility of young scientists or researchers, mutual recognition of competences, giving overall a new impetus, high incentives and perspectives for E&T within Europe and Internationally.

XI. Conclusion

Today's Research Infrastructures include major scientific equipment, scientific collections, structured information, ICT-based infrastructures, they are single sited or distributed throughout several countries. GIF Member States are faced with a wide spectrum of issues, from infrastructures, which are globally, unique to many regionally distributed. Many stakeholders are involved, from ministries to researchers and industry, with an underlying and growing use of e-infrastructures. They are opportunities but also

difficulties of interaction between basic research, academic organisations and industry, public and private funding is always lacking, and single countries do not have the critical mass or the dimension to implement large research infrastructures. There is a real need to cooperate on a wide International level.

Substantial Research, Development and Demonstration (RD&D) systems' conceptual/detailed design and analysis are needed. Refurbishment and/or construction of research infrastructures and facilities are increasingly complex and costly.

An opportunity exists, by identifying the latest R&D needs and mapping of infrastructures, to plan for the shared use of existing ones, and to undertake the development of others. Most important are within the areas of fuel cycle, fuels and materials irradiation, reactor safety, dedicated loops, mock-ups and test facilities, advanced simulation and validation tools, transnational access to infrastructures, and education, training and knowledge management of scientists and engineers.

All contributions are the result a common effort of all partners involved and it is very appreciated by the entire scientific community. GIF Member States can only strongly support a coordinated revitalisation of nuclear Research, Development and Demonstration and Innovation (RD&D&I) infrastructures worldwide to a level that would once again move a new generation forward quickly.

Acknowledgements

This research was supported by institutions, companies or individuals involved in GIF research projects and its Task Force on research Infrastructures. We are also thankful to colleagues who provided expertise that greatly assisted the research provided in this paper.

Nomenclature

Within the text of the paper

References

- [1] Generation IV International Forum (GIF) <http://www.gen-4.org/>
International Atomic Energy Agency <http://www.iaea.org/>
OECD Nuclear Energy Agency <http://www.oecd-nea.org/>
- [2] GIF Publications https://www.gen-4.org/gif/jcms/c_9373/publications
GIF Technology Roadmap update, January 2014, <https://www.gen-4.org/gif/upload/docs/application/pdf/2014-03/gif-tru2014.pdf>
GIF R&D Outlook, August 2009, https://www.gen-4.org/gif/upload/docs/application/pdf/2013-10/gif_rd_outlook_for_generation_iv_nuclear_energy_systems_2013-09-30_15-49-32_599.pdf, an update will be published in October 2018.
IAEA Databases www.iaea.org/resources/databases
OECD/NEA NI2050 initiative <https://www.oecd-nea.org/ndd/ni2050/>
- [3] OECD/NEA NEST initiative <https://www.oecd-nea.org/science/nest/>
IAEA International Centres based on Research Reactors (ICERRs) <https://www.iaea.org/about/partnerships/international-centres-based-on-research-reactors-icerrs>
CORDIS, European Community Research and Development Information Service http://cordis.europa.eu/home_en.html
- [3] IAEA database of Facilities in Support of Liquid Metal-cooled Fast Neutron Systems Facilities <https://nucleus.iaea.org/sites/lmfns/Pages/default.aspx>
IAEA Advanced Reactor Information System (ARIS) <https://aris.iaea.org/>
IAEA Research Reactor database (RRDB) <https://nucleus.iaea.org/RRDB/RR/ReactorSearch.aspx>
OECD/NEA Research and test facilities database (RTFDB) <https://www.oecd-nea.org/rtfdb/>

- OECD/NEA Task Group on Advanced Experimental Facilities (TAREF) on SFR <https://www.oecd-nea.org/globalsearch/download.php?doc=77089> and GFR <https://www.oecd-nea.org/globalsearch/download.php?doc=8901>
- OECD/NEA Task Group on Support Facilities for Existing and Advanced Reactors (SFEAR), 2007, <https://www.oecd-nea.org/globalsearch/download.php?doc=6450>
- EU/Euratom project ADRIANA roadmap, 2010, https://cordis.europa.eu/docs/projects/files/249/249687/adriana-final-report_en.pdf
- [4] M.A. Fütterer, C. Auriault, O. Baudrand, G. Brinkmann, D. Hittner, S. Knol, Th. Mull, K. Stehlik, D. Vanvor, K. Verfondern, R&D and Industrial Infrastructures, Deliverable D2.21 of the EU NC2I-R project, 9 September 2015.
- [5] S. Knol, F. Roelofs, M.A. Fütterer, P-M. Plet, D. Hittner, Report on Gap Analysis, Deliverable D2.31 of the EU NC2I-R project, 11 November 2015.
- [6] L.K.H. Leung, Y.-P. Huang, R. Novotny, S. Penttilä, A. Sáez-Maderuelo and M. Krykova, "R&D Experimental Capabilities for Advancing GIF SCWR System in the Next Decade", Proc. 2018 GIF Symposium, Paris, France, Oct. 16-17, 2018.
- [7] Serp, J., et al., The molten salt reactor (MSR) in generation IV: Overview and perspectives, *Progress in Nuclear Energy*, 77, November, (2014) 308-319, <https://www.sciencedirect.com/journal/progress-in-nuclear-energy>
- [8] Dolan, T., "Molten salt reactor and thorium energy", WP, Elsevier (2017)
- [9] Ignatiev, V., et al., Molten salt reactor as necessary element for closure of the nuclear fuel cycle for all actinides, *Atomic energy*, 122 (5), (2018) 250-253
- [10] ALLIBERT, M., et al., "Chapter 7 - Molten Salt Fast Reactors", *Handbook of Generation IV Nuclear Reactors*, Woodhead Publishing Series in Energy (2016)
- [11] UHLÍŘ, J., et al., "Current Status of Experimental Development of MSR and FHR Technologies", *Transactions of the American Nuclear Society*, 117, (2017) 1105
- [12] Yoder Jr., G.L., et al., An experimental test facility to support development of the fluoride-salt-cooled high-temperature reactor, *Annals of Nuclear Energy*, 64, February (2014)
- [13] Kun Chen, DEVELOPMENT AND LICENSING OF A MOLTEN SALT TEST REACTOR, TMSR-LF1, In Proc. of GIF Symposium – Paris (France) – 16-17 October 2018

TRACK 5: SAFETY AND SECURITY

NEW SAFETY MEASURES PROPOSED FOR EUROPEAN SODIUM FAST REACTOR IN HORIZON-2020 ESFR-SMART PROJECT (J. GUIDEZ ET AL)

Joel Guidez⁽¹⁾, Janos Bodi⁽²⁾, Konstantin Mikityuk⁽²⁾, Andrei Rineiski⁽³⁾, Enrico Girardi⁽⁴⁾

(1) CEA, GEN, France

(2) Paul Scherrer Institut (PSI), Switzerland

(3) Karlsruhe Institute of Technology (KIT), Germany

(4) EDF Lab Paris-Saclay, France

Abstract

Following up the previous European projects EFR and CP-ESFR, a new Horizon-2020 project, called ESFR-SMART, was launched in September 2017. This project, starting from the CP-ESFR design, will apply the new safety rules taking into account the lessons learned from the Fukushima accident, in order to increase the safety level of this European Sodium Fast Reactor (ESFR). In order to reach these new safety objectives, propositions are made to simplify as much as possible the design by using all the positive features of the Sodium Fast Reactors (SFR), i.e. low coolant pressure; high level of natural convection; possibility of decay heat removal by atmospheric air; high thermal inertia and long grace time before the human intervention.

These new safety objectives are presented in the paper from viewpoint of severe accidents prevention, defence in depth principles, extreme natural events to take into account, mitigation measures, etc. In all the cases, even in case of severe accident, early or significant radioactivity release requiring evacuation of the population will be avoided.

This paper gives a first list of propositions about ESFR, e.g.:

Improved primary sodium confinement: The new design of the pit will be able to receive and confine the sodium in case of leak from the primary vessel, which allows suppressing the guard vessel. The level of sodium in the primary vessel in this case will remain high enough to assure natural convection through the core. A massive metallic roof above the pit assures the sodium containment even in the case of the worst severe accidents. Other measures are taken to avoid, even in this case of severe accident, primary sodium leaks in the above roof area.

Secondary loops design efficient in natural convection: Even in case of loss of feed water in the steam generators and loss of electricity supply for the secondary pumps, the measures taken on the secondary loops aim at ensuring an efficient decay heat removal by active or passive ways. These measures will include an optimised geometry of the secondary loops to promote the natural convection of the secondary sodium, the use of passive thermal pumps to increase the cooling flow rate, and the use of the steam generators modules to promote the cooling of their external surfaces by the natural convection of atmospheric air.

Core design with improved safety parameters: special geometry and composition will significantly decrease a global void reactivity effect, and contributes to prevention of the severe accidents and mitigation of their consequences. Three types of control rods will be considered, including active and passive measures, i.e. activated by physical parameters, e.g. sodium temperature or flowrate.

Three different systems will allow safe decay heat removal in all situations aimed to achieve the practical elimination of the loss of this function.

In conclusion, the paper gives a first review of the new propositions to enhance the ESFR safety. Some of these safety measures need additional R&D work for validation and some of them will be assessed in more details at the next phases of the ESFR-SMART project. The compliance of this new design with all safety rules has not yet been established at this stage of the project and will be studied later in dedicated tasks.

1. Introduction

A conceptual design of the 1500 MWe European Sodium Fast Reactor was studied in the FP7 CP-ESFR project [1]. It features an integrated reactor concept with six secondary loops. The Horizon-2020 EU ESFR-SMART project aims at proposing a Sodium Fast Reactor, with different safety improvements on the design, trying to take into account the recommendations following the Fukushima accident and the safety objectives envisaged for Generation-IV reactors.

The paper gives a first review of the improvements proposed to enhance this ESFR safety. These safety measures have been integrated into a whole plant design reassembly and will be later calculated and assessed in more details during the next phases of the ESFR-SMART project.

At the end of this project, the additional R&D needed for implementation of the promising safety measures will also be recommended.

2. General Safety Objectives for Generation-IV SFRs

For Generation-IV SFRs, a probabilistic objective of the core-meltdown accident prevention is proposed, with the same value as for Generation-III Pressurised Water Reactors (i.e., a core damage frequency below 10^{-5} per reactor-year for all events including external hazards, with considerations of uncertainties). An additional and prescriptive reduction of the core-meltdown probability is not justified and might be even counterproductive. Indeed, the current probabilistic objectives are already ambitious and at the edge of representativeness. De facto, the probabilistic objective hardening, for already highly unlikely events, could increase complexity of the plant and its operation, and then reduce its everyday-life safety, for a marginal gain in terms of core-meltdown probability.

We remind that, despite this high level of core-meltdown prevention, mitigation provisions for this accident are adopted under the fourth level of defence in depth. In the event of a core-meltdown accident, the objective is to have very low radiological releases, and according to current thresholds, such that no off-site measures have to be implemented. If measures are nevertheless needed (e.g. restrictions on the consumption of crops), these must be limited in time and space, with sufficient time for their

implementation. The even-temporary evacuation of populations should not be necessary and only their sheltering, limited in time and space, would be possible.

On the other hand, the effort for Generation-IV SFRs should focus on the safety demonstration. In particular, for Generation-IV SFRs, for which limited experience feedback is available, the safety demonstration will rely primarily on deterministic methods so as to cover the defence-in-depth levels and to implement the core-meltdown-accident prevention and mitigation provisions. Probabilistic methods, whenever relevant, will provide an additional insight.

The Fukushima accident lessons have led to new guidelines so as to make the plant more robust against natural hazards:

- to ensure that sufficient design margins are available on the equipment necessary to avoid cliff edge effects in terms of off-site radiological consequences, for natural hazards more severe than those considered in the plant reference design domain;
- to favour a significant plant autonomy, regarding the amounts of time necessary for a possible external intervention;
- to promote the provisions enabling the implementation of internal or external means of intervention, on the site in a damaged state.

In general, the intended objectives are similar to those of the Generation-III PWR reactors. For Generation-IV SFRs, these lessons are considered from the design early stages, taking into account the concept specificities, for example by promoting passivity or grace period in operation. These and other measures for reactivity control are described in more detail in the following sections. For Generation-IV reactors the methodology of practical elimination is to be applied since the beginning of the design studies, to identify all severe accident situations possibilities and to make them extremely rare with a high level of confidence through appropriate design and operating provisions.

3. Reminders of the SFR Assets and Sensitive Points

The document produced by IRSN in preparation of the 2014 Permanent Group [3] presents a

review of the assets and of the sensitive points of each type of Generation-IV reactors and in particular of the SFRs.

The SFRs safety demonstration benefits from many positive aspects:

- the capability to remove the reactor core decay heat by natural convection, without intake of external water and with the atmospheric air as the final heat sink;
- the large margin between the sodium temperature during normal operations and its boiling point;
- the favourable character of the concept towards dosimetry and environmental impact, during operation;
- the primary circuit significant thermal inertia, which provides significant grace periods before need of human intervention;
- the absence of pressurisation of the primary circuit and of the secondary circuits;
- the simplicity of core operations and the absence of neutron poisons in normal operations (no xenon effect unlike thermal-spectrum reactors);
- the efficient trapping by sodium of the main fission products (in particular iodine and caesium).

On the other hand, the reactor design will have to take into account the SFRs sensitive points identified in the previous projects, and which deserve special attention, namely:

- At nominal conditions, the core is not in its most reactive configuration.
- The power density is generally high.
- A significant portion of the core may have a positive sodium void effect.

Sodium reacts chemically with many elements, in particular with water, air and concrete, resulting in energy releases that may be significant, as well as in hydrogen production in case of reaction with water. In contact with air, the aerosols coming from a sodium fire will turn into sodium hydroxide and then into sodium carbonate, before being found relatively quickly under the form of sodium bicarbonate, completely harmless.

The liquid sodium opacity and temperature make it difficult to inspect the structures under sodium.

Although some components may be designed with provisions so as to facilitate interventions and replacements, these are still difficult for sodium circuits and components.

Unloading sub-assemblies from the core lasts longer than in a water reactor.

It is proposed for ESFR-SMART to fulfil the achievement of safety objectives:

- on the one hand, by controlling the SFRs sensitive points such as the core neutron reactivity potential, the sodium chemical reactivity, the under sodium inspection;
- on the other hand, by relying upon the SFRs favourable characteristics, the plant natural behaviour and the passivity facilitated by the coolant efficiency, the grace and autonomy periods, etc.

We will detail in the following chapters a list of new safety measures for the ESFR reactor, aimed to improve implementation of the three main safety functions (plus some provisions for sodium chemical reactivity control).

4. Safety Measures to Improve the Control of the Reactivity

Several measures are proposed for further studies in the ESFR-SMART R&D framework, with the goal to ensure that the core reactivity control in ESFR-SMART is even better than in CP-ESFR.

New core concept with reduced sodium void effect

In order to prevent core power excursion in case of loss of flow transients, it is proposed to adopt, at the first stage, a core with a lot of various innovations, including increase of the fuel pin diameter, introduction of a sodium plenum above the fuel assemblies, axial heterogeneity (fertile and fissile parts) of the core, etc., described in ref 7 and allowing a close-to-zero global sodium void effect. This new core concept may provide a more favourable natural behaviour on most of the maximal accidental transient sequences, as for example the ULOF (loss of flowrate without drop of any control rods)

Passive control rod

Passive control rods are proposed as self-actuated reactivity control devices for the core. The absorber insertion into the reactor is thus passively obtained, i.e. without any use of instrumentation and control (I&C), when some criteria on physical parameters are met, e.g. low primary sodium flow rate or high primary sodium temperature.

Ultra-sonic measurements for knowledge of the core geometry

It is suggested to study the potential of ultrasonic means at the core periphery to monitor its global geometry during operations and to verify the absence of significant gaps between subassemblies (thus further preventing the risk of significant core compaction).

5. Safety Measures to Improve the Confinement of Radioactive Materials

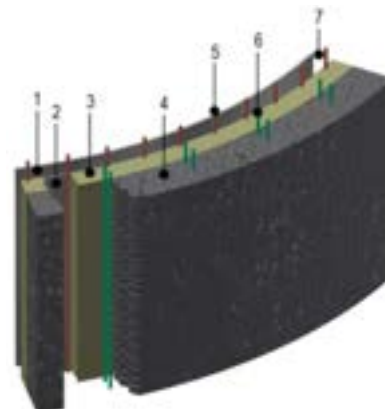
Recovery of the safety vessel functions by the reactor pit

The CP-ESFR safety vessel function was to contain the sodium in the event of the main vessel leakage, while maintaining in it a level of sodium sufficient to allow the sodium inlet into the intermediate heat exchanger (IHX) and keeping a sodium circulation for the core cooling. To recover this function by the reactor pit (hence suppressing the safety vessel), it is necessary to overlay the reactor pit with a metal-sheet liner so as to withstand the reception of a possible sodium leak and to bring it closer to the main vessel so that the volume between vessel and pit shall be lower than the sodium volume leading to uncover the IHX inlet. This option will be studied trying to take benefit from the following anticipated advantages:

- The replacement of the safety vessel by a liner with a DHR system attached, which can favour increased decay heat removal capabilities through the reactor pit.
- The simplification of the safety demonstration with respect to a potential question related to the double leak of the two vessels.
- A fault tolerant structure well adapted to the mitigation functions.
- The main vessel in-service inspection remains possible, as the main vessel still remains accessible from the reactor pit, by the top of the space between vessel and liner).

A special arrangement of the reactor pit is necessary in order to be able to operate in normal conditions, to deal with an accidental sodium leak of the primary vessel and to be able to cope with severe accident mitigation. A steel-concrete structure for the reactor pit is proposed for ESFR-SMART. A sacrificial material is provided between this steel concrete structure and the metal sheet liner. This material has to be chemically compatible with sodium and must protect the mixed structure even in case of leak through the inner sheet liner. For the liner material, an expansion coefficient is recommended as low as possible. Two independent active cooling systems will be installed in the reactor pit. The first system is an oil DHR circuit attached to the liner. Conversely to water, oil is able to support high temperature, but is likely to decompose in case of too high temperatures. The feasibility of implementation of an oil circuit close to the reactor vessel needs to be investigated both in case of normal operation and considering of all plausible accidents. Two possibilities have to be studied: this oil circuit located inside or outside of the liner. The second system is water active cooling circuits installed inside the concrete pit wall. This system is able to maintain the concrete temperature under 70°C in all situations, and even if the oil circuit is lost. Studies will notably be led as regards the thermomechanical constraints on the metal sheet liner in case of a main vessel leak. The sacrificial material could be, for example, an inert-to-sodium concrete, as studied and developed in the EFR project, or another material with good thermal properties as insulating and refractory material.

Figure 1. Detail of the ESFR-SMART reactor pit



1 – Reactor vessel; 2 – Liner; 3 – Insulation with sacrificial material; 4 – Steel concrete structure; 5 – Oil decay heat removal system (DHRS-3.1); 6 – Water concrete cooling system (DHRS-3.2); 7 – Gap

Massive metallic roof

Superphenix experience feedback [4] leads to the recommendation that the roof is hot at its bottom part (so as to minimise the aerosol deposits) and has no water cooling. This last recommendation will be a key point for demonstrating the practical elimination of a huge entry of water into the primary circuit. The EFR massive metallic roof is therefore taken over, which presents many other advantages such as neutron shielding and mechanical resistance. Its thickness will be defined by the industrial manufacturing contingencies, but should be about 80 cm. In the upper part, a heat insulator will eventually be installed so as to limit the heat flux to be evacuated during nominal conditions by air flow in forced convection or even natural convection.

Leak tightness of roof penetrations

It is proposed to study penetrations featuring improved leak tightness during operation with the goal to avoid primary sodium leakage through the roof in case of an energetic core meltdown scenario. Such leakages are very difficult to determine, and can thus lead to very conservative estimations and then to conservative calculations of overpressures in the containment. That makes necessary to implement systems such as dome or polar table which are expensive, quite complex and complicating the reactor operation.

To overcome these difficulties, the following options will be studied:

- For large components, pump and heat exchanger penetrations: they are already firmly bolted for earthquake issues. It is proposed to weld a sealing shell so as to ensure the leak tightness in fast overpressure transient. These components are not intended to be frequently handled, but if this handling is required, a grinding will enable to remove them easily.
- For rotating plugs: independently of the possible inflatable seals, the leak tightness with eutectic seals, which are liquefied during the handling phases so as to enable the rotation [4, 5], is recommended. Conversely, when operating the reactor, these seals are solidified and the design retained should eventually be such that there is no leakage possibility in the case of a severe accident with energy release. The design

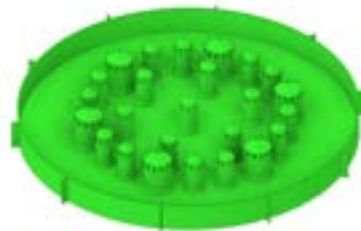
and safety investigations will be necessary to reach this goal.

- Consistently with this strategy, to improve the primary sodium confinement in the main vessel, it is also proposed to consider:
 - an integrated primary cold trap, likewise at Superphenix, so as to avoid any primary sodium circulation outside the vessel;
 - a sufficiently low argon pressure in the cover gas to avoid any sodium-fountain effect of a plunging pipe.

In-vessel core catcher (Figure 2).

The mitigation of a severe accident with core meltdown will be achieved by means of a corium receiver, also called core catcher, located at the bottom of the vessel, under the core support plate Transfer tubes, coming from the core, emerge above the core catcher so as to channel the molten corium. The use, as in the Russian reactor BN 800, of molybdenum, characterised by a high melting temperature, will notably be studied as regards its potential for avoiding melting of the core catcher structure and facilitating the power removal by conduction. The use of hafnium-type poisons will be studied as regards avoidance of any potential re-criticality. The core catcher will be designed for the whole core meltdown.

Figure 2. ESFR-SMART core catcher



6. Safety Measures to Improve Heat Removal from the Core

Hydraulic diodes

The possibility will be studied to equip the primary pump or diagrid connection with hydraulic diodes (anti reverse flow devices) enabling to limit the return flow towards a primary pump in case of spurious stopping and thus to increase the residual flow rate in the core.

Decay heat removal (DHR)

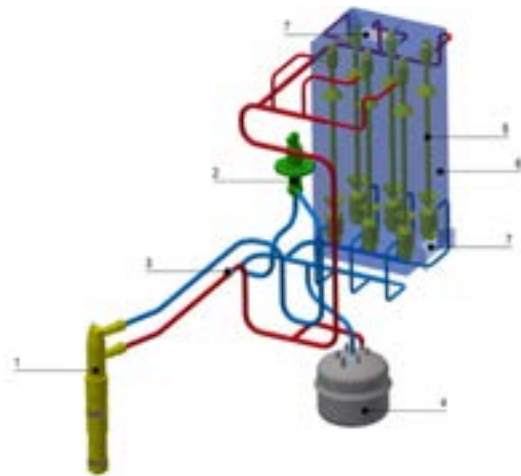
The secondary circuits are the normal power removal circuits. Their use for DHR in case of all primary pumps trip is very useful since that allows creating, in the IHX, a cold column essential for the establishment of a good natural convection in the primary circuit. The secondary circuit design will be optimised so as to enable a good heat removal by air in natural convection, that is to say, in the extreme situation when both the feed water and the electrical power supply have been lost.

For this purpose, several provisions are taken:

- A loop design enabling an easy establishment of natural convection will be adopted.
- The CP-ESFR design for steam generators (SGs), with six modules per loop will be kept. We will take advantage of the large exchange surface, related to the SG modular design, to have opportunities for cooling these modules by air in natural or forced convection (through hatch openings, likewise at Phenix reactor, as shown in ref 5). This will be the heat sink for the secondary loop. We will call this system DHRS-2 (Decay Heat Removal System) (see Figure 5).
- Finally it is foreseen to add one or more thermal pumps in the secondary circuits (see 3 in Figure 3). Thermal pumps are passive electromagnetic pumps using thermoelectricity provided by the difference in temperatures and with no need of external electricity supply (Figure 6). They provide the flow rate also in nominal conditions.

In addition to the secondary DHR loops, there will be two independent cooling circuits in the reactor pit, one with oil system brazed on the liner and one with water inside the concrete (see red and green tubes in Figure 1), capable to maintain the whole pit at temperatures below 70°C. Suppressing the safety vessel will make these devices attached to the liner much more efficient, and should be able to assure a large part of the Decay Heat Removal, maybe 100% or close to 100%. We will call this system DHRS-3.

Figure 3. View of the ESFR-SMART secondary loop (DHRS 2)



1 – Intermediate heat exchanger; 2 – Secondary pump; 3 – Thermal pump; 4 – Sodium storage tank; 5 – Steam generator; 6 – Decay Heat Removal System (DHRS-2); 7 – Openings for air circulation

If the safety analysis (demonstration of practical elimination of loss of DHR function) establishes that these DHR systems are not sufficient, it is proposed to add cooling circuits by sodium/air heat exchangers connected to the IHXs piping. These circuits, which we will call DHRS-1 or primary DHRS (see Figure 4), have several advantages compared to independent systems located in the primary circuit (formerly used in the CP-ESFR design):

- No additional roof penetrations are required (gain on the main vessel diameter).
- The cold column is maintained in the IHX, which is the guarantee of a good natural convection in the primary circuit through the core.
- This circuit can use the already existing purification circuit of the corresponding secondary loop and minimises the number of sodium circuits to be managed by the operator.
- It is still available even when the secondary loop is drained.

The DHRS-1 circuit ability to operate in natural convection will be assessed together with the possible addition of a thermal pump (Figure 4) to further increase its capabilities and help for the starting of the operation.

General view of ESFR-SMART primary and secondary DHRS systems is shown in Figure 5.

Figure 4. General view of ESFR-SMART secondary systems with DHRS-1

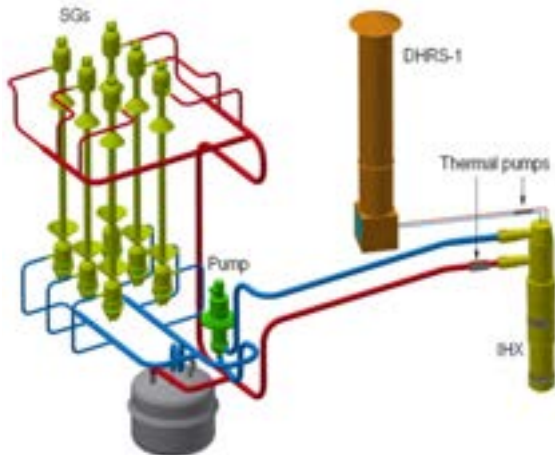
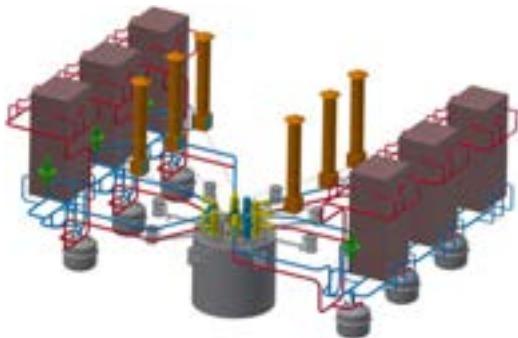


Figure 5. General view of ESFR-SMART primary and secondary DHRS systems



7. Safety Measures to Improve Control of Sodium Fires

As the provisions to prevent any leakage of primary sodium have already been outlined in Section 5, this chapter will only focus on the risks related to a secondary sodium leakage. In this sense, it should be noted that releases are mainly a chemical risk considering that no or very little radioactivity is present in the secondary sodium circuit. Possible impacts of sodium fires on other safety systems should also be addressed.

Figure 6. Thermal pump concept with permanent magnets shown in red and electrodes in grey

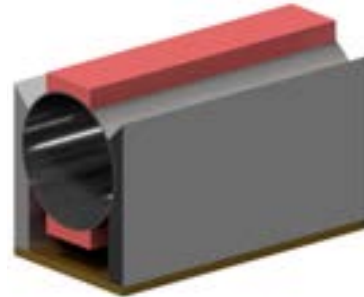


Figure 7. View of the double-wall piping with insulation/detection



Double wall for piping with quick sodium fire detection

All secondary sodium circulation loops are protected against leakage by a double wall piping (Figure 7). The piping itself is covered with an insulation including quick sodium fire detectors. Complementary sodium smoke detectors can be added between the two walls. This set of provisions will be studied with regard to its potential for justifying the secondary sodium fire control and its integration in a coherent set of design options aiming at simplifying the general arrangement of the plant organisation against secondary sodium fires.

8. Sodium/Water Reaction Control

Rather conventional devices enable to efficiently control this risk. Modular SGs are retained for studies, considering the possibility to quickly detect sodium water reaction, followed by the depressurisation/isolation and draining of the faulty module. The choice of modular SG allows also minimising the theoretical envelope accidents. In case of water/sodium reaction, the consequences on the plant operations are limited and the

operation can continue with remaining modules. Mitigation means against risk of sodium-water-air reaction will have also to be studied.

9. Severe Accident Mitigation

A more robust design than CP-ESFR is proposed for severe accident mitigation studies:

- A core catcher is provided at the bottom of the vessel, designed for the whole core meltdown (see a starting design to be further developed in Figure 2).
- The new core with a close to zero global sodium void effect allows a better mechanical behaviour in case of severe accident with reduced energy release.
- Mitigation devices inside the core (corium discharge tubes) will channel the molten fuel to the core catcher.
- The re-criticality of this core should be made impossible by disposition of dedicated material such as hafnium inside the core catcher.
- The reactor pit () should accept sodium leakage and, with its upper thick metal roof, should form a solid, tight and that-can-be-cooled containment system.
- This corium long-term cooling will be managed by the diversified cooling measures provided in the SG and in the pit (DHRS-2 and DHRS-3).
- The use of DHRS-1 circuits may be done as a supplement so as to continue the reactor block cooling even with the three secondary circuits being drained.

10. In-service Inspection

Although not yet addressed by the ESFR-SMART project, recent advances on in-sodium ultrasonic sensors and on robotics will be expected to enable inspections during periodic outages. Partial sodium draining (such as realised at Phenix) should enable visual inspections of the upper part, if required.

11. Dosimetry and Releases

It is known that, during normal operations, the SFR radiological releases are almost zero for gas. The only liquid radioactive release is the liquid used to wash fuel subassemblies or for washing

and decontamination of components [4, 5]. In terms of the personnel dosimetry, this reactor design leads to a dosimetry much lower than on the water reactors [6]. This benefit will be kept for ESFR-SMART.

12. Simplicity and Human Factor

Starting from the CP-ESFR design [2], our approach has consisted in proposing the simplest possible reactor, while keeping the necessary lines-of-defence. It is expected that this simplicity should contribute to the whole reactor safety, by making it easier to operate. Compared to CP-ESFR, the following simplifications will be studied in that frame:

- dome (or polar table) suppression;
- safety-vessel functions taken over by the reactor pit;
- primary sodium containment improvement;
- natural convection cooling enhancement in the secondary side;
- optimised and simplified DHR dedicated circuits.

Passive and redundant systems which are independent of instrumentation and control or of the operators' action will enable the reactor reactivity control and its cooling by natural convection, even in the most severe cases of simultaneous loss of cooling water and electrical power supply. With all those improvements, the new design is then more forgiving; both with respect to the reactivity control, as well as at the intervention time required from the operator (enhanced grace period).

Conclusion

The paper gave the first ideas about possible new safety measures proposed for European Sodium Fast Reactor studies in the frame of the Horizon-2020 EU ESFR-SMART project. The global view of the ESFR SMART primary system is shown in Figure 8.

The general principle of the studies was to increase the safety in operation, by increasing the simplicity of the design, avoiding adding new systems. For this purpose we tried to use at maximal level the possibilities given by the liquid metal coolant in terms of passivity, simplifications, operation and mitigation of the severe accident consequences:

In terms of passivity:

- A low sodium void reactivity effect, to reduce drastically any energy release, even in case of accidental sodium boiling. That was obtained by a lot of various innovations, including increase of the fuel pin diameter, introduction of a sodium plenum above the fuel assemblies, axial heterogeneity (fertile and fissile parts) of the core, etc.
- Passive control rods able to control the reactivity without human intervention or active protection measures, but only passively at the abnormal variation of such physical parameters as coolant temperature or flow rate.
- Better design to enhance natural convection of sodium in the secondary loop, even without feed water supply and without electrical supply.
- Possibility of decay heat removal without feed water supply, but only by natural convection of atmospheric air through the casing containing the six modules of the steam generators (DHRS-2).
- A passive decay heat removal system (DHRS-1) on each loop connected to the intermediate heat exchanger and able to remove decay heat by passive way with atmospheric air, even if the secondary loop is drained.
- Thermal pumps, totally passive, able to maintain permanent flow rates in the secondary loops and in the DHRS-1, even without any electrical supply.

In terms of simplifications:

- Suppression of the safety vessel.
- Suppression of dome or polar table.
- Suppression of separated DHRS inside the primary vessel.
- Minimisation of the number of sodium circuits.
- Very simple and massive reactor roof.

In terms of operation:

- New measures against sodium leaks and better protection of the building with strong separation of water and sodium circulation areas.

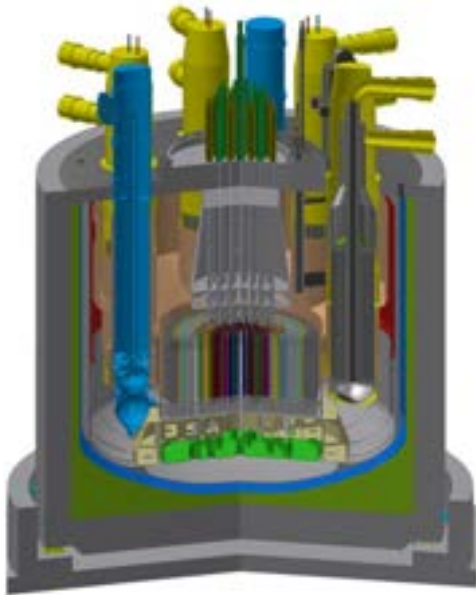
- Better concept to avoid any primary sodium leakage.
- Better access for handling operations (no polar table).
- Quick water sodium reaction detection and good protection against consequences based on choice of modular steam generators.
- Use of hydraulic diode to reduce in case of one pump failure the reverse flow through this pump and therefore reduce the core bypass.
- Mechanical measures at the level of the strongback to avoid any subsidence of the core support.
- Several design measures to avoid gas entrainment in the core.
- The reactor is very forgiving with a high inertial capacity and can stay stable a long time without operator actions.

In terms of mitigation of the severe accident consequences:

- Use of discharge tubes inside the core to drive the corium to the core catcher in mitigation situation.
- Low energy release with a new core conception with a close to zero global sodium void effect and big margins with the massive solid roof and the pit able to receive sodium leaks.
- Ability to cool the primary vessel during long mitigation situations with two cooling circuits inside the pit and one dedicated in case of loss of the first one (DHRS-3).
- A dedicated core catcher able to receive a significant part of the fissile core, with materials against ablation, with efficient natural convection cooling and without any recriticality possibilities.

The proposed set of the modifications compared to the CP-ESFR design aims at consistency with the main lines of safety evolutions for Generation-IV SFRs since the Fukushima accident, but needs, as indicated in introduction, to be calculated and validated by other tasks during this four-year project

Figure 8. Global view of the ESFR SMART primary system



Acknowledgement

The work has been prepared within EU Project ESFR-SMART which has received funding from the EURATOM Research and Training Programme 2014-2018 under the Grant Agreement No. 754501.

References

- [1] G.L. Fiorini, A. Vasile, "European Commission – 7th Framework Programme The Collaborative Project on European Sodium Fast Reactor (CP-ESFR)", Nuclear Engineering and Design 241 (2011) 3461–3469.
- [2] K. Mikityuk, E. Girardi, J. Krepel, E. Bubelis, E. Fridman, A. Rineiski, N. Girault, F. Payot, L. Buligins, G. Gerbeth, N. Chauvin, C. Latge, J.-C. Garnier. "ESFR-SMART: new Horizon-2020 project on SFR safety", IAEA-CN245-450, Proceedings of International Conference on Fast Reactors and Related Fuel Cycles: Next Generation Nuclear Systems for Sustainable, Development FR17, 26-29 June 2017, Yekaterinburg, Russia.
- [3] IRSN Report N° 2014 "Overview of Generation-IV Nuclear Systems (GEN IV)"
- [4] J. Guidez and G. Prêle "Superphenix. Technical and scientific achievements", Edition Springer, 2017, ISBN 978-94-6239-245-8.
- [5] J. Guidez "Phenix experience feedback", Edition EDP Sciences, 2014, EAN13: 9791092041057.
- [6] J. Guidez and A. Saturnin, "Evolution of the collective radiation dose of nuclear reactors from the 2nd through to the 3rd generation and Generation-IV sodium-cooled fast reactors", IAEA-CN245-016, Proceedings of International Conference on Fast Reactors and Related Fuel Cycles: Next Generation Nuclear Systems for Sustainable, Development FR17, 26-29 June 2017, Yekaterinburg, Russia.
- [7] A.Rineiski, C. Meriot, M. Marchetti, and J. Krepel, Core Safety Measures in ESFR-SMART, Proc. of PHYSOR 2018, Cancun, Mexico, April 22-26, 2018

APPLICATION OF PRACTICAL ELIMINATION APPROACH FOR GEN IV REACTORS DESIGN (J. GUIDEZ ET AL)

Joel Guidez, Laurent Costes, Paul Gauthé, Pierre LoPinto⁽¹⁾
Stephane Beils, Bernard Carluéc, Etienne Courtin⁽²⁾
Lionel Bourgue⁽³⁾

- (1) CEA
- (2) Framatome
- (3) EDF

Abstract

An essential objective of the design of all new reactors GEN III as GEN IV is to limit, the radiological consequences on the environment and populations in the event of a severe accident. For Gen IV reactors, in the event of a severe accident, evacuation of populations should not be necessary and only sheltering limited in time and space would be conceivable.

The fundamental safety principle applied to the design of GEN IV reactors is the defense in depth. The application of this principle leads to provisions to ensure the prevention of severe accidents in a highly reliable manner. This is the object of the first three levels of defense in depth.

Despite these provisions, the fourth level requires to postulate severe accidents and the provision of sufficiently reliable means to mitigate their consequences. The reactor design aims to put in place mitigation provisions with regard to all possible situations of severe accident.

Nevertheless, there may still be situations of severe accidents which cannot be reasonably covered by these provisions and which could lead to early large radiological releases, which would make impossible to organise measures for the protection of the population, or to massive radiological releases leading to displacement of populations over a significant period of time or in an extended area. These are situations that need to be identified soon in order to make them extremely unlikely by appropriate design during the reactor design studies.

Practical elimination is an approach which, in first, identifies these severe accident situations that cannot be mitigated under reasonable conditions. Then, appropriate design and operating provisions have to make them extremely unlikely with a high level of confidence. This methodology should be applied preferably for reactors in conceptual phase.

This paper issued from the GCFS (the French group EDF/CEA/FRAMATOME on safety of generation IV reactors) proposes an approach to apply, to establish a list of situations to be practically eliminated. This list should be confirmed by the safety authority, at the first stage of the design activities. Then guidelines are given to ensure demonstrations for all these situations. These demonstrations are mainly based on deterministic approach, by seeking, as a priority, to make these situations physically impossible.

Then an example of application of this methodology, used for the sodium fast reactor project ASTRID during its conceptual phase, is given. A list of eight situations practically eliminated is explained, with some examples of design improvements associated.

In conclusion it appears that, in addition to taking into account the severe accident under the fourth level of defense-in-depth, the implementation of a practical elimination approach, from the early stages of design studies of generation IV reactors is an important element to improve their safety.

Definition of Practical Elimination

An essential objective of the new reactor design is to limit, in the event of a severe accident, the radiological consequences on the environment and on the population. For Gen IV reactors, in the event of a severe accident, there should be no need for population evacuation and sheltering shall be limited in time and space.

The safety fundamental principle applied to reactor design is the Defense-in-Depth. The application of this principle leads to provide provisions enabling to prevent, in an extremely reliable way, the severe accident; it is the object of the defense-in-depth first three levels. Despite these provisions, the fourth level requires to take into account severe accidents, even unlikely, and to provide for sufficiently reliable mitigation means so as to manage them.

The design aims at setting up mitigation provisions towards all the possible situations of severe accident. Nevertheless, there may still exist some severe-accident situations that cannot be reasonably covered by these provisions and which may lead to either early radiological release with insufficient duration to organise the population protection measures, or massive ones, requiring the displacement of population over a significant period of time or in an extended area. These are the situations that require to be identified so as to make them extremely unlikely thanks to appropriate design and organisational provisions.

As such situations being an exception to the complete implementation of the defense-in-depth principle, there should be only in a limited number.

The practical elimination approach requires identifying, from the beginning of the reactor design studies, the situations that would not be reasonably possible to manage, in order to make them extremely unlikely with a high level of confidence through appropriate design and operating provisions.

This methodology is explained in the chapter 5 of the WENRA report in reference 1 and more recently, IRSN has given his position in a report in 2017 in reference 2. These two references are more dedicated to GEN III reactors.

Identification of the Situations to be Practically Eliminated

The question is to identify, at the very beginning of the project, the situations

resulting from phenomena, involving the concept characteristic risks, which could not be reasonably controlled, and to provide, as soon as possible from design studies, the provisions that will make these situations extremely unlikely with a high level of confidence.

In order to list the situations to be practically eliminated at an early stage of the design, the phenomena leading to significant radiological releases are first identified ("top down" type approach). Such an approach leads to look for all the hazardous phenomena, without getting limited to the only direct effects that could result from material failure. A limited number of situations to be practically eliminated must result from this identification phase. It is reminded that this phase aims to identify the situations to eliminate practically and not the sequences leading to them, since a situation is generally likely to be caused by several sequences.

In order to carry out the identification of the situations to eliminate practically, three types of severe-accident situations can be distinguished:

- Type 1: the severe accidents leading to a violent energetic phenomenon likely to damage the containment in an irreversible manner (e.g. a serious accident leading to a hydrogen explosion);
- Type 2: the situations leading successively to an unacceptable deterioration of the mitigation means and then to the severe accident (e.g. for some reactors, the extended loss of the decay heat removal function);
- Type 3: the severe accidents occurring whereas the mitigation means are not available or sufficiently efficient (e.g. during some handling operations).

As a reminder, severe accident situations, whose consequences can be managed under acceptable technical and economic conditions, must be dealt with.

However, the following situations are not covered by the practical elimination demonstration:

- The situations corresponding to a severe accident combined with a failure of the severe-accident mitigation measures, independently from the accident consequences or from the events that may have caused it: indeed, the

application of the defense-in-depth principle up to the fourth level is sufficient;

- The situations physically impossible or deemed as not plausible by expert consensus. For example, fall of a big meteor on brutal collapse of the containment.

Finally, the situations with a non-radiological environmental impact such as the releases of toxic chemical substances, are studied with specific methods, and are not a matter for the practical elimination demonstration.

Demonstration of Practical Elimination

Practical elimination demonstrations concern a limited number of situations, defined by the approach presented in the previous chapter. Each of these demonstrations is indeed a particular case, but it is possible to give some general indications. These demonstrations will explicitly be made in the plant safety report.

This demonstration challenge is to get sure of the extremely unlikely nature of the dreaded situation with a high level of confidence. The design first examines the possibility to make this situation physically impossible under reasonable conditions.

When the physical impossibility is not achieved, the demonstration relies on the following deterministic approach:

- First, the identification of the plausible sequences that may lead to the dreaded situation,
- Then the definition of an adequate set of independent and sufficiently reliable provisions for the prevention of the situation to be practically eliminated, covering all the plausible sequences identified and considering the uncertainties.

The provision adequacy can be evaluated as follows:

- A good practice, used in France for SFRs, is to implement the equivalent of three independent lines of defence. These lines-of-defence can correspond to a safety system, a structure, an operating provision or a favorable natural behavior. A low occurrence probability event can also be valued as a line-of-defence.

- Arguments related to the quality level of the equipment ensuring the function, to their technical specifications, to the monitoring, to the accident progressiveness, to the tolerance towards some faults, ... can also be used.

Whenever relevant, probabilistic insights may help to strengthen the sufficiently unlikely nature of sequences leading to the dreaded situation. There is no defined frequency criterion which could be used for the demonstration.

Finally, it will have to be taken care, so as to practically eliminate a situation, not to select provisions which could lead to new sequences that could significantly impact the safety. For example if you suppress any water in the containment building to provide a strong demonstration of practical elimination of big sodium/water reaction in this building, you will need to increase the number of handling during operation of the plant to clean the components in the washing pits out of the building. It is perhaps better to maintain the necessary washing pits inside the building, but with limited water quantities available.

Example of Application During the Design of French SFR Project ASTRID

During the conception and design work on the French SFR project ASTRID, eight cases of practical elimination were identified in accordance with safety authority:

Situations likely to lead to a core-disruptive accident with unmitigable mechanical energy releases	Important gas passage through the core
	Significant core compaction
	Collapse of the core support structures
Situations likely to lead to a containment failure and to fission product release	Massive water ingress into the primary circuit
	Generalized Hydrogen deflagration in the containment
	Loss of the decay heat removal function
Significant core damage situations when the containment provisions may not be efficient	Core loading errors leading to fuel melting
	Fuel-sub-assembly meltdown in the spent fuel storage

Without entering into the details, it appears, from the ASTRID experience that a number of design choices make it possible to prepare these practical elimination demonstrations.

As an example, it can be mentioned the case of important gas passage through the core, with the following provisions in the reactor design:

- Design of the hot-pool hydraulics with no significant vortex formation at the free surface.
- No gas retention zone possible in the primary circuit structures (inner vessel, strong back, etc.).
- No gas retention zone formation in the diagrid even with the pumps at low speed.
- No gas seal devices for the intermediate heat exchangers.

All these provisions contribute to make extremely unlikely an important gas passage through the core.

Conclusion

In addition to consideration of the severe accident under the defense-in-depth fourth

level, the implementation of a practical elimination approach, and this since the design study early stages, represents an essential element as part of the safety improvement for - generation IV reactors. This approach comes as a complement to the usual approach, which consists in defining a list of operating conditions and hazards, the consequences of which have to be limited.

It makes it possible to highlight the situations, whose prevention must be the subject of priority attention.

The practical elimination approach aims for this purpose to identify the severe accident situations which cannot reasonably be dealt with.

It strongly drives the design.

For situations to practically eliminate, the issue is indeed to ensure that, by design, they are physically impossible or extremely unlikely with a high level of confidence.

It contributes to the safety objectives achievement.

The practical elimination approach enables to strengthen the general safety objective, namely to avoid any severe accident leading to early or large important radiological releases.

References

[1] WENRA Report "Safety of new NPP design", Study by Reactor Harmonization Working Group RHWG, March 2013.

[2] "The "practical elimination" approach of accident situations for water-cooled nuclear power reactors" [Rapport PSN-SRDS n°2017-00004].

GIF RISK AND SAFETY WORKING GROUP: APPLICATION OF THE ISAM METHODOLOGY TO GEN-IV NUCLEAR SYSTEMS (Y. OKANO ET AL)

Yasushi Okano⁽¹⁾, Luca Ammirabile⁽²⁾, Tanju Sofu⁽³⁾

(1) Japan Atomic Energy Agency, Japan

(2) Joint Research Centre, European Commission

(3) Argonne National Laboratory, U.S.A.

Abstract

GIF promotes a consistent approach on safety, risk, and regulatory issues of Gen-IV reactor systems. Following the first report “Basis for the Safety Approach for Design & Assessment of Generation IV Nuclear Systems” in 2008, the Risk and Safety Working Group issued the “Integrated Safety Assessment Methodology (ISAM)” in 2011. ISAM is useful for safety assessments and serves as a “design driver”. The safety architecture of newly designed nuclear systems can be improved by repeatedly using ISAM in the entire design process from a pre-conceptual stage to licensing stage. The ISAM is solely intended to provide a useful methodology that contributes to the attainment of Gen-IV safety objectives, yields insights into the nature of safety and risk of the systems, and provides meaningful safety evaluations. In recent years, the ISAM has been applied in the design process of six Gen-IV reactor systems, and the results of the pilot application are being summarised in the RSWG’s White Papers as self-assessments reported by six system steering committees to provide guidance on improving safety features and upgrading safety related system design.

The ISAM includes five analytical tools: QSR (Qualitative Safety features Review), PIRT (Phenomena Identification and Ranking Table), OPT (Objective Provision Tree), DPA (Deterministic and Phenomenological Analyses), and PSA (Probabilistic Safety Assessment). It is intended that each tool be used to answer specific safety-related questions with different levels of detail during various design stages and the ISAM as a whole offers flexibility and a graded approach to analyse technical issues of complex system architectures. The five individual tools are well integrated, as evidenced by the fact that the output of each analysis tool supports preparation of input for other tools. Although each tool can be selected for individual and exclusive use, the full value of the integrated methodology is derived from using all tools, in an iterative fashion and in combination with the others, throughout the design process.

The paper describes what is ISAM (e.g. how to use it in the system design, when to apply it in the design process, and how the inputs and outputs be combined) and pilot examples of individual use of QSR, PIRT and OPT and also combination application of DPA-PSA.

I. Introduction

The Risk and Safety Working Group (RSWG) of the Generation IV (Gen-IV) International Forum (GIF) primarily focuses on the development and introduction of a harmonised common methodology for the evaluation and assessment of the safety of Gen-IV nuclear systems. In 2008, the RSWG issued its first report “Basis for the Safety Approach for Design

& Assessment of Generation IV Nuclear Systems”[1] presenting fundamental standpoints to achieve the safety goal of Gen-IV systems. Following this report, the second document “Integrated Safety Assessment Methodology (ISAM)”[2] was issued in 2011 to provide a common methodology for qualitative and quantitative assessment on the safety of the Gen-IV nuclear systems throughout their design processes. Since then, the ISAM has

been fully or partially used in Gen-IV design processes.

Early generations of nuclear reactors were designed, built, and operated before current system safety analysis tools were applied to identify and evaluate safety vulnerabilities. Safety vulnerabilities newly discovered through operating experiences, safety analyses, or new knowledge have been considered to be “added on” in the next phase updates of the nuclear systems or “backfitted” to existing nuclear systems to reduce vulnerabilities as necessary. On the other hand, Gen-IV nuclear systems have new design that allows the designers to modify or upgrade the nuclear system’s safety-related architecture throughout the design process based on safety assessments. The GIF RSWG has developed the ISAM to support the achievement of safety concepts in which the safety has to be “built in”, rather than “added on” the existing safety systems.

II. Overview of ISAM

The ISAM is a kind of toolkit to find/think/answer safety-related questions. The value of the toolkit is that the inputs of the several tools are shared and the outputs from them are used in others, and their mutual connections are iterated to improve the design through the whole process. The results are expected not only to improve safety design but also to reduce time spent on the development of the reactor systems by optimising equipment in its redundancy and diversity while achieving a target safety level. For this purpose, the ISAM tools will be used in three principal ways:

- The ISAM is intended to be used throughout a development stage. The use of ISAM will provide more detailed understandings of under-designed safety related vulnerabilities and of resulting contributions to risk. Thus new concept or new design improvements can be identified, developed, and implemented relatively early.
- Selected tools from the ISAM are applied at various phases in the design process. Each tool will provide understanding of risk contributors, safety margins, effectiveness of safety-related design measures, and sources and impact of uncertainties. These pieces of information will be used for decision making on design choices.

- The ISAM examines design maturity by measuring risks against safety objectives or by licensing criteria, including various potentially safety-related metrics or figures of merit, at a late design stage.

It is not intended that the application of the ISAM constrains designers to narrow down the selection of safety related tools. The ISAM cannot provide safety design criteria which should be developed by designers/regulators outside safety assessments. The sole intent of the ISAM is to provide a useful methodology that contributes to attain safety objectives, that yields useful insights into the architecture of safety systems, and that provides meaningful evaluations of the reactor concepts.

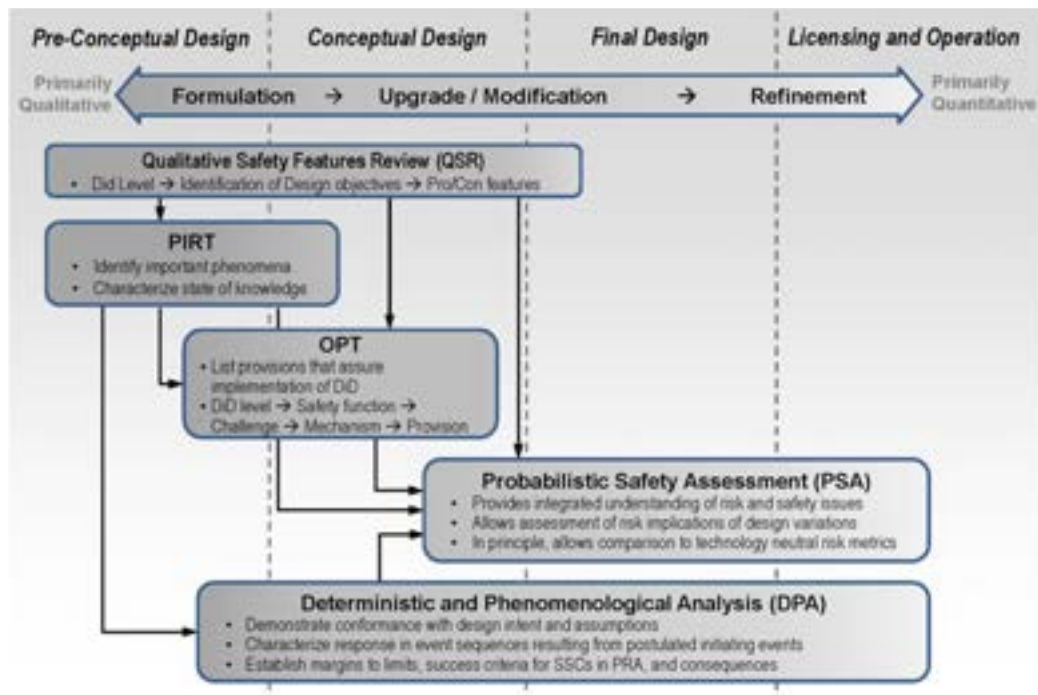
The ISAM consists of five distinct elemental tools that can be tailored to answer specific types of questions at various design stages and is essentially converged on a probabilistic safety assessment (PSA) based safety assessment. Each of the five analytical tools, three qualitative and two quantitative, is used to answer specific kinds of safety-related questions in different degrees of detail and at different stages of design maturity. At the same time, the diversity of the respective five tools and the integrated use of them with feedback obtained among them will ensure that the assessment results are complete and robust. The ISAM as a whole offers flexibility to allow a graded approach according to the design’s technical complexity and importance.

The methodology is well integrated to facilitate the input of results from one tool into the other tools. To take full advantage of the integrated methodology, the tools need to be used in combination with the others repeatedly. The ISAM report provides general instructions on why to use (e.g. objective, benefit), when and which to use (e.g. selection and timing of tool to be used during a design process), how to use (e.g. preparation, analysis), and what to make of (e.g. documentation).

III. Five Tools of Isam

Figure 1 shows an overall task flow of the ISAM and indicates which tools are intended to be used in a design stage of Gen-IV system development. The tools of ISAM are briefly described below.

Figure 1. Task Flow of GIF Integrated Safety Assessment Methodology (ISAM) in Design Process



III.1 Qualitative Safety Features Review (QSR)

The Qualitative Safety features Review (QSR) is a comparatively new tool, which provides a systematic means of ensuring and documenting desirable or undesirable safety-related attributes and characteristics. The QSR is a qualitative, not quantitative, tool used in pre-conceptual to conceptual design stages. The QSR also provides a useful means of identifying really important features (e.g. explicit/implicit advantage, double bind) from the multidisciplinary viewpoints and of sharing designers' approaches to extend the features, to avoid potential risks and to balance a trade-off. The assessment will be performed by engineers and designers in multidisciplinary fields through discussions on interested concepts and/or targeted structures, systems and components (SSCs). The QSR is a kind of "checklist" for technical features expected to be obtained and for general issues that can be involved. The use of a structured template of the checklist that facilitates the assessment process will help concept developers and designers consider and share their perspectives on respective concepts and SSCs, like how the attributes of defence in depth (DiD), high reliability, minimisation of sensitivity to

human error, and other important safety characteristics can be incorporated well. The QSR also serves as a useful preparatory step for the other ISAM tools by facilitating a multidisciplinary and comprehensive understanding of safety issues or vulnerabilities, which will be analysed in depth in latter steps by using other tools.

III.2 Phenomena Identification and Ranking Table (PIRT)

The Phenomena Identification and Ranking Table (PIRT) is a technique that has been widely used in both nuclear and non-nuclear applications[3]. The PIRT is a *qualitative*, not *quantitative*, technique, which is used in a pre-conceptual stage. It is used to identify a spectrum of safety-related phenomena or scenarios and to rank the phenomena or scenarios in order of their importance (e.g. potential consequences) and the state of knowledge related to associated phenomena (i.e., causes and magnitudes of phenomenological uncertainties).

The PIRT is performed by participants of engineers and designers in multidisciplinary fields. It relies heavily on elicitation of knowledge and background information from participants. The PIRT partially uses outputs

from the QSR in relation to safety features, potential risks, and trade-off had been identified. These QSR outputs are broken down into elemental or multiple phenomena, and the list of such phenomena is used as inputs for PIRT. The results from the PIRT can be used to

- prioritise confirmatory research activities to address safety-significant issues;
- inform decisions on the development of analytical tools for safety analysis;
- assist in defining test data needs for validation and verification of analytical tools; and
- provide insights for the review of safety analysis and supporting databases.

The PIRT can be focused on very general issues or on specific detailed design issues, depending on the need.

The PIRT provides a disciplined way of identifying technical issues that the developers will face in more accurate analyses in later design stages. As such, the PIRT forms inputs to both the Objective Provision Tree (OPT) analyses and the PSA. The issues identified in the PIRT and resolved in related research will be incorporated in the modelling used in the Deterministic and Phenomenological Analysis (DPA). In this context, the PIRT is particularly helpful in defining accident sequences and safety system success criteria. The PIRT is also essential to identify items to which additional research needs to reduce uncertainties.

III.3 Objective Provision Tree (OPT)

The Objective Provision Tree (OPT) is a relatively new analytical tool, now increasingly used. The OPT, promoted by the International Atomic Energy Agency (IAEA)[4], is a *qualitative*, not *quantitative*, tool which is used in pre-conceptual to conceptual design stages. The OPT is used to ensure and document provisions by using essential combination of multidisciplinary mechanisms so that phenomena that could potentially damage a nuclear system can be successfully prevented, controlled or mitigated.

There is a natural interface between the OPT and the PIRT; the PIRT identifies phenomena and issues that could potentially challenge the safety function, while the OPT focuses on mechanisms that could arise the challenge and on design provisions to prevent, control, or mitigate the consequences of these phenomena.

The OPT is an entirely qualitative tool to formulate a “tree diagram” that contains mechanisms and corresponding provisions in relation to the foreseen challenge on specific safety functions. As such, the purpose of OPT in the ISAM is to inform designers the challenges (e.g. against maintaining core cooling) in a structural manner and to identify effective design provisions for prevention and mitigation of phenomena that pose challenges to the reactor safety. The OPT output will eventually be referred to the PSA (e.g. formulation of fault trees and event trees including identification of possible accident initiators).

III.4 Deterministic and Phenomenological Analyses (DPA)

Traditional deterministic and phenomenological analyses collectively constitute an indispensable part of ISAM, including thermal-hydraulic analyses, computational fluid dynamics (CFD) analyses, reactor physics analyses, accident transient numerical simulation, materials behaviour models, and structural analysis models. These analyses will be used as needed to understand a wide range of safety issues, and its output will form inputs to the PSA. By using a statistical approach related to the DPA, a number of outputs (e.g. peak temperatures during accident transients) form distribution of quantitative values, and the probability of the outputs go beyond or below a target value is obtained from the distribution. The results are used in the PSA as success/failure probability branch, for example. It is anticipated that DPA are performed from a late pre-conceptual design stage through licensing stage.

III.5 Probabilistic Safety Assessment (PSA)

Today, PSAs are widely used in nuclear fields. It is an integrated and systematic method, and therefore the ISAM output as a whole converges on a PSA. The main difference between PSA in industrial nuclear applications and that in the ISAM is that, in the former case, it is used to evaluate core damage frequency (CDF) and to present dominant accident sequences contributing to risks in a licensing stage of a nuclear power plant, for example. In the latter case, it is used to improve safety related-designs via combination and iterative feedback with the DPA. The PSA in the ISAM can be meaningfully applied to design that has reached a minimum level of detail on safety-related architecture and related system design, thus it is performed in a late pre-conceptual design stage through to a final design stage.

In relation to so-called living PSA in which PSA results are often updated to reflect changes in design and system configuration, the idea of ISAM is to apply PSA at the earliest practical design stage to develop a new safety concept to be built in safety system architectures and also to continuously perform PSAs as a key decision tool throughout the design process. Although the other elements of the ISAM have significant values as stand-alone analysis methods, their values can be enhanced by being used for a PSA once the design proceeds to a point where the PSA can be applied.

The PSA provides a structured means to answer three questions, or "risk triplet": what can go wrong? (i.e. accident scenario), How likely is it to occur? (i.e. frequency, probability), and What will be the outcome? (i.e. consequences). A centrepiece of the ISAM is a full scope PSA, whereas non-full scope one will be used to assess the capability of risk reduction measures when applying new design SSCs, for example. One of the key strengths of the PSA is that it facilitates a systematic understanding of uncertainties related to risks of a reactor system. Uncertainties arise from a number of causes. One of the traditional general outlooks of safety-related uncertainties has been the provision of additional safety margin in the design. It is often based largely on engineering judgments to provide assurance so that severe core damage will not occur. Adding too much safety margins is, of course, expensive, and it may also lead to an inappropriate focus on some specific aspects of the design instead of other important and dominant risk contributors. On the other hand, the PSA provides systematic understanding of sources and a range of safety-related uncertainties, and it will help developers ensure that safety design considering reliability, economics, and such is optimised.

IV. Integration of ISAM Elements

IV.1 Design process and ISAM tools

It is intended that the five tools of the ISAM are diverse in their features. Some are primarily qualitative but others are quantitative. Some are probabilistic but others are deterministic. Some are inductive but others are deductive. Some focus on high-level issues, but others focus on more detailed issues. The diversity in the ISAM tools provides deeper, more complete, and more precise understanding of safety issues. The use of all the tools in an integrated way will improve and optimise safety related

design, but at the same time the designers will have total flexibility to attach importance on one of the specific tools for the best way to solve design issues at the moment depending on design maturity and their understanding on the design of target SSCs.

General steps for applying the ISAM tools are summarised as follows:

- a) The QSR can be performed any design phase although it is suitable from pre-conceptual to final design stages to support designers to ensure general characteristics including safety features to be extended in the following design development and also to identify possible safety vulnerabilities to be addressed and resolved with higher priority in the following design stages. Possible issues identified and documented via the QSR will be referred in PIRT, OPT, and PSA.
- b) The PIRT is employed from a pre-conceptual to conceptual design stages to identify specific issues and phenomena that may be important to a particular concept, by using the output (i.e. pro/con features) from the QSR. The PIRT output is documented, then will be directly used in the OPT and PSA. It will also be referred to numerical modelling and associated R&D for DPA tools like transient numerical codes.
- c) The OPT is employed from pre-conceptual to conceptual design stages to ensure and document that design under development incorporates adequate provisions, based on the understanding of the phenomena and issues that have been highlighted in the PIRT and also of pro/con features obtained from the QSR output. The output obtained from an OPT is documented and will be used in the following PSA to formulate fault and event trees and to identify postulated initiating events, for example.
- d) The DPA are performed throughout design stages to investigate safety issues to check correct implementation of deterministic principles such as a single failure criterion or needed redundancy and diversity of SSCs. In an early design stage, numerical models that had been identified to be newly developed by using the PIRT need to be included in DPA numerical codes.

- e) The PSA requires inputs from the outputs of the OPT to formulate fault and event trees and of the DPA results to justify success or failure criteria, for example. In order to investigate the uncertainty of PSA results which stem from input parameter ranges, not only DPA results but also QSR and PIRT results would be referred. By propagating uncertainties accompanied by models and analyses used, the PSA yields answers to, and displays the impacts of, the uncertainties. Importance analyses like Fussell-Vesely worth and RAW (Risk Achievement Worth) in the PSA identify vulnerable and important SSCs and will indicate which SSCs should be improved to reduce overall risks. Then, a new concept or modification of the SSCs (e.g. component types, the number, locations of) to minimise risks will be input to the QSR or OPT for next iteration.

The five independent tools are not of equal interest during developing stages. They are expected to be used in successive design development steps from purely qualitative to a more quantitative analyses.

IV.2 Resources required to implement ISAM

In addition to up-to-date plant concepts and designs, resources for practitioners and reviewers are certainly required to implement the ISAM tools and to ensure the outputs from the tools.

- QSR: Checklist provided and updated by system design teams, and finally reviewed by external experts.
- PIRT: Facilitated by experienced practitioners of PIRT, with expert teams comprised of system designers, supplemented by external experts as required.
- OPT: Led by experienced practitioners of OPT with system designers involved, and finally reviewed by external experts.
- DPA: Performed by system design and safety analysis teams supplemented by external experts as required.
- PSA: Performed by a team of internal event and external hazard specialists with recognised expertise of PSA, supported by system designers as necessary.

V. Examples of ISAM Application

In the following simple examples to envisage practices of the ISAM tools, three are stand-alone utilisation and one is combinational iterative utilisation. Other pilot applications of the ISAM are also explained in the Guidance Document of ISAM, named GDI[5], issued by the RSWG in 2014. The ISAM has been practically applied to the Gen-IV reactor systems in recent years, and the results are summarised in Risk and Safety Assessment White Paper reports [6]-[10].

V.1 QSR example

Table 1 shows QSR for decay heat removal (DHR) function of a new structural design concept, "Stratified REDAN" for a pool-type SFR. The idea of the concept is to enhance the capability of DHR under accident conditions by optimising the natural circulation of coolant. The "Stratified REDAN", shown in Figure 2, is a fixed in-vessel passive structural plate, and the flow path under natural circulation condition is simple. Such favourable features are marked with "X" in the Table. On the other hand, minimising leak-flow under normal operation would be more complex (marked in 1.1.2.1 in Table 1), and therefore the number of electromagnetic pump (EMP) in an intermediate heat exchanger (IHX) would increase (marked in 1.1.2.6 in Table 1).

Figure 2. Schematic of Stratified REDAN and flow patterns of a pool-type SFR

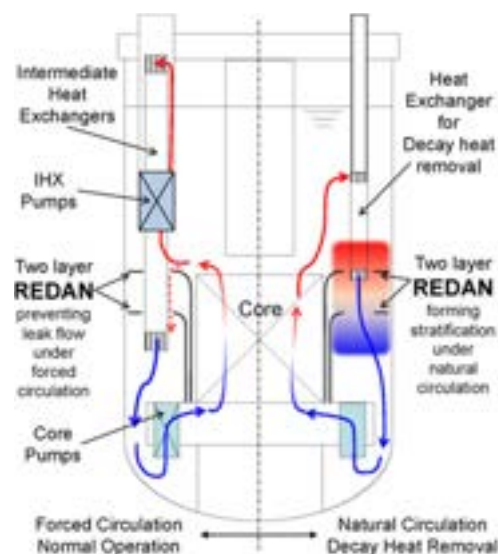


Table 1. QSR for Decay Heat Removal Function on New Concept: “Stratified REDAN” for Pool-type SFR

CLASS 3: Detailed & Technology Neutral Recommendations Applicable to a given Safety Function	F	N	U	Qualitative Assessment F: Favourable, N: Normal, U: Unfavourable
1 1st level PREVENTION: “Prevention of abnormal operation and failures”				
1.1. Work out & Set up Simple Design for operation & safety behaviour				
1.1.1. Simple neutronic design				
1.1.2. Simple thermal-hydraulic design				
1.1.2.1. Simplify thermal-hydraulic for normal operating conditions (heat removal at nominal operating conditions and during nominal operational transients)			X	<i>Thermal-hydraulic behaviour of primary circuit in pool-type SFR reactor vessel (RV) will be more complex due to the need of specific EMP (Electromagnetic Pump) control for stable stratification in internal volume of “REDAN” in RV</i>
1.1.2.2. Simplify thermal-hydraulic for normal DHR (decay heat removal)		X		DHR loop through DHX (direct heat exchanger) is conventional technology
1.1.2.3. Simplify thermal-hydraulic for safety DHR	X			Hydraulic loop to establish and maintain natural convection is significantly simple
1.1.2.4. Separate normal operating DHR function from safety DHR		X		Such design is already conventional
1.1.2.5. Increase available range covered by functionally redundant DHR systems (from only forced convection to natural convection)	X			Overlapping between “forced convection heat removal through IHX and DHX” and “natural convection heat removal via DHC” is achieved gradually and without significant modifications of hydraulic flow path
1.1.2.6. Minimize the number of components per system			X	<i>Increase the number of EMP installed on IHX</i>
1.1.3. Simple thermo-mechanic design				
1.1.4. Simple information and control design				
1.2. ...				
2. ...				

As a whole, pro/con features due to the installation of new design concept were identified, and the reasons to judge such features have objectivity from multidisciplinary viewpoints. Pro features will be informed to designers in order to take into account such pro features in quantitative analyses (e.g. margin to design limit), and con features will be examined in an early design stage so that it will be resolved before starting a regulation process in future, for example.

V.2 PIRT example

Table 2 shows a PIRT for the new concept of a passive mechanism embedded in a backup reactor shutdown system, named Self-Actuated Shutdown System (SASS). The PIRT was compiled by two designers, who are marked with “A” and “B” in the Table; one is an SFR engineer and the other is an LWR engineer newly participated an SFR project. The importance ranking is represented by “H” for high, “M” for medium, “L” for low, and “I” for insignificant. The two designers ranked many items in the Table as the same; however the ranking of some items differed as shown in yellow. This results from the difference in background information and/or large uncertainties of the new concept. The “Before” and “After” in the Table indicate when the PIRT was compiled, before or after the R&D of SASS

started. The numbers listed below the “Before” and “After” represent self-assessment rates on the knowledge: from “1”, very limited knowledge or uncertainty cannot be characterised, to “4”, fully understood or small uncertainty. The knowledge on the new concept was developed after the R&D started.

As a whole, the importance ranking identified which phenomena to be accurately modelled/counted in a safety demonstration for licencing, and the diversity (i.e. ranking discrepancy between designers) indicates on which SSCs, in relation to such phenomenon, fundamental experiments should be performed in order to reduce uncertainty of quantitative analyses, for example.

V.3 OPT example

Figure 3 depicts an OPT for heat removal from a reactor core under design basis accident in a loop-type SFR. The objective and barriers in this case is to control accidents within design basis, e.g. prevention of an accident within partial failure of fuel pins and maintenance of reactor core cooling. The safety function is heat removal from the reactor core, and its acceptance criteria for this safety function are adequate cooling of fuel, reactor vessel internals, reactor vessel, and reactor cavity. There are more safety functions excluded in this example, such as reactivity control to keep

subcriticality. The heat removal is achieved by using active and passive cooling systems that transfer decay heat from the reactor core to the ultimate heat sink to ensure the integrity of reactor core geometry and reactor vessel (or reactor coolant boundary). A challenge to the heat removal is degradation or disruption of heat transfer path by physical phenomena or mechanical failures of short-/long-term loss of forced convection, coolant leakage, and/or loss of intermediate heat transport path to ultimate heat sink. There will be provisions to prevent the advent of each mechanism. Provisions for the DiD Level 3 should be identified and selected under a condition that provisions for lower DiD levels (provisions for Levels 1 and 2 in this case) were insufficient because the plant condition had already progressed to Level 3.

As a whole, the mechanisms and associated provisions were identified with objectivity, and designers will take into account this information in the designs of SSCs. It is also utilised in a licencing process to explain that all the potential challenges in relation to each DiD level are resolved by the designs, for example.

V.4 DPA-PSA combination example

DPA are a kind of traditional analysis, which constitute an indispensable part of the overall ISAM. The objectives of DPA are, for example, to confirm operational limits, to evaluate specific accident sequences, and to conduct sensitivity and uncertainty analyses of accident transients. The specific features of PSA are from, for example, systematic analysis of risk, information integration, consideration of complex interactions of SSCs, development of quantitative measures for decision making. When DPA and PSA are used together, it can allow a new concept and/or SSCs to be built in

the safety architecture. An example for a loop-type SFR is shown in Figure 4. A designer team developed a DHR system concept by deterministic considerations: one Direct Reactor Auxiliary Cooling System (DRACS) in the reactor vessel and two Primary Reactor Auxiliary Cooling Systems (PRACS) at the primary coolant circuits. Both DRACS and PRACS are designed as safety grade, and the final heat sink is air. Both systems are available in not only forced circulation mode by using external power but also in natural circulation mode even under total loss of AC or DC power. An event sequence analysis, as a part of PSA, is performed for such DHR system, although determination of success or failure needs time-dependent transient results against the success criteria (simple and conservative criteria are used in this case), which are analysed by a series of numerical calculations in DPA. Then, success/failure of respective sequences is determined, and CDF is quantified by PSA. A dominant contributor to the CDF is identified as short-term loss of DHR sequences. The designer team can make risk-informed design modification such that installation of air-blowers at air coolers might be a good solution because the blower needs a power supply for only short time and small DC batteries are sufficient. The blowers and batteries are needed to cope with DEC but not with DBA, which makes it possible, although depending on a national regulation, to use non-safety grade blowers and batteries. As a result, based on the CDF calculations for modified design, the revised CDF became significantly lower, around 1/50 of the previous one. Such design can be upgraded via combination use of DPA and PSA through conceptual to final design stages.

Table 2. Preliminary PIRT on New Concept: Self-Actuated Shutdown System for Loop-type SFR

System / Component	Phenomena / Characteristics / State variables <i>(only selected items are listed)</i>	Ranking		Before		After	
		A	B	A	B	A	B
Self-actuated shutdown system (SASS)	Actuation (Cure-point) temperature of passive mechanism (gravity dropping) of absorber rods assembly (named SASS)	H	H	1	2	3	4
Upper core region in reactor vessel	Delay (lag) time of coolant transport from core outlet height to around SASS	H	H	3	2	3	3
	Delay of temperature response from coolant to Cure-point magnetic alloy	M	M	1	2	3	3
Reactor core and Fuel	Coolant temperatures of fuel assemblies' outlet around SASS	H	H	3	3	3	3
	Fuel temperature reactivity coefficient	L	M	4	3	4	3
	Coolant temperature reactivity coefficient	H	H	4	4	4	4
	Bulk coolant temperature at the core inlet and outlet	L	L	4	4	4	4
Coolant system	Fuel pellet thermal conductivity	I	I	4	4	4	4
	Coolant temperature instrumentation for reactor power control	M	L	4	4	4	4
	Pressure loss in the reactor core and primary coolant system	M	M	4	4	4	4

Figure 3. OPT on Heat Removal Safety Function under DiD Level 3: Design Basis Accident for Loop-type SFR

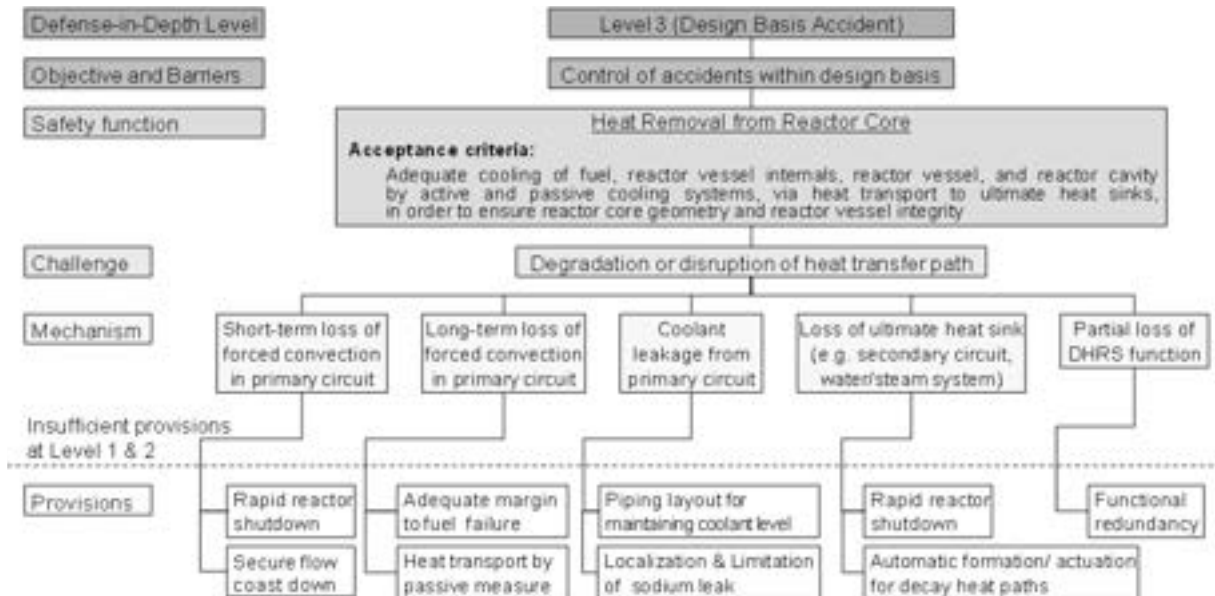
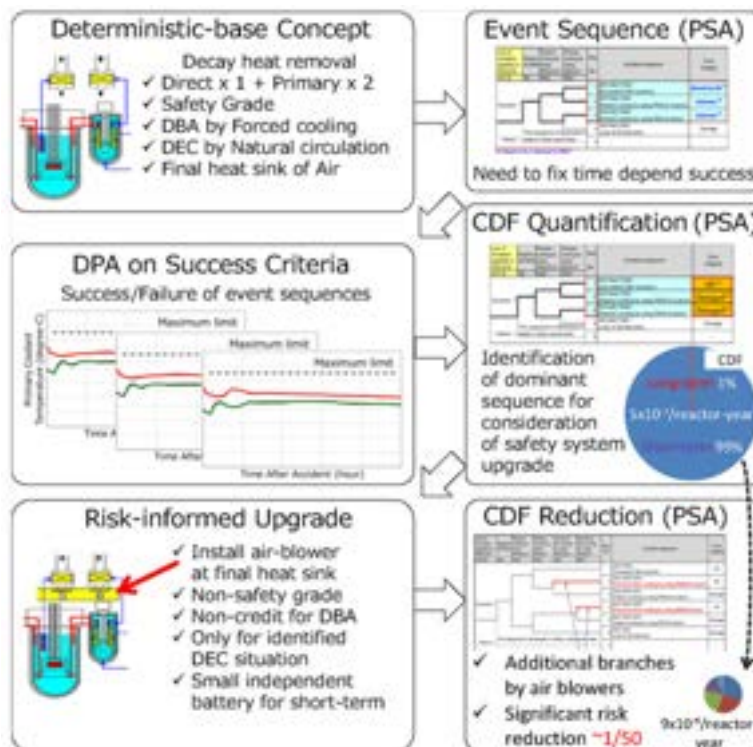


Figure 4. DPA-PSA Combination Use for Decay Heat Removal System in Conceptual Design Stage; [The picture shows an example for loop-type SFR]



VI. Concluding Remarks

This paper presents the five ISAM tools' respective roles in the design and assessment process of Gen-IV reactor systems, together with the task flow of ISAM and appropriate phases when the tools should be used. Specific examples are also included to show the relevance and usefulness of the ISAM. The ISAM will support developers and designers in designing, upgrading, and assessing new concepts and safety-related SSCs as well as overall safety architectures for all Gen-IV

reactor systems and other advanced reactor concepts. The ISAM is a user-oriented methodology and constructive feedback from ISAM users will be sincerely appreciated.

Acknowledgements

The authors, as the GIF Risk and Safety Working Group co-chairs, wish to show acknowledgement to Messrs. Tim LEAHY, INL, Gian Luigi FIORINI, CEA, Hajime NIWA and Ryodai NAKAI, JAEA as the former leaders on the development of the ISAM methodology.

References

- [1] GIF Risk and Safety Working Group, "Basis for the Safety Approach for Design & Assessment of Generation IV Nuclear Systems", Revision 1, GIF/RSWG/2007/002, 24 Nov. (2008). Available at https://www.gen-4.org/gif/jcms/c_9366/risk-safety (as of July 2018).
- [2] GIF Risk and Safety Working Group, "An Integrated Safety Assessment Methodology (ISAM) for Generation IV Nuclear Systems", Revision 1.1, GIF/RSWG/2010/002/Rev 1, June (2011).
- [3] M. Aoyagi, "Identification of important phenomena under sodium fire accidents based on PIRT process", CN245-93, FR17, 26-29 June, Yekaterinburg (2017).
- [4] IAEA, "Proposal for a Technology-Neutral Safety Approach for New Reactor Designs, IAEA TECDOC 1570, Vienna, pp.22-23 (2007).
- [5] GIF Risk and Safety Working Group, "Guidance Document for Integrated Safety Assessment Methodology (GDI)", GIF/RSWG/2014/001, 12 May (2014).
- [6] GIF RSWG and SCWR System Steering Committee, "Super-Critical Water-cooled Reactors (SCWR) Risk and Safety Assessment White Paper", January (2017).
- [7] GIF RSWG and GFR System Steering Committee, "Gas-cooled Fast Reactor (GFR) Risk and Safety Assessment White Paper", August (2016).
- [8] GIF RSWG and SFR System Steering Committee, "Sodium-cooled Fast Reactor (SFR) Risk and Safety Assessment White Paper", August (2016).
- [9] GIF RSWG and VHTR System Steering Committee, "Very High Temperature Reactor (VHTR) Risk and Safety Assessment White Paper", April (2015).
- [10] GIF RSWG and LFR System Steering Committee, "Lead-cooled Fast Reactor (LFR) Risk and Safety Assessment White Paper", April (2014).

TRACK 6: FUELS AND MATERIALS FOR GEN-IV SYSTEMS

HTR-STAP PROGRAM PACKAGE: SOURCE TERM ANALYSIS CODES FOR PEBBLE-BED HIGH-TEMPERATURE GAS-COOLED REACTOR (H. CHEN ET AL)

Chen Hongyu, Xing Haoyu, Li Chuan, Fang Chao

Institute of Nuclear and New Energy Technology, Tsinghua University, China

Abstract

Source term analysis is important in the design and safety analysis of advanced nuclear reactor and also provides a radiation safety analysis basis for High Temperature Gas Cooled Reactor (HTR). High Temperature Reactor-Pebble bed Modules (HTR-PM) design by China is a typical Gen-IV and due to different safety concepts and systems, the implements of source term analysis in light water reactors are not entirely applicable to HTR-PM. To solve this problem, HTR-STAP (HTR-PM Source Term Analysis Package) has been developed and related V&V has been finished. HTR-STAP consists of five units, including PCSA (Primary Circuit Source term Analysis code), NCSA (Normal Condition Airborne Source term Analysis code), ARCC (Accident Release Category Calculation code), CSA (C-14 Source Term Analysis code) and TSA (Tritium Source Term Analysis code). PCSA and NCSA may be used as calculating primary circuit coolant radioactivity and the release of airborne radioactivity to the environment under normal operating conditions of HTR-PM, respectively. The code ARCC composed of several source term analysis program in different typical accidents scenario, including SGTR (Steam Generator Tube Rupture), LOCA (Loss of Coolant Accident) and the transient process is compiled based on the results given by PCSA and NCSA. CSA and TSA are developed to calculate the productions of C-14 and H-3 through a different mechanism. Furthermore, the V&V has been performed on HTR-10 (10 MW High Temperature Gas-cooled Test Reactor), showing some positive results and it is shown that with limited adjustment, HTR-STAP could also be applied to the source term analysis of HTR-PM and 600MW High Temperature Reactor-Pebble bed Modules (HTR-PM600).

I. Introduction

Modular High Temperature Gas Cooled Reactor (HTR) could fulfill the safety goals of Gen-IV nuclear reactors and its fuel characteristics provide high confidence in the practical elimination of large radioactive release from nuclear power plants. Following the concept of design to safety, the first demonstration project of modular HTR in the world (HTR-PM) is under construction in Shidao Bay (in Shandong, China) and is planned to operate at the end of 2019. [1][2] Although HTR-PM is a kind of advanced reactor with inherent safety, the assessment of radioactivity during the operation, which play an essential role in the radiation protection, is still important. [3][4] Source term analysis may supply a radiation safety analysis basis for HTR and could provide the generation, quantity,

release and radiation hazard of radionuclides in a nuclear power plant under normal and accident conditions, which is make the design and safety assessment solid and credible.

With the development of nuclear reactor technology, many source term analysis codes have been developed and broad used. MELCOR, which is developed at Sandia National Laboratories, is an engineering-level computer code that models the progression of severe accidents in light water reactor [5]. KORIGEN, which is developed at FZK on the basis of the Oak Ridge Isotope Generation and Depletion code ORIGEN is used for radionuclides inventory estimation in the reactor core [6]. The French Institut de Radioprotection et de Sûreté Nucléaire (IRSN) and the German Gesellschaft für Anlagen und Reaktorsicherheit mbH (GRS) have developed a system of calculation codes,

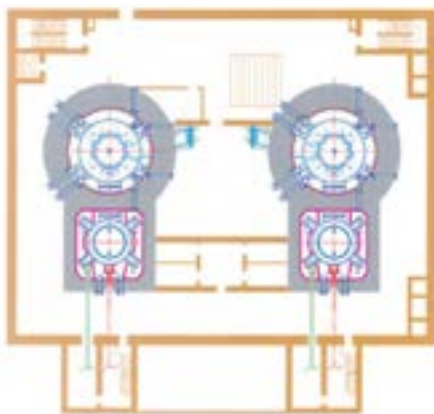
Accident Source Term Evaluation Code (ASTEC), to study source term of a hypothetical severe accident in a nuclear light water reactor [7-9]. The Japan Atomic Energy Agency (JAEA) has developed an integrated severe accident analysis code THALES2 and keep extending function via adding modules like KICHR (Kinetics of Iodine Chemistry in the Containment of Light Water Reactors) [10] [11]. Nevertheless, most source term analysis codes focus on water reactor and are not entirely applicable to HTR.

Source term analysis of HTR-PM has been performed by several commercial software and empirical formula before its construction. All results adopt conservation estimations and have been appraised by the National Nuclear Safety Administration (NNSA) of China. At present, commercial software used to study HTR source term only focuses on the radioactivity inventory and release of reactor core while another source term of the primary circuit and the release of airborne radioactive materials are not involving. Recently, the design of commercial 600MW High Temperature Reactor-Pebble bed Modules (HTR-PM600) is processing. In order to build a more systematic HTR source term analysis program package for the following commercial pebble-bed HTR design, a software package named HTR-STAP (HTR-PM Source Term Analysis Package) is developed. In this article, some prominent features of HTR-STAP are described and the code assessment is also be given.

II. The Features of HTR

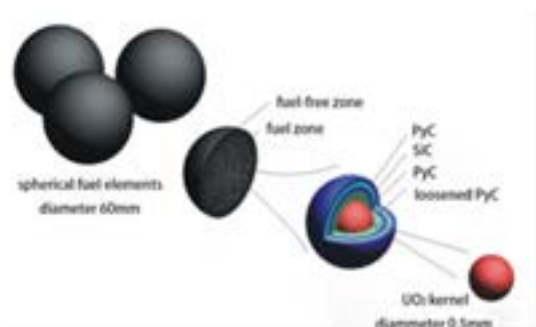
HTR-PM is taken for example to introduce some most important features of HTR.

Figure 1. Top view of HTR-PM



As shown in Figure 1, HTR-PM consists of two pebble-bed reactor modules coupled with a 210 MW steam turbine. Each reactor module includes a reactor pressure vessel; graphite, carbon, and metallic reactor internals; a steam generator; and a main helium blower. HTRs use graphite as a moderator as well as structural material and helium as a coolant which could reach 750°C at the core outlet. [12] Spherical fuel element with a diameter of 60 mm (Figure 2) is used in HTR-PM. Each fuel element contains about 12 000 coated particles which are uniformly embedded in a graphite matrix of 50 mm in diameter and an outer fuel-free zone of pure graphite surrounds the fuel graphite matrix. A coated fuel particle is composed of an UO_2 kernel of 0.5 mm diameter and three pyrolytic carbon (PyC) layers and one SiC layer (TRISO). [13] Experimental results show that the spherical fuel element will effectively be retained under 2200°C, which exceeds the safety limit of 1620°C for any operating or accident condition. The Heat-resistant property of spherical fuel element ensures core would not melt down.

Figure 2. Spherical fuel element of HTR-PM



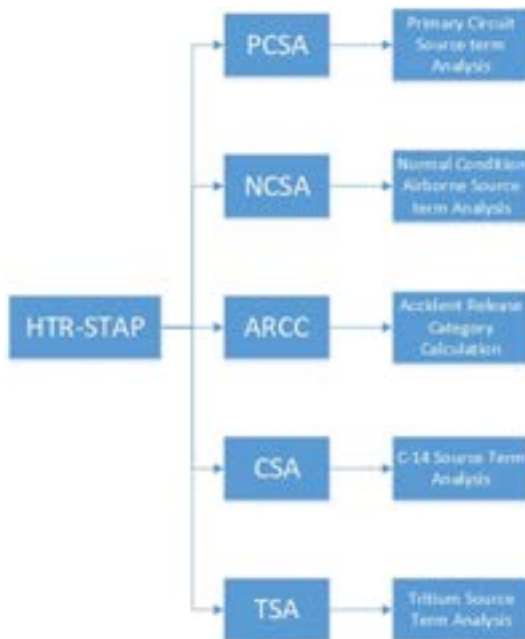
A unique fuel-discharge system allows the operation mode of HTR-PM to adopt continuous fuel loading and discharging. Fuel elements go through the core by gravity from up and down and are discharged through a fuel extraction pipe at the core bottom. The discharged fuel elements would be measured one by one to check their states of burn-up. A fuel element will be transported into the spent fuel storage tank if it reaches the design burn-up, otherwise, it will pass the core once again.

Average core power density of HTR-PM is about 3 MW/m³ while pressurised water reactor about 100 MW/m³. Lower power density means greater thermal-inertia and a slower rise of core temperature under accident conditions.

Besides, two independent shutdown systems are installed in HTR-PM: a control rod system and a small absorber sphere (SAS) system. They could drop into the graphitic side reflector borings by gravity and shutdown the core, making HTR-PM safer.

III. HTR-STAP Description

Figure 3. Construction of HTR-STAP



The objective of HTR-STAP is to study the accumulation and release of several significant nuclides, such as cesium, strontium, silver, iodide, tritium, etc., in normal and accident condition of pebble-bed HTR. The structure of HTR-STAP is modular and it consists of five units, including PCSA (Primary Circuit Source term Analysis code), NCSA (Normal Condition Airborne Source term Analysis code), ARCC (Accident Release Category Calculation code), CSA (C-14 Source Term Analysis code) and TSA (Tritium Source Term Analysis code). Each unit can be run independently for separate tests or coupled to take the overall evaluation. The programming language is Python and the code runs on a PC in diverse environments such as Linux and Windows.

III.A PCSA

To estimate the effect of the most serious accident, i.e. the core melt accident, amount of core radioactivity has been a significant issue

for reactors for a long time. Based on the special design, the special spherical fuel element will be perfect under any accidental condition and there is no melt down of the reactor core. However, fission product (FP) still release from fuel elements would transport in the primary circuit via helium cycle. The primary radioactivity could release slowly under the normal operating condition and would be a major source of radioactivity release during an accident. Hence, the primary circuit coolant radioactivity under normal operating conditions of HTRs should be studied and PCSA aims to do that.

FPs in helium is mainly generated in two ways: coated fuel particles failure and uranium contamination. It is found that a very small amount of TRISO particles with a defect layer in spherical fuel elements during the fabrication process and the irradiation would also induce few coated fuel particles failure [14]. Uranium contamination mainly exists on the surface of the coating layer, matrix graphite, sometimes also on natural graphite. Furthermore, the continuous reductions of FPs caused by atom decay, helium purification system and deposition on the primary circuit surface should be considered in the calculation. The dynamic equation of FPs in primary circuit could be addressed as:

$$\frac{dC_i(t)}{dt} = \frac{R_i}{V} - (\lambda_i + \varepsilon_i \frac{Q}{V} + \frac{\delta_i}{T} + \omega + \sigma_{ai} \phi_e \frac{t_v}{T}) C_i(t)$$

C_i The concentration of nuclide FP i ($\text{Bq}\cdot\text{m}^{-3}\cdot\text{s}^{-1}$)

R_i The release rate of FP i from the core fuel element ($\text{Bq}\cdot\text{s}^{-1}$)

V Volume of primary circuit air space (m^3)

λ_i The decay constant of FP i (s^{-1})

Q Purification flow of the helium purification system ($\text{m}^3\cdot\text{s}^{-1}$)

ε_i Purification efficiency of helium purification system of FP i (%)

δ_i The deposition rate of FP i per cycle (%)

T Cycle time of primary circuit helium (s)

ω Leak rate of primary circuit helium volume ($\%\cdot\text{s}^{-1}$)

σ_{ai} Neutron absorption cross section of FP i (cm^2)

ϕ_e Core average neutron fluence rate, ($\text{cm}^{-2}\cdot\text{s}^{-1}$)

t_v Time for helium to pass through the core per cycle (s)

FP i generated by activation of materials inside the primary circuit are also considered, and the dynamic equation is given by:

$$B_i = \frac{\rho A_0 f_n f_m}{A} \cdot \sigma \phi$$

B_i The generation rate of FP i in per unit volume of material ($\text{m}^{-3}\cdot\text{s}^{-1}$)

ρ Material density ($\text{g}\cdot\text{cm}^{-3}$)

A_0 Avogadro's constant (mol^{-1})

f_n Natural abundance of target nuclide (%)

f_m The weight percentage of the target element in the material (%)

A Molar mass of target nuclide t ($\text{g}\cdot\text{mol}^{-1}$)

σ Neutron activation cross section of target nuclide (cm^2)

ϕ Neutron fluence rate ($\text{cm}^{-2}\cdot\text{s}^{-1}$)

Due to the concerned FPs are long-lived nuclides, the decay of them are not considered. However, the code can be updated if it is necessary for some situation.

Based on these equations, PCSA calculates several radioactive nuclides amount chosen by user in primary circuit coolant, i.e., coolant source term analysis under normal operating conditions.

III.B NCSA

During the operation of pebble-bed HTR, the airborne radioactive material is considered to be the main source of radioactive discharge. It is essential to study this issue for safe areas division and radiation level assessment. Therefore, NCSA has been developed to study the release of airborne radioactive materials to the environment under normal operating conditions.

Six airborne radioactivity sources are considered (taking HTR-PM as instance shown in Fig.4) and calculated individually in NCSA, including:

- A. Air activation inside the cavity
- B. Leakage of primary coolant
- C. Venting of contaminated He tank
- D. Venting of fuel-discharge system
- E. Leakage of secondary loop steam
- F. Leakage of equipment room during maintenance

A cavity negative pressure air exhausting system has been installed in HTR-PM to discharge cavity air after filtration. However, Ar-41, a radionuclide generated by neutron activation from Ar-40, which shares 0.93% of air, cannot be filtrated and would release to atmosphere through the system at the same time. The dynamic equation is given by:

$$C(t) = \frac{\rho A_0 f_n f_m}{A} \cdot \frac{\sigma_c \phi}{\lambda + W + \sigma_a \phi}$$

$C(t)$ The concentration of Ar-41 at time t (m^{-3})

ρ Air density ($\text{g}\cdot\text{cm}^{-3}$)

A_0 Avogadro's constant (mol^{-1})

f_n Natural abundance of Ar-40 (%)

f_m The weight percentage of element Ar in the air (%)

A Molar mass of Ar-40 ($\text{g}\cdot\text{mol}^{-1}$)

λ Decay constant of Ar-41 (s^{-1})

σ_c Neutron absorption cross section of Ar-40 (cm^2)

ϕ Cavity average neutron fluence rate, ($\text{cm}^{-2}\cdot\text{s}^{-1}$)

W Removal constant due to negative pressure (s^{-1})

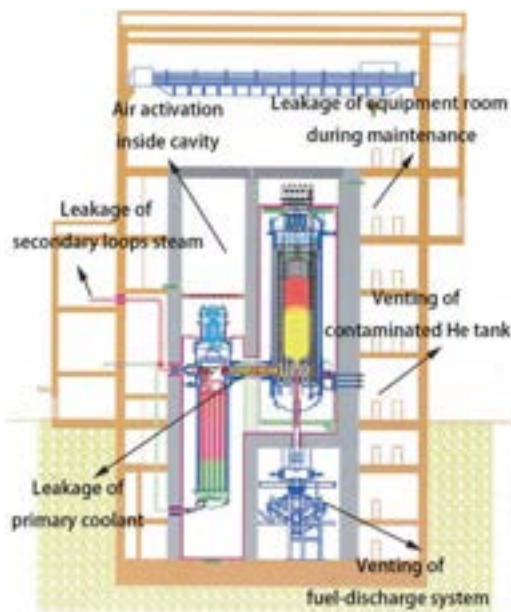
σ_a Neutron absorption cross section of Ar-41 (cm^2)

A little helium leaking from primary coolant and some radioactive gas generated by fuel-discharge system and maintenance of equipment room also release through negative pressure air exhausting system with filtration.

Waste helium in contaminated helium tank is mainly produced in the regeneration of helium purification system. Because of the decline of purification equipment's ability to transform or adsorb impurities, helium purification system needs regeneration after ten days. Desorption of parts of absorbed radioactive nuclides in this process makes contribute to airborne radioactivity, too.

Due to the activation and penetration of some radioactive materials, the secondary loop steam also has certain radionuclides and they are mainly tritium. The amount of airborne radioactivity leaked from the secondary loop steam is related to the concentration of tritium in the secondary loop and the operating status of the turbine.

Figure 4. Airborne radioactivity sources of HTR-PM



NASA estimates the six parts' air activation and presents an output result including each part's radioactivity and total evaluation.

III.C ARCC

PCSA and NASA perform normal condition source term analysis while ARCC study accident release category. The calculation results make a great contribution to safety estimation and Emergency Planning Zone division.

SGTR (Steam Generator Tube Rupture), LOCA (Loss of Coolant Accident) and transient process (an accident which causes a turbine trip) are three typical accidents on pebbled bed HTR. They are all considered in ARCC code and could represent most design basic accidents (DBA) in HTR. However, the source term analysis of beyond design basic accidents (BDBA) needs to be proceeded by a different way so they are not included in ARCC.

Generally speaking, there are two release processes in the accident progress. One is transient release and the other is long-term release. ARCC firstly classifies accidents by several input accident parameters and then outputs instant release, long-term release and a total release, respectively. Input parameters describe the characteristic and states of an accident, including fuel temperature, valve state, filtration efficiency, flooding quantity, etc. The long-term release comes from radioactive

fission products in fuel elements caused by the heat up of the core after accidents and it is mainly decided by core temperature. However, instant release varies from accident to accident and should be studied case by case.

(1) SGTR

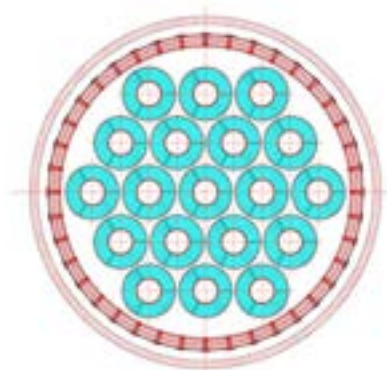
Steam Generator of HTR-PM has 19 heat exchange pipes. The pressure of primary circuit of HTR-PM is lower than the secondary circuit, so once a break occurs, water and water vapour in the secondary circuit would rapidly flow into the primary circuit and wash out radioactivity deposited on the steam generator and primary circuit. A higher pressure would trigger safety valves by which radioactivity release through. According to the size of the tube break, SGTR falls into three types:

- A. A small break of the heat pipe, represented by the double-end fracture of one heat pipe.
- B. Large break of the heat pipe, represented by the double-end fracture of several heat pipes.
- C. Complete rupture of the generator tube, which means the steam generator heat transfer tube plate ruptures.

Radioactivity instant release in SGTR consists of three parts:

- A. The primary circuit coolant radioactivity during steady operation before the accident which could be studied by PCSA.
- B. The radioactivity deposited on the inner surface of the steam generator washed into the primary coolant.
- C. The radioactivity caused by the reacts between water vapour and matrix graphite or broken fuel element.

Figure 5. Cross section of a steam generator with 19 assemblies [11]



(2) LOCA

LOCA of HTRs is the same as water reactors except the coolant is helium instead of water. The high-pressure helium with radioactive materials discharged into the containment vessel through a primary circuit break will cause a pressure increase and then trigger rupture discs so that airborne radioactivity would release to the environment.

The accident severity levels of LOCA is decided by the break size of primary circuit tube. Radioactivity instant release in LOCA also consists of three parts:

- A. The primary circuit coolant radioactivity during steady operation before the accident, the same as SGTR;
- B. Desorption of adsorptive radioactivity deposited on the inner surface of the primary circuit;
- C. Desorption of adsorptive radioactivity in helium purification system.

(3) Transient process

The transient process is an accident which causes a turbine trip in addition to SGTR and LOCA. Transient also causes a pressure increase and the radioactivity instant release in the transient process is the same as LOCA, but release through safety valve instead of break pipe.

III.D CSA and TSA

C-14 and tritium are two special radionuclides in HTR which needed to be studied separately. C-14 exists mainly in the form of carbon dioxide in the environment, could be easily entered into human body through carbon cycling and a 5730 years half-life makes its influence cannot be ignored. Tritium oxide (HTO, DTO, or T₂O) can be inhaled and can combine with organic matter and hard to excrete, resulting in internal irradiation, which is very harmful to the human body, too. C-14 and tritium are generated by two ways: ternary fission and neutron reactions (Table 1, 2). CSA and TSA study the cumulative quantity and cumulative rate of C-14 and tritium of each reaction in a specified time which can be set by users.

Table 1. C-14 generated in HTR-PM

Reaction type	Reaction formula	Reaction zone
Ternary fission reaction	U-235 (n, f) C-14	fuel elements and matrix graphite
Neutron activation reaction	N-14(n, p) C-14	coolant and fuel elements
	O-17 (n, α) C-14	fuel elements and matrix graphite
	C-13 (n, γ) C-14	matrix graphite, graphite reflector and fuel elements

Table 2. Tritium generated in HTR-PM

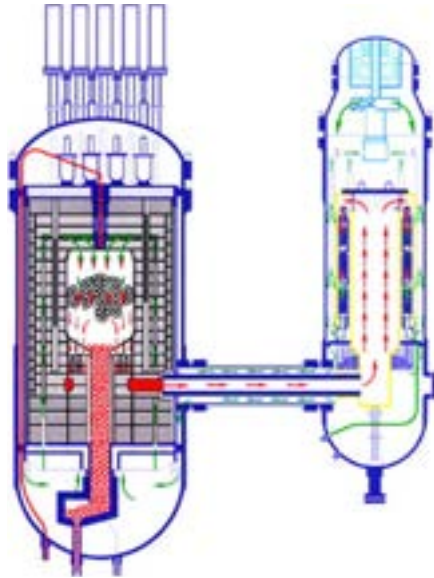
Reaction type	Reaction formula	Reaction zone
Ternary fission reaction	U-235 (n, f) H-3	fuel elements and matrix graphite
Neutron activation reaction	He-3 (n, p) H-3	Coolant
	Li-6 (n, α) H-3	matrix graphite, graphite reflector and carbon brick
	Li-7 (n, $n\alpha$) H-3	matrix graphite, graphite reflector, Boron containing carbon brick, control rod and absorber ball;
	B-10 (n, 2α) H-3	Boron-containing carbon brick, control rod and absorber ball;

IV. HTR-STAP Code Assessment

All the subprograms of HTR-STAP have been performed code validation. Due to HTR-PM is still under construction, real operation data of it is lacking. HTR-10 (10 MW High Temperature Gas-cooled Test Reactor), which is designed and constructed in the 1990s, brought to criticality in 2000, and reached full power operation in 2003 [15], is chosen to be the validation reactor. The Institute of Nuclear and New Energy Technology (INET), Tsinghua University has performed several data-collection campaigns on HTR-10, such as source term experimental analysis of irradiated graphite in the core, sampling of the radioactive graphite dust in the primary loop and R&D of helium sampling loop [16-19]. INET also has studied many theoretical calculation approaches like the Monte Carlo method and differential equations to predict

the radioactivity in HTR-10 [20-22]. Based on those theoretical predictions and experimental data, the validation is performed.

Figure 6. Primary circuit of HTR-10



As an example, the comparison of experiment result, theoretical calculation and HTR-STAP result of tritium in the primary loop of HTR-10 are showed in table 3. The theoretical calculation result is about 20 times higher than experiment data, which shows a conservatism for the evaluation of the activity concentration of tritium in the primary loop of HTR-10. The calculation result of HTR-STAP is also conservative and closer to actual data, which indicates that HTR-STAP is valid and more adopted than previous theoretical calculation. The discrepancy between HTR-STAP data and theoretical result may come from the most conservative input parameters, especially the concentration of He-3 in the helium coolant and Li-6 in the graphite.

Table 3. The comparison of experiment result, theoretical calculation and HTR-STAP result of tritium in the primary loop of HTR-10

Method	Value (Bq/m ³ STP)
Experiment [22]	1.09×10^4
Theoretical calculation [22]	2.31×10^5
HTR-STAP	1.28×10^5

Due to the safely running of HTR-10, accidental experimental data cannot be obtained. And more validations are conducted based on the safety analysis report of HTR-PM, which is appraised by NNSA. In the future, more assessment of HTR-STAP would be performed both on HTR-10 and HTR-PM.

V. Conclusion and Remarks

HTR-STAP is a composite source term analysis package for pebble-bed HTR, consisting of PCSA, NCSA, ARCC, CSA and TSA. Each subroutine of HTR-STAP could run independently or unites together and all of them are performed code validation and the comparison between HTR-STAP analysis results and experimental results shows great practicability.

Source term analysis of HTR-PM has done before the development of HTR-STAP and the results are reliable. Many algorithms, empirical formulae and assumptions during the design and safety analysis of HTR-PM are also applied in HTR-STAP. HTRs share the same operation model and physical process so that HTR-STAP could systematically perform source term analysis for most HTRs conveniently and flexibly. In the near future, more pebble bed HTRs will be design and HTR-STAP will make source term analysis of HTRs more reliable and accurate and would make a great contribution to the design and promotion of pebble-bed HTR.

Acknowledgements

This work has been supported by the National S&T Major Project (Grant No. ZX069).

Nomenclature

ASTEC	Accident Source Term Evaluation Code
ARCC	Accident Release Category Calculation code
CSA	C-14 Source Term Analysis code
FP	fission product
GRS	Gesellschaft für Anlagen und Reaktorsicherheit mbH
HTR-STAP	HTR-PM Source Term Analysis Package
HTR	High Temperature Gas Cooled Reactor

HTR-10	10 MW High Temperature Gas-cooled Test Reactor	LOCA	Loss of Coolant Accident
HTR-PM	High Temperature Reactor-Pebblebed Modules	NNSA	National Nuclear Safety Administration
HTR-PM600	600MW High Temperature Reactor-Pebble bed Modules	NCSA	Normal Condition Airborne Source term Analysis code
INET	Institute of Nuclear and New Energy Technology	PCSA	Primary Circuit Source term Analysis code
IRSN	Institut de Radioprotection et de Sûreté Nucléaire	PyC	Pyrolytic carbon
JAEA	Japan Atomic Energy Agency	SGTR	Steam Generator Tube Rupture
KICHR	Kinetics of Iodine Chemistry in the Containment of Light Water Reactors	TSA	Tritium Source Term Analysis code
		TRISO	Spherical fuel element with three PyC layers and one SiC layer

References

- [1] Fang Chao., et al. "Safety Features of High Temperature Gas Cooled Reactor", Science and Technology of Nuclear Installations, Vol. 2017, 9160971:1-3, 2017.
- [2] Zhang Zuoyi, et al. "The Shandong Shidao Bay 200 MWe High-Temperature Gas-Cooled Reactor Pebble-Bed Module (HTR-PM) Demonstration Power Plant: An Engineering and Technological Innovation." Engineering 2.1(2016):112-118.
- [3] Michael. A. F., et al. "Is tritium an issue for high temperature reactors?" Nuclear Engineering and Design 306(2016):160-169.
- [4] Liu. Y., et al. "Fission product release and its environment impact for normal reactor operations and for relevant accidents" Nuclear Engineering and Design 218(2002): 81-90.
- [5] Summers R. M., et al. "MELCOR 1. 8. 0: A computer code for nuclear reactor severe accident source term and risk assessment analyses." NUREG/CR-5531 and SAND 90-0364(1991).
- [6] Muswema, J. L., et al. "Source term derivation and radiological safety analysis for the TRICO II research reactor in Kinshasa." Nuclear Engineering & Design 281.281(2015):51-57.
- [7] Dorsselaere, J. P. Van, et al. "The ASTEC Integral Code for Severe Accident Simulation." Nuclear Technology 165.3(2009):293-307.
- [8] Chatelard, P., et al. "ASTEC V2 severe accident integral code main features, current V2.0 modelling status, perspectives." Nuclear Engineering & Design 272.6(2014):119-135.
- [9] Chatelard, P., et al. "Main modelling features of the ASTEC V2.1 major version." Annals of Nuclear Energy 93(2016):83-93.
- [10] Watanabe, Norio. "Development of THALES-2, a computer code for coupled thermal-hydraulics and fission product transport analyses for severe accident at LWRs and its application to analysis of fission product reevaporation phenomena." British Journal of Cancer 59.3(1991):439-440.
- [11] Kiyofumi M., et al. "Kiche: A simulation tool for Kinetics of iodine chemistry in the containment of light water reactors under severe accident conditions." JAEA-Data/Code 2010-034.
- [12] Zhang Zuoyi., et al. "Current status and technical description of Chinese 2 × 250 MWth, HTR-PM demonstration plant." Nuclear Engineering & Design 239.7(2009):1212-1219.
- [13] Tang Chunhe, et al. "Design and manufacture of the fuel element for the 10

- MW high temperature gas-cooled reactor." Nuclear Engineering & Design 218.1(2002):91-102.
- [14] Li Hong, et al. "Experimental study on the content and distribution of Key nuclides in an irradiated graphite sphere of HTR-10." Nuclear Engineering & Design 323(2017):39-45.
- [15] Wu Zongxin, D. Lin, and D. Zhong. "The design features of the HTR-10." Nuclear Engineering & Design 218.1(2002):25-32.
- [16] Xie Feng , et al. "Design and Study of Radioactive Graphite Dust Experimental System in Primary Loop of HTR-10." Atomic Energy Science & Technology 49.04(2015):744-749.
- [17] Xie Feng, et al. "Experimental research on the radioactive dust in the primary loop of HTR-10." Nuclear Engineering & Design 324(2017):372-378.
- [18] Liu Xuegang, et al. "Source Term Analysis of the Irradiated Graphite in the Core of HTR-10." Science and Technology and Nuclear Installations, 2017 (2017):1-6.
- [19] Fang Chao, et al. "The R&D of HTGR high temperature helium sampling loop: From HTR-10 to HTR-PM." Nuclear Engineering & Design 306(2016):192-197.
- [20] Jeong Hyedong, et al. "Development of a method of evaluating an inventory of fission products for a pebble bed reactor." Annals of Nuclear Energy 35.12(2008):2161-2171.
- [21] Xu Yi, et al. "Source Term Analysis of Tritium in HTR-10." Fusion Science & Technology 71.4(2017):671-678.
- [22] Xie Feng , et al. "Study of tritium in the primary loop of HTR-10: Experiment and theoretical calculations." Progress in Nuclear Energy 105(2018):99-105.

**THE GIF PROLIFERATION RESISTANCE AND PHYSICAL PROTECTION WORKING GROUP
(PRPPWG): ACHIEVEMENTS AND PERSPECTIVES (G. G. M. COJAZZI ET AL)**

G.G.M. Cojazzi⁽¹⁾, G. Renda⁽²⁾, L. Cheng⁽³⁾, P. Peterson⁽⁴⁾, R. Bari⁽⁵⁾, B. Boyer⁽⁶⁾, A. Chebeskov⁽⁷⁾,
G. Edwards⁽⁸⁾, D. Henderson⁽⁹⁾, E. Hervieu⁽¹⁰⁾, K. Hori⁽¹¹⁾, H. Kim⁽¹²⁾, F. Padoani⁽¹³⁾ on behalf of
PRPPWG.

See the acknowledgements section for the list of PRPPWG members & observers.

- (1) European Commission, Joint Research Centre, Italy
- (2) European Commission, Joint Research Centre, Italy
- (3) Brookhaven National Laboratory, United States of America
- (4) University of California Berkeley, United States of America
- (5) Brookhaven National Laboratory, United States of America
- (6) International Atomic Energy Agency, Austria
- (7) Institute for Physics and Power Engineering, the Russian Federation
- (8) Canadian Nuclear Laboratories, Canada
- (9) OECD-Nuclear Energy Agency, Paris, France
- (10) Commissariat à l'énergie atomique et aux énergies alternatives, France
- (11) Japan Atomic Energy Agency, Vienna office, Austria
- (12) Korea Atomic Energy Research Institute, Republic of Korea
- (13) ENEA, Italy

Abstract

The Generation IV International Forum (GIF) “Technology Roadmap” identified proliferation resistance and physical protection (PR&PP) as one of the four goal areas to advance nuclear energy into its next, “fourth” generation. It recommended the development of a methodology to define measures for PR&PP and to evaluate them for the six nuclear energy systems selected by GIF. Accordingly, the Forum formed a PR&PP Working Group (PRPPWG) to develop a methodology and to define the parameters against which PR&PP would be measured.

The PRPPWG developed the methodology through a series of development and demonstration case studies, by use of a hypothetical “Example Sodium Fast Reactor” (ESFR). The PR&PP ESFR assessment was the first opportunity to exercise the full methodology on a complete system, and many insights were gained from the process. The PRPPWG and representatives of the GIF System Steering Committees (SSCs) for each of the six GIF design concepts carried out a study on the PR&PP aspects of the six GIF designs. This interaction allowed the PRPPWG to engage the designers and to raise awareness about PR&PP. A number of international workshops have also been held which have introduced the methodology to design groups and other stakeholders.

In this paper, we first summarise the technical progress and the major accomplishments of the PRPPWG: the evaluation methodology and the ESFR case study used to develop and test the methodology. The interaction with the GIF System Steering Committees and the relaunching of the activity is then presented. Finally, an outline of the future challenges is provided along the lines identified in the GIF R&D outlook 2018 report.

I. Introduction

Following the publication of the Generation IV International Forum (GIF) Roadmap [1] in 2002, the Proliferation Resistance and Physical Protection Working Group (PRPPWG) was established, and charged with developing measures for expressing proliferation resistance and physical protection, and incorporating these into an associated evaluation methodology. Overall, the method would enable evaluation of the performance of different Generation IV systems (or options for a given system) against the GIF PR&PP goal. Successive developments and iterations taking benefit of ad hoc case studies [2] culminated in the methodology in its current revision [3].

As the 2002 Roadmap outlines, each GIF design would support R&D on material deployed, potential vulnerabilities, protective barriers, safeguards approaches, potential misuse, material protection, control and accounting for each step in the fuel cycle, etc.. As reported in the 2014 GIF Technology Roadmap update, each GIF design has not yet formally explicitly addressed all nine areas given in the 2002 Roadmap for PR&PP R&D [1]. Over the years there has been interaction between each of the six GIF System Steering Committees (SSCs) and provisional System Steering Committees (p SSCs) and the PRPPWG on the status of designs with regard to PR&PP R&D, resulting in a joint report between the PRPPWG and the SSCs [4].

Since the issuing of the GIF Roadmap and the establishment of the PRPPWG, the importance of considering safeguards needs as early as possible in the technology design process ("Safeguards by design", SbD) has become widely recognised. In this respect the interaction of the SSCs with the PRPPWG, the engagement of the individual design teams with the PR&PP process, and the dual consideration of security and safeguards concerns within the PR&PP process, demonstrate the alignment and leadership of GIF in the area of international PR&PP development over the last decade.

A summary of the work of the PRPPWG over the past decade appears in a special issue on PR&PP of the ANS journal Nuclear Technology in July 2012 [5], where several papers are derived from contributions to Global 2009 International Conference. A status paper on the PR&PP methodology and its application appeared in the GIF 2012 Symposium [6] with updated versions later presented at various international conferences [7-10]. Several national programs

have adapted the PR&PP methodology to their specific needs and interests see e.g. [11-19]. The PRPPWG has assembled a comprehensive bibliography (publicly available on the GIF-PR&PP web site) comprised of its papers and reports by the group as well as related documents prepared by others [20]. The bibliography is updated yearly.

In this paper, we first summarise the technical progress and the major accomplishments of the PRPPWG: the evaluation methodology [3] and the ESFR case study [2] used to develop and test the methodology. The interaction with the GIF System Steering Committees and the relaunching of the activity is then presented. Finally, an outline of the future challenges is provided along the lines identified in the GIF R&D outlook 2018 update.

II. The PR&PP Evaluation Methodology & Lessons Learned from Case Study

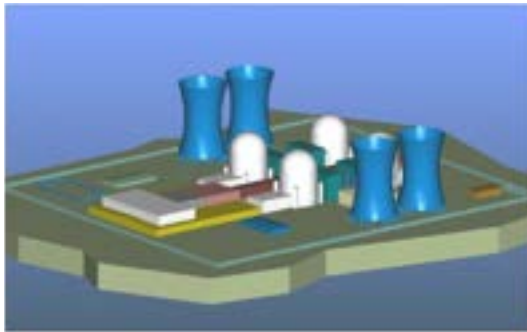
In a succession of revisions beginning in 2004, the PRPPWG has developed a methodology for PR&PP evaluation for all GIF systems, including measures and associated metrics. Consensus was achieved amongst all participating GIF members and observers (IAEA), and Revision 6 of the methodology report was approved by GIF for open distribution in 2011 [3]. Figure 1 illustrates the methodological approach at its most basic form. For a given system, analysts define a set of challenges, analyse system response to these challenges, and assess outcomes.

Figure 1. Basic Framework and evaluation steps for the PR&PP Evaluation Methodology [3].



The methodology was developed, demonstrated, and subsequently illustrated by use of a hypothetical “Example Sodium Fast Reactor” (ESFR, see Figure 2), by members of the PRPPWG. The ESFR assessment was the first opportunity to exercise the full methodology on a complete system, and many insights were gained from the process. In particular, the approach of breaking the assessment into subtasks, each focusing on a separate area of PR&PP (for PR: diversion, misuse, breakout; for PP: theft and sabotage) handled by a dedicated subgroup with diverse international membership, was useful in generating new insights and concept development [2].

Figure 2. The ESFR 3D rendering [2.]



The ESFR case study report [2] found key lessons in starting each PR&PP evaluation with a qualitative analysis, allowing scoping of the study, of the assumed threats, and identification of system elements, targets, etc. The ESFR study also noted a need to include a) detailed guidance for qualitative analyses in methodology, b) a role for experts with the necessary subject matter expertise (e.g. nuclear engineering, both reactor and fuel cycle technology, safeguards and security), c) inclusion of PR&PP experts and the use of expert elicitation techniques. The qualitative analysis already offers valuable results, even at the preliminary design level.

Completeness in identifying potential diversion pathways is a key goal. It was found that it is possible to systematically identify targets and potential pathways for each specific threat, and to systematically search for plausible scenarios that the proliferating host state could potentially implement to divert the target material. A set of diversion pathway segments can be developed and the PR measures for each pathway can be determined. The methodology can compare and distinguish how different design choices affect PR.

The diversion pathways analysis can provide a variety of useful information to stakeholders, including regulatory authorities, government officials, and system designers. This information includes how attractive the material is to potential proliferators for use in a weapons program; how difficult it would be to physically access and remove the material; and whether the facility can be designed and operated in such a manner that all plausible acquisition paths are covered by a combination of intrinsic (related to the design) features and extrinsic measures (related to safeguards and institutional arrangements).

The misuse pathways analysis requires consideration of potentially complex combinations of processes to produce weapons-usable material; i.e., it is not a single action on a single piece of equipment, but rather an integrated exploitation of various assets and system elements.

It was found that, given a proliferation strategy, some measures are likely to dominate the others, and within a measure some segments will dominate the overall pathway estimate.

The breakout pathways analysis found that breakout is a modifying strategy within the diversion and misuse threats and can take various forms that depend on intent and aggressiveness, and ultimately the time to complete the pathway, which PRPPWG describes as the proliferation time required by a proliferating state. Furthermore, measures can be assessed differently within the breakout threat, depending on the breakout strategy chosen. Note that some additional factors related to global response and foreign policy were identified as being relevant to the breakout threat, but those factors are not included in the PR&PP methodology.

The theft and sabotage pathways analysis found that multiple target and pathways exist. The most attractive theft target materials appeared to be located in a few target areas. For example, for the ESFR, the most attractive theft target areas with the most attractive target materials were found to be the light water reactor (LWR) spent-fuel cask parking area, the LWR spent-fuel storage and fuel cycle facility staging-washing area, the fuel cycle facility air cell (hot cell), and the inert hot cell.

III. Workshops & Outreach

The methodology was intended for three types of generic users: system designers, program

policy makers, and external stakeholders. Workshops with GIF designers and other stakeholders, to familiarise them with the methodology and to understand their needs for the design process, were held in the years in the USA, Italy, Japan, the Republic of Korea, the Russian Federation and France. This has helped to address one challenge with PR&PP, which is the engagement of technology designers; PR&PP has typically been a topic tackled in the latter stages of design, and at the initiation of external bodies like the IAEA. These workshops have spread awareness of the PR&PP methodology beyond the GIF community, which is appropriate since the methodology itself is applicable to the whole range of nuclear technology.

In addition to the workshops dedicated to the designers and stakeholders, workshops targeted to scholars and students and to the broader community have been also done [21, 22].

The PRPPWG produced a set of Frequently Asked Questions (FAQ) about its methodology and applications [23], intended for a broad audience wishing to know about the methodology at an introductory level.

IV. Interactions with the SSCs

Starting in 2007, the PRPPWG and the six SSCs conducted a series of workshops on the PR&PP characteristics of their respective designs and identified areas in which R&D is needed to further include such characteristics and features in each design. A common template was developed to systematically collect design information, including PR&PP-related features. This work culminated with reports, internally referred to as white papers, written jointly by the PRPPWG and the SSCs for each design. An overall report was approved by GIF for open distribution in 2011 [4]. The intent is to generate preliminary information about the PR&PP merits of each system and to recommend directions for optimising their PR&PP performance.

The report captures the current salient features of the GIF system design concepts that impact their PR&PP performance. It identifies crosscutting studies to assess PR&PP design or operating features common to various GIF systems; and it suggests beneficial characteristics of the design of future nuclear energy systems, beyond the nuclear island and power conversion system, that should be addressed in subsequent GIF activities.

The PRPPWG is strengthening its interaction with the SSCs to support the “PR&PP-by-design” process for each of the six GIF nuclear energy systems. This increased effort began in 2016 with the preparation by PRPPWG of a questionnaire addressed to all the GIF SSCs and is a follow-on effort to the joint study by the PRPPWG and the SSCs carried out between 2007 and 2011.

As one of the measures identified by means of the preparatory questionnaire, in April 2017, the PRPPWG held a joint workshop with representatives of the six systems to provide an overview of the purpose and principles of PR&PP and to discuss developments and design changes that have occurred since 2011. Hosted by the NEA in Paris, the workshop saw also the participation of representatives of the IAEA and the GIF Senior Industry Advisory Panel (SIAP). During the workshop the SSCs and the PRPPWG presented the current status of the six GIF system concepts and of the PR&PP Evaluation Methodology and of its application to get a better understanding of the SSCs needs and to convey the existing methodology. In most cases, it was clear that the design options under consideration had changed since the issue of the PR&PP Compendium Report of Gen IV systems in 2011. The SSCs and the PRPPWG discussed the next steps to develop a regular and sustained interaction between the groups. The workshop paved the way to additional face-to-face interactions with the SSCs, possible updates to the PR&PP Methodology, and most importantly to the increased use of the methodology during the design process for each of the six GIF concepts. The participants agreed to update the Systems PR&PP white papers from 2011 to be consistent with the current scope of the SSCs, and the PRPPWG offered to engage with SSCs as much as possible where there is interest in more substantial interaction. Currently the white papers are being updated and the target is to produce an updated version in 2019.

V. Interactions with the IAEA

The PRPPWG has coordinated closely with the IAEA since its inception; i.e. there has always been an IAEA representative in the PRPPWG who has contributed to the work and direction of the group.

In terms of methodology development there has been considerable interaction between GIF and the IAEA’s INPRO program [24], beginning with a comparison of the respective PR methodologies [25] of the two organisations

with an aim towards understanding how prospective users could benefit from each or from a joint application of the approaches. INPRO projects, such as PRADA (Proliferation Resistance: Acquisition/diversion Pathways Analysis) [26] and PROSA (Proliferation Resistance and Safeguardability Assessment) as well as other IAEA projects in nuclear energy or safeguards [27], involved some experts that were also members of the GIF PRPPWG. This has provided a useful catalyst to further cooperation.

There are, in fact, several benefits that accrue from continued interaction between GIF and the IAEA, and there is a strong argument for the complementary nature of the two methodologies:

- The IAEA/INPRO methodology for non-proliferation provides “rules of good practice” for design concepts. It thus provides a checklist that ensures that technology assessors “did things right”.
- The GIF/PR&PP methodology is a systematic approach to evaluating vulnerabilities in designs. It thus provides the assessment approach that ensures that assessors “did not do things wrong”. Together, both products are potentially useful in national programs.

GIF-IAEA-INPRO Interface meetings were held yearly till 2017. The meetings were focused on exchange of information on the respective evaluation methodologies. GIF and the IAEA decided in 2018 to broaden the scope of these interface meetings for promoting GIF-IAEA wider interaction.

VI. Current Situation Assessment & near Future PR&PP Activities

Today the PR&PP methodology is likely the most comprehensive publicly available evaluation methodology for any nuclear technology – despite being developed specifically to meet GIF goals. The PR&PP methodology is reasonably complete as an overarching framework; however, specificity of techniques and applications are needed, primarily as determined by the user.

With the interaction with designers, a need has emerged for simplified scoping PR&PP evaluations. Such scoping applications are a valid application of the methodology, and in fact support the view that PR&PP can be implemented at the earliest stages of design when a focused and simplified approach is appropriate. The application of the PR&PP

methodology in Canada [15], was a pared down implementation in this category. The application of the PR&PP framework within the European CP-ESFR project is another example in this direction [17].

In the international safeguards community, the concept of “Safeguards by Design” (SbD) has emerged as a key “cultural shift” to be encouraged amongst designers, and as noted earlier GIF was one of the first development organisations to embrace this concept through its creation of the cross-cutting PRPPWG. There are ongoing and planned efforts both in national programs and internationally, by the IAEA and by the European Commission, to promote and implement SbD in the nuclear facility design process. IAEA has efforts underway on SbD. The IAEA published generic guidance document in 2013 [28] and the facility-specific documents dedicated to nuclear reactors [29], fuel fabrication plants [30], uranium conversion plants [31] and long term spent fuel management facilities [32] in 2014 through 2018. The IAEA will soon follow these documents up with facility-specific guidance for both enrichment and reprocessing facilities. These volumes provide guidance for all parts of the fuel cycle which GEN IV systems may need new and innovative conversion, fuel fabrication, enrichment, and recycling technologies depending on the design and use and demands for certain nuclear materials.

Robust safeguards are essential to the PR&PP characteristics of all of the emerging GIF designs. In conjunction with the PRPPWG effort with the SSCs, the PRPPWG will maintain cognisance of technology developments and good practices that would foster SbD in the GIF designs. Since the beginning, the PRPPWG acknowledged the importance of supporting designers in conceiving systems that could be efficiently and effectively safeguarded. Rev. 5 of the PR&PP Evaluation methodology introduced the concept of *Safeguardability* as “*the ease with which a system can be effectively [and efficiently] put under international safeguards*” [33] The concept gave light to various related investigation efforts inside and outside the PRPPWG [33-35]. While the Safeguardability concept is of narrower scope than the full PR&PP methodology, it can play an important role in the PR&PP by Design process and its analysis can be used to inform a full PR&PP study or, alternatively, a Safeguards by Design effort. Safeguards by Design, as noted, is an area the IAEA desires to reach out and assist the designers of nuclear facilities to integrate safeguards early in the design process and is an

area [36, 37] where the IAEA and PRPPWG can build relationships with the design teams.

In addition, it is important to maintain cognisance of post-Fukushima lessons-learned for their potential relevance to PR&PP and linkage of safety to security and safeguards. During the Fukushima Dai-ichi Nuclear Power Station (NPS) accident, the failures of the safety systems during the flooding of the plant caused catastrophic damage to the facility. The damage to the plant created radiation and other hazards and destruction to the fuel elements in the cores and in the spent fuel pools with the relocation of their nuclear materials as debris. This destruction deeply affected the safeguards and security systems. Damage to the surveillance cameras and sealing systems combined with high radiation levels and industrial hazards making areas of the plant inaccessible made monitoring and access of cores and spent fuel pools for safeguards and sensitive areas of the plant for security nearly impossible during the period of the accident and for a few weeks after the accident. This accident showed that site safeguards and security both need to have contingency plans for accident scenarios that allow for reverifying nuclear material damaged and made inaccessible for long periods and for maintaining security of the plant during the accident and recovery period to protect the plant's assets and the public from harm. Gen IV designers while pushing for robust designs also need to address potential scenarios after accidents to recover safeguards verification of nuclear materials and security of the site and its nuclear and radioactive materials.

The PR&PP evaluation methodology considers cyber threats a mode of attack or strategy in the domain of physical protection. The development of appropriate measures and metrics to characterise the robustness of a nuclear energy system against cyber threats extends beyond the traditional realm of physical security. In addition to theft of information cyber-attacks could lead to physical damages with radiological consequences. Cyber security is a topic area that highlights the interface between Safety and Security.

There is an increased emphasis worldwide on the development and deployment of small modular reactors (SMRs). Since some of the GIF designs are in the SMR category it is important for PRPPWG to maintain cognisance of SMR issues and developments as they pertain to PR&PP. While some SMRs share with

conventional reactors many characteristics of relevance to PR&PP, others – particularly those with advanced fuel cycles or those destined for remote operation – represent novel designs or implementations that will benefit from a consistent and comprehensive PR&PP evaluation at various stages of the design process.

To the extent that it is relevant to GIF designs, the PRPPWG will maintain cognisance of this area and enable the incorporation of robust PR&PP features in the SMRs. To have reasonable physical security force size and costs, SMRs must include design features that increase intrinsic security characteristics, such as use of passive safety systems, and take into consideration the possibility of a multi-unit site. The emergence of SMRs as a major design consideration in the second decade of GIF, with potential impact on the GIF designs themselves (particularly in scaling of designs, as required) indicates the importance of crosscutting evaluation methodologies that are as generic as possible. The flexibility allowing non-GIF users to apply the PR&PP methodology also maintains the methodology's relevance to GIF design teams as specifications change

The GIF Senior Industry Advisory Panel (SIAP) has developed a questionnaire for Gen-IV system review which has been successfully tested on two pilot cases submitted by VHTR SSC. PRPP related questions, not originally present in the questionnaire, were added to the questionnaire revision issued in late 2017.

Coordination with the Risk and Safety Working Group (RSWG) and with the Economics Modeling Working Group (EMWG) should be pursued to assure effective implementation of approaches in the GIF design. To this aim joint meetings have been organised by the RSWG and PRPPWG groups, with the decision to strengthen the collaboration by focusing on the interface between Safety and Security. In particular, one aim will be to identify the possible inconsistencies and conflicts between safety and PR&PP objectives, and to propose a way to deal with them.

VII. Outlook

In the next decade, most Gen IV systems will reach the performance phase, and one or more will enter in their demonstration phase. In the performance phase, a safeguards strategy and a physical protection strategy will have to be identified, with an estimate of the related cost for extrinsic features. In the demonstration

phase, the full approaches will have to be developed [1].

Going forward, the primary emphasis of the PRPPWG activity will be to support this by developing a sustained and structured interaction between the SSCs and PR&PP experts.

The PRPPWG will concentrate its future R&D activities on five broad goals, here substantiated with an indication of possible aspects that might have to be investigated:

To capture the salient features of the design concepts that impacts their PR&PP performance. As the design progresses, the room for major design modifications dictated by PR&PP requirements will shrink considerably. The PRPPWG will liaise with the SSCs to support their need to take the PR&PP of the systems design into account. With time, the analysis might shift its focus from design modification suggestions to highlighting the safeguards challenges that the designs entail, so that the safeguards community could be better informed on future safeguards R&D needs. This might require the development of a different or complementary approach to the analysis of the GIF design. Collaboration with the IAEA will be essential.

To facilitate PR&PP crosscutting studies of relevance for several of the Generation IV systems. While every GIF design concept has unique design characteristics and peculiarities, there are aspects that are common to two or more design concepts. It is important to be able to address them in an effective, efficient and consistent way. Areas where ad hoc methodological R&D might be needed could include the analysis of a) the Gen IV systems fuels with potential similarities and b) the common nuclear fuel cycle front-end and back-end steps of the fuel cycles with which they will operate.

To identify insights for enhancing PR&PP characteristics of future nuclear energy systems. The PRPPWG foresees the in depth application of the "PR&PP-by-design" concept to at least one of the SSC designs. This would be done cooperatively between the PRPPWG and the particular designers.

The SSCs expressed the wish that PR&PP design guidelines might be developed to help systems designers incorporating PR&PP features into the design from the early design stages. Collaboration with the IAEA will be essential also in this respect as IAEA Safeguards by

Design outreach to designers is a leading safeguards initiative. Furthermore, PRPPWG through interactions and inputs received by SSCs, can provide the IAEA with insights on emerging GEN IV technologies needing development of new safeguards technologies and approaches.

PR&PP aspects are intertwined with many other aspects related to the other three GIF goals in which the design concepts will have to excel. An area where important synergies could be exploited is the interface between safety and security. Together with the Risk and Safety Working Group, a potential R&D area is to further investigate this interface and propose methods to correctly address it.

To foster the implementation of a PR&PP culture into the earliest phases of design. To meet this challenge, it is important to make sure that PR&PP is addressed in the right way at the right stage of each of the system's conception, design and construction. Not all the PR&PP aspects are to be taken into account at the same moment or within the same design stage, and as the design matures the focus will have to move from one set of aspects to another one. There might be a need to further investigate what aspects are to be addressed at which design stage and how to do it in order to maximise effectiveness and synergy with the rest of the design activities.

To keep cognisance of and to benefit from PR&PP activities outside GIF. There are several international initiatives outside GIF in the PR and PP areas. It is important that the PRPPWG will continue to maintain cognisance and, where possible, interaction with these activities and, when needed, include and adapt relevant findings and methods to make them useful for GIF designers.

The PRPPWG expects that all these activities will lead to a refinement of the PR&PP evaluation methodology and its application. This will streamline and focus the approach to PR&PP aspects to address issues of interest to the GIF and thus enhance decision making in the GIF program. Last but not least, PRPPWG will continue to seek opportunities to work on cross-cutting issues within GIF that will enable sound and robust designs.

VIII. Conclusion

The PRPPWG has developed an evaluation methodology that likely represents the most comprehensive publicly available PR&PP tool

that can inform the design process of any nuclear technology. This paper has summarised first the technical progress and the major accomplishments of the PRPPWG: the evaluation methodology and the ESFR case study used to develop and test the methodology. The interaction with the GIF System Steering Committees and the relaunching of the activity was then presented. Finally, an outline of the future challenges was provided along the lines identified in the GIF 2018 R&D outlook.

The PRPPWG will continue to work with the SSCs to implement pilot applications of the PR&PP methodology, as well as maintain cognisance of international developments and engagement with other groups within the international non-proliferation community. The PR&PP methodology will be maintained as necessary to retain its relevance and applicability to the development of new and emerging nuclear systems, primarily within GIF but also for the broader nuclear community.

Acknowledgements

The efforts and ideas of the many members and observers of the PR&PP working group over the past dozen years are the foundation of this summary paper which builds on and updates previous papers [6-10]. The full list of authors and contributors to the PR&PP methodology

appears in its rev. 6 report [3]. The corresponding authors would like to thank all the other PRPPWG members and observers: J. Bolholo (NECSA, South Africa), K.K. Choe (KINAC RoK), B. Cipiti (Sandia, US), S.H. Jeong (KINAC, RoK), H. Liu (CIAE, China), J.H. Ku (KAERI, RoK), G. Pshakin (IPPE, Russia), T. Shiba (JAEA, Japan), L. Wang (SNSTC, China), Y. Zhao (CIAE, China), B. Zong (SNSTC, China).

Nomenclature

EMWG	Economics Modelling Working Group
ESFR	Example Sodium Fast Reactor
SbD	Safeguards by Design
SSCs	System Steering Committee(s)
GIF	Generation IV International Forum
PRPPWG	Proliferation Resistance and Physical Protection Working Group
IAEA	International Atomic Energy Agency
RSWG	Risk and Safety Working Group
SMRs	Small Modular Reactor(s)
SIAP	Senior Industry Advisory Panel

References

- [1] GENERATION IV INTERNATIONAL FORUM (GIF), "A Technology Roadmap for Generation IV Nuclear Energy Systems", GIF-002-00, (2002). Available at: https://www.gen-4.org/gif/jcms/c_9352/technology-roadmap. Updated in 2014: https://www.gen-4.org/gif/jcms/c_60729/technology-roadmapupdate-for-generation-iv-nuclear-energysystems
- [2] GIF PRPPWG, "ESFR Case Study Report", GIF/PRPPWG/2009/002, (2009). Available at: https://www.gen-4.org/gif/jcms/c_40415/esfrcase-study-report
- [3] GIF PRPPWG, "Evaluation Methodology for Proliferation Resistance and Physical Protection of Generation IV Nuclear Energy Systems", Rev. 6, GIF/PRPPWG/2011/003 (2011). Available at: https://www.gen-4.org/gif/jcms/c_9365/prpp
- [4] GIF PRPPWG, "Proliferation Resistance and Physical Protection of the Six Generation IV Nuclear Energy Systems", GIF/PRPPWG/2011/002, (2011). Available at: https://www.gen-4.org/gif/jcms/c_9365/prpp
- [5] AMERICAN NUCLEAR SOCIETY, "Special Issue on Safeguards", Nuclear Technology, 179(1), (2012).
- [6] BARI, R.A., WHITLOCK, J.J., THERIOS, I.U., PETERSON, P.F., "Proliferation Resistance and Physical Protection Working Group: Methodology and Applications." in

- proceedings of GIF Symposium, San Diego, CA, USA, 14-15 November 2012.
- [7] J. WHITLOCK, et al., "Status of the Gen-IV Proliferation Resistance and Physical Protection (PR&PP) Evaluation Methodology," Proc. IAEA Symposium on International Safeguards: Linking Strategy, Implementation and People, CN-220-289, IAEA, Vienna, (2014).
- [8] J. CAZALET et al., "Status of the Generation IV Proliferation Resistance and Physical Protection (PR&PP) Evaluation Methodology", Paper 5460, Proc. of Global 2015, September 20-24, 2015, Paris (France), (2015).
- [9] G. COJAZZI et al, "The GIF Proliferation Resistance and Physical Protection (PR&PP) Evaluation Methodology: Status and Outlook," Proceedings of Advances in Nuclear Nonproliferation Technology and Policy Conference: Bridging the Gaps in Nuclear Nonproliferation. September 25-30, 2016, Santa Fe, NM, USA
- [10] CHEBESKOV A., COJAZZI G.G.M., BARI R., WHITLOCK J., PETERSON P., CAZALET J., KWON E., HORI K., The GIF Proliferation Resistance and Physical Protection (PR&PP) Evaluation Methodology: Status, Applications and Outlook. International Conference on Fast Reactors and Related Fuel Cycles: Next Generation Nuclear Systems for Sustainable Development (FR17). June 26-29, 2017, Yekaterinburg, Russian Federation.
- [11] R. BARI, et al., "Proliferation Risk Reduction of Alternative Spent Fuel Processing Technologies," Proc. 50th Annual Meeting of Institute of Nuclear Materials Management (INMM), (2009).
- [12] M. ZENTNER, et al., "An Expert Elicitation Based Study of the Proliferation Resistance of a Suite of Nuclear Power Plants," Proc. 51st Annual Meeting of Institute of Nuclear Materials Management (INMM), Baltimore, MD, USA, (2010).
- [13] GLASER, L. B. HOPKINS, M. V. RAMANA, "Resource Requirements And Proliferation Risks Associated With Small Modular Reactors," Nuclear Technology, 184, 121, (2013).
- [14] M. YUE, L.-Y. CHENG, R. A. BARI, "A Markov Model Approach to Proliferation-Resistance Assessment of Nuclear Energy Systems," Nuclear Technology, 162, 26 (2008); see also M. YUE, L.-Y. Cheng, and R. A. Bari, "Relative Proliferation Risks for Different Fuel Cycle Arrangements," Nuclear Technology, 165, 1 (2009).
- [15] J. WHITLOCK, "Incorporating the GIF PR&PP Proliferation Resistance Methodology in Reactor Design", Proc. 51st Annual Meeting of Institute of Nuclear Materials Management (INMM), Baltimore, MD, USA, (2010).
- [16] F. ROSSI, "Application of the GIF-PR&PP methodology to a fast reactor system for a diversion scenario," Proc. IAEA Symposium on International Safeguards, Vienna, (2014), See also ESARDA Bulletin, 52, p. 98-113-143, (2015).
- [17] G. RENDA, G. COJAZZI, F. ALIM, "Proliferation Resistance and Material Type Considerations within the Collaborative Project for a European Sodium Fast Reactor." EUR 26996, JRC92844. Publications Office of the European Union, Luxembourg, Luxembourg, (2014). Also in ESARDA Bulletin 52, p. 124-143, (2015).
- [18] R. ROSSA, K. VAN DER MEER, A. BORELLA, "Application of the PR&PP methodology to the MYRRHA research facility", ESARDA Bulletin, 49, p. 82-94 (2013).
- [19] S.K. AHN, E.H. KWON, H.L. CHANG, H.D. KIM, "A proliferation resistance evaluation for a pyroprocessing facility design", INMM 55th Annual Meeting (2014).
- [20] GIF PRPPWG, "Bibliography", Revision 06, (2018). available at: https://www.gen-4.org/gif/jcms/c_101559/gif-prppwg-bibliography-rev06-2018-07-18-final
- [21] GIF PRPPWG "Workshop on the PR&PP Methodology for Generation IV Nuclear Energy Systems", Univ. of California, Berkeley, California November 4 2015, https://www.gen-4.org/gif/upload/docs/application/pdf/2015-11/prppwg_nov_2015_2015-11-20_14-39-49_203.pdf
- [22] GIF PRPPWG "International Workshop on the Proliferation Resistance and Physical Protection Evaluation Methodology for Generation IV Nuclear Energy Systems", Jeju Island, Republic of Korea, October 12 2016, https://www.gen-4.org/gif/jcms/c_87571/prppwg-presentations-seoul-2016
- [23] GIF PRPPWG, "Frequently Asked Questions (FAQ) on Proliferation Resistance and Physical Protection", available at:

- https://www.gen-4.org/gif/jcms/c_44998/faqon-proliferation-resistance-and-physicalprotection
- [24] IAEA, "Guidance for the Application of an Assessment Methodology for Innovative Nuclear Energy Systems, INPRO Manual – PR", IAEA-TECDOC-1575 Rev.1, Vol. 5, Vienna, November (2008).
- [25] G. POMEROY, et al., "Approaches to Evaluation of Proliferation Resistance of Nuclear Energy Systems," Proc. 49th Annual Meeting of Institute of Nuclear Materials Management (INMM), Nashville, TN, USA, (2008).
- [26] IAEA, "INPRO Collaborative Project: Proliferation Resistance: Acquisition/diversion Pathways Analysis (PRADA)", IAEA TECDOC-1684, Vienna, (2012).
- [27] IAEA, "Options to Enhance Proliferation Resistance of Innovative Small and Medium Sized Reactors", IAEA, Nuclear Energy Series, NP-T-1.11, Vienna, (2014).
- [28] IAEA, "International Safeguards in Nuclear Facility Design and Construction", IAEA Nuclear Energy Series, NP-T-2.8, Vienna, (2013).
- [29] IAEA, "International Safeguards in the Design of Nuclear Reactors", IAEA, Nuclear Energy Series, NP-T-2.9, Vienna, (2014).
- [30] IAEA, "International Safeguards in the Design of Fuel Fabrication Plants", IAEA, Nuclear Energy Series, NF-T-4.7, Vienna, (2017).
- [31] IAEA, "International Safeguards in the Design of Uranium Conversion Plants", IAEA, Nuclear Energy Series, NF-T-4.8, Vienna, (2017).
- [32] IAEA, "International Safeguards in the Facilities for Long Term Spent Fuel Management", IAEA, Nuclear Energy Series, NF-T-3, Vienna, (2018).
- [33] GIF PRPPWG, Evaluation Methodology for Proliferation Resistance and Physical Protection of Generation IV Nuclear Energy Systems, Technical Addendum to Revision 5, January 31, 2007, Revised April 13, 2007, GIF/PRPPWG/2006/005-A.
- [34] COJAZZI, G.G.M., RENDA, G., SEVINI, F., Proliferation Resistance Characteristics of Advanced Nuclear Energy Systems: a Safeguardability Point of View. ESARDA Bulletin - Special Issue on Proliferation Resistance (39), p. 31-40, (2008).
- [35] BARI R.A., HOCKERT, J., WONDER, E.F., JOHNSON, S.J., WIGELAND, R., ZENTNER, M.D, Overview of the Facility Safeguardability Analysis (FSA) Process. PNNL-21698, Pacific Northwest National Laboratory, Richland, WA, (2012).
- [36] POIRIER, S., Lessons Learned from Safeguards Implementation for Facilities under Construction, Proceedings of the Fourth International Conference on Nuclear Power Plant Life Management, 23–27 October 2017 -Lyon, France.
- [37] POIRIER, S., J. WHITLOCK, B. BOYER, Safeguards Considerations in the Design of Nuclear Facilities, Proceedings of the Fourth International Conference on Nuclear Power Plant Life Management, 23–27 October 2017 - Lyon, France.
- [38] GENERATION IV INTERNATIONAL FORUM (GIF), "GIF R&D Outlook for Generation IV Nuclear Energy Systems: 2018 Update", to be published.

REPORT ON MANUFACTURING EXPERIMENTAL APPARATUS TO INVESTIGATE SWR PHENOMENON IN THE PCSG (S. SEO ET AL)

Siwon Seo ^(1,2), Jaeyoung Lee ⁽²⁾, Sangji Kim ^{(3)*}

(1) Atomic Creative Technology Co., Ltd., Republic of Korea

(2) School of Control and Mechanical Engineering, Handong Global Univ., Republic of Korea

(3) Korea Atomic Energy Research Institute, Republic of Korea

Abstract

The Sodium-cooled Fast Reactor (SFR) is one of the most promising Generation-IV nuclear reactors. Unfortunately, the SFR has possibility of the sodium-water reaction (SWR) inherently because two fluids (water and liquid sodium) exchange heat each other through heat transfer tube wall in steam generator (SG). So developing methodologies to reduce probability of the SWR accident and limit the SWR consequences are important. Until now, some approaches such as double walled SG tubes and using a Brayton cycle are suggested and studied. However, some problems such as degraded heat transfer efficiency and increased fabrication cost exist in the double walled approach. Heat transfer efficiency problem also exists in the Brayton cycle. Using a PCSG (Printed Circuit Steam Generator) could be good approach to reduce probability of the SWR and to limit the SWR consequences.

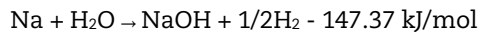
The PCSG is being considered as one of the candidate SGs to substitute conventional shell and tube SG in Korea due to safety and economic characteristics of the PCSG. The PCSG has much higher heat transfer surface area to volume ratio than the conventional shell and tube SG. It means the PCSG has high heat transfer efficiency. And if the shell and tube type SG can be replaced to the PCSG, size of the SG can be decreased considerably. Also manufacturing costs can be reduced. Although advantages of the PCSG comparing with the conventional SG are not only economics but also safety, integrity, performance, and reliability, only a safety feature of the PCSG against the SWR will be dealt with in this study.

The most limiting case of the SWR occurred in shell and tube SGs is multiple tube failure. If the SWR occurs, steam jet discharged into sodium pool can attack neighboring tubes. In this case, they could be damaged by corrosion and erosion. However, it could be indicated that, even if the second wall of the sodium channel is damaged by the SWR due to a leak through the first wall, there will be no propagation to the other channels. Very short target distance and absence of sodium pool could be expected as reasons of the SWR resistance of the PCSG. Objective of this work is showing that the PCSG has the SWR resistance. Manufacturing of experimental apparatus have been completed for this purpose and now it is tested by using water and sodium simulant. In this paper, only concept and design of experimental apparatus, and manufacturing status will be addressed. Experiment will be performed at the end of July or beginning of August, 2018.

I. Introduction

The Sodium-cooled Fast Reactor (SFR) is one of the most promising Generation-IV nuclear reactors. The SFR is liquid metal reactor using sodium as a coolant. Typically, two fluids (water and liquid sodium) exchange heat each other through heat transfer tube wall in a steam

generator (SG). For this reason, the SFR has possibility of sodium-water reaction (SWR) inherently. If boundary between sodium and water, in case of steam generator tube, is ruptured by any reason, sodium and water will contact. Then exothermic chemical reaction will occur according to mainly the following chemical formula [1].



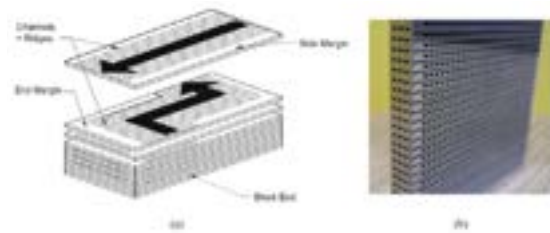
If SWR is happened, pressure and temperature in SG are increased because of highly exothermic reaction. And SG integrity is degraded by reaction product, NaOH, due to its corrosive property. In addition, hydrogen is generated by this chemical reaction. The SG integrity is severely threatened by the hydrogen explosion if venting of SG cannot be implemented. For these reasons, the SWR have always been a safety issue of the SFR. So, developing approaches to reduce probability of the SWR accident or limit the SWR consequence are very important. Until now, many researches [2~11] for prevention, detection, and mitigation of SWR have been performed to overcome this inherent risk. In point of design, two approached are suggested and studied to totally prevent the SWR. These methodologies are double walled SG tubes [12] and using a Brayton cycle [13] suggested in JSFR and ASTRID, respectively. However, some problems such as reduced heat transfer efficiency and increased fabrication cost exist in the double walled approach. Heat transfer efficiency problem also exists in the Brayton cycle. Using a PCSG (Printed Circuit Steam Generator) could be good approach to reduce probability of the SWR and to limit the SWR consequence.

The PCSG is a kind of PCHEs (Printed Circuit Heat Exchanger). The PCHE is manufactured by using diffusion bonding between chemically etched steel plates. Etching channels on steel board are shown in Figure 1. Schematic and cross-section of the PCHE are shown in Figure 2 [14].

Figure 1. PCHE platelet configuration



Figure 2. (a) plate stacking for diffusion bonding, (b) bonded printed circuit core



The PCSG is being considered as one of the candidate SGs to substitute the shell and tube SG in Korea due to safety and economic characteristics of the PCSG. The PCSG has much higher heat transfer surface area to volume ratio than the conventional shell and tube SG. It means the PCSG has high heat transfer efficiency. And size of the SG can be decreased considerably. Also manufacturing costs can be reduced. Although advantages of the PCSG comparing with the conventional SG are not only economics but also safety, integrity, performance, and reliability, only a safety feature of the PCSG against the SWR will be dealt with in this study. The PCSG could be expected to have strong points against the SWR accident comparing with shell and tube SGs. These expected advantages are as follows.

- Exclusion of damage propagation by impingement wastage
- Effective accident management by modularization of the PCSG
- Low background noise caused by laminarisation of SG flow due to small size tubes can facilitate acoustic detection of SWR.

Among above advantages, exclusion of damage propagation by impingement wastage and acoustic detection will be demonstrated by the experimental study. In this paper, only concept and design of experimental apparatus and manufacturing status will be addressed. Concept and design of the test facility will be expressed in chapter II. In chapter III, it will be explained that how experimental conditions are derived. Manufacturing status of the experimental apparatus also will be addressed in chapter IV. Finally, Chapter V summarises the these all processes.

II. Design of the Test Facility

Designed PCSG is shown in Figure 3, (a). Sodium flow directs from upper nozzle to lower nozzle of the PCSG (red arrows in Figure 3, (a)). Water flows into bottom side of the PCSG and steam is discharged from top side of the PCSG (blue arrows in Figure 3, (a)).

Figure 3. Designed PCSG (a), schematic of the SWR in the PCSG (b).

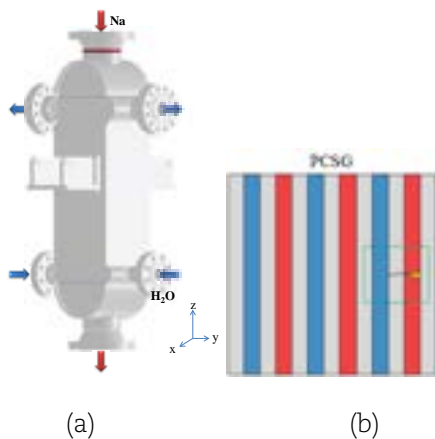
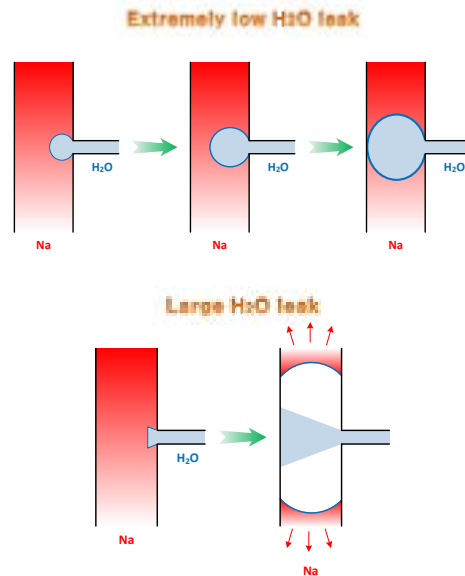


Figure 3, (b) represents cross-sectional area (y - z plane) of the PCSG and schematic of the SWR in the PCSG. Yellow indicates discharged steam. Water and sodium channels are expressed by blue and red respectively. Gray is body of the PCSG. Pressurised water can be discharged into the sodium tube when crack is generated between sodium side and water side. It is depicted in green dotted-line of Figure 3, (b).

If the SWR occurs, physical phenomenon in failed sodium channel depends on crack size dominantly. Expected physical phenomenon is described in Figure 4. If leak rate is extremely low, small size bubble (diameter < 4 mm) and slug could be formed in sodium tube. In this case, SWR can occur inside of the sodium tube. Corrosive reaction product, NaOH, might be generated near the sodium tube wall and crack tip. It causes impingement wastage and self-wastage. If larger crack is generated between sodium and water channel than previous case, high pressurised water can be discharged into the sodium channel. And sodium is expelled to both ends of the channel. In this case, SWR occurs in header of the PCSG, not inside of the sodium channel. Experimental apparatus is designed to identify these phenomena and to measure extent of wastage.

Figure 4. Expected two-phase (steam and liquid sodium) flow pattern forming by the SWR in the PCSG



Design of the test section of the apparatus is shown in Figure 5. Vertical and horizontal pipe of the test section represent sodium and water channel, respectively. Rupture disc is mounted between sodium side and water side. If pressure higher than 10 bar is exerted on the rupture disc, it is partially torn. Then pressurised water injected into the sodium channel through torn rupture disc and small hole.

Figure 5. Test section modeling and design

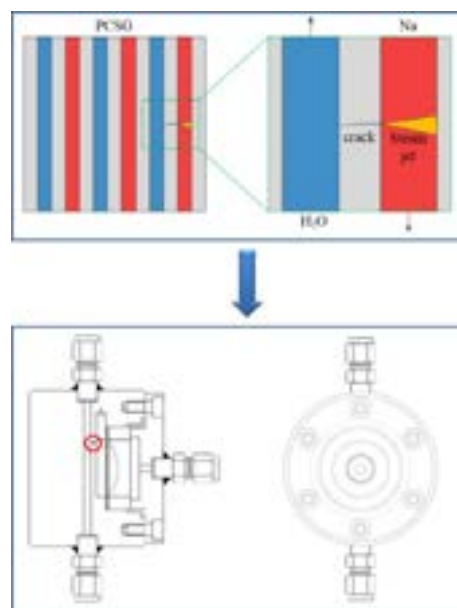
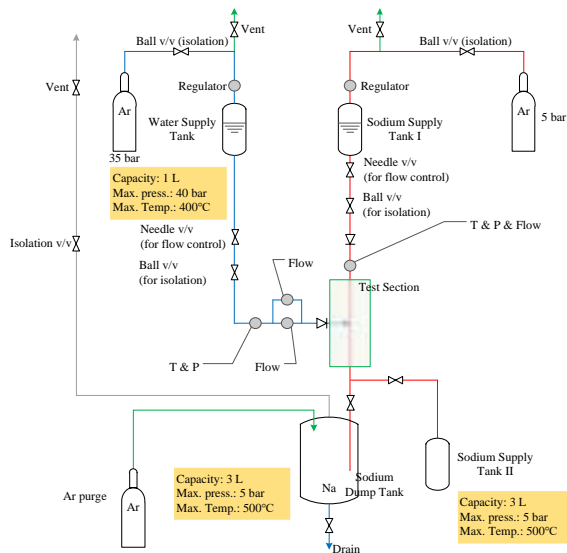


Figure 6. Result of rupture disc test



Some extra space between sodium pipe and rupture disc must be existed because opening of the rupture disc. In this test section, gap of the extra space is 5 mm. And this value which is minimum gap to tear rupture disc properly is determined through test. Test result is shown in Figure 6. In this test, it is confirmed that diameter of holes smaller than 1 mm are generated (red circle in Figure 6) when high pressure exerted on the rupture disc. Piping, tanks, and many measuring instruments are also designed as shown in Figure 7.

Figure 7. Schematic of the SWR experimental apparatus



III. Experimental Condition

III.1 Failure location of the PCSG

It is reported that most SG tube failures in SFR had occurred at welding area between tube sheet and U-tube. In practice, total five SWR

accidents occurred in Phenix during its life time [15]. First four accidents are happened by fatigue crack at welding area. These examples are for shell and tube type SG.

However, the PCSG is different from the conventional SG. There is no experience of applying PCSG to the SFR. There are no research results about the SWR in the PCSG. So there is no report about possible location of the SWR in the PCSG. Theoretically, possible reason of the boundary failure between sodium and water is stress by high pressure difference. Stress formula used to estimate mechanical integrity of the PCSG is as follow [16].

$$E = \Delta P \left(\frac{1}{N \cdot t} - 1 \right) \text{ (Eq. 1)}$$

E is stress exerted on heat transfer wall. ΔP is pressure difference between two fluids. N and t are the number of channel wall per unit length and wall thickness between two fluids, respectively. Minimum wall thickness and pitch for maintaining mechanical integrity under operating condition can be derived by using above formula. Maximum allowable stress is fixed according to materials. N and t are also fixed value by design of the PCSG. It means possibility of the failure between sodium and water channel is maximised in maximum pressure difference region of the PCSG.

Typically, the highest pressure difference is applied at water inlet region of the PCSG. Generally, operating pressure of the water inlet and sodium outlet are approximately 180 and 1 bar, respectively. Therefore, operating conditions of the water inlet region of the PCSG will be considered as test conditions of this experiment. Operating conditions of the PCSG are presented in table 1.

Table 1. Operating conditions of the PCSG

Input Parameters	Water side	Sodium side
Press. (MPa)	18 ~ 16.7	0.5
Temp. (°C)	240 ~ 503	528 ~ 332
Flow rate (kg/s) (single channel)	0.001483	0.0229

III.2 Temperature condition

Temperature conditions of water inlet and sodium outlet of the PCSG are 240°C and 332°C, respectively. Fluid components such as flow

meter and valves must be selected to meet these temperatures. In this test facility, flow meters that can be operable at 400°C are selected. And rated temperature of selected valves is minimum 350°C.

III.3 Pressure condition

Operating pressure of water inlet region is very high (18 MPa), whereas size of reaction zone of this experimental apparatus is small. Sodium channel diameter is just 4 mm and planned to use sodium less than 2 kg. Generally, size of fluid components tend to increase as operating pressure and temperature are increased. It means that it is very hard to apply high pressure and temperature to small size apparatus. Therefore, lower pressure than operating one should be applied in this experiment.

In case of the SWR, choked flow is formed in sodium channel because high pressurised water is injected into the almost non-pressurised sodium channel. Critical mass flux can be expressed by following formula [17].

$$G = \rho_0 \sqrt{2c_p T_0 \left[\left(\frac{P_b}{P_0} \right)^{\frac{2}{\gamma}} - \left(\frac{P_b}{P_0} \right)^{\frac{\gamma+1}{\gamma}} \right]} \quad (\text{Eq. 2})$$

γ is specific heat ratio and is expressed by c_p/c_v . P_b and P_0 are the downstream (i.e., sodium channel) and the upstream (i.e., water channel) pressure, respectively. The mass flux varies with the ratio P_b/P_0 so long as the downstream pressure, P_b , is higher or equal to a critical pressure (P_{cr}). For lower values of P_b than critical pressure, the mass flux stays constant. The value of critical pressure can be obtained by differentiating G of above formula with respect to pressure.

$$\frac{\partial G}{\partial P} = 0 \quad (\text{Eq. 3})$$

which leads to

$$\left(\frac{P_b}{P_0} \right) = \left(\frac{2}{\gamma+1} \right)^{\frac{\gamma}{\gamma-1}} \quad (\text{Eq. 4})$$

If pressure of sodium channel is 5 bar and heat capacity ratio (γ) with steam at 100°C is 1.324, following critical pressure can be obtained.

$$\left(\frac{P_b}{P_0} \right)_{cr} = \left(\frac{2}{1.324} \right)^{\frac{1.324}{0.324}} = 0.5414 \quad (\text{Eq. 5})$$

$$P_0 = \frac{1}{0.5414} P_b = 9.2653 \text{ bar}$$

As a result of above calculation, higher pressure than about 10 bar must be applied to the water side of the test apparatus to form a choked

flow. Saturation pressure at 240°C (water inlet temperature of the PCSG) is 33.4 bar. It means water side pressure of this experiment is at least above 33.4 bar to maintain liquid phase at 240°C. Therefore, 35 bar will be applied to water side of the experiment apparatus.

III.4 Preliminary test matrix

In summary, following experimental conditions, Table 2, will be applied to the test. Three kinds of hole will be prepared. In addition, tests with various flow rate under the same hole size will be performed. So, discharged steam flow rate effect on wastage rate will be checked.

Table 2. Preliminary test conditions of the SWR test in the PCSG

Test No.	Water Side Press (MPa)	Water side Temp. (°C)	Sodium Side Press (MPa)	Sodium side Temp. (°C)	Hole size (I.D., mm)
Test A1	3.5	240.0	0.5	332.0	Crack
Test A2					0.2
Test A3					0.3

IV. Manufacturing the SWR Test Facility

Figure 8. The front view of the experimental apparatus



According to above experimental condition, appropriate components are selected. And now, manufacturing experimental apparatus is finished. Various tests such as pressure and sealing test, temperature test and so on are performing now. The front view of finished apparatus is shown in Figure 8.

Two tanks (blue box in Figure 9) located above glove box is storage tank. Left and right tank are water storage tank and sodium storage tank, respectively. These two tanks are enveloped by heater. And pneumatic isolation valves are installed at downstream of two tanks. Sodium and water pipe (orange box in Figure 9) are located in the glove box for safety. Flow meters, thermocouples, and manometers are mounted on the both side piping. Sodium dump tank and sodium storage tank II (red box in Figure 9) is located beneath the glove box. These main components are assembled into a SWR test facility. Control panel and Control PC screen are presented in Figure 10.

Figure 9. Main components of the SWR test facility



Figure 10. Control Panel and monitoring system



V. Conclusion

An experimental apparatus is designed and manufactured to verify the safety feature of the PCSG against the SWR. To show it, impingement wastage rate will be measured to confirm expected wastage resistance of the PCSG. Also acoustic signals will be measured to estimate feasibility of the acoustic detection

system for the PCSG. Manufacturing experimental apparatus had been completed. Now, various tests excluding sodium are performing. Tests including sodium will be performed after all preliminary tests are completed. The SWR in the PCSG is not studied until now. Therefore, it is expected that safety feature of the PCSG is verified through this experimental study.

Acknowledgements

This work was supported by the National Research Foundation of Korea (NRF) grant funded by the Korea government (MSIP). (No.2017M2A8A4018812 and No.2017M2A8A4018812).

Nomenclature

SFR	Sodium-cooled Fast Reactor
SG	Steam Generator
SWR	Sodium-Water Reaction
PCSG	Printed Circuit Steam Generator
PCHE	Printed Circuit Heat Exchanger

References

- [1] Baldev Raj, P. Chellapandi, P. R. Vasudeva Rao, Sodium Fast Reactors with Closed Fuel Cycle, CRC Press, 2015.
- [2] H. V. Chamberlain, Project Summary – Sodium-Water Reactions Related to LMFBR Steam Generators, APDA-257, Atomic Power Development Associates, 1970.
- [3] N. Kanegae et al., Wastage and self-Wastage Phenomena Resulting from Small Leak Sodium-Water Reaction, PNC TN941 76-27, Power Reactor & Nuclear Fuel Development Corporation, 1976.
- [4] M. Nisimura et al., Sodium-Water Reaction Test to Confirm Thermal Influence on Heat Transfer Tubes, PNC TN9400 2003-014, Power Reactor & Nuclear Fuel Development Corporation, 2003.
- [5] K. Shimoyama, Wastage-Resistant Characteristics of 12Cr Steel Tube Material, PNC TN9410 2004-009, Power Reactor & Nuclear Fuel Development Corporation, 2004.
- [6] Y. Deguchi et al., Experimental and Numerical Reaction Analysis on Sodium-Water Chemical Reaction Field, Mechanical Engineering Journal Vol.2, No.1, 2015.
- [7] S. Kishore et al., An Experimental Study on Impingement Wastage of Mod 9Cr 1Mo Steel due to Sodium Water Reaction, Nuclear Engineering and Design 243 (2012) 49-55
- [8] S. Kishore et al., Impingement Wastage Experiments with 9Cr 1Mo Steel, Nuclear Engineering and Design 297 (2016) 104-110
- [9] H. Nei et al., Acoustic Detection for Small leak Sodium-Water Reaction, Journal of Nuclear Science and Technology, 14(8) 558-564, 1977.
- [10] Acoustic Signal Processing for the Detection of Sodium Boiling or Sodium-Water Reaction in LMFRs, IAEA-TECDOC-946, 1997.
- [11] T. Kim, J. Jeong, S. Hur, Performance Test for Developing the Acoustic Leak Detection System of the LMR Steam Generator, Transaction of the KNS Autumn Meeting, 2005.
- [12] Mari Marianne Uematsu et al., Comparison of JSFR design with EDF requirements for future SFR, Journal of Nuclear Science and Technology, Vol. 52, No. 3, pp.434-447, 2015.
- [13] D. Plancq et al., Progress in the ASTRID Sodium Gas Heat Exchanger development, IAEA-CN245-286. 2017.
- [14] J. Nestel et al., ASME code consideration for the compact heat exchanger, ORNL/TM-2015/401, 2015.
- [15] J. Guidez, G. Prele, Superphenix: technical and scientific achievements, 2017.
- [16] Hesselgreaves, J. E., "Compact Heat Exchangers: Selection, Design and Operation (2nd)", Pergamon Press, 2001.
- [17] N. E. Todreas, M. S. Kazimi, "Nuclear System I – Thermal Hydraulic Fundamentals", 1989.

STUDY ON RISK ANALYSIS METHODOLOGY OF FIRE BARRIER FAILURE CAUSED BY SEISMIC-INDUCED SODIUM FIRE IN SODIUM FAST REACTOR (J. JIANG ET AL)

Jiang Jingke, Wang Mingzheng, Yan Han

China Institute of Atomic Energy, China

Abstract

The Fukushima accident warns that the risk of multiple hazards occurring requires deeper insights. The presentation considers the risk and safety of seismic-sodium fire in a Sodium Fast Reactor (SFR). Combining existing seismic probabilistic safety analysis (PSA) with fire PSA methodology in pressurised water reactor (PWR), the correlation between seismic and sodium fire is studied, and the methodology is proposed for quantifying the risk level of fire barrier failure caused by seismic induced sodium fire in a SFR room.

I. Introduction

In 2011, an earthquake measuring 9.0 on the Richter scale occurred in Fukushima Prefecture, Japan. This seismic induced huge tsunami. Finally, the seismic-induced tsunami event caused core damage and radioactive release in the Fukushima nuclear power plant. The lessons learned from this accident shows that an external event can cause serious consequences, so the risk of multiple events cannot be ignored, even the occurrence frequency is low.

After the Fukushima nuclear accident, the nuclear industry at home and abroad began to pay more attention to considering the risk of multiple hazards, such as seismic-induced fire, seismic-induced flood, seismic-induced tsunami, and so on. [1] Many countries, the United States, Japan, and China, have successively conducted research work about safety analysis for multiple hazards in nuclear power plant. The study of PSA methodology with an external event and a multiple hazard has become an important research direction in reactor safety research.

The SFR uses metal sodium as coolant. Liquid metal sodium exists in pipelines or equipment. Sodium leakage may cause sodium fire accident.

Under seismic conditions, the possibility of sodium leakage will increase, and seismic-induced sodium fire is likely to occur, which may eventually cause core damage or other serious consequences in a nuclear power plant. Therefore, it is necessary to investigate the risk of seismic-induced sodium fire in SFR.

Based on the existing seismic PSA and fire PSA standards and guides in PWR, this paper analyses the correlation of seismic-induced sodium fire and identifies some key steps of risk analysis of seismic-induced sodium fire in a SFR sodium room. Finally, the paper proposes a set of procedure for the risk analysis of fire barrier failure caused by seismic-induced sodium fire in a SFR sodium room.

II. Seismic-induced Sodium Fire Correlation Analysis

The cause of sodium fire is sodium leakage. In the process of sodium fire risk analysis, it can be conservatively assumed that if sodium leaks, sodium fire will inevitably occur. Seismic could cause sodium leaks (or breaks) in sodium-related equipment and pipelines and induces sodium fire. This section analyses the seismic PSA process provided in related guides and the fire PSA process provided in the fire PSA guide NUREG-6850 to determine whether these sub-

tasks need to be implemented in the risk analysis of seismic-induced sodium fire in a SFR sodium room. [2]With analysing the correlation between seismic and sodium fire, the analysis results are shown in Table 1.

Table 1. Seismic-induced sodium fire correlation analysis

The sub-tasks of seismic PSA or fire PSA	Seismic-induced sodium fire correlation analysis
Seismic PSA sub-tasks	
Seismic hazard curve	Seismic hazard curve reflects the frequency of seismic, which is the initiation event of seismic-induced sodium fire. The sub-task should be as the sub-task of the risk analysis of seismic-induced sodium fire.
Component fragility analysis	Component fragility analysis is to know component failure condition probability under seismic condition. It should be implemented in the risk analysis of seismic-induced sodium fire.
Power plant response	This sub-task should be considered in the risk analysis of seismic-induced sodium fire. As seismic PSA plant response, it should be integrated with fire PSA plant response.
Fire PSA sub-tasks	
Task 1: Determining the analysis boundary and fire compartment	Nuclear power plant system is as analysis unit in seismic PSA, and fire compartment is as analysis unit in fire PSA. Seismic-induced sodium fire risk analysis should select the most convenient analysis unit, and it is proposed to make fire compartment as analysis unit.
Task 2: Screening fire PSA components	Seismic-induced sodium fire risk analysis should consider and screen fire PSA components and seismic PSA components.
Task 3: Screening fire PSA cables	Seismic-induced sodium fire risk analysis should consider and screen fire PSA cables.
Task 4: Qualitative screening	Fire compartments that are not related to fire PSA and seismic PSA should be screened out in seismic-induced sodium fire risk analysis process.
Task 5: Fire risk model	The sub-task, fire risk model, should be integrated with seismic risk model in seismic-induced sodium fire risk analysis process.

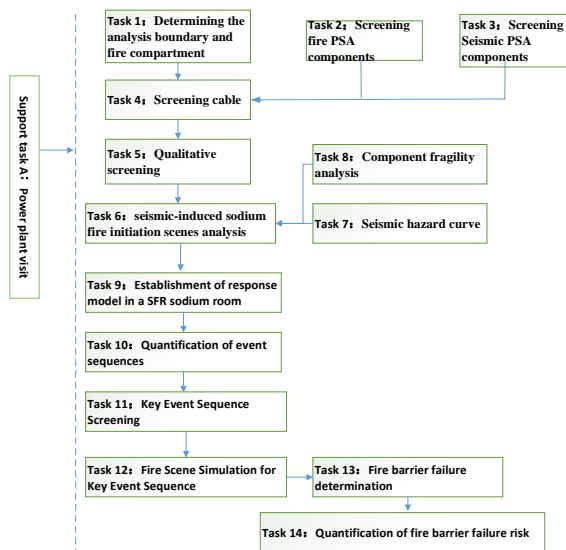
Table 1. Seismic-induced sodium fire correlation analysis (cont'd)

The sub-tasks of seismic PSA or fire PSA	Seismic-induced sodium fire correlation analysis
Task 6: Fire frequency analysis	Seismic increases the likelihood of sodium leakage, and induce sodium fire. Sodium fire frequency will increase. It should be implemented to analyse seismic-induced sodium fire initiation scenes and calculate their frequency.
Task 7: Quantitative screening	This sub-task must consider not only the impact of the fire but also the impact of the seismic, and screen fire compartments based on quantitative results.
Task 8: Determining the scope of fire modeling	The ignition source of seismic-induced sodium fire is sodium-related equipment and pipelines, so ignition identification is simple and easy. There is no need to identify the ignition source again and determine the modelling range like fire PSA. This sub-task is not needed to be considered in the seismic-induced sodium fire risk analysis.
Task 9: Detailed cables failure analysis	This sub-task should be considered in the seismic-induced sodium fire risk analysis.
Task 10: Cables failure modes and probability analysis	This sub-task should be considered in the seismic-induced sodium fire risk analysis.
Task 11: Detailed fire modeling	This sub-task should be integrated with seismic modeling.
Task 12: Human reliability analysis after fire	This sub-task should be integrated with human reliability analysis after seismic.
Task 13: Quantification of fire risk	This sub-task should be integrated with quantification of seismic risk.
Task 14: Complete fire PSA report	Complete fire PSA report.

III. The Risk Analysis of Seismic-induced Sodium Fire in a SFR Sodium Room

According to Table 1, 14 subtasks and 1 support task are identified as the method flow for seismic-induced sodium fire risk analysis, as shown in Figure 1.

Figure 1. the method flow for seismic-induced sodium fire risk analysis



Task 1: Determining the analysis boundary and fire compartments

The purpose of this task is to determine the scope of power plant analysis, define the analysis boundary, and divide fire compartments, which should be convenient for implementing risk analysis. There are separate sodium fire detection systems in each SFR sodium room, which is proposed to be as a separate fire compartment.

Task 2: Screening fire PSA components

This task is to identify all components that affect the safety of a fire compartment under fire accident, Such as components of fire detection and fire protection systems.

Task 3: Screening seismic PSA components

This task is to identify the components which affect the safety of a fire compartment under seismic but have not been considered in task 2, such as passive components or mechanical components.

Task 4: Screening cables

This task is to analyse related cables for powering these components of task 2 or task 3, and to identify the cables which affect the safety of a fire compartment under seismic-induced sodium fire.

Task 5: Qualitative screening

Task 5 is to filter out some fire compartments of very low risk level. The screening criteria is as follows.

1. There is no components or cables affecting the safety of a fire compartment which are identified in task 2, task 3 and task 4 in the fire compartment.

Task 6: Seismic-induced sodium fire initiation scenes analysis

Various sodium fire scenes may occur under seismic. This task includes two parts that are seismic-induced sodium fire initiation scenes and their frequency.

The first step is to divide peak ground acceleration (PGA) intervals. the second step is to analyse seismic-induced sodium fire initiation scenes under different intervals.

Seismic-induced sodium fire initiation scenes mainly include different sodium fire modes, sodium leak locations and break sizes. Sodium fire modes are related to sodium leak locations and break sizes, which generally include spray sodium fire, pool sodium fire and mixed sodium fire. By using event tree and fault tree method, it is to analyse seismic-induced sodium fire initiation scenes and their frequency of different PGA. [3]

Task 7: Seismic hazard curve

One of the output of seismic hazard analysis is seismic hazard curve which reflects the frequency of different PGA at a site. The X-axis is PGA. The Y-axis is the annual frequency of exceedance.

Task 8: Component fragility analysis

The output of component fragility analysis is component fragility curve, which reflects the conditional probability of component failure of different PGA. The abscissa is PGA. The ordinate is the conditional probability.

Task 9: Establishment of response model in a SFR sodium room

Seismic-induced sodium fire will cause the seismic or sodium fire protection system response. Operators may do the manual or automatic draining of the leaking sodium equipment. Seismic or sodium fire detection system may alarm. This task is to establish response model for each seismic-induced sodium fire initiation scenes in the fire

component and identify various possible event sequences after seismic-induced sodium fire, considering seismic or sodium fire protection system response.

Task 9 includes the following two parts:

1. Grouping task 6 “seismic-induced sodium fire initiation scenes”. The grouping principle is that The corresponding plant response for each group is the same, such as success criteria, Personnel operating behavior, or automatic power plant response.
2. Establishing the response model for each group. It is to analyse event sequences after seismic-induced sodium fire initiation scenes with event tree method, and to analyse the probability of function event of event tree with fault tree method.

Task 10: Quantification of event sequences

This task is to calculate the frequency of event sequences of task 9. Seismic hazard curve, component fragility curve, and response model are integrated to get the frequency of event sequences of task 9.

Task 11: Key event sequence screening

Key event sequence is event sequence with high risk level. This task is to screen out key event sequences from task 9 by excluding event sequences with severe consequences but very low frequency as well as high frequency but minor consequences.

Quantitative safety goal of nuclear power plants is generally characterised by CDF (core damage frequency) and LERF (early large radioactive release). The Chinese nuclear safety regulation "Nuclear Power Plant Safety Evaluation and Verification" requires that the new nuclear power plant CDF should be less than 10^{-5} per reactor year, and the LERF should be less than 10^{-6} per reactor year. It is known that CDF should be lower than 10^{-5} per reactor year, and this paper believes that the frequency of fire barrier failure should also be less than 10^{-5} per reactor year. In PSA technical analysis, the cutting set cut-off value is usually three to four orders of magnitude lower than the risk target value,[4] [4]so this paper make 10^{-9} per reactor year as cut-off value, which means that these event sequences below 10^{-9} per reactor year has little impact on the frequency of fire barrier failure and can be ignored, as the key event sequence screening principle.

Task 12: Fire scene simulation for key event sequence

Task 12 is to simulate key event sequence of task 11 and determine whether the event sequence will cause the fire barrier failure.

Task 13: Fire barrier failure determination

Fire barriers are things that limit the consequences of fire. That includes walls, floors, ceilings or closing devices (such as doorways, gates, penetrations and ventilation systems).

Under seismic-induced sodium fire, the causes of fire barrier failure include three aspects. The first is that the seismic causes the damage of the fire barrier structure, including firewall cracks, collapse and other failure modes, which makes the fire barrier lose its ability to block sodium fire. The second is that the thermal effect of seismic-induced sodium fire exceeds the acceptable range of the fire barrier, contribution to fire spreading. The third is that seismic reduce the fire resistance of the fire barrier, and eventually the fire barrier is disabled by the combination the sodium fire and seismic effect.

There are two ways to determine whether a fire can cause fire barrier failure.

1. If the maximum temperature of the room exceeds the rated temperature, it is assumed that the fire barrier has failed. This criterion is based on the determination of the fire barrier failure in the analysis of fire hazards, and fire barriers are characterised by fire resistance rating, expressed in hours.

The relationship exists between the fire resistance rating and the maximum temperature of the sodium room, as shown in the following formula. The fire resistance rating can be converted to the maximum temperature of the sodium room. [5]

$$T - T_0 = 345 \log_{10}(8t + 1)$$

$T(^{\circ}\text{C})$ —the temperature of the sodium room at time t ;

$T_0 (^{\circ}\text{C})$ —the initial temperature of the sodium room;

$t (\text{min})$ —time;

1. If the maximum temperature of the wall exceeds the rated temperature, the fire barrier is assumed to be ineffective. In the reference [5], the degree of damage to the

wall concrete structure can be divided into four types. [6]

- When the concrete temperature is below 400°C, the concrete structure is slightly damaged, and the strength is not reduced.
- When the concrete temperature is in the range of 400°C to 600°C, the concrete structure is moderately damaged and the strength is reduced to some extent.
- When the concrete temperature is in the range of 600°C to 800°C, the concrete structure is seriously damaged and its strength is significantly reduced.
- When the concrete temperature is above 800°C, the concrete structure is seriously damaged and the strength is completely lost.

When the concrete temperature is above 400°C, the concrete structure is moderately damaged. It can be conservatively considered that if the maximum temperature of the wall is above 400°C, the fire barrier will fail.

Regarding the influence of the seismic, it can be considered conservatively. Assuming that the fire barrier structure fails under seismic-induced sodium fire, the fire barrier will fail.

In addition to the effects of temperature, the high pressure caused sodium fire may contribute to fire barrier failure.

Task 14: Quantification of fire barrier failure risk

Task 14 is to calculate the frequency of fire barrier failure caused by seismic-induced sodium fire in a SFR sodium fire.

Support task A: Power plant visit

Power plant visit is an important part of seismic-induced sodium fire risk analysis process. The inspection team go to the site of the power plant to collect and verify the information of the power plant. Power plant visit can judge whether the information collected is consistent with the actual condition of the power plant, and can help learn about some information that cannot be clearly displayed on a drawing or document.

For the risk analysis of seismic-induced sodium fire, the focus of the power plant visit is as follows:

- Component location
- Component anchor
- Cable layout path
- Weld distribution
- Space and other forms of interaction

IV. Conclusion

The risk analysis of multiple hazard, like seismic-induced sodium fire, are one of the directions of nuclear power plant PSA research. In-depth insight into the risks is an inevitable requirement to ensure the safety of nuclear power plants. Seismic-induced sodium fire risk analysis in a SFR sodium room is part of the SFR seismic-induced sodium PSA study. This paper presents some key research elements for the risk analysis of seismic-induced sodium in a SFR sodium room, to speed up the development of risk quantification for multiple hazards.

Acknowledgements

The paper has been written with major contributions by Jiang Jingke, Wang Mingzheng and Yan Han from CIAE, China. Wang Jing from CIAE brought significant support at improving the paper.

Nomenclature

SFR	Sodium Fast Reactor
PSA	Probabilistic Safety Analysis
PWR	Pressurised Water Reactor
PGA	Peak Ground Acceleration
CDF	Core Damage Frequency
LERF	Early Large Radioactive Release

References

- [1] Katsumi Ebisawa. Concept for developing seismic-tsunami PSA methodology considering combination of seismic and tsunami events at multi-units, Proceedings of the International Symposium on Engineering Lessons Learned from the 2011 Great East Japan Earthquake, March 1-4, 2012, Tokyo, Japan.
- [2] USNRC. NUREG/CR-6850. Fire Probabilistic Risk Assessment Methods Enhancements. 2010.
- [3] China Institute of Atomic Energy. Fast reactor sodium fire analysis. 2000.
- [4] Chen Yan. The Application of PSA Importance in Risk-informed Management. Nuclear Science and Engineering, 2012 , 32 (4) : 379-384.
- [5] China Institute of Atomic Energy. China Experimental Fast Reactor Fire Hazard Analysis Report. 2009.
- [6] Wang Ankun. A summary of fire temperature determination methods for concrete buildings. Engineering Quality, 2005(3),37-39.

DESIGN AND SAFETY STUDIES OF THE MOLTEN SALT FAST REACTOR CONCEPT IN THE FRAME OF THE SAMOFAR H2020 PROJECT (E. MERLE ET AL)

E. Merle⁽¹⁾, M. Allibert⁽¹⁾, S. Beils⁽²⁾, A. Cammi⁽⁶⁾, B. Carlucci⁽²⁾, A. Carpignano⁽⁵⁾, S. Delpéché⁽⁷⁾, A. Di Ronco⁽⁶⁾, S. Dulla⁽⁵⁾, Y. Flauw⁽³⁾, D. Gerardin⁽¹⁾, A. Gerber⁽²⁾, D. Heuer⁽¹⁾, A. Laureau⁽¹⁾, S. Lorenzi⁽⁶⁾, M. Massone⁽⁴⁾, A. Rineiski⁽⁴⁾, V. Tiberi⁽³⁾, A. C. Uggenti⁽⁵⁾

- (1) LPSC-IN2P3-CNRS, UGA, Grenoble INP, France
- (2) FRAMATOME, France
- (3) IRSN, France
- (4) KIT, Germany
- (5) NEMO group, DENERG, Politecnico di Torino, Italy
- (6) Politecnico di Milano, Italy
- (7) Institut de Physique Nucléaire-IN2P3-CNRS, France

Abstract

Since more than 15 years, the National Centre for Scientific Research (CNRS, France) has focused R&D efforts on the development of a new molten salt reactor concept called the Molten Salt Fast Reactor (MSFR) selected by the Generation-IV International Forum (GIF) due to its promising design and safety features. Studies are performed to ascertain whether MSFR systems can satisfy the goals of Generation-IV reactors.

Molten salt reactors are liquid-fueled reactors, allowing a large flexibility in terms of operation (load-following capabilities...) or design (core geometry, fuel composition, specific power level...) choices. They are characterised by features different in terms of design, operation and safety approach compared to solid-fueled reactors. In the frame of the European SAMOFAR (Safety Assessment of Molten Salt Fast Reactors) project of Horizon2020, dedicated studies are performed on these topics. An overview of these studies will be presented in this article.

Firstly, an innovative design of the MSFR fuel circuit (defined as the circuit containing the fuel salt during power generation) and of the emergency draining system has been defined and is under optimisation in terms of safety. Such reactors also call for the definition of dedicated operational procedures different from that of solid-fueled reactors, requiring the use of specific modelling tools (multiphysics and system codes). A system code is thus under completion and validation in the frame of SAMOFAR to define the start-up and load following procedures of the MSFR, including the evaluation of safety transients. Finally, a safety approach dedicated to liquid circulating fuel reactors has been developed on the basis of the ISAM methodology of the GIF taking into account other safety methodologies and guidelines. An application procedure and the required tools have been proposed. The approach is being applied to the MSFR, allowing a preliminary identification of initiating events, lines of defence and confinement barriers for the concept.

I. Introduction

Since more than 15 years, the National Centre for Scientific Research (CNRS, France) has focused R&D efforts on the development of a new molten salt reactor concept called the Molten Salt Fast Reactor (MSFR) selected by the Generation-IV International Forum (GIF) due to

its promising design and safety features [1,2,3]. Studies are performed to ascertain whether MSFR systems can satisfy the goals of Generation-IV reactors.

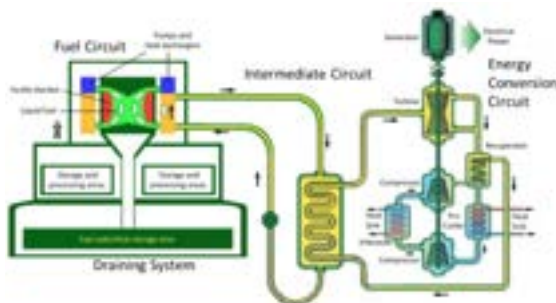
Molten salt reactors are liquid-fueled reactors, allowing a large flexibility in terms of operation (load-following capabilities...) or design (core geometry, fuel composition, specific power

level...) choices. They are characterised by features different in terms of design, operation and safety approach compared to solid-fueled reactors [4,5]. In the frame of the European SAMOFAR (Safety Assessment of Molten Salt Fast Reactors) project of Horizon2020, dedicated studies are performed on these topics. An overview of these studies and results will be presented in this article.

II. Integrated Design of the MSFR

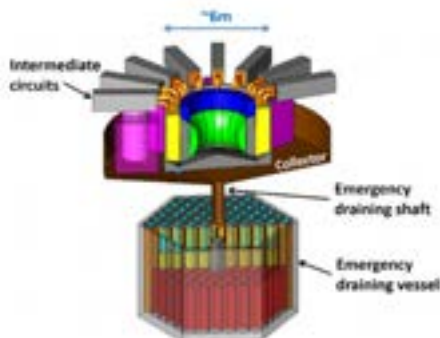
The MSFR plant includes three main circuits involved in power generation (see Figure 1): the fuel circuit, the intermediate circuit and the power conversion circuit. These circuits are associated to other systems composing the whole power plant: an emergency draining system, a routine draining system and storage areas, and bubbling and chemical processing units.

Figure 2. MSFR power plant



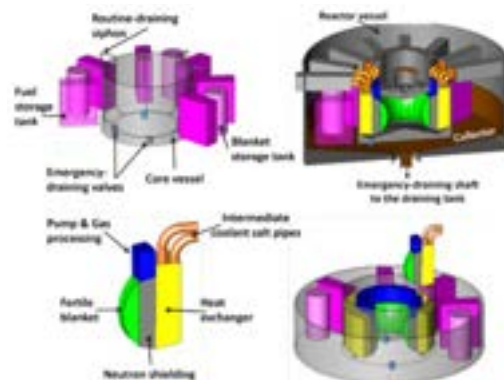
The main characteristic of the MSFR is the fuel in the form of a molten salt. This fuel salt circulates in the fuel circuit where it is cooled down and plays therefore the role of coolant as well.

Figure 2. New design of the MSFR system, including the fuel circuit and the Emergency Draining System (EDS)



The fuel circuit is defined as the circuit containing the fuel salt during power generation and includes the core cavity and the cooling sectors allowing the heat extraction. An integrated geometry of the fuel circuit [2,3] (see Figure 3) has been developed in order to prevent the risk of fuel leakages highlighted by preliminary safety and optimisation studies [5].

Figure 3. Schematic view of the integrated design of the MSFR fuel circuit



This integrated geometry includes a vessel used as container for the fuel salt, in which the 16 cooling sectors are disposed circumferentially. Each sector comprises a heat exchanger, a circulation pump, a gas processing system, and a fertile blanket tank. A neutron shielding in B_4C is positioned between the blanket and the heat exchangers to protect the heat exchangers from the neutron flux and to increase the breeding ratio. In addition, thick reflectors made of nickel-based alloys are located at the bottom and at the top of the vessel to protect the structures located outside the core.

Finally, in case of incident/accident during power production, the fuel can be drained gravitationally toward an emergency draining tank designed to passively remove the residual heat over a short to long period of time (the residual heat associated to the fuel salt, at reactor shutdown, represents around 3.8% of the nominal power). The fuel circuit is connected to this Emergency Draining System (EDS) through active and passive gates or plugs located in the bottom reflector.

III. System Code and Procedure Definitions

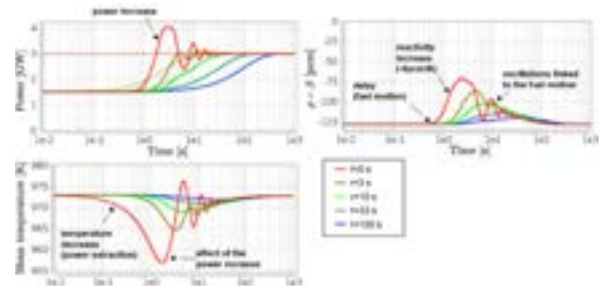
As mentioned, the characteristics of the MSFR require also dedicated studies and definition of specific operation procedures.

For example, the core negative feedback coefficients (density effect and Doppler Effect) are both negative and act rapidly since the heat is produced directly in the coolant. Although the fuel circulation drifts the delayed neutron precursors in low importance areas, reducing the effective fraction of delayed neutrons, the core presents a very intrinsically stable behaviour to reactivity insertions [4,6].

Within the framework of the design and the safety assessment of a complex system such as the MSFR, a fundamental role is played by the power plant simulator. This tool has to be able to properly model all the power plant subsystems and to simulate efficiently their coupled dynamic behaviour, from the reactor core to the electrical grid. In the framework of the SAMOFAR project, the development of a power plant simulator aims at (i) the analysis of the MSFR plant dynamic behaviour, (ii) the definition of the control strategies and operational procedures for the different reactor operation modes (full power, start-up, shut-down, load following, ...). The simulator is developed conjointly by LPSC/CNRS (fuel circuit) and POLIMI (intermediate and conversion circuits).

For the fuel circuit modelling, to take into account the dynamics due to the delayed neutrons, the LiCore (Liquid Core) code has been developed. The code uses the Java language and is based on a point kinetics neutronic model that can take into account the precursor position [6]. The precursors are followed with this code even during an evolution of the state of the reactor over time, i.e. during transients. The LiCore code is able to calculate a transient faster than real-time which is a very important point for the MSFR system code. Load following transients from 1.5 to 3 GW have been calculated with several time constants as displayed in Figure 4. One can notice the excellent behaviour of the MSFR core in case of an important load following solicitation, as already established by precise multiphysics core calculations [4]. The main limitations will come from the intermediate circuit that will have to be designed to perform such load following transients.

Figure 4. Load following transients from 1.5 to 3 GW, calculated with the LiCore code by varying the power extracted in the heat exchangers with different time constants



The LiCore code may also be used to calculate incidental transients, for example loss of flow transients. A dedicated pipe composed of empty cells representing the emergency draining tank has been added in the LiCore code to allow also calculations of incidental transients leading to a draining of the fuel salt if a given mean fuel temperature is reached. An instantaneous loss of the intermediate flow at 10 s is illustrated in Figure 5, with a draining occurring when the fuel reaches a temperature chosen by the user (1000 K on this example).

Figure 5. Loss of intermediate flow at 10s leading to an emergency draining of the fuel in the emergency draining system: view of the MSFR circuits modelled (top) and results of the calculations (bottom)

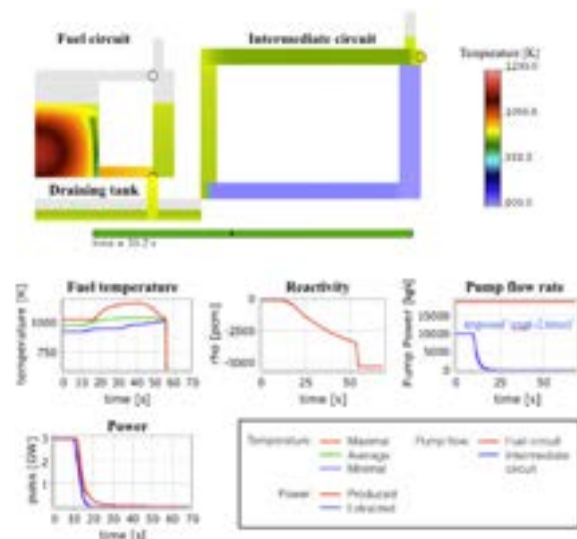
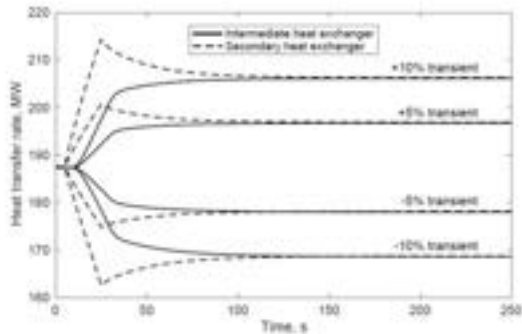


Figure 6. Evolution of the heat transfer rates in the heat exchangers for gas mass flow rate transients in the intermediate circuit



Regarding the modelling of the intermediate and the energy conversion systems of the MSFR, the chosen approach is the object-oriented modelling, which allows satisfying the modularity and efficiency requirements. The adopted modelling language is Modelica [7]. It allows a description of single system components (or objects) directly in terms of physical equations and principles, and to connect different components through standardised interfaces (or connectors). Different studies of the behaviour and the design of the intermediate and energy conversion circuits are done as shown in Figure 6.

IV. Safety Analysis Methodology for Liquid Fuel ED Reactors

Driven by the IRSN, a safety approach dedicated to liquid circulating fuel fast reactors has been developed, together with the definition of its application procedure and of the required tools for the application to the MSFR. The objective was to define a risk assessment methodology which could be applied from the earliest stages of design to licensing, operation and decommissioning. This methodology takes into account the Generation-IV safety requirements, the international safety standards, the available return of experience and the peculiarities of this kind of reactor with the help of available risk analysis tools. The idea is to achieve a safety which is “built-in” and not “added on” providing with a detailed understanding of safety related design vulnerabilities, and resulting contributions to risk. As such, new safety provisions or design improvements as well as R&D needs could be identified, developed, and implemented if necessary. The MSFR technology being at its first stages of design will benefit from such an

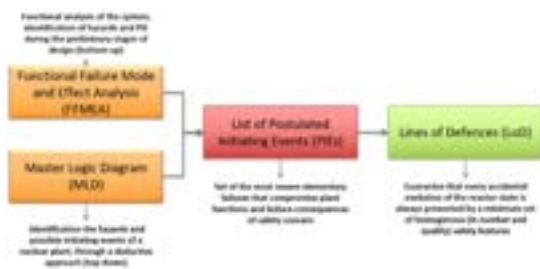
approach. The methodology is based on the Integrated Safety Assessment Methodology (ISAM) developed in the framework of the GIF [8]. ISAM is a tool kit of useful analysis tools for Gen IV systems. Some of these tools are primarily qualitative, others quantitative. Some are primarily probabilistic, others deterministic. Some focus on high-level issues such as systemic response to various phenomena, others focus on more detailed issues. This diversity helps to provide a robust guidance based on a good understanding of risk and safety issues.

The ISAM tools have been reviewed, completed and adapted, when needed, to better reflect the European standards/rules, the available return of experience and to better fit the scope of the SAMOFAR project. In addition, review of the usual risk analysis methods (HAZOP, FMEA, etc.) has been performed to analyse how they can be integrated within the ISAM framework (see Figure 7). This adapted method has then been declined to be applied to the MSFR technology. A focus has also been made on the safety-related subjects to be examined as a priority at the basic design stage of the MSFR.

Figure 7. Flowchart of the MSFR design/safety assessment and relevance of the different tools



Figure 8. Complementarity between the FFMEA and the MLD methods



Finally, this methodology and the related recommendations are currently applied on the MSFR for the reactor by POLITO, CNRS and Framatome. The analysis using the Functional Failure Mode and Effects Analysis (FFMEA) and the Master Logical Diagram (MLD) has been done on the plant state corresponding to the nominal power production of the MSFR (see Figure 8) and a list of Postulated Initiating Events has been identified [9, 10].

These studies have also been used to provide a list of design key-points that are relevant for safety and should be further investigated such as the type of pumps used for the fuel circulation, the definition of the decay heat removal system or the components of the fission product removal systems. The need to further define the operation and accidental procedures has also been highlighted. For instance, the cases in which the emergency draining system, the routine draining system or in-core shutdown are used should be defined [9, 10].

The method of the Lines of Defence (LoD) is under completion for the MSFR during nominal power production. The main objective is to ensure that every accidental evolution of the reactor state is always prevented by a minimum set of homogenous (in number and quality) safety features - called Lines of Defence - before a situation with potentially unacceptable consequences may arise. It can therefore help the designer to determine whether sufficient safety provisions are put in place for a given risk.

Finally, first proposals of confinement barriers definition have been made.

V. Conclusion

Molten salt reactors with a liquid circulating fuel, like the MSFR concept developed initially at CNRS and now in the SAMOFAR European project, are very different in terms of design and safety approach compared to solid-fueled reactors. Dedicated tools and methods are required for their study and optimisation, more general than the existing ones. An overview of the work performed to date on the MSFR in terms of design, simulation and safety approach has been presented in this article. In the future, the full application of these methodologies and tools will lead to a more refined definition of the concept up to its validation, the first step for industrialisation.

Acknowledgements

This project has received funding from the Euratom research and training programme 2015-2018 under grant agreement No 661891.

Nomenclature

CNRS	National Centre for Scientific Research
GIF	Generation IV International Forum
IRSN	Institute for Radiological Protection and Nuclear Safety
ISAM	Integrated Safety Assessment Methodology
MSFR	Molten Salt Fast Reactor
POLIMI	Politecnico di Milano
POLITO	Politecnico di Torino
SAMOFAR	Safety Assessment of Molten Salt Fast Reactors

References

- [1] J. Serp, M. Allibert, O. Beneš, S. Delpech, O. Feynberg, V. Ghetta, D. Heuer, D. Holcomb, V. Ignatiev, J.L. Kloosterman, L. Luzzi, E. Merle-Lucotte, J. Uhlíř, R. Yoshioka, D. Zhimin, "The molten salt reactor (MSR) in generation IV: Overview and Perspectives", Prog. Nucl. Energy, 1-12 (2014)
- [2] M. Allibert, M. Aufiero, M. Brovchenko, S. Delpech, V. Ghetta, D. Heuer, A. Laureau, E. Merle-Lucotte, "Chapter 7 - Molten Salt Fast Reactors", Handbook of Generation IV Nuclear Reactors, Woodhead Publishing Series in Energy (2015)
- [3] D. Gérardin et al , "Design Evolutions of the Molten Salt Fast Reactor", Proceedings of the Fast Reactors 2017 International Conference, Jekaterinburg, Russian Federation (2017)
- [4] A. Laureau et al., "Transient coupled calculations of the Molten Salt Fast Reactor using the Transient Fission Matrix approach", Nucl. Eng. and Design, Volume 316, Pages 112-124 (2016)
- [5] M. Brovchenko, D. Heuer, E. Merle-Lucotte, M. Allibert, V. Ghetta, A. Laureau, P. Rubiolo, "Design-related Studies for the Preliminary Safety Assessment of the Molten Salt Fast Reactor", Nuclear Science and Engineering 175, 329-339 (2013)
- [6] A. Laureau, "Développement de modèles neutroniques pour le couplage thermohydraulique du MSFR et le calcul de paramètres cinétiques effectifs", PhD Thesis, Grenoble Alpes University, France - in French (2015)
- [7] The Modelica Association, "Modelica 3.2.2 Language Specification", <http://www.modelica.org/> (2014)
- [8] GIF/RSWG, "An Integrated Safety Assessment Methodology (ISAM) for Generation IV Nuclear Systems", version 1.1 (2011)
- [9] A. C. Uggenti, D. Gerardin et al., "Preliminary Functional Safety Assessment for Molten salt Fast Reactors in the Framework of the SAMOFAR Project", Proceedings of the PSA2017 Conference, Pittsburgh, USA (2017)
- [10] D. Gerardin, A.C. Uggenti et al, "Identification of the Postulated Initiating Events with MLD and FFMEA for the Molten Salt Fast Reactor", submitted to Nuclear Engineering and Technology (2018).

DEVELOPMENT OF ODS TEMPERED MARTENSITIC STEEL FOR HIGH BURN UP FUEL CLADDING TUBE OF SFR (S. OHTSUKA ET AL)

S. Ohtsuka, T. Tanno, H. Oka, Y. Yano, Y. Tachi, T. Kaito, R. Hashidate, S. Kato, T. Furukawa, C. Ito, T. Yoshitake

Japan Atomic Energy Agency, Japan

Abstract

This paper describes the on-going efforts in Japan atomic energy agency (JAEA) on the development of oxide dispersion strengthened (ODS) steels for the long-life fuel cladding tube of sodium-cooled fast reactor (SFR), the use of which can be conducive to volume and hazardousness reduction of radioactive waste. ODS steel, which is highly strengthened by nano-sized oxide dispersion, has been noticed as a core material used in neutron irradiation condition at high-temperature. ODS steel cladding tubes for SFR application developed by JAEA are categorised into two types: martensitic ODS steel with ferritic-martensitic duplex matrix and ferritic ODS steel with recrystallised ferritic matrix. JAEA has focused on development of martensitic ODS steel cladding tube (9Cr-ODS steel), which is advantageous over ferritic ODS steel (12Cr-ODS steel) in terms of irradiation resistance and tube manufacturability; tempered martensitic matrix provides high density of trapping site for irradiation defects; it can be easily softened by intermediate heat treatment in the course of tube manufacturing process. Out-of-pile creep rupture tests of 9Cr-ODS steel demonstrated the excellent strength at high-temperature for long duration. The execution of neutron irradiation test up to 30 dpa at temperatures from 420-835°C using Joyo revealed that microstructure and mechanical strength were maintained under this neutron irradiation condition in 9Cr-ODS steels. It should be noted that the high burnup fuel cladding tube should possess corrosion resistance in addition to high-temperature strength and irradiation resistance. For improvement of corrosion resistance, increasing the content of Cr is effective. Based on the extensive research on high-temperature strength of 9Cr-ODS steels, important microstructural factors controlling high-temperature strength and microstructure stability were shown to be high population of nano-oxide particle dispersion and duplex microstructure (incorporation of residual ferrite having fine nano-oxide dispersion as reinforcement phase). In the light of this knowledge, a new specification of 11Cr-ODS steel was determined, where thermodynamic calculation technique was tentatively used for duplex microstructure control. As a result, the microstructure of 11Cr-ODS steel including the duplex matrix and nano-sized oxide particle dispersion was successfully controlled equivalent to that of 9Cr-ODS steel. Tube manufacturability and out-of-piles mechanical strength of 11Cr-ODS steel were demonstrated. For enhancing the flexibility of ODS martensitic steel development, 11Cr-ODS steel is ranked as a prospective choice of SFR fuel cladding tube in addition to 9Cr-ODS steel in JAEA

I. Introduction

Oxide dispersion strengthened (ODS) ferritic steel has been developed as high-strength and radiation-tolerant steel used for cladding tubes of fast reactor (FR) fuel and light water reactor accident-tolerant fuel, and fusion reactor material [1-12]. Japan atomic energy agency (JAEA) has been developing ODS steels for

sodium cooled fast reactor (SFR) high burn-up fuel cladding tube [1-4]. Application of high burn-up fuel to SFR core can contribute to improvement of economical performance of SFR in conjunction with volume and hazardousness reduction of radioactive waste. Cladding tube for SFR high burn-up fuel should be well-balanced in terms of several properties, i.e. manufacturability, mechanical property,

irradiation resistance, and corrosion resistance. In the reactor core, the cladding tube will be exposed to high energy neutron irradiation at high temperature, thus requiring adequate irradiation resistance (i.e. dimensional and microstructural stability, resistance to mechanical properties degradation under neutron irradiation). It also needs to possess substantial compatibility with flowing sodium and HNO_3 solution in the reprocessing process.

In the frame of the feasibility study from 1999 to 2005 [13], JAEA advanced the fabrication technology development in laboratory scale and derived out-of-pile and in-pile properties data on two types of ODS steels: the 9Cr-ODS tempered martensitic steel (TMS) having main matrix of tempered martensite and 12Cr-ODS ferritic steel (FS) having recrystallised ferritic matrix. Eventually, JAEA chose ODS TMS as primary candidate to attach importance to irradiation resistance and manufacturability. In the following project named FaCT from 2006 to 2010 [14], JAEA worked on the core technology development of large scale manufacturing process along with fuel pin and material irradiation tests for demonstrating in-reactor performance of 9Cr-ODS TMS. The fuel pin irradiation test using BOR-60 revealed unsatisfactory microstructure homogeneity of 9Cr-ODS TMS, thus led JAEA to improve the fabrication process [15,16]. Additionally, to improve conformity of ODS TMS with fuel cycle system, JAEA has started developing high Cr-ODS TMS, which is expected to have better corrosion resistance than 9Cr-ODS TMS [17-19]. This paper described the current status and future prospects of ODS TMS development in JAEA for SFR fuel application.

II. Current Status

II.A Required properties for high burn-up fuel cladding tube of SFR

For SFR high burn-up fuel cladding tube, several properties are required as shown in Table 1. ODS TMS is highly strengthened by nano-sized oxide particles dispersed in matrix. This nano-structure leads to high hardness of mother tube and difficulty in tube manufacturing without cracking. Therefore, development of tube manufacturing technology dedicated to ODS TMS is an unavoidable task. In the reactor core, the fuel cladding tube is exposed to high-dose neutron irradiation at high-temperature for a long duration. For example, in JSFR (Japan Sodium Fast Reactor), mid-wall maximum temperature of fuel cladding tube (hot-spot

temperature) is assumed to be 700 oC; the life time period approximately 9 years, and the peak irradiation dose 250 dpa in order to achieve peak burn-up of 250GWd/t [13,14]. Stress loaded to the tube is mainly hoop stress produced by accumulation of fission product gas; the stress at end of life is dependent of fuel design, typically around 100 MPa. For ensuring the integrity of fuel pin under reactor operation, fuel cladding tube should have substantial high-temperature strength and irradiation resistance; it specifically needs to keep adequate mechanical strength including creep rupture strength, and dimensional stability under irradiation (i.e. resistance to swelling). In addition to these properties, cladding tube requires sufficient conformity with fuel cycle system.

Table 1. Required properties for SFR fuel cladding tube.

Required properties	Individual properties
1) Manufacturability	i) Tube manufacturability
	ii) Weldability
2) Out-of-piles Performance	i) Creep strength
	ii) Tensile strength
	iii) Ductility
3) In-Reactor performance	i) Dimensional stability (resistance to swelling)
	ii) Compatibility with sodium
	iii) Irradiation resistance: - No pronounced high-temperature strength degradation - No pronounced embrittlement
4) Compatibility with fuel cycle system	i) Resistance to FCCI
	ii) HNO_3 corrosion resistance in reprocessing

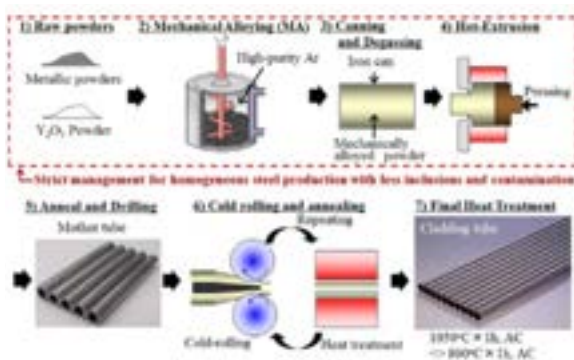
II.B Specifications and fabrication technology

JAEA has developed two types of ODS steel cladding tubes: ODS TMS (9 wt% Cr) and ODS FS (12 wt% Cr). In terms of irradiation resistance, ODS TMS is expected to be advantageous over ODS FS due to the presence of a lot of sink sites for irradiation-induced point defects in the matrix. Disadvantage of ODS TMS is limitation of Cr concentration lower than 12wt% for retention of tempered martensitic matrix. ODS FS can contain high Cr concentration, thereby having an advantage in corrosion resistance

over ODS TMS. JAEA placed importance on irradiation resistance including tolerance to swelling and embrittlement, thus choosing ODS TMS as primary candidate material.

Figure 1 is the schematic view of basic fabrication process of ODS steel cladding tube [1-4]. In the first half of the process, mother tube is fabricated by mechanical alloying (MA) and the following powder consolidation process of MAed powder (e.g. hot-extrusion, hot-isostatic pressing, etc.). In the second half, mother tube is processed to thin-walled tube by means of multiple pass of cold-rolling and heat treatment. JAEA classifies the fabrication process of consolidated ODS steel into three types: pre-mix, partially pre-alloy and full pre-alloy process. In the pre-mix process, elemental powders (Fe, Cr, C, W, Ti, etc.) and Y_2O_3 powder are used as raw material powder. In partially pre-alloy process, major raw material powder are pre-alloy powder and Y_2O_3 powder, however, small amount of elemental powder is added for minor control of chemical composition. The pre-alloy powder used is produced by vacuum melting followed by Ar-gas atomisation method. In full pre-alloy process, only the pre-alloy powder and the Y_2O_3 powder are used as raw material powder [15,16]. In addition, the strict management for homogeneous steel production with less inclusions and contamination is adopted throughout the process. In past years, JAEA has adopted the full pre-alloy process as standard fabrication process for ODS steel fuel cladding tube, and fabricated approximately a hundred of 9Cr,11Cr-ODS TMS cladding tubes with this process [3].

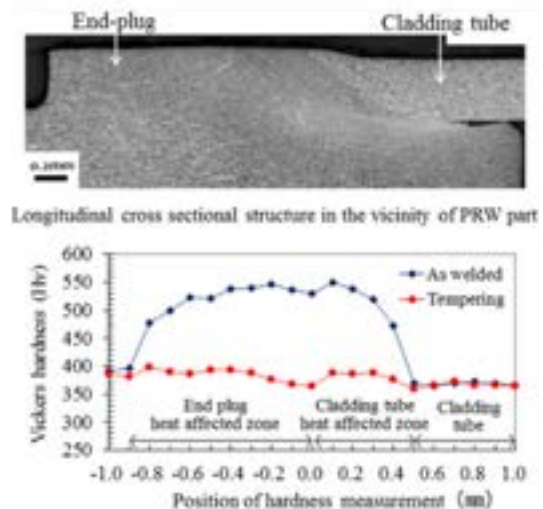
Figure 1. Schematic view of fabrication process of ODS TMS cladding tube.



For bonding between cladding tube and end-plug, JAEA established the pressurised resistance welding (PRW) technology [20]. Figure 2 shows a microstructure in the vicinity

of interface between tube and end plug in 9Cr-ODS TMS fuel pin. The bonding part has a homogeneous structure, making the interface difficult to identify. It is clearly shown that tempering heat-treatment at 800°C for 15 min restored the hardened region to its original value (340-400 Hv). JAEA has conducted a plenty of internally pressurised creep tests (over a hundred of tests) of 9Cr-ODS TMS specimens, where the end plugs made of 9Cr-ODS TMS were joined to 9Cr-ODS TMS cladding tube by the optimised PRW technology. The creep test temperatures were from 650 to 1000°C. The creep tests showed that creep rupture occurred at tube part, thereby demonstrating the integrity of PRW part. The fuel pin irradiation test at BOR-60 also proved the integrity of PRW part of 9Cr-ODS TMS fuel pin, where the irradiation test was conducted to the peak burn-up of 11.9at%, and irradiation time of 15,446 h, at the maximum temperature of 700°C (calculated value) [15].

Figure 2. PRW test result between cladding tube and end plug of 9Cr-ODS TMS [20].



II.C Microstructure and high-temperature strength of 9Cr-ODS TMS

Figure 3 shows the typical microstructures of 9Cr-ODS TMS cladding tube. Microstructure of 9Cr-ODS TMS is controlled to be duplex consisting of tempered martensitic and residual- α ferritic phases. The residual- α ferrite contains dense and uniform dispersion of nano-sized oxide particles, thus acting as reinforcement phase contributable to high-temperature strength improvement of 9Cr-ODS TMS [2-4, 27].

Figure 3. Typical metallograph of 9Cr-ODS TMS cladding tube

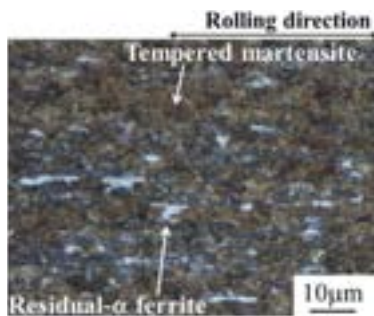


Figure 4. Internally pressurised creep rupture test results of 9Cr-ODS TMS cladding tube

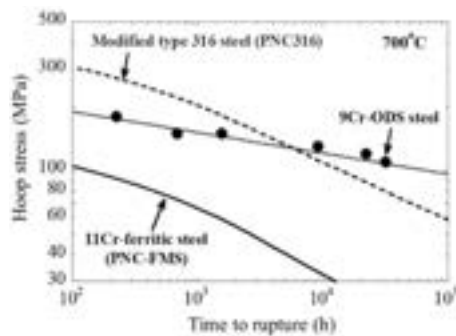
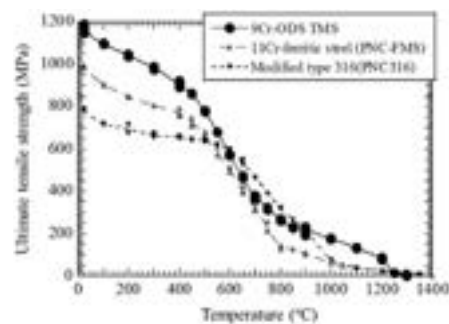


Figure 4 shows the internally pressurised creep test results of 9Cr-ODS TMS cladding tube at 700°C [1-3]. The 9Cr-ODS TMS shows satisfactory creep rupture strength in hoop direction. The noticeable feature in creep rupture behaviour is that there is no significant drop in creep rupture strength in long time region, in contrast to conventional steels such as modified type 316 steel and 11Cr-ferritic steel. The 9Cr-ODS TMS has much longer creep life time compared to the conventional core materials in the stress range lower than 100 MPa, which is typical assumed level for FR cladding tube in reactor operation. As shown in Figure 5, tensile strength of 9Cr-ODS TMS cladding tube was evaluated by ring tensile test in hoop direction up to 1300°C [21]. The tensile strength of 9Cr-ODS TMS was superior to that of 11Cr-ferritic steel in the whole temperature range. At temperatures from 1000 to 1200°C, 9Cr-ODS TMS showed the prominent strength roughly 3 times as high as that of modified type 316 steel and 11Cr-ferritic steel. In the high-temperature neutron irradiation environment, the superior strength of 9Cr-ODS TMS was maintained; neutron irradiation test using Joyo revealed that the adequate tensile strength was

kept even after neutron irradiation at 835°C to 26 dpa while significant strength degradation occurred for 11Cr-ferritic steels such (PNC-FMS) at temperature exceeding 650°C [22]. In addition, in-pile creep rupture test using material testing rig with temperature control (MARICO) indicated that there was no strength degradation caused by neutron irradiation to a few dpa at temperatures from 700 to 730°C [23]. These data proves the prominent irradiation resistance of 9Cr-ODS TMS. This is attributable to nano-sized oxide particle dispersion improving microstructure stability and tolerance to deformation and rupture. The nano-sized oxide particles were stable at high temperature and neutron irradiation environment according to TEM characterisation in the irradiation conditions tested [24].

Figure 5. Ring tensile strength of 9Cr-ODS steel cladding tube [21]



JAEA studied microstructure and high-temperature strength of 9Cr-ODS TMS towards the reliable and consistent production of high strength cladding tube made of 9Cr-ODS TMS, then revealed that mechanical strength and toughness of 9Cr-ODS TMS were largely influenced by three types of factors: concentration of minor alloying elements, powder consolidation condition, and type of fabrication process [4, 18,19,25-27]. Figure 6 shows the nano-structure analysis results of 9Cr-ODS TMS model alloys containing different concentrations of Ti, and excess oxygen (Ex.O), where the combined analysis using small angle neutron and X-ray [26] was applied. Ex.O is defined as the value subtracting oxygen coupled with Y as Y_2O_3 from the total oxygen in steel. Except for hot-extrusion temperature, all the model alloys were fabricated with the same process [25]. This combined analysis offers the average information of nano-structure in bulk material; measured volumes were roughly 10^{11} and $10^7 \mu\text{m}$ for neutron and X-ray analyses, respectively [25,26]. Small change of Ti and Ex.O

concentrations, and hot-extrusion temperature was shown to have pronounced effects on nano-sized oxide particle dispersion. Figure 7 shows the correlation between creep rupture strength and nano-sized oxide particle dispersion, which was evaluated by the combined analysis [25]. A parameter in vertical axis $\sqrt{d \cdot Np}$ is in inverse relation to average interspacing of nano-sized particles. Creep strength had a certain relationship with this parameter. The model alloys having higher fraction of residual- α ferrite had smaller average inter-particle spacing contributable to improved creep strength. The strength of 0.46wt% Ti-containing steel achieving largest $\sqrt{d \cdot Np}$ and residual- α ferrite fraction was not highest among the model alloys. This would be due to the presence of inclusions acting as crack initiation sites, which were formed by excessive titanium addition [26]. These analyses mean that, for stable and consistent production of high strength 9Cr-ODS TMS tube, allowable specifications of Ti and Ex.O concentrations along with consolidation temperature should be carefully determined. JAEA revealed the importance of inclusion control in ODS steel fabrication. In Charpy impact tests, full pre-alloy steel was shown to be much superior to pre-mix steel: approximately four times upper shelf energy and apparently lower ductile-brittle transition temperature. Fractographic investigation revealed that this improvement was caused by reduction of inclusions by applying the full pre-alloy process [19].

Figure 6. Small angle neutron and X-ray analysis result of 9Cr-ODS steel model alloys containing different concentrations of Ti, and Ex.O [25]

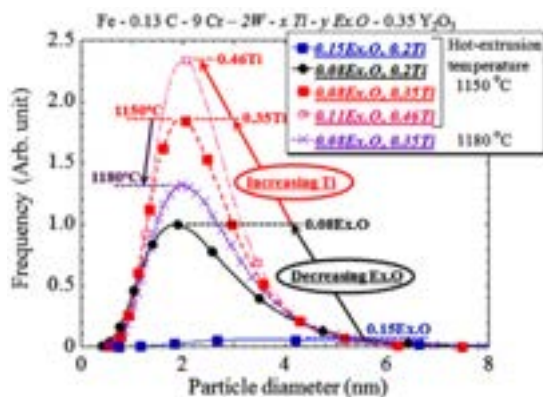
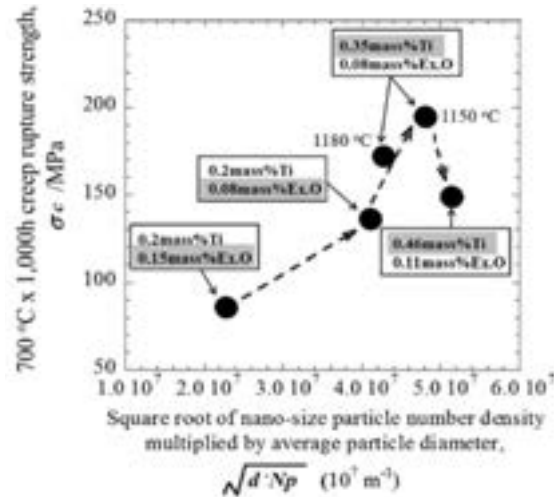


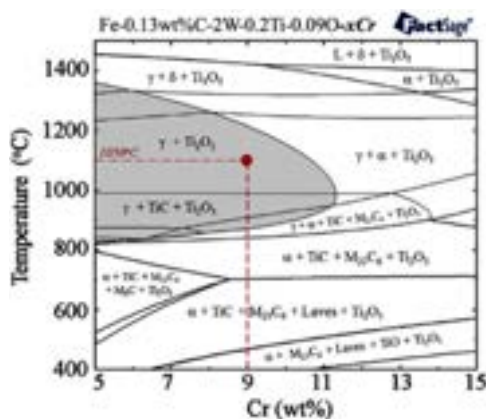
Figure 7. Correlation between creep rupture strength and condition of nano-sized oxide particle dispersion, which was evaluated by small angle neutron and X-ray analysis. α is volume fraction of residual- α ferritic phase evaluated by EPMA analysis [25]



II.D Development of high Cr-ODS TMS

It has been demonstrated that the 9Cr-ODS TMS cladding tube had notably improved strength. On the other hand, corrosion resistance of 9Cr-ODS TMS has been a concern for use as high burn-up fuel cladding tube. Higher Cr concentrations are preferable in terms of fuel-cladding chemical interaction (FCCI) and compatibility with HNO₃ solution in spent fuel reprocessing. JAEA started developing high Cr-ODS TMS cladding tube to increase the flexibility of ODS TMS development for SFR fuel. Basic chemical composition of high Cr-ODS TMS was studied on the basis of the information on microstructural studies of 9Cr-ODS TMS. Modification of the chemical composition other than Cr was examined to minimise the trade-off effect produced by increasing the Cr concentration (i.e. degradations in mechanical properties). Increasing Cr concentration from 9 wt% to 11-12 wt% is known to be effective for improvement of corrosion resistance. JAEA 12Cr-ODS steel and the conventional heat-resistant steels HT9 and PNC-FMS, contain 11-12 wt% Cr.

Figure 8. Phase diagram of Fe-0.13 wt%C-2 W-0.2Ti-0.09O-xCr system calculated by FaCTsage code with FSstel database [29]

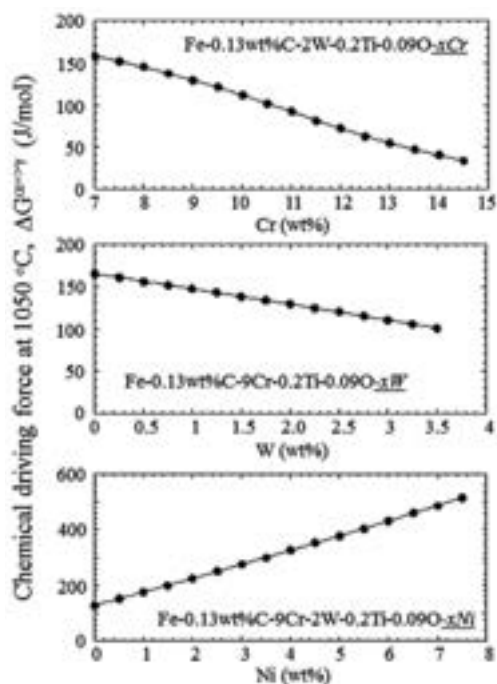


It was reported that they had adequate mechanical properties including ductility after neutron irradiation from 16 to 43 dpa at temperature from 420 to 835°C [22, 28]. Thus, the Cr concentration of the high Cr-ODS TMS was set to 11wt%. Figure 8 shows the phase diagram of Fe-0.13 wt%C-2 W-0.2Ti-0.09O-xCr system calculated by FaCTsage code with FSstel database [29]. It clearly indicates that α ferritic phase is stabilised with increasing Cr at 1050°C. In the composition containing Fe-0.13wt%C-9Cr-2W-0.2Ti-0.09O-0Ni, the heat treatment at 1050°C annealing produces fully γ - phase matrix, and following rapid cooling leads to the martensitic single phase matrix (i.e. no residual- α ferrite). However, residual- α ferrite is actually formed in the ODS TMS with this composition [4, 17, 18, 25, 27]. It has been believed that pinning of the α - γ interface by oxide particles suppresses the α to γ reverse transformation and produces the residual- α ferrite in the non-equilibrium state [30]; the formation of duplex matrix in ODS TMS is easier than in the conventional TMS produced without oxide particle dispersion.

Thus, it follows that the minor adjustment of chemical composition (e.g., decreasing the ferrite-forming element and increasing the austenite-forming element) is required to prevent excessive formation of residual- α ferrite in 11Cr ODS TMS. For controlling residual- α ferrite proportion, the parameter “chemical driving force for α to γ reverse transformation” was tentatively used in this study. In the first step, the Gibbs energy at 1050°C was calculated for the compositions of

ODS TMS in which, according to the calculation, the main matrix was austenite. In the next step, the austenite phase was set to be dormant to get the Gibbs energy of the ferrite matrix system at 1050°C. The chemical driving force for α to γ reverse transformation ($\Delta G_{\alpha \rightarrow \gamma}$) at 1050°C was calculated by subtracting the calculated Gibbs energy of the austenite matrix system from that of the ferrite matrix system. The calculated results are shown in Figure 9, where the calculated $\Delta G_{\alpha \rightarrow \gamma}$ at 1050°C was plotted as a functions of Cr, W and Ni concentrations. Increasing the concentrations of Cr and W (ferrite-forming elements) lowered the $\Delta G_{\alpha \rightarrow \gamma}$ while increasing Ni concentration (austenite-forming element) elevated the $\Delta G_{\alpha \rightarrow \gamma}$. Chromium is a strong ferrite-forming elements, so that increasing Cr concentration from 9 to 11 wt% leads to excessive formation of residual- α ferrite. As shown in Table 2, carbon contained in 9Cr-ODS TMS is an austenite-forming element, however, increasing C concentration was excluded as an option because increasing C concentration produces Cr carbides, thus decreasing matrix solute Cr.

Figure 9. Calculated chemical driving force for α to γ reverse phase transformation at 1050 °C as a function of Cr, W, and Ni concentration



Nickel is often used as an additive to suppress formation of δ -ferrite phase in conventional ferritic steels. For 11Cr-ODS TMS, Ni was added to control residual- α ferrite proportion. Addition of Ni is known to lower Ac1 temperature as calculated in Figure 10. It was reported that nano-sized oxide particle dispersion elevated the Ac1 temperature of 9Cr-ODS TMS [30]; indeed, Ac1 point of JAEA 9Cr-ODS TMS was measured to be 880°C [31], which was roughly 40°C higher than the equilibrium value estimated from Figure 9. On the basis of this measurement result, Ni concentration of 0.4 wt% was selected to keep the Ac1 temperature higher than 850°C in 11Cr-ODS TMS with the intention of keeping microstructure stability in the transient event. For controlling the residual- α ferrite proportion in 11Cr-ODS steel, concentrations of ferrite-forming element should be decreased in addition to Ni addition. Among main constituent elements of 9Cr-ODS TMS, ferrite-forming element except for Cr was W. Figure 11 shows the calculated $\Delta G_{\alpha \rightarrow \gamma}$ as a function of W concentration in the 11Cr-0.13C-0.4Ni-0.2Ti-0.07O-xW system, where the $\Delta G_{\alpha \rightarrow \gamma}$ for 9Cr-ODS TMS was shown for comparison. For obtaining the duplex microstructure equivalent to 9Cr-ODS TMS, the appropriate W concentration for 11Cr-ODS TMS was estimated to be 1.4wt%.

Figure 10. Change of Ac1 temperature as a function of Ni concentration calculated by FactSage code with FSstel data [3]

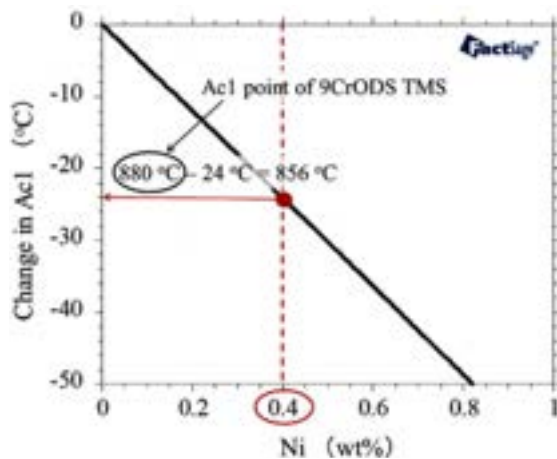


Figure 11. Calculated chemical driving force for α to γ reverse phase transformation as a function of W concentration in the 11Cr-0.13C-0.4Ni-0.2Ti-0.07O-xW system [3]

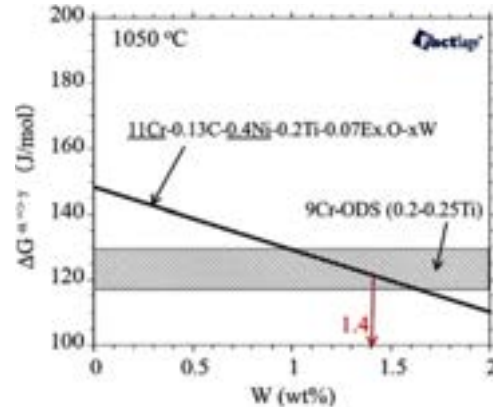


Figure 12. Ac1 point measurement result of 11Cr-ODS TMS (Chemical analysis result : Fe-0.14wt%C-10.8Cr-1.3W-0.4Ni-0.22Ti-0.34Y2O3-0.06Ex.O) using TMA

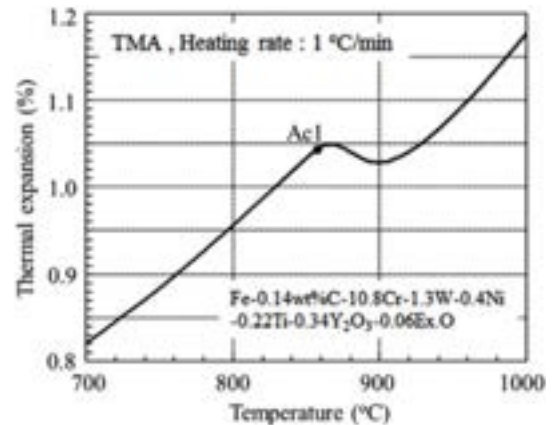


Table 2. Basic chemical composition of JAEA 9Cr,11Cr-ODS TMS cladding tube

	Chemical composition* (wt%)						
	Cr	C	Ni	W	Ti	Y ₂ O ₃	Ex.O
9Cr-ODS	9	0.13	-	2.0	0.2-0.3	0.35	0.04-0.10
11Cr-ODS	10-12	0.13	0.4	1.4	0.2-0.3	0.35	0.04-0.10

* Ferrite-forming element : Cr, W, Ti, Austenite-forming element : C, Ni

As discussed in section II.C, dispersion control of nano-sized oxide particle is essential for high-temperature strength improvement of ODS TMS. The concentrations of Ti, Ex.O and Y_2O_3 selected for 9Cr-ODS TMS was adopted for those of 11Cr-ODS TMS (Table 2).

Figure 13. Internally pressurised creep rupture strength of 11Cr-ODS TMS fuel cladding tube [3]

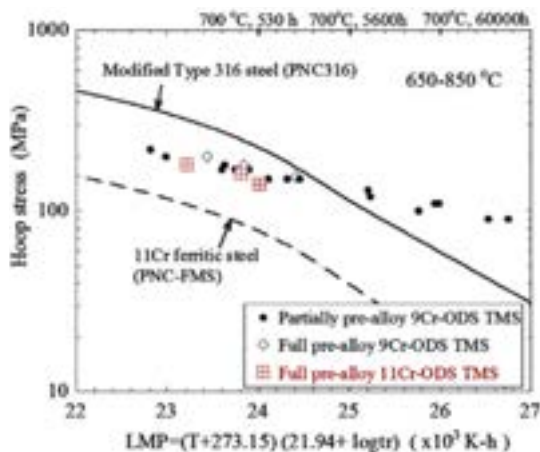
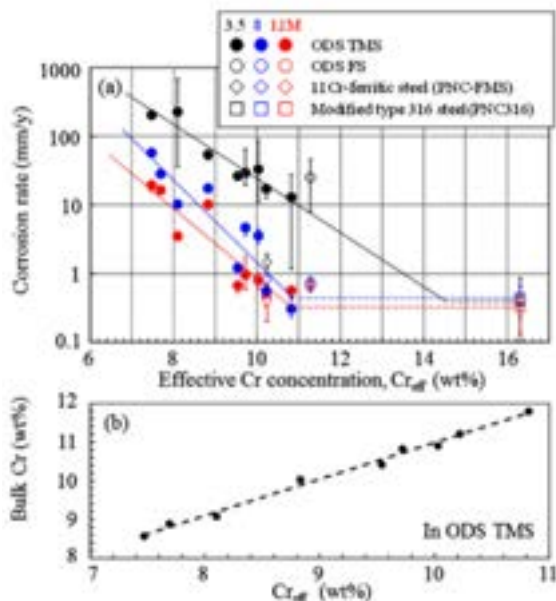


Figure 14. HNO₃ corrosion test results, (a) corrosion rate in nitric acid solutions for 30 min at 95 °C as a function of Cr_{eff} , and (b) Correlation between Cr_{eff} and bulk Cr concentration [32]



Multi-scale microstructural analysis (i.e. TEM, small angle X-ray scattering analysis, metallography, SEM/EPMA, high-temperature XRD) showed that the duplex matrix and nano-structure of 11Cr-ODS steel were successfully controlled as equivalent to 9Cr-ODS TMS [3, 18], e.g. 15-20 vol.% of residual- α ferrite proportion according to high temperature XRD characterisation, nano-sized oxide particle dispersion with the number density of around $5 \times 10^{23} \text{ m}^{-3}$ and the average diameter of roughly 3nm according to small angle X-ray scattering analysis [3, 18]. As for high temperature phase stability, dilatometric analysis of 11Cr-ODS TMS using thermo-mechanical analyser (TMA) showed that A_{c1} point of 11Cr-ODS TMS is sufficiently high (i.e. $A_{c1} > 850^\circ\text{C}$) (Figure 12) as designed by thermo-dynamic calculation. High-temperature strength of 11Cr-ODS TMS was shown to be comparable to that of 9Cr-ODS TMS (Figure 13) [3]. Figure 14 shows corrosion rate of 9Cr,11Cr-ODS TMS in nitric acid solutions for 30 min at 95°C on effective Cr concentration (Cr_{eff}) [32], where Cr_{eff} of 11Cr-ODS TMS was around 10wt%. Cr_{eff} means matrix solute Cr concentration estimated by chemical equilibrium calculation at tempering temperature (800°C). A part of Cr in ferritic steels is precipitated as Cr carbides, so that Cr_{eff} is slightly lower than bulk Cr concentration. This test result clearly demonstrated the improvement of compatibility with HNO₃ solution by increase of Cr concentration from 9 to 11wt%.

JAEA has already demonstrated adequate manufacturability of 11Cr-ODS TMS; three lots of full pre-alloy 11Cr-ODS TMS cladding tube were successfully manufactured without any cracks and quality problems. Total number of manufactured tube were 36. PRW test between 11Cr-ODS TMS cladding tube and 9Cr-ODS TMS end-plug proved that 11Cr-ODS TMS had adequate bondability equivalent to 9Cr-ODS TMS [3]. From the results of comprehensive study, JAEA rates the 11Cr-ODS TMS as a promising material for high burn-up fuel cladding tube of SFR along with 9Cr-ODS TMS. For development and qualification of 11Cr-ODS TMS, derivation of neutron irradiation data and long term creep rupture data are important issues in the future.

III. Future Plan

There are three important tasks for ODS TMS development after this; the development of large scale manufacturing technology for future mass production, the demonstration of

irradiation performance in the high burn-up condition and the establishment of material strength standard. Towards the development of mass production process, scaling up R&D of the mechanical alloying process is on-going in JAEA. The knowledge for producing high performance tubes including the full pre-alloy process has been accumulated through laboratory scale manufacturing tests of 9Cr-ODS TMS so far. These knowledge will be applied to development and optimisation of large scale manufacturing process. Planning of neutron irradiation test of 9Cr,11Cr-ODS TMS is on-going towards their irradiation performance evaluation after Joyo restart. These data will be used for performance comparison and selection of two types of ODS TMS. They will be also used for preparation of the material strength standard of these steels for fuel pin designing.

IV. Summaries

JAEA has developed ODS TMS as prospective material for high burn-up fuel cladding tube. Development of laboratory scale manufacturing technology has completed for ODS TMS. Development of mass production process is on-going in JAEA. Neutron irradiation data to approximately 30 dpa using Joyo showed that 9Cr-ODS TMS cladding tube had notable irradiation tolerance. On the basis of knowledge on 9Cr-ODS TMS studies, JAEA has started developing a new type of high Cr-ODS TMS, i.e. 11Cr-ODS TMS. JAEA is planning to

derive neutron irradiation data of 9Cr,11Cr-ODS TMS after Joyo restart.

Acknowledgements

The authors wish to offer their special thanks to Dr. M. Fujiwara, Mr. T. Nakai, and Dr. T. Okuda, KOBELCO Research Institute, and Mr. T. Kobayashi, Nippon Steel & Sumikin Technology for their support and contribution to ODS steel development.

Nomenclature

Ex.O	EXcess Oxygen
FaCT	Fast reactor Cycle Technology development
FCCI	Fuel-Cladding Chemical Interaction
FR	Fast Reactor
MA	Mechanical Alloying
ODS	Oxide Dispersion Strengthened
PRW	Pressurised Resistance Welding
SFR	Sodium cooled Fast Reactor
TMA	Thermo-Mechanical Analyser
JAEA	Japan Atomic Energy Agency
MARICO	MATERIAL testing RIG with temperature Control

References

- [1] S. Ukai, M. Fujiwara, J. Nucl. Mater. 307–311 (2002) 749–757.
- [2] T. Kaito, S. Ohtsuka, M. Inoue, Progress in the R&D on oxide dispersion strengthened and precipitation hardened ferritic steels for sodium cooled fast breeder reactor fuels, in: Proc. GLOBAL 2007, Boise, Idaho, September 9-13, 2007, pp.37–42 (CD-ROM).
- [3] T. Asayama, S. Ohtsuka, Development of core and structural materials for fast reactors, in: Proc. of International Conference on Fast Reactors and Related Fuel Cycles (FR17), Yekaterinburg, Russian Federation, June 26 – 29, 2017, IAEA-CN245-077.
- [4] S. Ohtsuka, S. Ukai, H. Sakasegawa, M. Fujiwara, T. Kaito, T. Narita, J. Nucl. Mater. 367–370 (2007) 160–165.
- [5] P. Dubuisson, Y. de Carlan, V. Garat, M. Blat, J. Nucl. Mater. 428 (2012) 6–12.
- [6] D. T. Hoelzer, K. A. Unocic, M. A. Sokolov, T. S. Byun, J. Nucl. Mater. 471 (2016) 251–265.
- [7] A. Das, H.W. Viehrig, F. Bergner, C. Heintze, E. Altstadt, J. Hoffmann, J. Nucl. Mater. 491 (2017) 83–93.

- [8] D. Kumar, U. Prakash, V.V. Dabhade, K. Laha, T. Sakhivel, *J. Nucl. Mater.* 488 (2017) 75-82.
- [9] J. H. Kim, T. S. Byun, J. H. Lee, J. Y. Min, S. W. Kim, C. H. Park, B. H. Lee, *J. Nucl. Mater.* 449 (2014) 300-307.
- [10] H. Dong, L. Yu, Y. Liu, C. Liu, H. Li, J. Wu, *J. Alloys Comp.* 702 (2017) 538-545.
- [11] N. H. Oono, S. Ukai, S. Hayashi, S. Ohtsuka, T. Kaito, A. Kimura, T. Torimaru, K. Sakamoto, *J. Nucl. Mater.* 493 (2017) 180-188.
- [12] A. Kimura, R. Kasada, N. Iwata, H. Kishimoto, C. H. Zhang, J. Isselin, P. Dou, J. H. Lee, N. Muthukumar, T. Okuda, M. Inoue, S. Ukai, S. Ohnuki, T. Fujisawa, F. Abe, *J. Nucl. Mater.* 417 (2011) 176-179.
- [13] Y. Shimakawa, S. Kasai, M. Konomua, M. Toda, *Nucl. Technol.* Vol.140 (2002) 1-17.
- [14] M. Ichimiya, T. Mizuno and S. Kotake, *Nucl. Eng. and Technol.*, Vol.39 No.3 (2007) 171-186.
- [15] T. Kaito, Y.Yano, S.Ohtsuka, M.Inoue, K.Tanaka, A.E. Fedoseev, A.V. Povstyanko, A. Novoselov, *J. Nucl. Sci. Technol.* Vol. 50, No. 4, pp.387-399 (2013).
- [16] S. Ohtsuka, T. Kaito, Y. Yano, S. Yamashita, R. Ogawa, T. Uwaba, S. Koyama, K. Tanaka, *J. Nucl. Sci. Technol.* Vol. 50, No. 5, pp.470-480 (2013)
- [17] S. Ohtsuka, T. Kaito, T. Tanno, Y. Yano, S. Koyama, K. Tanaka, *J. Nucl. Mater.* 442 (2013) S89-S94.
- [18] T. Tanno, S. Ohtsuka, Y. Yano, T. Kaito, Y. Oba, M. Ohnuma, S. Koyama, K. Tanaka, *J. Nucl. Mater.* 440 (2013) 568-574.
- [19] T. Tanno, S. Ohtsuka, Y. Yano, T. Kaito, T. Kenya, *J. Nucl. Mater.* 455 (2014) 480-485.
- [20] M. Seki, K. Hirako, S. Kono, Y. Kihara, T. Kaito, S. Ukai, *J. Nucl. Mater.* 329-333 (2004) 1534-1538.
- [21] Y. Yano, T. Tanno, H. Oka, S. Ohtsuka, T. Inoue, S. Kato, T. Furukawa, T. Uwaba, T. Kaito, S. Ukai, N. Oono, A. Kimura, S. Hayashi, T. Torimaru, *J. Nucl. Mater.* 487 (2017) 229-237.
- [22] Y.Yano, R.Ogawa, S.Yamashita, S.Ohtsuka, T.Kaito, N.Akasaka, M.Inoue, T.Yoshitake, K.Tanaka, *J. Nucl. Mater.* 419 (2011) 305-309.
- [23] T.Kaito, S.Ohtsuka, M.Inoue, T.Asayama, T.Uwaba, S.Mizuta, S.Ukai, T.Furukawa, C.Ito, E.Kagota, R.Kitamura, T.Aoyama, T.Inoue, *J.Nucl.Mater.* 386-388 (2009) 294-298.
- [24] S.Yamashita, Y.Yano, S.Ohtsuka, T.Yoshitake, T.Kaito, S.Koyama, K.Tanaka, *J.Nucl.Mater.* Vol.442 (2013) 417-424
- [25] S.Ohtsuka, T.Kaito, S.Kim, M.Inoue, T.Asayama, M.Ohnuma, J.Suzuki, *Mater. Trans.* Vol. 50, No. 7 (2009) 1778-1784.
- [26] M. Ohnuma, J. Suzuki, S. Ohtsuka, S.-W. Kim, T. Kaito, M. Inoue, H. Kitazawa, *Acta Mater.* 57 (2009) 5571-5581.
- [27] H. Oka, T. Tanno, S. Ohtsuka, Y. Yano, T. Uwaba, T. Kaito, M. Ohnuma, *Nucl. Mater. Energy* 9 (2016) 346-352.
- [28] Y. Yano, T. Yoshitake, S. Yamashita, N. Akasaka, S. Onose, S. Watanabe and H. Takahashi, *J. Nucl. Sci. Technol.* Vol. 44(12) (2007)1535-1542.
- [29] C. Bale, E. Belisle, P. Chartrand, S. Decterov, G. Eriksson, A. Gheribi, K. Hack, I. Jung, Y. Kang, J. Melancon, A. Pelton, S. Petersen, C. Robelin, J. Sangster, P. Spencer, M. Vanende, *CALPHAD* Vol.54, pp.35-53 (2016).
- [30] M. Yamamoto, S. Ukai, S. Hayashi, T. Kaito, S. Ohtsuka, *J. Nucl. Mater.* 417 (2011) 237-240.
- [31] S.Ukai, S.Mizuta, M.Fujiwara, T.Okuda, T.Kobayashi, *J. Nucl. Sci. Technol.* Vol. 39, No. 7 (2002) p. 778-788.
- [32] T. Tanno, M. Takeuchi, S. Ohtsuka, T. Kaito, *J. Nucl. Mater.* 494 (2017) 219-226.

PHYSICAL PROPERTIES OF NON-STOICHIOMETRIC (U, PU)O₂ (M. WATANABE ET AL)

Masashi Watanabe⁽¹⁾, Taku Matsumoto⁽²⁾, Shun Hirooka⁽³⁾, Kyoichi Morimoto⁽⁴⁾,
Masato Kato⁽⁵⁾

(1) & (5) Fuel Cycle Design Department, Japan Atomic Energy Agency, Japan
(2-4) Fuel Technology Department, Japan Atomic Energy Agency, Japan

Abstract

Studies on the physical properties of uranium and plutonium mixed oxide (U, Pu)O_{2±x} have been performed to further the development of advanced nuclear fuels. Knowing the physical properties of the nuclear fuels is essential for evaluating the fuel performance. It is well known that (U, Pu)O_{2±x} has a fluorite structure and it is a non-stoichiometric compound that stably exists in both regions of hyper- and hypo-stoichiometry. Its physical properties such as diffusion coefficient and thermal conductivity are strongly affected by its non-stoichiometry. Various physical properties of (U, Pu)O_{2±x} have been studied as a function of the oxygen-to-metal (O/M) ratio.

Recently, a research group studying at the Japan Atomic Energy Agency's Plutonium Fuel Development Facility (PFDF) has systematically measured a vast number of physical properties of (U, Pu)O_{2±x}; the lattice parameter, elastic modulus, thermal expansion, oxygen potential, oxygen chemical diffusion coefficient and thermal conductivity were successfully measured as function of Pu content, O/M ratio and temperature; moreover, the effects of Pu content and O/M ratio upon such physical properties were evaluated. In this work, these experimental data are reviewed, and the latest experimental data set for (U, Pu)O_{2±x} is presented. These data can be used in the development of a fuel-performance code.

I. Introduction

The physical properties of uranium-plutonium mixed-oxide (MOX) fuels, which are non-stoichiometric compounds, are significantly affected by the Pu content and the O/M ratio [1-8]. Therefore, it is important to understand the effects of these parameters to evaluate the properties and irradiation behaviour of MOX fuels.

Many studies on the physical properties of MOX fuel were performed from the 1960's to 80's, but their findings varied because the O/M ratio of MOX fuel readily changes with temperature and oxygen partial pressure. Therefore, we have carried out systematic and accurate measurements of the lattice parameter, elastic modulus, thermal expansion, oxygen potential, oxygen diffusion, and thermal conductivity of MOX fuels, and we summarise the results in

this paper. The effects of Pu content, O/M ratio and temperature upon these physical properties are evaluated.

II. Lattice Parameters

Lattice parameters are basic data for expressing material characteristics. These are used to evaluate the thermal properties of MOX such as thermal conductivities and heat capacities. In addition, the theoretical density of MOX is obtained from the lattice parameters and it is used to determine the quality of the fuel pellets in the fabrication process. Thus, lattice parameters are essential for developing nuclear fuels.

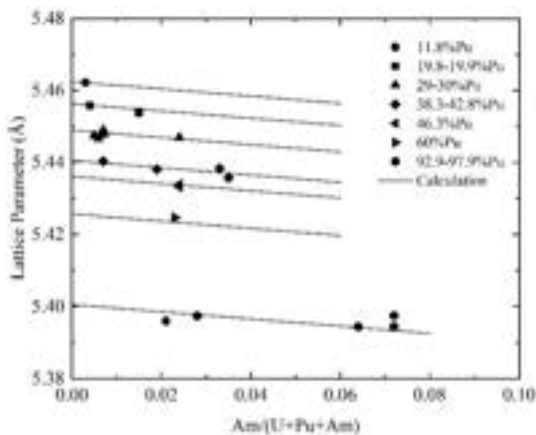
Previous works [9, 10], have updated the database of lattice parameters of MOX fuels containing minor actinides (MAs). There are about 120 data points relating to the Pu, Am,

and Np content and the O/M ratios. The lattice parameters were analysed using the database, with the result suggesting that MOX-containing Np and Am formed a substitutional solid solution. The lattice parameters of MA-MOX fuels obeyed Vegard's law, and increased with decreasing O/M ratio. An equation for calculating the lattice parameter of $(U_{1-z-y'-y''}Pu_zAm_yNp_y)O_{2.00-x}$ was derived by using the ionic-radius model, which is described as follows:

$$a = 4/\sqrt{3} [(r_U(1-z-y'-y'') + r_{Pu}z + r_{Am}y' + r_{Np}y'')(1 + 0.112x) + r_a], \quad (1)$$

where r_U , r_{Pu} , r_{Am} , r_{Np} and r_a , are 0.9972, 0.9642, 0.9539, 0.9805 and 1.372 Å respectively. Fig. 1 shows the calculation results in $(U_{1-z-y'-y''}Pu_zAm_y)O_{2.00}$. The lattice parameter decreased with increasing Pu and Am contents.

Figure 1. The lattice parameters of $(U_{1-z-y'-y''}Pu_zAm_y)O_{2.00}$



III. Elastic Modulus

The mechanical properties of MOX fuel are needed to evaluate various irradiation behaviours of fuel pellets, such as pellet-cladding mechanical interaction. The literature only reports Young's modulus data for MOX with 20% Pu content [11, 12]. In these studies, the Young's modulus of MOX was consistently higher than that of UO_2 . However, the number of data points with Pu content was limited and the trend of the Pu effect was not clearly quantified.

In a previous study [13], the sound speed of longitudinal and transverse wave in the MOX were measured as functions of porosity, O/M

ratio and Pu content. The effect of each parameter was well fitted by a linear function and the following equations were obtained for calculating the sound speeds:

$$v_L = 5358(1 - 1.3172p)(1 - 0.7279x)(1 + 0.040C_{Pu}); \quad (2)$$

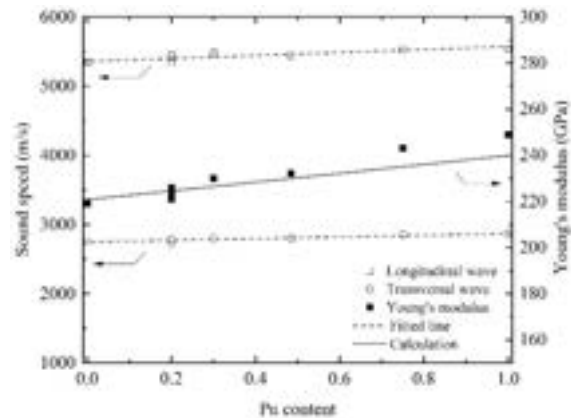
$$v_T = 2750(1 - 0.8945p)(1 - 1.0545x)(1 + 0.043C_{Pu}); \quad (3)$$

here p is the porosity, x is the deviation from stoichiometry, and C_{Pu} is the Pu content. From the sound speeds, the Young's modulus was calculated as

$$E = \rho v_T^2 [(3v_L^2 - 4v_T^2)/(v_L^2 - v_T^2)], \quad (4)$$

where ρ is the density of the specimen. Figure 2 shows the effects of Pu content for O/M = 2.000. The sound speeds and Young's modulus were higher for specimens with higher Pu content, and a linear relationship was obtained.

Figure 2. Sound speeds and Young's modulus in the MOX pellets with an O/M ratio of 2.000 as a function of Pu content.



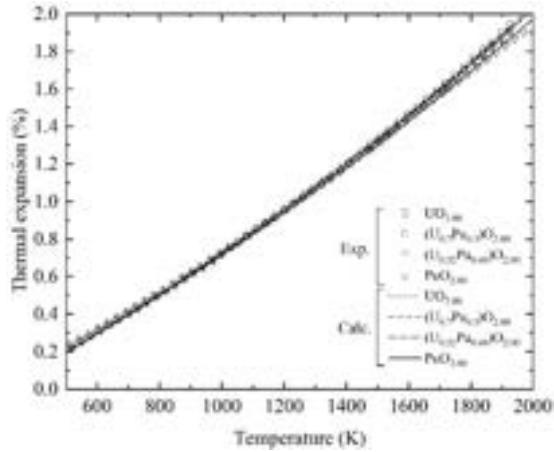
IV. Thermal Expansion

Thermal expansion has been measured by high-temperature X-ray diffractometry and thermal dilatometry [14, 15]. However, the data show variations, and it was observed that the O/M ratio was observed to change during the measurements. The measurement of MOX is difficult because this ratio changes readily with temperature and oxygen partial pressure.

In a previous study [16], the thermal expansion of MOX was successfully measured in an oxygen partial pressure controlled atmosphere and expressed as a function of O/M ratio, Pu content, and temperature. A relational

equation was derived to represent the thermal expansion. Figure 3 shows measured thermal expansions and calculated results. The thermal expansion of MOX increased slightly with decreasing Pu content.

Figure 3. Thermal expansion of $UO_{2.00}$, $(U, Pu)O_{2.00}$ and $PuO_{2.00}$.



V. Oxygen Potential

The oxygen potentials of the MOX fuels are important for evaluating the chemical behaviour of the fuel pins. Fuel-cladding chemical interaction (FCCI) occurs on the inner surface of the cladding during high burn-up and it limits the fuel’s lifetime.

Recently, we have measured the data of $(U_{0.88}Pu_{0.12})O_{2+x}$, $(U_{0.8}Pu_{0.2})O_{2+x}$ and $(U_{0.7}Pu_{0.3})O_{2+x}$, especially in the near stoichiometric region [17]. The oxygen potentials of MOX fuels were evaluated based on the defect chemistry using past results and data sets, and Brouwer diagrams were constructed for $(U_{0.88}Pu_{0.12})O_{2+x}$, $(U_{0.8}Pu_{0.2})O_{2+x}$ and $(U_{0.7}Pu_{0.3})O_{2+x}$. A relational equation to determine the O/M ratio was derived in terms of the oxygen partial pressure, Pu content and temperature as follows:

$$O/M = 2 - \left\{ \exp\left(\frac{44.0+55.8C_{Pu}}{R}\right) \exp\left(-\frac{376000}{RT}\right) P_{O_2}^{-1/2} \right\}^{-5} + \left(\left(\exp\left(\frac{68.8+131.3C_{Pu}}{R}\right) \exp\left(-\frac{515000}{RT}\right) \right)^{1/2} P_{O_2}^{-1/4} \right)^{-5} + \left(2 \exp\left(\frac{153.5-96.5C_{Pu}+331.0C_{Pu}^2}{R}\right) P_{O_2}^{-1/3} \right)^{-5}$$

$$\left(\frac{1}{2} C_{Pu} \right)^{-5} \left\{ \exp\left(\frac{-22.8-84.5C_{Pu}}{R}\right) \exp\left(\frac{105000}{RT}\right) P_{O_2}^{1/2} \right\} \cdot (5)$$

This equation cannot be applied to MOX containing more than 50%Pu, because there was not enough data in the high Pu content range. Figs. 5-7 show the measured oxygen potential data of MOX and calculation results of eq. (5). The calculation results shown in Figs. 5-7 are consistent with experimental data.

Figure 4. Oxygen potential of $(U_{0.88}Pu_{0.12})O_{2+x}$ as a function of O/M ratio for various temperatures.

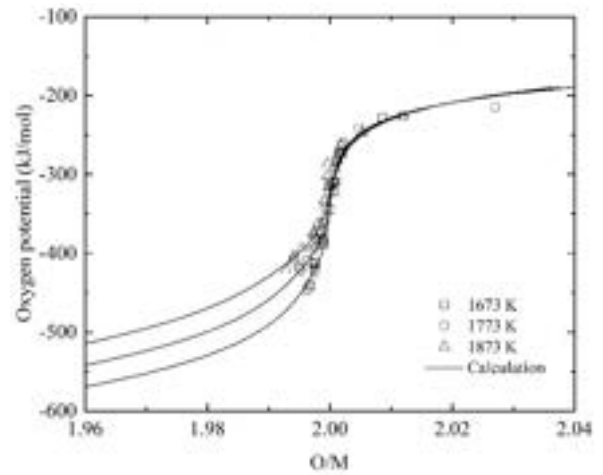


Figure 5. Oxygen potential of $(U_{0.8}Pu_{0.2})O_{2+x}$ as a function of O/M ratio for various temperatures.

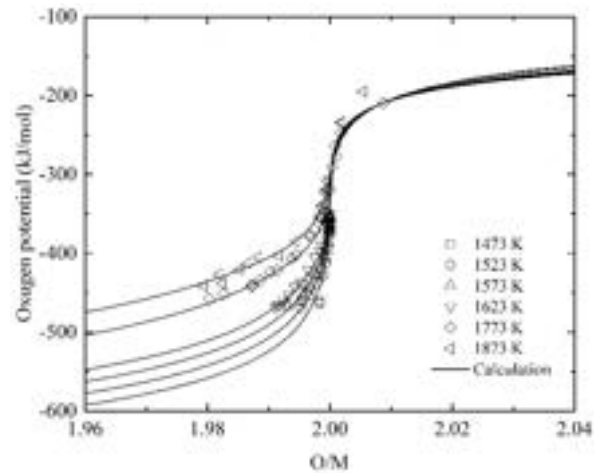
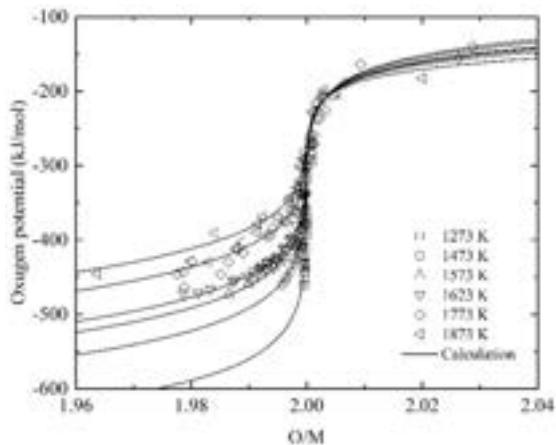


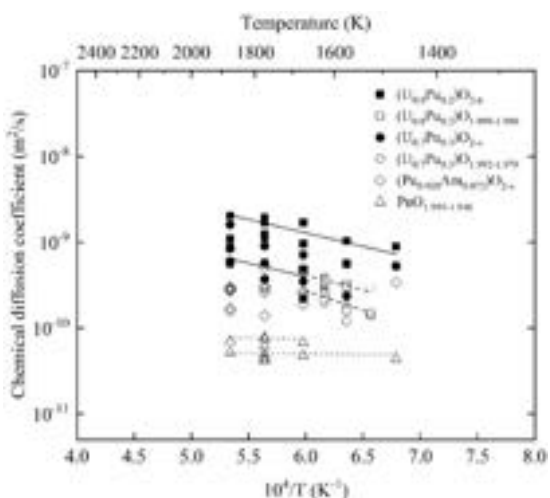
Figure 6 Oxygen potential of (U_{0.7}Pu_{0.3})O_{2+x} as a function of O/M ratio for various temperatures.



VI. Oxygen Chemical Diffusion

The change in the O/M ratio in MOX is dominated by the oxygen chemical-diffusion coefficient, which has been investigated by thermo-gravimetry and dilatometry. In early studies, the oxygen chemical-diffusion coefficient in the MOX was determined from the oxidation curves [3, 18]. Then, we measured the oxidation and reduction curves for MOX, and showed that the oxygen chemical diffusion coefficient cannot be determined by the oxidation curve because of the oxidation rate was much faster than the reduction rate [19].

Figure 7. Oxygen chemical-diffusion coefficients of (U_{0.8}Pu_{0.2})O_{2-x}, (U_{0.7}Pu_{0.3})O_{2-x}, (Pu_{0.928}Am_{0.072})O_{2-x}, and PuO_{2-x}.



The oxygen chemical-diffusion coefficients of MOX were measured as functions of O/M ratio, Pu content, and temperature [19-22]. All measurements were performed in the range of hypo-stoichiometric range and in the reduction process. Fig. 7 shows the oxygen chemical-diffusion coefficients of MOX and PuO₂ measured in our group. These oxygen chemical diffusion coefficients decrease with increasing Pu content.

VII. Thermal Conductivity

The thermal conductivity of MOX fuel is well known to vary significantly with density, O/M ratio and temperature. In previous studies [23-25], the influences of density and O/M ratio upon the thermal conductivities of MOX fuel have been evaluated. The sample densities and O/M ratios were controlled in the ranges of 85-95%TD and 1.916-2.000, respectively. The dependence of the thermal conductivities upon the density could be represented by the Maxwell-Eucken equation with a correction coefficient of 0.5. The thermal conductivities were measured to decrease significantly with decreased O/M ratio, as shown in Fig. 8. The thermal conductivities can be expressed by following equation:

$$\lambda = \frac{1}{3.31x + 9.92 \times 10^{-3} + (-6.68x + 2.46) \times 10^{-4}T}, \quad (6)$$

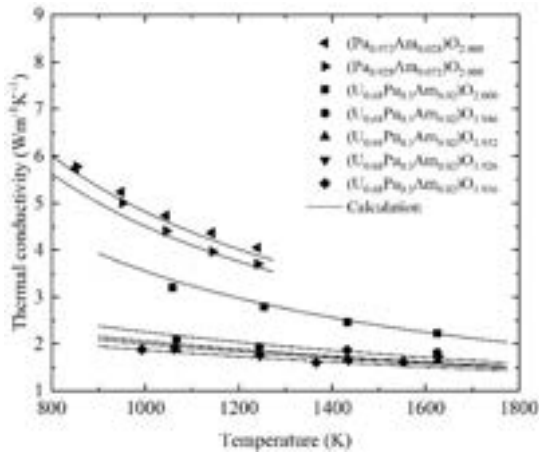
where x is deviation from the stoichiometric composition and T is the temperature.

Recently, the thermal conductivity of (Pu, Am)O₂ was successfully measured in the temperature range from 750 K to 1450 K [10]. The Am content dependences of (Pu, Am)O₂ were well explained by the phonon scattering model. The calculated thermal conductivity could be expressed by the following equation:

$$\lambda = \frac{1}{7.80 \times 10^{-5}C_{Am} + 1.49 \times 10^{-3} + 1.98 \times 10^{-4}T}, \quad (7)$$

where C_{Am} is the Am content in the (Pu, Am)O₂. This equation can be applied to PuO₂ which contains up to 7.2% Am.

Figure 8. Measured thermal conductivity together with the calculated results for MOX and PuO₂.



VIII. Conclusion

The lattice parameter, elastic modulus, thermal expansion, oxygen potential, oxygen chemical diffusion coefficient and thermal conductivity

of MOX fuels were successfully measured as function of Pu content, O/M ratio and temperature. The effects of Pu content and O/M ratio upon these physical properties were evaluated. The lattice parameters of MA-MOX fuels obeyed Vegard's law, and increased with decreasing O/M ratio. The sound speeds and Young's modulus were higher for specimens with higher Pu content, and a linear relationship was obtained. The thermal expansion of MOX increased slightly with decreasing Pu content. The oxygen potentials were evaluated based on the defect chemistry using past results and data sets, and Brouwer diagrams were constructed. The oxygen chemical diffusion coefficients decrease with increasing Pu content. The thermal conductivities decrease with increasing temperature and larger deviations of the O/M ratios from 2.00.

The relational equations of each physical property were derived from these experimental results. These equations can be managed easily managed by fuel performance codes because they have simpler representations than other reported models.

References

- [1] C. Sari, U. Benedict, H. Blank, *J. Nucl. Mater.*, 35 (1970) 276-277.
- [2] T. L. Markin, R. S. Street, *J. Inorg. Nucl. Chem.*, 29 (1967) 2265-2280.
- [3] C. Sari, *J. Nucl. Mater.*, 78 (1978) 425-426.
- [4] T. D. Chikalla, *J. Am. Ceram. Soc.*, 46 (1963) 323-328.
- [5] D. G. Martin, *J. Nucl. Mater.*, 110 (1982) 73-94
- [6] T. M. Bessman, T. B. Lindemer, *J. Nucl. Mater.*, 130 (1985) 489-504.
- [7] C. Guéneau, N. Dupin, B. Sundman, C. Martial, J. -C. Dumas, S. Gossé, S. Chatain, F. D. Bruycker, D. Manara, R. J. M. Konings, *J. Nucl. Mater.*, 419 (2011) 145-167.
- [8] E. Moore, C. Guéneau, J. -P. Crocombette, *J. Nucl. Mater.*, 485 (2017) 216-230.
- [9] M. Kato, K. Konashi, *J. Nucl. Mater.*, 385 (2009) 117-121.
- [10] T. Matsumoto, T. Arima, Y. Inagaki, K. Idemitsu, M. Kato, K. Morimoto, M. Ogasawara, *J. Alloys Comp.* 629 (2015) 92-97.
- [11] A. W. Nutt Jr., A. W. Allen, J. H. Handwerk, *J. Am. Ceram. Soc.*, 53 (1970) 205-210.
- [12] A. Padel, C. H. De Novion, *J. Nucl. Mater.*, 33 (1969) 40-51.
- [13] S. Hirooka, M. Kato, *J. Nucl. Sci. Tech.* 55 (2018) 356-362.
- [14] R. Lorenzelli M. El Sayed Ali, *J. Nucl. Mater.*, 68 (1977) 100-103.
- [15] P. J. Baldock, W. E. Spindler, T. W. Baker, 18 (1966) 305-313.
- [16] M. Kato, Y. Ikusawa, T. Sunaoshi, A. T. Nelson, K. J. McClellan, 469 (2016) 223-227.
- [17] M. Kato, M. Watanabe, T. Matsumoto, S. Hirooka, M. Akashi, 487 (2017) 424-432.
- [18] A. S. Bayoğlu, R. Lorenzelli, *Solid State Ionics* 12 (1984) 53-66.

- [19] M. Kato, K. Morimoto, T. Tamura, T. Sunaoshi, K. Konashi, S. Aono, M. Kashimura, J. Nucl. Mater., 389 (2009) 416-419.
- [20] M. Kato, T. Uchida, T. Sunaoshi, Phys. Status Solidi C, 10 (2013) 189-192.
- [21] M. Watanabe, T. Matsumoto, M. Kato, NEA/NSC/R(2015)2 376-380.
- [22] M. Watanabe, T. Sunaoshi, M. Kato, Defect and Diffusion Forum, 375 (2017) 84-90.
- [23] K. Morimoto, M. Kato, M. Ogasawara, M. Kashimura, J. Nucl. Mater., 374 (2008) 378-385.
- [24] K. Morimoto, M. Kato, M. Ogasawara, M. Kashimura, T. Abe, J. Alloys Comp., 452 (2008) 54-60.
- [25] K. Morimoto, M. Kato, M. Ogasawata, J. Nucl. Mater., 443 (2013) 286-290.

OXYGEN POTENTIAL AND SELF-IRRADIATION EFFECTS ON FUEL TEMPERATURE IN AM-MOX (Y. IKUSAWA ET AL)

Yoshihisa Ikusawa⁽¹⁾, Shun Hirooka⁽²⁾, Masayoshi Uno⁽³⁾

(1-2) Japan Atomic Energy Agency, Japan

(3) Research Institute of Nuclear Engineering, University of Fukui, Japan

Abstract

Research and development of Minor actinides (MAs) bearing MOX fuel for fast reactor has been proceeding from the viewpoint of reducing radioactive waste. In order to develop, MA bearing MOX, it is indispensable to clarify the influence of MA addition on irradiation behavior. The addition of Americium (Am) to MOX affects vapor pressure and thermal conductivity, which are important properties from the perspective of evaluating fuel temperature. This is because vapor pressure affects fuel restructuring, and thermal conductivity affects fuel temperature distribution. Focusing on these physical properties, this study evaluates the influence of Am on fuel temperature using irradiation behavior analysis code to contribute to the development of MA-bearing MOX fuel.

An increase in Am content decreases the thermal conductivity and increases the oxygen potential of oxide fuel. Because vapor pressure increases with increasing Am content, pore migration is accelerated, and the central void diameter increases with increasing Am content. As a result, after formation of the central void, the influence of Am content on the fuel center temperature is mild.

Alpha particles generated by radioactive decay of transuranium elements cause lattice defects in the oxide fuel pellets. It is well known that this phenomenon, which is called self-irradiation, affects thermal conductivity. Since americium is the typical alpha radioactive nucleus, to evaluate fuel temperature of Am-MOX is necessary to take account of the influence of self-irradiation damage on thermal conductivity. Self-irradiation decreases thermal conductivity, and as the Am content increases, the rate of decrease in thermal conductivity is accelerated. Because it recovers with temperature rise, the decrease in thermal conductivity due to self-irradiation damage has little effect on the fuel center temperature.

These results suggest that Am-MOX fuel could be irradiated under the same conditions as conventional MOX fuel.

I. Introduction

Radioactive waste is generated from nuclear power plant and hazardous to life and environment. Minor actinides (MAs) are included in radioactive waste and have long life times. Therefore, reducing MAs is one of the solutions to this problem. One thing we can do is to use MA-containing nuclear fuels in fast reactors. [1] MA-MOX fuel is one of the candidate fuels for fast reactor systems. The addition of MA to MOX affects the physical properties of fuel such as thermal conductivity, melting point, and oxygen potential. [2-4] For

developing MA-MOX, it is necessary to clarify the influence of MA addition on the irradiation behavior. In the present study, we evaluate the influence of changes in fuel properties owing to the addition of Americium (Am) on the fuel temperature during irradiation from the calculation results of irradiation behavior analysis code.[5]

II. Fuel Properties and Analysis Code

Vapor pressure and thermal conductivity are important properties from the viewpoint of evaluating fuel temperature. Vapor pressure affects fuel restructuring, and thermal conductivity affects fuel temperature distribution. Therefore, it is necessary to clarify the influence of Am addition on these physical properties.

Fuel restructuring is caused by evaporation-condensation processes. The vapor pressure of UO_3 , the dominant vapor species in MOX, strongly affects fuel restructuring. [6] Am addition increases the oxygen potential of MOX. [4] Since it leads to an increase in the vapor pressure of UO_3 , an increase in oxygen potential due to Am addition might affect fuel restructuring.

Alpha decay of Am induces lattice defects which is called self-irradiation. It is known that self-irradiation affects various fuel physical properties, and it decreases the thermal conductivity of fuel. [7,8] This is one of the most important behaviors from the viewpoint of fuel temperature evaluation.

In this study, the influence of Am content on change in vapor pressure and change in thermal conductivity by self-irradiation damage on fuel center temperature were evaluated based on the calculation results obtained using an analysis code. In the following section, we explain the vapor pressure and thermal conductivity model used in this study.

II.A Dependence of vapor pressure ON americium

Because fuel center temperature in MOX fuel pellets is higher than 2273 K during irradiation in a fast reactor, the existing pores in the as-fabricated MOX fuel pellet move toward the fuel center by evaporation-condensation processes under a radial temperature gradient. This pore migration causes the fuel restructuring, namely, a central void and columnar grains are formed. Because the fuel center temperature decreases with the formation of the central void and columnar grains, fuel restructuring is the most important behavior from the viewpoint of evaluating fuel thermal behavior. The vapor pressure of Am-MOX fuel can be evaluated using the Rand-Markin model. [5,9] Figure 1 shows the relationship between Am content and vapor pressure calculated using this model. The dominant vapor species in the figure is UO_3 ,

and its quantity increases with increasing Am content. This change in vapor pressure derives from the relationship between Am content and oxygen potential, as follows.

$$p(\text{UO}_3) = \exp\left(-\frac{\Delta G_{\text{UO}_2/\text{UO}_3}^0}{RT}\right)p(\text{UO}_2)p(\text{O}_2)^{1/2} \quad (1)$$

$$\Delta G_{\text{O}_2} = RT \ln p(\text{O}_2) \quad (2)$$

$p(\text{UO}_3)$: Vapor pressure of UO_3

$p(\text{UO}_2)$: Vapor pressure of UO_2

$p(\text{O}_2)$: Oxygen partial pressure

ΔG_{O_2} : Oxygen potential

R : Gas constant

T : Temperature

Thus, the vapor pressure of UO_3 depends on the vapor pressure of UO_2 and the oxygen partial pressure. Figure 2 shows the measured oxygen potentials of PuO_2 , AmO_2 , MOX, and Am-MOX. As shown in this figure, the oxygen potential of AmO_2 is higher than that of PuO_2 . [4] Because Am addition increases the oxygen potential, and the Am-MOX fuel has higher oxygen potential than that of MOX fuel, such a change suggests that Am addition leads to high UO_3 vapor pressure and accelerates fuel restructuring.

Figure 1. Am content dependence of vapor pressure at 2073 K (Pu = 32wt.%, O/M = 1.98)

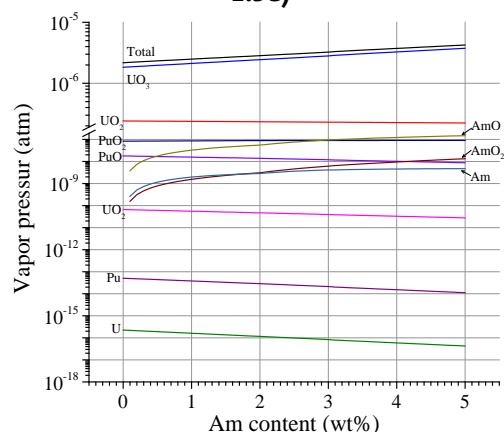
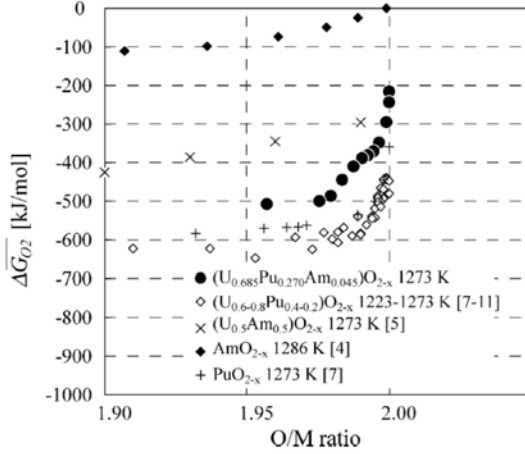


Figure 2. Measurement results of oxygen potentials of PuO₂, AmO₂, MOX, and Am-MOX[4]



II.B Reduction of thermal conductivity by self-irradiation damage

The thermal conductivity of oxide fuel can be evaluated using the following phonon transport model.

$$k = \frac{1}{A+BT} \quad (3)$$

In previous studies, we found that the change in MOX fuel thermal conductivity due to self-irradiation damage depends on the Pu content, its isotopic composition, storage time, and temperature. [8] This phenomenon for Am-MOX can be formulated as the effect of the coefficient A as follows.

$$A_{irr} = A_{irr0} \cdot \tau \cdot h(T) \quad (4)$$

$$\tau = 1 - \exp(-12000 \times \lambda t_s) \quad (5)$$

$$\lambda = C_{Pu} \sum \lambda_i C_i + C_{Am} \lambda_{Am} \quad (6)$$

$$h(T) = \frac{1}{1 + \beta \exp(-\gamma/T)} \quad (7)$$

A_{irr} : Influence of self-irradiation damage on coefficient A (mK/W)

T: Temperature (K)

C_{Pu} : Plutonium content (-)

λ_i : Decay constant of plutonium isotope (s⁻¹)

C_{Am} : Am content (-)

λ_{Am} : Decay constant of Am241 (s⁻¹)

t_s : Storage time from fabrication (s)

A_{irr0} , β , and γ : Coefficients

To account for the Am content, the above equation (6) added the Am term to the MOX fuel equation.[8] In this study, we propose the following equation for applying the term A_{irr} , which represents the effect of self-irradiation damage, to the thermal conductivity equation of MOX fuel [10] for fast reactors.

$$k = \frac{1-p}{1+0.5p} \cdot k_0 \quad (8)$$

$$k_0 = \frac{1}{A+B/T} + \frac{1.541 \times 10^{11}}{T^{2.5}} \exp\left(-\frac{15220}{T}\right) \quad (9)$$

$$A = 0.01595 + 2.713 \cdot x + 0.3583 \cdot C_{Am} + 0.06317 \cdot C_{Np} + A_{irr} \quad (10)$$

$$B = (2.493 - 2.625 \cdot x) \times 10^{-4} (11)$$

Here, k_0 is the thermal conductivity of a specimen with 100%TD, k is that of a real specimen with porosity p , x is deviation in 2.00- x , C_{Am} is Am content, C_{Np} is Np content, and T is temperature in Kelvin.

Figure 3 shows the change in the thermal conductivity with time relative to the production value, as evaluated using the above equation. As shown in the figure, the rate of decrease in thermal conductivity increases as the Am content increases. By contrast, Figure 4 shows the temperature dependence of the thermal conductivity. Because the defects due to self-irradiation recover upon the heat treatment, there is almost no influence of self-irradiation at temperatures higher than 1200 K.

Figure 3. Reduction of thermal conductivity by self-irradiation damage at 873 K (Pu = 32wt.%, O/M = 1.98)

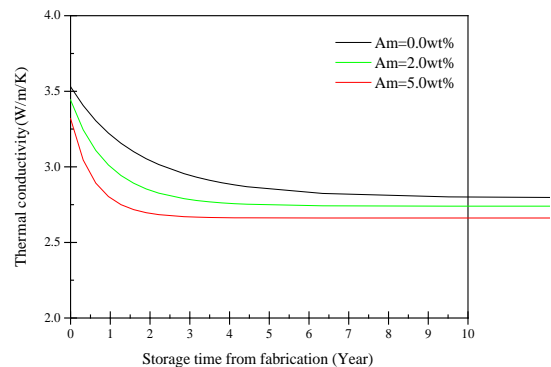


Figure 4. Temperature dependence of thermal conductivity (Am = 5.0 wt.%, O/M = 1.98)

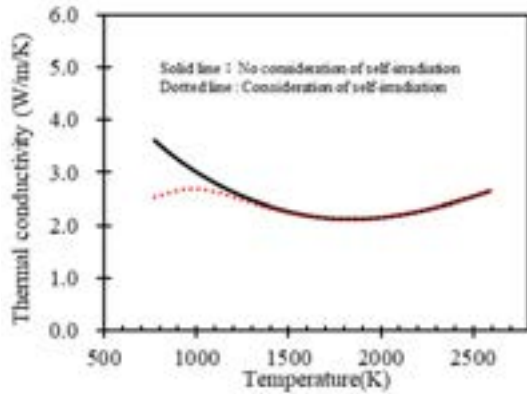
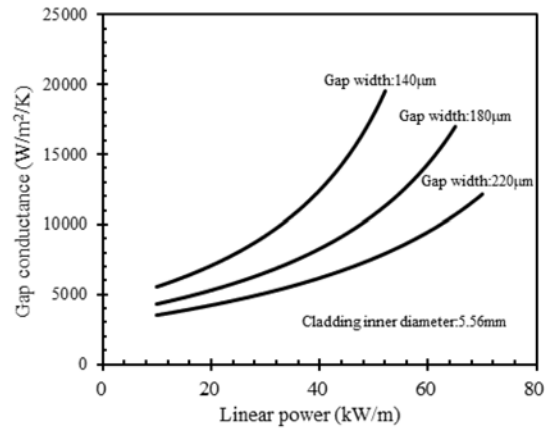


Figure 5. Linear power dependence of gap conductance calculated using equation (12)



II.C Fuel pin irradiation behavior using analysis code

We evaluated the influence of Am on fuel center temperature by using the DIRAD-TRANSIT code, [5] which can evaluate fuel temperature by using the above fuel property model. In fuel temperature evaluations, gap conductance is an important model. Herein, we used the following engineering model adapted for this code.

$$h_g = \frac{C_1 + C_2 Q}{G_0 - C_3 D_{pin} Q + C_4} \quad (12)$$

h_g : Gap conductance

$C_1 \sim C_4$: Calibration parameters

Q : Linear power

G_0 : As-fabricated gap width

D_{pin} : Cladding inner diameter

The above equation is an engineering model that is simplified to depend on linear power, as-fabricated gap width, and cladding diameter based on the Ross & Stoute [11] model. Figure 5 shows the linear power dependence of gap conductance at various gap widths calculated using this equation. The figure shows that the gap conductance increases with linear power and depends on the gap width.

III. Analysis Conditions and Results

Fuel specifications and irradiation conditions for the analysis was a reference to the B11 irradiation test fuel which was Am-bearing MOX fuel irradiated at the experimental fast reactor JOYO. [12] The influence of changes in thermal conductivity and vapor pressure on the Am content to fuel center temperature was evaluated. The presence or absence of the self-irradiation effect was evaluated as a parameter as well. The analysis conditions are listed in Table 1, and the linear power and cladding temperature history are shown in Figure 6.

Figure 6. History of linear power and cladding temperature

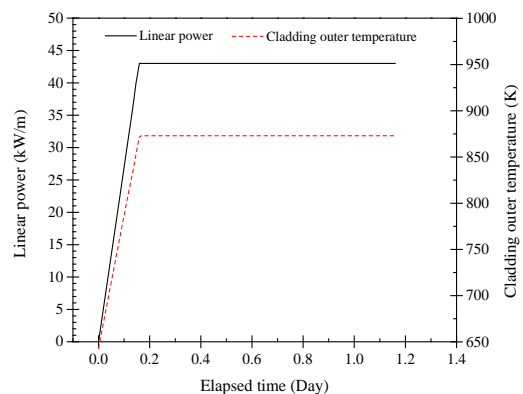


Table 1. Analysis conditions

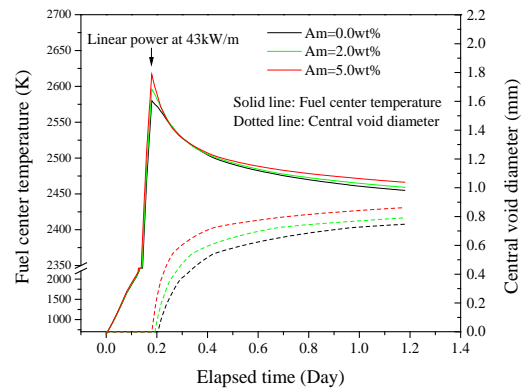
Items	Am content (wt.%)		
	0.0	2.0	5.0
Cladding outer diameter (mm)	6.5	←	←
Cladding inner diameter (mm)	5.56	←	←
Pellet outer diameter (mm)	5.42	←	←
Gap width (μm)	140	←	←
O/M (-)	1.98	←	←
Pellet density (%TD)	93	←	←
Pu content (wt.%)	32	←	←
U content (wt.%)	68	66	63
Decrease in thermal conductivity by self-irradiation damage	Considered / Not considered		
Maximum linear power (kW/m)	43		
Maximum cladding outer temperature (K)	873		

The influence of the change in vapor pressure due to the addition of Am on the fuel center temperature and the center void diameter was evaluated. After that, we evaluated the influence of decrease in thermal conductivity due to self-irradiation damage on the fuel center temperature.

III.A Fuel center temperature and Central void diameter

Figure 7 shows the history of the fuel center temperature and the central void diameter. At 43 kW/m, the fuel center temperature was the highest. Moreover, the fuel center temperature increased with increasing Am content. However, this figure shows that the fuel center temperature decreases with the passage of time owing to formation of the central void. In addition, the formation rate and the final central void diameter increased with increasing Am content. Table 2 shows a comparison of fuel temperatures before and after formation of the central void. As shown in the table, the fuel center temperature after void formation is lower than that before void formation, and this difference increases with increasing Am content, although the difference in fuel center temperature before formation of the central void is over 30K, it is about 10K after formation of the central void. Therefore, after formation of the central void, the influence of increase in Am content on the fuel center temperature is mild.

To clarify the reason underlying this analysis result, the pellet radial temperature distribution, pore migration velocity, and vapor pressure are shown in Figure 8 and Figure 9.

Figure 7. Calculation results of fuel center temperature and central void diameter**Table 2. Comparison of fuel temperatures before and after central void formation**

Am content (wt%)	Fuel center temperature (K)	
	Before central void formation	After central void formation
0.0	2580	2455
5.0	2617	2466

Figure 8 shows the fuel temperature in the radial direction and the pore migration velocity at 43 kW/m. The fuel temperature and the pore migration velocity increase with increasing Am content at all radial positions. Such an increase in the pore migration velocity leads to an increase in the diameter of the central void. The pore migration velocity “v” controlling the fuel restructuring can be calculated using the following equation:

$$v = \Omega \cdot D \frac{dn}{dT} \left(\frac{dT}{dr} \right)_{pore} \quad (14)$$

where v is the migration velocity of pores, Ω is the molecular volume, D is the diffusion coefficient, and the term (dn/dT) is expressed as

$$\left(\frac{dn}{dT} \right) = \frac{d}{dT} \left(\frac{p}{kT} \right)_{pore} \quad (15)$$

where n is the number of molecules, p is the vapor pressure of the mixed oxide, T is the temperature, and k is the Boltzmann constant. [6]

Thus, the central void diameter depends on the vapor pressure “p.” Figure 9 summarizes the evaluation results of vapor pressure at the

radial position 0.2, where the pore migration velocity is the highest in Figure 8. The vapor pressure increases with increasing Am content, as shown in Figure 9. Because the increase in Am content increases the vapor pressure of UO_3 , the total vapor pressure increases as the Am content increases, as described in II.A.

As a result, Am addition decreases thermal conductivity and increases the fuel center temperature. However, because the vapor pressure is increased, fuel restructuring is accelerated, and the diameter of the central void increases. After formation of the central void, the influence of Am content on the fuel center temperature is mild.

Figure 8. Radial distribution of fuel temperature and pore migration velocity in fuel pellet (at 47 kW/m)

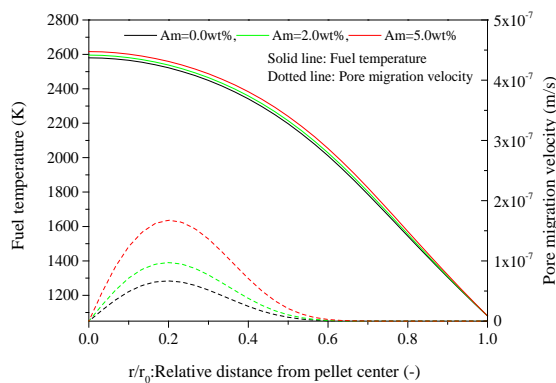
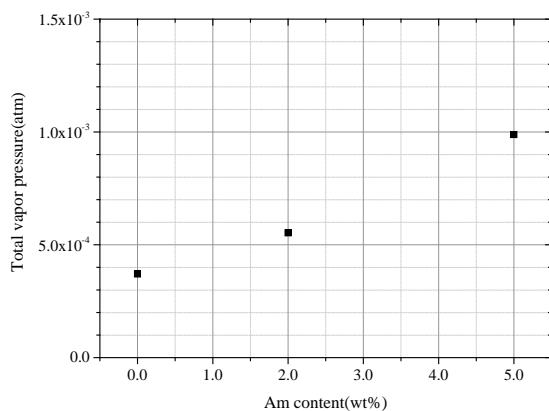


Figure 9. Am content dependence of vapor pressure at $r/r_0 = 0.2$

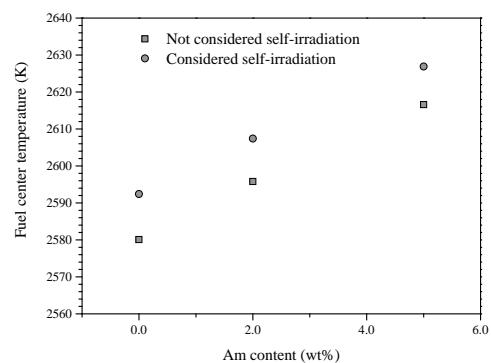


III.B EFFECT of self-irradiation on Fuel center temperature

In this evaluation, τ in equation 4 was set to 1.0, which is its saturation value. By using this value, equation 10 can be used to determine the lowest thermal conductivity due to self-irradiation damage. Therefore, the fuel temperature can then be determined under the condition that the thermal conductivity at its lowest due to self-irradiation damage.

Figure 10 shows the results of a comparison of the fuel center temperature with and without self-irradiation damage at 43 kW/m, as in Figure 6. The influence of self-irradiation on the fuel center temperature is only about 10 K because the decrease in the thermal conductivity due to self-irradiation damage is compensated for by the increase in temperature, as shown in Figure 4. This analysis result shows that although thermal conductivity during storage decreases due to self-irradiation damage, thermal conductivity recovers due to temperature rise during irradiation. Therefore, the decrease in the thermal conductivity due to self-irradiation damage has little influence on the fuel center temperature.

Figure 10. Influence of self-irradiation on fuel center temperature



IV. Conclusion

To contribute to the development of MA-bearing MOX fuel, the effect of Am on MOX fuel temperature was evaluated using an irradiation behavior analysis code.[5]

An increase in Am content decreases the thermal conductivity and increases the oxygen potential of oxide fuel. Because vapor pressure

increases with increasing Am content, pore migration is accelerated, and the central void diameter increases with increasing Am content. As a result, after formation of the central void, the influence of Am content on the fuel center temperature is mild.

By contrast, self-irradiation decreases thermal conductivity, and as the Am content increases, the rate of decrease in thermal conductivity is accelerated. Because it recovers with temperature rise, the decrease in thermal conductivity due to self-irradiation damage has little effect on fuel center temperature.

These results suggest that Am-MOX fuel could be irradiated under the same conditions as conventional MOX fuel.

Acknowledgements

The authors would like to express their appreciation to Mr. H. Nakajima (NESI Inc.) for

his considerable assistance with the code verification and development.

Nomenclature

FR	Fast Reactor
MOX	Mixed oxide
MA	Minor Actinide
Am	Americium
Pu	Plutonium
U	Uranium
Np	Neptunium
UO ₃	Uranium trioxide
PuO ₂	Plutonium dioxide
AmO ₂	Americium dioxide

References

- [1] N. Kasahara et al., Fast reactor system design, Springer, (2017), p18.
- [2] M. Kato et al., "Solidus and liquidus temperatures in the UO₂-PuO₂ system", Journal of Nuclear Materials 373 (2008) 237-245.
- [3] K. Morimoto et al., "Thermal conductivity of (U, Pu, Np)O₂ solid solutions", J. Nucl. Mater. 389 (2009) 179-185.
- [4] M. Osaka et al., "Oxygen potentials of (U_{0.685}Pu_{0.270}Am_{0.045})O_{2-x} solid solution", Journal of Alloys and Compounds 397 (2005) 110-114.
- [5] Y. Ikusawa et al., "Development and verification of the thermal behavior analysis code for MA containing MOX fuels", ICONE22, July 7-11, 2014, Prague, Czech Republic.
- [6] Y. Ikusawa et al., "Oxide-metal ratio dependence of central void formation of mixed oxide fuel irradiated in fast reactors", Nuclear Technology, vol. 199. (2017) 83-95.
- [7] D. Staicu et al., "Impact of auto-irradiation on the thermophysical properties of oxide nuclear reactor fuels", J. Nucl. Mater. 397, Issues 1-3, (2010), 8-18.
- [8] Y. Ikusawa et al., "The effects of plutonium content and self-irradiation on thermal conductivity of mixed oxide fuel", Nuclear Technology, (2018) in press.
- [9] D.R. Olander, Fundamental aspects of nuclear reactor fuel elements, TID-26711-P1, Energy Research and Development Administration, US, 1976, pp.155-160.
- [10] M. Kato et al., "Physical Properties and Irradiation Behavior Analysis of Np- and Am-Bearing MOX Fuels", J.Nucl.Sci.Technol. 48 (2011) 646-653.
- [11] A.M. Ross and R.L. Stoute, Heat Transfer Coefficient between UO₂ and Zircaloy-2, Atomic Energy of Canada Limited, AECL-1552 (1962).
- [12] K. Maeda et al., "Short-term irradiation behavior of minor actinide doped uranium plutonium mixed oxide fuels irradiated in an experimental fast reactor", J. Nucl. Mater. 385 (2009) 413-418.

HEAT CAPACITY OF UC FROM FIRST PRINCIPLES (D. LEGUT ET AL)

D. Legut⁽¹⁾ and U. D. Wdowik^(1,2)

(1) IT4Innovations, VSB – Technical University of Ostrava, Czech Republic

(2) Institute of Technology, Pedagogical University, Poland

Abstract

Uranium monocarbide is a potential fuel material for the generation IV reactors. Its electronic, magnetic, elastic, and phonon properties are determined using state-of-the-art quantum mechanical calculations based on density functional theory[1]. Obtained results are analysed and discussed in terms of spin-orbit interaction and localised versus itinerant behavior of the 5f electrons. The localisation of the 5f states is tuned by varying the local Coulomb repulsion interaction parameter. We demonstrate that the theoretical electronic structure, elastic constants, phonon dispersions, and their densities of states can reproduce accurately the results of x-ray photoemission and bremsstrahlung isochromat measurements as well as inelastic neutron scattering experiments only when the 5f states experience the spin-orbit interaction and simultaneously remain partially localised. The partial localisation of the 5f electrons could be represented by a moderate value of the on-site Coulomb interaction parameter of about 2 eV. The results of the present studies indicate that both strong electron correlations and spin-orbit effects are crucial for realistic theoretical description of the ground-state properties of uranium carbide.[2] In this paper we extend our result by analysis of the thermodynamical properties like heat capacity with both contribution coming from lattice dynamics as well as from the electronic subsystem. Our results are compared with the recorded data and show good agreement. Based on this comparison the mass-enhancement factor was refined.

I. Introduction

Recently about 130 concepts of novel nuclear reactors were evaluated and six reactor technologies were chosen for further research and development [3]. For the three of them, namely Gas-cooled Fast Reactor (GFR), Molten Salt Reactors (MSR) and Sodium-cooled Fast Reactor (SFR) the novel optimised nuclear fuels is searched for. Materials based on Pu/U carbides/nitrides are suitable for GFR, minor actinides (Np, Am, Cm) for the SFR and the actinides fluorides for the MSR. Overall, the advantage over standard fuels like U and Pu oxides and their mixture (MOX) are higher thermal conductivity, higher actinides density, higher fission temperatures, lower equilibrium vapor pressure and much better structural stability [4-6]. For the SFR the actinide fluorides serve as well not only as the fuel but also as the coolant, i.e. heat transfer medium [3]. Many of those compounds are highly radioactive and therefore it is desirable to investigate the thermophysical properties of the above

compounds using the quantum-mechanical calculations utilising the HPC resources. The main aim of our research is to determine the contributions (lattice vibrations, electrons, etc.) to the heat transfer and dilatation of the novel nuclear fuels like those based on actinide carbides and to develop a methodology for the accurate description of the electronic structure of those materials. These allow us to calculate the optimum fuel materials for various reactor designs. The key physical quantities are the thermal expansion and thermal conductivity of various actinide carbides, nitrides, and fluorides, i.e. mainly systems in Ac-Pa-U-Th-Np-Pu/C,N, and F. Let us point out the number of the compounds is related to the effect of weak vs. strong localisation of dual behavior of f-electrons, i.e. Ac-C behaves differently than Pu-C (commonly referred to the most complex actinide system). To achieve thermal expansion and thermal conductivity one needs very precise description of the electronic structure and phonon density of states and dispersion relation. Here we extend our pioneering study [1] for uranium carbide (UC), where for the first

time the correct description of optical phonon branches were obtained. This was only possible if the both spin-orbit coupling (SOC) and partly localisation using Hubbard U technique [7] was at the same time taken into account. In this paper we analyse thermodynamical properties such as heat capacity and its contribution by electron and phonon subsystems.

II. Methodology

Quantum mechanical calculations are based on the spin-polarised DFT method implementing the projector-augmented-wave (PAW) formalism for the treatment of the electron-ion interactions and the generalised gradient approximation parametrised by Pedrew, Burke, and Ernzerhof (GGA-PBE) for the exchange-correlation potential [8,9]. The cutoff energy of 520 eV for the wave functions expanded into plane waves was used. The valence electrons of uranium and carbon atoms are represented by configurations of $(6s^2 6p^6 5f^3 6d^1 7s^2)$ and $(2s^2 2p^2)$, respectively. Both the spin-orbit coupling and additional on-site Coulomb repulsion interaction are considered at the same time. The latter are taken into account within the rotationally invariant form of the GGA+U approach [7], where the localised 5f electrons experience a spin- and orbital-dependent potential (U) and the exchange interaction J, while the other orbitals are delocalised and treated by the conventional GGA approximation. As shown in our study [2] we adopt $J = 0.5$ eV and $U = 2.5$ eV, i.e. $U_{\text{eff}} = 2.0$ eV for the most accurate description of electronic structure (ES) and phonon dispersion relation see Figs. 3,6,7 of Ref. [2]. Uranium carbide holds a stable rocksalt structure (space group No. 225) within a wide range of temperatures and stoichiometries [10]. Its unit cell contains 8 atoms (4U and 4C atoms). Calculations are performed with the $10 \times 10 \times 10$ Monkhorst-Pack mesh of k-points. The convergence criteria for the system total energy and residual Hellmann-Feynman (HF) forces are set to 10^{-7} eV and 10^{-5} eV/Å respectively. The type-I antiferromagnetic order (AFM-I), in which the magnetic moments on the U atoms are aligned within the (100) layer and opposite to the moments of the next (100) layer, is considered. The dynamical properties of the UC lattice are obtained within the harmonic approximation and the direct method [11], which utilises the DFT calculated HF forces acting on all atoms in a given 64-atom supercell [2]. The Brillouin zone integration is performed with the reduced number of k points ($4 \times 4 \times 4$). The nonvanishing HF forces required to construct respective dynamical matrix $D(\mathbf{k})$ are generated by displacing the symmetry nonequivalent U

and C atoms from their equilibrium positions by the amplitude of ± 0.02 Å with number of 4 displacements.

III. Results

Based on the phonon density of the states and phonon dispersion relation well reproducing experimental results, see Figs. 3,6,7 of Ref. [2] the lattice heat capacity at constant volume was determined using

$$C_{ph} = Nrk_B \int d\omega D(\omega) \left(\frac{\hbar\omega}{k_B T} \right) \frac{\exp\left(\frac{\hbar\omega}{k_B T}\right)}{\left[\exp\left(\frac{\hbar\omega}{k_B T}\right) - 1 \right]^2}$$

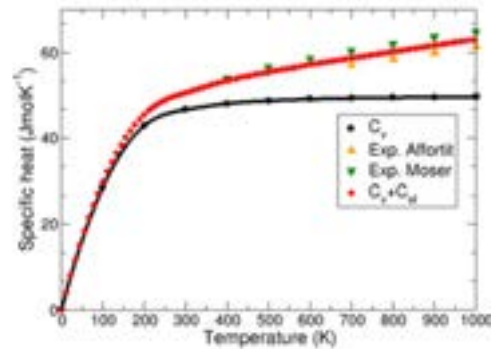
where, N is number of primitive cells, r is number of degrees of freedom, ω denotes vibration frequency, $D(\omega)$ is phonon density of states, \hbar and k_B stand for Planck and Boltzmann constants, respectively.

For more details see Ref. [12,13]. From the calculated electronic density of states at Fermi level $N(E_F)$ for the GGA+PBE +SOC with $U_{\text{eff}} = 2.0$ eV, i.e. $N(E_F) = 1.673$ states/eV one can deduce the electronic contribution

$$C_{el} = \left(\frac{\delta S_{el}}{\delta T} \right)_V = (2\pi^2/3 N(E_F)(1 + \lambda_{el-ph})k_B^2 T)$$

where λ_{el-ph} is a correction factor due to the many-body electron-phonon interactions [12].

Figure 1. Heat capacity of UC calculated for $U_{\text{eff}} = 2.0$ eV + SOC at constant volume



Both calculated contribution (electronic and phononic) to the heat capacity for the temperature range $T = 0-1000$ K are shown in Figure 1 together with experimental data of Affortit [14] and Moser [15]. To fit to the experimental data we used $\lambda_{el-ph} = 0.7$. We are aware that for the higher temperatures the

phonon anharmonicity can play a role and increase its contribution to the heat capacity and therefore the electron-phonon many body enhancement factor λ_{el-ph} will be lower and for the temperature above the Debye temperatures of 305-366K[16] will rapidly decrease.[12] Also a slight increase of calculated heat capacity is expected if the quasi-harmonic approximation (volume expansion) is taken into account and this allows of more precise heat capacity determination (C_p). This as well as the anharmonic effects are aims of our current investigations.

IV. Conclusion

Based on the DFT calculations of electronic structure and lattice dynamics (phonons) of uranium monocarbide we determine those system contributions to the heat capacity and compared to the available experimental data. Here, we have demonstrated the influence of the mass-enhancement electron-phonon factor on the electron contribution of the heat

capacity in case of uranium monocarbide. It amounts to ca. $\lambda_{el-ph}=0.7$, which leads to heat capacity at $T=1000K$ to about 22% stemming from electron subsystem and 78% from the phonons.

Acknowledgements

This work was supported by the European Regional Development Fund in the IT4Innovations national supercomputing center – Path to Exascale project, No. CZ.02.1.01/0.0/0.0/16_013/0001791 within the Operational Programme Research Development and Education and by Czech Science Foundation project No.17-27790S and grant No. 8J18DE004 of Ministry of Education, Youth, and Sport of the Czech Republic.

Nomenclature

GIF	Generation IV International Forum
HPC	High Performance Computing

References

- [1] P. Hohenberg and W. Kohn, *Phys. Rev.* 136, B864 (1964).
- [2] U. D. Wdowik, P. Piekarczyk, D. Legut, and G. Jaglo, *Phys. Rev. B* 94, 054303 (2016).
- [3] https://www.gen-4.org/gif/jcms/c_40473/a-technology-roadmap-for-generation-iv-nuclear-energy-systems
- [4] X.-Y. Liu, D. A. Andersson, B. P. Uberuaga, *J. Mater. Sci.* 47, 7367 (2012).
- [5] D. Petti, D. Crawford, and N. Chauvin, *MRS Bull.* 34, 40 (2009).
- [6] R. W. Stratton, G. Ledergerber, F. Ingold, T. W. Latimer, and K. M. Chidester, *J. Nucl. Mater.* 204, 39 (1993); D. C. Crawford, D. L. Porter, and S. L. Hayes, *J. Nucl. Mater.* 371, 202 (2007).
- [7] S. L. Dudarev, G. A. Botton, S. Y. Savrasov, C. J. Humphreys and A. P. Sutton, *Phys. Rev. B* 57, 1505 (1998).
- [8] G. Kresse and J. Furthmüller, *Comput. Mater. Sci.* 6, 15 (1996); G. Kresse and D. Joubert, *Phys. Rev. B* 59, 1758 (1999); <http://cms.mpi.univie.ac.at/vasp/>
- [9] J. P. Perdew, K. Burke, and M. Ernzerhof, *Phys. Rev. Lett.* 77, 3865 (1996); 78, 1396 (1997).
- [10] U. Carvajal-Nunez, L. Martel, D. Prieur, E. L. Honorato, R. Eloirdi, I. Farnan, T. Vitova, and J. Somers, *Inorg. Chem.* 52, 11669 (2013); U. Carvajal-Nunez, R. Eloirdi, D. Prieur, L. Martel, E. L. Honorato, I. Farnan, T. Vitova, and J. Somers, *J. Alloys Compds.* 589, 234 (2014).
- [11] K. Parlinski, Z.-Q. Li, and Y. Kawazoe, *Phys. Rev. Lett.* 78, 4063 (1997), A. Togo, L. Chaput, I. Tanaka, G. Hug, *Phys. Rev. B* 81, 174301 (2010).
- [12] G. Grimvall, *Thermophysical properties of materials*, Elsevier (1999)
- [13] U. D. Wdowik and D. Legut, *J. Phys.: Condens. Matter* 21, 275402 (2009)
- [14] J. B. Moser and O. L. Kruger, *J. Appl. Phys.* 38, 3215 (1967).
- [15] Ch. Affortit, *J. Nucl. Mater.* 34, 105 (1970).
- [16] E. Westrum, Y. Takahashi, and N. D. Stout, *J. Phys. Chem.* 69, 1520 (1965).

**OPTIMISATION OF MANUFACTURING PROCESS OF FUNCTIONALLY GRADED
COMPOSITE STEELS FOR LEAD-BISMUTH COOLED FAST REACTOR CLADDING
APPLICATION (J. LEE ET AL)**

Jeonghyeon Lee⁽¹⁾, Taeyong Kim⁽²⁾ and Ji Hyun Kim⁽³⁾

(1-2) Ulsan National Institute of Science and Technology (UNIST), Republic of Korea

(3) Department of Nuclear Engineering, School of Mechanical, Aerospace and Nuclear Engineering, Ulsan National Institute of Science and Technology (UNIST)

Abstract

Liquid metal coolants such as lead, lead-bismuth eutectic (LBE), and sodium also have the benefits of higher thermal conductivities and heat capacities than most other coolants. The advantages of lead or lead-bismuth eutectic, which has attractive thermal, hydraulic, and nuclear-physics properties, make these coolants ideal for fast-reactor and accelerator-target applications. However, at temperatures of interest for advanced reactor applications, such as high-efficiency electricity generation or producing process heat for high temperature electrolysis, the corrosion of cladding and structural materials becomes the limiting factor.

To increase corrosion resistance, the weld overlay technique is a widely used approach in nuclear industries; light water reactors typically use this hybrid layer technique in pressure vessels and fuel cladding. Weld overlaying of stainless steel inside the pressure vessel serves as a corrosion-resistant layer for the vessel. In fuel cladding tubes, which hold the fissile fuel in a core, pure zirconium is clad inside a zirconium alloy such as Zircaloy and advanced zirconium [2, 3].

Nuclear reactor cladding tubes are manufactured using the extrusion, drawing, and pilgering process, which is commonly known as a manufacturing process. Pilgering is a cold working operation where the outside diameter, inside diameter, and wall thickness of tubes are simultaneously reduced over the working length under a pair of dies with semi-circular tapered grooves cut on them. The goal of this paper is to further develop the functionally graded metallic composite (FGC). This functionally graded metallic composite will ultimately be available to be used as piping and fuel cladding in a lead-bismuth cooled nuclear reactor. The tasks provide a detailed description of the work completed within this paper. One of the tasks is to complete a detailed microstructural analysis of the piping product using optical microscopy. The second one is to optimise the microstructure and mechanical properties of the T91 and Fe-12Cr-2Si layers in the piping product through heat treatment.

I. Introduction

Liquid metal coolants such as lead, lead-bismuth eutectic (LBE), and sodium also have the benefits of higher thermal conductivities and heat capacities than most other coolants. The advantages of lead or lead-bismuth eutectic, which has attractive thermal, hydraulic, and nuclear-physics properties, make these coolants ideal for fast-reactor and accelerator-target applications. However, at temperatures of interest for advanced reactor applications (>500 °C), such as high-efficiency

electricity generation or producing process heat for high temperature electrolysis, the corrosion of cladding and structural materials becomes the limiting factor.

Heavy liquid metals are adequate coolants for transmutation of nuclear waste and spent fuel, as their heavy nuclei make it possible to obtain a very fast neutron spectrum, and nuclear safety and nuclear waste problems are important issues to consider. Long-lived minor actinides, such as neptunium or americium, which occur in nuclear waste, can be burned.

The weld overlay technique is a widely used approach in nuclear industries to increase corrosion resistance; light water reactors typically use this hybrid layer technique in pressure vessels and fuel cladding. Pressure vessels are usually made of carbon steels, which will endure the pressure. Weld overlaying of stainless steel inside the pressure vessel serves as a corrosion-resistant layer for the vessel [1]. In fuel cladding tubes, which hold the fissile fuel in a core, pure zirconium is clad inside a zirconium alloy such as Zircaloy and advanced zirconium [2, 3]. The pure zirconium serves as the corrosion-resistant layer, while the zircaloy serves as the structural layer. Occasionally, the zirconium liner on the inside of this type of fuel cladding, known as a fuel barrier, helps prevent fuel-cladding interactions. These approaches are not suitable for fast reactor applications.

Nuclear reactor cladding tubes are manufactured using the extrusion, drawing, and pilgering process, which is commonly known as a manufacturing process [4, 5]. Pilgering is a cold working operation where the outside diameter, inside diameter, and wall thickness of tubes are simultaneously reduced over the working length under a pair of dies with semi-circular tapered grooves cut on them [6]. Pilgering is often characterised by a Q-factor that is the ratio of the strain due to change in thickness to the strain resulting from reduction in diameter of the tube. It has been found that there is an improvement in the quality of the final product with increase in Q value (Ref.7). The Q ratio is variously defined as

$$Q = \frac{\Delta t/t_0}{\Delta D/D_0} = \frac{\Delta t/t_0}{\Delta D_{MW}/D_{0MW}} \quad (1)$$

where t is the thickness, D is the diameter and the subscript refers to the original or starting values. The right-hand side of the above equation with subscripts MW specifies mid-wall.

The goal of this paper is to further develop the functionally graded metallic composite. This FCG will ultimately be available to be used as piping and fuel cladding in a lead-bismuth cooled nuclear reactor. The chapters provide a detailed description of the work completed within this paper. One of the tasks is to complete a detailed microstructural analysis of the piping product using optical microscopy. The second one is to optimise the microstructure and mechanical properties of the T91 and Fe-12Cr-2Si layers in the piping product through heat treatment.

II. Experimental and Methodology

II.A. Selection of composite materials

Lim et al. proposed the Fe-Cr-Si alloy system as a high-temperature, corrosion-resistant material. From corrosion tests with a series of alloys based on the Fe-Cr-Si system, it has been verified that Fe alloys with suitable levels of Cr (>12 wt%) and Si (>2.5 wt%) will be protected by either a tenacious oxide film (over a wide range of oxygen potentials above the formation potential for Cr and Si oxides) or by a low solubility surface region at low oxygen potentials. Experimental results obtained from model alloys after LBE exposure at 600°C demonstrated the film formation process. The hypothesis that Si addition would promote the formation of a diffusion barrier was confirmed by the actual reduction of oxide thickness over time. The Si effect was enhanced by the addition of Cr to the system [6].

Based on their extensive characterisation study, they proposed the concept of an FGC consisting of two layers, a thin Fe-12Cr-2Si layer as a corrosion-resistant layer and T91—chosen for its strength and radiation resistance—as a structural layer [7]. Also, other ferritic/martensitic steels, like HT9 or Gr.92, can be selected for structural layer materials for various reactor applications. HT9 and Gr.92 have already showed good mechanical properties in a high-temperature sodium environment (Ref.8). Table 1 shows the chemical compositions of Fe-12Cr-2Si and T91 steels.

Table 1. Chemical composition of Fe-12Cr-2Si weld wire and T91 in wt.%

	Fe	Cr	Mn	Mo	Ni	Si	V	W	N	C
T91	Bal.	9.4	0.51	1.0	0.28	0.35	0.19	0.07	-	-
Fe-12Cr-2Si	Bal.	13.11	0.02	-	0.006	2.0	-	0.17	-	0.01

II.B. Hot extrusion and cold pilgering

The hot extrusion process was performed at MIT. The composite design consists of an T91 base structural layer with a Fe-12Cr-2Si corrosion resistant barrier. The weld wire from the Fe-12Cr-2Si was overlaid on the long cylindrical billets of T91 steel which is 23.4 cm outer diameter and 60.9 cm length. For the fuel cladding the Fe-12Cr-2Si weld wire was weld overlaid on the outer diameter of the T91

cylindrical billet that had been center drilled. These billets were then extruded into Tube Reduced Extrusions (TRES) 9.52 cm (3.75") OD 518 cm (408") long (TRES) tubing at $\sim 1200^{\circ}\text{C}$.

The cold pilgering test of the tube was conducted using the reducing schedule below, and the reduction rate of first pilgering is 53%. The reduction rate was maintained under the 60% for the safe process. And the Q factor of first pilgering was set as 1.58 for the similar value. Those factors are reviewed by the Korea Institute of Materials Science.

The procedure of manufacturing of an FGC tube consists of 3 steps. The first scheme is the overlay welding of Fe-12Cr-2Si to the T91. The choice of T91 as a structural layer in the composite was originally based on material availability. The purpose of the development effort was to take corrosion off the issue so that future versions of the composite might use a higher strength alloy. It has also been shown that for a fractured pipe one will see no disbonding between the Fe-12Cr-2Si layer and the T91 layer. This task was performed at MIT. The second scheme was a hot extrusion. The hot extrusion process of the FGC tube is manufactured from the mechanical FGC billet. And the final scheme was a cold pilgering to the FGC tube for reducing the tube size. The 1st step of pilgering was performed recently. And the next step of pilgering will be performed, sequentially.

The cold pilgering test is performed using a typical 125 VMR type mill manufactured by Manesmann Meer. A feed step of 3 mm per stroke cycle was used for all pilgering processes. And the stroke rate is 30 strokes per minute.

III. Results and Discussion

III.A. Microstructure after hot extrusion

Fig. 2 shows the optical microscopy result of an FGC tube after the hot extrusion including the microstructure of Fe-12Cr-2Si materials on the T91 cladding and the out surface of cladding. The thickness of the Fe-12Cr-2Si layer is 1500 μm . In the inner part, a ferritic/martensitic phase and, an austenitic grain boundary on Fe-12Cr-2Si were observed. Extrusion forming involves placing billet into a container and then applying pressure to them cause plastic deformation. Materials with small grain size has an increased yield strength, higher ultimate strength, according to Hall-Petch strengthening.

Figure 1. Microstructure after hot extrusion

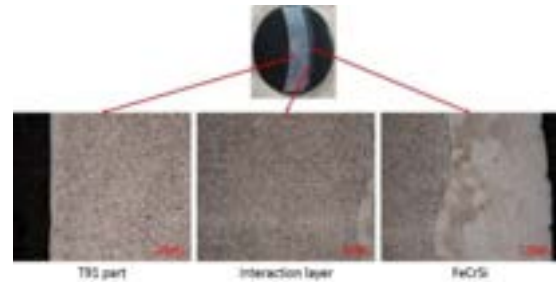
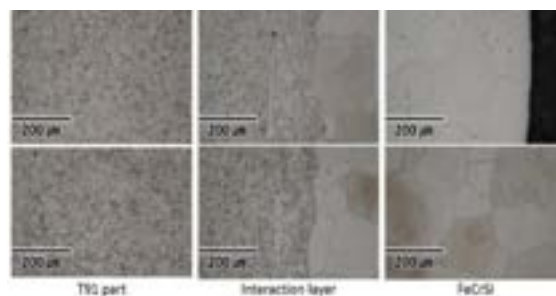


Figure 2. Microstructure of FGC tube after hot extrusion



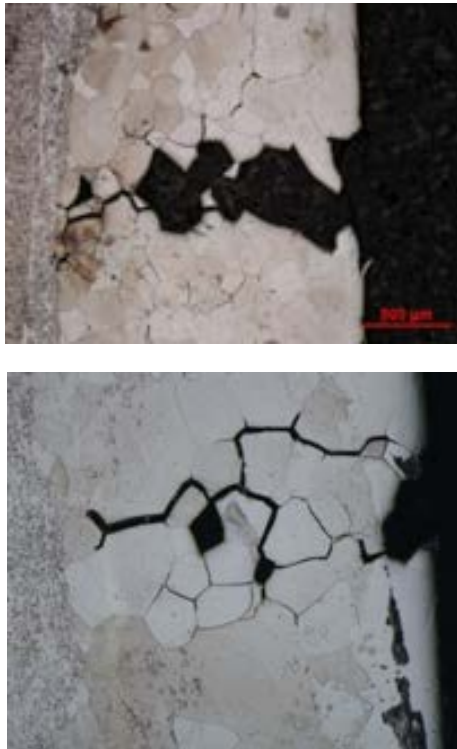
During the hot deformation process, the flow stress is sensitive to the work hardening and the dynamic softening. At the beginning of the deformation, the flow stress increases with the increasing strain. The material is under an unstable status due to the increasing dislocation density. The stored energy turns into a driving force for the dislocation migration. When the strain reaches to the critical strain, the dynamic recovery occurs and the flow stress increases owing to the conflation between softening and hardening. Moreover, with the strain continuing to increase, the work hardening and softening reach to a certain balance and the flow stress reaches to a plateau as well. Thus, the critical strain and work hardening are the significant parameters for the flow stress and should be considered in the constitutive models.

III.B. Crack examination after hot extrusion

The FGC billet was then preheated to 816°C in a reducing gas furnace for one hour, followed by an induction preheat between $1,193$ and $1,224^{\circ}\text{C}$ for 15 minutes. The billet was then immediately rolled out of the furnace and onto a fiberglass blanket. Glass lubricant was poured into the inner diameter, glass endcaps were melted on, and the billet was extruded within 15 seconds.

Fig. 3 shows the microstructure of Fe-12Cr-2Si materials on the FGC cladding with a small amount of intergranular pores tend to be more prone to grain boundary cracking after hot extrusion processing.

Figure 3. Microstructure of crack on Fe-12Cr-2Si



There are many reasons for the surface cracking during the hot extrusion processing which are i) grain boundary segregation ii) surface cracking by hot extrusion iii) hot cracking iv) reheat cracking by welding and extrusion v) crack of overlay weld metal by residual stress.

To investigate the near crack zone in specimens that were exposed to hot extrusion, electron probe micro analyser X-ray mapping was also used. In fig. 4, scattered electron (SE) image shows the specimen (excluding the left margin, which is the mounting resin containing O and C). In the image from the Cr and Si X-ray peak, those elements were enriched by the hot extrusion.

According to S. Hofmann et al., the temperature dependencies of silicon segregation to two grain boundaries exhibit a maximum near 627°C (Ref.9). In the bicrystalline steel (Fe-Si

steel), it has {112} and {013} symmetrical grain boundaries. Both the decrease of silicon segregation at 500°C and a relatively wide in-depth range of the silicon enrichment at all temperatures independent of the values of diffusion length estimates, are found for both grain boundaries. The annealing temperatures and times are presented in table 2.

Figure 4. Microstructure of crack on Fe-12Cr-2Si

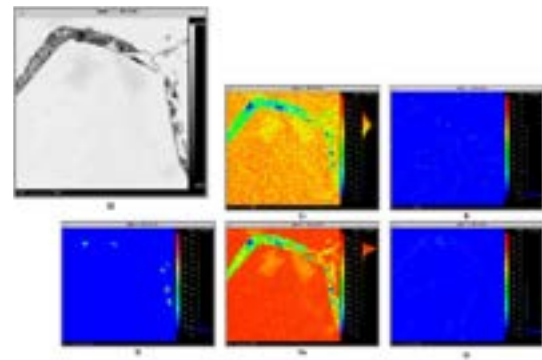


Table 2. Values of silicon diffusivities were calculated from data (?) of Si diffusion from data⁹.

Temperature (K)	1173	1073	973	873	773			
Time, t (h)	24	24	48	96	120	168	240	1440
\sqrt{Dt} (μm)	89	34	15	5	6	1	1.4	2.5

Surface cracking from high work-part temperatures that causes crack to develop at the surface. They often occur when the extrusion speed is too high, leading to high strain rates and associated heat generation. Both solidification cracking and hot cracking refer to the formation of shrinkage cracks during the solidification of weld metal, although hot cracking can also refer to liquation cracking. The cracking which occurred in the heat material was located exclusively at grain boundaries. Further, temperature variations across the billet during hot extrusion can also lead to inhomogeneous deformation.

III.C. Effect of heat treatment for FGC tube

The residual stress of the process finished FGC tubes was determined by the Sachs method; the process FGC tube exhibited changing residual stress across the wall thickness and tensile and

compressive stresses near the outer and inner sides.

The Vickers hardness of the FGC tube subjected to heat treatment and cold pilgering will be measured at a load of 10 N; the hardness will be measured using a HM-220 hardness testing machine.

The extrusion process was stopped before the ram reached the dead zone. In order to study the effect of the hot extrusion process on the extruded material hardness, Vickers hardness will be measured in dead and extruded zones for samples of each step.

According to Westbrook (Ref.10), the temperature dependence of hardness of metals and alloys has been reviewed. The summary of his equation for hardness by temperature is that the temperature dependence of hardness is best represented by the following relation of the type

$$H = A \exp(-BT) \quad (2)$$

where constants A and B are called the intrinsic hardness (i.e. the value of hardness at 0 K) and softening coefficient, respectively. The specimen of hardness will be analysed.

The heat treatment affects the carbide/precipitation phases and microstructures such as type, size, and volume of defects. It plays a decisive role in changing the mechanical properties such as hardness, creep property, and strength. According to literature, the austenite grain and ferrite grain might change at temperature higher than 1150°C because of the dissolution of carbide and precipitation in alloy steel. Heat treatment can be improved by removing of carbide/precipitation. Precipitation removes these materials from solid solution, which are thus no longer available for interaction cracking and solid solution hardening. The heat treated specimen will be analysed.

Precipitation removes these species from solid solution, and thus they are no longer available for interaction and solid-solution hardening.

IV. Conclusion

The functionally graded metallic composite (FGC) will ultimately be available to be used as piping and fuel cladding in a lead-bismuth cooled nuclear reactor. The present paper

provides a detailed description of the work completed. A detailed microstructural analysis of the piping product using optical microscopy has been completed. Although the solution-precipitation reaction is fundamentally reversible with temperature change, in many alloys transition structures form during precipitation but not during solution (dissolution?).

The main results are as follows:

- i) The microstructure of Fe-12Cr-2Si materials on the FGC tube with small amount of intergranular pores tend to be more prone to grain boundary cracking after hot extrusion processing.
- ii) There are key factors for cracking at overlay weld materials. Surface cracking is closely related to the temperature rise during extrusion. Hot cracking is the reason of cracking in Fe-12Cr-2Si weldment.
- iii) After the heat treatment, the Si phase grows to granular grain, so that the stress contraction can be avoided, which eliminates the tearing effect on the matrix.

To optimise the manufacturing process of cladding tubes, it is important to identify and resolve problems at each step of the manufacturing process. If the problems of each process can be solved, mass production of FGC cladding tubes will be possible. The crack on the tube surface can be solved by heat treatment and the cold pilgering process.

The cold pilgering is in progress and the microstructure change has been analysed. Also, the hardness will be measured using a HM-220 hardness testing machine.

Acknowledgements

This work was supported by the National Nuclear R&D program funded by the Ministry of Science, ICT and Future Planning, and by the National Nuclear R&D program (NRF-2017M2A8A1092492) organised by the National Research Foundation (NRF) of South Korea in support of the Ministry of Science, ICT and Future Planning, and by the Human Resources Development Project of the Korea Institute of Energy Technology Evaluation and Planning grant (No. 20174030201430) funded by the Korea Government Ministry of trade, Industry and Energy.

References

- [1] J. Lim, H.O. Nam, I.S. Hwang, and J.H. Kim, *Journal of Nuclear Materials*, 407, 205 (2010)
- [2] N.P. Gurao, H. Akhiani, J.A. Szpunar, *Journal of Nuclear Materials*, 453, 158 (1967)
- [3] P. Platt, V. Allen, M. Fenwick, *Corrosion Science*, 98, 1 (2015)
- [4] Vanegas-Márquez, K. Mocellin, L. Toualbi, Y. de Carlan, and R.E. Logé, *Journal of Nuclear Materials*, 420, 479 (2012)
- [5] K. Linga Murty, and I. Charit, *Progress in Nuclear Energy*, 48, 325 (2006)
- [6] G. Müller, G. Schumacher, D. Strauß, *Surface and Coatings Technology*, 135, 196 (2001)
- [7] Weisenburger, A. Heinzl, G. Müller, H. Muscher, and A. Rousanov, *Journal of Nuclear Materials*, 376, 274 (2008)
- [8] Heinzl, M. Kondo, and M. Takahashi, *Journal of Nuclear Materials*, 350, 264 (2006)
- [9] S. Hofmann, P. Lejck, *Journal de Colloques*, 51 (1990) C1-179
- [10] J. H. Westbrook et al., *Trans. Am. Soc. Met.* 45 (1953) 221.

EVALUATION OF PILGERING PROCESS OF FUNCTIONALLY GRADED COMPOSITE TUBE FOR LEAD-BISMUTH EUTECTIC COOLED FAST REACTOR THROUGH FINITE ELEMENT ANALYSIS (T. KIM ET AL)

Taeyong Kim, Jeonghyeon Lee, Ji Hyun Kim [†]

Ulsan National Institute of Science and Technology, Republic of Korea

Abstract

To prevent corrosion of the cladding in Lead-Bismuth Eutectic (LBE) cooled nuclear reactors, an innovative coating material; Fe-12Cr-2Si has been developed at Massachusetts Institute of Technology. By applying the oxidation resistance material to an existing cladding for LBE service, we can develop Functionally Graded Composite(FGC) cladding that merges the mechanical advantages of structured alloy. The coated alloy; Fe-12Cr-2Si is functionally served with a corrosion barrier, and the substrate; T91 has properties such as a low dimensional change at fast neutron environment or good strength at high-temperature. For manufacturing the FGC cladding, Fe-12Cr-2Si material is coated onto T91 billet by using overlay-welding technique. To shape the tube into cladding, outer diameter and thickness of the FGC tube need to be reduced by cold pilgering process. However, double layers of the FGC tube expect to occur different deformation processes because they have different mechanical properties. Distortion in interface between coated and substrated layer will make crack and then reduce the utilisation of products. To improve utilisation of cold pilgering process, we should evaluate the process in terms of stress/strain distribution and morphology of each layer. There are many factors for pilgering process affecting the stress/strain distribution and morphology. In this study, applying various Q-factor values, 3-dimensional computational simulation of the pilgering process of FGC tube have been made using a finite element analysis to describe that. From the simulation, behavior of circumferential and radial strain is evaluated in order to analyse crack characteristic. At low Q-factor value, the tube underwent repetitive and compressive circumferential strain during the pilgering process. However, pilgering process having high Q-factor value shows tensile circumferential strain as well as compressive in the tube. Therefore, the strain accumulation is moderated at high Q value and high Q value is appropriate for pilgering process. Later, the Q value is planned to be further specified.

It is necessary to develop a cladding to prevent oxidation in LBE cooled fast reactor, which is a IV generation reactor. FGC cladding is one of the innovative cladding that requires the evaluation of manufacturing processes for production. Because the pilgering process changes the microstructure and mechanical properties of the material, it should be considered in the evaluation of cladding material. The presentation is relevant to the development of a new coated cladding in the fuel and material track, which will be able to exchange of opinion and information on the appropriate topics.

I. Introduction

To prevent corrosion of the cladding in Lead-Bismuth Eutectic(LBE)-cooled nuclear reactors, an innovative coating material; Fe-12Cr-2Si has been developed at Massachusetts Institute of Technology. By applying the oxidation

resistance material to an existing cladding for LBE service, we can develop Functional Graded Composite(FGC) cladding that merges the mechanical advantages of structure alloy. The coated alloy; Fe-12Cr-2Si is functionally a corrosion barrier, and the substrate; T91 has properties such as a low dimensional change at

fast neutron environment or good strength at high-temperature [1].

For manufacturing the FGC cladding, Fe-12Cr-2Si material is coated onto T91 billet by using overlay-welding technique. To shape the tube into cladding, outer diameter and thickness of the FGC tube need to be reduced by cold pilgering process. The cold pilgering process involves a pair of grooved rolls and a mandrel to reduce both the wall thickness and the diameter of the mother tubes. The cold pilgering processed tube has advantages that close-dimensional tolerances and very high reductions in both wall thickness and tube diameter are possible. It can eventually lead to reduction in manufacturing coasts [2].

However, double layers of the FGC tube expect to occur different deformation processes because they have different mechanical properties. Distortion of the joint will make crack at interface and then reduce the utilisation of products [3]. To improve utilisation of cold pilgering process, we should evaluate the process in terms of stress distribution and morphology of each layer. There are many factors for pilgering process affecting the stress/strain distribution and morphology. In this study, applying various Q-factor values, 3-dimensional computational simulation of the pilgering process of FGC tube have been made using a finite element analysis to describe that. From the simulation, behavior of circumferential and radial strain is evaluated in order to analyse crack characteristic.

II. Pilgering Process Factor

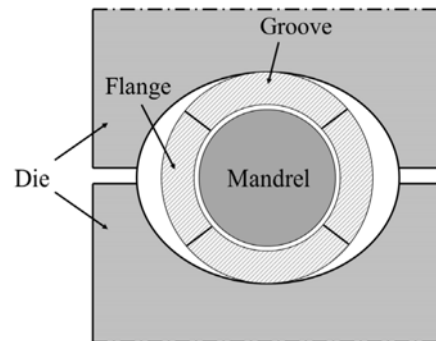
The Q-value is an important parameter in the pilgering process and expressed as the ratio of the decrease of the outer diameter and the decrease of the thickness of the tube [2-4].

$$Q \text{ value} = \frac{\ln\left(\frac{OD_{\text{final}}}{OD_{\text{initial}}}\right)}{\ln\left(\frac{r_{\text{final}}}{r_{\text{initial}}}\right)} \quad (1)$$

It is known that cracks can occur and grow within the cladding inner or outer diameter depending on the Q-value. As shown in Fig. 1, the section of the tube is divided into a groove portion directly contacting the die and a flange portion not directly contacting the die [5]. The crack initiation was evaluated as the accumulation of the strain of the circumference of the groove and flange part, which was confirmed to be influenced by the Q-value. In this paper, several Q-values were applied to

evaluate whether the crack growth was reduced by the result of the calculated strain.

Figure 1. Cross-section of pilgering tool



Other parameters are variables related to the movement rate of the equipment. Stroke rate is the reciprocating speed of the die that undergoes a linear reciprocating motion, which means the number of reciprocations per hour, usually expressed as 'stroke # / min'. Also, when the die is not in contact with the tube while the die is reciprocating, the tube is inserted while rotating at 90 ° and the insertion rate is called the feed rate. The insertion of the tube is carried out at the entrance or end of the die mandrel, and depending on the type of the pilgering machine, both types are inserted at both ends and only one type is inserted. In this study, the tube is inserted at the end of the mandrel, and the insertion speed can be expressed as 'mm / stroke #', which is the length inserted during one round trip of the die. In this paper, stress and strain were evaluated for the variables by applying the case used in the pilgering process.

III. Modeling and Simulation

Pilgering process accompanies metal plasticity which requires large deformation and nonlinear material behavior analysis. Therefore, finite element method is conducted for calculation of stress distribution and morphology of each layer. Material nonlinearities by pilgering process can be analysed with deformation, stress, strain by finite element method [2].

Before pilgering process simulation, it should be configured material nonlinearities about Fe-12Cr-2Si and T91 layers. Pilger process needs physical, mechanical and thermal properties information [6]. This values of Fe-12Cr-2Si and T91 are shown at Table 1.

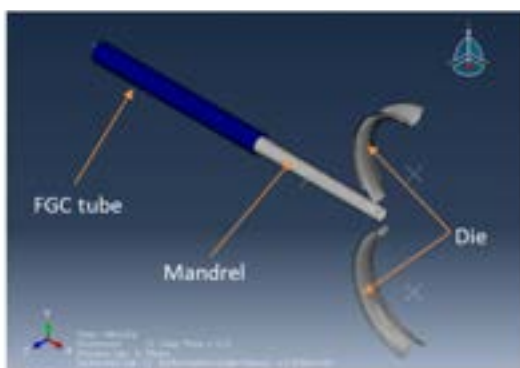
After setting the properties, the FGC tube model is composed of inner T91 and coating Fe-12Cr-2Si layers at outside from Fig. 2. The outside diameter is 95 mm. Thickness of T91 is 7.14 mm and coated Fe-12Cr-2Si layer has 1.18 mm thickness. The other parts for pilgering process simulation are mandrel and a pair of dies. In the case of mandrel and die, 'discrete rigid body' condition was applied as assuming no deformation.

For running simulation, contact conditions between different material are configured. Fe-12Cr-2Si and T91 are adjoined with overlay-welding. This condition is set with bonded type. And surfaces of coated Fe-12Cr-2Si layers adjoin with 'Surface-to-Surface' condition with 0.1 frictional coefficient [7].

Table 1. Thermal and mechanical properties of Fe-12Cr-2Si and T91

Property	Fe12Cr2Si	T91
Density (g/cm ³)	7.76	7.75
Young's modulus (GPa)	180.1	214.5
Poisson's ratio	0.31	0.33
Yield strength (MPa)	253.8	195.9
Tensile strength (MPa)	386.5	312

Figure 2. FEA model for pilgering process



There are variables determined by the dimensions of the equipment such as the Q-factor. Also, the know-how such as the operation schedule, heat treatment and so on become process variables. This FGC pilgering process uses the existing 125VMR pilgering equipment. In addition, the behaviour of the die

and the insertion speed of the tube are independent of the dimensions and material variables. Therefore, the model analysis was performed according to the feed rate related to the tube insertion, and the stroke rate related to the die motion in the pilgering process variables. The stroke rate is 195 stroke #/min and feed rate is 9 mm/stroke #. Based on this analysis, we will derive the optimal Q-factor and reduction rate by changing the later dimensional parameters. The dimension change is followed by Table 2 in this simulation. The area reduction of two case is same with 58%.

Table 2. Q-factor control for FGC pilgering process

	Step 1	Step 2	Q value
Case 1	95 ϕ \times 9.5t	53.8 ϕ \times 7.34t	2.2
Case 2		49.9 ϕ \times 8.15t	4.2

V. Simulation Analysis

The strain variation was analysed for pilgering process evaluation. For conservative evaluation, it is necessary to carry out the analysis in the circumferential direction where the compressive stress is greatest. Fig. 2 shows the stress in the circumferential direction applied depending on the position of the mandrel. Die was directly contacted, and a high compressive stress was generated at about 190 mm for the weak groove, so the analysis was carried out at that part. The results of the strain measurements in the circumferential and radial directions are shown in Fig. 3. In the flange part, it shows compressive strain in the circumferential direction. In the grooved section, the circumferential strain in the Q-value of 4.2 was compressible after stretching, whereas in the Q-value of 2.2, there was only compression for the circumferential strain. The results show that there is a risk of crack growth if the Q-value is less than 2.2 when sustained pressure is applied. However, the Q-value of 4.2 seems to reduce crack growth by repeatedly compressing and stretching the strain. In addition, the strain in the radial direction increases in the groove, which is reduced because the die increases while pushing the tube and decreases after passing.

Figure 3. Distribution of circumferential stress along mandrel

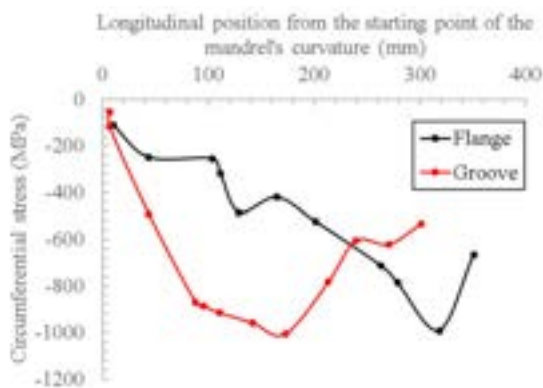
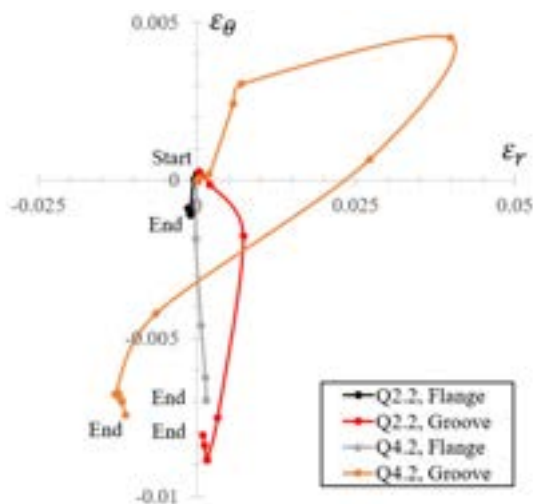


Figure 4. Distribution of circumferential and radial strain on 194 mm of mandrel at Q=2.2 and 4.2



V. Conclusion

In this paper, the finite element analysis of the multi-metal composite layer cladding, which is one of the accident-resistant fuel cladding, was discussed. The strain was measured in the circumferential and radial directions with different Q-values. In Q-value 2.2, there is a risk of crack growth due to compressive strain in both the flange part and the groove part. On the other hand, in the high Q value of 4.2, tensile is generated in the groove part, it seems to be beneficial to the process.

Acknowledgements

This work was financially supported by the International Collaborative Energy Technology R&D Program (No. 2016854000030) of the Korea Institute of Energy Technology Evaluation and Planning (KETEP) which is funded by the Ministry of Trade Industry and Energy.

This work was supported by the National Nuclear R&D program funded by Ministry of Science, ICT and Future Planning, and by the National Nuclear R&D program (NRF-2017M2A8A1092492) organised by the National Research Foundation (NRF) of South Korea in support of the Ministry of Science, ICT and Future Planning.

Nomenclature

- σ engineering stress
- ϵ_{θ} engineering strain along circumferential direction
- ϵ_r engineering strain along radial direction

References

- [1] Short, M., Zhang, Jinsuo, Whyte, D. Tonks, M., Hanninen, H. and Ehrnsten, U., 2015, "Multilayer Composite Fuel Cladding for LWR Performance Enhancement and Severe Accident Tolerance," Nuclear Energy University Programs, U. S. Department of Energy. N.P. Gurao, H. Akhiani, J.A. Szpunar, Journal of Nuclear Materials, 453, 158 (1967)
- [2] Hofstetter, S., 1993, Process improvement through designed experiments, Massachusetts Institute of Technology, pp. 1~120. E. Vanegas-Márquez, K. Mocellin, L. Toulbi, Y. de Carlan, and R.E. Logé, Journal of Nuclear Materials, 420, 479 (2012)
- [3] Verlinden, B., Driver, J., Samajdar, I. and Doherty, R., 2007, "Forming Techniques," Thermo-Mechanical Processing of Metallic Materials, Cahn, R. W.(Ed.), Elsevier, pp. 289~297. G. Müller, G. Schumacher, D. Strauß, Surface and Coatings Technology, **135**, 196 (2001)
- [4] Krishna A. Y V, 2014, "Complexity of pilgering in nuclear application," Journal of Engineering Research and Application, Vol. 4, No. 5, pp. 41~46. A. Heinzl, M. Kondo, and M. Takahashi, Journal of Nuclear Materials, **350**, 264 (2006)
- [5] Abe, H., Tarui, H., Honji, M. and Konishi, T., 1991, "Deformability of Zirconium-Lined Cladding tube in cold Pilgering," STP25497S Zirconium in the Nuclear Industry: Ninth International symposium, Ed., ASTM International, West Conshohocken, pp. 35~47.
- [6] Fray, E. S., 2013, Materials Testing and Development of Functionally Graded Composite Fuel Cladding and Piping for the Lead-Bismuth Cooled Nuclear Reactor, Massachusetts Institute of Technology, pp. 91~112.
- [7] Mulot, S., Hacquin, A., Montmitonnet, P. and Aubin J. L., 1996, "A fully 3D finite element simulation of cold pilgering," Journal of Materials Processing Technology, Vol. 60, pp. 505~512.

DEVELOPMENT AND ASSESSMENT OF MATERIALS FOR THE GENERATION IV NUCLEAR REACTORS: A BRIEF OVERVIEW OF RESEARCH IN AUSTRALIA (O. MURANSKY ET AL)

Ondrej Muránsky, Hanliang Zhu, Dhriti Bhattacharyya, Meng Jun Qin, Zhaoming Zhang, Gregory Lumpkin, Mihail Ionescu, Lyndon Edwards

ANSTO, Australia

Abstract

The Australian Nuclear Science and Technology Organisation (ANSTO) and its predecessor, the Australian Atomic Energy Commission has a long history in nuclear-based research and development. This is continuing through Australia's recent membership of the Generation IV International Forum (GIF). Australia's R&D contribution to GIF is concentrated on nuclear materials engineering in its widest context, including high-temperature, molten salt and radiation damage of materials, manufacturing, system structural integrity assessment, and prediction of component life in in-service conditions. Australia is supporting the Very High Temperature Reactor (VHTR) and Molten Salt Reactor (MSR) systems within GIF but most of the research undertaken is applicable to all advanced nuclear reactor systems. The present paper provides a brief overview of ANSTO's recent research outcomes focused on the experimental and numerical understanding of alloy development, high-temperature creep, radiation damage, and molten salt corrosion of materials for Generation IV nuclear reactor systems as well as a recent initiative to investigate how advanced manufacturing could reduce the time to deployment of Generation IV systems.

I. Introduction

Australia has abundant resources of uranium and other minerals, sophisticated engineering capabilities, and considerable current and past experience in many aspects of the nuclear fuel cycle, particularly at the front and backend. It produces approximately 11% of the world's uranium, and has more than 40% of the world's low-cost uranium reserves. In conjunction with INVAP, ANSTO designed, developed, constructed and now operates what is arguably the most modern research reactor in the world. OPAL, a truly multi-purpose reactor, provides state-of-the-art facilities for neutron diffraction, radiopharmaceutical production and materials irradiation. Australia also has a long and distinguished history of innovation in waste conditioning and is the world leader in the use of Synroc, an Australian invention. ANSTO is currently building the world's first industrial scale Synroc plant.

There has also been a long history of research into reactor systems undertaken by ANSTO and its predecessor, the AAEC. Australia has recently (2017) joined the Generation IV International Forum (GIF) and is undertaking research on the Very High Temperature Reactor (VHTR) and Molten Salt Reactor (MSR) systems [1].

VHTR - High or Very High Temperature Reactors were developed and operated between the 1960s-1990s, two are currently operational (HTR-10 is running and HTTR awaits regulator approval to restart) and two reactors are under construction (HTR-PM). They are characterised by fully ceramic coated particle fuel, the use of graphite as neutron moderator and helium as coolant. All modern designs feature passive decay heat removal capability resulting in inherent safety. They are generally conceived as modular SMRs and are particularly suitable for the highly efficient cogeneration of process heat and power. Several such reactors have already operated routinely in the reactor outlet

temperature range 700-850°C. Furthermore, operational experience has also been gained in two reactors for longer periods of time up to 950°C which is presently considered a limit for today's structural alloys. Beyond this temperature, new structural materials are required [1].

VHTR - High or Very High Temperature Reactors were developed and operated between the 1960s-1990s, two are currently operational (HTR-10 is running and HTTR awaits regulator approval to restart) and two reactors are under construction (HTR-PM). They are characterised by fully ceramic coated particle fuel, the use of graphite as neutron moderator and helium as coolant. All modern designs feature passive decay heat removal capability resulting in inherent safety. They are generally conceived as modular SMRs and are particularly suitable for the highly efficient cogeneration of process heat and power. Several such reactors have already operated routinely in the reactor outlet temperature range 700-850°C. Furthermore, operational experience has also been gained in two reactors for longer periods of time up to 950°C which is presently considered a limit for today's structural alloys. Beyond this temperature, new structural materials are required [1].

MSR Concept - has attracted worldwide interest owing to its inherent safety, high efficiency of fuel utilisation and low production of nuclear waste [2, 3]. MSR research was first established in the 1950s and 1960s at ORNL, and was revitalised when chosen as one of the six most promising reactor systems by GIF in 2002 [1]. Although initial progress on the MSR system since then has been relatively slow, there is a very substantial increase in interest in recent years. The community of national nuclear laboratories, university researchers and large nuclear companies that have typically led research and development of advanced reactor systems have been joined by an ever-increasing number of small and medium sized private companies worldwide including many dedicated to the design and deployment of MSR-based systems [4]. The vast majority of these are start-ups and in an era where many large public Nuclear Companies find market conditions challenging, they collectively have attracted very significant amounts of private capital and some governmental support. Furthermore, Shanghai Institute of Applied Physics (SINAP) has recently finished the design of a solid-fuel and liquid-fuel MSRs [5], and it currently planning to start construction of a demonstration 2MW molten salt reactor.

Materials Engineering Challenges - The rapid development and deployment of commercial VHTR and MSR systems is however still hindered by the development and standardisation of suitable materials (graphite, advanced nickel- and iron- based alloys, as well as composite ceramics). These materials are expected to withstand a combination of challenging operation conditions: (i) high-temperature damage, (ii) radiation damage, and (iii) molten salt corrosion (in case of MSR) [1, 6-9]. Therefore suitable structural materials have to exhibit a combination of unique properties [8]: high-temperature strength, microstructure stability, creep resistance, radiation tolerance, fatigue resistance, minimum tritium retention, low activation, and corrosion resistance. Most of these requirements apply to any structural materials used in any types of nuclear reactors, however the molten-salt corrosion in MSR system and high outlet temperature in VHTR system are particularly challenging [6-8, 10].

Over the past decades, a number of advanced nickel-based alloys: Hastelloy-N, GH3535, MONICR, Alloy-NM, HN80, EM-721 [5, 6, 8, 11, 12] and fine-grained nuclear graphite grades (NG-CT-50, NG-CT-10) have been developed specifically for applications in MSR systems. However, the high cost has severely limited their application and in turn hindered the development and deployment of MSRs. In addition, the time required to qualify new alloys in design codes such as ASME III Subsection NH, RCC-MRX and the UK code R5 can take decades, thus imposing further delays to the deployment of MSR technology. On the other hand, the structural materials for VHTR system are much further along the way of the development and standardisation process. The 9Cr1Mo (P91) alloy was identified as a promising candidate material for pressure vessel (400 - 450°C) and advanced nickel-based alloys 617, 800H and 230 were identified for used at temperatures between 700 and 1000°C for thermo-mechanically loaded components (e.g. heat exchangers, hot gas duct, process components) [1].

Due to the clear importance of structural materials in development and rapid deployment of novel nuclear reactor systems, ANSTO joined a number of international partners (SINAP, EDF, INL, etc.) in development and assessment of alloys for applications in the Generation IV nuclear reactors. This paper gives a brief overview of ANSTO's unique infrastructure and GIF-related research focused on (i) alloy development, (ii) high-temperature creep, (iii) radiation damage, (iv) molten salt

corrosion, (v) computer simulations and (vi) opportunities to use advanced manufacturing to reduce the time to deployment of Gen IV reactor systems.

II. ANSTO's Unique Research Infrastructure

ANSTO is home to a research reactor, accelerators, and synchrotron. These represent ANSTO's landmark infrastructure, which provides scientists and engineers with specialised experimental tools. The Open Pool Australian Lightwater (OPAL) reactor at ANSTO is a multi-purpose research reactor. It is used for scientific research, production of medical radioisotopes, and the irradiation of Si used in microelectronics and other specialised irradiations for research and industry. A suite of neutron beamlines are available for neutron diffraction, neutron scattering and neutron tomography, as part of the Australian Centre for Neutron Scattering, (ACNS). Similar to the OPAL reactor, the Australian Synchrotron (AS) offers a suite of beamlines with a wide range of unique analytic capabilities to facilitate specialised research as well as to meet industrial needs. For example, the intense, high energy X-ray beam can reveal the structure and composition of materials with a level of detail, speed and accuracy not possible in conventional X-ray laboratories.

ANSTO further operates four accelerators, the 10MV Australian National Tandem Research Accelerator (ANTARES), the 6MV SIRIUS Tandem Accelerator, the 2MV STAR Tandem Accelerator and the 1MV VEGA Accelerator, as part of the Centre for Accelerator Science (CAS). These are used for ion irradiation of materials for the use in future fusion and fission-based power-generation systems (see below). In addition, the accelerators are used for accelerator mass spectrometry (AMS) and ion beam analysis (IBA) to analyse materials to determine their elemental composition and age, and are fundamental to advancing knowledge in areas such as climate science, nuclear forensics, biology, electronics and materials.

In addition to the above landmark infrastructure (research reactor, synchrotron and accelerators), ANSTO operates specialised active laboratories to allow the fabrication, testing and analysis of radioactive materials. This includes dedicated post irradiation examination hot cells that are also used for OPAL reactor surveillance program.

III. Alloy Development

SINAP and ANSTO researchers have worked on the characterisation of the SINAP-developed Ni-SiC [13, 14] and NiMo-SiC [15, 16] composites with varying amount of SiC (0.5 – 2.5 wt.%) for applications in MSR systems. These novel materials were prepared at SINAP by powder metallurgy route consisting of (i) high-energy ball milling of initial powder mixtures (mechanical alloying), (2) spark plasma sintering (1150°C/50 MPa), (3) rapid cooling, (4) high-temperature annealing, and (5) water quenching. The microstructural analysis revealed that the Ni-SiC composites consist of Ni-matrix and unreacted SiC nano-particles, while the microstructure of NiMo-SiC composites is more complex consisting of NiMo matrix, Mo₂C agglomerates, Ni₃Si nano-precipitates, and unreacted SiC nano-particles from the initial powder mixture. It has been shown [15-17] that these newly developed materials have superior strength, but limited ductility. The strength of these materials stems from the combination of various strengthening mechanisms: (i) dispersion strengthening (SiC), (ii) precipitation strengthening (Ni₃Si), (iii) solid-solution strengthening (Mo in NiMo matrix), and (iv) Hall-Petch strengthening (matrix grain refinement). On the other hand, the low ductility is likely the consequence of porosity present in these materials [15-17]. Further work is therefore focused on the reduction of porosity.

IV. High Temperature Creep

The structural integrity, lifetime and ultimately the cost-effectiveness of power generating systems is directly dependent on the expected lifetime of its high temperature components in service. This is defined by the creep resistance of the employed materials. Creep damage is a significant problem for high temperature reactor components, which for MSR system is expected to be up to 700°C, while for VHTR system it is expected to be up to 950°C. Alloy 617 has been selected as the main high-temperature material for VHTR systems, while GH3535 alloy alongside Hastelloy-N are intended to be used in the experimental MSR currently under construction in China. Hence, ANSTO has focused on the creep damage phenomenon in these high-temperature alloys.

Kan et al. [18] have used uniaxial creep data of 617 alloy collected at various loads and temperatures 800°C, 900°C and 1000°C from Idaho National Laboratory to assess the

accuracy of a number of creep damage models: (i) Ductility Exhaustion (DE) [19], (ii) Stress-Modified Ductility Exhaustion (SMDE) [20], and (iii) Strain-Energy Ductility (SED) [21] in predicting creep time-to-failure. These creep damage models were used in conjunction with creep strain model to predict the creep time-to-failure. Kan et al. have shown in Ref. [18] that the SED model calibrated using reversed damage approach [20] provides the most accurate prediction of time-to-failure, while still being relatively conservative. Hence, the SED model shows potential for real world applications as a tool to assist in predicting remaining life of components.

Shrestha et al. [22] performed a number of creep tests on Chinese-developed GH3535 alloy at different temperatures (650°C, 700°C and 750°C) under applied loads between 85 and 380 MPa. Based on the obtained results it has been determined that the maximum allowable design stress of the GH3535 alloy at 700°C is 35 MPa according to the ASME BPVC guidelines. This stress is above the operating stresses expected in the MSR system. In addition, the formation of secondary precipitates along the grain boundaries was observed during the creep testing. The chemical analysis revealed that these precipitates contain Ni, Mo, Cr, Si and C. The combination of microscopy and diffraction techniques revealed that secondary precipitates are $M_{12}C$ type precipitates [22, 23], while the primary precipitates found in the as-received material as well as in the GH3535 welds are M_6C type [23, 24].

V. Radiation Damage

Neutron irradiation research programmes are complicated, time consuming and, since they require large capital nuclear infrastructure, are very expensive. Indeed, there is arguably a shortage of reactors and spallation sources with fast neutron fluxes large enough to produce the radiation damage seen in nuclear structural materials over the expected lifetime of operational Gen IV reactors. Hence, the majority of the initial radiation damage science on new materials is usually undertaken using ion irradiation. Although a new alloy or process is highly unlikely to be qualified for reactor use through ion irradiation studies alone, the technique provides fast irradiation times and, importantly, usually does not significantly activate the sample, simplifying the post-irradiation analysis. It is these features that are the key reasons for its increasing popularity. A

variety of ion species can be used as seen by the work described below.

Radiation damage research at ANSTO follows two main themes. The first is study of the radiation damage mechanisms through the study of the microstructure of ion irradiated materials. Reyes et al. [25, 26] studied the effect of krypton irradiation (100 dpa) at elevated temperature (450°C) on the microstructure of GH3535 alloy using TEM and molecular dynamics modelling. This study revealed that two different types of dislocation loops were formed in the alloy – the first $\frac{1}{2}\langle 100 \rangle$ (unfaulted loops) being away from pre-existing dislocations, whilst the second lying in $\{111\}$ plane being closer to pre-existing dislocations. Molecular dynamics simulations indicated that unfaulted $\frac{1}{2}\langle 100 \rangle$ dislocation loops may be formed inside the collision cascades during cascade relaxation, while the observed dislocation loops on $\{111\}$ planes form near pre-existing $\frac{1}{2}\langle 110 \rangle$ edge dislocations by absorption of atoms from the collision cascade, leaving behind $\frac{1}{3}\{111\}$ Frank loops, which could act as a nucleation site for $\frac{1}{6}\langle 112 \rangle\{111\}$ dislocations.

Huang et al. [27] studied the effect of nickel ion irradiation (0.5, 2, 12 dpa) at room and elevated temperature (600°C) on the microstructure of GH3535 alloy weld metal using XRD, TEM and nano-indentation. It was shown that nickel ion irradiation leads to formation of clusters or dislocation loops. Their size did not change with dose, while their number increased gradually. These irradiation-induced defects were found in both the matrix and also along pre-existing dislocations. There was clearly a lower density of irradiation-induced defects in samples irradiated at elevated temperature. It is believed that this is due to the higher diffusion rate of defects at elevated temperature. In addition, Huang et al. [27] have shown that ion irradiation leads to hardening of the material and that, as expected, this effect is more pronounced when the samples are irradiated at room temperature.

The second radiation damage research theme at ANSTO is assessment of how radiation damage effects the mechanical properties of irradiated components and structures and is designed to ameliorate the main deficiencies in ion irradiation since the range of ions into materials is orders of magnitude smaller than the penetration of neutrons. Thus, unless very expensive near relativistic accelerators are used, ion irradiation depth in samples is limited. Thus research is ongoing into the measurement

of mechanical properties using small micron-size ion-irradiated samples and how such measurements can be used to predict bulk properties.

Reichardt et al. [28] studied the effect of He ion irradiation on Ni single crystals using in-situ micro-tensile testing on samples with dimensions of $\sim 12 \mu\text{m}$ (thickness) $\times 10 \mu\text{m}$ (width) $\times \sim 25\text{-}30 \mu\text{m}$ (length). The obtained results clearly show that the fracture strength is proportional to damage dose. While the un-irradiated sample did not fracture even at 57% of strain, the sample irradiated to 10 dpa peak damage showed first rupture at a strain of about 1.7% and failed completely at about 26%. The sample irradiated to 19 dpa peak damage showed first rupture at a strain of about 2.2% and complete fracture at about 22.5%. The increase in strength was found to be almost linear with dose with the hardening/dose slope determined to be 230 – 240 MPa/dpa.

VI. Molten Salt Corrosion

Hastelloy-N, GH3535 alloy and NiMo-SiC composites were designed to withstand molten salt corrosion in MSR system. ANSTO and SINAP researchers studied the corrosion resistance of these alloys in FLiNaK molten salt at different temperatures.

Zhu et al. [29, 30] studied the effect of He ion-irradiation on corrosion resistance of GH3535 alloy in FLiNaK salt at 750°C. It was found that He bubbles acted as nucleation sites for corrosion cavities, and the bubbles and their surface defects increased the physical contact area between the sample and the molten salt, resulting in acceleration of the corrosion damage. Interestingly, it was also found that the corrosion-induced cavities acts as defect sinks and absorb the radiation-induced He bubbles, leading to the absence of large He bubbles in the corrosion-affected layer. Moreover, the segregation of Si at the bubble surfaces promoted the chemical reaction between the Si atoms and the molten salt and enhanced the localised corrosion. Once Ni-Si precipitates formed at the surfaces of big bubbles, galvanic corrosion occurred due to the difference in electrochemical potentials between the nickel matrix and Ni-Si precipitates. Hence, the significant segregation of Si enhanced the chemical corrosion damage to the alloy.

Yang et al. [31] have studied the corrosion resistance of NiMo-SiC composites containing

varying amount of SiC in FLiNaK salt at 650°C (200 h exposure). It has been found in Ref. [31] that the thickness of the corrosion layer and the material mass loss of these powder-metallurgy prepared NiMo-SiC composites during the corrosion testing was directly proportional to the volume fraction of the Mo_2C , which was found to be proportional to the SiC content in the initial powder mixture.

In addition to study of the molten salt corrosion of structural alloys, SINAP and ANSTO researchers studied infiltration of FLiNaK molten salt into different nuclear graphite (IG-10, 2114, G1, NBG-18, G2) under inert gas pressure (20h and 100h exposure). He et al. in Ref. [32] clearly showed that Chinese-developed fine-grained (G2) graphite displays the smallest weight gain suggesting the least FLiNaK salt infiltration. This work further shows the trend of increasing graphite weight gain during the molten salt exposure due to salt infiltration with increasing gas pressure, while increasing the exposure time from 20h to 100h had minimal effect.

VII. Computer Simulations

Computer simulation is a novel tool for the investigation of both the fundamentals of materials and their application within structures and components. Using a broad range of computer modelling techniques, researchers at ANSTO (i) design materials for nuclear energy at the atomic scale, (ii) investigate the fundamental structure-property relationships of nuclear materials, (iii) investigate material radiation-induced damage and have predicted the residual stresses in nuclear weldments.

Using atomistic modelling techniques Middleburgh et al. [33] investigated the formation and migration of intrinsic defects in the CrCoFeNi high entropy alloy (HEA) using ab-initio modelling. The ease of vacancy formation was found to vary depending on the element: vacancies formed by the removal of Fe, Ni and Co are positive while Cr has a negative vacancy formation energy and will precipitate out of the CrCoFeNi alloy. This mechanism may allow the formation of a corrosion passivating oxide layer, analogous to Cr behaviour in stainless steels. Hence, King et al. [34, 35] predicted the formation and stability of single phase high-entropy alloys, and phase transitions of HEAs for use in advanced nuclear applications.

Qin et al. [36, 37] performed molecular dynamics simulations to understand radiation-

induced phenomena, in particular radiation induced amorphisation and recrystallisation in crystalline ceramics, including the energetics of defect production, migration, and recombination, and the degradation of thermal and mechanical properties of nuclear materials under radiation damage. The simulations are currently being performed on nuclear structural materials to investigate the evolution of microstructure under radiation damage: nucleation and formation mechanism of radiation-induced defects, effects of microstructural features on the diffusion and clustering of radiation-induced defects, and effects of microstructural evolution on the mechanical properties. The simulations are combined with experimental approaches to understand and improve the properties of materials for the next generation of nuclear reactors.

ANSTO has also worked with EDF Energy, The University of Manchester and others in the NET consortium to make major advances in our ability to predict the residual stresses and distortion in both similar and dissimilar welds for nuclear applications [38]. It is important to quantify the residual stresses in welds found in nuclear power plants. It is, however, impractical and in most cases impossible to perform residual stress measurements for every welded component or assembly. Hence, validated finite element analyses are among the most often used methods for reliable prediction of residual stresses. Work in support of the UK Advance gas Cooled Reactor (AGR) fleet resulted in the development of sophisticated fully validated predictive models of welds in austenitic stainless steels and important advances were made, in particular, in our understanding of how plasticity affects development of weld residual stresses [39, 40].

Further work concentrated on the challenges that arise when attempting to predict weld residual stress in ferritic steel components, due to the influence of solid-state phase transformation (SSPT) kinetics that arise during heating and cooling of the sample. Subsequent modelling included consideration of the phase equilibria within the weld during the welding process and allowing validated models of ferritic steel welds to be produced [41].

The development of a full understanding of the requirements for validated modelling of both single phase, austenitic welds and multi-phase ferritic and bainitic steel welds allowed models of complex dissimilar nuclear welds to be developed [42, 43]. In particular, it enabled a

detailed comprehensive validated finite element modelling procedure, which made use of extensive manufacturing records to perform detailed pass-by-pass simulations of welds present in Safety Relief Valve (SRV) plant components. The models outputs were used by EDF Energy as part of a Safety Case for PWSGC mitigation at their Sizewell "B" plant, resulting in considerable savings to the company by proving that costly weld overlays are not required for SRV components and the principles underlying our weld residual stress simulation are currently being incorporated into the UK R6 code of practice for assessing structural integrity in nuclear plant.

VIII. Advanced Manufacturing

Operating Generation IV reactors will most probably require the successful utilisation of both traditional Nuclear Structural Materials and improved material designs resulting from recent advances in Materials Science. Furthermore, they are likely to utilise modern advanced manufacturing techniques where they can reduce cost or speed of construction. However, most nuclear design codes require the use of a restricted list of code qualified materials. Getting new materials or new manufacturing processes qualified can be a long and tortuous process because, for high temperature reactor designs, long-term material properties are required to establish safe design criteria. The long lead times involved in the material qualification process produce an effective and consequent barrier to market entry of new or optimised materials and processes at an industrial scale. It is clear, however, that a new material or manufacturing process is unlikely to be used in a safety critical application in the Nuclear Industry without fully characterised material behaviour and published and qualified design data.

Collectively, these issues present a barrier to market entry for Generation IV reactors and the development of materials and manufacturing solutions to benefit the six Gen IV reactor systems. Australia like many industrialised countries has recognised that novel technologies such as additive manufacturing have the potential to be both disruptive and transformative to many manufacturing industries [44].

These considerations have lead the GIF Policy Group to launch an investigation among GIF countries research institutions and nuclear companies assessing the interest in cross cutting activities supporting advanced

materials and innovative manufacturing development to a high technology readiness level (TRL). The assessment will address merits and difficulties of the collaboration on this topic, develop a priority list of R&D areas and the respective activities, and produce recommendations as to how to progress the area [45].

IX. Conclusion

This paper reports aspects of Australia's research on advanced nuclear reactors systems related to its Generation IV International Forum (GIF) membership. ANSTO, including through collaboration with its international partners

such as SINAP, has undertaken research on candidate structural materials for VHTR and MSR systems. The main focus of the research has been the development of new materials, and degradation of materials in in-service conditions (high-temperature, radiation, and molten salt).

The intent of ANSTO's research work is to reduce impediments to the design and deployment of both VHTR and MSR power-generation systems. This is being complimented by initiatives to investigate how recent advanced manufacturing techniques, such as additive manufacturing can be used to reduce the time to deployment of Gen IV systems

References

- [1] M. A. Fütterer, L. Fu, C. Sink, S. de Groot, M. Pouchon, Y. W. Kim, et al., "Status of the very high temperature reactor system," *Progress in Nuclear Energy*, vol. 77, pp. 266-281, 2014/11/01/ 2014.
- [2] M. M. Waldrop, "Nuclear energy: radical reactors," *Nature*, vol. 492, pp. 26-29, 2012.
- [3] T. J. Dolan, *Molten Salt Reactors and Thorium Energy*: Woodhead Publishing, 2017.
- [4] S. Brinton. (2015). *The Advanced Nuclear Industry*. Available: <http://www.thirdway.org/report/the-advanced-nuclear-industry>
- [5] D. Zhang, "14 - Generation IV concepts: China A2 - Pioro, Igor L," in *Handbook of Generation IV Nuclear Reactors*, ed, 2016, pp. 373-411.
- [6] V. Ignatiev and A. Surenkov, "5 - Corrosion phenomena induced by molten salts in Generation IV nuclear reactors A2 - Yvon, Pascal," in *Structural Materials for Generation IV Nuclear Reactors*, ed: Woodhead Publishing, 2017, pp. 153-189.
- [7] V. Ignatiev and A. Surenkov, "Material Performance in Molten Salts," in *Reference Module in Materials Science and Materials Engineering*, ed: Elsevier, 2016.
- [8] R. Yoshioka, M. Kinoshita, and I. Scott, "7 - Materials A2 - Dolan, Thomas J," in *Molten Salt Reactors and Thorium Energy*, ed, 2017, pp. 189-207.
- [9] H. Zhu, R. Holmes, T. Hanley, J. Davis, K. Short, and L. Edwards, "High-temperature corrosion of helium ion-irradiated Ni-based alloy in fluoride molten salt," *Corrosion Science*, vol. 91, pp. 1-6, 2015.
- [10] N. S. Patel, V. Pavlík, and M. Boča, "High-Temperature Corrosion Behavior of Superalloys in Molten Salts – A Review," *Critical Reviews in Solid State and Materials Sciences*, vol. 42, pp. 83-97, 2017/01/02 2017.
- [11] H. Yin, J. Qiu, H. Liu, W. Liu, Y. Wang, Z. Fei, et al., "Effect of CrF3 on the corrosion behaviour of Hastelloy-N and 316L stainless steel alloys in FLiNaK molten salt," *Corrosion Science*.
- [12] F.-Y. Ouyang, C.-H. Chang, and J.-J. Kai, "Long-term corrosion behaviors of Hastelloy-N and Hastelloy-B3 in moisture-containing molten FLiNaK salt environments," *Journal of Nuclear Materials*, vol. 446, pp. 81-89, 2014/03/01/ 2014.

- [13] H. Huang, C. Yang, M. d. l. Reyes, Y. Zhou, L. Yan, and X. Zhou, "Effect of Milling Time on the Microstructure and Tensile Properties of Ultrafine Grained Ni-SiC Composites at Room Temperature," *Journal of Materials Science & Technology*, vol. 31, pp. 923-929, 2015/09/01/ 2015.
- [14] H. F. Huang, W. Zhang, M. De Los Reyes, X. L. Zhou, C. Yang, R. Xie, et al., "Mitigation of He embrittlement and swelling in nickel by dispersed SiC nanoparticles," *Materials & Design*, vol. 90, pp. 359-363, 2016/01/15/ 2016.
- [15] C. Yang, O. Muránsky, H. Zhu, G. J. Thorogood, M. Avdeev, H. Huang, et al., "The effect of milling time on the microstructural characteristics and strengthening mechanisms of NiMo-SiC Alloys prepared via powder metallurgy," *Materials*, vol. 10, 2017.
- [16] C. Yang, O. Muránsky, H. Zhu, G. J. Thorogood, H. Huang, and X. Zhou, "On the origin of strengthening mechanisms in Ni-Mo alloys prepared via powder metallurgy," *Materials and Design*, vol. 113, pp. 223-231, 2017.
- [17] C. Yang, T. Wei, O. Muránsky, D. Carr, H. Huang, and X. Zhou, "The effect of ball-milling time and annealing temperature on fracture toughness of Ni-3 wt.% SiC using small punch testing," *Materials Characterization*, vol. 138, pp. 289-295, 2018/04/01/ 2018.
- [18] K. Kan, O. Muránsky, P. J. Bendeich, R. N. Wright, J. J. Kruzic, and W. M. Payten, "Assessment of Creep Damage Models in the Prediction of Time-to-Failure for Alloy 617 " presented at the HTR2018, Warsaw, Poland, 2018.
- [19] R. Ainsworth, "R5: Assessment procedure for the high temperature response of structures," 2003.
- [20] M. W. Spindler, "The prediction of creep damage in Type 347 weld metal: part II creep fatigue tests," *International Journal of Pressure Vessels and Piping*, vol. 82, pp. 185-194, 2005/03/01/ 2005.
- [21] W. M. Payten, D. W. Dean, and K. U. Snowden, "A strain energy density method for the prediction of creep-fatigue damage in high temperature components," *Materials Science and Engineering: A*, vol. 527, pp. 1920-1925, 3/25/ 2010.
- [22] S. L. Shrestha, D. Bhattacharyya, G. Yuan, Z. J. Li, E. Budzacoska-Testone, M. De Los Reyes, et al., "Creep resistance and material degradation of a candidate Ni-Mo-Cr corrosion resistant alloy," *Materials Science and Engineering: A*, vol. 674, pp. 64-75, 2016/09/30/ 2016.
- [23] T. Liu, J. S. Dong, L. Wang, Z. J. Li, X. T. Zhou, L. H. Lou, et al., "Effect of Long-term Thermal Exposure on Microstructure and Stress Rupture Properties of GH3535 Superalloy," *Journal of Materials Science & Technology*, vol. 31, pp. 269-279, 2015/03/01/ 2015.
- [24] D. Bhattacharyya, J. Davis, M. Drew, R. P. Harrison, and L. Edwards, "Characterization of complex carbide-silicide precipitates in a Ni-Cr-Mo-Fe-Si alloy modified by welding," *Materials Characterization*, vol. 105, pp. 118-128, 2015.
- [25] M. de los Reyes, R. Voskoboinikov, M. A. Kirk, H. Huang, G. Lumpkin, and D. Bhattacharyya, "Defect evolution in a NiMoCrFe alloy subjected to high-dose Kr ion irradiation at elevated temperature," *Journal of Nuclear Materials*, vol. 474, pp. 155-162, 2016/06/01/ 2016.
- [26] M. De Los Reyes, L. Edwards, M. A. Kirk, D. Bhattacharyya, K. T. Lu, and G. R. Lumpkin, "Microstructural evolution of an ion irradiated NiMoCrFe alloy at elevated temperatures," *Materials Transactions*, vol. 55, pp. 428-433, 2014.
- [27] H. Huang, X. Zhou, C. Li, J. Gao, T. Wei, G. Lei, et al., "Temperature dependence of nickel ion irradiation damage in GH3535 alloy weld metal," *Journal of Nuclear Materials*, vol. 497, pp. 108-116, 2017/12/15/ 2017.
- [28] A. Reichardt, M. Ionescu, J. Davis, L. Edwards, R. P. Harrison, P. Hosemann, et al., "In situ micro tensile testing of He+2 ion irradiated and implanted single crystal nickel film," *Acta Materialia*, vol. 100, pp. 147-154, 2015.
- [29] H. Zhu, R. Holmes, T. Hanley, J. Davis, K. Short, and L. Edwards, "High-temperature corrosion of helium ion-irradiated Ni-based alloy in fluoride molten salt," *Corrosion Science*, vol. 91, pp. 1-6, 2015/02/01/ 2015.
- [30] H. Zhu, R. Holmes, T. Hanley, J. Davis, K. Short, L. Edwards, et al., "Effects of bubbles on high-temperature corrosion of helium ion-irradiated Ni-based alloy in fluoride molten salt," *Corrosion Science*, vol. 125, pp. 184-193, 2017/08/15/ 2017.

- [31] C. Yang, O. Muránsky, H. Zhu, I. Karatchevtseva, R. Holmes, M. Avdeev, et al., "On Molten Salt Corrosion of NiMo-SiC Alloys Prepared via Powder Metallurgy " submitted to Corrosion Science, 2018.
- [32] Z. He, L. Gao, W. Qi, B. Zhang, X. Wang, J. Song, et al., "Molten FLiNaK salt infiltration into degassed nuclear graphite under inert gas pressure," *Carbon*, vol. 84, pp. 511-518, 2015/04/01/ 2015.
- [33] S. C. Middleburgh, D. M. King, G. R. Lumpkin, M. Cortie, and L. Edwards, "Segregation and migration of species in the CrCoFeNi high entropy alloy," *Journal of Alloys and Compounds*, vol. 599, pp. 179-182, 2014/06/25/ 2014.
- [34] D. J. M. King, S. C. Middleburgh, A. G. McGregor, and M. B. Cortie, "Predicting the formation and stability of single phase high-entropy alloys," *Acta Materialia*, vol. 104, pp. 172-179, 2016/02/01/ 2016.
- [35] D. J. M. King, S. C. Middleburgh, L. Edwards, G. R. Lumpkin, and M. Cortie, "Predicting the crystal structure and phase transitions in high-entropy alloys," *Jom*, vol. 67, pp. 2375-2380, 2015.
- [36] M. J. Qin, E. Y. Kuo, K. R. Whittle, S. C. Middleburgh, and M. Robinson, "Density and structural effects in the radiation tolerance of TiO₂ polymorphs," *J. Phys.: Condens. Matter*, vol. 25, p. 355402, 2013.
- [37] M. J. Qin, M. W. D. Cooper, E. Y. Kuo, M. J. D. Rushton, R. W. Grimes, G. R. Lumpkin, et al., "Thermal conductivity and energetic recoils in UO₂ using a many-body potential model," *J. Phys.: Condens. Matter*, vol. 26, p. 495401, 2014.
- [38] C. `Ohms, R. V. Martins, O. Uca, A. G. Youtsos, P. J. Bouchard, M. C. Smith, et al., "European Network on Neutron Techniques Standardization for Structural Integrity - NeT," presented at the American Society of Mechanical Engineers (ASME), 2008.
- [39] O. Muránsky, M. C. Smith, P. J. Bendeich, T. M. Holden, V. Luzin, R. V. Martins, et al., "Comprehensive numerical analysis of a three-pass bead-in-slot weld and its critical validation using neutron and synchrotron diffraction residual stress measurements," *International Journal of Solids and Structures*, vol. 49, pp. 1045-1062, 2012.
- [40] O. Muránsky, C. J. Hamelin, M. C. Smith, P. J. Bendeich, and L. Edwards, "The effect of plasticity theory on predicted residual stress fields in numerical weld analyses," *Computational Materials Science*, vol. 54, pp. 125-134, 2012.
- [41] C. J. Hamelin, O. Muránsky, M. C. Smith, T. M. Holden, V. Luzin, P. J. Bendeich, et al., "Validation of a numerical model used to predict phase distribution and residual stress in ferritic steel weldments," *Acta Materialia*, vol. 75, pp. 1-19, 8/15/ 2014.
- [42] P. J. Bendeich, O. Muránsky, C. J. Hamelin, M. C. Smith, and L. Edwards, "The impact of axi-symmetric boundary conditions on predicted residual stress and shrinkage in a pwr nozzle dissimilar metal weld," in *American Society of Mechanical Engineers, Pressure Vessels and Piping Division (Publication) PVP*, 2012, pp. 1139-1145.
- [43] O. Muránsky, M. C. Smith, P. J. Bendeich, and L. Edwards, "Validated numerical analysis of residual stresses in Safety Relief Valve (SRV) nozzle mock-ups," *Computational Materials Science*, vol. 50, pp. 2203-2215, 2011.
- [44] <https://www.business.gov.au/assistance/advanced-manufacturing-growth-fund>
- [45] https://www.gen-4.org/gif/jcms/c_42188/publications

TRACK 7: ADVANCED COMPONENTS

GEN WORKSHOP 64: AN INNOVATIVE WAY TO WORK ON A HARMONISED SET OF RULES FOR GEN-IV REACTORS (C. PETESCH ET AL)

Cécile Pétesch⁽¹⁾, Karl-Fredrik Nilsson⁽²⁾

(1) DEN-Service d'étude mécaniques et thermiques (SEMT), CEA, France

(2) European Commission DG-JRC, Directorate G4- Nuclear Reactor Safety and Emergency Preparedness

Abstract

In the nuclear industry, specific design and construction Codes provide a set of essential engineering tools for the design, construction, and integration of nuclear high safety class components and systems.

These Codes are the common reference between all actors involved in the design and construction of power plants and other nuclear facilities, starting from the main supplier of the technology, the engineer, the operator, manufacturers and suppliers of components, contractors, but also inspectors and safety authorities.

In the perspective of the implementation of Generation IV systems, a concerted effort was carried out in the European area to federate stakeholders in a common code elaboration process, in a frame of a CEN Workshop.

This Workshop is supported by the European Commission (EC) as an exercise of Europeanisation of a given standard (AFCEC codes). The first phase was carried out in 2011-2014 with the objectives:

- *integrate Modification Request from European experts and users with the aim to develop an European Code,*
- *identify the near and medium term fields of research and development to be explored for the development towards a European design code.*

The second phase, which started 2014 and ends in 2018 is extended with GEN II and GEN III mechanical components and civil work and focused on the medium and long-term code evolution and associated pre-normative R&D needs. The Code Evolution proposals will be integrated into the future version of the AFCEC codes whereas the R&D proposals provide a basis for joint European research activities. The presentation will describe the objective and organisation of the CEN WS064 and summarise some of the main Code Evolution and R&D proposals. The first two phases can already be considered as a success and a next phase of the workshop is now considered.

I. Introduction

In the nuclear industry, specific design and construction Codes provide a set of essential engineering tools for the design, construction, and integration of nuclear high safety class components and systems. These Codes are the common reference between all actors involved in the design and construction of power plants and other nuclear facilities, starting from the main supplier of the technology, the architect

engineer, the operator, manufacturers and suppliers of components, contractors, but also inspectors and safety authorities.

In the perspective of the implementation of Generation IV systems, a concerted effort was carried out in the European area to federate stakeholders in a common code elaboration process, in a frame of a CEN Workshop (WS).

II. Objectives and Organisation of the GEN Workshop 64

A GEN Workshop is a structure and an associated process, introduced by CEN in the standardisation area, which aims at bridging the gap between industrial consortia that produce de facto standards with the limited participation of interested parties, and the formal European standardisation process which produces standards through consensus under the authority of CEN member bodies. CEN Workshops have a flexible structure that benefits from the openness and consensus that are key values of CEN.

This Workshop is supported by the European Commission (EC) as an exercise of Europeanisation of a given standard (AFCEN codes). The first phase [1] was carried out in 2011-2014 with the objectives:

- integrate Modification Request from European experts and users with the aim to develop an European Code,
- identify the near and medium term fields of research and development to be explored for the development towards a European design code.

The second phase, which started 2014 and ends in 2018 was extended with GEN II and GEN III mechanical components and civil work. It focused on the medium and long-term code evolution and associated pre-normative R&D needs. The Code Evolution proposals will be integrated into the future version of the AFCEN codes whereas the R&D proposals provide a basis for joint European research activities. The first two phases can already be considered as a success and a next phase of the workshop is now considered.

III. Main Results of the First Phase of the GEN Workshop – Evolution Through the Phase 2

The first phase of the Workshop addressed innovative nuclear installations and the RCC-MRx code [2]. The purpose was to allow the Workshop members to appropriate the RCC-MRx and to propose modifications to meet their needs of ESNII projects. The workshop on RCC-MRx gathered the following members:

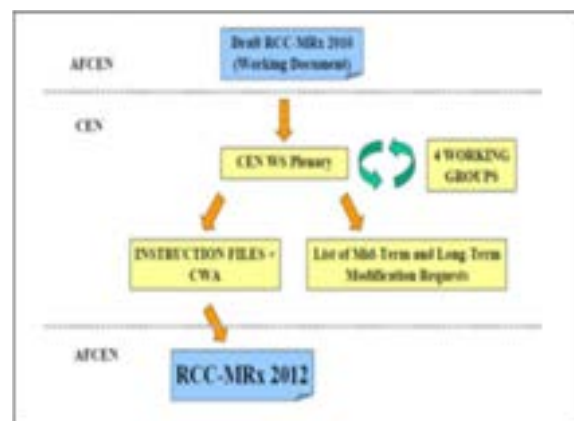
Table 1. Members involved in the first phase of the workshop

Company	Country
KIT	Germany
Bel V	Belgium
GDF Suez	Belgium
SCKCEN	Belgium
Vincotte	Belgium
EC	Europe
ITER	Europe
AFNOR	France
Areva NP	France
Areva TA	France
CEA	France
EDF	France
ANSALDO	Italy
ENEA	Italy
JRC	Netherland
NRG	Netherland
RCR	Czech Republic
ESSS	Sweden
FERRODAY	United Kingdom

A draft of the code was distributed to the members and at the end of the workshop, in December 2012, 33 modification requests (DMRx) have been proposed (20 short term, 7 middle term, 1 long term and 5 rejected).

These requests have been introduced through the existing dedicated AFCEN subcommittees through a channel defined in the workshop frame:

Figure 1. Flowchart



A brief overview of non-editorial modifications is given in the table 2.

Table 2. Modifications of the code issued from the first phase of the workshop

DMRx No.	Chap.	Purpose
11-122	RS	Further details concerning the maximum temperature for filler metals from the RS 2900 "reference sheets"
11-142	A16	Introduction of allias in the notations table
11-144	Tome 6 RPP	Introduction of a standards procedure for locating defects
11-145	A16	Further details concerning the method to be used to describe a defect with complex orientation
11-147	REC	Limiting the use of standards NF EN 13445 and 13480 to negligible irradiation and creep ranges
11-148	RB	Clarification of the text, addition of a sketch
11-149	A10	Development of models and options for strain hardening laws
12-219	RDG	Further details on the irradiation scope covered by the Code
12-220	Tome 6 RPP	Possibility of procuring very thick X10CrMoVn9-1 alloy steel sheets
12-223	RM	Incorporation of feedback confirming that Charpy tests are not necessary
12-232	RB	Clarification concerning analysis of S-type damage in the case of significant irradiation

The result of this first phase was thus direct modifications of the code, in order to bring it at a European level, and also more long term recommendations for further work (publication in the document [1]). It revealed also the need to go further in the in-depth work on the Europeanisation process, and to treat not only the short term evolutions but also to open to the definition of the research and development needs, which are crucial for the Generation IV reactors.

IV. Results of the Second Phase of the Workshop

A second phase of the workshop (2014-2018) was launched but with different targets and scope:

- Exploit the possibility to adapt an existing set of nuclear codes to the needs of a diversity of stakeholders from different European countries, "A European Code" with AFCEN codes as a pilot case,
- Identify the R&D programmes that could favour these adaptations.

The scope of the workshop was enlarged by two additional codes: RCC-M (PWR mechanical components) and RCC-CW (PWR civil work). For each code, a dedicated Working group (referred to as Prospective Group, PG) was created, which increased notably the number of stakeholders:

Figure 2. Workshop phase 2 organisation

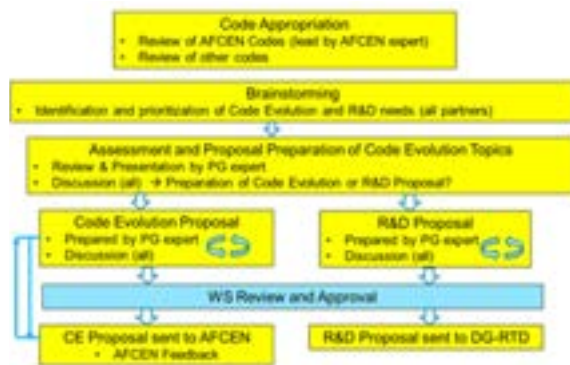


Table 3. Members involved in the second phase of the workshop

Organism	Country	Type of organisation
PG1		
IRSN	France	TSO
Tractebel	Belgium	Utility
VGB	Germany	Utility
AREVA (AFCEN)	France	Supplier
Vattenfall	Sweden	Utility
STUK	Finland	Safety Authority
JRC	EC	Research Entity
AMEC fw	UK	Supplier
PG2		
IRSN	France	TSO
Tractebel	Belgium	Utility
AREVA	France	Supplier
CEA (AFCEN)	France	Research Entity
EDF	France	Utility
SCK CEN	Belgium	Research Entity
JRC	EC	Research Entity
AMEC	UK	Supplier
ENEA	Italy	Research Entity
PG3		
Vattenfall AB	Sweden	Utility
Scanscot technology	Sweden	Research entity
Stuk	Finland	Safety Authority
Warsaw University Technology (WUT)	Poland	Research Entity
EDF (AFCEN)	France	Utility
VGB	Germany	Utility
AMEC	UK	Utility
IRSN	France	TSO
SCK CEN	Belgium	Research Entity
CEA	France	Research Entity
Tractebel	Belgium	Utility

The initial process used for the Phase 1 of the workshop evolved to integrate the new working groups and also a link with the EC for the research and development aspect of the phase 2 (illustrated in figure 3).

Figure 3. Workshop process



As a result for the three prospective groups, more than 30 code evolution proposals were submitted to AFCEN, most of them received a positive answer, and 9 R&D proposals were submitted to DG RTD. The R&D proposals were in compliance with the code evolutions and thus, strongly linked to future code needs. It should be stressed that for the innovative Gen IV reactors there is much less feedback experience and hence more need for pre-normative research.

The GEN IV prospective group, produced six Code Evolution proposals and six R&D proposals as summarised below.

In addition to the topics that resulted in CE or R&D proposals, numerous topics emerged during the last part of the workshop that could be studied and developed more in detail. For the Gen IV working group the following additional items were identified:

- the use of miniature tests in design and plant life management,
- the defect analysis of welded components,
- the leak-Before-Break for the small diameter sodium piping system,
- the Web based Data Management,
- The development and application of visco-plastic constitutive models,
- The flow Induced vibrations.

Table 2. Modifications proposals of the code issued from the second phase of the workshop

<p>PG2/CE-01: "Use of the code in innovative coolant environment"</p> <p>The designer (Prime Contractor) should verify four conditions related to its In-service inspection program and operating condition (mainly coolant chemistry) in order to insure structural integrity.</p>
<p>PG2/CE-02: "Consistent methodology for assessment of negligible creep curves"</p> <p>AFCEN is invited to integrate in RCC-MRx the method proposed by EN13445 for negligible creep curves.</p>
<p>PG2/CE-03: "Extension of Temperature range for Mechanical Properties of Specific Materials in RCC-MRx"</p> <p>AFCEN is invited to extend the range of the available mechanical property design data for the following alloys and temperatures to enable accident or fault events to be evaluated:</p> <ul style="list-style-type: none"> • Alloy 800H – maximum temperature – 1000°C • Alloy 316L – maximum temperature – 1000°C • Alloy Gr91 – maximum temperature – 850°C • Eurofer – maximum temperature – 850°C • Alloy IN718 – maximum temperature – 900°C
<p>PG2/CE-04: "Extension of creep strain and rupture data range for austenitic steel in RCC-MRx"</p> <p>AFCEN is invited to define a rupture model in the code capable of short term creep rupture predictions (restricted to the tensile strength).</p>
<p>PG2/CE-05: "Multiaxial Tubesheet Analysis"</p> <p>Calculate the primary membrane plus bending stress intensity from all the normal component stresses.</p>
<p>PG2/CE-06: "Re-introduction of 304LN SS in RCC-MRx"</p> <p>AFCEN is invited to re-introduce 304LN Stainless steel (X2CrNi19-10 with controlled Nitrogen) in the RCC-MRx by defining its properties group in Appendix A3, for fabrication of SFR components which are not in creep regime.</p>

Table 3. Research and development proposals issued from the second phase of the workshop

<p>PG2/RD-01: "Development of Design Rules and characterisation of Material Behaviour in Heavy Liquid Metal (HLM) Environments"</p> <p>The main objectives are to:</p> <ul style="list-style-type: none"> • Define borderlines separating negligible, acceptable, and unacceptable impact of the environment on structural materials; • Model properties and degradation of structural materials and welds in HLM; • Determine practical rules on the design material data to comply with the appropriate impact.
<p>PG2/RD-02: "Methodology for the design and life-assessment of components exposed to 60 years' service-life"</p> <p>The main objectives are to:</p> <ul style="list-style-type: none"> • Better understand long-term degradation of components, high temperature, low-dose long term irradiation and environmental effects; • Develop methodologies to predict long-term degradation from accelerated tests; • Generate data representative for long-term degradation; • Derive a methodology that allows design of components with a service life beyond 60 years.
<p>PG2/RD-03: "Irradiated Characteristic for Advanced Reactor in Upset and Safety State"</p> <p>The main goal is to complete the material properties database for the structural materials for future Gen IV reactor development in Europe (ASTRID, ALFRED, MYRRHA), mainly austenitic stainless steel 316 L(N). In a later stage, the program could also cover weldment.</p>
<p>PG2/RD-04: "Optimal weld design of 316 type steels for enhanced creep-fatigue endurance"</p> <p>The main objective is to find an "optimum" mix of factors to achieve good weldability, freedom of significant flaws, good ductility and "sufficient" weld metal strength in pursuit of enhanced long-term resistance to creep-fatigue damage and to feed the code development by improving the design data.</p>
<p>PG2/RD-05: "Creep/relaxation, creep-fatigue damage and their successful modelling for design rules application"</p> <p>The main objective is to settle best practices in relaxation, creep-fatigue and thermal fatigue modelling and how to combine these for optimally define design curves, design rules and assessment procedures.</p>
<p>PG2/RD-06: "Protective Coatings and Surface Alloys against corrosion in components working in Heavy Liquid Metal (HLM) Environments (Serena)"</p> <p>The main objectives are to:</p> <ul style="list-style-type: none"> • Demonstrate the feasibility and the effectiveness of the coating/surface alloy strategy at industrial scale as a tool to face corrosion in HLM-cooled nuclear reactors; • Provide scientific and engineering basis to extend the RCC-MRx Code.

V. Conclusion: Toward a Third Phase of the Workshop

The GEN/WS 64 phase 2 managed to create a community of experts, discussing and building consensus on a variety of aspects within a relatively short time. The technical result of the second phase of the workshop will be published before the end of 2018 [3].

The Workshop was also acknowledged by the EC as a major contribution to the

harmonisation of standards regarding NPP equipment [4], therefore, improving both their safety and competitiveness.

To conclude, there is an expectation from the experts involved in the Workshop 64 Phase 2 to fully tap its recommendations. In this respect, the process initiated with AFCEN needs to be continued. On the technical area, some consideration will be given to the reactor life extension aspects, for example the necessary provisions to be drafted in AFCEN code to supply spare parts on existing European reactors, originally designed with other codes, and to the suitability of using non-nuclear equipment complying with high quality industry standards. On the R&D point of view, the process initiated with EC DG "Research and Innovation" is also to be carried on. In this framework, the Workshop will have to ensure that its R&D recommendations will be integrated in the future European Commission Framework Program.

Acknowledgements

The contributors express their thanks to all the members of the CEN Workshop 64 and to the European Commission for its support.

Nomenclature

AFCEN	Association Française pour les règles de Conception, de construction et de surveillance en exploitation des matériels des Chaudières Electronucléaires (French Association for design, construction and in-service inspections rules for nuclear island components)
CEN	European Committee for Standardisation
DG	Directorate-General
DMRx	Modification request of the code
EC	European Commission
ESNII	European Sustainable Nuclear Industrial Initiative
RCC	Recueil de Conception et de Construction (Design and construction code)
R&D	Research and Development
SFR	Sodium Fast Reactor
TSO	Technical Safety Organisation
UK	United Kingdom
WS	Workshop

References

- [1] CWA 16519 (2012), "Design and Construction Code for mechanical equipments of innovative nuclear installations", CEN
- [2] RCC-MRx, 2015 edition, "Design and Construction Rules for Mechanical Components of Nuclear Installations: high temperature, research and fusion reactors", AFCEN
- [3] CEN/WS 064 PHASE 2, " Design and Construction Codes for Gen II to IV nuclear facilities (pilot case for process for evolution of AFCEN codes)", under preparation
- [4] Contract DG ENER 2014 – 376 "Feasibility Study on Harmonization of Nuclear Design and Construction Codes at EU level"

USE OF CAD MODELS IN ESFR-SMART EU PROJECT (J. BODI ET AL)

J. Bodi⁽¹⁾, K. Mikityuk⁽²⁾, A. Ponomarev⁽³⁾, J. Guidez⁽⁴⁾

(1-3) Paul Scherrer Institut, Switzerland

(4) CEA CEN Saclay, France

Abstract

As part of the Horizon 2020 European Union programme, research and development is under process on the European Sodium Fast Reactor in the framework of the European Sodium Fast Reactor Safety Measures Assessment and Research Tools (ESFR-SMART) project. In this project, a large commercial pool type sodium-cooled fast reactor is under development which requires state of the art research tools. One of the new approaches is the use of Computer Aided Design (CAD) software in which a 3D CAD model was developed, based on open literature, and has already proven its usefulness in many ways during the project. But the possibilities are only scratching the surface. As it is mainly a design tool, it has been used mostly to create the 3D design of the whole reactor system with its sub-systems. Through this process, the visualisation of the project gave an unprecedented ease to the understanding of different concepts for project members, allowed to improve communication between the partners and finally helped to decrease the time needed for the development of the reactor system. In particular, this ease of visualisation made it possible to assess new design ideas and whether they fit the existing space around the primary system of the ESFR. The CAD model serves as a basis for accurate physical measurements as well as to provide data on different physical properties such as material volumes, surfaces areas, etc. Next, this feature of the model has been used already in the project to provide information for the core catcher design's criticality calculation as well as data about sodium volume to facilitate the reactor pit preliminary design. Among further possibilities of the model is time saving by providing already available input information for other research tools and system codes. For instance, detailed geometrical data can be provided for thermal hydraulic CFD (e.g. OpenFOAM) or neutronics Monte Carlo (e.g. Serpent) codes. Furthermore, the model serves as a common base for any kind of design change to keep track of the latest version of the design which helps documenting the project, providing instant access to the needed information. In addition, the CAD software employs built-in modules which provide greater visualisation by making available the creation of videos of the reactor for demonstration purposes or even to use other technologies such as 3D printing to present the work on the project to the other researchers or to public. These possibilities show the originality and usefulness of a 3D CAD model and the new dimensions for future research activities.

I. Introduction

Research and development is under process on the European Sodium Fast Reactor in the framework of the European Sodium Fast Reactor Safety Measures Assessment and Research Tools (ESFR-SMART) project [1]. The subject of this EU project is a 3600MWth (1500MWe), pool type sodium-cooled fast reactor. In order to organise the work and to visualise the reactor design concepts, a Computer Aided Design (CAD) model is being

developed. Computer Aided Design is a computational tool which serves the purpose of developing, visualising, optimising and analysing different designs and concepts [2]. The CAD model being developed for the ESFR reactor can be used in multiple ways to help the research project and to provide information for various tasks and has already been a key player in providing multiple benefits for the design process.

The paper is focused on applications of the model and its potentials. First, due to the 3D product visualisation, the time for product development is greatly reduced by the improved communication between involved parties in the development process as it facilitates the understanding of the preliminary design concept. Second, the model offers a common source of information regarding to exact measurements of the system components and provides input information for simulation tools. Finally, it has also been used to analyse the possibility of 3D printing. These utilisation methods are described in more detail in this paper.

II. Design Visualisation

As a first step to modelling the ESFR system, relevant information was gathered from CP-ESFR [3] and EFR EU projects [4] as well as French ASTRID reactor research program [5]. Based on this information, a preliminary design of the reactor primary system, secondary circuits and decay heat removal systems was established for the ESFR-SMART project.

Having this initial design, there is a source for further design development and a mean to test whether new amendment ideas fit into the available space envelop without major modification on the whole system. In addition, the 3D visualisation with different colour codes helps to understand where the different system elements are and how they relate to each other. A visualisation example can be seen in Figure 1, which demonstrates the designed elements of the ESFR.

Figure 1. ESFR components overview

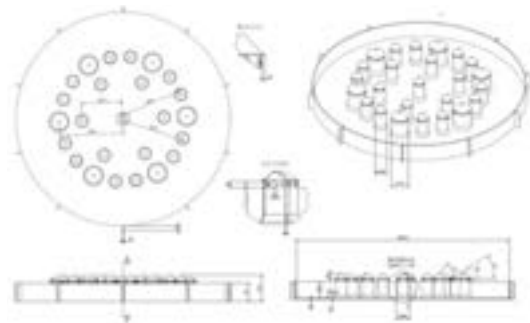


These coloured 3D figures help greatly the design iteration process by providing an unprecedented ease to understand how the different elements are interconnected.

III. Measurement and Input Information Provision for Simulation Tools

One further advantage of having the CAD model being developed is that information regarding to the geometry of the system or system elements can be quickly and easily obtained in either 2D or in 3D format for preparing the models for different simulation tools, i.e. MCNP [6], Serpent [7] or OpenFOAM [8].

Figure 2. ESFR core catcher working drawing



The 2D format, namely working drawing, can be used when the 3D geometry cannot be used for the actual problem. On these drawings, the components of interest are represented with different 2D views, as it is shown in Figure 2, with all the needed measurements plotted. In this way, it is not necessary to redraw the elements by 2D CAD software but the already existing 3D model can be used for the document, speeding up greatly the information exchange process.

Figure 3. Strongback mesh structure for simulation with OpenFOAM



Regarding 3D format, it is possible to provide the exact geometry from the CAD model in the format which directly can be used by the simulation code. For instance, 3D model geometry can be directly fed into OpenFOAM CFD code converting native CAD file into a specific format (such as STL). Figure 3 provides an example to this conversion, where the strongback of the reactor is converted into STL format to create the meshed geometry.

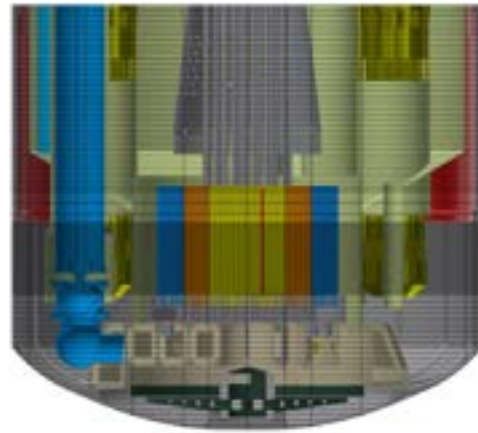
Figure 4. Measurement for core catcher criticality calculations



In addition to geometry information, the model provides many more useful data. By providing the material information to the model, the weight of the elements can be obtained. Surface and volume information can be derived from the model which is essential for accurate thermal hydraulic calculations. For instance, the necessary hydraulic diameter as well as the volume measure for specific elements can be derived. As an illustration, a volume measurement of a core catcher is given in Figure 4. Combined with core volume measurement this data was used to run criticality calculations with the MCNP code in order to assess the potential of anticipated recriticality in accident scenarios with the core meltdown, as an ongoing work within ESFR-SMART project.

A specific example of potential area where the model can be used for input information generation is application for the TRACE thermal hydraulic code, which capabilities has been extended in PSI [8] for treating of sodium coolant and, in particular, for modelling of transient accident behaviour of SFR. In Figures 5, 6 and 7, an example of this use is provided. In Figure 5, the primary system is shown after it has been divided up to axial and radial layers corresponding to the actual TRACE model set up. The elements formed after the division of the primary system, which are called nodes, represent a piece of the reactor with its surface, volume and porosity information.

Figure 5. Primary system subdivision in TRACE model



In Figure 6, one axial slice is shown being taken out from the primary system. On the bottom part of the figure, each of the different element slices can be seen such as the (blue) primary pump, the (yellow) intermediate heat exchangers, the (green) redan, (red) vessel cooling system unit and (grey) main vessel. On the upper part of the figure, the same slice is shown filled with sodium (grey).

As the axial layer is further divided into the actual node, which is the division on the azimuthal direction, Figure 7 is obtained. The components can also be seen with different colours on the right side of the picture, whereas the same node is shown on the left filled with sodium. After obtaining this node, it is very straightforward to extract and calculate the required information – volume, surface and porosity value, which is the ratio of the sodium volume in the node to total node volume. Applying the above-mentioned method the use of average data for system elements in the calculation can be substituted by use of accurate actual input data for all individual nodes aiming more accurate simulations to be performed.

Another important research project currently being under investigation is to use the CAD model to run different simulations on the model directly within the CAD software. There are various built-in simulation add-ons in most mainstream CAD software, such as the built-in CFD add-on, Finite Element Analysis (FEA), thermal simulation and electromagnetics analysis, just to mention a few possibilities.

Figure 6. Primary system axial slice in TRACE model

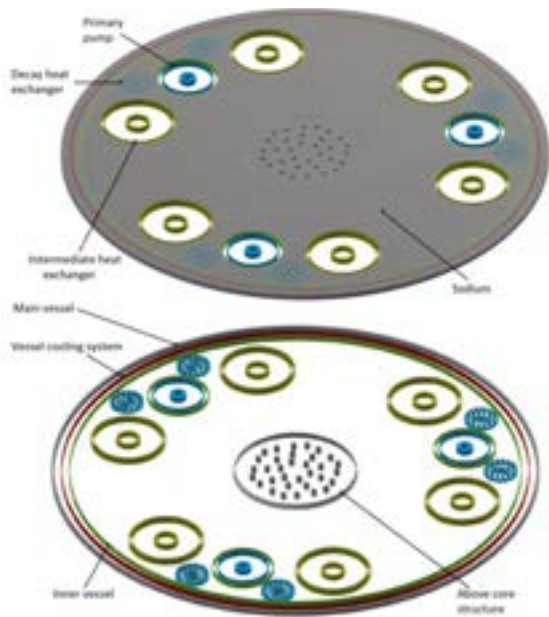
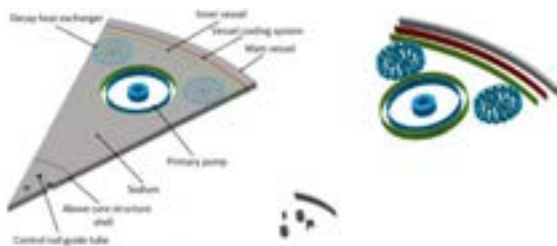


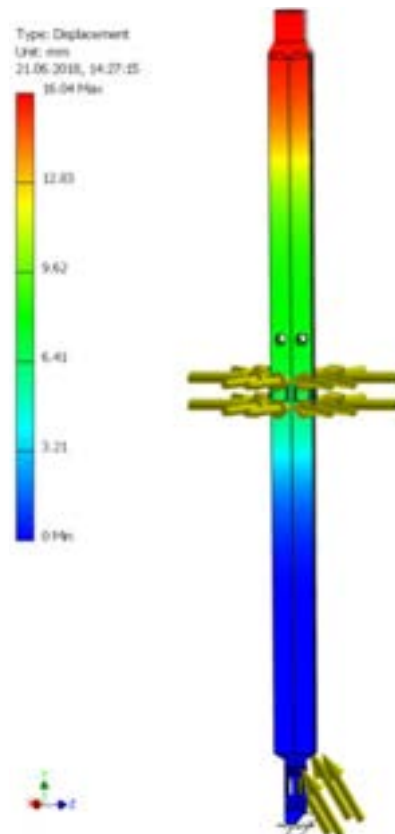
Figure 7. Primary system cells in TRACE model



Currently, efforts are being made to assess the capability of the built-in FEA for application in the modelling of mechanically deformed (perturbed) geometries in different Monte Carlo simulations. In FEA, different temperature distributions, forces and pressure are applied on the analysed nominal body geometry to calculate the resultant stresses, strain, and displacements in different directions. In principle, by using this method, different perturbed reactor core geometries could be accurately modelled and transferred into Monte Carlo neutron physics codes, such as Serpent. In this specific case for the transfer of the model, the deformed geometry has to be converted into STL format which can be used directly in Serpent. To do this conversion, Python scripts are openly available for this purpose or it can be done through commercial software packages also. The change of multiplication features of

the core can be analysed subsequently with respect to nominal conditions, for instance, an accurate subassembly bowing reactivity feedback effect can be simulated and the corresponding reactivity feedback can be assessed. Figure 8 illustrates the above-mentioned analysis presenting a deformed fuel subassembly.

Figure 8. Deformed fuel subassembly



Other major application of the CAD model is related to shielding problem and neutron - photon transport simulation to calculate activation and gamma heating for structural materials [10]. Although this application is currently not in the scope of the ESRF-SMART project it can be considered at later phase of design.

IV. 3D Printing Application

There are other applications of the model which are still in the beginning of their exploration. For example, some tests have been performed for the 3D printing of the model.

There are various ways in which a 3D printed component can be used. As an illustration, a 3D printed part is shown in Figure 9, which was used to test the achievable quality of a specific 3D printing technology serving demonstration purposes.

Figure 9. 3D printed strongback concept



Other future application for the CAD model could be to serve as a base for video creation. There are numerous different CAD software with built-in capability to create a video with different settings which can be used for demonstration purposes for the public or for project members.

V. Conclusion

In conclusion, the utilisation of the CAD model serves multiple purposes as part of the ESFR-SMART research project. Not only does it help the development of the reactor system itself by providing an easy concept visualisation which resulted in better understanding of the design, but also plays a key role in providing geometry and other input information for different simulations and nuclear codes at conceptual design phase. This geometry provision can lead to better simulation results as it represents the actual geometry of the system and not only a simplified version of it. Such a usage was shown for TRACE thermal hydraulic code and the OpenFOAM CFD code.

There are some usage possibilities being explored as well, such as the 3D printing or video creation for demonstration purposes or, perhaps in a more distant future, whole experimental set up printing based on the scaled version of the actual model.

These are few of the current applications of the prepared CAD model for the project. Nevertheless, in the future, more useful applications will arise as the technology evolves and opens up new possibilities.

Acknowledgements

The work has been prepared within EU Project ESFR-SMART which has received funding from the EURATOM Research and Training Programme 2014-2018 under the Grant Agreement No. 754501.

Nomenclature

3D	Three-dimensional
ASTRID	Advanced Sodium Technological Reactor for Industrial Demonstration
CAD	Computer Aided Design
CFD	Computational Fluid Dynamics
CP ESFR	Collaborative Project for a European Sodium Fast Reactor
EFR	European Fast Reactor
ESFR-SMART	European Sodium Fast Reactor Safety Measures Assessment and Research Tools
FEA	Finite Element Analysis
SFR	Sodium-cooled Fast Reactor
TRACE	TRAC/RELAP Advanced Computational Engine

References

- [1] Enhancing the Safety of Sodium Fast Reactors, <http://esfr-smart.eu> (accessed 17.04.2018)
- [2] Narayan, K. Lalit (2008), Computer Aided Design and Manufacturing, New Delhi, Prentice Hall of India, p. 3. ISBN 812033342X
- [3] G. L. Fiorini, A. Vasile, "European Commission – 7th Framework programme: The Collaborative Project on European Sodium Fast Reactor (CP ESFR)", Nuclear Engineering and Design, Vol. 241, Issue 9, pp. 3461–3469, September 2011
- [4] J. Recamier, EFR European Fast Reactor: Outcome of design studies, EDF, Lyon, 1999
- [5] 4th –Generation Sodium-cooled Fast Reactors – The ASTRID Technological Demonstrator, CEA, Nuclear Energy Division, 2012, Retrieved from: <http://www.cea.fr/english/Documents/corporate-publications/4th-generation-sodium-cooled-fast-reactors.pdf>
- [6] J. T. Goorley, et al., "Initial MCNP6 Release Overview – MCNP6 version 1.0", LA-UR-13-22934, 2013
- [7] J. Leppänen, M. Pusa, T. Viitanen, V. Valtavirta and T. Kaltiaisenaho, "The Serpent Monte Carlo code: Status, development and applications in 2013", Ann. Nucl. Energy, 82 (2015) 142-150
- [8] OpenFOAM, 2014. <http://www.openfoam.org/>
- [9] A. Chenu, K. Mikityuk, R. Chawla, "Analysis of selected Phenix EOL tests with the FAST code system – Part II: Unprotected phase of the Natural Convection Test", Ann. Nucl. Energy, 49 (2012), pp. 191-199
- [10] J. Leppänen, "CAD-based Geometry Type in Serpent 2 – Application in Fusion Neutronics", In proceedings of M&C + SNA + MC 2015, Nashville, TN, Apr. 19-23, 2015

STATUS OF THE ASTRID GAS POWER CONVERSION SYSTEM OPTION (D. PLANCQ ET AL)

D. Plancq⁽¹⁾, L. Cachon⁽¹⁾, A. Remy⁽²⁾, J. Quenaut⁽³⁾, Y. Fasel⁽³⁾, P. Gama⁽⁴⁾, A. Dauphin⁽⁴⁾, L. Raquin⁽⁵⁾

- (1) French Atomic Energy and Alternative Energies Commission (CEA), France
 (2) General Electric Belfort, France
 (3) General Electric Baden, Switzerland
 (4) Framatome, Lyon, France
 (5) NOX, Ivry sur Seine, France

Abstract

Within the framework of the French 600 MWe Advanced Sodium Technological Reactor for Industrial Demonstration (ASTRID) project, two options of Power Conversion System (PCS) were studied during the conceptual design phase (2010-2015):

- *the use of a classical Rankine water-steam cycle, similar to the solution implemented in France in Phenix and Superphenix, but with the goal of greatly reducing the probability of occurrence of a sodium-water reaction and limiting its potential consequences; chosen as the reference for the ASTRID Plant Model during the conceptual design phase due its high level of maturity,*
- *the use of a Brayton gas cycle, which has never been implemented in a Sodium Fast Reactor. Its application is mainly justified by safety and public acceptance considerations in inherently eliminating the sodium-water and sodium-water-air reaction risk existing with a Rankine cycle.*

The ASTRID conceptual design phase period allowed a significant increase of the maturity level of a standalone Gas Power Conversion System option. It has been thus decided to lay during the 2016-2017 phase the ASTRID Gas PCS integration studies on the same level with the ASTRID Water based PCS studies completed at the end of 2015.

The 2016-2017 period, in which the Gas PCS has been integrated in the overall layout of the reactor, has allowed a better specification of the technical and economic implications of the selection of gas PCS taking into account all the aspects of the integration of such an option. A well-documented comparison between the two systems is therefore facilitated.

This paper resumes progress in the integration of the Gas Power Conversion System in the ASTRID Reactor Plant Model. It describes the main characteristics defined particularly on the Balance-of-Plant (BOP), the turbomachinery, the Sodium Gas Heat Exchangers (SGHE) as well as expected performances, operability and safety analysis.

Introduction

The Sodium-cooled Fast Reactor (SFR) is one of the Generation IV reactor concepts selected to secure the nuclear fuel resources and to manage radioactive waste. Within the framework of the June 2006 act on the sustainable management of radioactive

material and waste, the French Government asked CEA to conduct design studies for the Advanced Sodium Technological Reactor for Industrial Demonstration (ASTRID) project [1] in collaboration with industrial partners [2].

ASTRID is a project of an integrated technology prototype designed for industrial-scale

demonstration of 4th-generation Sodium-cooled Fast Reactor (SFR) safety and operation aiming at improving safety, operability and robustness levels against external hazards compared with previous SFRs.

The pre-conceptual design phase – AVP1 conducted from mid-2010 to the end of 2012 – has been focusing on innovation and technological breakthroughs, while maintaining risk at an acceptable level. This phase was followed by the AVP2 conceptual design phase planned until the end of 2015 whose objectives were to focus on the design in order to finalise a coherent reactor outline and to finalise by December 2015 the Safety Option Report. The ASTRID conceptual design is based on a sodium-cooled pool reactor of 1500 MWth with an intermediate circuit in sodium generating about 600 MWe. Two Power Conversion Systems (PCS) were studied in parallel during the AVP2 conceptual design phase based on a Rankine steam cycle and a Brayton gas cycle.

The steam PCS option is the most mature option. As it is the power conversion system for all SFRs up to now, it benefits from a large experience and tens of unit-operating years. For this option, conventional 180bar/500°C steam cycle conditions have been selected. Nevertheless, the always present sodium-water and sodium-water-air reactions risk is a strong design and operation constraint to be overcome.

The closed Brayton Gas PCS option is generally considered as the likely choice for High Temperature Reactors (HTR), as it provides at 800°C temperature range better cycle net efficiency than the best Rankine cycle. Application of Nitrogen closed Brayton cycle for a sodium cooled fast reactor in the 500°C temperature range is mainly justified for safety and acceptance considerations by inherently eliminating the sodium-water reaction risk existing in a Rankine cycle.

Despite the capabilities of the supercritical CO₂ PCS to reach a high efficiency greater than 42% [3], the Nitrogen PCS option has been preferred due to its higher maturity. Nevertheless, s-CO₂ PCS remains an interesting option for commercial reactors, N₂ PCS being a first step towards operation feedback of a Brayton cycle. In particular, Na/s-CO₂ interaction characterisation has already been started, but some points need to be confirmed in terms of kinetics for example [4],

During the ASTRID AVP2 phase from 2013 to 2015, a strong R&D effort was focused on the

Gas PCS in order to increase its maturity level. This allowed a significant increase of the maturity level of a standalone Gas Power Conversion System option [5].

It has been thus decided to lay during the 2016-2017 phase the ASTRID Gas PCS integration studies on the same level with the ASTRID Water based PCS studies completed at the end of 2015. The 2016-2017 phase, in which the Gas PCS is integrated in the overall layout of the reactor, allows a better specification of the technical and economic implications of the selection of Gas PCS taking into account all the aspects of the integration of such an option. A well-documented comparison between the two systems is therefore facilitated.

This paper discusses progress in the integration of the Gas Power Conversion System in the Astrid Reactor Plant Model. It also describes the characteristics of the main systems particularly the turbomachinery, the Heat Exchangers (Sodium/Gas, Gas/Gas and Gas/Water) and the Gas Inventory Management System.

ASTRID Gas Cycle Performance

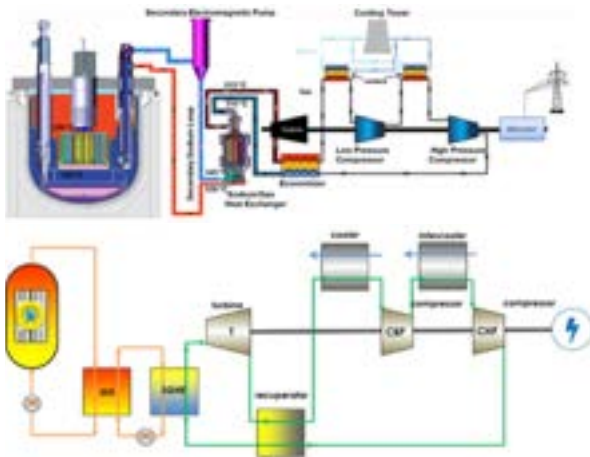
At the end of the AVP2 Phase (2013-2015), the reference cycle for the ASTRID Power Conversion System is a closed Brayton cycle in pure nitrogen at 180 bar (figure 1). The turbine and the compressors are placed on the same shaft line as the turbogenerator. Aiming at optimising the cycle, the gas is cooled before the high-pressure compressor inlet to limit the compression work and an economiser allows raising the temperature of the gas returning to the Sodium Gas Heat Exchangers (SGHE). The reference solution for the heat sink is a wet cooling tower. The closed cooling water system provides the cooling medium for the pre-coolers and coolers.

The main boundary conditions for the thermodynamic gas cycle calculations are the following:

- Thermal power delivered to the gas cycle: 1500 MWth
- Sodium gas heat exchanger outlet temperature: 515°C
- Sodium gas heat exchanger outlet pressure: 180 bar
- Sodium gas heat exchanger inlet temperature: 310°C
- Cooler outlet temperature: 27°C

The expected gross efficiency at the end of the AVP2 phase (2013-2015) is around 37.4%, not taking into account cooling requirements, sodium pumps and auxiliary power. Main operation procedures of ASTRID gas power conversion system have been defined [6].

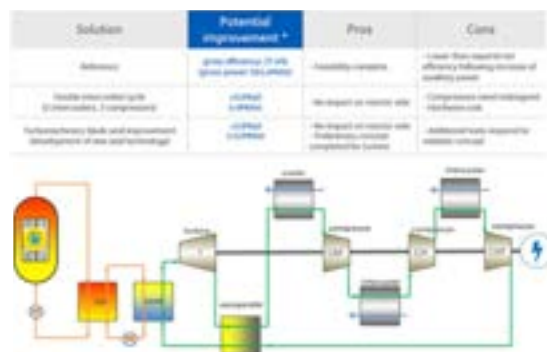
Figure 1. AVP2 Reference Brayton cycle



ASTRID Project Business Confidential Information, CEA and GE property designs

At the beginning of the phase 2016-2017, it has been asked to GE and CEA R&D to think about solutions to maximise the efficiency of the cycle. Different solutions were investigated (double intercooled cycle, reheated cycle, add CO₂ to Nitrogen, ORC solutions...). The double intercooled cycle appeared as the most robust solution as it deals no impact on reactor side and no significant modifications on turbomachinery and Heat Exchangers thermal load (except an increase of 10% for the modular economisers). Thus, this solution has been embedded in the new configuration together with turbomachinery blade seals improvement.

Figure 2. New Reference Brayton cycle



ASTRID Project Business Confidential Information, CEA and GE property designs

The Heat Exchangers

The Sodium Gas Heat Exchanger (SGHE)

Eight Sodium Gas Heat Exchangers bring the thermal power to the Gas PCS. Due to their very innovative design and operating conditions, the Sodium Gas Heat Exchanger (SGHE) is leading to a main technological challenge. The Sodium Gas heat exchanger is based on a compact plate heat exchanger technology investigated by the CEA [7] [8]. The SGHE concept is a component power unit of 190 MWth (2 components per secondary sodium loop), using a technology of plate assembly by high isostatic pressure diffusion bonding manufacturing process (HIP-DB) [8]. The principle of this design of SGHE is based on a component integrating 8 elementary modules of Compact Plate Heat Exchanger into a pressurised vessel which also plays the role of inlet manifold (Figure 3). These design options aim at:

- limiting the impact of a failure of the exchanger module towards the outside, the external vessel constituting the second sodium containment barrier,
- limiting the impact of a failure of the module on the secondary circuit: the maximal nitrogen leak section in the sodium is reduced, and the sodium manifolds are brought out the pressure vessel,
- limiting the thermo-mechanical stresses: the pressure vessel structures are maintained at the heat exchanger low temperature, i.e. 310°C, and the plates are maintained in compression,
- minimising the sodium inventory in the components,
- maximising compactness and minimising the pressure drop.

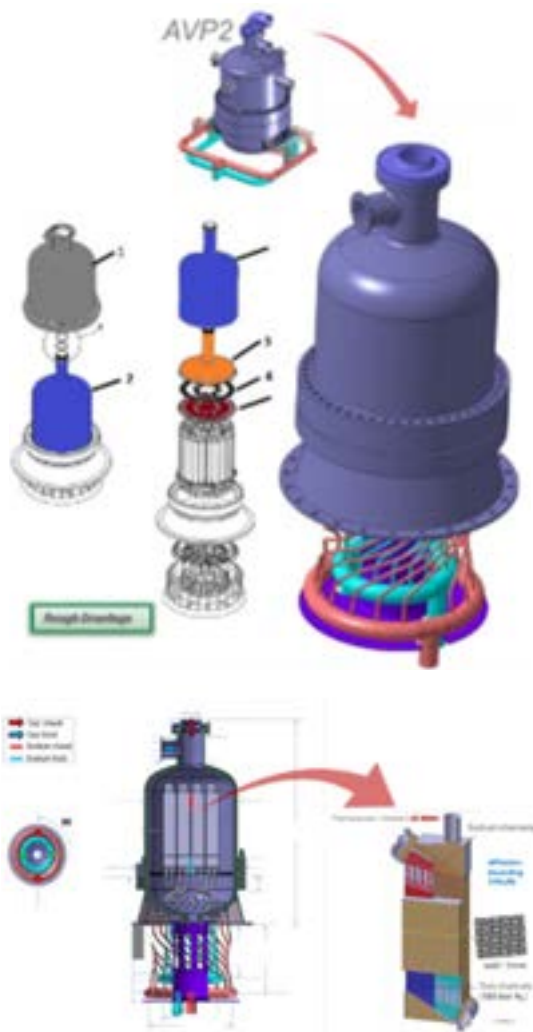
The significant weight of the pressure vessel and the fact that the internal sodium pipes are loaded by an external pressure are the main drawbacks of this concept.

Few mock-ups at small scale (40kW) have been manufactured and tested on the DIADEMO facility (CEA) in representative conditions [8].

The engineering of the SGHE general component was transferred to FRAMATOME in March 2016, CEA R&D pursuing design studies on exchange module because of its innovative nature [7]. A road map for the development, qualification and industrialisation of SGHE was

since developed in synergy between FRAMATOME and CEA R&D and two SGHE project reviews were performed. The principle to put the Compact Plate Heat Exchanger modules in a pressurised vessel, playing also a “header/gas pipes/safety containment” functions has been confirmed. The selection of a concept of a “on the floor” component has been made to authorise the disassembling of the upper part of the component.

Figure 3. Sodium Gas Heat Exchanger



ASTRID Project Business Confidential
Information, CEA and Framatome property
designs

In parallel to this concept, Alternative SGHE design solutions are studied to reduce the total mass of the SGHE.

SGHE: Alternative concept



Limitation of the consequence of internal nitrogen leak into the sodium

The absence of sodium-water at the interface between the secondary fluid and tertiary is an undeniable advantage of the Gas PCS for the safety demonstration. Gas PCS also allows to make possible the exclusion of large sodium-water reaction if it is removed in the way in the other places of the reactor, including washing facilities.

The impact of Gas PCS on key safety functions (reactivity control, cooling and containment) was analysed qualitatively and compared to steam PCS. Concerning the reactivity control, the Gas PCS takes the advantage in the fact that core gas ingestion and core compaction are easier to manage with a suitable design of the Intermediate Heat Exchangers, as a SGHE leakage behavior is physically less severe than a sodium water reaction in a steam generator. Concerning the containment, the Gas PCS inherently eliminates the sodium-water-air reactions risk in the exchanger buildings. In addition, there is no risk of leakage self-evolution (no wastage), no production of hydrogen or soda.

Various measures are envisaged to limit the consequences of a possible internal failure of the exchangers that could occur despite the quality provided to the manufacture of the modules and their integration in the exchangers. Passive arrangements to limit the pressure rise in the secondary loop are under study (rupture disks,...).

First EUROPLEXUS calculations of pressure wave propagation were carried out to evaluate, according to the layout of the secondary loop, the effectiveness of the arrangements put in place to avoid the consequences of such events. They will be supplemented by mass transfer calculations.

Preliminary results show that there are effective solutions to reduce the pressure peaks in the secondary loop and consequently at the intermediate heat exchanger. However, these solutions are very dependent on the architecture of the secondary loops and the design of the exchangers. Studies must be continued on this subject.

Monitoring systems are being investigated (eg, monitoring the nitrogen content in the gaseous skies of reservoirs on the secondary loop) to detect early degradation of the exchange zone and prevent its evolution towards failures more important.

The other exchangers

The new Brayton thermodynamic cycle with a double intercooled cycle leads to the choice of:

- An economiser between the high pressure and low pressure lines of the cycle increasing the average operating temperature of the SGHE.
- Three stages of compression with appropriate coolers to limit the compression work and the power input to the shaft-line.

The operating conditions of these heat exchangers in terms of pressure and temperature are less severe than those imposed on sodium / gas exchangers. The economiser (also called recuperator) is a gas / gas exchanger between the high-pressure and low-pressure lines that passively cools the expanded gas from the turbine outlet and heats the recompressed gas before the SGHE to raise the average temperature of the heat source and thus improve the cycle efficiency. The pre-design studies carried out on this high power component show that only a modular technology of compact exchangers could be feasible for reasons of compactness and allowable mechanical load.

The pre-coolers and coolers are gas / water exchangers for cooling of the compressor inlet gas to limit the compression work. They operate at the bottom pressure levels and temperature of the cycle (at pressures below 110 bar, temperatures below 100°C). The use of

compact plate heat exchangers for these coolers leads to a gain in thermal compactness of at least a factor 10 compared to the shell and tube concepts. Furthermore, without grid, penalising in terms of size and cost, it is not possible to implement exchangers based on plate&shell technology. Therefore, the modular technology of compact plate heat exchangers type should also be withheld for gas cycle coolers.

The engineering of these exchangers of the tertiary gas cycle has been addressed by the CNIM Company since September 2016.

The Turbomachinery

At the end of AVP2 Phase (2013-2015), the turbomachinery was based on 2 single-flow axial turbines, one Low-Pressure and one High-Pressure radial Compressors on the same shaft line as the turbogenerator. The design of the turbomachinery has been pre-defined together with the main ancillary systems. All key technologies have references in the industry and the feasibility of the turbomachinery is confirmed.

The turbines

The driving machinery is a pair of multi-stage axial nitrogen turbine arranged in opposite direction (split-flow concept) to balance the axial thrust. An innovative design for the turbine inlet guiding the flow from the two incoming pipes to the blade area has been developed to minimise the head loss. A similar concept is used for the turbine outlet, which guides the flow leaving the last stage blade to the 2 outlet pipes (Figure 5). A barrel outer casing ensures tightness while minimising thermal distortions. Several types of shaft-end seals such as mechanical seal, hydrodynamic seal, brush seal... have been investigated to minimise the shaft leakage. The bearings are conventional hydrodynamic tilt-pad bearings. These 2 elements are enclosed in the bearing housing.

A comparison between axial and radial technologies has been performed concluding that the axial technology was the most suitable for the turbine. Trade studies were performed between a single-flow turbine vs. split-flow turbine. Whilst the single-flow turbine aerodynamic efficiency was higher, the requirement for a balance piston to balance the turbine axial thrust makes the efficiency of the single-flow turbine at the same level of the split-flow turbine. In addition, a split-flow back-to-back turbine configuration reduces the risk

of thrust reversal during transient. This has also the benefit to lower blade gas bending loads due to shorter blades and twice the number of rows.

In the two shaft lines configuration, pipe lines connecting the turbine to the upstream and downstream components are limited to 4, with two inlet/outlet pipes per turbine casing. The reduction of the number of inlet / outlet piping simplifies penetrations and allows returning to more conventional solutions compared to the one shaft line configuration.

Turbine casings are subjected to high internal pressure, especially at the turbine inlet. To limit inner casing ovalisation causing leakage between turbine stages and a drop in performance, the current concept provides a double envelope with internal pressure balance.

Concerning the rotor, several construction technologies such as bolted rotors, monoblock rotor, welded rotor... have been investigated. A welded hollow rotor has been chosen to minimise the mass/moment of inertia ratio and to ensure a good behavior when going through the turbine critical speed during speeding up/slowing down, and thus allowing the minimum radial clearances to be set. Thermal, thermomechanical and rotor dynamic analysis confirmed the feasibility of the rotor.

Figure 5. Nitrogen turbine



ASTRID Project Business Confidential
Information, CEA and GE property designs

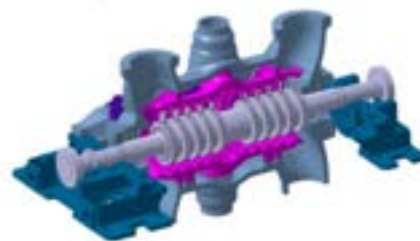
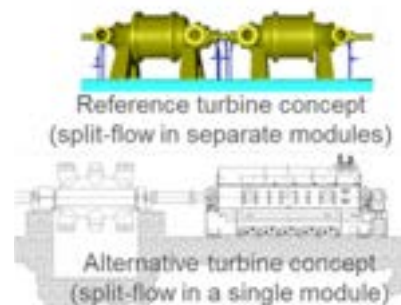
During 2016, the GE team paid particular attention to the consolidation of the turbomachinery concept, especially on the turbine design. With the first concept completed, the team had sufficient insight to come back to the assumptions initially made and to ensure that they lead to the best concept. In parallel, GE has also investigated potential improvements proposed during the various GE internal design reviews and the ASTRID project

Gas PCS expert review held at the end of AVP2. Independent concept studies using alternative tools have confirmed the feasibility of the turbomachinery and the anticipated performances (figure 6). A new design of turbine derived from steam/water turbine technology has been embedded. This design deals with a double flow turbine in a single outer casing is now possible. So far, the concept was based on 2 single-flow turbines, each having half the mass flow. The main advantages of the double flow are:

- The module is internally thrust balanced and transmits no effort to the shaft line.
- There are only 2 shaft-end seals instead of 4 and no seals at 180 bars.
- Total length is smaller.
- There is only one intake chamber, which then acts as a collector and equalises the gas pressure from the 4 main pipes. This could potentially simplify operation with a secondary sodium loop unavailable.

However, a characteristic of the configuration of the dual flow turbine is that there are more penetrations in the outer shell (4 inlets and 4 outlets) than in the single flow turbine. Before confirming this design, the mechanical integrity of the envelope has to be verified by Finite Element analysis.

Figure 6. Alternative Nitrogen turbine concept



ASTRID Project Business Confidential
Information, CEA and GE property designs

Many aspects of the turbine design are already consolidated: axial technology, split-flow, hydrodynamic bearings, inner + outer casing construction, performance.

The compressors

Both axial and radial technologies were further analysed. The radial technology has been maintained for its simplicity and robustness, but a multi-stage configuration has been chosen to maintain a good efficiency (figure 7). Split-flow compressors and face-to-face mounting single-flow compressors have been studied to minimise residual axial thrust during all transients. Those options have been revisited in 2017 to take into account the new configuration with three compressors (HPC, IPC and LPC).

The new design still uses radial compressor technology from a proven family of wheels. On the other hand, the compressors are now double-flow, which minimises the residual thrust of each component. The other advantage is that the transmitted torque of the blades on the shaft is lower (increased number of wheels for the same total power), which makes it possible to mount the wheels on the shaft by tightening. The dual flow configuration also reduces the leakage rate at the shaft ends because both seals operate at the inlet pressure.

Figure 7. 2-stage compressor



ASTRID Project Business Confidential
Information, CEA and GE property designs

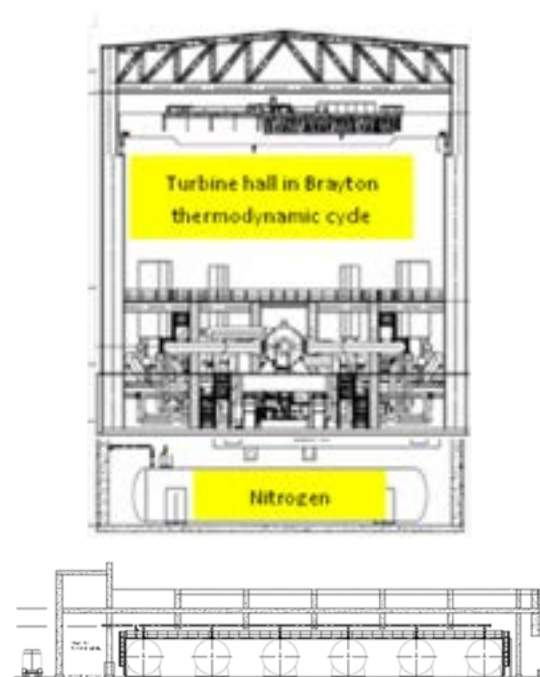
A good mechanical behavior of the wheels is expected even for maximum over-speed. Thermomechanical analysis of the staged pressure vessel shows that stress limits are widely observed. Only a few specific points are beyond the limits while remaining well below

the allowable stress limit. To confirm the mechanical integrity of the pressure vessel, an elasto-plastic analysis was performed in accordance with the European Unfired Pressure Vessel Standard. This analysis has shown that all criteria were passed with a minimum lifetime greater than 10000 cycles for the most-strained areas of the casings.

Gas Inventory Management System

Actual load of the shaft line is driven by the specific volume of the gas in the turbine. The Gas Inventory Management System allows the voiding and filling of the tertiary nitrogen circuit and allows management of the mass of gas in the tertiary circuit and thus the mean operating pressure according to the various operating conditions of the reactor. Note that rapid transients will primarily be managed by equipment bypasses. The Gas Inventory Management System, which is composed with 6 large gas storage vessels, 600 m³ under 50 bar each, is now implemented on the ground floor of the turbine building, below the Brayton cycle equipment. In addition, a liquid nitrogen storage unit, and a set of nitrogen cylinders under 200 bar, allow the first filling and a continuous make-up (to compensate leakage) of the Gas Inventory.

Figure 8. Gas Inventory Management System



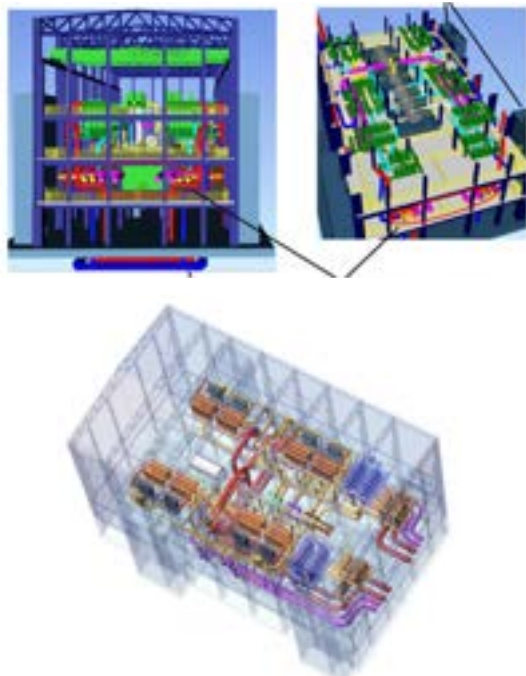
The General layout of the Gas PCS

During the AVP2 phase (2013-2015), a techno-economic analysis has been conducted on the ASTRID Gas PCS. A multiple parameters investigation concluded to an optimised configuration of the Gas PCS with two turbomachinery shaft lines in two separate turbine halls. This configuration led to a strong reduction of the number of gas lines and equipment, of the steel and nitrogen inventories (divided by a factor 2) and of the Gas Inventory Management System. In addition, the simplification of the gas piping layout allowed a better arrangement of the turbine hall with easier accessibility and maintainability.

At the end of the ASTRID AVP2 phase, the selection of the concept of two 300 MWe Turbomachinery shaftlines in two separate turbine halls was confirmed and a first design of the main components was defined.

The new cycle configuration with a double intercooled cycle does not change the number of Heat Exchangers but have consequence on their design.

Figure 9. Gas PCS General layout



ASTRID Project Business Confidential Information, CEA and GE property designs

Integration of the Gas PCS in the ASTRID General Model Plant

The integration of the Gas PCS in the ASTRID reference configuration has been performed with the introduction of Sodium-Gas Heat Exchangers in the nuclear island and their connections with the Secondary Sodium Loops and the tertiary system. Several configurations of implantation of SGHE in Heat Exchanger buildings and plots of the Secondary Sodium Loops and tertiary lines have been studied in parallel with the turbine halls disposal on the general plant model in order to obtain optimal ergonomics of the buildings, of the buildings layout and of the gas piping layout. The selection of a lateral disposition of the turbine halls oriented to the south and a longitudinal disposition of SGHE in two lateral Heat Exchanger buildings has been made.

Figure 10. ASTRID Project Business Confidential Information, CEA and FRAMATOME property designs



Control of the Gas PCS

During the 2016-2017 phase, significant progress has been made on Gas PCS control [6]. The team has performed numerous dynamic simulations to reach a high level of understanding on the various operating cases

of ASTRID and to specify a preliminary control system. In the current solution, 4 control functions are defined. The inventory management system is used to control large change of load, startup and normal shutdown. Acting on the inventory of the PCS is a slow process and a quicker and finer way of controlling the load (and the sodium return temperature) is also possible with the use of the SGHE bypass (sodium temperature increase) and of the recuperator bypass (sodium temperature reduction).

In addition, each compressor has also a bypass. This bypass has a threefold role. The first role is to act as a protection against turbomachinery overspeed after an unexpected grid disconnection by increasing the load of the compressors and reducing the power produced by the turbine. The second role is to protect the compressors against surge by increasing their volume flows when necessary. Finally, these bypasses are used when the generator is not connected to the Grid, i.e. house load, startup and shutdown to accurately control the speed of the turbomachinery.

The first investigations have demonstrated that all bypasses could use large high-pressure butterfly valves available on the market. The main difference would rely in the actuators. The compressor bypasses require a rapid opening of the valves to limit the shaft overspeed to a minimum. With fast hydraulic actuators, an opening time of about one second could be achieved.

Figure 11. ASTRID Control System



Conclusions

Progress in the integration of the Gas Power Conversion System in the Astrid Reactor Plant Model has been described together with the characteristics of main systems particularly the turbomachinery, the Heat Exchangers (Sodium/Gas, Gas/Gas and Gas/Water) and the Gas Inventory Management System.

Those studies allow a better specification of the technical and economic implications of the selection of the Gas Power Conversion System taking into account all the aspects of the integration of such an option, enabling a well-documented comparison between Gas PCS and conventional Steam PCS.

References

- [1] F. GAUCHE "The French Prototype of 4th Generation Reactor: ASTRID"; Annual meeting on nuclear technology, Berlin, May 17&18th; (2011).
- [2] J. ROUAULT et al. "ASTRID, The SFR GEN IV Technology Demonstrator Project: Where are we, where do we stand for?" Proceedings of ICAPP'15, Nice, France, May 03-06, (2015).
- [3] H.S.PHAM "Mapping of the thermodynamic performance of the supercritical CO2 cycle and optimisation for a small modular reactor and a sodium-cooled fast reactor"; Energy 87 412-424 (2015).
- [4] L. GICQUEL..., "Supercritical CO2 Brayton Cycle Coupled with a Sodium Fast Reactor: Na/CO2 interaction experiments and modeling", Proceedings of ICAPP '10, San Diego, CA, USA, June 13-17, 2010, Paper 10215.
- [5] D. PLANCO et al. "Status of studies on ASTRID gas power conversion system option"; Proceedings of ICAPP'16, San Francisco United-States, April 17-20, (2016).
- [6] D. BARBIER et al. "Main operation procedures for ASTRID gas power conversion system"; Proceedings of International Conference on Fast Reactors

- and Related Fuel Cycles, Yekaterinburg, Russian Federation, (2017).
- [7] D. PLANCQ et al. "Progress in ASTRID Sodium Gas Heat Exchanger Development", Proceedings of International Conference on Fast Reactors and Related Fuel Cycles, Yekaterinburg, Russian Federation, (2017).
- [7] L. CACHON et al. "Status of the Sodium Gas Heat Exchanger (SGHE) Development for the Nitrogen Power Conversion System Planned for the ASTRID SFR Prototype", Proceedings of ICAPP 2015, Paper 15439, SFEN, Nice, France (2015).
- [8] G. GAILLARD-GROLEAS et al., "the qualification process of simulation tools, components and systems within the frameworks of the ASTRID project – Description and examples" Proceedings of ICAPP'17, Fukui and Kyoto, Japan, (2017).
- [9] In addition, D. PLANCQ et al., "Progress in the ASTRID Gas Power Conversion System development". FR17 Paper IAEA-CN-245-285.
- [10] In addition, D. PLANCQ et al., "Progress in the ASTRID Sodium Gas Heat Exchanger development". FR17 Paper IAEA-CN-245-286.

CODES AND STANDARDS DEVELOPMENT FOR NEXT GENERATION SODIUM-COOLED FAST REACTORS IN JAPAN (T. ASAYAMA ET AL)

Tai Asayama, Masanori Ando, Satoshi Okajima, Takashi Onizawa, Shigeru Takaya, and Hiroki Yada

Japan Atomic Energy Agency, Japan

I. Introduction

This paper describes the current status and path forward of structural codes and standards development for next generation sodium-cooled fast reactors in Japan. The focus is on the development of codes and standards that fully extract the favourable features of sodium-cooled plants. To achieve this, the System Based Code (SBC) concept has been adopted as a basic principle. The concept allows optimised allocation of margins across various technological aspects in a plant life-cycle - materials, design, fabrication, operation, inspection and maintenance. Codes and guidelines that materialise the concept are being developed within the Japan Society of Mechanical Engineers (JSME). This activity involves a number of experts from various organisations including Japan Atomic Energy Agency (JAEA). The authors of this paper are members of the Subgroup on Elevated Temperature Codes of the JSME Subcommittee on Nuclear Power, which is in charge of codes for sodium-cooled fast reactors, with the first author its chair.

II. Code Development Strategy

The main point is to develop a system of codes and guidelines that fully extract favourable technical features of sodium-cooled fast reactor plants to overcome some of their downsides and allow them to meet the high goals of safety and reliability in a most effective way. The favourable technical features include 1) use of ductile materials for structural components, 2) operation under low pressures, and 3) high boiling point of sodium that allow high sub-coolness. The downsides include 1) sodium opacity and 2) possible sodium-water reaction.

The System Based Code (SBC) [1] concept has been adopted as a basic principle for the development. This concept was proposed based on the recognition that existing codes and standards structure had become unnecessarily rigid in the long history of development and through a number of revisions. The SBC concept presents a new framework that is flexible enough to reflect the state-of-the-art technologies and operation experiences of existing reactors. It encompasses a whole plant life cycle and is flexible enough to allow modification of design margins based on inspection methods when it is fully implemented.

Based on the SBC concept, a set of mutually related codes that encompasses a plant life is being developed as Japan Society of Mechanical Engineers (JSME) Codes for Electricity Generation Facilities (some of them have been published as described later). Those are design and construction code (this includes material strength standards), code for welding, fitness-for-service code (inservice inspection code), leak-before-break evaluation guidelines, and reliability evaluation guidelines for passive components.

III. Current Status and PATH Forward

III.A Design and construction code

The first version of the JSME Code for Design and Construction of Fast Reactors was published in 2005 [2]. Although the main structure of this code (hereinafter, JSME D&C FRs Code) was equivalent to the ASME Code Case N-47 [3], it incorporated design rules developed in Japan for the Japanese prototype fast reactor (FR) "Monju" [4][5]. One of the outstanding features is the incorporation of the

elastic follow-up concept, which allowed evaluation of inelastic behaviour of structural components based on conventional elastic analysis. The French RCC-MR [6] code and ASME Boiler and Pressure Vessel Code Section III Division 1 Subsection NH [3] followed suit. Also to note is that the allowable stresses were developed by using the material test data obtained in Japan.

Another point to note about the JSME D&C FRs Code is that it provides detailed commentaries on its rules, especially on the elevated temperature design rules and material strength standards. Concepts and background of each of the rules are described to help the user understand and use the rules correctly. The commentaries include equations for material behaviours (tensile, creep and fatigue curves) as well as creep strain rate with detailed descriptions of procedures for setting allowable stresses.

The rules and allowable stresses in the JSME D&C FRs Code have been updated since its first publication. Some parts of the Demonstration Fast Reactor Design Standard (DDS) [7][8] developed in the 1990s were reflected; two candidate materials for next generation reactors, 316FR steel and Mod.9Cr-1Mo steel, were covered in the 2012 Edition, through referring to the codification study [9] for the DDS. 316FR is a material originally developed in Japan for fast breeder reactors [10][11], and Mod.9Cr-1Mo steel is basically the same material as the ASTM/ASME Grade 91 steel. In parallel to this update, the applicability of the rules in the JSME D&C FRs Code to these materials was validated [10]. Especially, the appropriateness of creep-fatigue damage evaluation procedures was demonstrated using the material and structural test data of these materials [12][13][14].

Moreover, for Mod.9Cr-1Mo steel, timewise design factors for creep rupture strength to define S_R , time to creep rupture for design, were optimised by adopting the region splitting method. Statistical analysis of collected creep rupture data indicated that the values of 10 and 5, for short and long term regions, respectively, give the reliability equivalent to that for the conventional materials [15].

The JSME D&C FRs Code has been improved continuously. Items currently under consideration include 1) extension of time-dependent allowable stresses for the 316FR steel and Mod.9Cr-1Mo steel from 300,000 to 500,000 hours, 2) incorporation of Mod.9Cr-1Mo steel tube products, 3) buckling evaluation rules

for vessel that accounts for axial compression, developed in DDS [16], 4) external pressure chart for 2.25Cr-1Mo and Mod.9Cr-1Mo steels at elevated temperatures, developed originally, and 5) design evaluation procedures for weld joints at elevated temperatures.

Figure 1 and 2 indicate creep rupture test data and creep rupture curves that are under development for 500,000 hour design, for 316FR and Mod.9Cr-1Mo steels, respectively. For improving the accuracy of prediction in the long term regions, the region splitting method is applied to 316FR steel, too. The creep strain equations will also be revised reflecting the adoption of the region splitting method. Design factors to develop the values of S_R will also be optimised in same manner as Mod.9Cr-1Mo steel. These curves, which are applied up to 500,000 hours, will be implemented in the coming edition of the JSME D&C FRs Code.

Figure 1. Relationship between creep data and creep rupture equations of 316FR steel

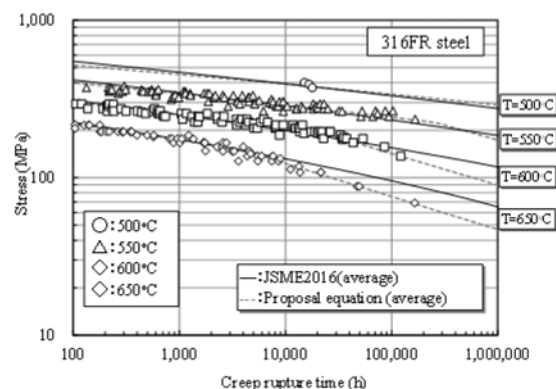
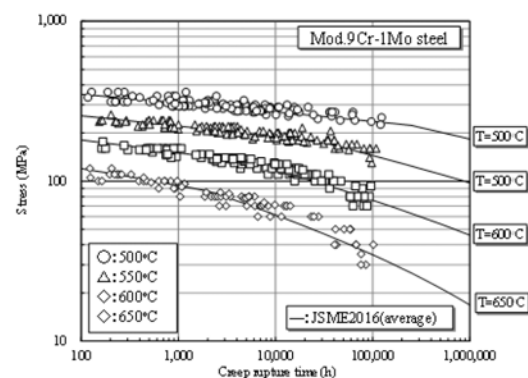


Figure 2. Relationship between creep data and creep rupture equation of Mod.9Cr-1Mo steel



III.B Fitness-for-Service code

A draft of fitness-for-service code (inservice inspection code) was developed for Class1 components and their support structures. It refers to the JSME Fitness-for-Service Code for light water reactors [17], ASME Boiler and Pressure Vessel Code, Section XI, Division 3 [18], and ASME Code Case N-875 which was published in 2017 [19]. The draft is being reviewed in JSME for publication. Proposed inservice inspection requirements are shown in Table 1.

Table 1. Proposed inservice inspection requirements in the draft of JSME fitness-for-service code (Class1 components and their support structures except core support structures)

Parts examined	Examination method
Liquid sodium retaining welds in vessels and piping	Continuous monitoring of sodium leak
Radioactive cover gas retaining welds in vessels and piping	Continuous monitoring of radioactive gas leak
Welds in support structures	Visual test (VTM-1)

*Note: VTM-1 examinations are conducted to detect discontinuities and imperfections including cracks, wear, corrosion, and erosion on the surfaces of components.

The draft code employs continuous leak monitoring for the inspection of coolant boundaries provided that Leak-Before-Break (LBB) is demonstrated to hold in the point of interest. This concept is consistent with the following features of sodium-cooled fast reactors:

- Excellent compatibility of structural materials with sodium.
- Low pressure coolant systems that preclude the possibility of loss of coolant due to flashing.
- Safety measures against coolant leakage that include guard vessels that limit the total amount of leakage, and liners for prevention of sodium-concrete reactions.

Guidelines on LBB assessment are concurrently developed and are also under review in JSME. The details of the guidelines will be explained in the next section.

Requirements for continuous leak monitoring are not included in the JSME Fitness-for-Service Code for light water reactors. Therefore, they were prepared mainly based on ASME Boiler

and Pressure Vessel Code, Section XI, Division 3 and the experience obtained in the prototype reactor in Japan, Monju.

JSME collaborates with ASME on the development of fitness-for-service rules for liquid-metal cooled reactors. A joint task group was established in 2012 to develop alternative requirements for ASME Boiler and Pressure Vessel Code, Section XI, Division 3 by utilising the System Based Code concept [20]. [21].

The joint task group discussed what would appropriate in-service inspection requirements be to meet the safety goals [22-24]. The discussion materialised as a new code case, N-875 which was issued in 2017. The Code Case provides a unique procedure to derive reliability targets for components from given plant safety goals. In the first stage, whether or not a component of interest has sufficient structural integrity to meet derived reliability targets without taking account of inspections. Then, in the second stage, the detectability of a possible flaw before the flaw reaches the maximum acceptable size, which is derived based on the safety evaluation of the plant, is evaluated. For coolant boundaries, if LBB is demonstrated to hold, continuous leak monitoring is selected as a measure for inservice inspection.

III.C Leak-Before-Break guidelines

The LBB guidelines are being developed in connection to the fitness-for-service code; the main purpose is to provide assessment procedures to determine if LBB holds in the point of interest.

The scope of the guidelines is to provide LBB assessment procedures for piping and vessels of fast reactor plants that retain sodium coolant. Design features of fast reactor plants, such as operation at elevated temperatures and low pressure coolant-systems, were taken into account.

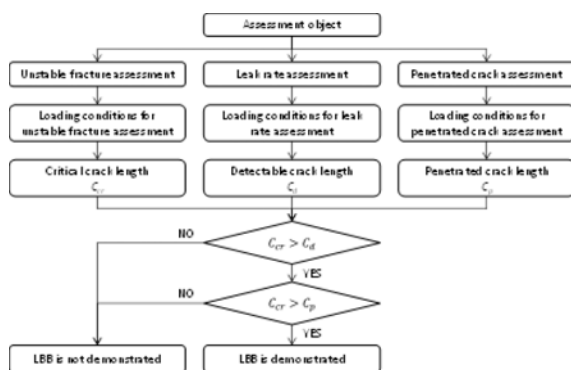
Figure 3 represents the LBB assessment flow. There are three main paths, which are "Unstable fracture assessment", "Leak rate assessment" and "Penetrated crack assessment". The path "Unstable fracture assessment" is to determine a critical crack length, C_{cr} , above which unstable fracture occurs under given loading conditions. The path "Leak rate assessment" is to determine detectable crack length, C_d , above which sodium leakage can be detected by given leak detectors. A new crack opening displacement evaluation method was developed for thin walled large diameter cylindrical structures [25].

The path “Penetrated crack assessment” is to C_p , the crack length when a crack penetrates the wall, under given transients virtually repeated enough cycles for the crack to penetrate the wall. A simplified method was developed to evaluate penetrated crack length both for axial and circumferential cracks as a function of the ratio of membrane and bending stresses and fatigue crack growth characteristics [26] [27]. In the method, penetrated crack length is evaluated by considering only fatigue crack growth mechanism because penetrated crack length without considering creep effects becomes longer [26].

If C_{cr} is longer than both C_d and C_p , LBB holds.

LBB assessments were performed for high stressed regions in major piping systems of Monju and JSFR by using the LBB guidelines, and in both cases, LBB was demonstrated to hold [28] [29].

Figure 3. LBB assessment flowchart for FBR [28]



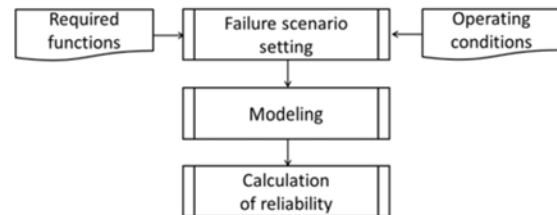
III.D Reliability evaluation guidelines

New guidelines on reliability evaluation of fast reactor passive components will be published from JSME in 2018 [30]. They are consistent with the risk-informed approach and the System Based Code concept [21]. For example, the Code Case N-875 explained above would require these guidelines: it provides a framework in which detailed structural reliability evaluation procedures such as the guidelines play an important role.

The guidelines consist of five chapters, which are “General rules”, “Overview of Reliability Evaluation”, “Failure Scenario Setting”, “Modeling” and “Calculation of Reliability”, corresponding to the evaluation procedure

shown in Fig. 4. The methods provided in these guidelines are “model-based”, because operation experience on sodium-cooled reactors is relatively limited, while experimental and analytical studies in Japan have reached to a point where reliable models based on them can be developed.

Figure 4 Reliability evaluation procedure



One of the difficulties in conducting structural reliability evaluation is how to determine probabilistic distributions of random variables. Material property is one of the most important random variables. Therefore, statistical properties of material strength such as creep rupture time, steady creep strain rate, yield stress, tensile stress, fatigue life and cyclic stress-strain curve were estimated for austenitic stainless steels, based on the material strength database used for developing the JSME D&C FRs Code [31]. A summary of the statistical properties of material strength is included in the guidelines for user's convenience. Loading condition is another important random variable. Methodologies and basic ideas to determine statistical parameters for loading conditions are also prepared [32].

Numerical calculation codes are also needed for model-based reliability evaluation. JAEA is developing a probabilistic fracture mechanics analysis code, REAL-P [33] in line with the development of the guidelines. Currently, verification benchmark analysis is being conducted with another computational code programmed independent of REAL-P.

Integrated development of the guidelines, tables of statistical parameters of random variables and REAL-P contributes to the implementation of the System Based Code concept.

V. Conclusion

For the next generation sodium-cooled fast reactors to meet the high goals of safety and reliability as well as economical requirements,

it is essential to use structural codes and standards that are most suitable for reactors. Sodium-cooled fast reactors have a number of technical features that relate to various aspects of a plant life-cycle. The codes and standards should be developed based on these features. Based on this recognition, a set of codes and standards is being developed within the Japan Society of Mechanical Engineers (JSME). The System Based Code (SBC) concept is used as a basic principle. The codes being updated or newly developed include design and construction code (this includes material strength standards), code for welding, fitness-for-service code (inservice inspection code), leak-before-break evaluation guidelines, and

reliability evaluation guidelines for passive components.

Acknowledgements

The authors are grateful to Mr. Koji Dozaki, vice-chair, Mr. Tomomi Otani, secretary, and the members of the Subgroup on Elevated Temperature Codes of the JSME Subcommittee on Nuclear Power. The authors are also thankful to the contributors to the JSME/ASME Joint Task Group for System Based Code of the ASME Boiler and Pressure Vessel Committee for intuitive discussions and useful suggestions.

References

- [1] Asada, Y., Japanese Activities Concerning Nuclear Codes and Standards – Part II, *Journal of Pressure Vessel Technology*, ASME 128 (2006) 64.
- [2] JSME S NC2-2005 “Code for Nuclear Power Generation Facilities, -Rules on Design and Construction for Nuclear Power Plants-Section II Fast Reactor Codes”, JSME (In Japanese)
- [3] (Recent edition) Boiler and Pressure Vessel Code, Section III, Division 5, Rules of Construction for High Temperature Reactors, ASME (2017).
- [4] Iida, K., et al., “Construction codes developed for prototype FBR Monju”, *Journal of Nuclear Engineering and Design*, Vol.98, pp.283–288, 1987.
- [5] Iida, K., et al., “Simplified analysis and design for elevated temperature components of Monju”, *Journal of Nuclear Engineering and Design*, Vol.98, pp.305–317, 1987
- [6] (Recent edition) RCC-MRx, Design and Construction Rules for Mechanical Components in high-temperature structures, experimental reactors and fusion reactors, Afcen (2015)
- [7] Kawasaki, N., et al., “Recent design improvements of elevated temperature structural design guide for DFBR in Japan”, *SMiRT15, Div. F, F04/4*, pp. IV 161-168, 1990
- [8] Kurome, K., et al., “Material strength standard of 316FR stainless steel and modified 9Cr-1Mo steel”, *Proceedings of ASME PVP 1999, PVP-Vol.391*, pp.47-54, 1999
- [9] Asayama, T., et al., “Development of 2012 Edition of JSME Code for Design and Construction of Fast Reactors — (1) Overview”, *Proceedings of ASME PVP 2013, PVP-2013 98061*, 2013
- [10] Nakazawa, H., et al., “Advanced type stainless 316FR for fast breeder reactor structures”, *Journal of Materials Processing Technology*, Vol.143-144, pp.905-909, 2003.
- [11] Onizawa, T., et al., “Development of 2012 Edition of JSME Code for Design and Construction of Fast Reactors — (2) Development of the Material Strength Standard of 316FR Stainless Steel”, *Proceedings of ASME PVP 2013, PVP-2013 97608*, 2013
- [12] Ando, M., et al., “Development of 2012 Edition of JSME Code for Design and Construction of Fast Reactors — (6) Design Margin Assessment for the New Materials to the Rules”, *Proceedings of ASME PVP 2013, PVP-2013 97803*, 2013
- [13] Nagae, Y., et al., “Development of 2012 Edition of JSME Code for Design and Construction of Fast Reactors — (5) Creep-Fatigue Evaluation Method for 316FR Stainless Steel”, *Proceedings of ASME PVP 2013, PVP-2013 97806*, 2013

- [14] Takaya, S., et al., "Development of 2012 Edition of JSME Code for Design and Construction of Fast Reactors — (4) Creep-Fatigue Evaluation Method for Modified 9Cr-1Mo Steel", Proceedings of ASME PVP 2013, PVP-2013 97609, 2013
- [15] Onizawa, T., et al., "Development of 2012 Edition of JSME Code for Design and Construction of Fast Reactors — (3) Development of the Material Strength Standard of Modified 9Cr-1Mo Steel", Proceedings of ASME PVP 2013, PVP-2013 97611, 2013
- [16] Akiyama, H., et al., "Outline of the Seismic Buckling Design Guideline of FBR Main Vessels", SMiRT13, Div. E, E013, pp. 445-456, 1995
- [17] JSME S NA1-2016 "Code for Nuclear Power Generation Facilities, -Rules on Fitness-for-Service for Nuclear Power Plants-", JSME (2016), in Japanese.
- [18] Boiler and Pressure Vessel Code, Section XI, Division 3, Rules for Inspection and Testing of Components of Liquid-Metal-Cooled Plants, ASME (2001).
- [19] Case N-875 "Alternative Inservice Inspection Requirements for Liquid-Metal Reactor Passive Components", Code Cases: Nuclear Components Supplement 1, ASME (2017).
- [20] Asayama, T., et al., "Elaboration of the System Based Code Concept -Activities in JSME and ASME- (4) Joint Efforts of JSME and ASME", Proc. of the 2014 22nd International Conference on Nuclear Engineering (2014) Paper ID: ICONE22-30572.
- [21] Asayama, T. et al., "Development of Structural Codes for JSFR Based on the System Based Code Concept", Proc. of the ASME 2014 Pressure Vessel and Piping Conference (2014) Paper ID: PVP2014-28853.
- [22] Kurisaka, K., et al., "Development of System Based Code (1) Reliability Target Derivation of Structures and Components", Journal of Power and Energy System, Vol. 5, No. 1 (2011) pp. 19-32.
- [23] Takaya, S., et al., "Application of the System Based Code Concept to the Determination of In-Service Inspection Requirements", Journal of Nuclear Engineering and Radiation Science, Vol. 1 (2015) Paper ID: 011004.
- [24] Takaya, S., et al., "Determination of In-Service Inspection Requirements for Fast Reactor Components using System Based Code Concept", Nuclear Engineering and Design, Vol. 305 (2016) pp. 270-276.
- [25] Wakai, T., et al., "Development of a Crack Opening Displacement Assessment Procedure Considering Change of Compliance at a Crack Part in Thin Wall Pipes Made of Modified 9Cr-1Mo Steel", Proc. of the 2018 26th International Conference on Nuclear Engineering (2018), Paper ID: ICONE26-82619.
- [26] Wakai, T., et al., "Development of LBB Assessment Method for Japan Sodium Cooled Fast Reactor (JSFR) Pipes (5) Crack Growth Assessment Method for Pipes Made of Mod.9Cr-1Mo Steel", Proc. of the ASME 2011 Pressure Vessel and Piping Conference (2011) Paper ID: PVP2011-57513.
- [27] Wakai, T., et al., "A study on evaluation method of penetrate crack length for LBB assessment of fast reactor pipes", The Proceedings of the Materials and Mechanics Conference (2015). (in Japanese)
- [28] Yada, H., et al., "Proposal on LBB evaluation conditions for sodium cooled fast reactor pipes and effects of pipe parameters", Transactions of the JSME, Vol.84, No.859 (2018). (in Japanese)
- [29] Wakai, T., et al., "Demonstration of leak-before-break in Japan Sodium cooled Fast Reactor (JSFR) pipes", Nuclear Engineering and Design, Vol. 269 (2014), pp. 88-96.
- [30] JSME S NX7-2017 "Code for Nuclear Power Generation Facilities, -Guidelines on Reliability Evaluation of Fast Reactor Components-", JSME, in press, in Japanese.
- [31] Takaya, S. et al, "Statistical Properties of Material Strength for Reliability Evaluation of Components of Fast Reactors -Austenitic Stainless Steels-", JAEA-Data/Code 2015-002 (2015), in Japanese.
- [32] Yokoi, S., et al., "Determination Methodologies for Input Data including Loads Considered for Reliability Evaluation of Fast Reactor Components", JAEA-Data/Code 2016-002 (2016), in Japanese.
- [33] Yoshimura, S. and Kanto, Y. eds., "Probabilistic fracture mechanics for risk-informed activities -Fundamentals and Applications-", The Japan Welding Engineering Society (2017) <http://www-it.jwes.or.jp/ae/free/ae-1402e/ae-1402e-00.pdf>

INNOVATIVE SODIUM FAST REACTORS CONTROL ROD DESIGNS (H. GUO ET AL)

Hui Guo, Laurent Buiron

CEA, DEN, Cadarache, France

I. Introduction

To guide the next generation fast reactor design, GIF defined global objectives in terms of safety improvement, sustainability, economy, non-proliferation and physical-protection [1]. Sodium Fast Reactor (SFR) is studied as potential industrial G-IV reactors in France. Many efforts in CEA have been made to achieve these challenging technological criteria [2]–[5].

Next generation self-breeder sodium fast reactors exhibit relatively low reactivity swing compared to past concepts, with the consequence that the core control rods have to be adapted to fulfil both reactivity control requirements, power map distribution and safety requirements [5]–[8]. The optimal design of such control systems is a complex and challenging task, as it involves a large set of target criteria and constraints to be simultaneously met, including boron depletion with irradiation, power peak localisation and maximum linear heat rate estimation, core shutdown margin, etc.

The most widely employed technique to control the core's reactivity in fast reactors is by inserting or removing absorber materials [9]. Boron, present in the form of boron carbide, B_4C , is the most generally used absorber in SFR because its relatively high neutron absorption cross-sections. The ceramic B_4C is available with relative low price with comparative ease of fabrication. Its simple reaction chain also raises the degradation of its reactivity worth especially for B_4C with low ^{10}B enrichment.

Currently, the absorber materials are enclosed in absorber pins and then packaged in movable cluster in controls rods sub-assembly. Although many improvements are achieved for design of control rods with B_4C as absorber, its residence

is still limited by effects of irradiation on B_4C : helium generation, decrease of thermal conductivity and pellet swelling. The burn-up of ^{10}B at 210×10^{20} at./ cm^3 generate 777 cm^3 of helium at standard pressure and hence its loading on the control clad would be important if the closed pin design is used. This could be solved by providing sufficient plenum volume or by using venting pin design. The venting pin design increases the thermal transfer but at same time diffusion of carbon to the steel structure i.e. pin clad. The melting temperature is higher than 2350°C but its chemical reaction with steel starts from 1000°C and becomes not acceptable beyond 1200°C [10]. The thermal conductivity decreases with increase of temperature (after a pic at about 100°C), ^{10}B enrichment and also the depth of irradiation. Under the irradiation, the thermal conductivity decreases and hence the thermal conductivity which will reduce its margin to melting temperature[11]. The irradiation also raises swelling of ceramic pellet which will finally trigger the Absorber-Clad Contact (ACC) which is the principal effect limiting the residence time of control rods in the core. In order to retard the swelling, the pellet with B_4C is enwrapped in steel shroud. And hence the maximal burn-up of ^{10}B is increased from 150×10^{20} at./ cm^3 (without shroud) to 210×10^{20} at./ cm^3 according to experiences from PHENIX and SUPER-PHENIX reactors.

After a preliminary study, there are several innovative designs directions to improve performance of control rods such as optimised pins size, alternative absorber materials, and application of moderators. These designs possess potentials to improve its neutronic characteristics safety margin, economical performance while its complete analysis requires notably more accurate calculation of

efficiency and evolution of isotopes' concentrations under irradiation. At same time, a determinist transport code called APOLLO3 is under development at CEA and it will replace ERANOS code[12] for fast reactors analysis. Unstructured adaptive mesh SN solvers (MINARET)[13], as well as 2D and 3D Method of Characteristic's (MOC) are already implemented in APOLLO3[14]. An important effort is invested to develop and validate schemes in APOLLO3. This recent neutronic transport code improves the simulation of control rods sub-assemblies in G-IV fast reactors and also for some challengeable design works.

II. Innovative Design Directions

According to previous study based on typical GIV-SFR, the margin to melting would limit largely the residence time of current control rods designs if high ^{10}B enrichment B_4C is used[15]. Hence, smaller pin size control rods are proposed to increase the margin to melting after irradiation by means of liner heat rating reduction. However, these works are based on ERANOS codes and more detailed and accurate study is needed.

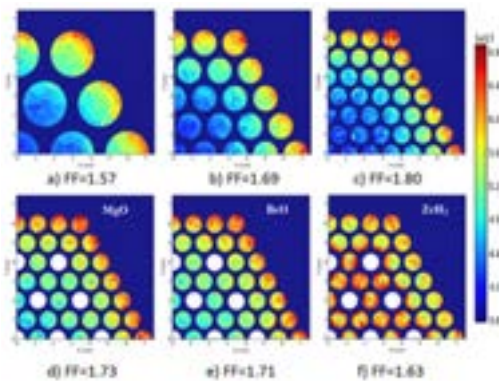
Different designs of control rods with B_4C are investigated under irradiation of typical G-IV SFR spectrum with Monte-Carlo (MC) TRIPOLI-4 code[16]. Fig 1 shows their distribution of ^{10}B absorption reaction rate and Form Factor (FF) is the ratio between maximal absorption rate and average absorption rate. Fig 1.a is the current control rods design where the reaction rate decreases largely from the absorber in the outer region to the inner region. Fig 1.b and Fig 1.c keep the same absorber volume as Fig 1.a but increase the number of pins. As show from Fig 1.a to Fig 1.c, the gradient of absorption becomes more important with decrease of pins' radius that may induce depletion pic in certain region and hence decrease its safety margin or limit its residence time.

As the absorption ability of these materials decreases with neutron energy, utilisation of moderator seems to be a good option to increase their reactivity worth or optimise reaction distribution. Several moderator materials are considered in this works. ZrH_2 is a good moderator because it contains two light hydrogen nuclei. Nevertheless, the dissociation temperature of ZrH_2 is very close the operation temperature of core[17]. In the future, the suitable stoichiometry of hydrogen should be considered and other hydrides with higher desorption temperature may be also studied.

The reason to give the preference to oxide, such as BeO and MgO , is their high fusion temperature.

Small pin designs also offer the flexibility to introduce moderator. As shown the white regions in Fig 1.d-f, certain B_4C pins in Fig 1.c are replaced by pins with moderator material. With less investment of absorber material, the use of moderator increases slightly the reactivity worth of control rods with higher average absorption rate. Furthermore, absorption distribution of ^{10}B become more homogenise with use of moderator. However, evaluation of these designs in the core is required.

Figure 1. ^{10}B Absorption Reaction Rate Distribution



One main function of control rods is to compensate reactivity loss during operating cycle. This requires important reactivity worth of control rods with only a small part inserted which limits the selection of absorber materials. G-IV industrial size SFR designs leads to reduce the reactivity loss to minimise inadvertent Control Rod Withdrawal (CRW) effects. At same time, this improvement enables the use of some other absorbers with less absorption ability but with advantage in other aspects. Hafnium, Gadolinium, Europium absorb neutron by (n, γ) reaction that generates less heat by comparing with B_4C and without any gas release. Furthermore, some materials such as metallic Hf and HfB_2 have better heat transfer ability and hence lower temperature in the centre of absorber[18]. These properties give the intuitive safety characteristics to control rods. In addition, their long depletion reaction chains would reduce its disappearance kinetic and hence increase their residence time. In this work, we validate their neutronic simulation method firstly and then investigate their

candidate forms: Gd_2O_3 , Eu_2O_3 , Dy_2TiO_5 , Hf, $HfH_{1.62}$ and HfB_2 .

III. Methodology

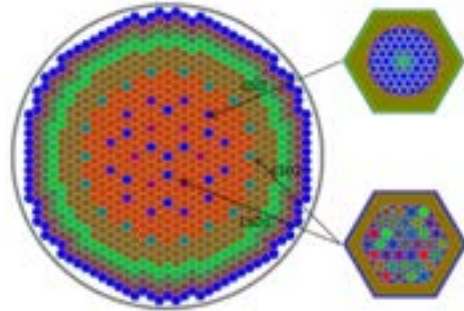
Accurate and high performance neutronic simulation is the key for the evaluation of these innovative designs of reactivity control system. The complex geometries of control rods should be treated in details because control rods are the most sub-critical structures in the core and hence with important flux gradient. The complex chains for different isotope should also be considered for their depletion calculation. After careful weighting of advantages and disadvantages of different tools, APOLLO3 is chosen for the neutronic simulation of these reactivity control systems design works.

The calculation scheme in this deterministic code includes two steps from lattice calculation to core calculation. The MOC based lattice calculation is able to simulate complex geometries with exact description thereby compute self-shielding effects in this step. The tabulated cross-section scheme improves significantly the accuracy of depletion calculation because it is able to transfer the variation on self-shielding from lattice step to core step, which is important for the absorber materials. Different from homogenous description of all structures in traditional deterministic codes, a heterogeneous description of control rods is proposed because MINARET is able to treat unstructured geometry. Such heterogeneous description improves further the accuracy but it needs more calculation time. Our development and validation works prove APOLLO3 has high level confidence to be used for innovative control rod designs[19].

By comparing with EFR and SUPER-PHENIX core types, SFR-V2B (3600 MWth) was the result of optimisation process especially toward reduced reactivity loss and sodium void effect. This concept is based on a bundle of tightly packed and large-diameter fuel pins designed to increase the fuel fraction in the core while reducing the sodium fraction[5], [20]. A reduction in the core volume power density was found to be the best solution for meeting the requested design parameters that imply a reduction of the sodium volume fraction together with an increase of the fuel volume fraction. SFR-V2B is a representative GIV SFR core and hence is chosen in this works. As shown in Fig 2, SFR-V2B has 267 inner core S/A and 186 outer core S/A. After one cycle

irradiation, 410 EFPD, about 1/5th fuel are recycled. The reactivity loss of SFR-V2B is about 450 pcm per equilibrium cycle.

Figure 2. Layout of SFR-V2B core and its original control rods designs

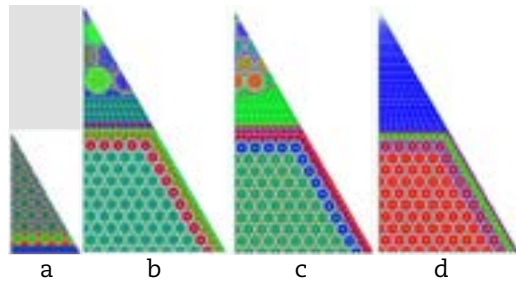


SFR-V2B has two independent control rods systems. The first system is designed for the operation of reactor (power management, burn-up compensation...) and also for shutdowns needs. This system is named CSD (Control Shutdown System) in SFR-V2B projects. This system include 24 control rods sub-assemblies: the first part CSD1 has 6 sub-assemblies which locate in the inner core and the second part CSD2 has 18 sub-assemblies that locate in the interface between inner and outer core. The second system is dedicated to the emergency shutdown. This system is named DSD (Diverse Shutdown System) which include 12 sub-assemblies. CSD and DSD are redundant, independent, and diverse in order to ensure a safe shutdown of a reactor at any time needed.

At Beginning of Equilibrium Cycle (BOEC), the core is set at critical state where CSD1 and DSD are kept at the top of fissile zone while CSD2 inserted about 25 cm into fissile zone. After one cycle irradiation, CSD is also completely withdrawn to compensate core's reactivity loss. The reactivity worth of CSD2 critical insertion is hence its ability to compensate reactivity loss. The reactivity worth of all control rods insertion at bottom of fissile zone is used to bring core from full power state to isothermal shutdown that includes: Doppler Effect (~1000 pcm); management of fuel handling errors (~2000 pcm); reactivity loss (~450 pcm); integration of uncertainty level (~750 pcm). That means the anti-reactivity of all control rods insertion should be higher than 4200 pcm. The original designs of CSD and DSD S/A are also shown in Fig 2. CSD was based B_4C and DSD use 90% ^{10}B enrichment B_4C . The geometries for sub-assembly calculation of SFR-V2B using

APOLLO3 are shown in Fig 3. The sub-assembly is normalised 50 W/g(HN) in fuel region with total irradiation time 3000 EFPD.

Figure 3. Geometries for SFR-V2B sub-assembly calculation a) 1/12th of Fuel sub-assembly. b) 1/12th CSD-Fuel cluster. c) 1/12th DSD-Fuel cluster. d) 1/12th Reflector-Fuel cluster.



In the core level calculation, two methods indicated previously, i.e. CR-HOMO and CR-HETE, are compared. These control rods are used for 5 cycles with total irradiation time 2050 EFPD. The efficiency in Table 1 is the reactivity worth of 25 cm insertion of CSD2 at BOEC. In this work, the Beginning of Life (BOL) for these control rods is 0 EFPD where all rods use new materials and the End of Life (EOL) is 2050 EFPD.

As shown in Table 1, for both original designs with natural B₄C and materials with absorption resonance and moderators, CR-HOMO scheme shows high coherence with CR-HETE scheme not only on the efficacy but also on its variation. Note that CR-HETE requires 6 times computation time as CR-HOMO. In following works, CR-HOMO is used and in the future the ideal candidate designs will be recomputed with CR-HETE scheme.

Table 1. Benchmark between CR-HETE and CR-HOMO

EFPD	Natural B ₄ C		HfH _{1,62}	
	HOMO	HETE	HOMO	HETE
0	509	510	672	665
410	491	493	659	652
820	483	484	659	651
1230	463	464	651	643
1640	445	447	646	647
2050	430	432	642	636

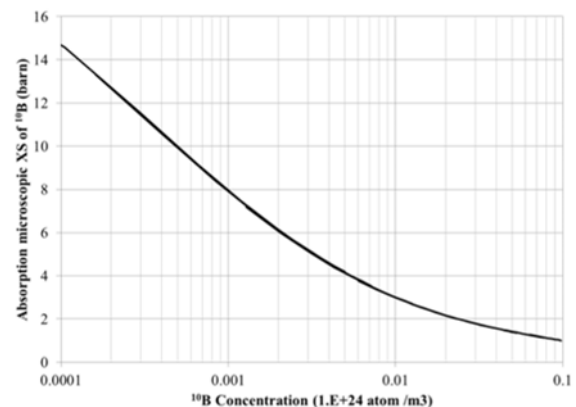
IV. Results and Discussions

IV.A. Different ¹⁰B enrichment

In this section, the absorber in Fig 3.b is replaced by different enrichment ¹⁰B to compute their effective microscopic cross-section using APOLLO3-TDT solver.

Fig 4 shows the variation of one-group effective microscopic absorption cross-section of ¹⁰B with concentration. The microscopic cross-section decreases with increase of ¹⁰B concentration because of the increase of spatial self-shielding effect. For new absorber, the concentration of ¹⁰B in 90% ¹⁰B enrichment B₄C is about 4.5 times of that in natural B₄C while its micro-cross-section is about 50% of that in natural B₄C.

Figure 4. Variation of ¹⁰B effective microscopic cross-section with ¹⁰B concentration

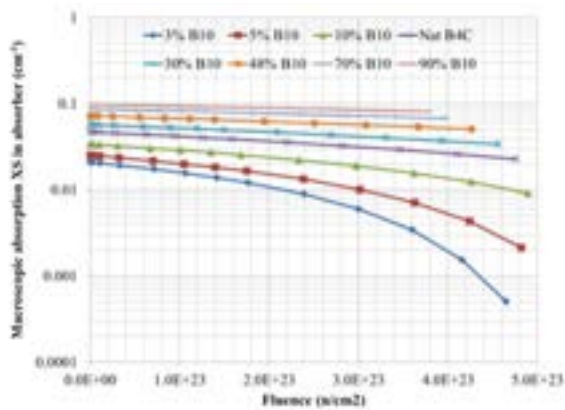


As shown in Fig 5, the absorption ability of 90% ¹⁰B enrichment B₄C increases only about 125% by comparing with natural B₄C. The absorption ability of ¹⁰B decreases under irradiation. For high ¹⁰B enrichment B₄C, its initial spatial self-shielding effect is important but it is reduced with depletion of materials that slows down the degradation of control rods' efficiency. The loss of efficiency in lower ¹⁰B enrichment B₄C is more important and hence it should be computed in details.

The burnable poisons (BP), independent to control rods system, are designed to compensate core's reactivity loss by its depletion, and hence decrease the insertion depth of control rods. The application of BP would reduce the surplus reactivity from CRs in CRW accidents or bring new degree of freedom

in core designs such as increase of cycle length. Furthermore, the efficiency requirement and the movement of control rods during operation would be reduced. BP requires absorbers with enough anti-reactivity at beginning but high depletion kinetic and small residual anti-reactivity at the end. As shown in Fig 4, the lower enriched B_4C has much higher microscopic cross-section. Although their initial macroscopic cross-section is small, their variation is close to natural and high ^{10}B enrichment B_4C . From this point of view, lower enriched B_4C is more suitable for BP purpose.

Figure 5. Variation of ^{10}B macroscopic cross-sections with fluency accumulated in absorber



IV.B. Different materials

In this section, B_4C in the original CSD design is replaced by different absorber materials. These different designs are calculated firstly by APOLLO3 TDT solver in cluster with fuel at lattice level and then APOLLO3 MINARET solver in SFR-V2B core.

In this work, complete chains of these isotopes are used. For instance, Lu, Hf, Ta and W are considered in the evolution of Hafnium. Fig 6 and Fig 7 show variation of concentration and macroscopic cross-sections in absorber with fluency accumulated according to sub-assembly calculation. The absorptions for hafnium are principally caused by (n, gamma) which generates higher order hafnium. The Hf181 is also generated in this chain while its half-life is only about 42 days and hence transform to Ta181 by beta- decay. As shown in Fig 6 and Fig 7, the total concentration of these isotopes is constant which proves the conservation of materials. The most important decrease in concentration and in absorption

ability is raised from disappearance of Hf177. The absorption cross-sections of Hf180 are much less important while its proportion is about 35% in the natural hafnium. Although the concentration of Ta and W generated from (n, gamma) and beta- reactions are not significant, their absorption ability becomes non negligible.

Figure 6. Variation of absorber compositions with fluency

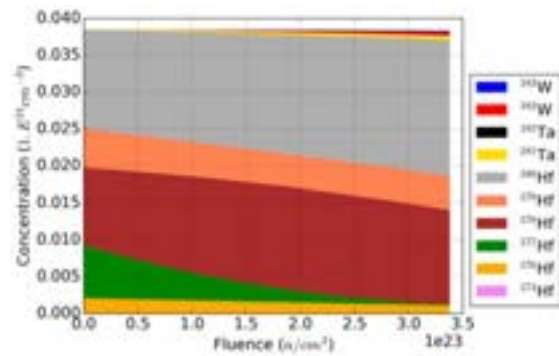
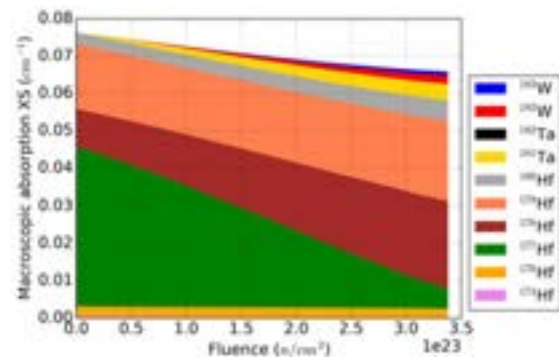


Figure 7. Variation of macroscopic cross-sections with fluency accumulated in absorber



In the core calculation, the natural B_4C in all CSD is replaced by alternative materials. The efficiency of all control rods insertion and solely CSD2 25 cm insertion are presented in Table 2. Among these materials, HfH_{1.62} has highest efficiency and least reactivity loss. The efficiencies of Eu_2O_3 and HfB_2 are close to natural B_4C with a slight slower degradation Kinetic.

However, the efficiency of metallic Hf, Gd_2O_3 or Dy_2TiO_5 is not comparable with natural B_4C . Although these rare earth elements have longer depletion chain than B_4C , their improvement on reducing loss of reactivity worth is not

significant as hafnium. The evolution of isotopes relieves more importantly spatial self-shielding effect in B_4C and $HfH_{1.62}$ because the outer region depleted firstly and then behaves as ‘moderator’ to slow down the neutrons that might improve the absorption ability in the inner region.

All rods insertion should be able to shut down reactors at any moment. The results in Table 2, is calculated only at BOEC. According to our calculation, with evolution of core, the power distribution shift from outer core to inner core and hence the efficiency of all control rods insertion at EOEC is more important than that BOEC. The reactivity loss of this efficiency is less significant because it comes from both CSD and DSD. However, some designs still not satisfy the requirement. Hence, we propose axially mixed control rods where the insertion part is replace by material with high residence to depletion and other part by material with high absorption ability. Several control rods S/A designs already adapt control rods with two axial regions with different ^{10}B enrichment B_4C . However, the axial connection with different materials should be investigated firstly and then detailed evolution of designs.

Table 2. Efficiency of different materials

	Reactivity worth of CSD2 25 cm insertion			Reactivity worth of all control rods insertion		
	BOL	EOL	Loss	BOL	EOL	Loss
Nat. B_4C	510	432	-15%	6396	6030	-6%
$HfH_{1.62}$	672	642	-4%	7955	7691	-3%
Eu_2O_3	457	403	-12%	5880	5565	-5%
Nat. HfB_2	442	381	-14%	5780	5449	-6%
Hf	252	235	-7%	4141	3984	-4%
Gd_2O_3	248	217	-12%	4136	3924	-5%
Dy_2TiO_5	210	186	-12%	3815	3636	-5%

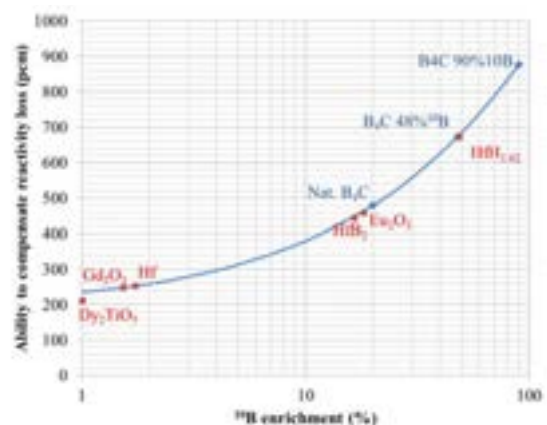
The ability to compensate reactivity loss of different materials is shown in Fig 8. This figure depend not only the characteristics of these absorbers but also the ‘architecture’ of control rods such as the number of control rods S/A, their position in the core, the insertion depth and so on. However, if the neutron spectrum is similar, the relative relation between different material and different ^{10}B enrichment would be still valuable. This figure is based on SFR-V2B core calculation but the lattice calculation in also able to get similar results because the reactivity worth of control rods in core is

proportional to the macroscopic cross-section calculated with Fig 3.b.

If core has low reactivity loss, natural B_4C even ‘depleted’ B_4C is able to compensate reactivity loss. Other alternative material are suitable but their economic performance should be evaluated because rare earth elements are more expensive than natural B_4C .

High reactivity loss core requires enriched B_4C . Reactivity worth of B_4C does increase slowly with ^{10}B enrichment. Furthermore, margin to melting will limit the residence time of enriched B_4C because its power density is proportional to ^{10}B enrichment. One solution is to use small pin design to improve heat transfer and moderators to homogenise absorption distribution, which will be presented in the next section. Another solution would be to replace B_4C with other material such as HfB_2 . The thermal conductivity of HfB_2 is much more significant than B_4C . The efficiency of natural HfB_2 is slight smaller than natural B_4C but their efficiencies would become closer with increase of ^{10}B enrichment. The third solution may be radially mixed designs where only certain B_4C pins replaced by alternative materials with higher margin to melting. The designs and evaluation of radially mixed control rods is in progress.

Figure 8. Ability to compensate cycle reactivity loss of different materials



IV.C. Moderator

As shown in Fig 9, the number of absorber pins is increased from original designs 37 pins to 127 pins with same volume of absorber and structure. Furthermore, moderator pins replace 19 small absorber pins and hence it saves about 15% investment of absorber.

Figure 9. Control rods with small pin size (left) and control rods with moderator pins (right)



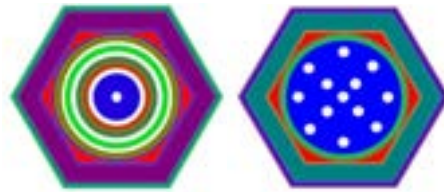
This design is charged with different absorber and moderator and is calculated in the same algorithm as previous designs. As shown in Table 3, the switch from big pin size to small pin size increase slightly the efficiency of control rods. ZrH₂ increases all absorber's absorption ability especially for metallic Hf. However, the use of moderator increases also the reactivity loss of control rods because of their higher average absorption rate. HfH_{1.62} has equivalent efficiency as 50% ¹⁰B enriched B₄C and very small reactivity loss but its melting temperature is close to SFR operation temperature. The direct mix of Hf and H is more effective than the introduction of independent moderator pins. However, as a metal, it has more flexibility on the geometries and introduction of moderators. As shown in Fig 10, several innovative geometries of control rods are proposed and would be evaluated in near future.

The BeO increase the average absorption rate in absorber but it is not able to increase the total absorption in control rods S/A because it also replaces a part of absorber. However, it is also able to homogenise the distribution of absorption with adequate positioning. In the future, the influence of moderator on the temperature distribution in the control rods under irradiation should be computed especially for high ¹⁰B enrichment B₄C.

Table 3. Efficiency of different designs with small pin size and moderator

Absorber	Moderator	BOL	EOL	Loss
Natural B ₄ C	Non	518	439	-15%
	BeO	497	408	-18%
	ZrH ₂	549	459	-16%
Hf	BeO	253	233	-8%
	ZrH ₂	344	321	-7%
Nat. HfB ₂	ZrH ₂	493	415	-16%

Figure 10. Innovative geometries for control rods with metallic Hf



V. Conclusion

Current control rods designs use B₄C as absorber but with multi limitations regarding for its safety margin, residence time and economic performance. Several innovative designs are proposed. Base on the validated APOLLO3 calculation schemes and Monte-Carlo codes, these designs are evaluated in our work.

The spatial self-shielding effect limits the absorption ability of high ¹⁰B enrichment B₄C but also slowdowns its degradation. With high-level capture cross-section, lower enriched B₄C is the most suitable materials for burnable neutrons poisons in SFR. Thanks to moderator, Eu₂O₃ and HfB₂ have improvement safety characteristics and equivalent efficiency to natural B₄C that would replace the B₄C in low reactivity loss cores. HfH_{1.62} has equivalent efficiency as 50% ¹⁰B enriched B₄C and low reactivity loss. Moderator may save investment of expansive absorber and even improve reactivity worth. It homogenises reaction distribution and hence reduces the absorption peak.

Several design directions are also proposed in this paper such as burnable neutrons poisons using lower enriched B₄C, radially or axially mixed control rods to improve local characteristics and innovative pins design for Hf. In the future, these designs will be studied in depth combining with more moderator designs and thermodynamic calculation.

Acknowledgements

The authors would like to thank the APOLLO3 development team for their efforts in developing the code. APOLLO3 R is a registered trademark of CEA. We gratefully acknowledge AREVA and EDF for their long term partnership and their support

Nomenclature

GIF	Generation IV International Forum
MOC	Method of Characteristics

References

- [1] I. L. Pioro, "2 - Introduction: Generation IV International Forum," in *Handbook of Generation IV Nuclear Reactors*, Woodhead Publishing, 2016, pp. 37–54.
- [2] F. V.-P. MARSAULT-Marie-Sophie, C.-B. B. CONTI, P. S.-C. V. FONTAINE, N. D.-L. MARTIN, and A.-C. S. VERRIER, "Pre-conceptual design study of ASTRID core," presented at the ICAPP12, Chicago, USA, 2012.
- [3] M. Chenaud et al., "Status of the ASTRID core at the end of the pre-conceptual design phase 1," *Nucl. Eng. Technol.*, vol. 45, no. 6, pp. 721–730, Nov. 2013.
- [4] P. Sciora et al., "Low void effect core design applied on 2400 MWth SFR reactor," in *Proceedings of ICAPP, 2011*, pp. 2–5.
- [5] B. Fontaine, N. Devictor, P. Le Coz, A. Zaetta, D. Verwaerde, and J.-M. Hamy, "The French R&D on SFR core design and ASTRID Project," presented at the *Proceedings of GLOBAL 2011*, Makuhari, JAPAN, 2011.
- [6] B. Fontaine, V. Marc, P. Sciora, and C. Venard, "ASTRID: an innovative control rod system to manage reactivity," presented at the ICAPP 2016, San Francisco, California, USA, 2016.
- [7] D. Blanchet and B. Fontaine, "Control Rod Depletion in Sodium-Cooled Fast Reactor: Models and Impact on Reactivity Control," *Nucl. Sci. Eng.*, vol. 177, no. 3, pp. 260–274, Jul. 2014.
- [8] L. Dujčiková and L. Buiron, "Development and analysis of SFR control rod design," *Int. J. Phys. Math. Sci.*, vol. 2, 2015.
- [9] A. E. Waltar, D. R. Todd, and P. V. Tsvetkov, Eds., *Fast Spectrum Reactors*. Boston, MA: Springer US, 2012.
- [10] R. Sasaki, S. Ueda, S.-J. Kim, X. Gao, and S. Kitamura, "Reaction behavior between B4C, 304 grade of stainless steel and Zircaloy at 1473 K," *J. Nucl. Mater.*, vol. 477, pp. 205–214, Aug. 2016.
- [11] M. Akiyoshi, T. Yano, Y. Tachi, and H. Nakano, "Saturation in degradation of thermal diffusivity of neutron-irradiated ceramics at $3 \times 10^{26} \text{n/m}^2$," *J. Nucl. Mater.*, vol. 367–370, pp. 1023–1027, Aug. 2007.
- [12] Gérald Rimpault, Danièle Plisson, Robert Jacqmin, Jean Tommasi, and Robert Jacqmin, "THE ERANOS CODE AND DATA SYSTEM FOR FAST REACTOR NEUTRONIC ANALYSES," presented at the *PHYSOR 2002*, Seoul, Korea, 2002.
- [13] J. Y. Moller, J. J. Lautard, and D. Schneider, "Minaret, a deterministic neutron transport solver for nuclear core calculations," presented at the *M&C 2011*, Rio de Janeiro, RJ, Brazil, 2011.
- [14] D. Sciannandrone, S. Santandrea, and R. Sanchez, "Optimized tracking strategies for step MOC calculations in extruded 3D axial geometries," *Ann. Nucl. Energy*, vol. 87, pp. 49–60, Jan. 2016.
- [15] L. Buiron and L. Dujčiková, "Low Void Effect (CFV) Core Concept Flexibility from Self-breeder to Burner Core," presented at the *Proceedings of ICAPP 2015*, Nice, FRANCE, 2015.
- [16] E. Brun et al., "TRIPOLI-4@, CEA, EDF and AREVA reference Monte Carlo code," *Ann. Nucl. Energy*, vol. 82, pp. 151–160, Aug. 2015.
- [17] M. Ma, W. Xiang, B. Tang, L. Liang, L. Wang, and X. Tan, "Non-isothermal and isothermal hydrogen desorption Kinetics of zirconium hydride," *J. Nucl. Mater.*, vol. 467, pp. 349–356, Dec. 2015.
- [18] M. M. Opeka, I. G. Talmy, E. J. Wuchina, J. A. Zaykoski, and S. J. Causey, "Mechanical, Thermal, and Oxidation Properties of Refractory Hafnium and zirconium Compounds," *J. Eur. Ceram. Soc.*, vol. 19, no. 13, pp. 2405–2414, Oct. 1999.
- [19] H. Guo, G. Martin, and L. Buiron, "Improvement of sodium fast reactor control rods calculations with APOLLO3," presented at the *ICAPP 2018*, Charlotte, North Carolina, USA, 2018.
- [20] G. Mignot et al., "Studies on french SFR advanced core designs," presented at the *ICAPP, Anaheim, CA, USA, 2008*.

TRACK 8: INTEGRATION OF GEN IV REACTORS IN LOW CARBON ENERGY SYSTEM

OPTIMAL ENERGY STORAGE SYSTEM FOR THE AHTR TECHNOLOGY (O. P. RAKERENG ET AL)

Okaeng P. Rakereng and Mmeli Fipaza

Eskom, South Africa

I. Introduction

Eskom, a South African electric utility company is exploring the feasibility of the re-launch of the Pebble Bed Modular Reactor (PBMR) programme in the form of an Advanced High Temperature Reactor (AHTR). The configuration entails single shaft helium driven gas turbo-generator machine with the energy storage system, and a steam cycle in the bottoming cycle with dry cooling tower. The AHTR reactor is intended to operate at constant thermal power (MWth), and the Brayton cycle will operate at base load power while the bottoming Rankine cycle with the energy storage system will be used for load following.

Operating at base load power at times does not meet grid power demand during peak times. Energy storage is one of the possible way to overcome the over demand of power during peak times.

The use of nuclear energy for cogeneration provides many economic, environmental and efficiency-related benefits [1]. The proposed AHTR cogeneration system is an energy storage which can be used for different applications, however in the Eskom plant will be used for load following during peak times of electricity demand.

Energy Storage is preferred over reactor load following (power variations based on grid demand) because NPPs are conventionally used as base load sources of electricity, and their technology has high fixed cost and low variable cost [2]. The other main issue with NPP load following is the reduction of the load factor since nuclear fuel represent a small fraction in

the generation of electricity compared to fossil fuels [3]. This makes operating at higher load factors favourable for NPPs since they are not making a saving on fuel cost when they not producing electricity.

Molten Salt energy storage system was the initial choice because of the operating experience Eskom has in the Concentrated Solar Power (CSP) plant with the same energy storage. The pre-feasibility of the programme however, realised there is a variety of energy storage techniques that could be applicable to the proposed gas cooled reactor.

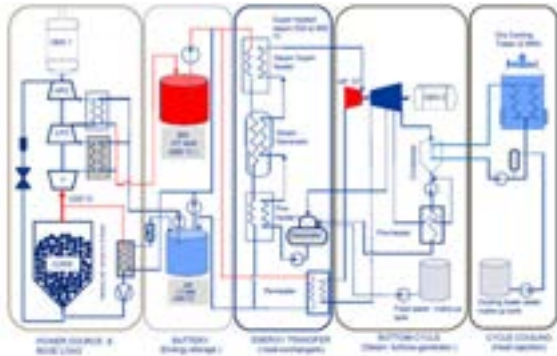
This paper is an effort to evaluate and determine the optimal energy storage system technique and/or medium for the developing AHTR programme or rather confirm if the molten salt is the best choice. The most optimal energy storage system is determined by employing a Multi Criteria Decision Making (MCDM) tool. MCDM is a valuable tool that can be applied to many complex decisions. It is most applicable to solving problems that are characterised as a choice among alternatives [4].

II. System Overview

The proposed AHTR plant has five systems as shown in Figure 1. System 1 is the Power Source (Brayton cycle) and consist of the reactor, turbine and the generator. System 2 is the Energy Storage which is used to absorb the rejected heat from the Brayton cycle. The energy absorbed/stored will be used by system 3 (Energy Transfer) to produce steam for System 4 (Bottom/Rankine Cycle) to produce electricity during peak times. System 5 (Cycle Cooling) is

used to absorb and dissipate the rejected heat from system 4 (Bottom Cycle).

Figure 1. Proposed AHTR Plant Design [5]



and High Temperature (HT) –TES are all developed EES technologies. These developed EES systems are commercially available; however, the actual applications, especially for large-scale utilities, are still not widespread.

Figure 2. Energy storage classification with respect to function [6].



III. Energy Storage Technologies

This section summarise alternatives of energy storage technologies considered for the AHTR. The Electrical Energy Storage (EES) technologies considered for the AHTR are listed in Table 1. Some of these technologies are currently available and some are still under development.

The various EESs can be categorised into two criteria: function and form. In terms of function, EES technologies can be categorised into those that are intended for high power ratings with a relatively small energy content making them suitable for power quality or Uninterrupted Power Supply (UPS); and those designed for energy management [6], as shown in Figure 2.

IV. Assessment and Comparison of the EES Technologies

This section summarises the literature of the assessment and comparison of the EES technologies from Chen et al [6] work.

Technical maturity

The technical maturity of the EES systems is shown in Figure 3. The EES technologies can be divided into three technical maturity groups; mature, developed and developing. The matured EES technologies are PHS and Lead-Acid battery. PHS was first used in the 1890's [7] and the Lead acid battery was invented in 1860 [8].

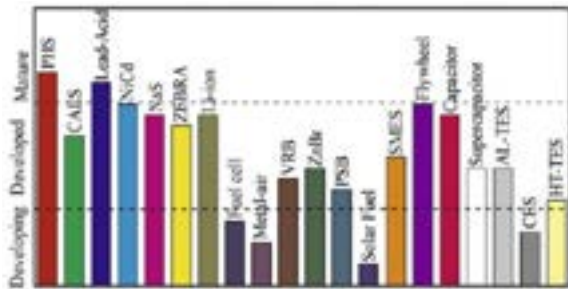
CAES; NiCd battery; NaS battery; ZEBRA battery; Li-ion battery; Flow Batteries; SMES; Flywheel; Capacitor; Supercapacitor; Aquiferous Low temperature (AL)-Thermal Energy Storage (TES)

Table 1. Forms of Electrical Storage Technologies.

Electrical energy storage	Electrostatic energy storage	Capacitors and Supercapacitors
	Magnetic/Current energy storage	Superconducting Magnetic Energy Storage system (SMES)
Mechanical energy storage	Kinetic energy storage	Flywheels
	Potential energy storage	Pumped Hydroelectric Storage (PHS) Compressed Air Energy Storage (CAES)
Thermal energy storage (TES)	Aquifers Low Temperature Energy Storage (AL-TES)	Aquiferous cold energy storage, Cryogenic Energy Storage (CES)
	High temperature energy storage (HT-TES)	Sensible heat systems (steam or hot water accumulators, graphite, molten salt, hot rocks and concrete)
		Latent heat systems (phase change materials)
Chemical energy storage	Electrochemical energy storage	Conventional batteries such as Lead-Acid, Nickel Metal Hydride, Lithium Ion and Flow-Cell batteries such as Zinc Bromine and Vanadium Redox)
	Chemical energy storage	Fuel cells, Molten-Carbonate Fuel cells (MCFCs) and Metal-Air batteries
	Thermochemical energy storage	Solar Hydrogen, Solar metal, Solar Ammonia Dissociation-Recombination and Solar Methane Dissociation-Recombination)

The developing technologies are Fuel Cells; Meta-Air battery; Solar Fuels; and CES. They are not commercially mature although technically possible and have been investigated by various institutions.

Figure 3. Technical maturity of the ESS technology [6]



Power rating and discharge time

The power ratings of various EES are shown in Table 4. PHS, CAES and CES are applicable for applications in scales above 100 MW with hourly to daily output durations. They can be used for energy management of large-scale generations such as load following.

Large-scale batteries, Flow batteries, Fuel Cells, Solar Fuels, CES and TES are suitable for medium-scale energy management with a capacity of 10–100 MW.

Flywheels, Batteries, SMES, Capacitor and Supercapacitor have a fast response (~milliseconds) and therefore can be utilised for power quality such as the instantaneous voltage drop and short duration UPS. The typical power rating for this kind of application is lower than 1 MW.

Flow batteries, Fuel Cells and Metal-Air Cells not only have a relatively fast response (≤ 1 s) but also have relatively long discharge time (hours), therefore they are more suitable for bridging power. The typical power rating for these types of applications is about 100 kW – 10 MW.

Energy density

Energy density (Wh/kg) is the amount of energy stored in a given system or region of space per unit volume

As shown in Table 4, the Fuel Cells, Metal-Air battery, and Solar Fuels have an extremely high energy density (~1000 Wh/kg).

Batteries, TESs, CES and CAES have medium energy density.

The energy density of PHS, SMES, Capacitor/Supercapacitor and Flywheel are among the lowest below ~30 Wh/kg.

Capital cost

Capital cost is one of the most important factors for the industrial take-up of the EES. All the costs per unit energy shown in Table 4 have been divided by the storage efficiency to obtain the cost per output (useful) energy.

CAES, Metal-Air battery, PHS, TESs and CES are in the low range in terms of the capital cost per kWh.

It is highly possible that the capital cost of energy storage systems can differ from the approximations presented here. Factors such as breakthroughs in technologies, time of construction, location of plants, and size of the system can affect the capital cost. The capital cost estimations presented should only be viewed as being preliminary.

Storage duration

Table 4 also indicates the self-discharge (energy dissipation) per day for the EES systems. It is evident that PHS, CAES, Fuel Cells, Metal-Air Cells, Solar Fuels and Flow batteries have a small self-discharge ratio so are suitable for a long storage period.

Lead-Acid, NiCd, Li-ion, TESs and CES have a medium self-discharge ratio and are suitable for a storage period not longer than tens of days.

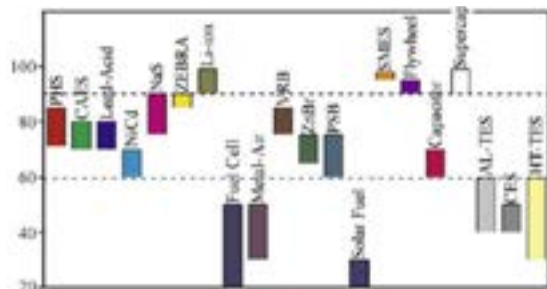
NaS, ZEBRA, SMES, Capacitor and Supercapacitor have a very high self-charge ratio of 10–40% per day. Flywheels will discharge 100% of the stored energy if the storage period is longer than about 1 day.

Cycle efficiency

The cycle efficiency of the EES systems during one charge discharge cycle is illustrated in Figure 4. The cycle efficiency is the “round-trip” efficiency defined as E_{out}/E_{in} , with E_{out} and E_{in} being the electricity input and output respectively. It is evident from Figure 4 the EES systems can be divided into three groups:

- Very high efficiency:
 - SMES, Flywheel, Supercapacitor and Li-ion battery have very high cycle efficiency of greater than 90%.
- High efficiency:
 - PHS, CAES, batteries (except for Li-ion), Flow batteries and conventional Capacitor have a cycle efficiency of 60 – 90%.
- Low efficiency:
 - Solar Fuel, TESs and CES have efficiency lower than 60%.

Figure 4: Cycle Efficiency of the EES Systems [6]



Influence on the environment

The influence of the EES on the environment is also specified in Table 4. Solar Fuel and CES have positive influences on the environment. PHS, CAES, Batteries, Flow Batteries, Fuel Cells and SMES have negative influences on the environment. Other EESs have relatively small influences on the environment as they do not involve fossil combustion, landscape damage and toxic remains.

V. EES Technologies Applicable for AHTR

The approximate desired storage duration and energy capacity of the proposed AHTR EES system is approximately 6 hours and 85 MW respectively [5]. The energy storage is intended for load following (energy management) as stated before. Capacitor, Supercapacitor, Flywheel and SMES as shown in Figure 2 are not applicable for load following or energy management and thus are not considered for the AHTR.

Fuel Cell, CES and Solar Fuels are still in the developing stages and will not be considered for the AHTR system.

The EES technologies applicable or considered for the AHTR system are then reduced to the following list:

- PHS
- CAES
- Large scale Battery (Lead-Acid, NiCd and Nas)
- Flow Batteries (VRB, ZnBr and PSB)
- TES (AL – TES and HT – TES)

VI. Ranking Method

A Multi Criteria Decision Making (MCDM) tool employed to rank the AHTR applicable EES

technologies is called 1000 minds. The MCDM assess the trade-offs between multiple criteria in order to rank, prioritise or choose from various EES.

1000 minds is an online suite of tools and processes that helps individuals or groups with their Decision-Making [9] and can be accessed on the site <https://www.1000minds.com>.

1000 minds involve four key components:

- Alternatives to be prioritised or ranked.
- Criteria by which the alternatives are evaluated and compared.
- Weights representing the relative importance of the criteria.
- Decision-makers and other stakeholders, whose preferences are to be represented.

1000 minds determine the relative importance (weights) of each criterion by using the PAPRIKA method [9]. The PAPRIKA method involves the decision-maker answering a series of simple questions, based on the expert knowledge and subjective judgment of the decision maker. Each question is based on choosing between two hypothetical alternatives defined on just two criteria or attributes at a time and involving a trade-off. The weights of the criteria are determined from these answers [9].

Table 4 shows the criteria and criteria levels of the different EES technologies. Table 3 shows normalised criterion weights and single criterion level scores. The criterion weights and the single criterion level score on this table are used to determine the total score of each EES technology. An illustration is shown on the Results section.

Criteria used to rank the EES technology

The eight criteria used to rank the EES technologies are listed below. Each criterion has three levels and the levels are ranked down the page from the lowest (least important) to the highest (most important).

- Technical Maturity
 - Developing
 - Developed
 - Mature
- Power Rating
 - Power Rating < 500kW
 - 500kW < Power Rating < 20MW
 - Power Rating > 20MW

- Energy Density
 - Power Density < 5Wh/kg
 - 5Wh/kg < Power Density < 75Wh/kg
 - Power Density > 75Wh/kg
- Capital Cost
 - Capital Cost > 1000USD /kWh
 - 100USD /kWh < Capital Cost < 1000USD /kWh
 - Capital Cost < 100USD /kWh
- Storage Duration
 - Storage Duration < Hour
 - Hour < Storage Duration < Day
 - Storage Duration > Day
- Self-Discharge
 - Self-Discharge > 15%
 - 1% < Self-Discharge < 15%
 - Self-Discharge < 1%
- Influence on the Environment
 - Negative
 - Small
 - Positive
- Cycle Efficiency
 - Cycle Efficiency < 60%
 - 60% < Cycle Efficiency < 90%
 - Cycle Efficiency > 90%

VII. Ranking Results

The first column of Table 4 show the ranking results of the EES technologies. Figure 5 show the criterion weights (importance) obtained from answering the trade-off questions. The criteria weights are capital cost (31.5%), technical maturity (15.5%), power rating (14.7%), power density (12.5%), storage duration (8.6%), influence to the environment (6.9%), cycle efficiency (6.5%) and self-discharge per day (3.9%).

Using the criterion levels of each ESS technology showed on Table 4, normalised criterion weights and single criterion level scores showed on Table 3, the different EES technologies can be ranked. The top three ranked EES technologies total score is calculated as follows:

$$\text{EES total score} = \sum (\text{criterion weight} \times \text{single criterion score})$$

Figure 5. Criterion Weights



As an example the top three ranked EES technologies total scores are calculated below:

HT TES total score

$$\begin{aligned} &= (0.155 \times 97.2) + (0.147 \times 100) \\ &+ (0.125 \times 100) + (0.315 \times 100) \\ &+ (0.065 \times 73.3) + (0.086 \times 100) \\ &+ (0.039 \times 100) + (0.069 \times 62.5) \\ &= \mathbf{95.343} \end{aligned}$$

AL TES total score

$$\begin{aligned} &= (0.155 \times 97.2) + (0.147 \times 85.3) \\ &+ (0.125 \times 100) + (0.315 \times 100) \\ &+ (0.065 \times 73.3) + (0.086 \times 100) \\ &+ (0.039 \times 100) + (0.069 \times 62.5) \\ &= \mathbf{93.1821} \end{aligned}$$

CAES total score

$$\begin{aligned} &= (0.155 \times 97.2) + (0.147 \times 85.3) \\ &+ (0.125 \times 72.4) + (0.315 \times 100) \\ &+ (0.065 \times 100) + (0.086 \times 100) \\ &+ (0.039 \times 100) + (0.069 \times 0) \\ &= \mathbf{87.1551} \end{aligned}$$

Table 2 shows the relative importance of the criteria, obtained by dividing the row criterion with the column criterion.

The EES technologies are ranked in this order with 1 being the most suitable and 10 being the least suitable.

- HT-TES
- AL-TES
- CAES
- PHS
- VRB
- ZnBr battery

- Lead-Acid Battery
- PSB Battery
- Nas Battery and
- NiCd Battery.

(molten salt energy storage/ HT TES) as the most optimal for the AHTR.

Table 2. Relative importance of criteria

	Capital Cost	Technical Maturity	Power Rating	Energy Density	Storage Duration	Influence to the Environment	Cycle Efficiency	Self-Discharge per Day
Capital Cost	2.0	2.1	2.5	3.7	4.6	4.9	8.1	
Technical Maturity	0.5	1.1	1.2	1.8	2.3	2.4	4.0	
Power Rating	0.5	0.9	1.2	1.7	2.1	2.3	3.8	
Energy Density	0.4	0.8	0.9	1.5	1.8	1.9	3.2	
Storage Duration	0.3	0.6	0.6	0.7	1.3	1.3	2.2	
Influence to the Environment	0.2	0.4	0.5	0.6	0.8	1.1	1.8	
Cycle Efficiency	0.2	0.4	0.4	0.5	0.8	0.9	1.7	
Self-Discharge per Day	0.1	0.3	0.3	0.3	0.5	0.6	0.6	

Table 3. Normalised criterion weights and single criterion scores

Criterion	Criterion weight (sum to 1)	Criterion level	Single criterion Level score (0-100)
Technical Maturity	0.155	Developing	0.0
		Developed	97.2
		Mature	100
Power Rating	0.147	Power Rating < 500kW	0.0
		500kW < Power Rating < 20MW	85.3
		Power Rating > 20MW	100
Energy Density	0.125	5Wh/kg < Energy Density	0.0
		5Wh/kg < Energy Density < 75Wh/kg	72.4
		Energy Density > 75Wh/kg	100
Capital Cost	0.315	Capital Cost > 1000USD /kWh	0.0
		100USD /kWh < Capital Cost < 1000USD /kWh	49.3
		Capital Cost < 100USD /kWh	100
Cycle Efficiency	0.065	Cycle Efficiency < 60%	0.0
		60% < Cycle Efficiency < 90%	73.3
		Cycle Efficiency > 90%	100
Storage Duration	0.086	Storage Duration < Hour	0.0
		Hour < Storage Duration < Day	85.0
		Storage Duration > Day	100
Self-Discharge per Day	0.039	Self-Discharge > 15%	0.0
		1% < Self-Discharge < 15%	22.2
		Self-Discharge < 1%	100
Influence to the Environment	0.069	Negative	0.0
		Small	62.5
		Positive	100

Conclusions

Eskom, a South African electricity utility company is developing AHTR. It has been realised that cogeneration provides economic, environmental and efficiency benefits, and thus the proposed cogeneration system for the developing AHTR is energy storage which will be employed for load following.

Various EES technologies have been evaluated to determine the most suitable EES technology for the AHTR. 1000 minds, an MCDM tool was used to rank the technologies and the top three (in order) EES technologies found to be suitable for the AHTR are HT-TES, AL-TES and the CAES.

This paper then confirms the initial choice of energy storage system chosen

Table 4: EES Characteristics and Ranking [6]

Rank	Technology	Technical Maturity	Power Rating	Energy Density	Capital Cost	Cycle Efficiency	Storage Duration	Self-Discharge per day	Influence to the Environment
1st	High Temperature Thermal Energy Storage (HT TES)	Developed	Power Rating > 20MW	Power Density > 75Wh/kg	Capital Cost < 100USD /kW	60% < Cycle Efficiency < 90%	Storage Duration > Day	Self-Discharge < 1%	Small
2nd	Aquifers Low-temperature TES (AL - TES)	Developed	500kW < Power Rating < 20MW	Power Density > 75Wh/kg	Capital Cost < 100USD /kW	60% < Cycle Efficiency < 90%	Storage Duration > Day	Self-Discharge < 1%	Small
3rd	Compressed Air Energy Storage system (CAES)	Developed	500kW < Power Rating < 20MW	5Wh/kg < Power Density < 75Wh/kg	Capital Cost < 100USD /kW	Cycle Efficiency > 90%	Storage Duration > Day	Self-Discharge < 1%	Negative
4th	Pumped Hydroelectric Storage (PHS)	Mature	Power Rating > 20MW	Power Density < 5Wh/kg	Capital Cost < 100USD /kW	Cycle Efficiency > 90%	Storage Duration > Day	Self-Discharge < 1%	Negative
5th=	VRB Battery	Developed	Power Rating > 20MW	5Wh/kg < Power Density < 75Wh/kg	100USD /kWh < Capital Cost < 1000USD /kWh	Cycle Efficiency > 90%	Storage Duration > Day	Self-Discharge < 1%	Negative
5th=	ZnBr Battery	Developed	Power Rating > 20MW	5Wh/kg < Power Density < 75Wh/kg	100USD /kWh < Capital Cost < 1000USD /kWh	Cycle Efficiency > 90%	Storage Duration > Day	Self-Discharge < 1%	Negative
7th	Lead-Acid Battery	Mature	Power Rating > 20MW	5Wh/kg < Power Density < 75Wh/kg	100USD /kWh < Capital Cost < 1000USD /kWh	60% < Cycle Efficiency < 90%	Storage Duration > Day	Self-Discharge < 1%	Negative
8th	PSB Battery	Developed	500kW < Power Rating < 20MW	5Wh/kg < Power Density < 75Wh/kg	100USD /kWh < Capital Cost < 1000USD /kWh	Cycle Efficiency > 90%	Storage Duration > Day	Self-Discharge < 1%	Negative
9th	Nas Battery	Developed	500kW < Power Rating < 20MW	Power Density > 75Wh/kg	100USD /kWh < Capital Cost < 1000USD /kWh	Cycle Efficiency < 60%	Hour < Storage Duration < Day	Self-Discharge > 15%	Negative
10th	NiCd Battery	Developed	Power Rating > 20MW	5Wh/kg < Power Density < 75Wh/kg	Capital Cost > 1000USD /kWh	60% < Cycle Efficiency < 90%	Storage Duration > Day	Self-Discharge < 1%	Negative

Acknowledgements

This paper has been written with contribution from M. Fipaza and L. Molele working at Eskom (a south african electricity utility company); they brought a significant support at improving this paper.

Nomenclature

AHTR	Advanced High Temperature Reactor
AL	Aquiferous Low temperature
CAES	Compressed Air Energy Storage
CES	Cryogenic Energy Storage

CSP	Concentrated Solar Power
EES	Electric Energy Storage
HT	High Temperatures
MCDM	Multi Criteria Decision Making
MCFC	Molten Carbonate Fuel Cells
NPP	Nuclear Power Plant
PBMR	Pebble Bed Modular Reactor
PHS	Pumped Hydroelectric Storage
SMES	Superconducting Magnetic Energy Storage
TES	Thermal Energy Storage
UPS	Uninterrupted Power Supply

References

- [1] Nuclear Power (NENP), "IAEA," 11 December 2015. [Online]. Available: https://www.iaea.org/NuclearPower/NEA_Cogeneration/index.html. [Accessed 28 June 2018].
- [2] A. Lokhov, "Load-following with nuclear power plants," NEA updates, NEA News, 2011.
- [3] NEA, "Technical and Economic," OECD/NEA online report, 2011.
- [4] "National Resources Leadership Institute," [Online]. Available: <https://projects.ncsu.edu/nrli/decision-making/MCDA.php>. [Accessed 26 June 2018].
- [5] D. R. Nicholls, "Advanced High Temperature Reactor Project – PBMR relaunch," Africa Utility Week, CTICC, 2017.
- [6] H. Chen, T. N. Cong, W. Yong, C. Tan, Y. Li and Y. Ding, "Progress in electrical energy storage system: A critical review," Progress in Natural Science, 2008.
- [7] L. Wegner, "Overview of energy storage methods," Research report, 2007.
- [8] P. Kurzweil, "Gaston Planté and his invention of the lead–acid battery—The genesis of the first practical rechargeable battery," Journal of Power sources, vol. 195, no. 14, 2010.
- [9] 1000 Minds, "Decision-Making Tool," [Online]. Available: <https://www.1000minds.com/decision-making>. [Accessed 08 May 2018].

BASE-LOAD NUCLEAR REACTORS WITH HEAT STORAGE TO BUY AND SELL ELECTRICITY: INTEGRATING NUCLEAR AND RENEWABLES (C. FORSBERG)

Charles W. Forsberg

Massachusetts Institute of Technology, USA

I. Introduction

In a low-carbon world (nuclear, wind, solar, and hydro) there is the need to replace fossil fuels in their role of providing variable assured generating capacity to match electricity production with demand. Base-load nuclear reactors can provide variable electricity including assured peak electricity production with power cycles that include (1) heat storage and (2) auxiliary heat generation using combustion heaters that in the near-term burn natural gas and in the long-term burn low-carbon fuels (biofuels or hydrogen).

The reactor operates at base-load. When electricity prices are low the turbine-generator operates at minimum electricity output with all other heat sent to storage. In a light-water reactor (LWR), the heat would be in the form of steam. For GenIV reactors the heat could be in the form of steam or an alternative reactor coolant (sodium, lead, salt, or helium). If there is excess electricity generation from wind or solar (low electricity prices), electricity from the nuclear plant and the grid can be converted into stored heat. At times of high electricity prices heat from the reactor and heat storage is sent to the power conversion system to produce peak electricity—more than base-load generating capacity. The combustion heaters replace the heat from storage when peak power is needed and heat storage is depleted. Because the heat storage system usually provides the heat for peak electricity production, the annual fuel consumption by the combustion system is low. For an LWR, the combustion heater is a water-tube steam boiler.

Heat storage is cheaper than electricity storage. Nuclear reactors produce heat and thus couple

to thermal energy storage systems (latent heat, sensible heat, etc.). Wind and solar photovoltaic produce electricity and thus couple to electricity storage systems (batteries, hydro pumped storage, etc.). A recent review [1] of future electricity storage systems concluded costs of USD 340 +/-60 per kWh of electricity when deployed at the terawatt-hour storage scale. The U.S. Department of Energy (DOE) long-term battery storage goal is USD 150/kWh for the battery and about double that when installed with power conversion and other required systems to couple to the grid. These storage costs would more than double electricity costs [2]. In contrast, the DOE thermal energy storage goal for concentrated solar power systems is USD 15/kWh of heat. Because heat storage is less expensive than electricity storage, storage economics favor nuclear reactors with heat storage to match electricity production with demand.

The other consideration is assured generating capacity. If storage is depleted, assured capacity can be obtained by adding a furnace or boiler to provide heat—at a rate equivalent to heat from storage for peak electricity production. If one buys a heat storage system coupled to a nuclear power plant, one increases the size of the turbine, generator, condenser and other equipment to enable peak electricity production—electricity output greater than a base-load nuclear plant. The cost of the added furnace or boiler is small. The fuel consumption is low because most peak electricity demand is met by heat storage. This is not an option for electricity storage technologies such as batteries and hydro pumped storage where a gas turbine or equivalent technology is required to provide an assured electricity supply.

This combination of characteristics may make nuclear power the enabling technology for (1) a low-carbon grid and (2) large-scale use of wind and solar by providing low-cost energy storage and assured electricity generation. We discuss herein markets, system design and technology options for heat storage coupled to nuclear power plants for assured variable electricity generation.

II. Electricity Markets

There are three electricity markets that are sources of revenue for electricity generators and storage systems [3]. We describe herein the market mechanisms for deregulated, competitive markets that define the economic requirements for any energy production or storage system with assured capacity. In theory, an ideal free market and an ideal regulated market will have similar outcomes. In practice, there are no fully free markets or ideally regulated utilities.

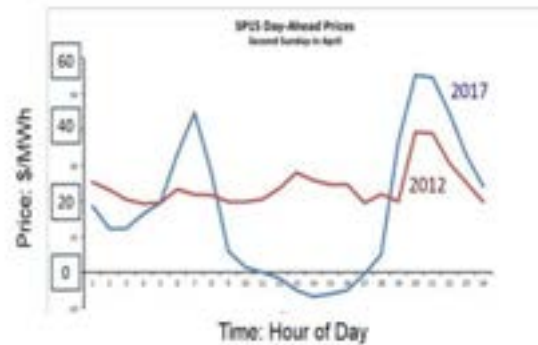
II.A. Energy markets

Energy markets pay per unit of electricity (MWh) delivered to the grid and are the primary source of revenue for storage systems. In deregulated electricity markets, electricity generators bid a day ahead on the price that they are willing to sell electricity into the market—typically for each hour of the day. These are also known as competitive wholesale electricity markets. Electricity generators bid their short-run operating cost [4] to produce electricity, including fuel costs and variable operations and maintenance (O&M) costs. The grid operator accepts electricity bids up to the expected electricity demand for each hour. The accepted bid (USD /MWh) with the highest electricity price sets the price for that hour, and everyone who bids below that price gets the same marginal price. Energy markets have existed for decades and are reasonably well understood with relatively stable market rules.

In a perfect market, wind and solar will bid near zero dollars per megawatt hour—their variable operating and maintenance costs. Figure 1 shows electricity prices in parts of California on a spring day in 2012 and 2017 [5]. Over a period of five years, large numbers of photovoltaic (PV) systems were installed that collapsed prices on days with good solar conditions and limited electricity demand. As more solar plants are built, electricity prices collapse more hours per year during times of high solar output when production exceeds demand. Experience in European countries shows that this limits solar

electricity production to less than 8% of total electricity consumption [6], even if there are large decreases in solar capital costs [7].

Figure 1. Price Impact of Adding Solar Between 2012 and 2017 on a Spring Day in California [5]



The same effect occurs with wind. Studies have quantified this effect in the European market [8-9]. If wind grows from providing 0% to 30% of all electricity, the average yearly price for wind electricity in the market would drop from 73 EUR/MWh (first wind farm) to 18EUR/MWh (30% of all electricity generated). There would be 1000 hours per year when wind could provide the total electricity demand, the price of electricity would be near zero, and 28% of all wind energy would be sold in the market for prices near zero.

II.B. Capacity markets

There are two strategies to assure sufficient generating capacity to avoid blackouts. The first strategy is to allow electricity prices to go to very high levels (USD 1,000s/MWh or more) at times of scarcity. Plants will be built whose revenue depends upon incomes during the sale of electricity for tens or hundreds of hours per year when prices are very high.

The second strategy is for the grid to offer forward capacity contracts for assured electricity supply (auctions for such contracts are known as a capacity market). This assures electricity supply even if there are multiday periods of low solar production, month-long periods of low wind (such as January 2017 in Europe) or extreme weather events (United States). Most electricity markets have capacity markets where the grid operator pays so many dollars per megawatt of assured capacity. The grid operator pays to lower the risks of blackouts because of the high costs of such

blackouts in terms of economics, public health risks (cold houses, summer heat exhaustion, etc.) and social disruption (crime waves, riots, etc.).

Historically capacity markets were not needed or the payments were low because the electricity was generated by nuclear and fossil units—dispatchable electricity sources. The addition of wind and solar have increased the use of capacity markets because these energy sources cannot assure production of electricity given their intermittency. Electricity storage systems (batteries, pumped storage) can be depleted and thus do not assure capacity. Heat storage systems with auxiliary combustion heaters coupled to nuclear plants for peak electricity production would receive capacity payments.

Capacity markets as a major source of revenue are relatively new—a consequence of adding wind and solar. The rules are evolving. There are other complications that have not been addressed. If one has a yearly market for capacity payments and a local economic recession, the peak electricity demand will go down, and capacity payments will be reduced. If the economy picks up, the electricity demand grows with the need for more capacity, but it takes more than a year to build more capacity.

There are also generating capacities that may appear to provide assured capacity but may not over a decade. For example, Brazil and parts of eastern Canada have large hydroelectric facilities that were thought to provide assured capacity; however, long periods of low rain resulted in capacity shortages. Large-scale wind was assumed to provide some assured capacity on the assumption that the wind will not disappear over distances of a 1,000 km; however, Europe recently had one such low-wind event. It may be a decade or more before stable capacity market rules are developed.

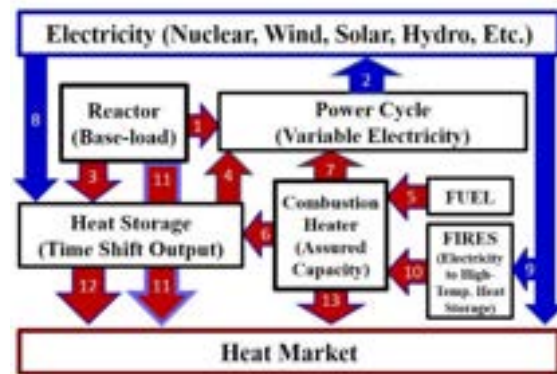
II.C. Ancillary/Auxiliary service markets

This refers to other electricity grid services such as frequency control, black start (start after power outage) and reserves for rapid response to grid emergencies such as another electrical generator failing. Most of the thermal storage technologies associated with LWRs have some capabilities to provide these services as described below, but this is not currently a large source of revenue in any electricity grid—typically 1–2% of total electricity revenue.

III. System Description

Figure 2 shows the system for variable electricity to the grid and heat to industry from a base-load nuclear plant with assured delivery of electricity to the grid and heat to industry. In the description below we include in parenthesis {} example technologies that are applicable to LWRs. Later we discuss other technologies applicable to sodium, helium or salt reactors. The top-level goal is variable electricity and heat with nuclear, solar, and wind facilities operating at full capacity—their most economic mode of operation.

Figure 2. Reactor System with Dispatchable Electricity to the Grid and Assured Capacity



The reactor operates at base-load with variable electricity (2) to the grid with the option of heat {steam} to industrial customers (11). The electricity grid may include wind or solar production facilities. When there is excess electricity production (low prices), some of the heat {steam} from the reactor is diverted to heat storage (3) {steam accumulators, oil, etc.}. Sufficient heat {steam} is sent the power cycle (1) to operate at minimum electricity output. By operating the power cycle at minimum load, the power cycle can quickly return to full base-load power by sending all heat {steam} from the reactor to the power cycle. When additional electricity is needed (high electricity prices), all heat {steam} from the reactor (1) is sent to the power cycle and additional heat {steam} from storage (4) is sent to the power cycle to produce added peak electricity.

The addition of heat storage enables variable electricity from a base-load reactor but does not assure peak electricity production at all times. The heat storage system can become depleted and electricity production will be limited to

base-load electricity production from the reactor operating at full power. To assure the capability of peak electricity production at all times, a combustion heater {water-tube boiler} burning natural gas, oil, biofuels or other fuels (5) can provide heat {steam} to the storage system (6) or directly to the power cycle (7). Where to add heat will depend upon the specific system design. For an LWR, a boiler provides saturated steam.

The cost of assured peaking capacity is small. If one has a 1000 MWe reactor and adds a storage system to produce an additional 200 MWe of peak power capacity, one has the extra power cycle equipment (added turbine, generator, electrical switchgear, condenser, cooling tower capacity) required to produce the added 200 MWe of peak power capacity. To provide 200 MWe of added assured generating capacity even if storage is depleted, a combustion heater {boiler} only needs to provide the heat for that peak 200 MWe capacity. Heat storage usually provides peak capacity; thus, the auxiliary heater {boiler} will likely be operated less than 100 hours per year. For the specific case of a LWR, the capital costs [Ref 10] for such a boiler are estimated at USD 100-300/kWe, less than the cost of a simple gas turbine (USD 500/kWe) to provide assured generating capacity.

If there is excess electricity production from wind and solar (Fig. 1), there are options to convert excess electricity from the reactor and the electricity grid into stored high-temperature heat rather than curtailing wind or solar resources. The first option (8) is to add electric resistance heaters to the heat storage system. The second option is to add Firebrick Resistance Heated Energy Storage (FIRES) [Ref 11] to convert excess electricity (9) into high-temperature stored heat in the form of hot firebrick. When there is a demand for peak electricity, cold air is blown through channels in the hot firebrick to produce hot air (10) that goes to the combustion heater {steam boiler}. The hot air from FIRES replaces the burning of fossil fuels to provide heat to the heat storage system or power cycle. FIRES operates as a second heat storage system except the energy into the FIRES system is in the form of electricity. If there are large amounts of excess electricity available from the grid, FIRES storage can be expanded to allow longer-term storage.

Regular heat storage and FIRES enables variable heat to industry. Heat from the reactor (11), heat from storage (12) and heat from FIRES via the combustion heater (13) can provide low-cost industrial heat {steam} produced at times

of low electricity prices. There have been only limited studies of such systems to understand strengths, weaknesses, and requirements for different components for an optimum system under different conditions.

IV. Heat Storage and Capacity Technologies

There are three options for variable electricity to the grid from a nuclear power plant: (1) vary reactor output [12-13], (2) hybrid systems where a base-load reactor coproduces electricity and one or more energy intensive products such as hydrogen and (3) base-load reactors with heat storage for variable electricity to the grid and heat to industry. We summarise options for reactors with heat storage coupled to steam cycles [14], in intermediate loops (sodium, lead, etc.) [15], (3) in HTGR reactor cores [16] and coupled to Brayton power cycles [2, 17-19].

Not all reactor types couple to each heat storage technology. The most important reactor characteristic in terms of heat storage is the temperature range over which heat is delivered (Table 1). However is it not the only important reactor characteristic. Some heat storage technologies are reactor specific—such as using the HTGR reactor core as the heat storage reservoir (see below).

Table 1. Typical Reactor Coolant Temperatures

Coolant	Average Core Inlet Temp. (°C)	Average Core Exit Temp. (°C)	Average Temp. of Delivered Heat.(°C)
Water	270	290	280
Sodium	450	550	500
Helium	350	750	550
Salt	600	700	650

IV.A. Heat storage in steam cycles

A recent workshop [20] examined heat storage coupled to LWRs. At times of low electricity prices, some steam is diverted to heat storage but sufficient steam is sent to the turbine to keep it on-line to enable quick return to full electricity output when needed. Turbine generator systems can be designed to operate reliably at 30% of full power with quick return to full power if electricity prices rise. Diverting

steam from an LWR to storage is a low-cost operation.

Heat storage has two major costs: (1) the heat storage system and (2) the power conversion system to convert stored heat back to electricity. The lowest cost strategy for converting stored heat to electricity is to send steam from storage to the main turbine or feed water heaters; that is, oversize the main turbine plant for peak power production. The capital cost of a somewhat larger power conversion system may be half the cost of a separate power conversion system to convert stored heat to electricity. For a new reactor plant, the turbine system could be designed for power outputs from 30 to 130% of base-load power output. The reactor core would operate at 100% load with variable steam to and from the storage system. Some of these heat storage technologies are applicable to high-temperature steam cycles that may be used with sodium, helium, and salt cooled reactors—but not all of these heat storage technologies would match higher-temperature GenIV steam cycles.

Latent heat storage. Heat is stored in a phase-change material:

- *Steam Accumulators.* A steam accumulator is a pressure vessel nearly full of water that is heated to its saturation temperature by steam injection. The heat is stored as high-temperature high-pressure water. When steam is needed, valves open and some of the water is flashed to steam that is sent to a turbine or feed-water heaters to produce peak electricity while the remainder of the water decreases in temperature. Steam accumulators for heat storage are commercially deployed in concentrated solar thermal power plants where the system produces steam. The efficiency decreases if one uses high-temperature supercritical steam as input.
- *Cryogenic Air Systems.* A cryogenic air energy storage system stores energy by liquefying air at times of low electricity prices. To produce electricity, the liquid air is compressed, heated using low-temperature heat (cooling water) from the power plant, further heated with steam from the LWR and sent through a gas turbine before being exhausted to the atmosphere. This technology can be coupled to any heat source. A pilot plant coupled to a biofuels power plant is now operating in the United Kingdom.

Efficiency increases with higher steam temperatures.

Sensible Heat Fluid Systems. Sensible heat storage involves heating a second material where heat is stored by raising the temperature of the second material.

- *Hot oil storage.* This technology is commercially deployed in concentrated solar thermal power systems where a heat-transfer oil is sent through the concentrated solar power system and the hot oil is sent to the power system or a large storage tank. Westinghouse is developing a low-pressure thermal storage system where a heat-transfer oil moves heat from the steam system to concrete that is the primary heat storage medium. Concrete in the form of thin plates in tanks are used for heat storage because of its low cost relative to the price of heat transfer oils. Different heat transfer fluids and heat storage media would be required if the input was higher-temperature steam from a GenIV reactor.
- *Packed-bed Thermal Energy Storage.* A packed-bed thermal energy storage system consists of a pressure vessel filled with solid pebbles with a steam valve at the top and water outlet at the bottom. Heat is stored as sensible heat in the pebbles. To charge the system, steam is injected into the pebble bed, condenses as the cold pebbles are heated and water exits from the bottom of the vessel. At the end of the charging cycle all pebbles are hot and there is hot water filling the voids at the bottom of the vessel. To discharge the system, water is injected into the bottom of the vessel and steam is produced by the hot pebbles.
- *Hot Rock Storage.* In a hot rock energy storage system²¹⁻²² a volume of crushed rock with air ducts at the top and bottom is created. To charge the system, air is heated using a steam-to-air heat exchanger delivering heat from the reactor, then the air is circulated through the crushed rock, heating the rock. To discharge the system, the airflow is reversed, and cold air is circulated into the crushed rock at the bottom. The discharged hot air can be used to (1) produce steam for electricity or industry or (2) hot air for collocated industrial furnaces to reduce natural gas

consumption. It has the lowest incremental heat storage costs per kWh. The technology is under development for heat storage in concentrated solar power systems that produce hot air. It can function with any temperature steam.

- *Geothermal Heat Storage Systems.* Thermal energy is stored by injecting hot water heated by steam from the reactor into the underground reservoir; energy is discharged by pumping hot water back to the surface for electricity production in a conventional geothermal plant. Only limited studies have been completed. It can provide seasonal energy storage but can only be deployed as a large system because there is no way to insulate rock deep underground. The underground surface area for heat losses goes up as the square while the storage volume increases as the cube resulting in low losses for systems with more than 0.1 Gigawatt-year of heat storage. Injected hot-water temperatures are limited to about 300°C because of the water chemistry of most types of rock.

Chemical heat storage. Chemical heat storage systems store heat in some type of chemical reaction. Relatively little work has been done on these systems relative to the options above.

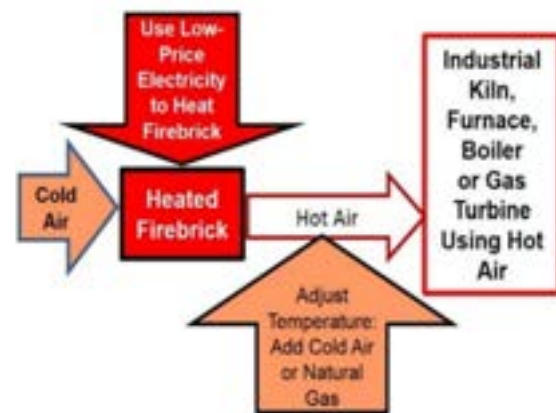
IV.B. Heat storage with electricity input

If there are times of low electricity prices (Fig. 1) that are below the price of fossil fuels, there are two options to divert low-price electricity from the nuclear power plant turbine that is running at minimum load and/or from the electricity grid to heat storage.

- *Heat storage system.* The electricity can be converted to heat using resistance heaters in most of the above heat storage systems. Where the heat is added depends upon the specific storage technology.
- *Firebrick Resistance Heated Energy Storage [11] (FIRES).* Low-price electricity can be sent to FIRES to heat firebrick to high temperatures. To convert this heat back to electricity, air is blown through FIRES creating hot air. In the case of a LWR, the hot air is sent to a water-tube boiler that produces steam, and the steam is sent to the reactor turbine or heat storage system.

FIRES (Fig. 3) is a general purpose technology to convert electricity less than the price of fossil fuels into high-temperature stored heat and then converting that heat into hot air to substitute for hot air produced by burning fossil fuels. The firebrick is heated with electric resistance heaters. Cold air is blown through channels in the firebrick to produce hot air that replaces hot air generated by burning natural gas, oil, biofuels and ultimately hydrogen in furnaces, boilers and other applications.

Figure 3. Firebrick Resistance Heated Energy Storage (FIRES)



Small FIRES units (<100 kWh) are used for home heating where utilities provide low-priced electricity during off hours for FIRES to be charged. Hot air is produced for home heating for a day or more. More recently the Chinese have deployed units up to 8 MWh with an electricity input rates at 1 MWe for heating large apartment complexes. FIRES is charged at night and the hot air is used to provide steam or hot water for building heat. For temperatures to 850°C and atmospheric pressure, FIRES is an off-the shelf technology. Heat storage can be provided by classical firebrick for higher performance applications or using hot rock [20-21] as the storage media rather than firebrick if storing heat for days or weeks where a very low-cost storage media is required.

IV.C. Heat storage with Brayton Power cycles

The advances in gas turbine technologies have resulted in ongoing work to couple gas turbines to sodium, helium, and salt reactors. There are many options but only a small subset have been investigated. Two options are discussed herein.

For HTGRs coupled to direct gas turbine cycles there is the option to use the reactor core to store heat. This option is being examined in Japan [16]. The reactor core power remains constant but electricity to the grid can be changed by allowing the reactor core temperature to go up and down in temperature with variable heat to the power cycle. This is unique to HTGRs with their relatively low power densities and large graphite reactor cores with massive high-temperature heat capacity.

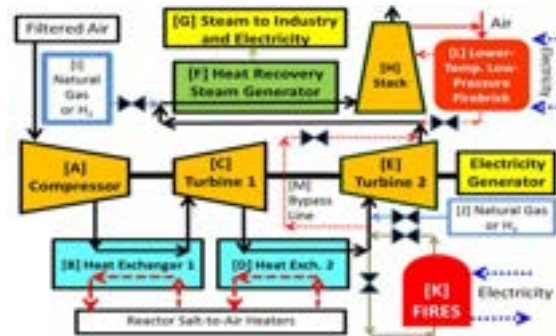
A second set of options [2, 17-19] are Nuclear Air-Brayton Combined Cycles (NACC) that couple to multiple types of high-temperature reactors (HTRs). Figure 4 shows such a cycle that includes a gas turbine and a heat recovery steam generator (HRSG) and two types of internal heat storage systems coupled to a salt-cooled reactor that delivers heat between 600 and 700°C. This specific NACC design is based on the GE F7B natural gas combined cycle (NGCC). The HRSG could also be coupled to the steam-cycle heat-storage technologies that were described earlier.

Base-Load Electricity (black lines and outlines). During base-load operation (1) outside air is compressed [A], (2) heat is added to the compressed air from the reactor through Heat Exchanger 1 [B], (3) hot compressed air goes through Turbine 1 [C] to produce electricity, (4) air is reheated in Heat Exchanger 2 [D] and sent through Turbine 2 [E] to produce added electricity, (5) the warm low-pressure exiting air goes through a HRSG [F] to generate steam [G] that is used to produce added electricity or sent to industry and (6) air and/or combustion gases exit up the stack [H].

Utility gas turbine compressors raise the gas inlet temperature to between 350 and 450°C. This requires that the nuclear heat input must be in the temperature range of 550 to 700°C. That implies that heat must be delivered to the power cycle in the range of 550 to 700°C—and determines what types of GenIV reactors can couple to this power cycle. Advanced reactors that can be coupled to Brayton power cycles include fluoride-salt-cooled high-temperature reactors (FHRs) with solid fuel and clean salt coolants, molten salt reactors (MSRs) with fuel dissolved in the salt coolant, high-temperature lead-cooled fast reactors, and HTGRs. There are variants with compressor intercoolers that can couple to sodium fast reactors. Almost all work to date in coupling NACC to a reactor has been with FHRs designed to deliver heat between 600 and 700°C using a modified GE 7FB gas turbine.

The base-load heat-to-electricity efficiency is 42% with the specific design described herein.

Figure 4. NACC with Two Heat Storage Systems and Use of Auxiliary Fuels



Peak Electricity Production. The maximum base-load temperature is determined by the materials of construction of the reactor-coolant gas-turbine heat exchangers. With existing commercial materials, that limit is near 700°C. While these are high temperatures for heat exchangers, they are low temperatures for gas turbines, where there are industrial gas turbines with peak temperatures over 1400°C. Higher temperatures are possible because gas turbine blades can be cooled from the inside and ceramic coatings placed on the outside to insulate the turbine blade from the high combustion temperatures. Consequently, in NACC there is the option of adding heat after the nuclear heating in Heat Exchanger 2 to further raise compressed gas temperatures before entering Turbine 2—a thermodynamic topping cycle. The added high-temperature heat can be provided by natural gas, hydrogen, another combustible fuel [J] or FIRES stored heat [K]. Auxiliary heating the compressed air after nuclear heating up to 1065°C results in an incremental heat-to-electricity efficiency of 66.4%—the most efficient system using existing technology to convert heat to electricity.

This design was optimised for base-load electricity. If optimised for peak power efficiency (radiant heat boiler section in HRSG, higher temperature gas turbine blades, etc.), the incremental heat-to-peak electricity efficiency would approach ~70%. The GE 7FB combined cycle plant running on natural gas that was used in this analysis has a rated efficiency of 56.9%. The first of the General Electric H-Class NGCC plants are now being deployed with efficiencies in excess of 62%. NACC with H-Class technology would have significantly

better performance with improvements in NGCC systems improving NACC performance.

The use of a high-efficiency thermodynamic topping cycle for peak electricity production has major economic implications. NACC converts natural gas to electricity with an efficiency of 66.4% versus an efficiency of ~60% for a stand-alone natural gas combined cycle plant and ~40% for a stand-alone natural gas turbine. That implies the first “natural gas” plant that is dispatched is a reactor with NACC, then the stand-alone natural gas combined cycle plants followed by the simple natural-gas turbines. As long as the reactors with NACC do not dominate the market, peak prices will be controlled most of the time by stand-alone less-efficient natural gas plants that set higher prices because of their lower efficiencies. A GenIV reactor with NACC in today’s Texas market would have 50% more revenue than a base-load nuclear plant. It also has major implications in a low-carbon grid because such topping cycles are the most efficient methods to convert hydrogen or biofuels into peak electricity.

Added Electricity Production Using High-Temperature Stored Heat for Turbine 2. In a low-carbon grid there will be times when electricity prices are low or negative (Figure 1). FIRES [K] uses this low-price electricity to replace natural gas in NACC. Electricity is bought whenever the electricity price is less than the price of natural gas and is used to heat firebrick up to temperatures that can approach 1800°C. When peak electricity is needed from NACC, the compressed air after nuclear heating in Heat Exchanger 2 is sent through FIRES to be heated to higher temperatures and then to Turbine 2. Exit temperatures from FIRES are controlled by either (1) cooler compressed air or steam from the HRSG to lower temperatures or (2) natural gas [J] (which self-ignites) to increase temperatures. In the long term, hydrogen may replace natural gas.

Added Steam Using Stored Heat for HRSG. Heat storage can be added between Turbine 2 and the HRSG in the form of a firebrick recuperator [L]. If electricity prices are low or heat (steam) demand is low, the hot air exhaust from Turbine 2 is partly or fully diverted from the HRSG into a low-pressure (near atmospheric) brick recuperator [L] where it heats firebrick and then is exhausted to the stack [H]. At times of high electricity or heat demand, fans send cold air through the firebrick recuperator [L] that is heated to provide added hot air for the HRSG. If electricity prices are low or negative,

there is the option to include electric resistance heaters to heat the recuperator firebrick [L] for later use to produce steam in the HRSG. However, the lower-temperature recuperator will have a lower heat-to-electricity efficiency than FIRES because lower-temperature heat is being delivered to the HRSG.

IV.D. Heat storage between reactor and power system

Heat storage [15] can be incorporated between the reactor and the power conversion system. In most cases this would be in the intermediate loop where the coolant depends upon the reactor type and the coolant properties drive the choice of heat storage system. Most of the work on these systems has been associated with concentrated solar thermal power systems. As with other storage systems, there is the option of using a combustion heater with heat exchanger in the heat storage system to provide assured peaking capacity if heat storage is depleted.

Sodium. Sodium is used in sodium fast reactors (SFRs), sodium-cooled solar power towers, and in the intermediate loop of some proposed salt-cooled reactors coupled to Brayton power cycles. The Aircraft Nuclear Propulsion Program in the 1950s and 1960s partly developed a MSR with a sodium intermediate loop to transfer heat to the jet engines because of the high performance of the sodium-to-air heat exchangers. Sodium in solar and salt reactor systems would be at higher temperatures than SFRs.

If sodium is in the intermediate loop, sodium can be used as the heat storage media. Assuming a 100°K hot to cold temperature swing, one gigawatt of heat storage requires 30,000 metric tons of sodium per GWh with heat storage costs of ~USD 100/kWh. The risks of sodium storage can be reduced by several orders of magnitude using a secondary media for heat storage that is compatible with sodium. The simplest option is storing heat in iron or steel, materials compatibility with sodium. One could fill a tank with rectangular or hexagonal billets 10 to 20 meters tall with vertical grooves in the sides of each billet for sodium flow. Assuming a 100°K hot to cold temperature swing, one requires 80,000 metric tons of iron per GWh or USD 40/kWh of heat storage. A GWh of heat storage is a little over 10,000 m³.

There are lower-cost filler materials such as quartzite (SiO₂) for sodium systems—but insufficient work to determine if these options meet requirements of a high-temperature heat storage system. A recent paper [23] reviews

heat storage options for sodium solar thermal systems over the temperature range of 400 to 750°C.

Salt. Work is underway to develop salt reactors using fluoride or chloride salts. This includes the fluoride salt cooled high-temperature reactor (FHR) with solid fuel and a clean salt and molten salt reactors (MSR) using fluoride or chloride salts with fuel dissolved in the salt. All MSRs have secondary loops. The concentrated solar power community [24] is examining chloride and carbonate salts for heat storage in the same temperature ranges with much of the current emphasis on sodium-potassium-magnesium chloride salts because of their low costs. Low-cost candidate fill materials for heat storage in salt tanks include steel and potentially graphite. The options are more limited because heat storage will be in the 600 to 800°C range.

Helium. HTGRs operate at high pressure with inlet temperatures near 350°C and exit temperatures in the 750 to 850°C range. If heat storage is at pressure, the likely heat storage mediums are steel, firebrick or graphite. As noted earlier, work is underway to use the graphite in the reactor core for heat storage. Such a system could be augmented with carbon in a second vessel or a larger primary vessel. If heat is to be transferred to a secondary heat storage system through a heat exchanger, the likely near-term candidate will be a chloride salt because this is the leading candidate for heat storage concentrated solar power systems designed to operate over a similar range of temperatures.

IV.E. Assured peak electricity capacity

Assured generating capacity for peak power production requires a combustion heater burning natural gas, oil, biofuels or ultimately hydrogen. For an LWR with heat storage, that combustion heater is a water tube steam generator producing saturated steam. For NACC it is a topping cycle that burns any combustible fuel in the gas turbine. For heat stored in an intermediate sodium or salt loop, it may be a combustion heater to heat the intermediate fluid. The technology depends upon the specific system.

V. Other Considerations

Economics depends upon the differences in electricity prices over time in specific markets and the cost of heat storage technologies. Recent studies²⁵ indicate storage coupled to

nuclear power plants is economic today in some markets—a market development that has only occurred in the last three to four years. A decade ago, there would have been no incentive for heat storage. A decade from now heat storage may be a standard feature of many nuclear reactors.

The industrial heat market in the U.S. is larger than the electricity market.²⁶ Heat storage coupled to nuclear reactors may create new opportunities for nuclear heat sales to industry.

- **Reliability.** Many industries have very high requirements for reliability of heat supplies that has necessitated multiple reactors.²⁷⁻²⁸ Heat storage with auxiliary heaters can meet those reliability requirements.
- **Lower cost heat.** A low-carbon electricity market implies large time variations in the price of energy. Heat storage coupled to reactors is a way to move some of that low-priced energy to the industrial sector.

It is unlikely that there will be a single optimum heat storage technology because of the different electricity markets. There are different requirements for heat storage with large-scale deployment of solar with daily cycles versus wind with multi-day cycles. The electricity demand on an hourly to seasonal basis is different in warm versus cold climates. These differences imply large differences in the ratio of heat storage (USD /kWh) versus peak power capacity (USD /kW).

Last, economics favor large-scale heat storage in the storage system and in the heat-to-electricity conversion system. There are large economics of scale associated with steam turbines and generators²⁹ up to about 500 MWe.

VI. Conclusions

Most nuclear plants have been operated to produce base-load electricity—the economically optimum solution in an electricity grid with a mixture of nuclear and fossil plants. The market is changing. The large-scale addition of wind or solar creates times of very low electricity prices because these technologies are non-dispatchable—driving prices down at times of high wind or solar inputs while raising prices at other times. Separately from addition of renewables, the goal of a low-carbon electricity grid creates the need for nuclear energy as a dispatchable form of electricity to replace fossil fuels in this role.

These changes create economic incentives for nuclear plants to operate at base-load to minimise costs while using heat storage to enable varying electricity production to maximise revenue. Heat storage with assured peak generating capacity using a combustion heat source can meet the capacity requirements of a low carbon world. These capabilities imply that nuclear energy may be the enabling technology for larger-scale use of renewables by providing economic dispatchable electricity with power plants that can buy and sell electricity. The change in requirements implies changes in the heat-to-electricity conversion systems and may imply changes in preferred reactor types—including

GenIV reactors. The economic and technology options for variable dispatchable electricity with assured capacity from nuclear power systems are only partly understood today.

Acknowledgements

We would like to thank the Shanghai Institute of Applied Physics of the Chinese Academy of Sciences, Exelon Corporation and the U.S. Department of Energy, Idaho National Laboratory (INL) for their support. Work supported through the INL National University Consortium (NUC) Program under DOE Idaho Operations Office Contract DE-AC07-05ID14517.

References

- [1] Schmidt, O. et al., “The Future Cost of Electricity Storage Based on Experience Rates”, *Nature Energy*, 2 (July 10, 2017).
- [2] Forsberg, C., Brick, S., and Haratyk, G., “Coupling Heat Storage to Nuclear Reactors for Variable Electricity Output with Base-Load Reactor Operation”, *Electricity Journal*, 31, 23-31 (April 2018), <https://doi.org/10.1016/j.tej.2018.03.008>
- [3] U.S. Department of Energy, Office of Electricity Delivery and Energy Reliability, *United States Electricity Industry Primer*, Washington, DC (2015).
- [4] U.S. Energy Information Agency, *Annual Energy Outlook 2016: Levelized Cost and Levelized Avoided Cost of New Generation Resources in the Annual Energy Outlook 2015* (7 July 2016). http://www.eia.gov/forecasts/aeo/electricity_generation.cfm.
- [5] California ISO, "California ISO: Renewables and emissions reports," (09 April 2017). <http://www.caiso.com/market/Pages/ReportsBulletins/RenewablesReporting.aspx>.
- [6] Sivaram, V., “A Tale of Two Technologies”, *The Breakthrough Journal*, 8. (Winter 2018).
- [7] MIT Energy Initiative, *The Future of Solar Energy: an Interdisciplinary MIT Study*, Massachusetts Institute of Technology, Cambridge, MA (2015).
- [8] Hirth, L., “The Market Value of Variable Renewables, the Effect of Solar Wind Power Variability on Their Relative Prices”. *Energy Economics*, 38, 218-236 (2013).
- [9] Hirth, L., “The Optimal Share of Variable Renewables: How the Variability of Wind and Solar Power Affects their Welfare-Optimal Development”, *The Energy Journal*, 36 (1), (2015).
- [10] Forsberg, C. and Varrin, R., “Light Water Reactors with Heat Storage and Auxiliary-Combustion Steam Generation to Maximize Electricity and Capacity Payment Revenue” *Proc. 2018 American Nuclear Society Annual Meeting*; Philadelphia, Pennsylvania (June 27-21, 2018).
- [11] Forsberg, C., Stack, D., Curtis, D., Haratyk, G. and Sepulveda, N. A., “Converting Excess Low-Price Electricity into High-Temperature Stored Heat for Industry and High-Value Electricity Production,” 30, 42-52, *Electricity Journal* (July 2017), <https://doi.org/10.1016/j.tej.2017.06.009>
- [12] Jenkins, J. D. et al. “The Benefits of Nuclear Flexibility in Power System Operations with Renewable Energy”, *Applied Energy*, 222, 872-884 (2018). <https://doi.org/10.1016/j.apenergy.2018.03.002>
- [13] International Atomic Energy Agency, *Non-Baseload Operation in Nuclear Power Plants: Load Following and Frequency Control Modes of Flexible Operation*, NP-T-3.23 (2018).

- [14] Forsberg, C. W., "Variable and Assured Peak Electricity from Base-Load Light-Water Reactors with Heat Storage and Auxiliary Combustible Fuels", Nuclear Technology March 2019 (Web published, paper version March).
<https://doi.org/10.1080/00295450.2018.1518555>
- [15] Forsberg, C., "Heat Storage for Variable Electricity Production from Base-Load Reactors with Sodium or Salt in the Secondary Loops", Proc. 2018 International Congress on Advances in Nuclear Power Plants (ICAPP 2018), Charlotte, North Carolina (April 8-11, 2018).
- [16] Forsberg, C. W. et al., MIT-Japan Study: Future of Nuclear Power in a Low-Carbon World: The Need for Dispatchable Energy, MIT-ANP-TR-171, Center for Advanced Nuclear Energy (CANES), Massachusetts Institute of Technology, September (2017), <http://energy.mit.edu/wp-content/uploads/2017/12/MIT-Japan-Study-Future-of-Nuclear-Power-in-a-Low-Carbon-World-The-Need-for-Dispatchable-Energy.pdf>
- [17] Andreades, C., Scarlat, R. O., Dempsey, L. and Peterson, P. F., June 2014. Reheating air-Brayton combined cycle power conversion design and performance under normal ambient conditions, J. of Eng. for Gas Turbines and Power, 136 (June 2014)
- [18] Forsberg, C. W. and Peterson, P. F., "Basis for Fluoride-Salt-Cooled High-Temperature Reactors with Nuclear Air-Brayton Combined Cycles and Firebrick Resistance-Heated Energy Storage", Nucl. Technol., 196, 1, 13-31 (October 2016)
<http://dx.doi.org/10.13182/NT16-28>
- [19] Fathi, N., McDaniel, P., Forsberg, C., and de Oliveria, C., "Power Cycle Assessment of Nuclear Systems, Providing Energy Storage for Low Carbon Grids," J. of Nuclear Engineering and Radiation Science, Vol. 4, ASME 020911 (April, 2018).
- [20] Forsberg, C. W. et al., Light Water Reactor Heat Storage for Peak Power and Increased Revenue: Focused Workshop on Near Term Options, MIT-ANP-TR-170, Massachusetts Institute of Technology, Cambridge, MA. (July 2017). <http://energy.mit.edu/2017-can-es-light-water-reactor-heat-storage-for-peak-power-and-increased-revenue>
- [21] Forsberg, C. W., Curtis, D., and Stack, D., "Light-water Reactors with Crushed-Rock Thermal Storage for Industrial Heat and High-value Electricity" Nuclear Technology, (2017).
<http://dx.doi.org/10.1080/00295450.2017.1294426>
- [22] McLachlan, N. R., Crushed Rock Thermal Energy Storage & Nuclear Technology: Option Space & Economics, MS Thesis, Department of Nuclear Science and Engineering, MIT (June 2018)
- [23] Niedermeier, K et al., "Assessment of Thermal Energy Storage Options in a Sodium-Based CSP Plant", Applied Thermal Engineering, 107, 386-397 (August 2016).
<https://doi.org/10.1016/j.applthermaleng.2016.06.152>.
- [24] Mehhos, M. et. al, Concentrating Solar Power Gen3 Demonstration Roadmap, NREL-TP-5500-67464, National Renewable Energy Laboratory (January 2017).
- [25] Mann, W. N. et al. Technoeconomic Modeling of Heat Storage with Assured Capacity for Steam-Cycle Nuclear Power Plants, UTEXAS/ME--2018-04-1, MIT-ANP-TR-173, Framatome 38-9284432-000 (2018).
- [26] Lawrence Livermore National Laboratory, "Estimated U.S. Energy Consumption in 2017," (April 2018).
https://flowcharts.llnl.gov/content/assets/images/energy/us/Energy_US_2017.png.
- [27] Herd, E. M. and Lommers, L. J., "HTGR Strategies to Meet Process Heat Reliability and Availability Needs," Proc. International Congress on Advances in Nuclear Power Plants (ICAPP'10), San Diego (2010).
- [28] Herd, E., Lommers, L. and Southworth, F., "Impact of Demand Load Size on Strategies for Reliable Process Heat Supply," Nuclear Engineering and Design, vol. 251, pp. 282-91 (2012).
- [29] Dawson, K. and Sabharwall, P., "A Review of Light Water Reactor Costs and Cost Drivers," INL/EXT-17-43273, Idaho National Laboratory, Idaho Falls, ID (2017)

SMALL MODULAR LFR: CONSTRUCTION COST FEATURES AND COMPARISON WITH PWR (S. BOARIN ET AL)

Sara Boarin⁽¹⁾, Kamil Tuček⁽²⁾, Craig F. Smith⁽³⁾

(1) Politecnico di Milano, Italy

(2) European Commission, Joint Research Centre, Directorate G – Nuclear Safety & Security, the Netherlands

(3) Naval Postgraduate School, Monterey, United States

Abstract

The Lead-cooled Fast Reactor (LFR) is a promising GEN-IV reactor concept, among the most advanced in the development track towards technological demonstration. Small Modular Reactors (SMRs) represent an attractive new investment paradigm in the nuclear power sector. SMR concepts are expected to bring advantages from the point of view of economics, safety, security, as well as environmental and societal aspects that are to a great degree independent of the specific reactor technology. Such benefits would arise from advantages of the reduced scale, which could, among others, enable factory fabrication, design simplification, and modular deployment. The SMR concepts are therefore receiving increasing interest and endorsement within the industrial and scientific community. In this context, several new SMR concepts based on lead-coolant technology are in their development phase worldwide.

Economic viability is a key enabling factor for these innovative concepts. Specific assessment must therefore accompany technology development, and increasingly refined economic analysis is needed as designs are progressively developed. The aim is to understand if and to what extent the economic paradigm generic to SMR concepts applies to lead-cooled SMR technology as well.

This work approaches the capital cost issue as a key factor affecting the economics and the integration of this innovative nuclear plant technology into an energy system. It presents an insight analysis of the construction cost structure of lead-cooled SMRs and focuses on the specific features that have an impact on the capital costs. The work also offers a comparison with respect to SMRs based on the PWR technology and highlights the benefits and the areas of needed improvement for lead-cooled SMRs to achieve even higher economic competitiveness and attractiveness for investors.

I. Introduction

Some recent literature considers nuclear power plants as megaprojects, each of them representing “an energy infrastructure with a budget of at least USD 1 billion with a high level of innovation and complexity, and with a long-term and far reaching effects on the environment” [1]. Among megaprojects, hydroelectric dams and nuclear reactors have the greatest amount and frequency of cost overruns, even when normalising the overrun per installed megawatt (MW) [2].

Some Generation III/III+ new build reactors give evidence of that, with poor delivery records in terms of both timeliness and budget [3]. Some

authors ascribe this to the increasing complexity of nuclear power plants (NPPs) as megaprojects that would lead to a “diseconomy of scale” and an inability to fully benefit from learning effects [4] [5]. Cost overruns and delays propagate to electricity generation cost because capital cost is the main component (60-85%) of Levelised Cost Of Electricity (LCOE) [6]. Smaller, modular, scalable systems have fewer cost overruns in terms of both frequency and magnitude and both in absolute and relative terms [1]. Coherently, SMRs are expected to cope with the issue of cost overruns and construction delays that undermines the economic sustainability of a NPP project. Their smaller size, design simplification and modularisation are expected

to streamline the Engineering, Procurement & Construction (EPC) and make construction cost more predictable. In the past, the SMR economic paradigm has been inferred and investigated primarily with specific reference to LWRs. While it is still to be proven by evidence from actual construction projects, some SMR concepts of the PWR type (GEN III+) are already in an advanced development stage and a few lead-cooled SMR concepts (GEN IV) are in a conceptual development stage.

This work constitutes the first attempt to calculate/assess the capital cost structure of the LFR SMR, based on the available data provided by the LFR system designers, and compares it with the cost structure of PWR SMRs to discern specific features and characteristics that could enable the application of the SMR economic paradigm.

II. Methodology

This work has been performed in the framework of the Euratom-US International Nuclear Energy Research Initiative (I-NERI) that allowed the collection of original data from the LFR system developers, by means of a questionnaire sent to the I-NERI project partners. The questionnaire sought information on a comprehensive set of economic parameters including tentative breakdown of capital costs.

The data on capital costs considered in this work concern First Of A Kind (FOAK) plants and do not include economies from series-production or fleet deployment. In this work, cost evaluation is performed on a quantitative basis, elaborating the preliminary cost estimates provided by the LFR system developers and does not integrate qualitative considerations on cost reduction potential. None of the SMR considered, either LFR or PWR-type, have ever been built; therefore the analysis makes use of budget costs in both cases.

Capital costs information has been processed according to the cost breakdown structure proposed in the Guidelines developed by the Economic Modeling Working Group (EMWG) of the Generation IV International Forum [7]. Whenever the cost classification was consistent, data have been averaged to highlight common features among the LFR SMR concepts. Due to the early development stage of LFR SMRs, cost information was somewhat incomplete and mainly focused on Capitalised Direct Costs (COA 20, according to [7]). Cost estimation capability for innovative projects is

facilitated as far as Capitalised Direct Costs (CDC) are concerned and fades beyond this perimeter. Indeed, CDC costs are those related to the fabrication and installation of specific equipment, according to the plant layout and preliminary technical specifications. The cost estimates of the equipment may rely on the availability of market prices or of specific quotations made by the industry. On the other hand, Capitalised Indirect Services Costs (CISC) and other complementary costs that summed up give the Total Capital Investment Cost, have either no market reference (e.g., Interests During Construction, escalation), or these costs are country-specific (e.g., insurance, taxes), or case-specific (e.g., land rights, transport costs), or are difficult to estimate at an early development stage of a new plant technology (e.g., staff-related costs, Project Management / Construction Management costs).

Note that the LFR SMR sample did not provide enough information to calculate meaningful results on Capitalised Pre-Construction and Owner's Costs. In the Supplementary Costs category, available information concerns the cost of Initial Fuel Core Load only. Naturally, no information on Financial Cost is meaningful at this stage. As a result, this analysis focuses on three cost categories: CDC (COA 20), Capitalised Indirect Services Costs (COA 30), and Initial Fuel Core Load (COA 55, included in Category 50 related to Capitalised Supplementary Costs).

The comparison with PWR SMRs focuses on CDC only and exploits a proprietary database of Politecnico di Milano [8]. This database contains a bottom-up cost estimation of CDC concerning several GEN III+ PWR SMRs. The PWR SMR sample includes the following types:

1. Integral-PWR, steel containment (pressure-suppression type), helical coil steam generator (SG), and internal primary pumps.
2. Integral-PWR, concrete containment (pressure type), straight tubes SG, and Reactor Pressure Vessel (RPV)-connected primary pumps.
3. Integral-PWR, steel containment (pressure-suppression type), helical coil SG, and natural circulation in the primary circuit.
4. Integral-PWR, steel containment (pressure-suppression type), straight tubes SG, and RPV-connected primary pumps.

A further classification is based on the underground location of the reactor vessel (RV)

that is deep underground (>20 m) for types 2) and 4) and <20 m for types 1) and 3). As a result, for the purpose of this study, the PWR SMR sample has been classified into two groups:

- PWR1 that represents the average cost features of plant types with helical coil SG and foundation < 20 m.
- PWR2 that averages cost features of plants with straight tubes SG and deep underground foundations (> 20 m).

The resulting comparison between LFR and PWR SMRs is consistent benefitting from the use of the same cost accounting structure as recommended in [7]. Figures do not include contingencies and represent expected (best-estimate) values of each cost account.

III. LFR SMR Designs Considered in the Analysis

GEN IV lead-cooled fast reactors include a number of design projects, some of which may be considered to have features typical of SMRs. The LFR concepts represented in the Generation IV International Forum (GIF) System Research Plan (SRP) are based on Europe's European Lead Fast Reactor (ELFR), Russia's BREST-OD-300, and the SSTAR system concept designed in the US.

In addition, a number of lead-cooled concepts (including also those making use of lead-bismuth eutectic) are under various stages of development in numerous countries including the US, EU, Russian Federation, China, Korea, and Japan.

Lead-cooled reactors tend to fall naturally in the SMR definition, since the electric output of the majority of these innovative projects is currently below 300 MWe. Those considered for the purpose of this work range from 3-10 MWe for SEALER and LFR-10, to 300 MWe for Westinghouse LFR prototype3. The use of lead-coolant generally limits somewhat the physical size of systems, due to the density of lead and related buoyancy and seismic isolation considerations.

This work elaborates the information provided by:

- ALFRED (Advanced Lead Fast Reactor European Demonstrator), developed in

the framework of the European Euratom collaboration project LEADER, as a milestone towards the development of a full scale, 600MWe European Lead Fast Reactor [9][10][11][12][13][14].

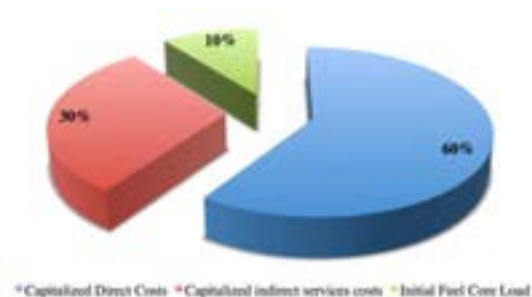
- ALFRED-based small modular LFR (FALCON consortium).
- LFR-AS-200 and its VSMR version LFR-10 (proprietary design of Hydromine Inc.) [15][16][17][18].
- Swedish SEALER (LeadCold Reactors) [19][20].
- Westinghouse LFR [21][22].

First hand information was drawn from the answers to the questionnaire mentioned in Section II (METHODOLOGY) and from [14]. In particular, [14] provides a bottom-up cost estimate of ALFRED.

IV. Results

The analysis of the available data provided by the LFR SMR concept developers results in the average cost structure at one-digit level shown in Figure 1. As can be seen, the Capitalised Direct Costs (CDC) are dominant compared to Capitalised Indirect Services Costs (CISC) and Initial Fuel Core Load cost. In other words, systems and equipment costs that compose CDC are significantly higher than the service costs (CISC) needed to manage and realise the EPC. Such a cost structure could be explained by high-expected shop-built content of LFR SMR projects that might reduce the site-specific work component and the related services.

Figure 1. Cost breakdown of LFR SMR into the three investigated cost macro-categories



³ "It is a lead-cooled, pool-type fast reactor targeting operation by 2030 for a ≤300 MWe prototype that will demonstrate basic feasibility during an initial phase of operation (Phase I). In Phase II the

same technology will be used to develop a ~450 MWe first-of-a-kind plant representative of the commercial fleet"[22]

Nevertheless, in the early development stage, the full identification, simulation and quotation of the activities needed to accomplish the EPC of a new plant concept are not straightforward. As a consequence it might also be that CISC are currently underestimated.

Figure 2 introduces a further breakdown of CDC into the two-digit level COA according to [7]. Error ranges are indicated, taking as a lower and upper bound the minimum and maximum cost record in the sample, respectively, per each cost item. The highest uncertainty is present for CDC, with an expected value of 60% in the cost breakdown structure, and a range of 27 percentage points between the minimum and the maximum values (that are 50% and 77% respectively). Inside the CDC category, the reactor equipment cost shows the highest uncertainty (i.e. 12 pp between the minimum and the maximum values, that are 25.6% and 37.4% respectively). This is not surprising, since the reactor equipment represents the most innovative part of the LFR plant. Moreover, quotation of new systems and materials has no easy reference to market prices. The cost of categories “structures and improvements” and “turbine generator equipment” shows lower uncertainty of the estimates. These costs refer to civil works & building construction, and to the secondary system, respectively. These plant parts have more conventional features and are less affected by the groundbreaking nature of the primary system. The interesting finding is the extent of the uncertainty and the fact that it is often skewed towards the higher end: e.g., [-9; +18 pp] with respect to the average value of CDC; [-0.4; +5.2 pp] with respect to the average cost of structures and improvements; [-4.4; +7.4 pp] with respect to the average cost of reactor equipment.

Interesting findings arise from the comparison of the three main cost accounts of CDC: i.e., structures and improvements, reactor equipment and turbine generator equipment. Figure 2 shows that reactor equipment cost is much higher than costs of structures & improvements and of turbine generator equipment. This is confirmed by results displayed in Figure 3, where CDC breakdown is represented in percentage terms and compared to the two reference PWR SMR designs (PWR1 & PWR2).

Results show that the LFR technology reverses the relative weight of the cost items: reactor equipment is by far the most expensive category (50% of CDC), followed by structures & improvements (24%) and turbine generator

equipment (19%). In the case of PWR SMRs, independently of the plant type, structures & improvements are the most expensive cost item (37-45%), followed by the reactor equipment and the turbine generator equipment, that have the same weight in the CDC composition (23-27% and 22-26% respectively) (Figure 3).

Figure 2. Cost breakdown of a LFR SMR into the one-digit COA (black-outlined bars) and breakdown of CDC into the two-digit COA (light blue bars)

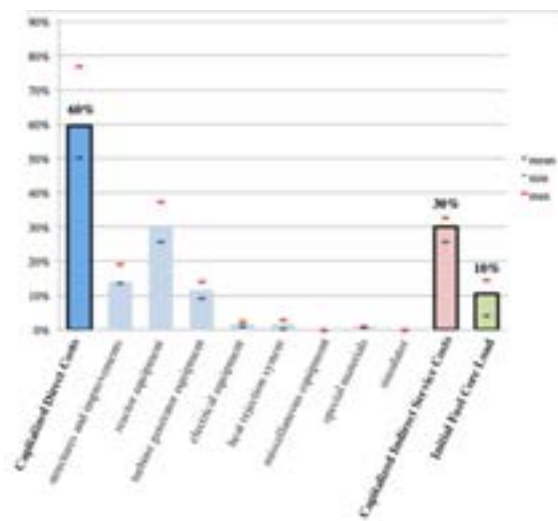
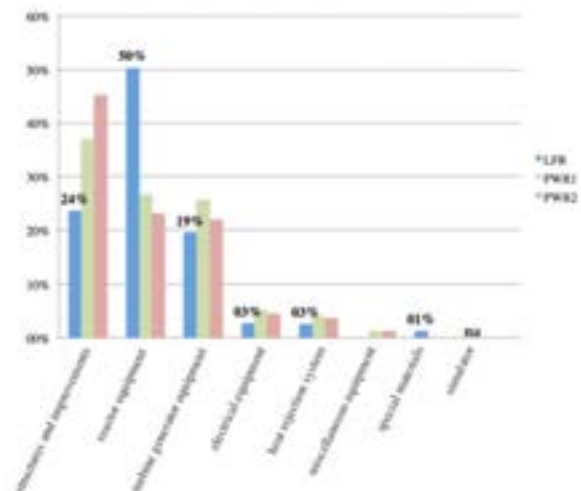


Figure 3. Two-digit cost breakdown of CDC of a LFR SMR and the two defined PWR SMR types

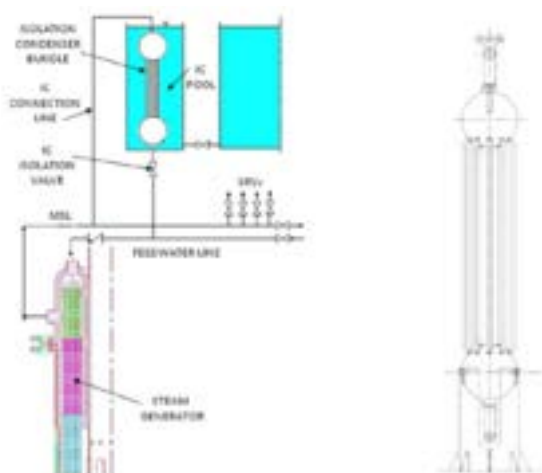


The following considerations may provide further understanding of these findings.

1) Primary system costs include costs for safety systems, that in the available economic information are often accounted separately as “auxiliary systems”, while they must be properly accounted in the reactor equipment cost. Auxiliaries deal with primary coolant purification and related liquid and gaseous waste processing systems, fuel transfer machine and fuel handling, and safety systems. Conceptual designs show that LFR safety relies on diverse and redundant decay heat removal (DHR) heat exchangers. As an example, ALFRED is equipped with eight Isolation Condenser (IC) systems connected to the secondary side of SGs (Figure 4) [10].

Strategies that contribute to the safety of PWR SMR, such as reactor vessel flooding, automatic depressurisation system, borated water delivery to the RV[23][24], are less expensive than heat exchangers. On the other hand, it should be highlighted that lead-alloy coolants have excellent cooling properties (specifically high natural convection capability, thermal inertia as well as boiling point/1749°C for lead) that result in a substantial improvement of passive safety. Nevertheless, some LFR designs aim at an unprecedented level of safety, thereby implementing higher redundancy and featuring thus a higher number of emergency heat exchangers per reactor unit than PWR SMRs.

Figure 4. ALFRED, representation of one of the eight isolation condenser safety systems, connected to a SG (left), and IC bundle (right)



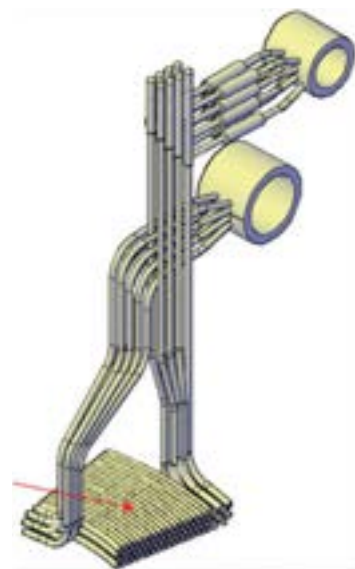
2) Different design and safety criteria (aiming at improved redundancy & independence) drive in turn the primary system arrangement. Some LFR SMRs feature a higher number of SGs compared to their PWR counterparts. The SEALER small power unit (3-10 MWe) has eight SGs with a primary pump (PP) integrated in each SG; the same applies to ALFRED. By comparison, the PWR-type NuScale PWR module/unit (50 MWe) has two helical-coil SGs, while the mPower (125 MWe) and the Westinghouse PWR SMR (225 MWe) rely on a single SG per reactor unit. NuScale has no primary pumps and operates in natural circulation mode.

Nevertheless, despite the reduced speed of lead coolant, all types of LFR SGs have advantages in term of compactness with respect to LWR SGs, due to:

- (i.) generally, a higher temperature difference between primary coolant and water/steam coolant,
- (ii.) a higher heat transfer coefficient,
- (iii.) in the case of the spiral tubes SG, a reduced pitch among the tubes, resulting in a tube bundle with half the volume of a helical-tube bundle.

The mass of LFR SG tubes is reduced with respect to LWR SG; also, in the case of a spiral-tube SG, the primary pressure loss is limited to half the pressure loss of a helical-tube SG[15].

Figure 5. Spiral-tube SG (STSG) is made of superposed plane tube-spirals



However, if compact SGs allow reducing the LFR primary system volume and the mechanical load, on the other hand their fabrication might be more expensive in terms of assembly and auxiliary activities, such as engineering, quality control and stress analysis.

This can be inferred by the following considerations. For a helical-coil SG of a PWR SMR, the cost of material and fabrication of SG components represents 50% of total SG cost; the cost for the assembling of SG components accounts for some 20% and, mainly due to the tubes bending, the cost for engineering, quality control and stress analysis is about 30%. However, in this context, it has been estimated that the cost of auxiliary activities decreases significantly over a batch of eight SGs, down to 10%, due to series production economies, while the decrease in the assembling cost is not relevant [8].

On the contrary, a single, straight tube SG for PWR SMR has 81% cost for material and components fabrication, 7% cost of assembling and 12% cost of engineering, quality control and stress analysis.

Further analysis is therefore needed to evaluate the economics of fractioning the heat exchange surface into multiple short-height/compact SGs with integrated primary pumps : on one side, there is a loss of economy of scale compared to PWR SGs and the duplication of fabrication tasks and components for multiple SG/PPs; on the other side, there is a higher standardisation potential for smaller sized SGs and consequent cost reduction from series production.

3) The LFR primary system requires the qualification of innovative special alloys and surface coatings (e.g., Alumina-Forming Austenitic or Oxide Dispersion Strengthened steels) for structural materials and for the most thermally-loaded components such as fuel claddings, steam generators, and/or heat exchangers. These materials must cope with environmental conditions of high-temperature molten lead and related corrosion-erosion effects, together with irradiation damage.

The cost for the supply and qualification of innovative materials as compared to the steels used in PWR has not been considered yet in the cost evaluation and will need further investigation to understand whether it will correspond to a higher price. Special material technological solutions are needed for the primary pumps as well, where the pump impeller may be exposed, in some designs, to a coolant velocity up to 10 m/s.

4) Benefitting from low partial vapor pressure of molten lead ($2.9 \cdot 10^{-5}$ Pa at 400°C), lead primary coolant can be maintained at near atmospheric pressure, avoiding the need to maintain complex (and expensive) structures to provide pressure boundaries in LWRs. The studied LFR SMRs have low-pressure integrated primary systems, with reduced vessel height compared to PWR SMRs. RV height in a LFR SMRs ranges from 3.5 m for the LFR-10 concept to 10 m for ALFRED. Average RV height in a PWR SMRs is around 20 m, even for very small power units. Nevertheless, the vessel diameter in the currently investigated LFRs is relatively larger and the result is a higher volume-to-power ratio of LFR SMRs compared to LWR [25]. LFR primary system compactness depends on the equipment arrangement and on other innovative solutions such as extended fuel assemblies to be handled by ex-vessel refueling machine, ex-core control rods, self-sustaining core, etc. Short-height SGs with integrated mechanical pump are a key provision to achieve the goal of design compactness. Nevertheless, volume-to-power ratios are generally above $3 \text{ m}^3/\text{MWe}$ in the current LFRs (with the exception of LFR-AS-200 whose primary systems design would correspond to about $1 \text{ m}^3/\text{MWe}$) and often below $2 \text{ m}^3/\text{MWe}$ in LWR SMR [25].

Figure 6. Cross-cut view of the very compact SEALER Reactor Vessel (2.7x6.0 m)



5) To improve security and safety of the nuclear island, some PWR SMR developers foresee the deep underground siting of reactor containment with associated primary systems.

While this solution might improve social acceptance, it poses, on the other hand, significant realisation drawbacks, in particular due to the need for dewatering in order to ensure long-term structural resistance to buoyancy. Underground foundations deeper than 20 m translate to very high costs [8]. As a consequence, in PWR SMRs the cost of “structure and improvements” category increases such that it overweights the relative contribution of “reactor equipment” cost, especially for PWR type 2. Note that PWR type 1 shows high cost for structures and improvements as well, compared to LFR; foundation cost is also of significance even though it is lower than for PWR2. It has to be noted that in the bottom-up cost estimate of every PWR SMR, foundation and dewatering have been accounted for, while in the cost estimate of some LFR SMR concepts, this cost has been explicitly excluded, cf. [14]. However, even if LFR concepts do not currently propose deep underground foundation, data gathered for LFR do not allow drawing meaningful conclusions on the full extent of structures and improvement costs.

6) Finally, the reactor equipment cost includes a “special material” cost account that, in LFRs, represents the coolant lead inventory. This cost is only 1% of CDC, while coolant cost is not included in PWRs.

V. Conclusion

This work contributes to the economic assessment of the innovative LFR SMR concepts currently under development. In particular, the results aim at providing LFR developers with useful input to assess the plant layout and system & component design from an economic perspective.

The analysis points out interesting differences in the cost structure of studied LFRs compared to PWR SMRs: namely, the LFRs show a relatively higher cost of the reactor equipment in comparison to costs of structures and improvements and of the Balance of Plant (BoP).

To gain better insight into the different cost composition, this work examined the safety approach and configuration of primary systems (DHR system, RV and SG size and layout) implemented in the considered PWR and LFR SMR concepts. Additionally, supply and qualification of innovative structural materials as well the impact of potential underground siting were also considered.

As far as the primary system equipment is suitable for factory-fabrication and for the application of the “economy of replication”, with mini-serial production, standardisation, improved quality and wider supply chain options, these aspects might be particularly beneficial for LFR SMRs. A deployment of fleet strategy would cut these costs more than those of structure and improvements, unless the cost of special materials and special technical solution would hamper the cost reduction.

It should be noted that the comparison of the cost structures of LFRs and PWR SMRs is made on a relative (percentage) basis only and it is therefore not meaningful and not intended to derive conclusions about absolute cost competitiveness of the two plant categories, but only about their different relative cost structures.

At the same time, while the cost of the reactor equipment appears as a dominant cost category for LFR SMRs, it is also recognised that additional data would be necessary to assess the full extent of the structures and improvement costs, as well as of Construction Indirect Services Costs for LFR SMRs.

Further research should also be devoted to the consideration of non-fully quantifiable advantages of the LFR SMRs, that contribute to the economic benefit on a broader societal perspective, or that provide complementary benefits other than economic (e.g., security, sustainability, development objectives, environmental compatibility).

Acknowledgements

The authors wish to acknowledge the I-NERI partners that participated to this work providing technical-economic information on the LFR SMR concepts under development and giving fruitful contribution to the review of this paper.

Nomenclature

ALFRED	Advanced Lead Fast Reactor European Demonstrator
BoP	Balance of Plant
BREST-OD-300	Bystryi REactor so Svintsovym Teplonositelem
CDC	Capitalised Direct Costs
CISC	Capitalised Indirect Service Costs

COA	Code Of Account	LEADER	Lead-cooled European Advanced Demonstration Reactor
DC	Dip Cooler		
DHR	Decay Heat Removal	LFR	Lead-cooled Fast Reactor
ELFR	European Lead Fast Reactor	LFR-AS-200	Lead Fast Reactor-Amphora Shaped-200
ELSY	European Lead System		
EMWG	Economic Modeling Working Group of the Generation IV International Forum	LWR	Light Water Reactor
		NPP	Nuclear Power Plant
EPC	Engineering, Procurement & Construction	PP	Primary Pump
		PWR	Pressurised Water Reactor
FOAK	First Of A Kind	RPV	Reactor Pressure Vessel
GEN-IV	Generation IV	RV	Reactor Vessel
GEN III+	Generation III+	SEALER	Swedish Advanced Lead Reactor
GIF	Generation IV International Forum	SG	Steam Generator
IC	Isolation Condenser	SMR	Small Modular Reactor
I-NERI	International Nuclear Energy Research Initiative	SRP	System Research Plan
LCOE	Levelised Cost of Electricity	SSTAR	Small Secure Transportable Autonomous Reactor
		VSMR	Very Small Modular Reactor

References

- [1] M. Mancini and G. Locatelli, "Power Plants as Megaprojects: Using Empirics to Shape Policy, Planning and Construction Management", *Utilities Policy*, vol. 36, pp. 57-66, October 2015.
- [2] A. Gilbert, D. Nugent and B.K. Sovacool, "An international comparative assessment of construction cost overruns for electricity infrastructure", *Energy Research and Social Science*, vol. 3, pp. 152-160, 2014.
- [3] M. Mancini and G. Locatelli, "Looking back to see the future: building nuclear power plants in Europe", *Construction Management and Economics*, vol. 30, no. 8, pp. 623-637, 2012.
- [4] A. Gilbert, D. Nugent, B.K. Sovacool, "Risk, innovation, electricity infrastructure and construction cost overruns: testing six hypotheses", *Energy*, vol. 74, pp. 906-917, 2014.
- [5] A. Grubler, "The costs of the French nuclear scale-up: a case of negative learning by doing", *Energy Policy*, vol. 38, no. 9, pp. 5174-5188, 2010.
- [6] W.D. D'haeseleer, "Synthesis on the Economics of Nuclear Energy", Study for the European Commission, DG Energy 2013.
- [7] The Economic Modeling Working Group Of the Generation IV International Forum, "Cost Estimating Guidelines for Generation IV Nuclear Energy Systems", Revision 4.2 GIF/EMWG/2007/004, 2007.
- [8] S. Boarin and G. Dodich, "SMRs cost evaluation: from Top-Down to Bottom-Up", Politecnico di Milano, Graduate Thesis <https://www.politesi.polimi.it/handle/10589/84726>, 2013.
- [9] A. Alemberti, "ALFRED", Santa Fe, Mexico City, Consultants' Meeting: Education

- Training Seminar on Fast Reactors, 29 June -03 July 2015.
- [10] M. Frogheri, L. Mansani and A. Alemberti, "The Lead Fast Reactor Demonstrator (ALFRED) and ELFR Design", In International Conference on FAST REACTORS AND RELATED FUEL CYCLES: Safe Technologies and Sustainable Scenarios - FR13, Paris, France, 4-7 March 2013.
- [11] M. Tarantino on behalf of Falcon Consortium, "ALFRED Project: Energy Conversion System", in ESNI Biennial Conference, Brussels, Belgium, 17-18-19 March 2015.
- [12] A. Alemberti (Ansaldo Nucleare), "Final Report Summary - LEADER (Lead-cooled European Advanced Demonstration Reactor)", LEADER Report Summary, 2014.
- [13] A. Alemberti, L. Mansani and M. Frogheri, "The Advanced Lead Fast Reactor European Demonstrator (ALFRED)", in The 15th International Topical Meeting on Nuclear Reactor Thermal - Hydraulics, NURETH-15, May 12-17, 2013, Pisa, Italy.
- [14] M. Vasquez and F. Roelofs, "Cost Estimation for the LFR and the ETDR", 092-219-E-S-00001, LEADER DEL 30, 2013.
- [15] L. Cinotti, "Designs for Fast Reactors: Spiral-Tube Steam Generators for compact integrated reactors - The ELSY project", Vienna, IAEA Technical Meeting on Innovative Heat Exchanger and Steam Generator Designs for Fast Reactors, December 21-22, 2011.
- [16] L. Cinotti, "Novelty of the LFR-AS-200 project", February 9, 2017, Presentation for invited audience.
- [17] L. Cinotti, "Simplification, the atout of LFR-AS-200", in International Conference FR17, Yekaterinburg, (Russia), June 27, 2017.
- [18] L. Cinotti, "The innovations of the LFR-AS-200 project", July 12, 2016, Presentation to invited audience.
- [19] "Lead-cooled reactors for electricity generation in Arctic areas", in Energiforsk, Stockholm, 2017.
- [20] LeadCold. www.leadcold.com. [Online]. <https://www.leadcold.com/sealer.html>
- [21] Westinghouse. <http://www.westinghousenuclear.com>. [Online]. http://www.westinghousenuclear.com/Portals/0/new%20plants/LFR/ECOE-0002_LeadFastReactor.pdf
- [22] F. Franceschini. (2018, January) The Westinghouse Lead Fast Reactor. [Online]. <https://www.ne.ncsu.edu/event/westinghouse-lead-fast-reactor/>
- [23] R. F. Wright and M. C. Smith, "Westinghouse Small Modular Reactor Passive Safety System Response to Postulated Events", in ICAPP '12, Chicago, USA, 2012.
- [24] NuScale Power. <http://www.nuscalepower.com>. [Online]. <http://www.nuscalepower.com/smr-benefits/safe/reactor-modules>
- [25] D. T. Ingersoll, "Chapter 7: Expanding Nuclear Power Flexibility - Section 7.1: Size matters", in "Small Modular Reactors: Nuclear Power Fad or Future?", Woodhead Publishing, vol. 90, 2016.

EMWG POSITION PAPER ON THE IMPACT OF INCREASING SHARE OF RENEWABLES ON THE DEPLOYMENT OF GENERATION IV NUCLEAR SYSTEMS (A. MENDOZA ET AL)

Alberto Mendoza⁽¹⁾, Ramesh Sadhankar⁽²⁾, and Michel Berthélemy⁽³⁾

(1-2) Canadian Nuclear Laboratories, Canada

(3) French Alternative Energies and Atomic Energy Commission, France

I. Introduction

In the past several decades, market liberalisation and climate change policies are two key factors that introduced changes in the electricity sector.

Across the globe, the market structure of electricity is characterised by liberalisation, which began in the 1980s [1-3]. An outcome of market liberalisation has been a greater focus on wholesale (generation) and retail competition. In some cases, this has led to lower prices; thus, a lower incentive to invest in new capacity and energy conservation [4] [5].

Over a similar period, nations introduced climate change policies to pursue lower greenhouse gas emissions, which included the adoption of renewables. Some countries, for example, Canada, France, Germany, and the United States [6-8], experienced an increasing share of renewable sources for electrical power generation as part of their climate change policies.

The adoption of variable renewables was incentivised in part by subsidies [9] [10]. Technology improvements and the resulting lower investment costs for renewables also led to increasing capacity, particularly for solar photovoltaic generators. The increasing use of variable renewables creates grid management challenges [11]. Renewables are being given priority when connecting to the grid; in which case, dispatchable generation sources are required to load follow to meet the residual demand. This could lead to forced outages of nuclear plants and in some cases early retirements due to unfavourable economics [12].

The Economic Modeling Working Group (EMWG) of the Generation IV International Forum (GIF) has been looking at the challenges of deploying Generation IV reactors in markets with a significant share of renewable resources. The paper will discuss EMWG's work related to economic assessments and methodologies, and will highlight and identify the requirements for the advanced reactors for integration with renewable resources.

The paper will first discuss the key grid management challenges (section II). Section III identifies the economic impact of integrating renewables in a grid. Section IV discusses recent policies that may enable the deployment of advanced reactor systems. Recommendations are made in the concluding section (V).

II. Reliability and Flexibility

The key grid management issues are reliability and flexibility of power supply to the consumers [12] [13]. Reliability refers to the resource adequacy and operation capability of an electrical system [13]. In an electrical system, reliability operates at different timescales ranging from the short-term to long-term scale [13].

Power system flexibility is defined as the ability of a resource, whether any component or collection of components of the power system, to respond to the known and unknown changes of power system conditions at various operational timescales [14].

The reasons for needing flexible and reliable operations stem from demand variation, matching generation to demand, generators

providing reserve, and the adoption of variable renewable generation [15].

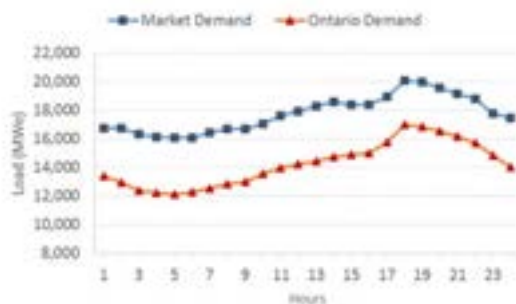
The case of nuclear power generation in Canada (in particular, Bruce Power Station in Ontario) is used to highlight the need for flexibility, and implementation of operational flexibility. Ontario's current electricity mix is summarised in Table 1 [16].

Table 1. Ontario's Electricity Mix in 2016

	Installed Capacity	Production in 2016
Total (GWe)	36.5	17.2 (avg.)
Nuclear	35%	61%
Hydro	23%	24%
Gas/Oil	28%	9%
Renewable (Wind/Solar/Biofuels)	13%	6%

Figure 1 (data from [17]) shows the load for market (includes net exports) and Ontario demand for electricity over a 24 hour period. The load profile in this example indicates a peak load is reached in the evening (around 18 h), which was typical for Ontario from 2002-2016 [18].

Figure 1. Market and Ontario Demand for Electricity (January 1, 2016)



During this period, hourly nuclear power generation at Bruce Power Stations fluctuated (Figure 2, data from [19]) in a similar manner to adjust for hourly demand changes.

In addition, nuclear power generation in Ontario fluctuates monthly (Figure 3, data from [20]) over the year to adjust for seasonal changes in demand.

Figure 2. Nuclear Power Generation at Bruce Power Stations (January 1, 2016)

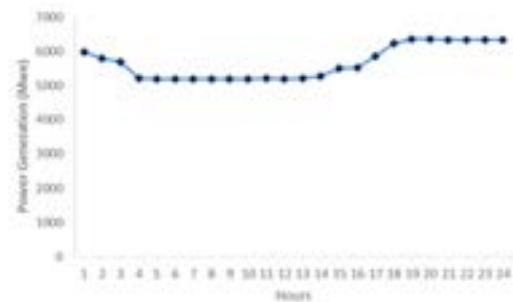
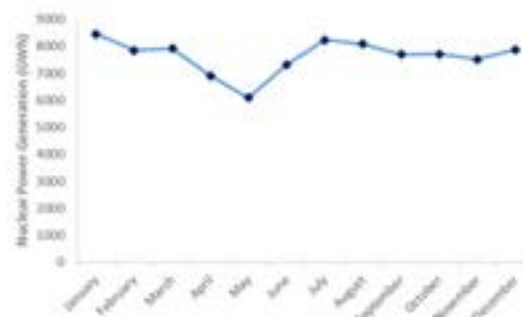


Figure 3. Monthly Nuclear Power Generation in Ontario, Canada in 2016



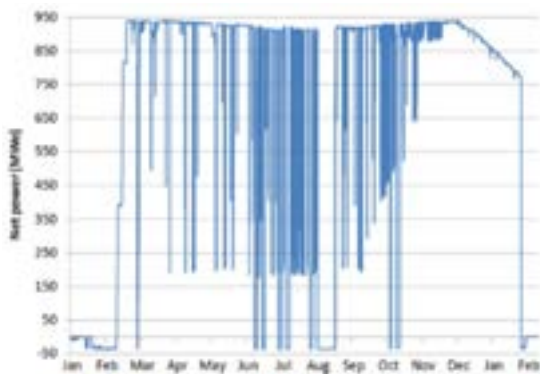
The increasing share of renewable sources of electrical power generation has led to surplus baseload electricity generation, which has resulted in baseload sources operating at a lower capacity [21] [22]. In 2016, there were 393 nuclear reductions due to surplus baseload generation, and two shutdowns which accounted for approximately 1% loss in the total base-load generation capacity of nuclear power plants in Ontario [25].

Furthermore, the grid operator, Independent Electricity System Operator (IESO) performed a review of the operability of the grid assuming the variable renewable capacity increased to 10 GWe from the current capacity of about 5 GWe [23]. This study noted that additional flexible resources will be required to compensate for inaccuracies in hour-ahead forecast of variable generation resources 95% of the time. Another IESO study [24] found that small amounts of energy storage could be useful to help manage the generation fleet by providing flexibility to address demand fluctuations and overcoming the inflexibility of the intermediate fleet brought about by high minimum loading points and long minimum run-times.

In France, 80% of the electricity is currently produced by nuclear reactors of the Électricité de France (EDF) fleet. Therefore, the entire French nuclear fleet participates in frequency services (primary and secondary reserves) and two-third of the plants are used for load-following (Figure 4).

In EDF reactors, load-following is implemented through control rods supplemented with grey rods that have a lower neutron capture effectiveness. Grey control rods and primary coolant temperature variation allows significant operating flexibility for French nuclear plants (down to 20% of rated power during two third of the fuel cycle). The combination of load-following capabilities with the size of the nuclear fleet allows EDF to achieve significant shifting of the nuclear load that can reach more than 12 GWe of nuclear capacity over a few hours (i.e., 20% of France installed nuclear).

Figure 4. Annual Load Following Profile of Blayais 2 Nuclear Power Plant in France



France plans to reduce the share of nuclear power to 50% and to increase that of renewable power to 40% by 2030 [21]. This may put additional demand of flexibility on French nuclear reactors but also impact the overall management of the fleet. For instance, there may be a trade-off between level of load-following and the planning of plants outages during the period of low electricity demand.

In Germany, the renewable resources generate about 30% of the total electricity. Large variations in renewable generation requires nuclear plants to have enhanced load-following capabilities, which adversely affects the economics of nuclear power generation. The load-following capabilities were built-in at the construction of the German nuclear fleet, but

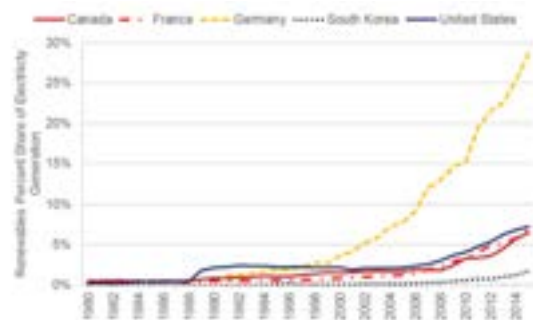
have only started to be used recently in response to renewables intermittency.

Operational flexibility depends on technical, regulation and electricity market structure aspects of generating power. For more details on the technical and economic aspects of flexible nuclear power generation, the reader is deferred to [26-30], which include a discussion on international operating experience.

III. Cost & Price of Electricity Effects on Baseload

Over the past several decades, OECD nations such as Canada, France, Germany, South Korea, and the United States experienced an increasing share of variable renewable power generation (Figure 5, data from [31]).

Figure 5. Increasing Share of Renewables (Non-Hydro)



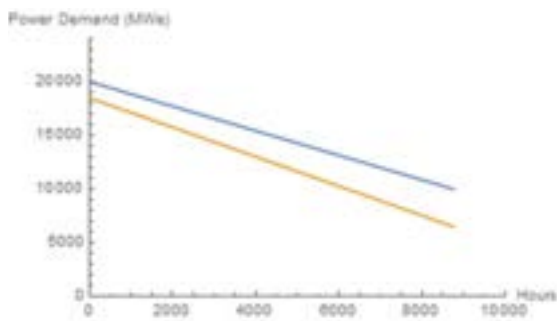
In the last few decades, the share of nuclear power generation declined in Germany and South Korea, while Canada, France, and the United States experienced relatively stable shares of nuclear power generation (Figure 6, data from [31]).

Figure 6. Share of Nuclear Power Generation



The reduction in the capacity factor for nuclear generation plants in part stems from renewable sources receiving preferred treatment in supplying electricity to the grid. As a consequence, baseload generation sources must compete amongst themselves for residual demand, shown in Figure 7 (based on a linear approximation of load and residual load curve [22] [32]).

Figure 7. Load and Residual Demand



The significance for surplus baseload power generation is lower capacity factors. In turn, lower capacity factors mean higher unit costs of generating electricity, which reduces profitability [33]. For example, baseload technologies with higher variable costs have greater losses [33]. Thus, surplus baseload electricity generation reduces the economic feasibility of baseload electrical power generation sources, such as nuclear energy.

Table 2 (data from [34]) provides a list of OECD nations that have also implemented liberalisation policies in electricity markets, such as competition in wholesale pricing.

Table 2. Deregulated Electricity Markets

Country (and Province or State, if applicable)	Year of Deregulation
Canada (Alberta)	2001
Canada (Ontario)	1999
France	2001
Germany	2000
South Korea	2000
USA (Texas)	2002
USA (New York)	1999

The list in Table 1 is not exhaustive, since nations such as Canada and the United States have provincial or regional electricity markets, which are not included in the table.

Baseload power generation may experience lower wholesale prices as shares of renewables increase and as liberalised market policy is implemented; as illustrated by the example below.

Figure 8 shows the ranking of power generation according to price bids entered in the wholesale market auction. Each technology's power capacity is ordered from lowest to highest bid price – the merit order. In Figure 8, renewables offer the lowest bid price, and coal the highest bid price. Each technology is assumed to have equal generating capacity. The market price is determined by the highest bid that fulfills market demand for electricity.

Figure 8. Merit Order Pricing

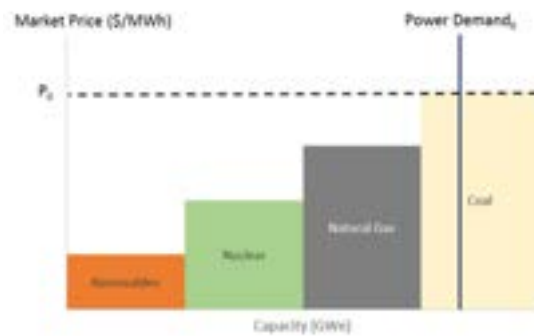
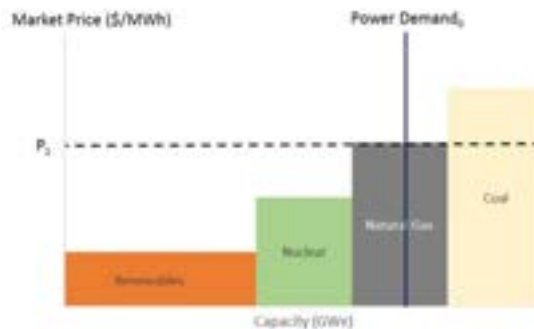


Figure 9 shows the impact of doubling the renewables generation. As the capacity of renewables increases, other power sources are displaced, such as coal, and the wholesale market price declines, but the nuclear generation might not be affected. The reduction in price means potentially lower revenue for electric utilities.

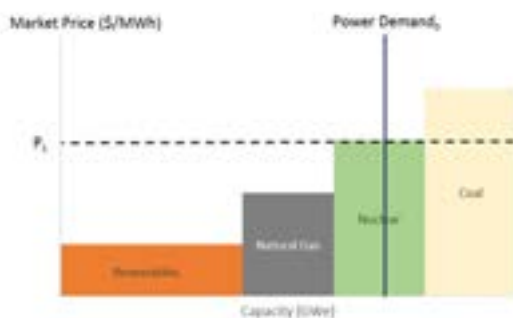
Figure 9. Merit Order Pricing with no Effect on Nuclear by Increasing the Share of Renewables



This example also illustrates the impact of generation mix. If the current generation is predominantly dominated by nuclear, for example up to 75% in the case of France, an increase in renewables by up to 25%, with priority dispatch will adversely affect the load factor and hence the economics of nuclear generation. For a medium but dominant share of nuclear on the grid (for example up to 60% in case of Ontario, Canada) nuclear may or may not be adversely affected depending on the generation capacity of other dispatchable sources like gas turbines and on the potential for demand side management.

Figure 10, like Figure 9, shows the impact of doubling the renewables generation, but unlike Figure 9, Figure 10 shows that nuclear generation is adversely affected. Figure 10 depicts a merit order scenario that is consistent with current nuclear power generation economics in the United States. A Department of Energy study concluded that “low-cost, abundant natural gas and the development of highly-efficient NGCC plants resulted in a new baseload competitor to the existing coal, nuclear, and hydroelectric plants”, and are the biggest factors contributing to coal and nuclear plant retirements [12].

Figure 10. Merit Order Pricing Effect with an Effect on Nuclear by Increasing the Share of Renewables



Since the integration of variable renewable energy sources into a grid requires taking into account more than just the cost associated with generation, the use of levelised costs of electricity (or full life-cycle costs (fixed and variable) of a power generating technology per unit of electricity) as a metric for comparing alternative energy sources is considered flawed [35-39]. When grid system costs are addressed explicitly, several cost issues may be observed, for instance: (1) increasing costs due to higher curtailment [37] [40]; (2) increasing costs for

balancing services through higher operating reserves [41]; and (3) additional investment in grid upgrades [33].

The OECD NEA evaluated the additional cost imposed on grid system costs by integrating renewables, such as wind onshore, wind offshore, and solar for six OECD countries (Finland, France, Germany, South Korea, United Kingdom, and United States). In a grid system with 10% penetration level of three types of renewables (onshore wind, offshore wind, and solar), the average annual cost of electricity supply is greater compared to that for the reference grid mix consisting of conventional dispatchable technology [33]. As the penetration level of renewables increases to say 30%, system grid costs will still increase [33].

IV. Trends in Policies to Make Nuclear Deployment Competitive

Various policies have been tried out and/or implemented in different jurisdictions to encourage greenhouse gas emission reduction. As discussed in Section III, some of the policies such as market liberalisation and priority dispatch for renewables adversely affects the economics of nuclear generation. However, some other policies may improve the economics of nuclear generation and could be conducive to future nuclear deployment. Policy issues to enable nuclear deployment are taxes and credits, electricity pricing, and financial arrangements.

IV.1 Zero emission credits and carbon taxes

In response to the possibility of a premature closure of nuclear power plants some regions in certain countries considered implementing zero emission credits (which are similar to renewable energy credits [38]), for example, New York, Illinois, Connecticut, New Jersey, Ohio, and Pennsylvania in the United States that allows utilities with nuclear power plants to apply for such credits [12] [42]. The value of the zero emission credits ranges from USD 10 per megawatt-hour (MWh) in Illinois to USD 17.48 per MWh in New York [42]. In the case of New York, the zero emission credits are first purchased by the load serving entity, and the cost of the credit is recovered from customer bills [42]. Such a program has been challenged, and in some cases, the challenges have been dismissed though there continues to be opposition to such programs [43].

A potential issue for nuclear is that zero emission credits are based on power generation

in a given year [44]. If the share of renewables increases, then the total value of the zero emission credit from nuclear power generation may decline over time, especially in jurisdictions that provide priority for renewables. Another potential issue is that the timing of receiving the credit may not come quickly enough to offset the rising costs of generating power as the renewable share of electricity generation rises, which may require additional debt load if revenues are declining and there is insufficient working capital.

A carbon tax is a tax set by government in terms of dollars per ton of carbon dioxide (CO₂) emitted [45]. The carbon tax is part of annual costs incurred by a utility. The introduction of a carbon tax would likely make nuclear more competitive [21] [46]. Different carbon taxes may be adopted by different OECD regions to enable nuclear power more competitive. Regional differences can reflect different manufacturing culture, environments for regulation and public acceptance of nuclear plants [47]. Furthermore, break-even carbon tax will depend on the prices of fossil fuels in different regions of the world.

IV.2 Financing and electricity pricing

Financing nuclear power project remains a challenge today [48]. Raising capital for new nuclear plants will be more challenging in markets where nuclear is required to be integrated with renewable resources on the grid causing low capacity utilisation of the plant.

The underlying trend is that government support is still used and is the leading source of finance in the nuclear industry for the deployment of new nuclear reactors [48]. Three prominent ways government provides financial support to the nuclear industry are:

- 1) loan guarantees, for instance, Vogtle nuclear power plant in the United States, and Wylfa nuclear power plant in the United Kingdom [48] [49];
- 2) guaranteed long term electricity contractual agreements, for example, strike price in the United Kingdom, and Power Purchase Agreement for Bruce Power in Canada [48] [49]; and,
- 3) export credit agency financing, for instance, Rosatom uses Vnesheconombank (state-owned bank) to finance the exporting of Water-Water Energy Reactor (VVER) [48-50].

Even though the government's financial role still dominates the deployment of new reactors, governments are looking for private sector participation [48]. Private financing schemes used are corporate financing, investor financing, and vendor financing [48]. Private sector financing has gained some momentum but is still constrained by the consequences of the 2017-2018 global financial crisis, which limits financing, still seeks government support, and puts a risk premium on nuclear projects based on past performance [48]. Reducing project and liquidity risks are, therefore, important factors to consider for future research. New financing mechanisms will be vital for the deployment of future nuclear builds [48]. In this regard, the regulated asset base model has been proposed in the United Kingdom as an alternative to using a strike price and direct investment for financing a new nuclear reactor deployment [51].

Another issue associated with financing the deployment of new capacity in the context of liberalised markets is the price of electricity [52]. In order to offset the volatility of wholesale market prices and potential decline in prices, a fixed contract may be used when an electric utility with nuclear power generation has to use load following mode. As an example, the case of Bruce Power will be provided.

In 2015, Ontario's Independent Electricity System Operator signed an agreement with Bruce Power to secure 6,300 MWe from Bruce Power Stations (A and B), with an initial (starting January 1, 2016) price of electricity of USD 65.73/MWh, and an average price over the agreement lifetime of about USD 77/MWh [53] [54]. The higher price over the lifetime of the agreement accounts for refurbishment costs [53].

Figure 11 shows that Bruce Power Stations power level was typically below baseload capacity (6,300 MWe) during a 24 hour period on January 1, 2016.

Figure 11. Load Following (January 1, 2016) versus Baseload Power Generation

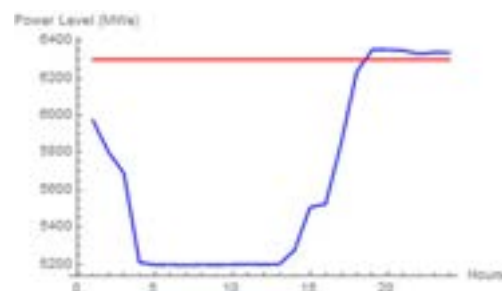
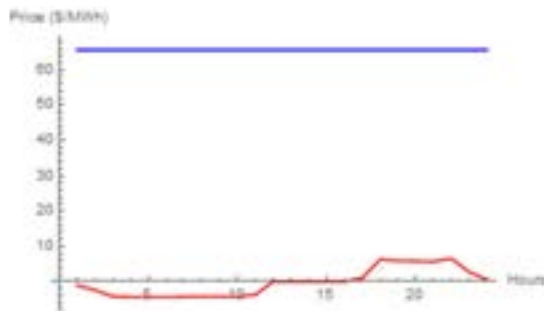


Figure 12 shows the initial contract price for Bruce Power was higher than the hourly wholesale electricity price in Ontario.

Figure 12. Fixed Price for Bruce versus Hourly Prices in Ontario Electricity Market on January 1, 2016



In order to show that a fixed price has benefited Bruce Power, Table 3 calculates the daily revenue for four cases, each case consisting of a price type and power mode. In the fixed price cases, the initial contract price was assumed, while the hourly price is based on the hourly wholesale electricity price on January 1, 2016 (see Figure 12). Note that the cases II, III, and IV are hypothetical, since they did not materialise.

Table 3. Daily Revenue for Different Types of Pricing and Power Modes

Cases	Price Type and Power Mode	Daily Revenue (Canadian Dollars)
I	Fixed Price and Baseload Power	USD 9,441,457
II	Fixed Price and Load Following	USD 8,933,956
III	Hourly Price and Baseload Power	USD 44,648
IV	Hourly Price and Load Following	USD 4,860

The daily revenue from load following with a fixed price would be USD 8,933,956 (CDN), while the daily revenue from baseload with a fixed price would have been USD 9,441,457 (CDN) at the initial price of USD 65.73/MWh. If on the other hand, an hourly price were used for both baseload and load following, then the daily revenue would have been lower than with a fixed price of USD 65.73/MWh.

The financial impact on consumers in the short-term (during refurbishment) will likely be an increase in electricity costs; however, the agreement is “projected to provide ratepayers with a long-term supply of relatively low-cost, low emissions electricity [54].

Other measures have been proposed to ensure viability of baseload generation and to ensure reliability and resiliency of the grid. These include compensation for reliability of generation including on-site fuel supply and requiring grid operators to include a level of nuclear generation [12].

V. Conclusion

Increasing share of renewable resources, supported by government incentives, and having priority for dispatch are creating new challenges for grid management requiring increasingly more flexible operation of other generators including nuclear plants. Currently, some of the nuclear plants (e.g., in France and Germany) already operate in flexible mode. Recognising the projected growth in renewable resources on the grid, the utilities have drafted requirements for flexible operation for new nuclear reactors. This will require Generation IV advanced reactors for future deployment to be more flexible compared to current generation reactors to be able to operate in a system with significant intermittent renewable sources.

New nuclear reactors, being capital intensive, will need to achieve a sufficiently high capacity factor to be economically viable, while simultaneously offering the flexible output that the grid operator would demand. In addition, advanced reactors will need the capabilities to generate revenues from sources in addition to electricity sales, such as heat sales [46].

Increasing share of renewables, with priority dispatch could also lead to grid instabilities, as the renewables currently are not obligated to provide frequency and voltage regulation services. To maintain the reliability of supply, an optimum mix of renewable, nuclear, other generators, demand side management and energy storage is required. This will require significant policy changes. Apart from reliable power supply, consumers also expect economic power supply. Contrary to the belief that the renewable sources provide economical electricity, the total cost of supply to the consumers is likely to increase with increasing share of renewables when the system effects of integration of renewables into the grid are

accounted for [33]. Grid-scale energy storage will help improve the grid stability and overall economics of nuclear integrated with renewables on the grid. Decision makers should be aware of long term consequences [55] of introducing significant amount of renewables into the grid and consider reliability.

Growth of renewable and natural (shale) gas generation in some deregulated markets is contributing to the premature closure of nuclear plants, particularly in concert with the current low cost of natural gas in the United States (e.g. the Kewaunee nuclear power plant in Wisconsin was shut down in mid-2013 due to unfavourable economics in light of low natural gas prices [12]). Deregulated markets require all generation sources to compete to sell electric energy and services to meet grid demand. Adequate policies will be required to correct the market to benefit consumers from a grid-based power supply that is reliable, resilient and economical.

Nuclear-renewable hybrid energy systems have been suggested as a solution to achieve the required flexibility. These are defined as integrated facilities comprised of nuclear reactors, renewable energy generation, energy storage, and flexible industrial processes that can simultaneously address the need for grid flexibility, greenhouse gas emission reductions, and optimal use of investment capital. New developments in nuclear technology, including small modular reactors, are also providing renewed attention toward nuclear generation, which could spur the development of novel hybrid energy systems. Viability of such systems will depend on the optimum mix of nuclear, renewable and an adequate industrial process and the business model to operate such systems.

The requirement of flexible operation for Generation IV reactors will necessitate addressing the technical challenges with advanced power conversion cycles, improved materials to withstand stresses of cyclic operation, and adequate instrumentation and control to allow flexible operation. At a minimum, the utilities requirements for advanced new reactors include automatic frequency control in response to grid signals.

It would appear that designing future nuclear reactors to be flexible enough for integration with significant renewable resources on the

grid might be a relatively easier technical challenge compared with the bigger market- and policy-driven challenges for deployment of new nuclear capacity. Recent experiences in implementing new nuclear units in the OECD countries have not been positive in terms of cost over-runs and delays. Reducing the nuclear project cost would require creative approaches to project management and technological solution to reduce the fabrication costs. Nevertheless, current power market designs remain a formidable challenge to current and future nuclear deployment. Market flaws hurt nuclear power, grid diversity and economy; and will require a major policy shift.

Acknowledgements

The authors gratefully acknowledge the assistance provided by the CR Library staff, S. Gimson, A. Smith, M. Moore, L. Leung, D. Majoor, A. van Heek, F. Carré, members of the GIF Economic Modeling Working Group, and participants at the 38th Experts Group Meeting Cape Town, South Africa October 18, 2017. This study was funded by Atomic Energy of Canada Limited, under the auspices of the Federal Nuclear Science and Technology Program.

Nomenclature

CDN	Canadian
EDF	Électricité de France
EMWG	Economic Modeling Working Group
GIF	Generation IV International Forum
IESO	Independent Electricity System Operator
NEA	Nuclear Energy Agency
NGCC	Natural Gas-fired Combined-Cycle
OECD	Organisation for Economic Co-operation and Development

References

- [1] UNCTAD Secretariat, "Competition in Energy Markets", TD/B/COM.2/CLP/60, 26 April 2007.
- [2] M. G. Pollitt, "The role of policy in energy transitions: lessons from the energy liberalisation era", CWPE 1216 & EPRG 1208, March 2012.
- [3] F. P. Sioshansi, Editor, *Evolution of Global Electricity Markets*, Academic Press, London, 2013.
- [4] P. L. Joskow, "Lessons Learned From Electricity Market Liberalization", *Energy Journal*, pp. 9-42, 2008.
- [5] Public Sector Consultants, "Electric Industry Deregulation", March 2014.
- [6] National Energy Board, "Canada's Renewable Power Landscape", NE2-17E-PDF, 2016.
- [7] Eurostat, "Share of energy from renewable sources", nrg_ind_335a, Statistical Office of the European Union; <http://ec.europa.eu/eurostat/web/energy/data/database> (accessed September 2017).
- [8] U. S. Energy Information Administration, "Monthly Energy Review", DOE/EIA-0035(2017/09), September 2017.
- [9] D. Helm, Editor, *Climate-change Policy*, Oxford University Press, Oxford, 2005.
- [10] J. Cavicchia, "Rethinking government subsidies for renewable electricity generation resources", *The Electricity Journal*, 30, pp. 1-7, 2017.
- [11] L. E. Jones, Editor, *Renewable Energy Integration: Practical Management of Variability, Uncertainty, and Flexibility in Power Grids*, Academic Press, London, 2014.
- [12] U. S. Department of Energy, "Staff Report to the Secretary on Electricity Markets and Reliability," August 2017.
- [13] E. Hsieh, and R. Anderson, "Grid flexibility: The quiet revolution", *The Electricity Journal*, 30, pp. 1-8, 2017.
- [14] E. Ela et al., "Evolution of Wholesale Electricity Market Design with Increasing Levels of Renewable Generation", National Renewable Energy Laboratory, NREL/TP-5D00-61765, September 2014.
- [15] D. Ward, "Definition and Reasons for Flexible Operations", Technical Meeting on Flexible (non-baseload) Operation Approaches for Nuclear Power Plants, 4-6 Sep 2013, L'Aéro-Club de France, Paris, France, International Atomic Energy Agency, 2013; <https://www.iaea.org/NuclearPower/Meetings/2013/2013-09-04-09-06-TM-NPE.html> (accessed December 2017).
- [16] Independent Electricity System Operator, "Supply Overview"; IESO: <http://www.ieso.ca/power-data/supply-overview/transmission-connected-generation> (accessed September 2017).
- [17] Independent Electricity System Operator, "Hourly Demand Report", 2016; IESO: <http://reports.ieso.ca/public/Demand/> (accessed June 2018).
- [18] National Energy Board, "Market Snapshot: Why is Ontario's electricity demand declining?", March 2018; <https://www.neb-one.gc.ca/nrg/ntgrtd/mrkt/snpsht/2018/03-03ntrlctrctdmnd-eng.html> (accessed July 2018).
- [19] Independent Electricity System Operator, "Generator Output and Capability Report", 2016; IESO: <http://www.ieso.ca/power-data/data-directory> (accessed June 2018).
- [20] Independent Electricity System Operator, "Generator Output by Fuel Type Monthly Report", 2016, <http://reports.ieso.ca/public/GenOutputbyFuelMonthly/> (accessed June 2018).
- [21] C. Cany et al., "Nuclear and intermittent renewables: Two compatible supply options? The case of the French Mix", *Energy Policy*, 95, pp. 135-146, 2016.
- [22] D. Most, "Economics of Energy Storage: The Role of Storage in Energy System Flexibility", TU Dresden.
- [23] Independent Electricity System Operator, "2016 IESO Operability Assessment –

- Summary: Review of the Operability of the IESO-Controlled Grid to 2020”, June 2016.
- [24] Independent Electricity System Operator, “Report: Energy Storage”, March 2016.
- [25] Independent Electricity System Operator, “2016 Year-End Data”; IESO: <http://www.ieso.ca/corporate-ieso/media/year-end-data> (accessed September 2017).
- [26] A. Lokhov, “Technical and Economic Aspects of Load Following with Nuclear Power Plants”, Nuclear Energy Agency, OECD, 2011.
- [27] A. Lokhov, “The Economics of Long-term Operation of Nuclear Power Plants”, NEA No. 7054, Nuclear Energy Agency, OECD, 2012.
- [28] International Atomic Energy Agency, “Non-baseload operation in nuclear power plants: load following and frequency control modes of flexible operation”, No. NP-T-3.23, International Atomic Energy Agency, Vienna, 2018.
- [29] C. Bruynooghe, A. Eriksson, and G. Fulli, “Load-following operating mode at Nuclear Power Plants (NPPs) and incidence on Operation and Maintenance (O&M) costs. Compatibility with wind power variability”, 2010; Joint Research Centre: <https://ses.jrc.ec.europa.eu/publications/reports/load-following-operating-mode-nuclear-power-plants-npps-and-incidence-operation> (accessed September 2017).
- [30] H. Ludwig et al., “Load cycling capabilities of German Nuclear Power Plants (NPP)”, International Journal for Nuclear Power, Volume 55, Issue 8/9, August/September 2010.
- [31] U. S. Energy Information Administration, International Energy Statistics; www.eia.gov/cfapps/ipdbproject/IEDIndex3.cfm (Accessed June 2018).
- [32] P. Joskow, “Competitive Electricity Markets and Investment in New Generating Capacity”, AEI-Brookings Joint Center Working Paper No. 06-14, 2006; SSRN: <http://dx.doi.org/10.2139/ssrn.902005> (accessed May 2018).
- [33] OECD Nuclear Energy Agency, “Nuclear Energy and Renewables: System Effects in Low-carbon Electricity Systems”, NEA No. 7056, OECD, 2012.
- [34] K. Mayer, and S. Trück, “Electricity markets around the world”, Journal of Commodity Markets, 9, pp. 77-100, 2018.
- [35] P. L. Joskow, “Comparing the Costs of Intermittent and Dispatchable Electricity Generating Technologies”, American Economic Review, Volume 101, No. 3, pp. 238-241, 2011.
- [36] F. Ueckerdt, L. Hirth, G. Luderer, and O. Edenhofer, “System LCOE: What are the costs of variable renewables?”, Energy, Volume 63, pp. 61-75, 15 December 2013.
- [37] U. Helman, “Economic and Reliability Benefits of Large-Scale Solar Plants”, in Renewable Energy Integration: Practical Management of Variability, Uncertainty, and Flexibility in Power Grids, pp. 83-99, L. E. Jones (Ed.), Academic Press, London, 2014.
- [38] Nuclear Energy Institute, “Zero-Emission Credits”, April 2018.
- [39] J. P. M. Sijm, “Cost and revenue related impacts of integrating electricity from variable renewable energy into the power system - A review of recent literature”, ECN--E-14-022, ECN, May 2014.
- [40] B. Matek, and K. Gawell, “The Benefits of Baseload Renewables: A Misunderstood Energy Technology”, The Electricity Journal, Volume 28, Issue 2, pp. 101-112, March 2015.
- [41] B. Kirby, E. Ela and M. Milligan, “Analyzing the Impact of Variable Energy Resources on Power System Reserves”, in Renewable Energy Integration: Practical Management of Variability, Uncertainty, and Flexibility in Power Grids, pp. 83-99, L. E. Jones (Ed.), Academic Press, London, 2014.
- [42] C.-H. Tsai, and G. Gülen, “Are zero emission credits the right rationale for saving economically challenged U.S. nuclear plants?”, The Electricity Journal, Volume 30, pp. 17-21, 2017.
- [43] J. Anderson, “Power Producers Ask Appeals Court to Invalidate New York’s ZEC Program”, Nucleonics Week, Volume 58, Number 42, October 19, 2017.
- [44] Illinois Power Agency, “Zero Emission Standard Procurement Plan – Final”, October 31, 2017.

- [45] J. E. Aldy and R. N. Stavins, "The Promise and Problems of Pricing Carbon: Theory and Experience", FEEM Working Paper No. 82.2011, January 18, 2012). Available at SSRN: <https://ssrn.com/abstract=1987487> or <http://dx.doi.org/10.2139/ssrn.1987487>.
- [46] J. Bistline and R. James, "Exploring the Role of Advanced Nuclear in Future Energy Markets", Technical Report 3002011803, Electric Power Research Institute, March 2018.
- [47] Nuclear Energy Agency, "Carbon Pricing, Power Markets and the Competitiveness of Nuclear Power", NEA No. 6982, OECD, 2011.
- [48] N. Barkatullah, and A. Ahmad, "Current status and emerging trends in financing nuclear power projects", Energy Strategy Reviews, Volume 18, pp. 127-140, 2017.
- [49] F. P. Lucet, "Financing Nuclear Power Plant Projects A New Paradigm?", Institut français des relations internationales, May 2015.
- [50] V. Ivanov, "ROSATOM: Financing Opportunities and Challenges", May 2017.
- [51] D. Helm, "The Nuclear RAB Model", Energy Futures Network Paper 27, June 2018; <http://www.dieterhelm.co.uk/enregy/energy/the-nuclear-rab-model/> (accessed July 2018).
- [52] Public Sector Consultants Inc., "Electric Industry Deregulation: A Look at the Experience of Four States", March 2014.
- [53] Independent Electricity System Operator, "Media Backgrounder: Amended and Restated BPRIA", December 3, 2015.
- [54] Financial Accountability Office, "An Assessment of the Financial Risks of the Nuclear Refurbishment Plan", Queen's Printer for Ontario, Toronto, 2017.
- [55] Nucleonics Week, Volume 58, Number 39, September 28, 2017.

TRACK 9: DECOMMISSIONING & WASTE MANAGEMENT

(No papers were received for this track)

TRACK 10: OPERATION, MAINTENANCE, SIMULATION, TRAINING

IN SERVICE INSPECTION AND REPAIR DEVELOPMENTS FOR SFRS (F. BAQUÉ ET AL)

F. Baqué⁽¹⁾, R. Marlier⁽²⁾, J.Fr. Saillant⁽³⁾, M.S. Chenaud⁽⁴⁾

(1) CEA, France

(2) FRAMATOME, France

(3) FRAMATOME/INTERCONTROLE, France

(4) CEA, France

Abstract

Within the framework of large R&D studies performed since 2010 for future sodium-cooled reactors, with a first prototype called ASTRID, in-service inspection and repair (ISI&R) has been identified as a major issue to be taken into account in order to improve the reactor's safety, to consolidate its availability and to protect its related investment.

Development, improvement and qualification of the ISI&R tools and processes for structures immersed in sodium at about 200°C have been performed since early pre-conceptual design phase of ASTRID. This work is based on a set of consolidated specifications and a qualification process involving increasingly more realistic experiments and simulations mainly performed with the Non Destructive Examination CIVA code platform.

ISI&R items (in sodium telemetry and vision, Non Destructive Examination, Laser repair, associated Robotics) are being developed and qualified as part of a multi-year program which mainly deals with the reactor block structures and primary components, and sodium circuit with the power conversion system.

This program is ensuring the strong ties needed between the reactor designers and inspection specialists since the aim is to optimise inspectability and repairability. This has already induced specific rules for design in order to shorten and facilitate ISI&R operations. These new rules have been merged into the RCC-MRx rules in its first 2012 edition.

Current R&D deals with the following ISI&R items:

- Under-sodium non-destructive examination (NDE) of Stainless Steel thick welded joints: specific ultrasonic transducers are developed and used for sodium testing, and associated simulations are being performed.
- NDE of in-sodium welded joints, from outside of the main vessel (through the main vessel wall): modeling, water testing and simulation are being performed..
- Under-sodium telemetry and vision of immersed structures and components: improved techniques of short distance (less than 200mm) and far distance (up to some meters) scanning are being studied. Water and sodium testing, and simulations are being performed.
- Methods for in-situ repair: a single laser technique has been selected for sodium sweeping before machining and welding.
- Associated in-sodium robotics: a sodium-proof material and technology is being developed and tested. In sodium tight bell is looked at for repair application.

This paper is an up-dated version of the paper presented in 2015 at the ICAPP international conference [1] and provides the main testing and simulation results for telemetry, vision and NDE applications.

R&D for inspection and repair of SFRs faces challenging requirements and is progressing towards available technological solutions, associated with demonstrated performance levels: the basic inspection techniques are expected to reach level 6 of 'technological readiness' by the end of detailed design phase: proof of principle with Pilot-scale, similar (prototypical) subsystem validation in relevant environment.

The 'integrated readiness level' is also discussed in this paper with respect to access within the reactor block, fluids, positioning and maintenance aspects.

I. Introduction

Within the framework of the future Generation IV reactors, a project of a sodium-cooled fast reactor prototype called ASTRID was launched by France. A specific large R&D program¹ has been defined on In-Service Inspection and Repair (ISI&R) which has been identified as a difficult task to be performed² (as sodium coolant is opaque, hot and highly chemically reactive) on the basis of experience feedback (French Phenix and Superphenix SFRs, as well as foreign power plants). ISI&R is thus considered to be a major issue to be taken into account in order to improve the reactor's safety (as inspection gives information on the actual reactor structure health), to consolidate its availability and to protect its associated investment.

Since 2009, R&D studies for ISI&R are parted into four levels. These levels are related to the specific rules for design applicable to SFRs3 (Figure 1.).

Figure 1. French ISI&R organisation for SFRs



A number of general options were chosen at the end of the ASTRID pre-conceptual design phase. Now we are focusing on improving the ISI&R tool⁴ for the ASTRID reactor block structures immersed in sodium at about 200°C (ISI&R operations are performed at shut-down conditions). This is being done on the basis of consolidated specifications and a pre-qualification process involving increasingly more realistic experiments using acoustic techniques⁵ and simulations performed with the patented CIVA code.

ISI&R items (inspection: ultrasonic sensors, telemetry, vision and volumetric control, repair, associated robotics) are being developed and qualified within the scope of a multi-year program⁶ which mainly deals with the reactor block systems, structures and components, and the power conversion system. One has to note that repair aspect is considered to be less important than inspection one.

This program is ensuring the strong ties needed between the reactor designers and inspection specialists since the aim is to optimise inspectability (and reparability). This has already induced specific rules for design in order to shorten and facilitate the ISI&R operations, and these new rules have been merged into the RCC-MRx rules (2012 edition).

Thus, ISI&R will participate to ASTRID prototype safety, as it will be able to face the standards associated to high level requirements for nuclear plants (assessment of nuclear power mastery, thermal balance release and respect of the environment).

In the present design phase R&D activities deal with general ISI&R objectives (for example: being able to perform NDE under sodium) which will then be declined for each case, depending on what is required for each component and structure.

II. R&D for ISI&R of ASTRID

The design of the ASTRID reactor prototype aims at minimising the inspection needs (e.g. the fewer welding joints, the better) and to facilitate access to areas which should be inspected due to their safety function. The in-service inspection of systems, structures and components will depend on their contribution to the reactor's defense and mitigation lines.

The inspection graduation applied to each system, structure and component is based on a set of parameters, among which are mainly the consequences in case of possible structure failure on the reactor safety and/or defense and mitigation lines ; but also the structure service and mechanical loading (design margins), its functions (containment, mechanical support...), its exploitation feedback...

The following sections deal with R&D on the improvement and qualification of inspection techniques: this is based on simulation and testing, first through feasibility assessments and then on the basis of increasingly more realistic tests for technological bricks and systems, i.e. the 'technological readiness level' and 'integrated readiness level' methodology.

R&D on repair focuses on a single laser technique for all applications while robotics is studied through architecture concepts, robot design, technological bricks and under-sodium leak tightness.

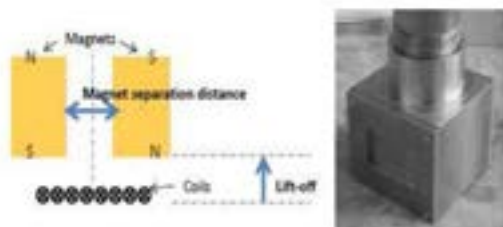
II.A. Under sodium ultrasonic sensors for telemetry and NDE

Development of in sodium ultrasonic sensors forms the basis of most of inspection techniques⁶. It is why both piezoelectric (TUSHT from CEA and TUCSS from FRAMATOME INTERCONTROLE) and electromagnetic acoustic (EMAT from CEA⁷) technologies are being investigated to provide solutions that are adapted to the ASTRID inspection needs.

Experimental tests performed in liquid sodium have already demonstrated the good performance of custom mono-element EMAT probes⁷. Telemetry measurements were also performed with good accuracy. The integrity of the immersed probes was assessed after testing and cleaning. It has thus been possible to validate the design of the probe casing based on a stainless steel container.

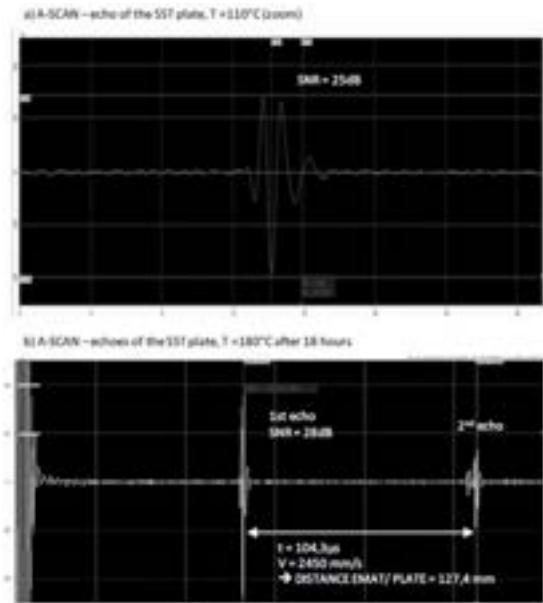
Developments have been continued to increase the performance and the capacity of the probe: an 8-elements EMAT probe has been designed and developed by INNERSPEC Technologies in accordance with the CEA specifications for under-sodium imaging (Figure 2).

Figure 2. Principle and photo of in sodium 8-phased array EMAT probe



As can be seen on Figure 3, under-sodium tests have shown the good performance of the probe for telemetry measurements with normal incidence. Deflection tests proved to be difficult due to the size of the focal spot compared with that of the targets. New developments are ongoing at the CEA to enhance the performance of this EMAT probe: acoustic beam deflection capacity and sensor sensitivity.

Figure 3. A-SCAN of the EMAT echoes (in sodium at 110°C and 180°C)



The high-temperature ultrasonic transducer (TUSHT) developed by the CEA is a lithium-niobate-based probe: LiNbO_3 piezoelectric crystal, enriched with $^7\text{LiNbO}_3$ for severe neutron irradiation conditions. The casing is made of AISI 304L stainless steel, as shown on Figure 4, and an efficient acoustic bonding between the casing and the crystal is provided via a hard-soldering technique. This provides stable high-frequency transmission (up to 5 MHz at least) in the temperature range applicable during both inspection (200°C reactor shutdown state) and continuous surveillance and monitoring (up to nearly 600°C reactor full power state) of SFRs.

Figure 4. Photo of the TUSHT (4540 standard model)

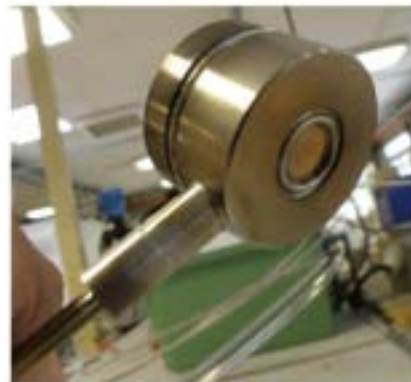
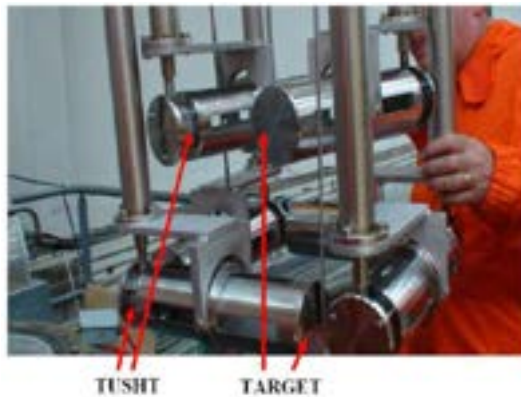


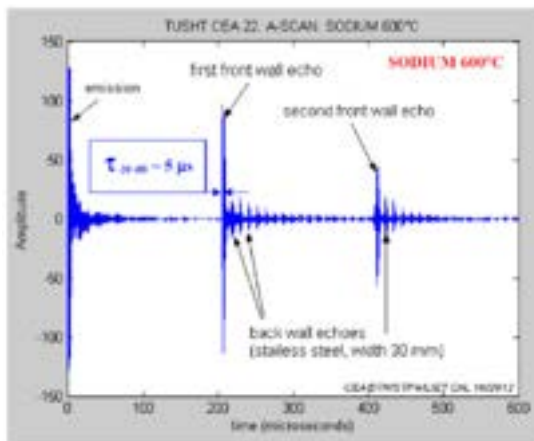
Figure 5 shows the arrangement of the six TUSHT samples which were tested in sodium in a pulse-echo mode, shooting on a target located at 230 mm. The target was a stainless steel plate with a thickness of 30 mm.

Figure 5. TUSHT and target setting for sodium test



As illustrated in the Figure 6, ringing echoes are visible, in particular those resulting from internal reflections inside the target. The front-wall and back-wall echoes of the target are detectable, with the echo duration being 5 microseconds (width at -20dB).

Figure 6. TUSHT acoustic signal during sodium test at 600°C



The adaptation of the TUSHT technology can also be considered to develop array transducers. The next in-sodium experiments will consist in testing focused transducers (with a curved front face) to verify that they can achieve the expected standard focusing features (as they do in water conditions). The acoustic wetting of

transducers machined with mirror-like polished front faces will also be tested.

FRAMATOME INTERCONTROLE is also developing transducers for specific applications regarding volumetric NDE under liquid sodium at 200°C. The objective of the development is to show that it is possible to detect a flaw inside a stainless steel structure immersed under liquid sodium.

The work reported here shows “immersion” NDT testing, where the transducer is not in contact with the entry face of the inspected part. This allows to search for potential flaws with different incident angles while keeping the same transducer.

The test block considered here is represented in Figure 7 left. It includes two reflectors R1 and R2 oriented in the x-direction and y-direction respectively. R1 should be detected using an L0° beam when scanning from x0 to x2, and R2 should be detected when scanning from x1 to x4 using an angled beam (tilted transducer). The test block was made of 316L stainless steel and the notches R1 and R2 were made by spark machining. The notches were 20 mm deep for a 0.2 mm opening width on the whole height of the block (100 mm), which is representative or conservative of the potential flaws that would be sought in ASTRID reactor structures.

Under-sodium tests were conducted in a glove box of CEA-DEN (Cadache, France) sodium facilities. A characterisation device, called DEFO (see Figure 7 – right), was specifically designed and fabricated in order to accurately move the TUCSS in front of the test block inside this sodium filled vessel. Figure 8 shows a photograph of a TUCSS transducer mounted on the DEFO device just before immersion under liquid sodium.

Figure 7. Sketch of the test block and scanning range (left) and view of the DEFO testing device (right)

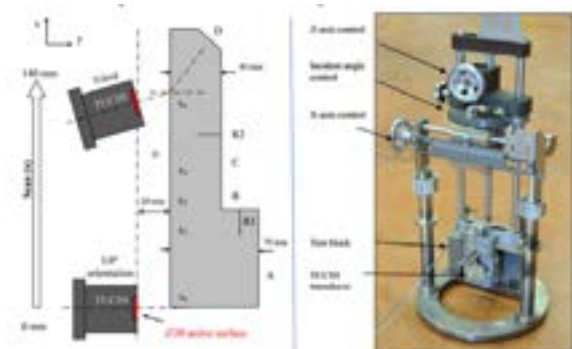


Figure 8. Photograph of a TUCSS transducer (left) and photograph of a TUCSS mounted on the DEFO device just before immersion under liquid sodium (right)

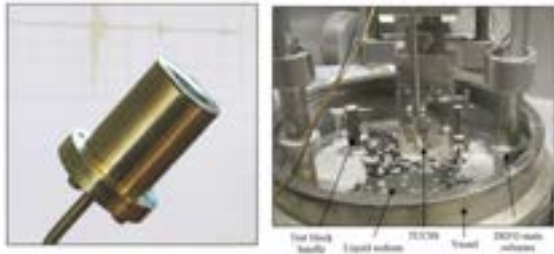


Figure 9 (left) shows a B-scan done under sodium at 200°C in normal incidence (i.e. with the orientation of the TUCSS transducer perpendicular to the surface of the test block). Interpretation is as follows:

- The red band from 0 to 10 μs is the saturated dead zone of the transducer.
- The red bands O and O' (at 18 μs and 36 μs) are respectively the block's entrance echo and its repetition (between the transducer and the block).
- The echo from surface A is visible at 45 μs .
- The echo from reflector R1 is visible at 40 μs .
- The echo from surface C is visible at 33 μs . The echo from surface C is disrupted when TUCSS passes the position of reflector R2.

Figure 9. Detection of R1 using longitudinal waves 0° (left) and detection of R2 using shear waves 38° (right) – under sodium at 200°C

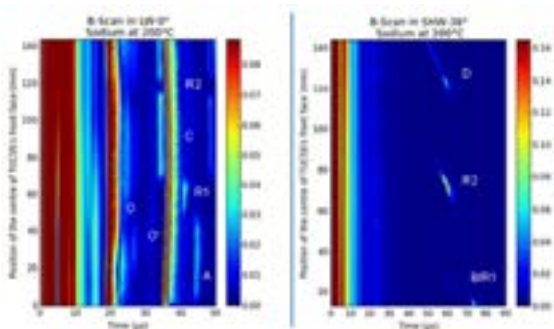


Figure 9 (right) shows a B-scan done in oblique incidence. The axis of the transducer was tilted to an incidence angle of 30°, producing pure shear waves with a 38° refraction angle (critical angle at 26.3°, therefore no longitudinal waves). Interpretation of this scan is as follows:

- The red band from 0 to 10 μs is the saturated dead zone of the transducer.
- The echo at 70 mm / 60 μs is the echo coming from R2.
- The echo at 15 mm / 73 μs is the echo from the corner between R1 and surface B.
- The echo at 120 mm / 60 μs is coming from the chamfered surface D.

These two scans clearly demonstrate that the TUCSS acoustical properties are sufficient to perform basic NDT using normal and oblique immersion techniques, under sodium at 200°C.

The B-scan made in oblique incidence looks much cleaner than that made in normal incidence. This is principally due to the fact that there is no echo from the block's entrance and no repetition echo. It is also due to the fact that shear waves are slower than longitudinal waves ($V_L=5608\text{m/s}$ and $V_S=3038\text{m/s}$ in 316L material at 200°C), delaying arrival time of echoes and pushing them further out from the dead zone. Inspection using normal incidence technique should therefore be done using a greater distance.

This transducer spent 27 days in total under sodium without physical degradation. It was noticed that amplitude of echoes gradually decreased with time. Nonetheless, its acoustical properties were finally still good enough to detect R2 with good signal to noise ratio.

These results demonstrate that basic immersion ultrasonic NDT techniques can be used in the chemically aggressive sodium environment during outages. Further work will consist of under-sodium tests with mockups including representative welds.

II.B. Under sodium NDE of welded joints within the ASTRID Supporting Core Structure (so called strongback)

Much is being done to improve and to propose the most suitable ISI&R strategy for the main ASTRID structures and equipment. The ISI&R strategy consists in proposing the appropriate mix of continuous monitoring, periodic

examinations and extra access/ repair abilities for each given structure. Various aspects have to be studied and taken into account to reach this objective.

These aspects are: i) design of the equipment, ii) associated damage modes, iii) behavior of the equipment when damaged, iv) probability of failures, v) capabilities of the surveillance/examination devices (existing or to be developed) and, vi) economic criteria (cost of the devices, impact on the plant's availability).

First of all, the supporting core structure (see Figure 10) is undergoing considerable analysis, as it is considered very important: a number of hypothetical inspection cases are being considered and simulated with the patented CIVA code which has been upgraded to meet SFR needs¹⁰.

As an example of CIVA simulation capacities compared with ASTRID extended accessibility issues, Figure 10 shows the hypothetical inspection of the welded joint between outlet skirt and upper plate. The arrow indicates the positions where the ultrasonic TUSHT sensor could be (assuming a simple rigid pole through the existing specific ISI&R access in the roof slab of the main vessel) and of an example targeted welded area where a hypothetical 100mm-long flat defect is located.

The effect of the relative position (internal/external) and depth (5/ 10/ 20 mm) of such a defect is studied. Figure 11 shows the simulated echo amplitude calculated by the CIVA code: detecting such defects should be possible since the signal-to-noise ratio is high enough.

Figure 10. CIVA code simulation of strongback inspection: example of NDE conditions

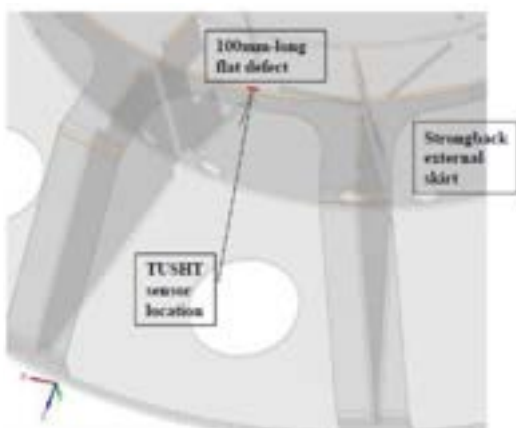
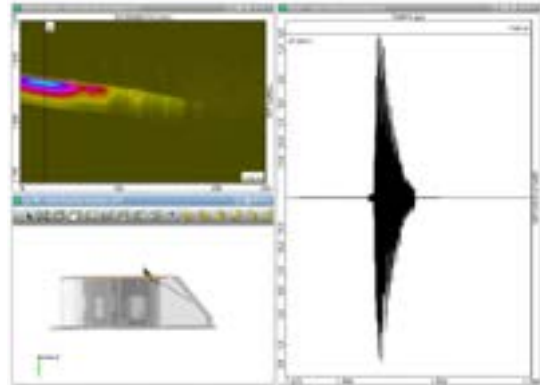


Figure 11. CIVA code simulation of strongback inspection: example of NDE results



In the frame of NDE studies, this demonstrates CIVA abilities to be a useful tool for extended accessibility verifications in ASTRID configurations.

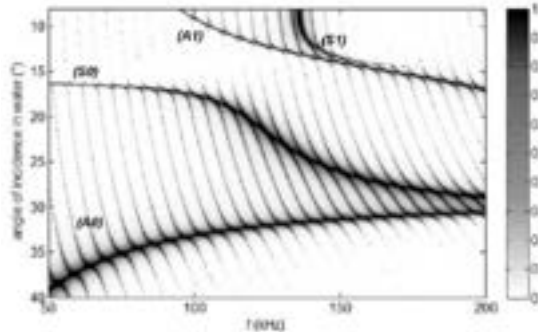
II.C. NDE of welded joints within the ASTRID strongback support skirt, from outside primary sodium (through main vessel wall)

Another important structure to be controlled is the strongback support skirt (see Figure 15 where "inspection branch" corresponds to it). Three techniques based on inspection from outside the primary sodium are being investigated: i) Lamb waves which could propagate in sodium from one structure to another, ii) guides waves within structures welded to the main vessel, and iii) conventional volumetric waves.

Lamb wave propagation in multilayers can be considered as they can propagate with low attenuation. A simplified mockup of typical SFR vessels and shells has been manufactured with parallel steel plates immersed in water (20 and 30 mm thick).

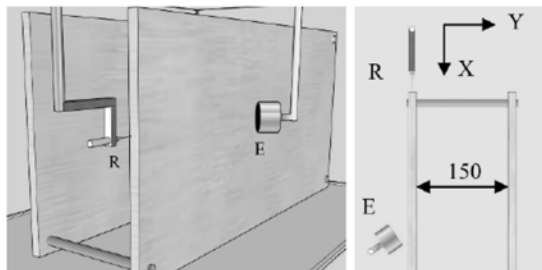
Austenitic stainless steel plates are immersed in water and separated by 150 mm of water: Lamb waves are produced as a function of the frequency and the angle of incidence of the pressure waves produced by sensors immersed in water.

Figure 12. Modulus of the transmission coefficients through a set of two plates, along frequency and incidence



The re-emission of such waves, from one plate to another, has been demonstrated. The behavior of waves can be predicted using the transfer matrix method together with the general equations for the dispersion curves, the normal displacements and the tangential displacements in the plate: acoustic modes can be determined as shown on Figure 12.

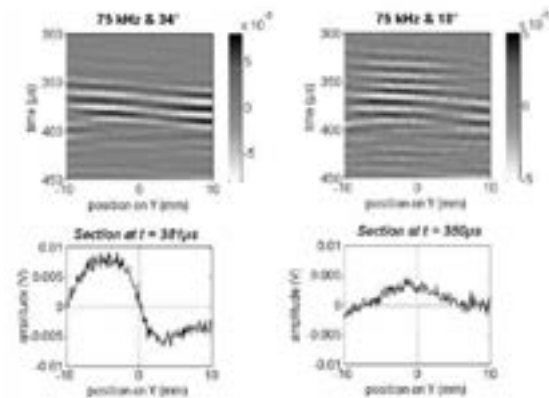
Figure 13. Experimental setup (left: 3D, right: 2D top view)



The acoustic emitter E was tilted to generate the expected Lamb mode in the first plate, while the receiver R (needle hydrophone) was positioned close to the edge of the plate. Thanks to its Y displacement, the emitted pressure waves could be recorded along the edge of both plates (see Figure 13).

As shown on Figure 14, A0 and S0 modes were observed in the first plate and identified by the measurements of celerity and displacements at the interface with water. The angles of radiated pressure waves were measured to ensure that the incident waves on the second plate could generate Lamb waves. Then the propagating modes were also observed and identified in the 'hidden' plate.

Figure 14. Pressure amplitudes measured along the edge of the second plate. Left: antisymmetric mode. Right: symmetric mode



Experimental validations show good agreement with theory and highlight Lamb wave propagation in the hidden plate. The A0 mode could be used for the non-destructive testing of the hidden plate⁹.

Experimental measurements were validated by comparison between theory, experimentation and finite-element simulations (using COMSOL Multiphysics® software) in the case of one immersed plate in water. These signal processing techniques proved to be efficient in the case of multi-modal propagation. They were applied to two immersed plates to identify the leaky Lamb mode generated in the second plate. When plates have the same thickness, leaky Lamb modes propagate from the first to the second plate without any mode change, with the apparent attenuation being weaker in the second plate. Considering that the second plate is continuously supplied in energy by the first one, an energy-based model (EBM) is proposed herein to estimate the apparent attenuation in the second plate. Despite our extremely simplifying assumption, this model proved to be in good agreement with both finite-element modelling (FEM) and experimentation.

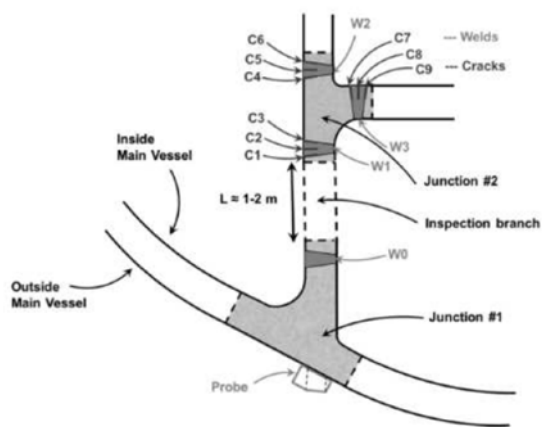
Guided waves can also be used, as the strongback support skirt is welded to the main vessel: this configuration implies a continuous stainless steel guide, from outside the main vessel up to the strongback¹⁰.

Guided wave modeling has been developed with a hybrid finite-element modal method for arbitrary waveguides. The method couples high-order finite elements that allow the interaction of guided waves with arbitrary defects with a modal expansion that permits semi-analytical

propagation along waveguide principal axes. Between the different modal decompositions, scattering matrix formalism is applied to easily chain complex geometries to each other with emission and scattering phenomena.

A case study featuring a branched steel structure representative of strongback supporting skirt welded on the main vessel was simulated to determine the effect of cracks on the pulse-echo inspected region. This is shown in Figure 15.

Figure 15. Case study for guided wave inspection (top) and inspection configurations used (bottom)



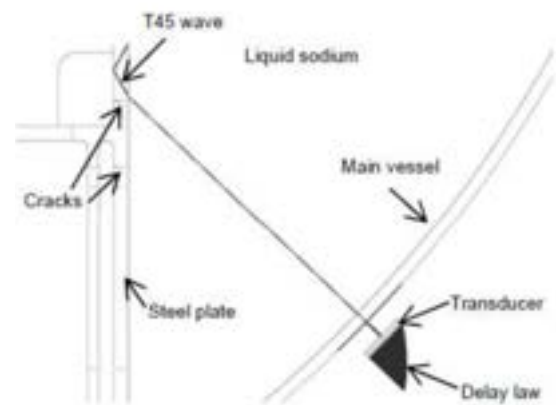
A parametric study was conducted for each emission configuration to determine the optimal location of the probe, its size and frequency of operation, depending on the modes generated in the control branch. After choosing the optimal set-up, pulse-echo ultrasonic guided wave simulation was carried out with cracks C1 to C9 present one at a time. These studies revealed the fact that modal contributions are strongly dependent on the emission configuration used. In the case of cracks C7, C8 and C9, which are located in a geometrically inaccessible region, a variation of 6 dB between the best and the worst inspection configuration can be observed.

Further work on this topic will include experimental validation of the simulation results relating to this type of complex branch-like structural inspection.

Volumetric waves seem less likely to be successful, as the distance to the reactor vessel and the amplitude decrease in successive echoes from a surface perpendicular to the incident ray direction limits the detectability of internals.

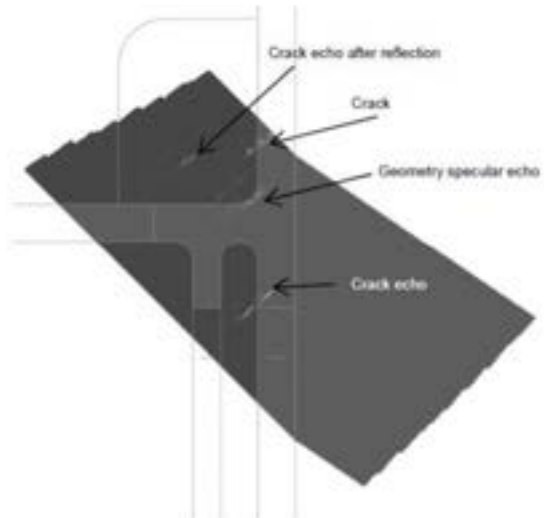
Nevertheless, simulation was performed to check the efficiency of different sensors for the upper part of the strongback supporting skirt inspection configuration: a non-destructive examination of two cracks inside the skirt was simulated, as illustrated on Figure 16.

Figure 16. Configuration of T45 volumetric inspection of strongback supporting skirt with two cracks, from behind the main vessel



A 45° shear wave inspection (T45) was simulated with CIVA code, assuming a phased array probe positioned outside of the main vessel. The resulting B-scan has been projected onto the geometry of the reactor in Figure 17.

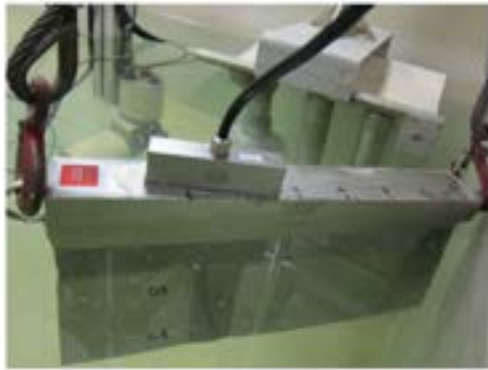
Figure 17. NDE simulation of volumetric T45 inspection of strongback supporting skirt with two cracks, from behind the main vessel



In the case of this inspection, the crack echoes show not only the specular corner reflection of the T45 beam, but also the tip diffraction echoes that make it possible to size the cracks. A validation case with steel plate mockup immersed in water will be set up to estimate whether this inspection technique is also adapted in practice.

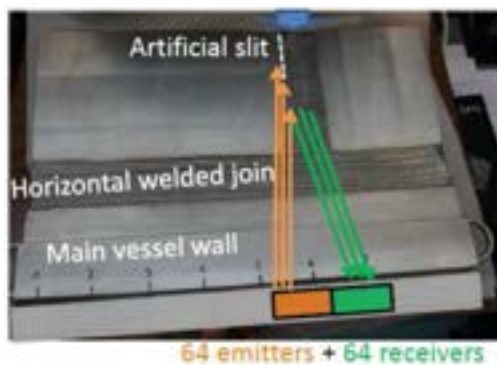
Another configuration is being studied for the inspection of vertical welded joints of the core supporting skirt: using out-of-sodium sensors, ultrasonic volumetric waves are likely to cross the main vessel wall and then propagate across the skirt where they have to cross a horizontal welded joint.

Figure 18. Core supporting skirt mock 'up, during water tests



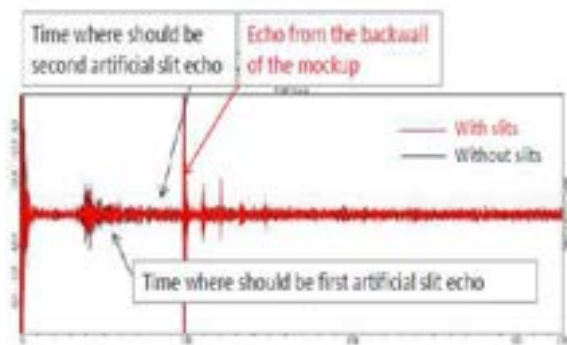
A first mock-up was designed and manufactured to check the detection of artificial cracks in its 40mm-deep welded joints, with the mock-up immersed in water as shown on Figure 18 (representing the surrounding sodium of the current ASTRID conditions) and using a single 128 phased-array 5 MHz sensor.

Figure 19. Under water test configuration for vertical welded joint inspection with one 128 elements sensor (plane wave case)



The NDE measurements corresponded to the time-of-flight diffraction (TOFD) on artificial slit edges: 64 elements of the phased-array sensor emitted plane waves or focused waves, thanks to the former CIVA code calculation of the corresponding time delay laws. The other 64 elements acted as receivers (see Figure 19).

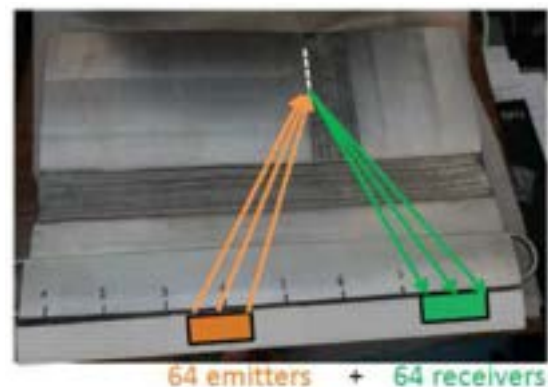
Figure 20. NDE of core supporting skirt mockup (water test results at room temperature with linear 128 element sensor)



The NDE of this mock-up was performed first without and then with some artificial slits which were machined in the welded joints or in their heat-affected zone.

The echoes of the slits to be detected could not be found: there was no specific response associated with the slits (see Figure 20). This is why these tests will be repeated with not one but two 64 element transducers, with each transducer being able to move along the length of the mock-up, so that incidence of acoustic beam on the slit to be detected will be larger (see Figure 21).

Figure 21. Under water test configuration for vertical welded joint inspection with two 64 element sensors (focused wave case)



Of course, CIVA code simulation will also be used to predict the echoes from the slit edges in order to use the best configurations for NDE.

II.D. Under sodium telemetry and vision of immersed structures and components

Complementary acoustic techniques such as in sodium imaging are also considered, even if they are less important than NDE ones. As sodium is opaque, visualising components and structures immersed in sodium could provide interesting information for some applications: accurate local vision for structure surface metrology, global vision of the primary circuit, detection of opened cracks, location and identification of loose parts, robotic navigation positioning, and identification of coding systems for fuel sub-assemblies. The study has been divided into several parts:

- Acoustic behavior of such systems, using the CIVA code simulation
- Development of associated transducers (phased-array systems)
- Signal treatment for 2D and 3D image reconstruction (advanced signal processing)
- Qualification by in-water then in-sodium tests using dedicated targets for each application.

This study is being carried out with the help of French and international partners.

In a preliminary phase, telemetry tests were performed in 2010 on a mock-up called MULTIREFLECTEUR in order to study ultrasonic diffractions and reflections in liquid sodium. It included a rotating TUSHT, a fixed target, rotating targets and thermocouples (see Figure 22). In order to reach the metrological objective, all the components were initially calibrated in air at room temperature, which resulted in a global uncertainty of ± 0.02 mm (20 μ m) for their location and $\pm 0.02^\circ$ for their angular position.

Figure 22. MULTIREFLECTEUR mockup for telemetry sodium tests



After under-water commissioning tests, the mock-up was dried and used in a 1m-diameter pot in isothermal 200°C static sodium conditions: the test parameters were the TUSHT frequency and 6 target positions. The global uncertainty on the ultrasonic distance measurement was checked and proved to be better than 100 μ m. The test results helped qualify the CIVA code.

In late 2013, PhD work was launched at the CEA to find the best techniques for visualising opened cracks and for optimising the related acoustic systems, based on numerical simulation and combined with experimental qualification.

Surface-breaking cracks and deep cracks were sought in the weld area as welds are more subject to defect initiation.

Traditional methods enabled us to detect emerging cracks of sub-millimeter size with the sodium-compatible high-temperature TUSHT transducer (water tests). The PhD work relied on making use of prior knowledge of the environment by implementing differential imaging and time-reversal techniques. This approach makes it possible to detect change by comparison with a reference measurement and by focusing back to any change in the environment. It provides a means of analysis and understanding of the physical phenomena, thus making it possible to design more effective inspection strategies. The differences in the measured signals revealed that the acoustic field was scattered by a perturbation (a crack for instance), which may have occurred between periodical measurements.

The imaging method relies on the adequate combination of two computed ultrasonic fields, one forward and one adjoint¹¹. The adjoint field, which carries the information about the defects, is analogous to a time-reversal operation. One of the advantages of this method is that the time-reversal operation is not done experimentally but numerically. Numerical simulations have been carried out to validate the practical relevance of this approach.

However, they still reveal a number of important limitations. Artifacts observed on the conventional topological energy image result from wave interactions with the boundaries of the inspected medium. A method was developed for addressing these artifacts, which involves forward and adjoint fields specified in terms of the boundary conditions. Modified topological energies were then defined according to the type of analysed flaw (open slit or inclusion). Comparison of the numerical results with the experimental data confirms the

relevance of the approach (see Figure 23). The water tests were performed in simplified conditions, with conventional sensors which were accurately moved with 5D systems (see Figure 24). With these test conditions, it was possible to detect machined slits (simulating opened cracks) whose width is only 800 μm (ASME specification for visual inspection) and letters whose size is more than 6 mm as shown on Figure 25).

Figure 23. Imaging results of the scattering topological energy of a 1-mm diameter hole delimited by the black hollow circle in a steel block. The medium was insonified (a) by one element and (b) by 64 elements on the upper surface of the block; 64 receivers were used. The resulting images are expressed in decibels and normalised

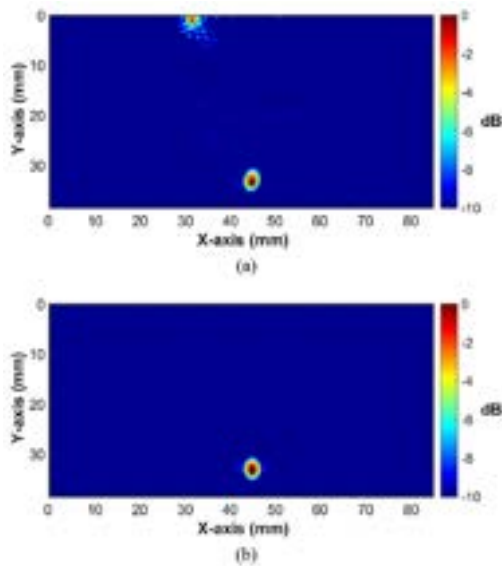
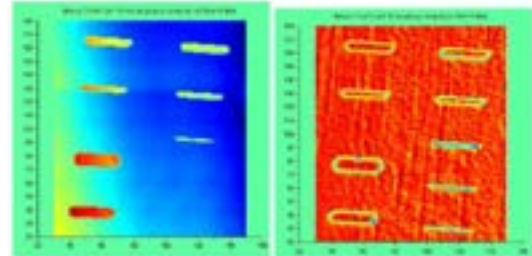


Figure 24. VISIO water facility (2 m long, 1 m large, 1 m height) devoted to ultrasonic visualisation study



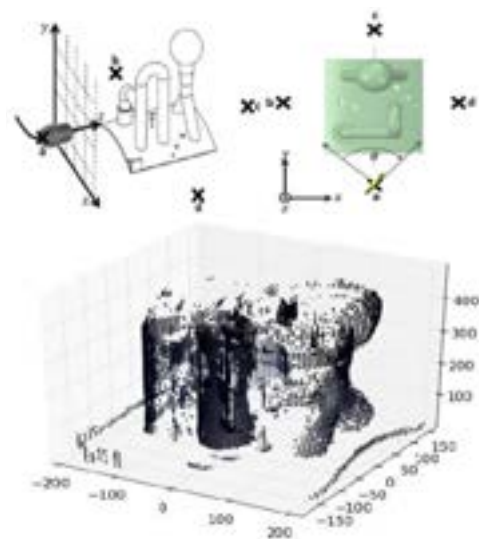
Figure 25. Acoustic imaging of a plate with slits. Left: time of flight. Right: amplitude (under water test at room temperature).



The main components of a 3D mock-up – a specially designed specimen that simulates various structure shapes found inside the ASTRID reactor block (pipe, elbow, reducer, plate and sphere) – have been identified through US scanning, but all its details are not always visible. For example, when the immersed object is not flat, only the specular echoes are useful for imaging, explaining why it is important to choose the right strategy for sensor positioning and displacement along the targets to be imaged.

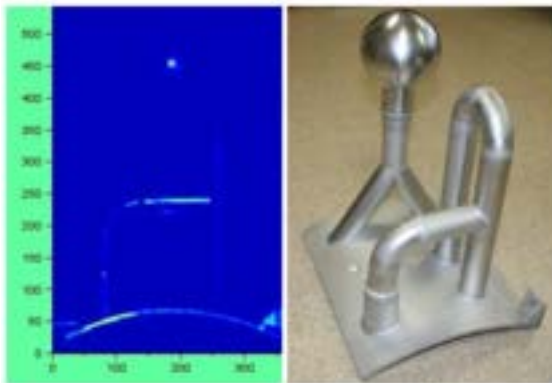
In addition to water testing, CIVA simulation was also carried out to obtain 3D images of the simulated specimen that were generated by XY raster and Z-theta approaches as shown on Figure 26.

Figure 26. XY raster and Z-theta approaches for CIVA code calculation of 3D mockup. Z-theta CIVA results



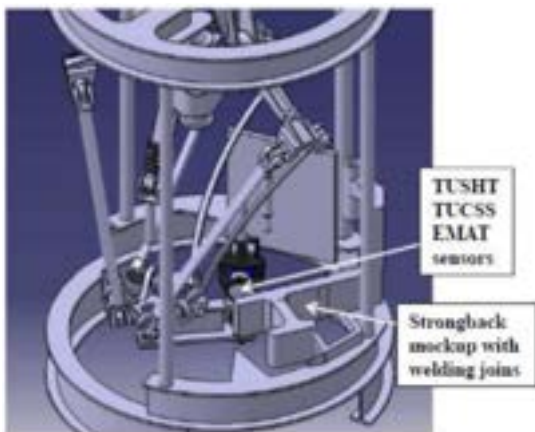
The simulation studies indicate that both XY raster (illustrated on Figure 27) and Z-theta scan can be used for deciphering the shapes.

Figure 27. In water 3D mockup ultrasonic imaging with sensor XY displacement in a vertical plan (echoes amplitude)



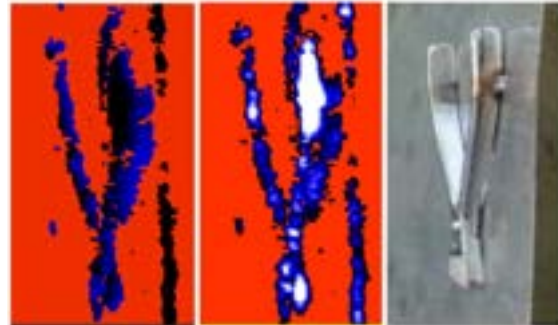
After the water-tests, in sodium-tests must be performed to validate the water/sodium transposition. For this purpose, a 3D scanning system (see Figure 28) has been used for under-sodium imaging of objects in a CEA test vessel. Two TUSHT transducers were moved with four degrees of freedom in a 1.5 m³ sodium vessel¹².

Figure 28. Specific positioning device for US sensors, and strongback mockup for future sodium close-range NDE tests¹²



In the meantime, the first raw imaging of 200°C sodium-immersed objects (bolt, hammer and pliers) was performed in 2013, as shown on Figure 29.

Figure 29. First in sodium acoustic imaging at 200°C: first plier raw reconstruction. Left: time of flight. Right: amplitude



Further under-sodium viewing tests were performed with the specific positioning device for US sensors (see Figure 28) and aimed at introducing C-scan images acquired thanks to this four degrees of freedom robot arm able to carry and precisely position high temperature ultrasonic transducers (TUSHT) under 200°C sodium. In the sodium pot, several mock-ups are positioned with different objectives: Imaging, NDT in ASTRID representative structures, sub-assembly identification and telemetry through screens.

Regarding under-sodium imaging, the VISION mock-up contains engraved letters and grooves, simulating open fissures, a small triangle with sharp edges and a portion of piping. It is initially a set of images obtained by targeting this mock-up that is reconstituted and compared with those obtained in water.

The ability to visualise objects in sodium under operational conditions was demonstrated¹³ by scanning objects using this robot with four degrees of freedom and high-temperature ultrasonic transducers (TUSHT). This was done by reconstructing a 3D image on the basis of ultrasonic sodium tests, as well as providing a representation of the letters and grooves simulating open cracks.

The grooves, including the thinnest which was only 500 µm wide, were detected by the Ø40mm TUSHT with a focusing lens (Figure 30).

The letters and engraved slits can be seen in these images (also see Figure 30). The letters "CEA", "SCK" and "IGCAR" can be read.

The engraved slits are also well represented. It is important to remember that the thinnest slit measured only 500 µm, while the focal diameter was only 2 mm.

These images were obtained with a scanning step of 0.5 mm, which gave us the image resolution.

By comparing the mockup's metrology model with the measurements on the images, the following is obtained:

- The depth of the engravings is 2 mm.
- The slot width is obtained at less than 0.5 mm, which corresponds to the resolution of our images.

Figure 30. In sodium imaging of a plate with slits and letters (VENUS tests with TUSHT transducers). Optical image (top left), rough acoustic echoes (top right, in blue) and enhanced signal treatment (bottom, orange zones).



II.E Control of sodium-gas compact heat exchangers

A non-destructive testing method has been tested for the inspection of innovative compact heat exchanger. One of its main innovations, compared to past sodium fast reactor heat exchangers, is to eliminate the risk of a sodium-water reaction by using high pressure nitrogen as a cooling fluid.

This innovation comes at the cost of new constraints on the thermomechanical and thermohydraulic design of this component and its non-destructive testing. The heat exchanger assembly procedure currently proposed involves high temperature and high pressure diffusion welding of grooved stainless steel plates, with the goal of reaching high compactness levels.

The aim of the non-destructive method presented herein is to characterise the quality of the welds obtained through this assembly process¹⁴. Following preliminary work on this topic, a quantitative method has been selected that can be applied to pulse-echo normal incidence ultrasonic scans of bonded specimens. This method should be extended to higher ultrasonic frequencies. This will allow to reach a higher resolution in some welded location as well as a more precise characterisation of the diffusion bond and hence the material state. Experimental results obtained on sample specimens are promising. This quantitative evaluation method should give special attention to the analysis of the narrow grooved regions and the precision attained in their ultrasonic image.

II.F Methods for in-situ repair

In the frame of ASTRID project, R&D effort for repair was lower than for inspection and mainly done during pre-conceptual and conceptual design phases (2010-2015).

The laser process was assessed as a possible repair tool¹⁵ because it has the advantage of being suitable for the steps to be performed (1. removal of sodium traces, 2. machining or gouging, and 3. welding of the stainless steel structural material), without generating any stress on the tool. Conventional tools (brush or gas blower for sodium removal, milling machine for machining, and TIG for welding) are only considered as back-up solutions.

The laser technology covers a wide range of applications: heat treatment (in solid phase), welding (in liquid phase), cutting, engraving,

machining, drilling, laser shock peening (LSP) and cold work without contact (with vapor phase). Three main parameters define the field of application for the laser beam: wave length (which determines the depth of photon penetration), power density (which controls the surface temperature) and the interaction time (which determines the power: from several Kilowatts for continuous waves up to several megawatts for a 'nanosecond' pulse).

Three types of requirements have been identified for applications using lasers to perform repairs:

- Stripping requirements: This involves removing the layer of sodium before an inspection or welding operation (particularly necessary for TIG welding due to the interaction of sodium vapors with the direct current plasma and ignition difficulties).
- Machining requirements: This usually involves gouging around a crack.
- Fusion welding requirements, with or without filler metal, fusion for the relief of internal stresses, closure of cracks, and refilling gouges or welding patches, etc.

For the removal of sodium traces (before other repair steps), a preliminary design phase assessed the capacity to evaporate the sodium deposited on stainless steel structures by heating, using the laser. However, for practical purposes, sodium was replaced with zinc since its evaporation temperature at 907°C is similar to that of sodium at 883°C. The BALTHAZAR test facility was designed for this reason: it is equipped with two induction heating systems as shown on Figure 31. The first was used to generate a molten pool of zinc in a refractory crucible. The second was used to control the temperature of the test sample.

The crucible and the test sample were housed in a vessel which ensures inert gas atmosphere of the surrounding environment. The thickness of the zinc deposition was around 100µm, as demonstrated by the metallographic cross-section in Figure 32.

Figure 31. BALTHAZAR laser test facility

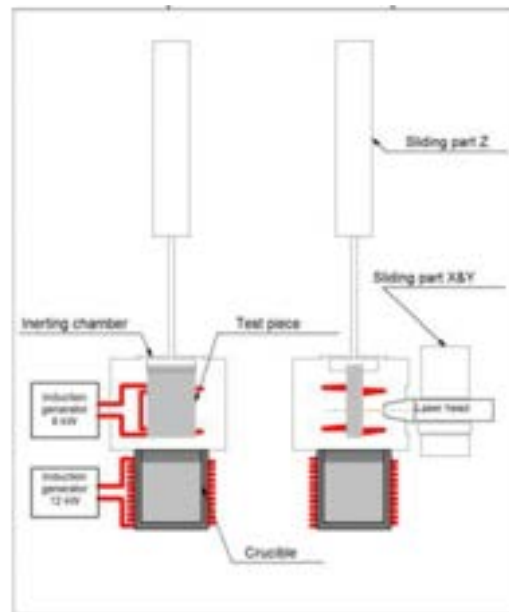
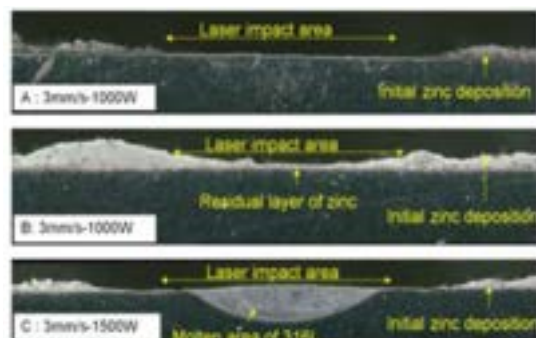


Figure 32. Metallographic cross-section – zinc deposition on 316L steel



Figure 33 shows the macrographic cross-sections corresponding to three tests performed with a laser head translation rate of 3 mm/s, in order to remove zinc traces.

Figure 33. Metallographic cross-sections - zinc evaporation



Test A carried out at a power of 1000 W made it possible to strip the zinc, without forming a molten area of 316L. With the same parameters, however, test B led to a different result as stripping was only partial. This difference is attributed to a difference in the initial thickness of the zinc deposition. For test C carried out at a higher power (1500 W), the removal of the zinc was combined with the formation of a molten area of 316 L steel. It is therefore possible to evaporate the zinc deposition before melting the 316L steel and thus create a melt run without filler metal on a stripped surface. The same should apply with filler metal: this will be demonstrated later.

Where prior visual examination of the steel surface under the deposition is necessary, controlling the energy source so the right amount is applied to evaporate the zinc deposition without melting its substrate proves to be a difficult operation. This would require the use of an adapted servo-system.

For the machining or gouging of damaged material, the evaporation of 316 L steel can be performed using a laser beam with sufficient power density. A test campaign of isolated laser shots – with the pulses repeated in a line and then with 2D scanning – made it possible to determine the impact of different process parameters in order to conduct the first excavation run: impact diameter, power, pulse duration, cycle time, overlap factor and type of surrounding gas. The displacement of a focused beam over a diameter of about 0.5 mm with a peak power of 4 kW made it possible to excavate out the first cavity with a depth of 2 mm at a rate of some cm³/hour.

The research must be continued in order to increase the excavation depth by means of successive runs. The metallurgical quality of the final results must also be checked to see whether it is possible to fill this cavity with a new supply of material.

The optical aspects must also be better controlled in terms of protection against the pollution generated by the process (high production of vapors and metal particles against the laser head window).

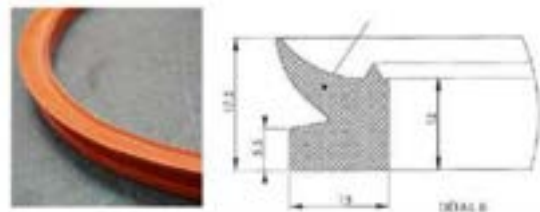
For the welding of damaged zones, it is considered that the laser process is now available through many industrial applications (technological materials: laser heads, optical fibers, simulation). The welding parameters will have to be optimised with respect to the related performance levels assessed before being qualified for realistic ASTRID structural repair

conditions (geometry, material, position, etc.). Two scenarios are envisaged: welding of a local plug (on plate with a hole) or sleeve (in leaking tube), and welding after gouging. Re-qualification after repair will also have to be considered.

These repair techniques are not applicable in a bulk sodium medium. This is why, except for the removable components, they will be performed in a gas environment: either in the upper dry zones of the reactor cover-gas plenum, or in a gas-tight volume, if the faulty zone is located under the sodium free level: such sodium-immersed bells will be positioned on the structure in order to perform local repairs. This system will have to contain the inspection and repair tools and protect them from the surrounding liquid sodium.

The design and water qualification of such a gas-tight system¹⁶ (using seals) was performed: a rigid bell, in contact with the structure to be repaired and having a seal formed by two flexible lips (see Figure 34), was investigated.

Figure 34. Profile of silicone sealing join

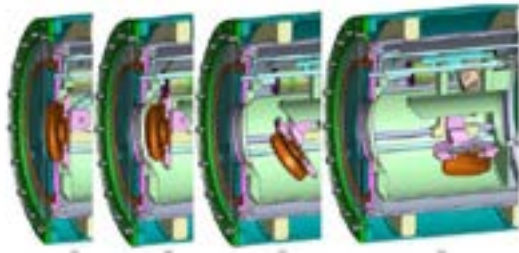


A first prototype bell is now being tested in a water tank which will be used for the later qualification of the entire repair kinematics (repair tools in the bell, sealing of the bell, associated fluids): its shutter kinematics is illustrated on Figure 35.

A silicone material (C85MTHT/60) was chosen for the seals after some test campaigns which were conducted to characterise this type of material. In terms of leaktightness, the tests showed that the irradiation campaigns had little influence on the performance of seals in the field in question (irradiation ageing with a cobalt γ source: 1.17 - 1.33MeV, inducing 600 - 6000 Gy cumulated dose). As far as ageing in sodium is concerned, the results are more controversial. In fact, the surface of aged samples was damaged by the sodium: cracks seriously affected the degree of leaktightness. Although improvement by a factor of 10 can be observed with grade C85MTHT/60, the degree of

leaktightness is still lower by a factor of 100 compared with the leaktight performance for the non-aged material.

Figure 35. Kinematic of the bell shutter: [A] Shutter closed, tight thanks to pressurised membrane [B] Depressurisation of membrane and opening of the shutter [C] Removal of the shutter [D] Shutter completely removed



R&D effort for repair techniques is now lower during conceptual design phase.

II.G In-sodium robotics

As mentioned before for repair activity, R&D effort for robotics is also lower than for inspection during pre-conceptual and conceptual design phases.

One of the ASTRID project goals is to demonstrate the feasibility of under sodium robotic inspection and repair. Indeed, under sodium operations would be preferred to sodium draining operation when possible (considering the potential caustic corrosion risk).

Running R&D is now focused on dedicated actions for specific applications within ASTRID reactor (see hereafter); the most important technical aspects to be resolved (in sodium tightness, irradiation and thermal effects...) were studied during pre-conceptual phase. Associated R&D effort for robotics is also lower during conceptual design phase.

Several work topics have been identified and distributed between the CEA, EDF and FRAMATOME teams:

- Generic studies on robotics for ASTRID (in sodium or not);
- Associated means for testing;
- Application 1: robotics within the gap between main and safety vessels (out of sodium);

- Application 2: inspection system for steam generator tubes;
- Application 3: pushed chain type robot; this has been specifically studied for the case of the bottom part of the strongback structure;¹⁷
- Application 4: pole and cable type robot;
- Application 5: on-wheels robot for large in-gaz equipments;
- Application 6: robot for repair tools;
- Repair techniques.

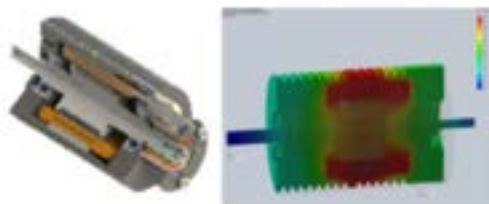
At a preliminary phase, three main configurations have been considered, depending on the adopted solution for robot component seclusion¹⁶:

- Leaktight surrounding shell cooled by an argon gas flow: the constraints are irradiation and 70°C temperature,
- Leaktight surrounding shell (not cooled) where the constraints are irradiation and 180°C-200°C temperature,
- No leaktight surrounding shell with the following higher constraints: irradiation and 180°C-200°C temperature and immersion within liquid sodium.

It appears that some technical solutions do exist for future in-sodium carriers, using available trade components, but not for all required materials. This is why development and qualification will be needed to confirm some specific components (such as polymers, greases, sensors, reducers, motors, bearings).

As an example, for electrical motor dedicated to 200°C operation, R&D work is leading to a first prototype with already available components, as shown on Figure 36.

Figure 36. Prototypic brushless motor working at 200°C



Validation tests on simplified geometries (see Figure 37), as well as on realistic robot articulations, are currently being

conducted to confirm the feasibility of using factory-produced or custom-made robots, insulated and cooled at 200°C, for repairing ASTRID.

Figure 37. Specific tight robot mockup with 2 degrees of freedom



Taking advantage of generic and technological studies for ASTRID robotics, specific ISI&R tool carriers are considered during conceptual and basic design phases. Development and qualification still remain for reaching demonstration level.

III. Conclusion

On the basis of available feedback and the high level safety requirements of nuclear plants, the ISI&R for SFRs has been identified as a major task: indeed, it gives actual information of structure plant health, in accordance with design rules.

The French R&D program for ISI&R improvement is developed along several aspects (with different R&D priorities): i) ensuring close collaboration between the reactor designers and inspection specialists (high priority), ii) developing inspection tools and techniques applicable in a sodium environment: US transducers, NDE, telemetry and imaging techniques (high priority), iii) developing repair laser tools applicable in a sodium environment (low priority), iiiii) developing in-sodium robotics: generic studies for associated materials and specific applications for ASTRID (medium priority). The inspection of compact sodium-gas heat exchangers is also looked at.

The key milestones of this ambitious R&D program are:

- Validation of ultrasonic transducers for under sodium conditions,
- Development and qualification of ultrasonic inspection techniques (Non Destructive Examination, telemetry, and imaging) under 200°C sodium conditions,
- Definition and solutions for inspecting compact sodium-gas heat exchangers,
- Definition of key components of the robotic equipment for operation in sodium,
- Preliminary validation of repair processes and techniques (cleaning, machining and welding),
- Development of specific repair and robotic solutions for specific applications, during basic design phase.

Acknowledgements

The authors would like to thank the following colleagues who provided information or checked certain sections of this paper: F. Navacchia, C. Lhuillier, G. Gobillot, K. Paumel, P. Kauffmann, M. Cavaro, L. Brissonneau, F. le Bourdais, L. Pucci, J-M. Decitre, F. Rey, T. Jouan de Kervénoaël, C. Chagnot and K. Vulliez from CEA, and S. Mensah, S. Rakotonarivo, G. Corneloup, M-A. Ploix and J-F. Chaix from Aix-Marseille University.

Nomenclature

EMAT:	Electro Magnetic Acoustic Transducer
ISI&R:	In Service Inspection and Repair
NDE:	Non Destructive Examination
R&D:	Research and Development
SFR:	Sodium Fast Reactor
TUCSS:	Ultrasonic Transducer for under sodium NDE
TUSHT:	High Temperature Ultrasonic Transducer
US:	Ultrasonic, UltraSound

References

- [1] F. Baqué, F. Jadot, R. Marlier, J.F. Saillant, V. Delalande, *In Service Inspection and Repair of the Sodium cooled ASTRID Reactor Prototype*, Paper 15041, ICAPP 2015 Conf., Nice, France (May 3-6, 2015)
- [2] F. BAQUE, F. JADOT, R.MARLIER, J. F. SAILLANT, and V. DELALANDE, *In Service Inspection and Repair of Sodium cooled ASTRID Prototype*, Paper 44, ANIMMA 2015 Conf., Lisboa, Portugal (April 20-24, 2015)
- [3] F. JADOT, F. BAQUE, J. SIBILO, J. M. AUGEM, V. DELALANDE and J. L. ARLAUD, *In-Service Inspection and Repair for the ASTRID Project: Main Stakes and Feasible Solutions*, Paper T1-CN-199/165, FR'13 Conf., Paris, France (March 4-7, 2013)
- [4] F. BAQUE, F. JADOT, F. LE BOURDAIS, J. SIBILO, J. M. AUGEM and O. GASTALDI, *ASTRID In Service Inspection and Repair: review of R&D program and associated results*, Paper 337, FR'13 Conf., Paris, France (March 4-7, 2013)
- [5] F. BAQUE, F. REVERDY, J. M. AUGEM and J. SIBILO, *Development of Tools, Instrumentation and Codes for Improving Periodic Examination and Repair of SFRs*, Hindawi Publishing Corporation, Science and Technology of Nuclear Installations, Volume 2012, Research Article ID 718034, 19 pages (2012)
- [6] F. Baqué, C. Lhuillier, F. Le Bourdais, F. Navacchia, JF. Saillant, R. Marlier, JM. Augem, *R&D status on in-sodium ultrasonic transducers for ASTRID inspection*, Paper 279, FR'17 Conf., Ekaterinburg, Russia (26-29 June, 2017)
- [7] F. LE BOURDAIS, J-M. DECITRE, L. PUCCI, C. REBOUD, *Accurate simulation of EMAT probes for ultrasonic NDT based on experimental measurements*, Quantitative Nondestructive Evaluation Conf., Baltimore, Maryland, USA (July 2016)
- [8] J. F. SAILLANT, R. MARLIER and F. BAQUE, *First results of non-destructive testing under liquid sodium at 200°C*, ANIMMA 2017 Int. Conf., Lièges, Belgium (June, 2017)
- [9] P. Kauffmann, M-A. Ploix, J-F. Chaix, G. Corneloup, C. Gueudré, F. Baqué, *Multi-modal leaky Lamb waves in two parallel and immersed plates: theoretical considerations, simulations and measurements*, JASA (Journal of the Acoustical Society of America) Manuscript number JASA-03004
- [10] G. TOULLELAN, R. RAILLON, S. MAHAUT, S. CHATILLON, S. LONNE, *Results of the 2016 UT Modeling Benchmark Obtained with Models Implemented in CIVA*, Quantitative Nondestructive Evaluation Conf., Baltimore, Maryland, USA (July 2016)
- [11] Lubeigt, S. Mensah, S. Rakotonarivo, J-F. Chaix, F. Baqué, G. Gobillot, *Topological imaging in bounded elastic media*, Ultrasonics 76 (2017) 145–153
- [12] G. GOBILLOT, E. SANSEIGNE, F. BAQUE, I. EL KHALLOUFI, *Under-Sodium Imaging of SFR Internals – Four degrees of freedom with a sodium transducer displacement system*, Int. Conf. Ultrasonics 2018, Lisbon, Portugal (June 2018)
- [13] G. GOBILLOT, E. SANSEIGNE, F. BAQUE, *Four degrees of freedom with a sodium transducer displacement system*, ANIMMA 2017 Int. Conf., Lièges, Belgium (June, 2017)
- [14] LE BOURDAIS, L. CACHON, F. BAQUÉ, E. RIGAL, *High Frequency Reflexion Measurements of Diffusion Bonded Steel Plates for the ASTRID Secondary Heat Exchanger*, ANIMMA 2017 Conf., Lièges, Belgium (June 19-23, 2017)
- [15] BAQUE, C. CHAGNOT, L. BRUGUIERE, J. M. AUGEM, V. DELALANDE, L. GUENAD and J. SIBILO, *Generation IV Nuclear Reactors : Under Sodium Repair for SFRs*, Paper 1256, ANIMMA 2013 Conf., Marseille, France (June 22-27, 2013)
- [16] K. VULLIEZ, L. BRUGUIERE, L. MIRABEL, A. BEZIAT, F. BAQUE, M. BERGER, B. DESCHAMPS, J. F. JULIAA, F. LEDRAPPIER, G. RODRIGUEZ and B. ROUCHOUZE, *R&D Program on sealing issues for in-service inspection and repair tools on ASTRID sodium prototype*, Paper 199/125, FR'13 Conf., Paris, France (March 4-7, 2013)
- [17] M. Giraud, R. Marlier, L. Gresset, F. Baqué, T. Jouan de Kervenoael, A. Riwan, K. Vulliez, JM. Augem, *Main R&D objectives and results for under-sodium inspection carriers – Example of the ASTRID matting exceptional inspection carrier*, Paper 417, FR'17 Conf., Ekaterinburg, Russia (26-29 June, 2017)

PAPERS WITH NO TRACK

DEVELOPING A MOLTEN SALT REACTOR SAFEGUARDS MODEL (B. CIPITI ET AL)

Benjamin Cipiti and Nathan Shoman

Sandia National Laboratories, USA

Abstract

Molten Salt Reactor (MSR) designs can be significantly different from a typical light water reactor. Current designs include solid fuelled cores with molten salt coolants, liquid fuelled drop-in core designs, and liquid-fuelled designs with on-site salt reprocessing. The liquid-fuelled designs in particular have unique materials accountancy challenges. Safeguards requirements for light water reactors are based on item accounting and containment and surveillance since the fuel assemblies are discrete entities. MSRs may have materials accountancy requirements similar to bulk processing facilities. In this work, a material tracking and safeguards model of a MSR was developed in order to better understand safeguards needs and develop initial materials accountancy system designs. The model is built using Matlab Simulink and is linked to the SCALE code to calculate depletion and decay at various points in the reactor salt loop as needed. This paper presents the modelling philosophy and technical challenges. Initial results will be presented, but more detailed analysis will be required before safeguards approaches can be considered.

I. Introduction

Recently, there have been a number of new vendors developing Molten Salt Reactors (MSRs) for commercial deployment. Of all the advanced reactors types, MSR designs vary the most since they can include liquid-fuelled or molten salt cooled designs with solid fuel. As such there are various safeguards challenges depending on the design. The purpose of this work is to develop a modelling capability to evaluate materials accountancy approaches for MSRs.

II. Background

Several variations of MSR designs exist, but they generally fall into three categories: liquid-fuelled designs with full on-site salt processing, drop-in liquid-fuelled core designs with limited on-site salt processing, and solid fuelled designs that use a molten salt coolant.

The first category are MSRs with liquid-fuelled cores and full on-site processing of the salt. These designs stem from the work on the

Molten Salt Reactor Experiment (MSRE) at Oak Ridge National Laboratory in the 1960's [1]. Molten salt is used as both the fuel and coolant, and salt processing is required to replenish actinides and remove fission products and gases. Typical designs can include a fuel salt and blanket salt for a breed and burn system, and can have a design life of up to 60 years. The Liquid-Fluoride Thorium Reactor (LFTR) design from Fluibe Energy appears to be the most mature current concept in this category [2]. These designs will have the most significant safeguards challenges since the actinide content may need to be determined through sampling and destructive analysis. The processing loops are similar to reprocessing plants, and in particular pyroprocessing salts.

The second category of MSRs are liquid-fuelled drop-in cores. These are designed as self-contained designs where the reactor module is replaced every 7-8 years or so. An example design is the Integral Molten Salt Reactor by Terrestrial Energy [3]. The salt is not processed on-site, but the entire core would be removed and processed at a centralised processing facility. One advantage of this design is to

reduce the risk of neutron damage to reactor materials. Materials accountancy measurements of the molten salt will still be required, but there may be advantages to self-contained cores.

The third category of MSRs are solid-fuelled cores with molten salt as the coolant. These designs are using TRISO fuel either in fixed assemblies or pebble bed designs. The Small Fluoride Salt-Cooled High Temperature Reactor, developed by Oak Ridge National Laboratory is an example of this type of design [4]. Fixed assemblies would have similar safeguards requirements as light water reactors (mainly based on item accounting and containment and surveillance). Pebble bed designs may have an added complication in keeping track of pebbles, but generally the requirement of obtaining large numbers of pebbles to get enough material for a significant quantity makes theft unrealistic.

This work is initially focused on modelling liquid-fuelled designs with on-site processing since they pose the greatest safeguards challenges. Future work will examine liquid-fuelled drop-in core designs based on lessons learned from this work.

III. Modelling Approach

The MSR safeguards model was built using Matlab Simulink, and pulls on past work developing the Separation and Safeguards Performance Model (SSPM). The SSPM has been used for safeguards analysis and design of both aqueous and electrochemical reprocessing plants, and is designed to evaluate accountancy systems for bulk handling facilities [5]. The architecture of the SSPM was used to build the salt processing loop for the MSR model; however, the model was linked with ORIGEN in order to approximate depletion in the core and decay calculations.

A key challenge of this work has been to correctly model the changing isotopic and elemental inventories as a function of time. Linking with ORIGEN provided a starting point upon which to build the rest of the model, but future work will integrate with more mature modelling efforts at Oak Ridge National Laboratory [6]. The work to date has focused on modelling the elemental and isotopic flows and inventories, but future work will add in various safeguards elements.

The MSR design and flowsheet that was used for the model was based on the Liquid-Fluoride

Thorium Reactor (LFTR) [2]. This design was a collaboration between the Electric Power Research Institute and Southern Company and pulls heavily on the MSRE work. The reactor is liquid-fuelled, graphite moderated, and utilises a thorium fuel cycle. U-233 is burned in the fuel salt, and a separate blanket salt is used to breed U-233 from thorium.

Reference 2 was used in part because it was the only one available which contained enough information about the salt processing loops to model. This reference included the processing steps and flow rates, which were directly used to build the Simulink model. The specific details will not be described here.

Simulink model

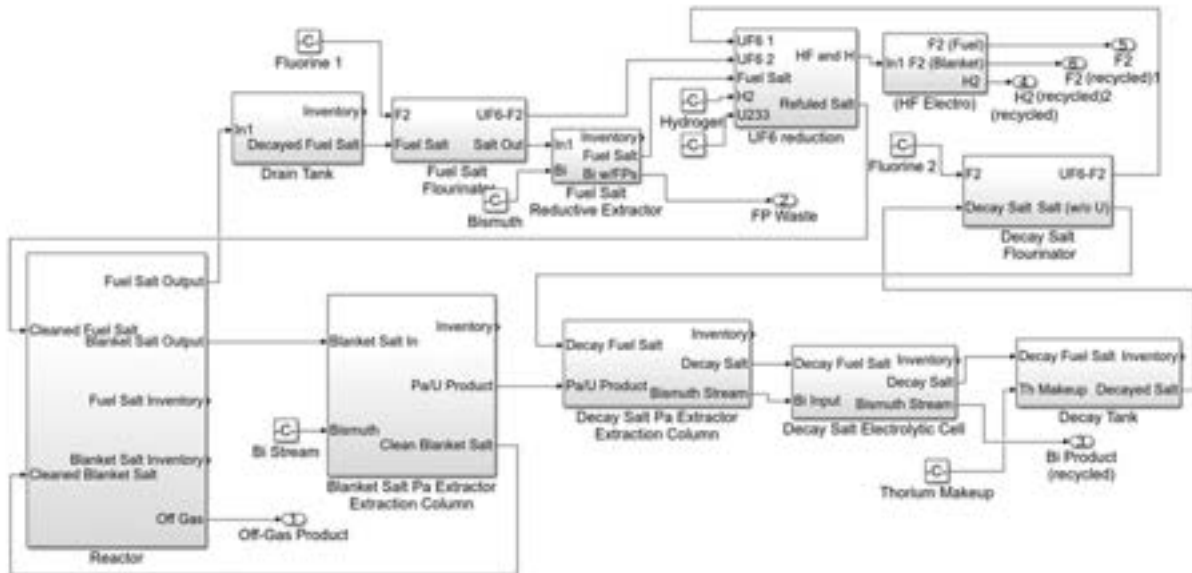
The preliminary MSR safeguards model is shown in Figure 1. The blocks in this figure represent the major unit operations. The most detail is included in the reactor subsystem, shown on the left. The rest of the blocks are various tanks and columns used for the salt processing.

The reactor design uses both a fuel salt and blanket salt. The fuel salt flow to the heat exchangers is not modelled (for simplicity) and because the flow rate is so large compared to the chemical processing loop. However, it is taken into account in the reactor model and in determining the correct off-gas production.

The top half of Figure 1 is the fuel salt processing loop. A small stream of the fuel salt goes to the drain tank where the material is held up for about 30 days to allow short-lived fission products to decay. Then the fuel goes through the remaining processing steps. The subsequent steps remove fission products and then re-fuel the salt with UF₆ from the blanket loop. The fuel salt is then returned to the reactor.

The bottom half of Figure 1 is the blanket salt processing loop. The blanket salt is first processed in an extraction column to remove the bred protactinium and replace lost thorium. The protactinium needs to decay in the Decay Tank for about 100 days so that most of the protactinium decays to U-233. That material is then transferred into the fuel salt for re-fuelling.

Figure 1. Molten Salt Reactor Safeguards Model



Reactor subsystem

The reactor subsystem consists of the fuel salt and blanket salt inventory terms. These inventory terms are periodically updated by calling the ORIGEN depletion code. Simulink constantly updates the blanket and fuel salt inventory terms as recycled salt is added from the various chemical processing systems. Every 20 simulation hours ORIGEN is called to update the salt terms. The Simulink calculation is paused as the inventory terms are formatted and written to an ORIGEN file.

Once ORIGEN has depleted the blanket and fuel salt, Matlab reads the ORIGEN output, formats the data, and updates the Simulink model. Transport delays are used in Simulink to ensure that the simulation time is then synchronised with the time elapsed during the depletion. After the inventory has been updated, the Simulink calculation continues to run until the next ORIGEN update.

Currently, the salt inventories are depleted separately. The salt depletion is calculated by ORIGEN using a library derived from the flux spectra and one-group cross-section library of a Westinghouse 17x17 pressurised water reactor assembly. This flux is probably a reasonable approximation for the fuel salt since the neutron spectra is expected to be thermal, but

the blanket salt will likely have a faster neutron spectra. In the future, the depletion model will be updated to be more representative of molten salt reactor conditions. The power applied to the fuel and blanket salt are tuned to provide a specified breeding ratio.

Salt processing loops

The salt processing loops consist of tanks and extraction columns. The drain tank and decay tank require unique programming since they take into account decay of the actinides and/or fission products. These are described more in the following section.

The extraction columns use bismuth to extract quantities of interest. The unit operation models in Simulink use gain blocks to determine the fraction of each element that goes into each output.

Starting with the blanket salt output, in the Blanket Salt Pa Extraction Column, the blanket salt is contacted with a metallic Bi stream that contains Th. The extraction essentially removes any Pa and U from the blanket salt and replaces it with Th. The Pa and U are then in the metallic state in the Bi stream. The cleaned and re-fuelled blanket salt is returned to the reactor.

The Decay Salt Pa Extraction Column and the Decay Salt Electrolytic Cell extract the Pa and U back into the decay salt and keep any Th in the metallic Bi stream. The decay salt with Pa and U then goes to the decay tank.

The decay tank provides enough time for most of the Pa to decay to U, and the U is then transferred to the fuel salt loop in the Decay Salt Fluorinator. The decay tank is also where fresh Th is added to the blanket—it ultimately gets transferred to the Bi stream which re-fuels the blanket in the Blanket Salt Pa Extraction Column.

Moving up to the fuel salt loop, the Drain Tank is used to allow time for short-lived species to decay. The slightly-cooled fuel salt goes to the Fuel Salt Fluorinator which temporarily removes U.

The fuel salt is then contacted with metallic Bi in the Fuel Salt Reductive Extractor to remove fission products as a waste.

The cleaned fuel salt, the temporarily removed U, and the U-233 from the blanket salt are combined in the UF₆ Reduction vessel and then returned to the reactor.

The loops also contain chemical reactors that use hydrogen and fluorine gas for various steps. The model does not track specific chemicals, instead it tracks the total elemental quantities in each stream.

Drain and decay tanks

The drain tank contains fuel salt that needs to decay before further processing. The fuel salt decays to reduce the short-lived (and high thermal output) fission product concentration. The material residence time in the drain tank is approximately 30 days.

The decay tank contains blanket salt and allows time for the Pa-233 to decay to U-233 which is later used as fuel. The material residence time in the decay tank is approximately 100 days, which provides enough time for four half-lives.

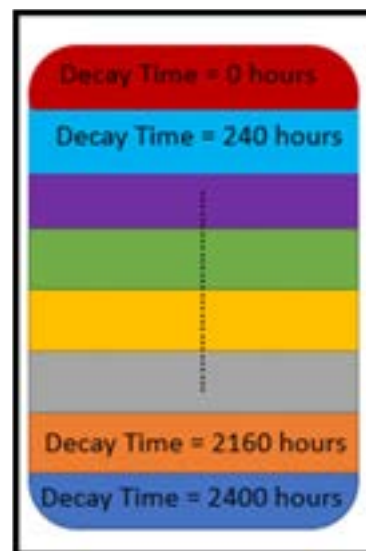
Both decay tanks are modelled exactly the same except for the length of time the material is in the tank. For illustrative purposes the blanket salt decay tank will be described.

Modelling the decay tank is challenging due to the constant change of the blanket material. As stated previously the blanket salt is depleted every 20 hours, which means that the composition of the blanket salt entering the decay tank is changing every 20 hours. The changing input fuel is approximated by

modelling the tank in 10 “slices” as seen in Figure 2. Initially, the decay tank is assumed to contain 10 slices of clean salt. The flow rate into the tank and the tank volume are given in the reference so it is possible to determine the length of time required to accumulate 1/10th of the tank volume or one “slice”.

Once enough time has elapsed to accumulate one slice, that material is written to an ORIGEN file for decay. The output of the ORIGEN file describes the decay of the given material in 10 evenly spaced intervals from the initial time $t=0$ to the final decay time $t=100$ days. This data is stored in a persistent Matlab array. This process repeats every time enough material enters the decay tank to create a slice. Every time a slice is created the inventory and decay tank output is updated.

Figure 2. Decay tank inventory



To summarise, the reactor subsystem and drain and decay tank subsystems are the more complex areas of the model. The calls to ORIGEN to calculate the depletion or decay calculations require the most computational time. The separation of elements in the salt processing loops is relatively straight-forward in comparison. The following sections describes the current status of the model and some preliminary results.

IV. Current Model Status

Currently the model is generating useful results. The model has been balanced so that the

actinide levels reach steady-state. Figure 3 shows the modelling results for the protactinium content in the blanket salt as a function of time. It takes on the order of ten days or so for the content to stabilise after start-up of the reactor.

The fission products build up considerably in the fuel salt, which is expected since only a small slip stream of the fuel salt is processed. Figure 4 shows the build-up of cesium in the fuel salt—even after 4000 hours the reactor is not in a steady-state condition. This buildup is typical of an MSR, but the acceptable build-up levels of fission products will be determined based on the effect on core neutronics and heat load. In future design work, the volume of the salt processing loop can be changed to accommodate design requirements.

Figure 3. Protactinium Content in the Blanket

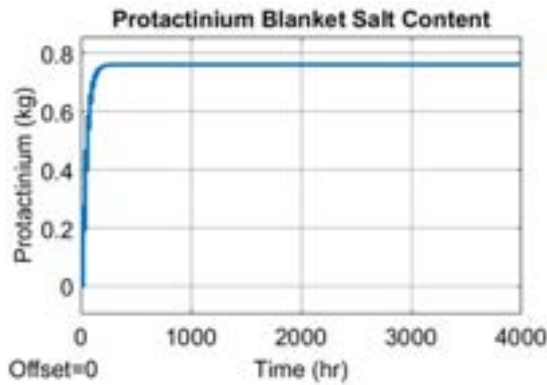
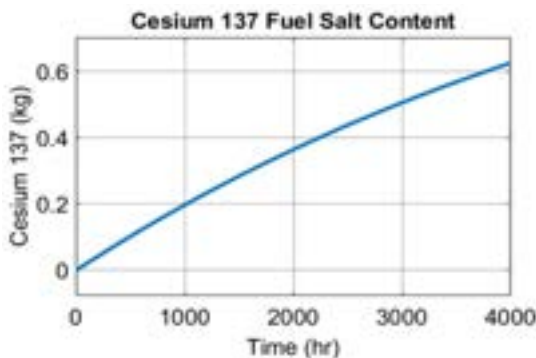


Figure 4. Cs-137 Content in the Fuel Salt

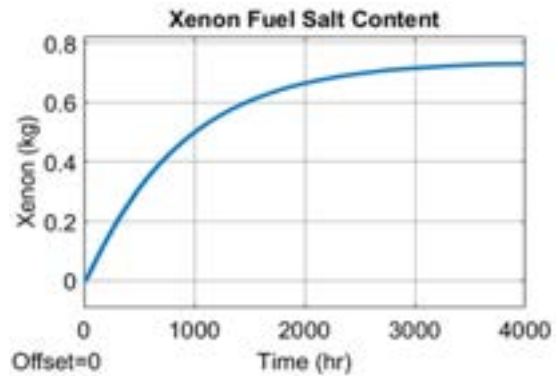


The xenon content in the fuel salt was also examined since it is important to minimise this poison. Since the xenon is removed in the main fuel salt heat transfer loop, considerably more

is removed as a function of time, and it reaches a steady-state condition sooner (as compared to the cesium which is removed in a much smaller processing loop). Figure 5 shows the xenon content as a function of time—by about 3000 hours, the xenon is near a steady-state condition.

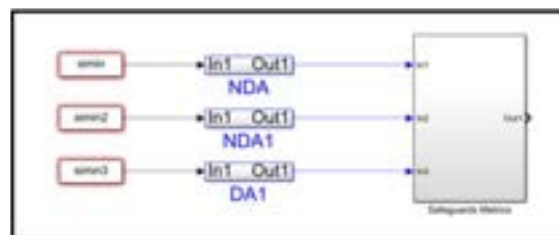
One challenge with the modelling is that the external calls to ORIGEN lead to significant computational times. Several hours are required to model one year of operation. Steady-state conditions in an MSR that occur after several years may take 24 hours of run time. This computational time cannot be improved through parallel processing since Simulink processes functions in series. However, future work will attempt to improve processing times.

Figure 5. Xenon Content in the Fuel Salt



Due to the lengthy computational times to run the model, the safeguards model is de-coupled from the plant model. The plant model will be used to generate data sets as function of time (inventories and flowrates) that feed into the safeguards model. Figure 6 shows basic architecture. The true values for inventories and flowrates will be used to inform safeguards measurements. Those measurements will then be used to calculate an overall material balance.

Figure 6. Safeguards Modeling Approach



The safeguards model is at a less mature point in development. One of the challenges is that regulatory requirements for MSRs are uncertain, so specific measurement locations will need to be determined. In the next year, safeguards measurements will be added to the model. Fortunately, past work on safeguards and process monitoring measurements for pyroprocessing can be leveraged since pyroprocessing facilities also work with molten salts. The models for these measurements as well as the material balance calculations exist in other SSPM models.

Moving forward, this work will be linked with on-going work at Oak Ridge National Laboratory to provide more realistic depletion calculations. This may involve updating cross-section libraries or directly linking to the ChemTriton depletion and transport code [6].

V. Conclusion

A preliminary MSR process and safeguards model has been generated in the Matlab Simulink platform. The model is designed for liquid-fuelled designs with on-site salt processing. The work in this past year focused on building the base of the model and correctly modelling flow rates, depletion, and decay. Future work will either use more robust code results from Oak Ridge National Laboratory or verify the existing calculations. The ultimate purpose of this work is to model the safeguards systems, so future work will add in safeguards and process monitoring measurements and propose preliminary safeguards system designs.

Acknowledgements

This work was funded by the Materials Protection Accounting and Control Technologies (mpaCT) working group as part of the Fuel Cycle Technologies Program under the U.S. Department of Energy, Office of Nuclear Energy. Sandia National Laboratories is a multitechnology laboratory managed and operated by National Technology and Engineering Solutions of Sandia LLC, a wholly owned subsidiary of Honeywell International Inc. for the U.S. Department of Energy's National Nuclear Security Administration under contract DE-NA0003525. This paper describes objective technical results and analysis. Any subjective views or opinions that might be expressed in the paper do not necessarily represent the views of the U.S. Department of Energy or the United States Government.

Nomenclature

LFTR	Liquid Fluoride Thorium Reactor
MSR	Molten Salt Reactor
MSRE	Molten Salt Reactor Experiment
ORIGEN	Oak Ridge Isotopic Generation
SCALE	Standardised Computer Analysis for Licensing Evaluations
SSPM	Separation and Safeguards Performance Model
TRISO	Tri-Isotropic

References

- [1] M.W. ROSENTHAL et al., "Molten Salt Reactor Program Semiannual Progress Report," Oak Ridge National Laboratory, ORNL-4191 (1967).
- [2] SOWDER, "Program on Technology Innovation: Technology Assessment of a Molten Salt Reactor Design: The Liquid-Fluoride Thorium Reactor," Electric Power Research Institute (2015).
- [3] "Status Report - IMSR-400," available at aris.iaea.org, Terrestrial Energy (2016).
- [4] "Status Report - SmAHTR," available at aris.iaea.org, Oak Ridge National Laboratory (2016).
- [5] CIPITI, "Separations and Safeguards Performance Modeling for Advanced Reprocessing Facility Design," *Journal of Nuclear Materials Management*, 40/3 pp. 6-11 (2012).
- [6] B.R. BETZLER, J.J. POWERS, and A. WORRALL, "Molten Salt Reactor Neutronics and Fuel Cycle Modeling and Simulation with SCALE," *Annals of Nuclear Energy*, pp. 489-503 (2017).

CORROSION BEHAVIOR OF 310S IN SUPERCRITICAL WATER (B. GONG ET AL)

Bin Gong, Jin-Hua Liu, Shan-Xiu Cong

Nuclear Power Institute of China, Chengdu, China

Abstract

The effects of dissolved oxygen and hydrogen at 620°C/25 MPa on the stress corrosion cracking sensitivity of 310S were studied by slow strain rate tensile tests. The main failure mode of stress corrosion test specimens is intergranular cracking at 620°C/25 MPa in oxidised SCW. Cracking sensitivity was increased by the increase of dissolved oxygen. Crack originated in the Cr-rich carbides and propagated along the grain boundary. Cr-rich oxide layer along the cracks formed in the supercritical water containing high concentration of dissolved oxygen is relatively discontinuous and non-uniform. Dissolved hydrogen cannot significantly decrease the crack propagation rate. Slow strain rate tensile tests results showed an increased transgranular cracking sensitivity of 310S in the supercritical water containing 1.0 mg/kg of H₂ at 620°C/25 MPa. General corrosion experiment on 310S was carried out in deaerated SCW at 550°C/25 MPa for 1000h. Thermal water quality measurement were carried out during the tests to observe the variation of water parameters in the pseudo critical zones. A hideout and hideout return process of the impurities caused a value peaks of conductivity at 385.8°C. General corrosion test results showed a low weight gain and the oxide layer was 180nm with multi-layer structures. The Cr-rich inner oxide layer that formed in deaerated SCW was thin and continuous, which was favorable to improve the oxidation resistance of 310S.

Keywords: Supercritical water, Stress corrosion cracking, Austenitic stainless steel

I. Introduction

A supercritical water reactor (SCWR) is considered a promising Generation IV nuclear reactor owing to its simple design and high thermal efficiency. SCWR is a high-temperature, high-pressure, and water-cooled reactor, which operates above the critical point of water (374°C, 22.1 MPa). The typical design of an SCWR is a once-through, direct-cycle system operating at a pressure of 25 MPa and temperature range from 280°C to 620°C. One of the major challenge problems is corrosion and stress corrosion cracking (SCC) of materials in supercritical water (SCW). The corrosion resistance of materials is important requirements for the life management of SCWR reactor internals.

Austenitic stainless steels have been widely used as structural materials in nuclear reactors

owing to their excellent high-temperature corrosion resistance, good mechanical properties and easy availability. Typical 310S stainless steel is considered a promising material for fuel cladding of the Chinese CSR1000^[1] and the Japanese SCWR design^[2]. For the applicability and reliability analysis, the research on corrosion and SCC properties of this kind of material is the one of important tasks. Effects of candidate water chemistry regions (oxygen, hydrogen, etc.) on corrosion behaviors were also investigated. This paper reviewed the corrosion test results in recent research by NPIC.

II. General Corrosion Behavior

The weight gain of 310S and 800H in SCW at 550°C and pressure of 25 MPa was investigated

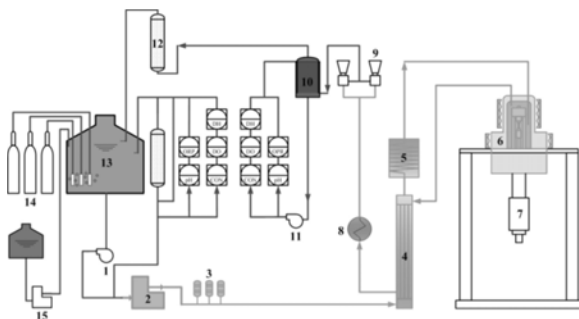
by a general corrosion test. The compositions of coupon specimens are listed as the Table 1. This research is also one part of the 2nd Round Robin exercise that was organised by JRC-IET in 2016. Also, similar experiment procedures and settings are used in each laboratory to evaluate the reproducibility of the results and the reliability of the test facilities.

Table 1. Chemical compositions of coupon specimens

Alloy	Fe	Cr	Ni	Mo	Mn
800H	bal	22.5	34.8	-	1.59
310S	bal	24.5	20.2	-	1.17
Alloy	Si	Al	C	Ti	
800H	0.95	0.45	0.08	-	-
310S	0.33	-	0.03	-	-

To investigate the general corrosion behavior of the specimens, the experiment was performed in a supercritical corrosion testing facility as schematically shown in Fig. 1. The testing facility consists an autoclave made from Hastelloy C 276 with the maximum testing temperature of 650°C at 30 MPa. A steady and reliable water chemistry environment in the autoclave was obtained during the testing. Water chemistry in the loop is controlled by extracting water from the loop. Running it through a chemistry system and re-injecting the water. Dissolved oxygen concentration, electronic conductivity, pH and ORP were measured by the chemistry system.

Figure 1. Flow chart of SCW Test Loop



1-feeding pump, 2-high pressure pump, 3-pressure storage, 4-heat exchanger, 5-preheater, 6-test cell, 7-loading system, 8-cooler, 9-pressure regulator, 10-outlet water storage, 11-measure pump, 12-purify column, 13-test solution storage, 14-gas cylinders, 15-chemicals feeding pump

The test cell volume was 2.5L and the flow rate of water was 1.2 L/h, resulting in refreshment of the test cell water approximately 0.48 times per hour. De-ionised water with conductivity less than 0.1 μ S/cm was pressurised to 25 MPa and heated to 550°C for establishing the SCW environment. The heat rate was controlled to be 50°C per hour in the range of 25-350°C and 5°C per hour in the range of 350-550°C for an observation of water parameters transition from subcritical to supercritical condition. The dissolved oxygen (DO) concentration in the SCW environment during the experiment was controlled less than 5 μ g/kg by bubbling high purity nitrogen. The Electronic conductivity was controlled under 55 nS/cm by ion exchange resin.

The dimensions of the samples were measured using microscope, which have accuracy of 0.1 μ m. Weighing of coupons was performed by a balance to an accuracy of 0.1 milligram, weighing of a specimen was repeated five times, datum of the weight is obtained as the average of these measured values. Weight and surface area changes were calculated after the experiment. The specimen was fixed in a holder made from Inconel 625 by 316L wires with a diameter of 0.5mm to ensure the surface area of the specimen in contact with holder was minimised (Fig. 2).

Figure 2. Coupons for general corrosion tests



Water chemistry parameters were monitored in a short term pre-test for observation the water quality affected by temperature. Metallic elements expected to be produced by corrosion of coupons, loop, and specimen holder. The non-metallic elements could be produced by ion-exchange resin and raw de-ionised water.

During the heating-up and cooling down, the purify system was closed and the release of ions caused a notable variation of electronic conductivity (EC), as shown in Fig. 3. A critical point of EC is at 385.8°C, the release of ions slow down above this point due to a hideout process and speed up above this point due to a hideout return process. With the purpose of maintain water quality, the purify system was working continually in the official test. Accumulation of elements could not be observed and had a low concentration constantly in the stable operation stage. The results of water samples for analysing dissolved metals and impurities were presented in Table 2, using Inductively-Coupled Plasma Atomic Emission Spectrometer. Notable among these data are relatively higher concentration of fluoride, chloride and sulfide, which are measured at 350~380°C during heating up and cooling down after 1000hrs test. Concentration of metal ions is lower than anion as expected due to purification and low corrosion rate of loop components.

Table 2. Element analysis in SCW during the experiment

Elements ($\mu\text{g}/\text{kg}$)	Heating-up ($^{\circ}\text{C}$)					
	25	350	380	450	500	550
F ⁻	1.96	0.16	5.08	0.43	0.55	0.21
Cl ⁻	1.42	14.49	9.39	2.56	1.08	3.26
SO ₄ ²⁻	0.05	0.68	0.52	0.17	1.92	1.48
Al	–	8	–	–	–	–
Si	–	–	–	–	–	–
Mg	–	–	–	–	–	–
Fe	–	–	–	–	4	5
Cr	–	–	–	–	–	–
Ni	–	13	6	4	6	8

Elements ($\mu\text{g}/\text{kg}$)	Experiment (hrs)			
	100	300	500	1000 (cooling down)
F ⁻	0.75	1.51	–	15.92
Cl ⁻	3.21	3.49	0.76	24.79
SO ₄ ²⁻	0.54	0.77	0.14	53.68
Al	3	–	–	–
Si	15	11	6	7
Mg	–	–	–	–
Fe	–	2	–	5
Cr	–	–	–	–
Ni	9	5	5	6

Figure 3. The conductivity of SCW measured in the short term pre-test

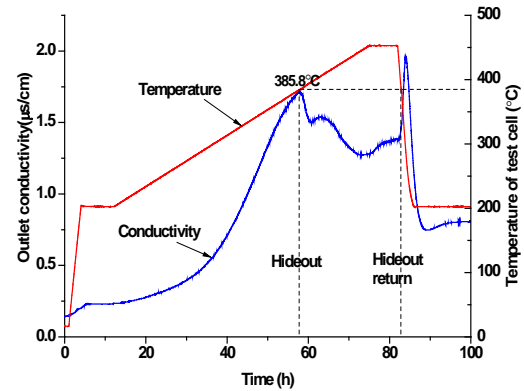


Table 3. Weight change of 310S and 800H after exposure in SCW at 500°C and 25 MPa for 1000h

Coupon Identification	Weight Change (mg)	Weight Change (mg/dm ²)
310S-1	0.12	6.309
310S-2	0.12	6.078
310S-3	0.14	7.116
310S-4	0.14	7.108
800H-1	0.14	7.098
800H-2	0.14	7.132
800H-3	0.18	9.183
800H-4	0.18	9.205

After exposure to supercritical water for 1000h at 550°C, the coupon weight change were measured and shown in Table 3 for 310S and 800H respectively. Weight gain was observed in all of specimens. 310S has gained 0.13mg mass in average, with the weight change rate of 6.65 mg/dm². 800H increased 0.16mg in average with the weight change rate of 8.15 mg/dm², which had greater weight gain co MPare to 310S.

Figure 4. Coupons after 1000hrs exposure in SCW

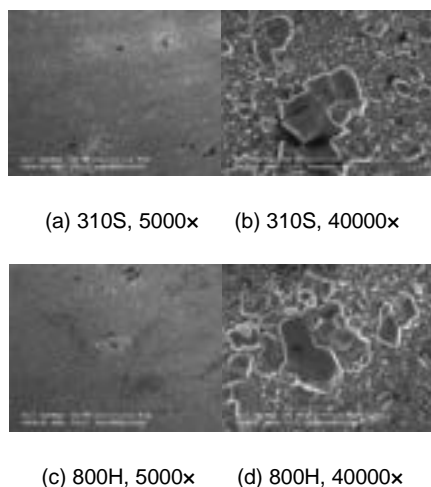


(a) 310S coupons



(b) 800H coupons

Figure 5. SEM morphology of coupons after exposure in SCW

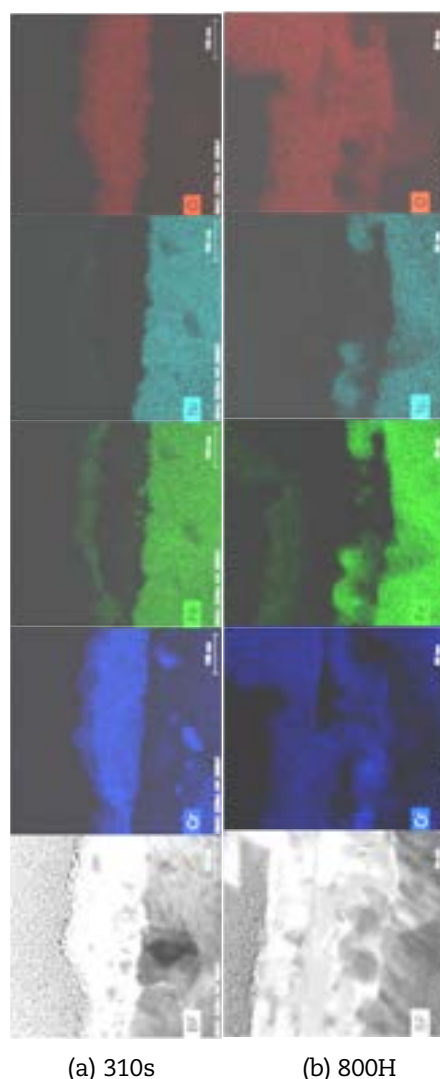


Visually, the 310S coupons have lost metallic color and turned into grey due to oxidation. The oxides of 800H coupons are typically in non-uniform metallic color, as shown in Fig. 4. There are dense oxide particles over the surface. The length of particles is less than ~ 200 nm. Some larger particles with length of ~ 1 μm can be observed and Cr is depleted, as shown in the SEM morphology (Fig.5). In Halvarsson's research [3], Cr in the oxide layer reacts with water and turns into $\text{CrO}_2(\text{OH})_2$ or $\text{CrO}_2(\text{OH})$, which is volatile and cause a loss of Cr in the oxide layer. The passivation of oxide layer decreases and results in the growth of oxide particles.

The elements distribution along the cross-section of oxide layers is shown in Fig.6. The oxide layer thickness is approximate 180 nm for 310S and 200nm for 800H. It is clear that a Two or three-layers structure. Cr is well distributed at all layers. Fe is detected in the outer layer. Ni enriches at the interface of the inter oxide layer and substrate, and small amount of Ni can be detected in the outer layer. The outer layer is $(\text{Cr}, \text{M})_3\text{O}_4$, spinel type Cr-rich oxide formed in high temperature water for austenitic stainless steels. This structure making it a dense and compact, preventing diffusion of environmental oxygen over the matrix. Formation of this protective film usually costs only a short period, but it can greatly slow down further corrosion rate. The middle layer is Cr_xO_y and Fe is depleted in the middle layer, which is a key role preventing the base metal element over the surface. The inter layer is $(\text{Fe}, \text{Cr}, \text{Ni})_3\text{O}_4$ spinel passivation of substrate. A

compact, stable Cr-rich oxide film is protective and essential in suppressing general corrosion in supercritical water.

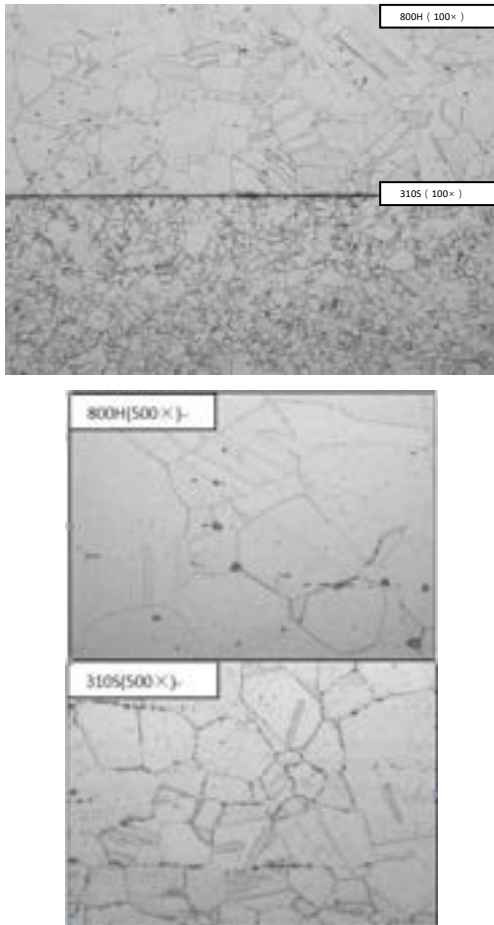
Figure 6. EDS images of cross-section of oxide layers after 1000hrs exposure in SCW



The metallographic structures of 310S and 800H were compared at same magnifications after exposed in SCW (Fig. 7). Larger grain size can be observed for 800H, and the grain boundary of 800H is pure with no obvious precipitates, only few discontinuous phase precipitations can be found on the surface of the metal. For 310S, the grain boundaries become clear and continuous because of precipitates, a kind of detrimental sigma phase, which is often observed in various series of stainless steels, being one of the main

reasons for the degradation of properties (mechanical, corrosion resistance, and weld ability). The sigma phase can be precipitated under elevated temperature and is difficult to prevent this phase when the Cr content is above 20 wt.% in stainless steels.

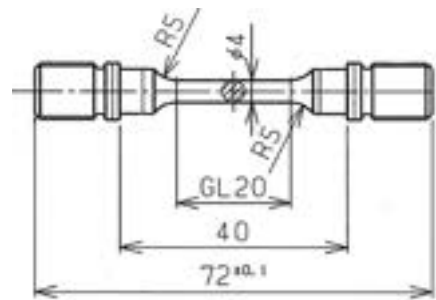
Figure 7. metallographic structures after 1000hrs exposure in SCW



III. Stress Corrosion Behavior

The specimens used for SCC susceptibility are extruded bars of 310S, which were subjected to solution heat treatment at 1050°C for 1 h, followed by quenching in water. The geometry of the round bar tensile specimen is shown in Fig. 8. The gauge section was burnished with 1000 grit emery paper, washed with ethanol in an ultrasonic cleaner, and cleaned with distilled water.

Figure 8. Dimensions of the tensile specimen (mm)



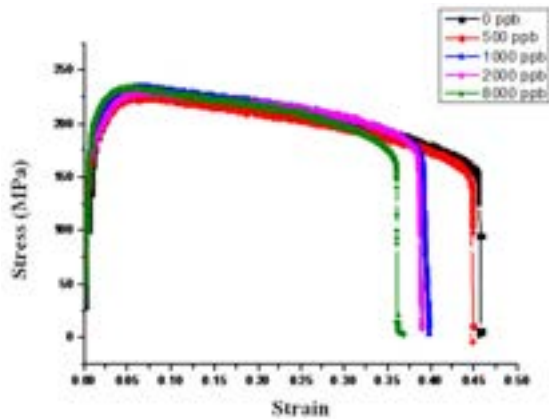
Slow strain rate tensile tests (SSRT) were performed on specimens in the SCW Test Loop installed with a loading system, as shown in Fig.1. Deionised water with conductivity less than 0.1 $\mu\text{S}/\text{cm}$ was pressurised to 25 MPa and heated to 620°C to establish the SCW environment. The DO concentration in the SCW during the SCC tests ranged from zero to 8000 ppb with continuously bubbling argon-oxygen mixture gases. The tensile load with the strain rate of $7.5 \times 10^{-7} \text{ s}^{-1}$ was applied to the specimen till fracture.

Table4. SSRT results of 310S in in SCW with 0-8000 ppb dissolved oxygen at 620°C and 25 MPa

DO (ppb)	UTS (MPa)	YS (MPa)	Elongation (%)	Fracture mode
0	229	186	45.6	IG
500	225	170	44.7	IG
1000	234	184	39.8	IG
2000	229	174	38.9	IG
8000	233	190	36.7	IG

The stress-strain curves of 310S obtained from the in SCW at 620°C are shown in Fig. 9 and the results are presented in Table 4. Elongation reduction was used as a quantitative method to evaluate the SCC susceptibility. It revealed that the elongation decreased with the increase of DO concentration, which indicates its dependence on DO concentration. This tendency follows the increase in the oxidation potential of SCW.

Figure 9. Comparison of stress ~ strain, obtained by SSRT tests on 310s in SCW with 0-8000 ppb dissolved oxygen at 620°C and 25 MPa



According to Zhu [4], dissolved oxygen change the oxidation potential of SCW, leading to an increase in the oxidation rate. The potential gradient between the crack mouth and crack tip increases with the increase of DO concentration. Crack growth rate also increases owing to the acceleration of the oxidation rate at the crack tip. A similar result was obtained by Zhang [5].

Fig.10 shows the SEM fractography in deaerated SCW. The failure surface exhibited intergranular fracture morphology. Intergranular facets appeared in both the center and edge regions of the fracture surface, which are characteristics of brittle fracture. These results are very close to the data of HR3C, tested in SCW at temperatures of 600°C and 650°C [6]. The specimens tested in SCW with different DO concentrations showed similar characteristics.

Fig. 11 shows that the cracks were widely distributed at the gauge surface near the fracture surface, and most of the cracks were perpendicular to the loading direction. By using energy dispersive spectrometer (EDS) analysis, chemical changes were observed in the oxide film at the crack mouth with different DO concentrations, as presented in Table 5. The Cr concentration increased with the increase of DO, which indicated that DO affects the composition of the oxide layer. When oxygen is present, the solvation of SCW increase the solubility of Fe-rich outer oxides, leading to the decrease of the concentration of iron and the opposite trend for Cr concentration.

Table 5. Results of EDS of oxide on specimen surfaces at different DO concentrations in SCW

DO (ppb)	Time to fracture (h)	Cr (wt%)	Fe (wt%)	O (wt%)
0	169	7.55	62.22	30.22
500	165	12.82	56.84	30.34
1000	147	16.60	52.83	30.36
2000	144	40.28	28.77	30.95
8000	133	63.91	4.61	31.48

Figure 10. Fracture surfaces of specimens tested at 620°C with DO at 0 ppb; position A is in the centre region and position B is in the edge region of the fracture surface.

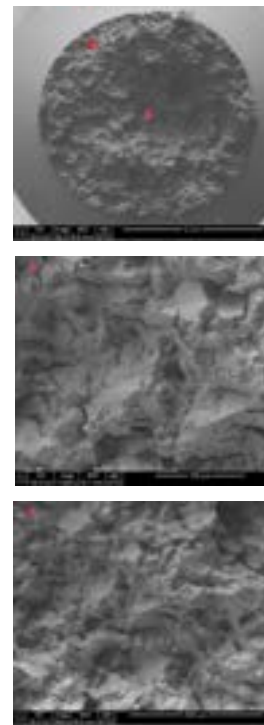


Figure 11. SEM images of 310S tested in SCW at 620°C with DO at 500 ppb

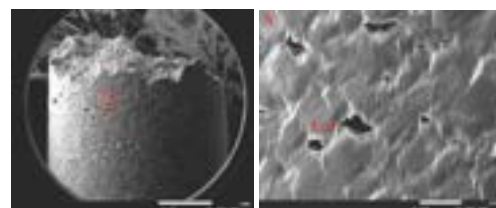


Figure 12. EPMA images of cracks after testing in (a, c) deaerated SCW and (b, d) SCW with DO of 8000 ppb

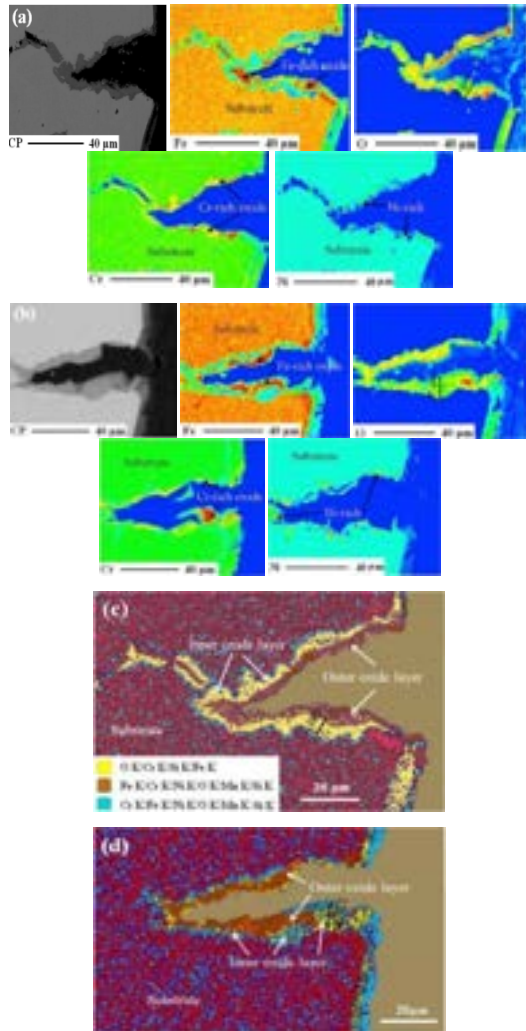


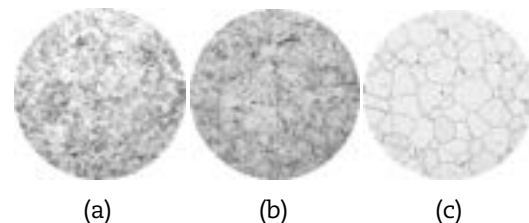
Fig.12 show the results obtained from EPMA using a wave length-dispersive spectrometer (EPMA-WDS) on the cross-section of the cracks. The Fe-Cr oxide was distributed along the crack and can be divided into two layers. The iron was enriched in the outer layer but was depleted in the inner layer, whereas the concentration of chromium exhibited the opposite trend. Ni enrichment was detected at the oxide/metal interface. This observation of a double oxide layer is consistent with the studies on 316 in the SCW^[6,7]. The oxide layer thickness in SCW with DO of 8000 ppb is 17 μm and greater than 10 μm formed in deaerated SCW.

The integrity of the Cr-rich inner oxide layer plays an important role in the SCC resistance. Figs. 12(c) and (d) show elements proportion in

the cross-section of cracks, obtained using EPMA with an EDS (EPMA-EDS). For the specimen exposed to deaerated SCW, the Cr-rich oxide layer (indicated by yellow zone) appears to be compact and continuous. In SCW with DO of 8000 ppb, the Cr-rich oxide layer is relatively discontinuous and non-uniform. It is expected that a thin and continuous Cr-rich oxide layer prevent further oxidation, whereas the discontinuous Cr-rich oxide layer may increase the SCC susceptibility.

The fractography indicates that the failure mode in the SCW containing dissolved oxygen and deaerated condition is dominated by intergranular brittle fracture. Thermal aging of metal structure, which is similar to the sensitisation behavior of austenitic steel above 600°C is considered to be a main cause of cracks origin. As shown in Fig. 13, a notable grain growth and chain precipitated phases had occurred after SSRT test. The precipitated phases were identified to be M_{23}C_6 , which were Cr-rich and also observed in the coupons after 1000 hrs exposure test. The M_{23}C_6 is brittle and form the stress concentration on the grain boundaries when specimen is loaded. It provides a germination conditions for micro pores that grow into micro cracks under effect of tensile stress. When the M_{23}C_6 is rich on the boundary, it comes along with the Cr depletion zone that cause preferentially oxidising of the boundary, and finally propagation into the intergranular stress corrosion cracking. Thermal aging tendency of 310S cannot be observed by the preliminary sensitising test of austenitic steel according to ASTM A262-10. The evolution of mental structure in the supercritical temperature zone will be long-term and accelerated by thermal stress.

Figure 13. Comparison of metallurgical structure (200 \times). a) Before test, b) sensitised at 650°C for 2 h, c) after SSRT test at 620°C and 25 MPa for 90 hrs



Two techniques are being considered for improving the SCC resistance of austenitic steels in SCW by using the modification of the

mental structure and the water chemistry environment.

Considering the intergranular cracking tendency of 310S caused by the high temperature aging effect, the metal chemical composition should be optimised. Reducing carbon content and adding the elements such as Ta and W can reduce Cr-rich precipitation of $M_{23}C_6$ in the grain boundaries. Refinement of grain structure [8] by cold work and thermal treatment helps improve the mechanical performance of austenitic steel. A fine grain structure spreads more easily chromium to metal and oxidant interface and form continuous internal Cr-rich oxide layer that helps to improve the resistance to oxidation of materials. Additional thermal treatment should be adopted for stabilisation of metal structure at supercritical temperature. Some researches [9] revealed a thermally treatment (TT) at 800°C for approximate 1000hrs have a significantly reduced susceptibility to IGSCC and no obvious Cr-depletion was present adjacent to the phase in the TT 310S.

For the water chemistry optimisation, the application experiences of hydrogen water chemistry (HWC) in BWR remains investigation for the control of internal SCC in SCWR. By present tests on 310S at 500°C and 25 MPa, the measured crack growth rate is 2.00×10^{-8} mm/s in the SCW containing 1.58 mg/kg of H_2 and 6.79×10^{-8} mm/s in the SCW containing 2.0 mg/kg of O_2 . It seems to be ineffective of hydrogen for inhibiting the propagation of cracks in the SCW. SSRT tests results indicated a notable decrease of elongation of 310S in the SCW containing 1.0 mg/kg of H_2 at 620°C and 25 MPa, as shown Fig.14. Transgranular cracking were observed on the edge of fracture surface at 400°C and the cracking of 310S is dominated by a blending mode of transgranular and intergranular cracking at 620°C when exposed to the SCW containing hydrogen, as shown in Fig.15.

For the test results in the hydrogen conditions, the inhibition effect of hydrogen on the SCC was lower than expected. The causes are summarised as follows: (1) the hydrogen concentration using in these tests may not be in an appropriate region to suppress the oxidation of cracks in the SCW. Previous research [10] identified SCC growth rate was a function of the critical hydrogen concentration for the nickel/nickel oxide transition. The critical hydrogen concentration increases with temperature and may be out of the specification of the current LWR plants when temperatures reach critical point. (2) Evolution

of microstructure at 620°C dominate the fracture process, which weaken the function of water chemistry factors and corrosion suppressing effect of hydrogen is not easy to detect; (3) The fracture caused by hydrogen embrittlement should be vigilance when using hydrogen chemistry, especially the excess diffusion of hydrogen into the metal substrate may not be avoided due to the weak passivation of oxide layer in the SCW.

Figure 14. Comparison of stress ~ strain, obtained by SSRT tests on 310s in SCW with 0-1000 ppb dissolved hydrogen at 620°C and 25 MPa

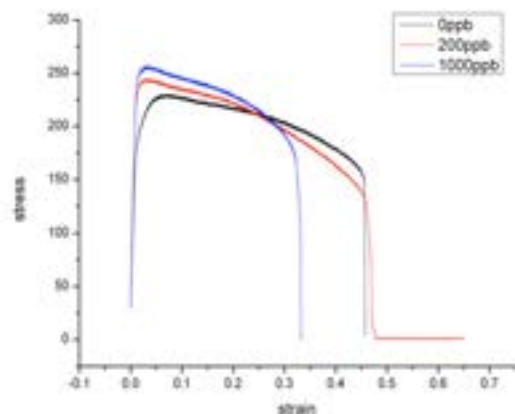
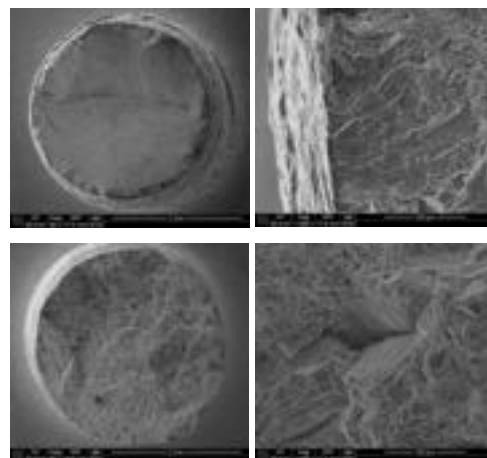


Figure 15: SEM fractography of specimen tested in the SCW, a) and b) 400°C, 200ppb dissolved hydrogen; c) and d) 620°C, 200ppb dissolved hydrogen



IV. Conclusion

The oxidation behavior of 310S and 800H exposed with supercritical water was investigated. After 1000hrs exposure to SCW at 550°C, both 310S and 800H present weight gain. The oxide layers of 310S are composed of a densely packed layer with three-layer structure. Iron and nickel enrichment occurred in the inner oxide layer while chromium is evenly distributed.

The transitions of the water parameters were observed near the critical point in the corrosion tests. The variation of water conductivity occurred during heating up and cooling process. This means that water quality control is challenging during the operation of SCWR. Hideout of impurities may decrease the purification efficiency and increase the accumulation of impurities in the core area where the temperature great than 385.8°C at 25 MPa. When the temperature is lower than this critical point, impurities release back to the coolant in hideout return process and increase the corrosion risk of internals due to the underestimate of conductivity especially combining effect of oxidised radiolysis.

SSRT tests of 310S were carried out in SCW at a temperature of 620°C. The tests were performed with various DO concentrations. The main results are as follows: (1) The elongation of SSRT specimens was dependent on the DO concentration, which indicated the effect of oxygen on the SCC susceptibility. (2) The intergranular brittle fracture mode was observed on the fracture surface, and dense cracks were observed on the gauge section. This failure mode was dominated by the evolution of microstructure due to thermal aging at the 620°C. (3) Oxides were observed inside the cracks with two-layered structures. The Cr-rich inner oxide layer inside the cracks was more continuous in deaerated SCW compared with that in oxygenated SCW.

The SSRT and crack growth test results indicated weak inhibition of hydrogen on SCC in SCW. Possible causes are summarised for the future investigation on the relationship between the materials and hydrogen water chemistry in SCW.

Acknowledgements

This work was supported by the National Natural Science Foundation of China (No. 51271171). Parts of specimens in this research were provided free by JRC-IET. The authors express their immense appreciation to them.

Nomenclature

DH	Dissolved Hydrogen
DO	Dissolved Oxygen
EC	Electronic Conductivity
EDS	Energy Dispersive Spectrometer
EPMA	Electron probe micro-analyzer
GIF	Generation IV International Forum
HWC	Hydrogen Water Chemistry
IGSCC	Intergranular Stress Corrosion Cracking
JRC-IE	Joint Research Centre-Institute for Energy and Transport
LWR	Light Water Reactors
NPIC	Nuclear Power Institute of China
ORP	Oxidation-Reduction Potential
SCC	Stress Corrosion Cracking
SCWR	Super Critical Water-Cooled Reactor
SCW	Supercritical Water
SEM	Scanning Electron Microscope
SSRT	Slow Strain Rate Tensile
TT	Thermally Treatment
WDS	Wave Length-Dispersive Spectrometer

References

- [1] P. Wu, J.L. Gou, J.Q. Shan et al., Preliminary safety evaluation for CSR1000 with passive safety system. *Ann. Nucl. Energy.* 65, 390-401 (2014). doi:10.1016/j.anucene.2013.11.031
- [2] D. Guzonas, R. Novotny, Supercritical water-cooled reactor materials - Summary of research and open issues. *Prog. Nucl. Energy.* 77, 361-372 (2014). doi:10.1016/j.pnucene.2014.02.008
- [3] Halvarsson. M, Tang J E and Johansson L G. Microstructural investigation of the breakdown of the protective oxide scale on a 304 steel in the presence of oxygen and water vapour at 600°C. *Corrosion Science* 48(8) 2014-2035,2006
- [4] Z.L. Zhu, H. Xu, D.F. Jiang et al., The role of dissolved oxygen in supercritical water in the oxidation of ferritic-martensitic steel. *J. Supercrit. Fluids.* 108, 56-60 (2016). doi:10.1016/j.supflu.2015.10.017
- [5] L.T. Zhang, J.Q. Wang, Effect of dissolved oxygen content on stress corrosion cracking of a cold worked 316L stainless steel in simulated pressurized water reactor primary water environment. *J. Nucl. Mater.* 446, 15-26 (2014). doi:10.1016/j.jnucmat.2013.11.027
- [6] Z. Shen, L.F. Zhang, R. Tang et al., The effect of temperature on the SSRT behavior of austenitic stainless steels in SCW. *J. Nucl. Mater.* 454(1), 274-282 (2014). doi:10.1016/j.jnucmat.2014.08.006
- [7] H. Je, A. Kimura, Stress corrosion cracking susceptibility of candidate structural materials in supercritical pressurized water. *J. Nucl. Mater.* 455(1), 507-511 (2014). doi:10.1016/j.jnucmat.2014.08.016
- [8] Yusaku Murano, Junya Kaneda, Shigeki Kasahara, et al. Evaluation of Weight Loss of Stainless Steels in Supercritical Water[C]. ICAPP 2009, Tokyo, Japan, May 10-14, 2009.
- [9] Y. Jiao & J. Kish ,Intergranular Corrosion Resistance of Thermally-Treated Type 310S Stainless Steel, the 7th International Symposium on Supercritical Water-Cooled Reactors ISSCWR-7-2029 15-18 March 2015, Helsinki, Finland.
- [10] Steven, A. A., and David, S. M., 2003, "Measurement of the nickel/nickel oxide transition in Ni-Cr-Fe alloys and updated data and correlations to quantify the effect of aqueous hydrogen on primary water SCC," Technical Report No. LM-03K049; TRN: US2004111%203, Lockheed Martin Corporation, Schenectady, NY 12301 (US).

THE USA'S ADVANCED REACTOR TECHNOLOGIES (ART) GRAPHITE R&D PROGRAM (W. WINDES ET AL)

William Windes⁽¹⁾, Tim Burchell⁽²⁾, Michael Davenport⁽¹⁾

(1) Idaho National Laboratory, United States

(2) Oak Ridge National Laboratory, United States

Abstract

The USA DOE Advanced Reactor Technologies (ART) graphite R&D program supporting HTR design is one of the longest running nuclear graphite R&D programs. Significant progress has been made in several areas of research within this extensive program including unirradiated and irradiated testing of nuclear graphite, oxidation results and modeling, fracture behavior, irradiation damage studies, and several international collaboration studies. The latest results in these research areas as well as a discussion of a new direction in nuclear graphite irradiation for the USA program will be presented. Recently, the USA made a decision to support moderate to high dose irradiation of nuclear graphite (0.5 to 15 dpa). This will provide irradiation data for graphite HTR core components up to 15 dpa for numerous nuclear graphite grades. The irradiation plan and a tentative schedule for this new irradiation direction will be presented in detail.

I. Introduction

High-purity, synthetic nuclear grade graphite is the core structural material of choice for high temperature reactor (HTR) designs, due to its capacity as both neutron moderator and reflector, its stability at high temperature, machinability, and relatively low cost. Thus, a thorough understanding of the material properties for these nuclear graphite grades is critical to the development of robust commercial HTR designs. Unfortunately, while the general manufacturing processes necessary for producing nuclear grade graphite are well documented, historical nuclear-grades are no longer produced [1] and new grades must be considered for the new HTR designs. This requires the new grades to be thoroughly characterised, tested, and irradiated to demonstrate that they exhibit acceptable irradiated and unirradiated behavior for the thermomechanical design of HTR core components. Accordingly, the DOE Advanced Reactor Technologies (ART) program initiated a Graphite R&D program in 2005 to provide

graphite material data (both unirradiated and irradiated) necessary for the eventual utilisation of these new grades for nuclear core components in HTR applications.

The ART graphite R&D program is one of the longest running nuclear graphite programs in support of the new HTR design with one of the largest graphite irradiation programs attempted in recent years. The Advanced Graphite Creep (AGC) experiment has been operating since 2009 [2] and is approximately 60% complete. At completion, over 2000 graphite specimens from 7 major nuclear grades will have been irradiated to dose levels of up to 15 dpa (displacements per atom) and irradiation temperatures between 600°C to 800°C [3].

Currently, an unirradiated material property characterisation effort (Baseline activity) is underway to establish the as-fabricated material properties for the AGC major nuclear grades in support of the irradiation program. This test program will yield a large amount of unirradiated material property data

encompassing all the major AGC nuclear grades and providing a large statistically accurate sample population. Once the baseline material property values are established, the measured change to the properties from the AGC experiment will be used to determine statistically accurate irradiation induced material properties for each grade of graphite tested.

Other significant areas of research include degradation studies (oxidation, fracture, and fundamental irradiation damage studies), model development, and ASME code development as well as several national and international graphite collaborations. The latest results in selected research areas as well as a discussion of a new direction in the USA's graphite irradiation program will be discussed.

II. Irradiated and Unirradiated Graphite Characterisation Testing

Material property testing within the ART graphite program is focused on two primary activities: the graphite irradiation experiment (AGC) and the unirradiated Baseline activity. These are considered essential to providing data necessary for the accurate determination of irradiation response of graphite under HTR operating conditions.

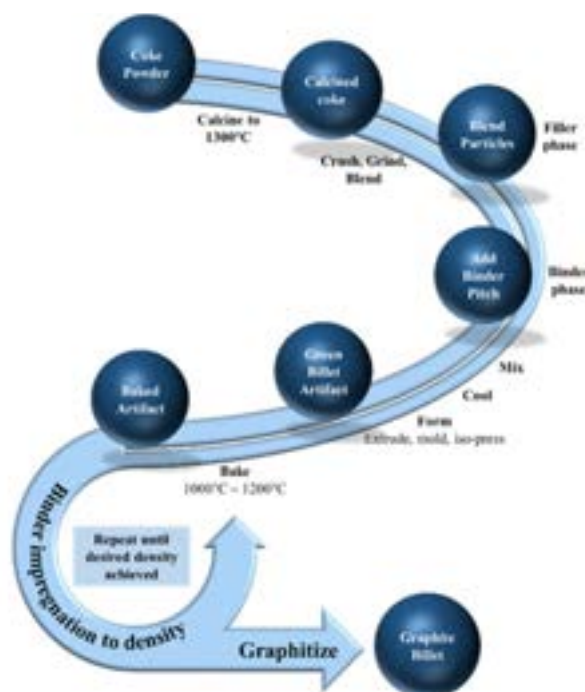
II.A. AGC irradiation experiment

The AGC experiment is currently underway to determine the in-service behavior of numerous new graphite grades for gas-cooled as well as molten salt reactor HTR designs. This irradiation experiment will examine nuclear graphite property changes and behavior at two different irradiation temperatures (600°C and 800°C) over a spectrum of irradiation dose up to 15 dpa. Half of the graphite specimens are subjected to a mechanical stress to induce irradiation creep strain over the 15 dpa neutron dose range. The irradiation creep rate coefficient for each tested grade can then be determined by comparing the dimensional changes between stressed and unstressed specimens.

The experiment is comprised of six planned capsules irradiated in the Advanced Test Reactor in a large flux trap located at Idaho National Laboratory (INL). Each irradiation capsule consists of over 500 graphite specimens that are characterised before and after irradiation to determine the irradiation induced material properties changes and life-limiting irradiation creep rate for nuclear graphite.

The AGC experiment was designed to provide irradiation response data over a wide variety of different nuclear graphite fabrication methods [4]. Generally, nuclear grade is manufactured from petroleum or coal-tar derived cokes which are formed to impart near-isotropic or isotropic material properties, Figure 1. However, the raw material, forming processes, and densification processes impart unique property variations which yield different irradiation response for each selected grade of graphite. The AGC experiment is investigate the irradiation response in the various grades.

Figure 1. Typical process steps in the manufacture of nuclear graphite.



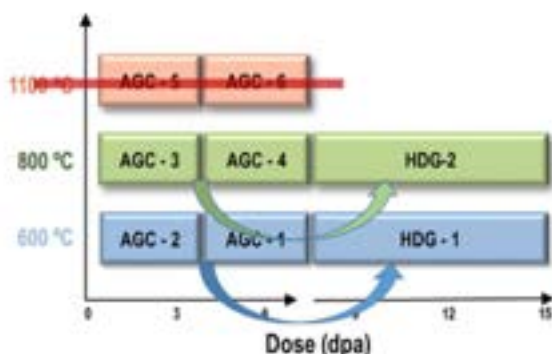
It should be noted that a wide range of graphite properties will be necessary to satisfy the requirements of the unique HTR core design (i.e., differences in the required structural strength, grain/pore size, final component size, billet cost, and most obviously irradiation response). The design of AGC investigates many of these fabrication parameters of interest but the experiment focuses on the irradiation creep response to ascertain this life limiting irradiation parameter. The influence of factors such as grain size (pore structure), coke source, isotropy, and fabrication method on the creep response and measured creep rate are of primary importance for the AGC. Of course,

irradiation changes such as dimensional change, density, thermal diffusivity, thermal expansion, strength, and isotropy will also be determined across the neutron dose range for both irradiation temperatures. Thus, the irradiation effects across a wide range of fabrication parameters should provide core component behaviour information for most of the HTR designs currently being considered for commercial application.

Currently, irradiation and post-irradiation examination (PIE) testing of the capsules irradiated at 600°C up to a maximum dose of 7 dpa have been completed. Irradiation and PIE analysis of the 800°C/7 dpa specimens will be complete by early 2020.

In 2018, a significant change to the AGC irradiation experiment was initiated. Previously the AGC had been focused on very high temperature, low dose irradiations (~7 dpa) in support of the original Very High Temperature Reactor (VHTR) design with an anticipated outlet temperature of 1000°C. However, these low dose, very high temperature designs have little current interest for graphite vendors who are pursuing reactor designs with anticipated outlet temperature of only 750°C but with much higher received dose levels for the graphite core components (i.e., HTR operating conditions). To support this new reactor design direction the AGC experiment was altered to eliminate the very high temperature irradiations in place of a higher dose irradiation, Figure 2.

Figure 2. AGC graphite irradiation experiment illustrating recent changes to a higher dose level and elimination of high temperature irradiations



Thus, the original very high temperature capsules (AGC-5 and AGC-6) will now be used to re-irradiate the preceding AGC-2, AGC-3, and

AGC-4 specimens to a total fast neutron ($E > 0.1$ MeV) dose range of 0.5 – 15 dpa. These new higher dose capsules have been designated High Dose Graphite (HDG) capsules and are expected to complete irradiation by 2023 and 2026, respectively. HDG-1 will be irradiated at 600°C and HDG-2 at 800°C, Figure 2.

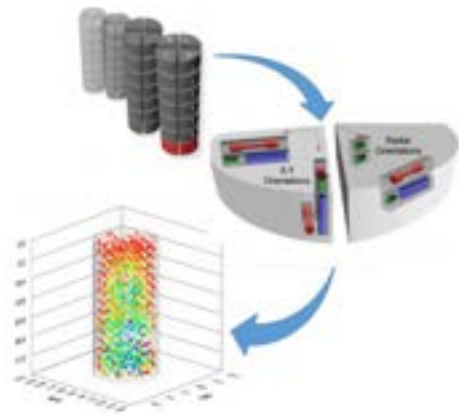
Once the AGC experiment is complete the data is intended to be incorporated in the American Society of Mechanical Engineers (ASME) Boiler Pressure Vessel Code. This will provide an extensive irradiated material property database for multiple nuclear graphite grades up to dose levels of 15 dpa and 600°C to 800°C temperatures. It is anticipated that this data will be extremely useful for future design, licensing, and safe operation of HTR designs.

II.B. Unirradiated baseline activity

To accurately determine the irradiation induced material property changes, the AGC results will be compared to data within the large Baseline unirradiated material property database. The Baseline program utilises full-sized ASTM test specimens, the extensive levels of testing will provide a large sample population, and it uses established test standards to obtain the as-manufactured material properties for the major (production ready) nuclear grades [5]. None of this is possible for the small, limited number of irradiated specimens in the AGC experiment. Material property testing across intra-billet, inter-billet, and batch-to-batch for all major grades will establish the inherent data variation for each particular grade and provide greater accuracy when determining the irradiation induced material property values. An extensive sampling plan with multiple specimens machined from all regions of the billet is used to determine the inherent location variability within each billet, Figure 3.

To date, the Baseline program is approximately 60% complete with intra-billet testing for all major grades complete and batch-to-batch testing well under way. The program is expected to be completed by 2023 providing the baseline material property values for multiple billets across at least two different batches for seven current nuclear grades.

Figure 3. Baseline sample extraction strategy ensures all locations and grain orientations within a billet are tested to provide complete volumetric assessment of material properties within a billet (intra-billet testing). Density variation as a function of location within a PCEA billet (GrafTech, Inc.) is shown to illustrate the material property variability throughout the billet volume (red = 1.86 g/cm³, blue = 1.74 g/cm³)



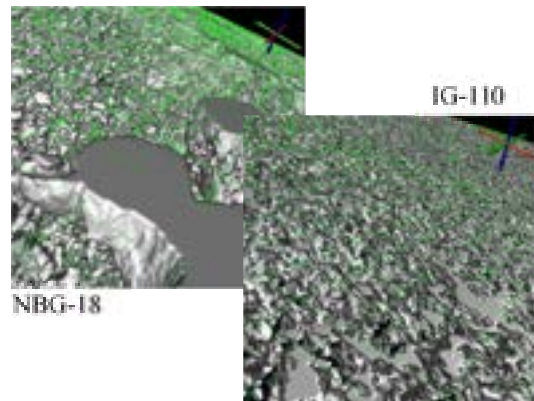
III. Analysis of Graphite Behavior

Based upon the initial results, the irradiated and unirradiated graphite behavior is complex. Several fundamental material science studies have been initiated to assist in the analysis of the material behavior. Fundamental studies through national and international collaborations have been established to ascertain the underlying mechanisms responsible for these complex analyses.

III.A. Analysis and fundamental material science studies

Several more fundamental research studies have been initiated to assist in understanding the irradiated data results from the AGC experiment. Because there is a large inventory of irradiated graphite specimens from the AGC capsules, a number of specimens have been shared between material research laboratories to facilitate microstructural studies on irradiated graphite. Of specific interest are the underlying mechanisms responsible for irradiation damage in graphitic crystallite structures and irradiation creep. Initial results from these studies have provided interesting and unique insight in both the crystal structure and microstructural changes, Figure 4, after irradiation [6, 7, 8].

Figure 4. X-ray computer tomography (CT) image of vibrationally molded NBG-18 and isostatically molded IG-110 grades illustrating pore sizes differences between the two graphites



Observations from these irradiation studies have shown that damage within the anisotropic graphite structure will cause expansion within the c-axis crystallographic direction (direction perpendicular to the stacked graphene basal planes). This expansion will continue with increasing dose filling the available accommodating porosity generated during fabrication. After the accommodating porosity has been filled the c-axis expansion will continue until new cracks, triple points between crystals, and eventually larger pores within the microstructure begin to grow. While crystal damage from irradiation is understood to change the material properties within graphite, the effects from pore/crack formation within the larger microstructure are not as well understood. These irradiation damage induced and microstructure evolved changes are under investigation by the ART Graphite program in order to understand graphite behavior under irradiation. A thorough understanding of these effects will be required to predict the behavior of the core components over the lifetime of the graphite core.

III.B. Graphite degradation studies

A significant portion of the ART Graphite program is investigating degradation of graphite during both normal and off-normal operations. Structural integrity of the graphite components is critical to ensure protection of the fuel, control rod insertion, and proper coolant flow within the core. The major degradation issues of concern are acute (accident) oxidation, chronic (normal

operational) oxidation, fracture behavior, and irradiation performance. While the AGC experiment will address the irradiation performance, significant progress in oxidation and fracture have also been accomplished.

Uniaxial and multiaxial fracture studies have been conducted for a variety of graphite grades [9] with a specified minimum value for graphite mode I critical stress intensity factor, K_{Ic} , for nuclear component applications. Of particular interest is the recent development of an ASTM standard test method for the determination of fracture toughness of graphite [10]. The ART graphite program was the lead laboratory in the development of this fracture standard created to ensure compatibility and a common testing method for easy comparison of fracture results. A microstructure dependent fracture model has been initiated which now accounts for the characteristics of filler particles, binder phase, and the distribution of pores and voids [11]. While still under development, this phase-field based model has been demonstrated to accurately reproduce results from the experimental testing on various grades of graphite.

Tremendous progress in the areas of acute and chronic oxidation in nuclear graphite has brought about a new level of understanding in the underlying mechanisms and kinetics for the graphite-oxygen reaction, Figure 5. Extensive experimental results for acute air oxidation [12, 13], chronic oxidation in moist Helium environments to more accurately mimic the normal operating environment of a gas-cooled core [14, 15, 16], and even fundamental studies to produce new oxidation resistant or protective coating grades have been actively investigated [17]. Based upon these experimental results and our enhanced understanding of the oxidation behavior of nuclear graphite we have begun development of a new chronic oxidation model based upon work by Langmuir-Hinshelwood [18]. This new Boltzmann-enhanced Langmuir-Hinshelwood (BLH) model vastly improves the prediction of oxidation for multiple nuclear grades especially at the higher temperature and partial pressures of water anticipated for the HTR design [19].

In addition, sophisticated models of both acute (accident) and chronic oxidation of graphite components have been developed which accurately predict air oxidation behavior for multiple graphite grades, Figure 6. Results from this oxidation-transport model correctly calculate the penetration depth, mass loss rate, and oxidation performance for acute air and

air-He mixtures in both fine and medium grain grades.

Figure 5. Gas diffusion pathways within the extruded PCEA grade graphite used to assist in determining the effective gas diffusion. The interconnected pathways and resulting tortuosity within the graphite microstructure are determined using advanced 3D CT image analysis techniques

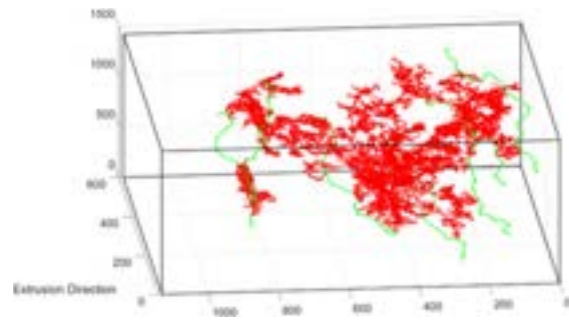
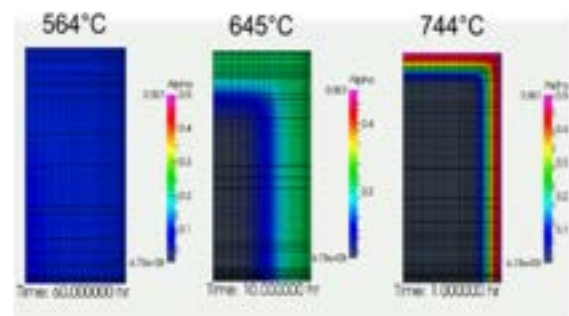


Figure 6. Penetration depth calculations for a fine grain graphite specimen as a function of oxidising temperature. Samples were oxidised to the same total mass loss with color graded scale indicating the level of oxidation at specific penetration depths (blue indicating ~ 7% and red ~ 45% mass loss)



The eventual goal of the ART graphite program will be to build similar graphite behaviour models based upon the extensive data available from the AGC and Baseline data. New comprehensive behavior models have been initiated which combine fracture, oxidation, and mechanical strength models for nuclear graphite. Finally, the effects from irradiation will be incorporated to allow irradiation performance of graphite core components within a variety of reactor environments. These

comprehensive models will eventually be used to assist in improving the ASME code used for licensing and safe operation of these HTR designs.

IV. Licensing and Code Development

Finally, a new graphite based code in Section III, Division 5 of the ASME is being developed for the use of graphite components within nuclear applications in support of the anticipated new high temperature reactor designs [20]. Previous HTR designs used deterministic codes and performance models, while the new HTR designs will utilise new graphite grades and risk-derived (probabilistic) performance models and design codes, such as that being developed by the ASME. To assist in the development of this new graphite HTR design code the ART graphite program has volunteered to provide the irradiated and unirradiated graphite data from the AGC experiment and Baseline program, respectively. The Baseline data is being used to ascertain the viability and usability of the code for future commercial vendors and license applicants for USA NRC consideration. Since the ART Baseline has one of the largest unirradiated property databases (over 15,000 material property data values) for numerous nuclear graphite grades we have volunteered to use this data to “proof test” the new graphite ASME code. By following the code requirements and using actual material property data from the Baseline database, the code is being evaluated for any potential gaps or missing data requirements that most commercial license applicants would need for licensing a future HTR design in the USA.

The irradiated AGC data will be utilised directly by the ASME code since it provides the largest

irradiated graphite database of multiple and currently available nuclear graphite grades. The ART graphite program is currently working with the ASME graphite working group committees to incorporate the AGC data within the code. It is expected that the changes of the AGC experiment to higher dose levels will assist in extending the graphite code requirement to neutron dose levels beyond Turnaround.

Acknowledgements

The authors wish to acknowledge that this work was performed at Idaho National Laboratory (INL) by Battelle Energy Alliance, LLC under contract DE-AC07-05ID14517 and Oak Ridge National Laboratory (ORNL) by UT-Battelle, LLC, under contract DE-AC05-00OR22725.

Nomenclature

AGC	Advanced Graphite Creep
ART	Advanced Reactor Technologies
ASME	American Society of Mechanical Engineers
ASTM	American Society for Testing and Materials
BLH	Boltzmann-enhanced Langmuir-Hinshelwood
CT	Computer Tomography
DOE	Department of Energy
HDG	High Dose Graphite
HTR	High Temperature Reactor
GIF	Generation IV International Forum

References

- [1] T.R. Allen, K. Sridharan, L. Tan, W.E. Windes, J.I. Cole, D.C. Crawford, G.S. Was, Materials challenges for generation IV nuclear energy systems, Nuclear Technology, v162, p.342, 2008.
- [2] S.B. Grover, D. A. Petti, M. Davenport, Status of the Third NGNP Graphite Irradiation AGC-3 in the Advanced Test Reactor, Proceedings of the 2013 21st International Conference on Nuclear Engineering - ICONE21, Chengdu China, July 29 – August 2, 2013.
- [3] T.D. Burchell and W.E. Windes, A Comparison of the Irradiation Creep Behavior of Several Graphites, Transactions of the American Nuclear Society, v115, 2016.
- [4] T.D. Burchell, R. Bratton, and W.E. Windes, NGNP Graphite Selection and Acquisition

- Strategy, ORNL Technical Manuscript, ORNL/TM-2007/153, September 2007.
- [5] M.C. Carroll, W.E. Windes, D.T. Rohrbaugh, J.P. Strizak, and T.D. Burchell, Leveraging comprehensive baseline datasets to quantify property variability in nuclear-grade graphites, *Nuclear Engineering and Design*, v307, p.77, 2016.
- [6] C. Karthik, J. Kane, D.P. Butt, W. Windes, and R. Ubic, Microstructural characterization of next-generation nuclear graphites, *Microscopy and Microanalysis*, v18, p.272, 2012
- [7] C. Karthik, J. Kane, D.P. Butt, W. Windes, R. Ubic, Neutron Irradiation Induced Microstructural Changes in NBG-18 and IG-110 Nuclear Graphites, *Carbon*, v86, p.124, 2015.
- [8] H. Freeman, B. Mironov, W. Windes, M. Alnairi, A. Scott, A. Westwood, R. Brydson, Microstructural changes in neutron irradiated nuclear graphites PCEA and PCIB, *Journal of Nuclear Materials*, v491, p.221, 2017
- [9] T.D. Burchell, D. Erdmann III, R.R. Lowden, J. Hunter, C. Hannel, The Fracture Toughness of Nuclear Graphites, ORNL Technical Manuscript ORNL/TM-2016/678, 2016.
- [10] ASTM D7779, Standard Test Method for the Determination of Fracture Toughness of Graphite at Ambient Temperature, Annual Book of ASTM Standards, Vol. 5.05, Petroleum Product, Lubricants, and Fossil Fuels, p. 832. Pub. ASTM International, West Conshohocken, PA, 2016.
- [11] P. Chakraborty, P. Sabharwall, and M.C. Carroll, A phase-field approach to model multi-axial and microstructure dependent fracture in nuclear grade graphite, *Journal of Nuclear Materials*, v475, p.200, 2016.
- [12] R.E. Smith and W.E. Windes, NNGP Graphite Oxidation Studies, 12th International Nuclear Graphite Specialists Meeting (INGSM-12), Jeju South Korea, September 2011.
- [13] J.J. Kane, C. I. Contescu, R.E. Smith, G. Strydom, and W. E. Windes, Understanding the Reaction of Nuclear Graphite with Molecular Oxygen: Kinetics, Transport, and Structural Evolution, *Journal of Nuclear Materials*, v493, p.343, 2017.
- [14] C.I. Contescu, T. Guldan, P. Wang, T.D. Burchell, The effect of microstructure on air oxidation resistance of nuclear graphite, *Carbon*, v50, p.3354, 2012
- [15] J.J. Kane, A.C. Matthews, C.J. Orme, C.I. Contescu, W.D. Swank, and W.E. Windes, Effective Gaseous Diffusion Coefficients of Select Ultra-fine, Super-fine and Medium Grain Nuclear Graphite, *Carbon*, v136, p.369, 2018
- [16] R.P. Wichner, T.D. Burchell, C.I. Contescu, Penetration depth and transient oxidation of graphite by oxygen and water vapor, *Journal of Nuclear Materials*, v393, p.518, 2009.
- [17] J.W. Park, E.S. Kim, J.U. Kim, Y. Kim, and W.E. Windes, Enhancing the oxidation resistance of graphite by applying an SiC coat with crack healing at an elevated temperature, *Applied Surface Science*, v378, p.341, 2016.
- [18] P.L. Walker Jr., F. Rusinko Jr., L.G. Austin, Gas reactions of carbon, *Advanced Catalysis*, v11, p.133, 1959
- [19] C.I. Contescu, R.W. Mee, Y. (Jo Jo) Lee, J.D. Arregui-Mena, N.C. Gallego, T.D. Burchell, J.J. Kane, and W.E. Windes, Beyond the Classical Kinetic Model for Chronic Graphite Oxidation by Moisture in High Temperature Gas-Cooled Reactors, *Carbon*, v127, p.158, 2018
- [20] ASME BPVC.III.5, American Society of Mechanical Engineers (ASME) Boiler and Pressure Vessel Code (BPVC), Section III, Rules for the Construction of Nuclear Facility Components, Division 5, High Temperature Reactors, New York, 2017.

DEVELOPMENT OF SAFETY DESIGN GUIDELINES ON STRUCTURES, SYSTEMS AND COMPONENTS FOR GENERATION IV SODIUM-COOLED FAST REACTOR SYSTEMS (S. KUBO ET AL)

Shigenobu Kubo⁽¹⁾, Ryodai Nakai⁽²⁾, Tanju Sofu⁽³⁾

(1-2) Japan Atomic Energy Agency, Japan

(3) Argonne National Laboratory, the United States of America

Abstract

The GIF Safety Design Criteria Task Force (SDC-TF) is updating the previously published SFR Safety Design Criteria (SDC) and the first SFR Safety Design Guidelines report (SDG on Safety Approach) based on external feedback. The SDC-TF is currently developing the second safety design guidelines report, "Safety Design Guidelines on Structures, Systems and Components for Generation IV (Gen-IV) Sodium-cooled Fast Reactor Systems (SDG on SSC)", which provides recommendations in considering the design of structures, systems, and components (SSCs) important to safety and supports practical application of the SDC and the SDG on Safety Approach to the design of safety-related SSCs. The SDG on SSC specifies 14 focal points related to three fundamental systems: (1) reactor core system, (2) coolant system, and (3) containment system. These recommendations on the specific SSCs are developed to clarify the safety requirements for the Gen-IV SFR systems. The SDC-TF intends to complete the SDG on SSC report and issue it in 2019. SFR developing countries such as Russia, France, India, China, US, Korea, EU, and Japan are striving to enhance the safety of next generation SFRs in the consistent manner with the SDC and SDGs.

I. Introduction

After TEPCO Fukushima Dai-ichi nuclear power plant accident, activities to enhance the safety of nuclear power plants have become conspicuous. Development of Sodium-cooled Fast Reactor (SFR) is vigorously being promoted especially in France, Russia, China and India, and therefore a demand for an international standard for ensuring the safety of SFRs is growing.

In the framework of the GIF, an effort to develop "Safety Design Criteria (SDC)" for SFR systems was initiated in 2011. For this purpose, an SDC task force (SDC-TF) was formulated in July 2011, with the aim of summarising and consolidating the SDC. The SDC-TF members consist of representatives of CIAE (China), CEA (France), JAEA (Japan), KAERI, KINS (Republic of Korea),

IPPE (Russia), ANL, INL, ORNL (United States of America), EC and IAEA.

Figure 1 shows the hierarchy of GIF safety standards, including the SDC and Safety Design Guidelines (SDGs). The SFR SDC report was completed in 2013 and distributed to international organisations, namely IAEA, MDEP, NEA/CNRA, and regulatory bodies of the GIF member states with active SFR development programs (China, EC, France, Japan, Korea, Russia and the United States) [1]. In 2017, the SDC-TF finalised responses to feedback from IAEA, U.S. Nuclear Regulatory Commission (NRC), China National Nuclear Safety Administration (NNSA), and the France's IRSN, and the SDC report was updated based on various comments on general matters e.g. safety approaches for Gen-IV reactor systems, the interface between safety and security (necessity of management system to take into

account the potential for adverse effects on safety or security) and suggestions on specific criteria for dealing with e.g. sodium fire, design basis accident (DBA), and design extension condition (DEC). The revised SDC also reflect the revision of IAEA SSR 2/1 [2].

In 2016, the SDC-TF completed the first SFR safety design guideline report titled “Safety Design Guidelines on Safety Approach and Design Conditions for Gen-IV Sodium-cooled Fast Reactor Systems (SDG on Safety Approach)” [3]. The guidelines are a set of recommendations on how to comply with the SFR SDC and address SFR-specific safety topics by clarifying technical issues and providing design options. The SDG on Safety Approach report was distributed to OECD/NEA's Ad-hoc Group on the Safety of Advanced Reactors (GSAR) and the IAEA for review. Leveraging the important and constructive feedback, the TF integrated the resolutions for GSAR and IAEA comments into the report in 2018.

Figure 1. Hierarchy of GIF safety standards, including safety design criteria and safety design guidelines



The SDC-TF is currently developing the second safety design guideline report, “Safety Design Guidelines on Structures, Systems and Components for Gen-IV Sodium-cooled Fast Reactor Systems (SDG on SSC)”, which provides recommendations on the design of structures, systems, and components (SSCs) important to safety and supports practical application of the SDC and the SDG on Safety Approach to the safety-related SSC designs. The SDG on SSC specifies 14 focal points related to three fundamental systems: (1) reactor core system, (2) coolant system, and (3) containment system. These recommendations on the specific SSCs have been developed to clarify the safety requirements for the Gen-IV SFR systems. The

TF intends to complete the SDG on SSC report and issue it in 2019.

These reports have been introduced at joint IAEA-GIF workshops on the safety of SFR and shared widely by GIF member countries, non-member countries like India, regulatory bodies and associated organisations, and plant manufacturers [4][5].

II. Safety Characteristics of SFR

The specific characteristics of SFR that are considered in the design are below.

Safety advantages of SFR

- Low-pressure primary and intermediate coolant systems
 - Guard vessel and guard pipes to maintain coolant inventory
 - No need of emergency core cooling systems, no risks of loss of coolant accident and control-rod ejection
- Inherent safety features with net negative reactivity feedback during an accident possibly raising core and coolant temperatures
 - A large margin to coolant boiling (~400 degrees C) to prevent coolant boiling and core damage
- Dedicated systems for decay heat removal to an ultimate heat sink
 - Liquid-metal coolant that has excellent thermal conductivity and natural circulation characteristics to facilitate reliance on passive systems
- Low-pressure design (~0.5 bar) for containment (mainly against heat from a sodium fire)
- Capability to retain non-volatile and some volatile fission products of liquid sodium in core damage situations
- Simple operation and accident management (long grace period for corrective actions)

Challenges to SFR

- High temperature (> 500 degrees C core outlet temperature) and high core power density

- Liquid sodium coolant in use that reacts with air, water and concrete
 - These reactions have to be prevented and/or mitigated to avoid their effects on SSCs important to safety.
- The core is not in its most reactive configuration.
 - Relocation of core materials may lead to positive reactivity insertion.
- For large cores, sodium void worth can be positive.
- Opaque sodium coolant could pose challenges to in-service inspection and maintenance.

III. SDC Report

The objective of the SDC is to present the reference criteria of the safety design of SSCs of the SFR system. The criteria are clarified systematically and comprehensively for adopting the GIF's basic safety approach established by the GIF Risk & Safety Working Group, with the aim of achieving the safety and reliability goals defined in the GIF Roadmap.

The contents of the SDC are grouped into four parts. The first part is the Chapters 1 and 2 in which the formulation principles of the SDC and the key viewpoints are described to interpret the GIF's safety & reliability goals and basic safety approaches to the criteria for the safety design. The second part is from Chapters 3 to 6 that describe 83 criteria for the overall plant design and specific SSC design. The format of the second part is consistent with that of the IAEA SSR 2/1 for the convenience of not only SFR concept developers under the GIF but also other R&D and regulatory entities interested in the SFR technology. The SDC refer to the basic text in the SSR 2/1 as SSR 2/1 is applied to Gen-IV SFR systems. The third part is a glossary and the fourth part is an appendix which includes examples of key items of the SFR system configuration and technical background to understand the SFR safety characteristics better.

To enhance the safety of Gen-IV SFRs, the SDC mainly focused on improving each level of defence-in-depth including the 4th level, with particular attention on the robust safety demonstration. The levels of defence-in-depth and plant states shown in Figure 2 are defined based on IAEA INSAG-12 & SSR-2/1 (Rev.1, 2016).

Figure 2. Defence-in-depth level and plant states

Defence-in-Depth Levels					
Level 1	Level 2	Level 3	Level 4		Level 5
Plant States (considered in design)					Off-site emergency response (out of the design)
Operational States		Accident Conditions			
Normal Operation	Anticipated Operational Occurrences	Design Basis Accidents	Design Extension Conditions		
			Without significant fuel degradation	With core melting	

IV. SDG on Safety Approach Report

The SDG on Safety Approach report outlines the main characteristics of SFR systems and provides general approaches to normal operation, anticipated operational occurrences (AOOs), and DBAs. However, the report places a greater emphasis on DECs and residual risk events (including the practically eliminated accidents) as infrequent and limited accidents for which the GIF SFR SDC call for new and additional requirements. General design approaches defined in the report are based on the use of (1) redundant engineered safety features to lower the probability and limit the consequences of DBAs, (2) passive/inherent features for reactivity control and core cooling during DECs. In addition to opportunities to exploit inherent design characteristics for enhanced safety, the report suggests specific prevention and mitigation measures against infrequent or limited events such as anticipated transients without scram (ATWS), loss of decay heat removal function, and reactor coolant level reduction. For limited cases, when a mitigation measure cannot be taken under acceptable conditions, the report outlines the considerations and principles for setting up a robust safety demonstration to support practical elimination of such cases from the design.

Postulated initiating events in each plant state are the design basis for the safety design of nuclear power plants. While the residual risk is excluded in the plant states, situations to be practically eliminated are considered to be the part of the residual risk (Figure 3). Design measures for prevention and mitigation of core damage should be provided against DECs in addition to the design measures against DBAs.

Figure 3. Illustration of design basis and residual risk



Specific provisions against DEC are as follows. Recommendations in this document are expressed as 'should' statements.

Against anticipated transient without scram (ATWS)

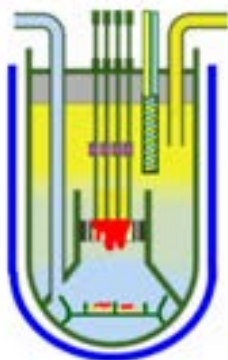
Prevention of core damage

- Means for maintaining the acceptable balance between reactor power and heat removal capabilities should be provided to avoid core damage, given an assumed failure of the active reactor shutdown function in AOOs. These capabilities should include inherent and/or passive means.

Mitigation of core damage

- SFR design should have preventive measures against large energy release that could threaten the integrity of the containment and measures for long-term cooling of a degraded core to avoid reactor coolant boundary failure so as to achieve in-vessel retention (IVR) against unprotected transients with core damage (Figure 4).

Figure 4. An image of design measure achieving in-vessel retention

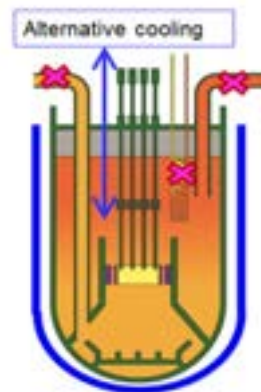


Against loss of safety systems for decay heat removal

Prevention of core damage

- Decay heat removal system (DHRS) with extended capability (normally designed for DBAs) should be considered, and other alternative cooling provisions should be available to prevent core damage and reactor coolant boundary failure due to overheating, given assumed causes of DHRS failure as a DEC. (Figure 5)

Figure 5. An image of alternative cooling provision



Against reactor coolant level reduction

Prevention of core damage

- Reactor Vessels (RVs) and Guard Vessels (GVs) should be designed, manufactured, installed, maintained and inspected to have the highest level of reliability to prevent double leakage from an RV and GV. If double leakage from an RV and GV cannot be practically eliminated, the situation has to be considered for implementing design provisions.

V. SDG on SSC Report

The SDG on SSC makes clear connection between the recommendations in the SDG on Safety Approach and each SSC design. In addition, the SDG on SSC provides recommendations on the requirements of the SDC report that were not elaborated in the SDG on Safety Approach. The recommendations in these guidelines include measures against ATWS for reactivity characteristics, and measures for practical elimination of core

uncovering and complete loss of decay heat removal function. The recommendations, which were out of the scope of the SDG on Safety Approach, are, e.g. for fuels and materials under high temperature and radiation conditions, measures against various hazards such as sodium fire, sodium-water reaction, and load factors on the containment system. Recommendations for addressing these issues are provided in the Chapters with guidelines for reactor core, reactor coolant and containment systems. Figure 6 shows the development process of the SDG on SSC. The objective of the SDG on SSC is to provide detailed guidelines for SFR designers to support the practical application of the SDC in design process to ensure the highest level of safety in SFR design. Although the SDG on SSC is currently focusing on issues related to the main parts of SFR, it will be extended to other issues such as fuel handling and fuel storage.

The SDG on SSC shows recommendations and guidance to comply with the SDC report and the SDG on Safety Approach with examples, which can be applied to Gen-IV SFR systems in general. The SDC-TF expects that these recommendations and examples will be appropriately considered in design according to each design characteristic. It is recommended to adopt the stated measures or equivalent alternative measures.

In the SDG on SSC, the three fundamental safety systems, core systems, coolant systems, and containment systems, together with selected 14 focal points on the systems are

described in particular. Table 1 lists the SFR-specific safety features of the systems. The TF referred to design features of the Gen-IV SFR systems, and the descriptions, definitions, and formats of IAEA NS-G series [6 to 8] to develop recommendations on the specific SSCs.

The SDG on SSC covers the recommendations of the SDG on Safety Approach, such as active and passive reactivity reduction mechanisms, and preventive measures against significant energy release in a severe accident. It also describes design measures to maintain the reactor coolant level and coolability of the core, to utilise the natural circulation of sodium, and to ensure its reliability for decay heat removal from the core. In addition, SFR-specific measures against sodium leakage and combustion and sodium-water reaction are included as internal hazard countermeasures. Measures against external hazards like earthquake are incorporated in each item individually. The design of fuel and of components of the coolant systems to withstand the high temperature conditions is also addressed.

Examples of design measures proposed by GIF SFR System Steering Committee member countries for the 14 focal points are presented in the SDC-TF. Common measures are described in the main text, while design concepts that can differ from one country to another are collected in Appendix as a part of the main text, as defined in the IAEA NS-G series.

Figure 6. The development process of SDG on SSC

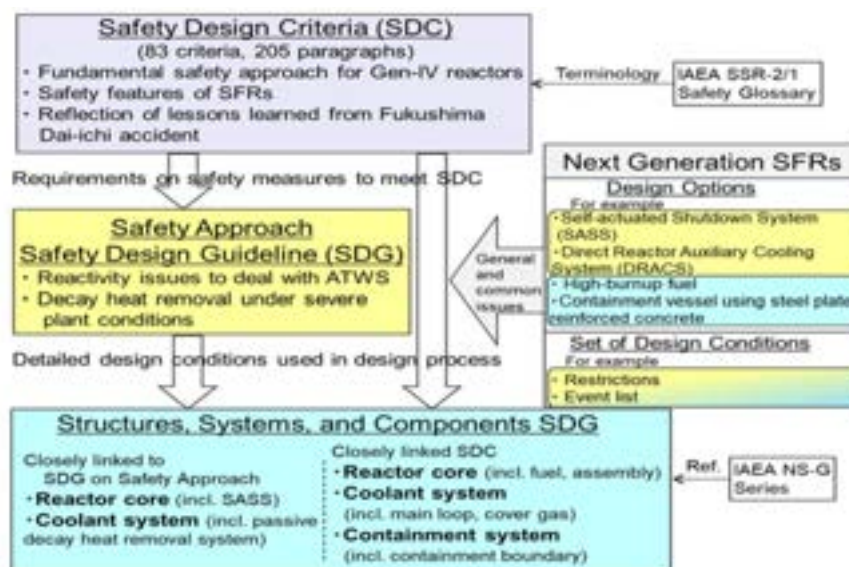


Table 1. 14 focal points in the SDG on SSC

Systems	Safety features	Focal points	SDC	SDG on Safety Approach
Reactor Core systems	Integrity maintenance of core fuels	1. Fuel design to withstand high temperature, high inner pressure, and high radiation conditions	✓	
		2. Core design to keep the core coolability	✓	✓
	Reactivity control	3. Active reactor shutdown	✓	✓
		4. Reactor shutdown using inherent reactivity feedback and passive reactivity reduction	✓	✓
		5. Prevention of significant energy release during a core damage accident, In-Vessel Retention	✓	✓
Coolant systems	Integrity maintenance of components	6. Component design to withstand high temperature and low pressure conditions	✓	
	Primary coolant system	7. Cover gas and its boundary	✓	
		8. Measures to keep the reactor level	✓	✓
	Measures against chemical reactions of sodium	9. Measures against sodium leakage	✓	
		10. Measures against sodium-water reaction	✓	
	Decay heat removal	11. Application of natural circulation of sodium	✓	✓
12. Reliability maintenance (diversity and redundancy)		✓	✓	
Containment systems	Design concept and load factors	13. Formation of containment boundary and loads on it	✓	
	Containment boundary	14. Containment function of secondary coolant system	✓	

There are four chapters in the SDG on SSC.

Chapter 1 “Introduction” describes the background and objectives together with the scope and structure of the SDG on SSC.

Chapter 2 “Guidelines for reactor core systems” includes recommendations on fuel elements and fuel assemblies for the integrity maintenance of the reactor core system, active reactor shutdown system, and reactor shutdown under a DEC with inherent reactivity feedback effects and/or passive feedback or reactivity reduction mechanisms.

Chapter 3 “Guidelines for coolant systems” provides recommendations on component design and reactor cover gas and its boundary, coolant level maintenance, and measures against sodium leakage and combustion in the primary coolant system. Fundamental functions, decay heat removal under a DBA, decay heat removal under a DEC are presented to give recommendations on DHRS. It shows application of natural circulation and safety considerations of tests and inspections. Measures against sodium leakage and combustion and measures against sodium-water reaction in the secondary coolant system are also described.

Chapter 4 “Guidelines for containment systems” presents containment systems and their safety functions, the general design basis of containment systems, and the design of containment systems to withstand accident conditions. Tests and inspections for the whole

system are included in this chapter. This chapter also describes the confinement function of the secondary coolant system, which is one of the SFR characteristics, under an accident condition.

VI. Examples of SDG on SSC

Reactor shutdown under a DEC, examples of “Guidelines for reactor core systems”

The SDG on Safety Approach describes that even if active reactor shutdown systems fail, core damage should be prevented by appropriate combination of inherent reactivity reduction capabilities and passive reactivity reduction mechanisms. The inherent reactivity reduction capabilities are naturally obtained negative reactivity effects in an upset core condition. The passive reactivity reduction mechanisms are activated in direct response to natural phenomena (such as increased coolant temperature or reduced coolant pressure) without any active signals, activation mechanisms or power source. To guide SFR designers, the SDG on SSC shows key points obtained from design and operational experiences, and current achievement of advanced SFR design and R&Ds. The examples of recommendations described below. Recommendations in this document are expressed as ‘should’ statements.

Inherent reactivity feedback

- In order to rely on inherent reactivity feedback to lower the reactor power and core temperature to a level that can be sustained without core damage or primary coolant system boundary failure during an accident with failure of all shutdown systems for the period of time necessary to actuate a complementary reactor shutdown measure, the total power coefficient, isothermal temperature coefficient and power/flow coefficient, should be negative.
- The net effect of a reactor's inherent reactivity responses should ensure the insertion of sufficient negative reactivity to the core to prevent core damage.

Passive reactivity reduction mechanisms

- In the design of passive reactivity reduction mechanism, the following factors should be considered for the rate of shutdown:
 - (a) The response time of the passive actuation system to initiate the means of passive reactivity reduction.
 - (b) Time required for shutdown elements to achieve shutdown after the actuation. For example, for a passive control rod insertion system, the factors may include the distance from the control rods to the active region of the core prior to the insertion, ease of entry of the control rods into the core including the fluid-dynamic effects, and the insertion speed of the control rods.
 - (c) The design should provide appropriate margin for the actuation to avoid spurious activation during normal operation. If the passive reactivity reduction system is based on passive means of release and insertion of the control rods, the number and the position of the control rods should ensure insertion of sufficient negative reactivity to the core to achieve subcriticality. The design should limit displacement between the control rods and control rod channels, and prevent their deformation to keep needed

clearance for passive insertion of the control rods.

- The passive reactivity reduction mechanisms should be designed as simple as possible. A diverse mechanism from reactivity control and active shutdown systems should be considered against common cause failures. They should be designed for fail-safe behavior, as appropriate, so that their failure does not jeopardise the performance of the intended safety function.

Measures against sodium-water reactions at steam generator, examples of “Guidelines for coolant systems”

The SDC requires design measures for prevention and mitigation of chemical reactions of sodium with water or other working fluids. Adequate margin should also be provided to cope with DECs even under multiple failure of mitigation measures so that the fundamental safety functions can be maintained. To guide SFR designers, the SDG on SSC presents key points obtained from design and operational experiences, and the current achievement of advanced SFR design and R&Ds. Examples are described below.

Prevention of sodium-water reaction

- The integrity of structures with sodium-water/steam interface should be maintained with sufficient margin against a comprehensive set of load conditions such as design basis earthquake, transient thermal loads, and flow induced vibrations.
- The concentration of impurities in the water/steam systems, as well as the interfacing sodium systems, should be controlled to prevent the boundary failure due to erosion or corrosion.
- The structures with sodium-water/steam interface should be designed so that measures for monitoring and inspection can be taken, such as continuous monitoring of water/steam leak, periodic inspections.

Mitigation of sodium-water reaction

- A water/steam leak detection system should be installed to detect any interaction with sodium as quickly as possible, such as an increase in the secondary coolant system pressure,

- accumulation of hydrogen gas, to conduct timely isolation of the leak and facilitate reactor shutdown.
- Means of isolation of sodium from steam/water following any failure of a sodium-steam/water interface should be provided, e.g., installation of shutoff valves and relief valves in the water-steam system, and injection of inert gas.
- A pressure relief system, such as rupture disks and connected discharge lines, should be installed in the secondary coolant system to ensure the integrity of primary coolant boundary at the interface with the secondary coolant system as well as the integrity of the secondary coolant system.

Load factors on the containment, examples of “Guidelines for containment systems”

The SDC requires controlling SFR-specific phenomena like sodium combustion and sodium-concrete reactions to ensure the integrity of a containment vessel. The SDG on SSC recommends SFR designers to consider the following items against potential SFR specific load factors on a containment.

- Events that may cause loads on the containment structure include the following.
 - Sodium leakage and combustion
 - Sodium-concrete reaction
 - Heat generation caused by gaseous fission product
 - Hydrogen combustion
 - Mechanical energy release induced by core melting and re-criticality
 - Core debris-concrete interaction

Prevention and/or mitigation measures against all of these events should be taken to reduce the uncertainty about conditions in the containment and the containment response. Design load conditions for the containment structure should be determined taking the effects of these prevention and/or mitigation measures into account.

- IVR should be applied to reactor core and primary coolant systems in order to reduce the following potential load factors on the containment:

- Mechanical energy release induced by core melting and re-criticality, which should be prevented by measures against severe re-criticality in core damage sequences resulting from an unprotected transient;
- Core debris-concrete interaction, which should be prevented by design measures for IVR in core damage sequences resulting from an unprotected transient, and by practically eliminating complete loss of heat removal function and core uncovering caused by sodium inventory loss.

VII. Latest SFR Safety Design Concepts in the World

The SDC and SDGs are beginning to be introduced in the safety design of SFRs in many countries through activities of GIF and IAEA. At the same time, these documents are being updated based on feedback from international organisations and national regulatory organisations.

This section describes recent SFR safety design concepts in the world regarding design measures against two types of DECs, namely ATWS, and loss of heat removal system. In the latest design, SFR-specific design measures, especially for prevention and mitigation of severe accidents, have been installed as consistent with the SDC and SDG. For example, the documents require or recommend that a reactor is shut down without damaging the core by using appropriate combination of inherent reactivity feedback and passive reactivity reduction mechanisms, and that even if core damage occurred, reactor coolant boundary failure is prevented—in other words, IVR is achieved—to maintain the containment function. Some recent SFRs will adopt or enhance the passive mechanisms among other design options. Hydraulically suspended rods (HSR) are installed in Russian BN-1200 [9]. A self-actuated rod insertion mechanism by means of curie-point magnets, as well as HSR are introduced into ASTRID of France [10]. Similar design concepts are under review for Indian CFBR [11]. Furthermore, those countries are considering installing a core catcher in their reactor vessels, aiming at IVR.

Regarding decay heat removal, the SDC and SDG require or recommend that the coolant level is maintained by ensuring structural

integrity of an RV and GV, and that the loss of decay heat removal function is practically eliminated by maintaining coolability through enhancement of the DHRs or highly independent alternative cooling measures. Latest SFRs are equipped with GVs that cover whole primary coolant systems with diverse and redundant DHRs and with natural circulation capability of the coolant to prevent core damage caused by loss of reactor level and loss of decay heat removal after reactor shutdown.

As exemplified above, SFR developing countries such as Russia, France, India, China, U.S., Korea, EU, and Japan are striving to enhance the safety of next generation SFRs in the consistent manner with the SDC and SDGs.

VIII. Conclusion

After TEPCO Fukushima Dai-ichi nuclear power plant accident, activities to enhance the safety of nuclear power plants have become conspicuous. Development of Sodium-cooled Fast Reactor (SFR) is vigorously being promoted especially in France, Russia, China and India, and therefore a demand for an international standard for ensuring the safety of SFRs is growing.

The SDC-TF has been contributed to establish such international safety standards through its activities for developing SDC and SDGs. The SDC and SDGs have been developed based on a consensus among member states of the TF that these documents should be international standards. The SDC and SDGs have been introduced to non-GIF SFR developing countries through international exchanges such as joint IAEA-GIF SFR safety workshops and FR17 (International Conference on Fast Reactors and

Related Fuel Cycles in 2017). Interaction with national regulatory organisations has also been made.

The second safety design guidelines report, "Safety Design Guidelines on Structures, Systems and Components (SDG on SSC)" is in the final stage of its development and external review will be started.

Nomenclature

AOO	Anticipated Operational Occurrence
ATWS	Anticipated Transients Without Scram
DBA	Design Basis Accident
DEC	Design Extension Condition
DHRs	Decay Heat Removal System
DiD	Defence-in-Depth
GIF	Generation IV International Forum
GV	Guard Vessel
IVR	In-vessel Retention
RV	Reactor Vessel
SDC	Safety Design Criteria
SDC-TF	Safety Design Criteria Task Force
SDG	Safety Design Guidelines
SFR	Sodium-cooled Fast Reactor
SDG on SSC	Safety Design Guidelines on Structures, Systems and Components

References

- [1] GIF, "Safety Design Criteria for Generation IV Sodium-cooled Fast Reactor System, Rev.1" GIF SDC-TF/2017/02 (2017).
- [2] IAEA, 'Safety of Nuclear Power Plants: Design', SSR-2/1 Rev.1 (2016)
- [3] GIF, "Safety Design Guidelines on Safety Approach and Design Conditions for Generation IV Sodium-cooled Fast Reactor Systems", GIF SDC-TF/2016/01 (2016).
- [4] Joint IAEA-GIF Technical Meetings/Workshops on the Safety of SFRs (June 2014, June 2015, Nov. 2016).
- [5] 7th Joint IAEA-GIF Technical Meetings/Workshops on the Safety of LMFRs (March 2018).
- [6] IAEA, "Design of the Reactor Core for Nuclear Power Plants", NS-G-1.12 (2005).

- [7] IAEA, “Design of the Reactor Coolant System and Associated Systems in Nuclear Power Plants”, NS-G-1.9 (2004)
- [8] IAEA, “Design of Reactor Containment Structure and Systems for Nuclear Power Plants”, DS-482, Step 8a (2016)
- [9] Marova1, et. al., “Results of BN-1200 Design Assessment for the Compliance with the Requirements of Generation IV and INPRO”, FR17, IAEA-CN-245-399 (2017)
- [10] VARAINE, et. al., “ASTRID Project General Overview and Status Progress, ICAPP 2018 Paper ID#23960 (2018)
- [11] P. Puthiyavinayagam, et. al., “Advanced Design Features of MOX Fuelled Future Indian SFRs”, FR17, IAEA-CN-245-300 (2017)

ECONOMIC AND FINANCIAL ANALYSIS OF A LEAD-COOLED SMALL MODULAR REACTOR (SMR) (C. PIETTE ET AL)

Célestin Piette⁽¹⁾, Mathias Schmit⁽²⁾

(1) Tractebel Engineering A.S., Belgium

(2) Solvay Business School, Belgium

Abstract

SMRs are one of the most promising response brought by the nuclear sector for de-risking its new build projects. In particular, in markets where: (1) the industry lost its “know-how” due to decades-long hiatus in nuclear development (e.g. Europe, North America...); the consequence being greater execution risks (delays and costs overrun). (2) Projects are financed through private investments rather than public one, there is a strong bias against long term and capital-intensive project, typically, nuclear projects. And (3) where electricity is openly traded based on merit order principle (almost) without consideration for system costs (e.g. grid, back-up...) and externalities (e.g. CO₂, pollution related disease...).

The SMR approach addresses these issues through three paths: (1) The finance ability with reduced up-front capital requirement and greater number of actors. (2) The constructability where the size reduction inherently eases the construction progress (e.g. field management, equipment size...), scale economies replaced by economies of mass production (several standardised autonomous modules under a common architecture) and design simplification due to easier passive safety implementation. And (3) the market flexibility because additional high-value applications: off-grid, small grid, load-following and heat applications (sea water desalination, industrial process heat...).

The hope of the approach is to have a life cycle cost advantage over other energy sources while presenting a level of financial risk comparable to other energy projects.

The present report screens the literature to condense an analysis methodology and deeps dive into the financial aspects of such new type of construction.

I. Introduction

This study takes place in the context of a final thesis of the complementary master in management of the Solvay Business School.

The present report exposes the methodology and the conclusions of an economic and financial analysis of a SMR using lead-cooled technology as a case study, at a conceptual screening level of details. Lead, a molten metal, has been chosen because of the disruptive properties it offers in comparison to conventional water-cooled reactors (see §0).

Because the costs of prototyping are not representative of the competitiveness of a mature technology, this cost estimation are for a Nth Of A Kind (NOAK) concept. It is those costs that should drive decision makers [11] because most representative of its final market competitiveness.

The cost estimates are rough and based on a top-down analysis from public literature (see §0) and professionals interviews.

Context

The present study is articulated in a broader picture than solely the nuclear sector which appears to affect us all.

The energy trilemma [1]

The energy is at the base of our industry and have allowed our modern development. Energy is of an infinite complexity and must meet a trilemma:

1. **Economical:** a source of energy must be both competitive and offer a level of risk comparable to those of its alternatives.
2. **Sustainability:** a sustainable energy source allows the present generation to meet its needs without compromising the ability of future generation to meet theirs. Meaning that:
 1. Long term availability of the energy resources must be promoted;
 2. Minimise wastes: greenhouse gas, micro-particles, nuclear wastes...
3. **Security of supply:** by being both available when required (dispatchable) and sufficiently diversified to prevent shortage caused by external events (including political ones).

To meet these challenges, a natural tendency is observed toward the electrification of the market: electric vehicles, domestic heat pumps and electric heaters... Together with a growing population and a growing energy demand linked to the increasing wealth of emerging countries; it appears as an evidence that electricity demand will almost double in the next decades [2].

Competitive environment of the electricity market [1]

The energy market is 200 years old; meaning that it is mature and highly competitive. Three main players compete for the electric supply:

1. **Fossil fuels:** mainly coal and gas whose appear to be cheap and exportable around the globe. This tendency will intensify with the rise of LNG (Liquid Natural Gas) and US unconventional (shale) gas. The main drawbacks being (1) the emission of greenhouse gas following the combustion of the fuel, (2) the volatility of prices of those resources and (3) the unequal repartition of resources on earth leading to geopolitical tensions.
2. **Renewable energies:** wind and solar whose drivers are (1) the absence of waste (when omitting those produced during the manufacture) and (2) the

inexhaustibility of its resources (sun, wind, rain, crops...). While the drawbacks are (1) the intermittency and (2) the unequal repartition of favourable wind-field and sun exposure.

3. **Nuclear energy:** exclusively pressurised water-cooled reactor which provide (1) a greenhouse gas free energy, (2) a long term stable energy prices and (3) low cost when upfront capital investments are absorbed. The main drawbacks being (1) the public fear of nuclear wastes and disasters and (2) large entry barriers due to large infrastructures and financial challenges introduced by enormous upfront capital requirements.

Objectives of the analysis

The SMR approach is more an economical challenge than a technical one. This drives us to the question: "Is a lead-cooled SMR a viable energy source?".

The aim of the present report is to condense the methodology analysis spread across the literature to study (1) the value creation of such project and (2) its resources requirement.

Value creation

It has been chosen to materialise the value creation through the cost of electricity production. Rothwell defines the levelised cost of electricity, or LCOE, "as the constant real price of electricity over the life of the plant that compensates debt and equity investors at their required rates of return. Interest on debt accrues during the construction period and debt holders are repaid with equal annual payments [in constant dollars] over the debt term. Equity holders invest during the construction period and receive profits after tax and debt payment over the plant life. The LCOE is the electricity price that yields the rate of return required by equity holders on the returns accruing to them" [25].

So, the LCOE in USD/MWh is that levelised cost, LC, such that the present value of equity investment (negative cash flows), during construction are equal to the present value of the positive cash flows to equity investors at their expected rate of return, r (or the WACC, see §0).

There is value creation if:

$$LCOE < \text{Electricity Price of Alternatives}$$

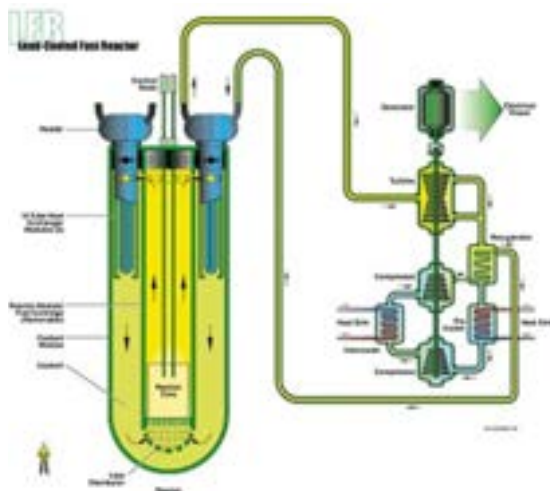
Resource requirements

The amount and timing of capital needs are analysed through the financial statements; combining (1) income statements, (2) balance sheet and (3) cash flow statements.

II. Value Proposition

The product studied in the present study is a technical innovation fostered by a business strategy U-turn.

Generation IV technologies [4]



The fourth generation of nuclear reactors is a selection of six technologies⁴ that present a disruptive approach to meet the criteria mentioned at §0. The research and development of such technologies is shared through an international collaboration including Europe, China, Russia, the US... This generation is radically different from the current generation of pressurised water reactor.

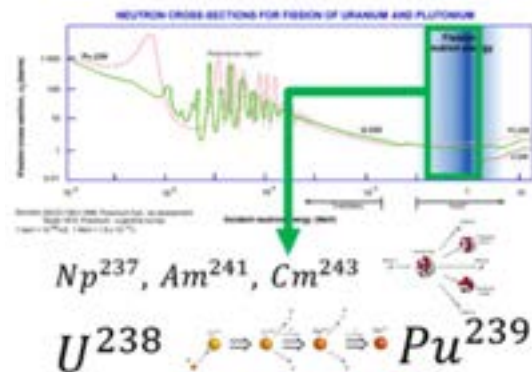
The present study focusses on Lead-Cooled Fast Reactor⁵ (LCFR) which use molten lead, a liquid metal, as coolant. The properties of lead allow:

- The use of “fast neutron” whose benefits are:
- The consumption (burning) of long living nuclear waste (the minor actinides) reducing their volume and

longevity by two to three orders of magnitude;

- The conversion of fertile material (such as uranium 238) into fissile product (such as plutonium 239); by doing so, the consumable fraction of uranium is theoretically multiplied by 60 to 100 making uranium resources virtually infinite for humankind.

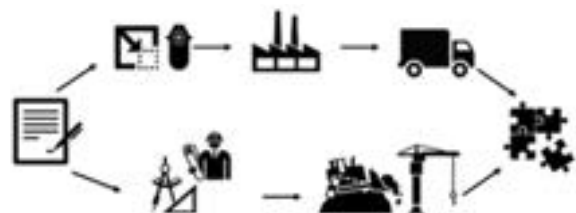
Figure 1. The use of fast neutron allows to (1) transmute minor actinide and (2) the conversion of Uranium 238 (fertile) into Plutonium 239 (fissile)



The elimination of the need of offsite emergency response in case Fukushima type accident because of better thermal and chemical properties: high boiling point, high thermal conductivity and radio-nuclide retention in case of leak.

The « SMR » approach [3]

Figure 2. Schematic illustration of the SMR philosophy. Source: Author creation



4 Super Critical Water Reactor (SCWR), Sodium Fast React (SFR), Lead Fast Reactor (LFR), Very High Temperature Reactor (VHTR), Gas Fast Reactor (GFR), Molten Salt Reactor (MSR).

5 Regardless of the promising properties of lead as coolant, it is also the technology selected by the Belgian National Nuclear laboratory SCK-CEN.

By the past nuclear reactors have been designed continuously bigger (up to 1650 MWe for the French EPR) to achieve economies of scale. Recent event such as problems at the Flamanville project [36], Olkiluoto (Finland) [35], and the bankruptcy of Westinghouse following the delays and cost overruns at the two US new constructions (VC Summer and Vogtle) [37] have demonstrated that those increases in size are accompanied with increased complexity which may wash-out the economies of scale.

The SMR (for Small Modular Reactor) is an innovative approach where [3]:

- The reactor is significantly smaller (from 50 to 300 MWe);
- The design is standardised and thought to be manufactured directly on an assembly line;
- The total power of the plant is spread among several independent modules (from 1 to 12 depending of the design).

The resultant benefits being:

- A drastically reduced upfront capital requirement which reduces barriers for new entrant and related financial burden. Rather than being purchased by governments, an association of electro-intensive consumers (for example heavy industries) could decide to purchase a nuclear power plan;
- Power build up by the addition of modules while demand increases;
- A well supplied order book would lead to a continuous flow of reactors manufacture leading to:
 - Talent and knowledge retention;
 - Reduced incertitude about manufacturing cost;
 - Economies of mass production.

Figure 3. Illustration of the NuScale concept where the total power of the plant is spread among several (12) autonomous modules that may be add and connected as demand arises



Source: NuScale Power [38]

Technical description of the studied SMR

The present Master Thesis is focused on a single nuclear power plan composed of six modules each producing 100 MW of electricity and is inspired by the SVBR-100 Russian design [22].

This is an integrated pool type SMR where primary pumps and steam generators are incorporated to the vessel. The end product works as a plug and play Nuclear Steam Supply System (NSSS).

The reactor is cooled by lead, a liquid metal, and operate in fast spectrum (see §0); however due to the lack of data, no credit is given to the fuel recycling and long living waste burning.

Figure 4. SVBR-100. Source: Aris database [22]



III. Methodology

The life cycle cost assessment of an innovative nuclear project is both complex and subject of wide uncertainties. Those may be kept under control through rigorous and systematic analysis. The following sub-sections detail the methodology constructed and the tools implemented to guarantee a degree of robustness in the analysis.

Literature-inferred approach

The characteristics of the studied reactor are obtained from a screening of the existing designs available on the IAEA database ARIS [22][23]. The hybrid reactor studied use blended characteristics of those designs with a large influence of the Russian SVBR-100 [65].

Cost categories

The apparent complexity of such project is tackled by the Economics Modelling Working Group of the Generation IV International Forum (GIF) [10]. They provide guidelines and a cost account codification with a gradual complexity: ranking from single to double and triple digits code. This allows a systematic decomposition of the distinct categories of costs that make up a nuclear project.

Figure 5. Cost Categories breakdown in Gen IV Accounting Framework [10]



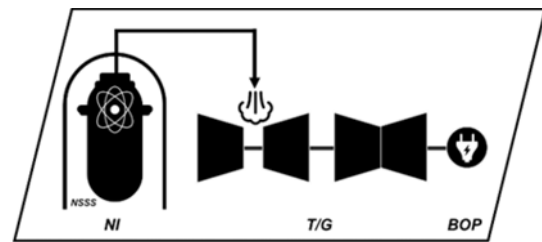
Benchmark & Top-down analysis [11][12][13][14][15][16][17][18][19][24].

A nuclear power plant can be subdivided in two main parts:

- **The Nuclear island (NI):** The part of the plant containing most of nuclear-related equipment and systems. Typically, it consists of containment, the reactor building, the fuel building and similar facilities.
- **The Balance of Plant (BOP) and Turbine & Generator Island (T/G):** All areas of the plant and systems not included in the nuclear island scope.

The BOP and T/G are not technology specific: once the steam is extracted from the reactor, the systems and equipment used for the electricity generation are conventional (meaning not dependant of the nuclear technology considered). Hence their cost may be estimated from the literature: from the existing pressurised water reactor fleet, or even conventional fossil fuel installation.

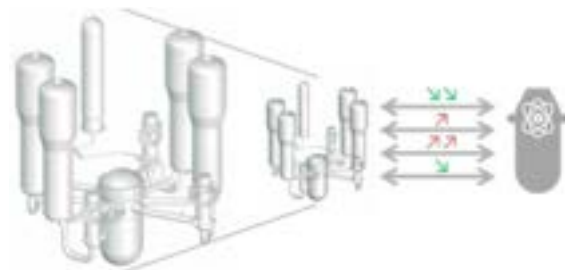
Figure 6. Schematic nuclear power plant subdivision



Source: Author creation

On the other hand, the NI is technology dependant. Hence, the estimation of the liquid metal cooled reactor is not straightforward. The following picture illustrates the strategy deployed: (1) a reference water cooled design is (2) scaled down using parametric analogies [9] and then (3) after split into the cost categories (defined in §0) following a certain repartition key [30], credit to specific technological advantages or drawbacks are allocated by cost categories (as detailed in §0).

Figure 7. Illustration of cost estimation strategy for the Nuclear Island as described in [30] and [24]



Technological balance of lead-cooled reactors [40]

Benefits (drawbacks) of the lead-cooled technology inherently lead to cost reduction (increase). Those are detailed, characteristic by characteristic, in the following two sections with a qualitative appreciation of the effect on cost.

- Benefits

Table 1. Costs implication of lead-cooled technology benefits

Property	Advantage	Possible design simplification	Cost category	Effect
High boiling point (1743°C at 1 bar)	Wide safety margins before onset of boiling	Coolant boiling very unlikely No need for pressurisation	Primary Vessel	↘↘
Inert with water and air	Reduced internal hazards Air/water usable as heat vector/sink	No need of intermediate circuit Air/water based DHRs	NSSS	↘
High density & volume expansion coefficient	Fuel dispersion potentially dominating Facilitated natural circulation	Potentially no core catcher needed Natural circulation even in unprotected accident	NSSS & Reactor structures	↘
High heat capacity	High thermal inertia transients	Primary side driving the time-scale	O&M	↘
Excellent neutronic properties	Low moderating power Hard neutron spectrum	Favoured breeding/transmutation	Fuel	↘
Excellent retention capabilities	Barrier against releases	Reduced confinement requirements	NSSS	↘↘
Excellent gamma shielding	Reduced need of engineered shielding	Simplified layout around the primary system	O&M Reactor structures	↘

- Drawbacks

Table 2. Costs implication of lead-cooled technology drawbacks

Property	Disadvantage	Necessary design provision	Cost category impacted	Effect
High melting point (327°C)	Investment protection concern	Reduced heat losses in shutdown Reliable heating systems	NSSS	↗
High density	Seismic risk Buoyancy of immersed components	Limited plant size 2D seismic isolators	Field preparation	↗
Corrosion	Dissolution of constituents Alteration of coolant	Limited temperature range Need for coolant treatment system	Vessel Auxiliary system	↗↗
Erosion	Limited bulk velocities	Need for specific materials where requirements cannot be met (pump)	Primary pumps	↗
Opacity	No visual inspection allowed Non-standard repair under lead	Need for alternative In Service Inspection devices Extractable components	O&M	↗

Hypotheses

The following hypotheses have been postulated, consistently with literature:

Table 3. Main hypotheses for cost estimation

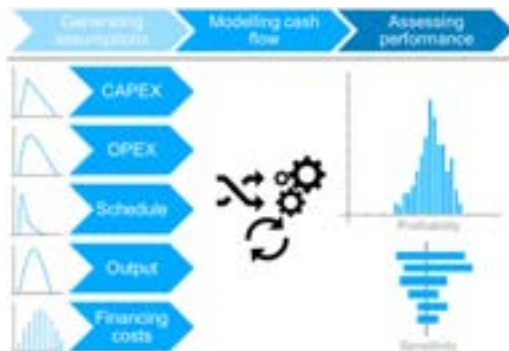
Parameters	Hypothesis
Reactor average capacity factor [25]	89%
Modules economic life ⁶ [23]	40 years
Plant economic life ⁷	Not constraining
Plant construction lead time ⁸ [25] [13]	3 years
Module construction lead time ⁹	2 years
Multiple modules production lines ¹⁰	Yes
Production rate ¹¹	1 module/month
Uranium enrichment [23]	16,5% in U ₂₃₅
Time between refuelling [23]	18 months
Fuel recycling	None
Depreciation [14]	20 years
Debt repayment ¹²	21 years

Contingency management

The present section describes the strategy implemented to increase the robustness of the model and manage uncertainties.

General approach

Figure 8. Input-related uncertainties management through Monte-Carlo simulation



Author creation adapted from [42]

In addition to the parameters defined in §0, economic cost estimation of equipments and infrastructures are modelled with a probabilistic distribution.

The economic model implemented by the author run **50+** economic parameters with an Excel based Add-In (@Risk). The software run a Monte Carlo algorithm that simulates **10.000** random scenarii based on the probabilistic distribution of the input data. The outputs are: (1) the profitability (VAN) of the project as a histogram and (2) the sensibility analysis that displays, ranking by magnitude, the most impactful variables.

Contingency is an adder account for uncertainty in the cost estimate. Contingency includes an allowance for indeterminate elements. In other words, it is the cost allocated to the uncertainty of the cost estimation.

In practice, literature [25] suggests that a proper value for contingency correspond to one standard deviation of the cost estimation (Overnight Cost) distribution.

Input distribution model selection

Uncertainties regarding inputs are fed to the model through probabilistic distributions with patterns fitted to their expected behaviour (often from empirical evidence).

CAPEX

CAPEX are fed to the model through a **triangular** distribution whose parameters are (1) the minimum, (2) maximum and (3) best estimate of the input variables.

The accuracy range for conceptual screening is taken between [-30%; +50%] coherent with the AACE suggestion [25].

The author has chosen to take unsymmetrical accuracy range to tackle optimism bias.

6 Due to corrosive behaviour of lead.

7 It is of common knowledge in the nuclear industry that the only component that can't be replaced is the Reactor Pressure Vessel (RPV). Therefore, the lifetime of the plant has been postulated not limiting.

8 There are some empirical evidences of construction lead time shorter than 5 years [5] [25] for large nuclear power plant. Some vendors are claiming schedule below 3 years [38] (between first concrete pouring and mechanical completion).

9 This value is based on engineering judgement only rather than specifications or vendors quote.

10 Meaning that more than one module at a time can be manufactured.

11 Informal interview with competent expert reports that SMR Vendors are targeting a production rate of 100MWe/month for a manufacturing facility costing about half a billion US dollars to construct.

12 Same conditions as the loan granted from the Russian government to Hungary for the construction of PAKS II [41].

▪ OPEX

OPEX comprising for fuel and Operation & Maintenance (O&M) costs are fed to the model through a **normal** distribution; the 17.000+ cumulative years of operational experience providing more robust estimates [43][25].

▪ Schedule

Schedule, in particular construction lead time, is fed to the model through a **Poisson** distribution as observed from empirical evidence with large scale reactors [25].

▪ Output

Operational performance that account for the capacity factor of energy production is fed to the model through a normal distribution. The reasoning is the same as for OPEX.

▪ Financing costs

The expected return (or discount rate) of the project is not a variable but a parameter that is agreed upon the signature of the project. Hence, its variations are discrete and depend of the contracting and financial scheme (see §0).

Cost analysis [10][25]

The annual total cost (TC) of a nuclear power plant is given by the following formula:

$$TC = A_c + Fuel + O\&M + D\&D$$

With:

$$A_c = CRF * KC$$

$$KC = OC + IDC$$

$$CRF = r * \frac{(1+r)^T}{(1+r)^F - 1}$$

Where:

- **A_c**: is an annual annuity payment to repay the construction capital's principal and interest;
- **CRF**: is the capital recovery factor;
- **KC**: is the total cost of construction (including interest during construction);
- **OC**: is the overnight cost;
- **IDC**: Interest During Construction;
- **Fuel**: annual cost of fuel, including interim storage and long-term disposal;
- **O&M**: cost for operation and maintenance;

- **D&D**: is the annual provision for decontamination and decommissioning of the plant;
- **r**: is the expected return or the WACC;
- **T**: is the economic life of the plant.

When norming TC by the annual mean electric production, we obtain the levelised cost of electricity (LCOE):

$$LCOE = \frac{TC}{E}$$

$$E = MW * TT * CF$$

Where:

- **E**: Electricity output;
- **MW**: is the power capacity of a specific plant;
- **TT**: is the total potential working hour during the economic life of the plan;
- **CF**: is the fraction of capacity at which the plant is operated during the period.

The following sections detail the above-mentioned costs.

Because some of the collected information are proprietary (i.e. confidential), the results of this section are presented at an aggregate level. Hence, the present report stays in the public domain.

Overnight costs

Overnight cost represents all the “up-front” expenses: base construction cost plus contingencies:

$$OC = BASE + Contingency$$

$$BASE = DIR + INDIR + OWN + SUPP$$

Where:

- **Contingency**: is the cost of incertitude (see §0);
- **DIR**: are the direct construction plus pre-construction cost (such as licensing);
- **INDIR**: indirect cost which include engineering and administrative costs that cannot be associated with specific cost category;
- **OWN**: owners' cost that include for example transmission cost;
- **SUPP**: supplementary cost which are mainly first core cost;

It is referred to as overnight cost in the sense that time value cost (Interest During Construction – IDC) are not included (i.e., as if

the plant were constructed “overnight” with no accrual of interest).

Table 5. Overnight costs breakdown summary

Code	Category	Result [MUSD]
10s	Pre-Construction Cost	140
+20s	Direct Cost (BOP + T/G + first module)	1322
	Direct Cost (SMR)	5x132
=	Direct Cost	= 2.122
+30s	Indirect Services Cost	500
=	Base Construction Cost	= 2.622
+40s	Owner's Cost	200
+50s	Supplementary Cost	0 ¹³
=	Overnight Construction Cost	= 2.822

Interests during construction

Interests during construction (IDC) are the interest accrued for up-front cost financing (i.e., it is accrued to the end of the construction and plant start up).

Once money is raised and the construction payments begin, an accumulated return (interest) to the construction loan, investors, or bank must be accrued until commercial operation.

The IDC rate used is the average cost of money (WACC or expected return), including both equity and debt.

IDC have been calculated using the following method [10][25]:

$$IDC = \sum_{j=1}^{j=J} C_j [(1+r)^{t_{op}-j} - 1]$$

Where:

- j = period #;
- J = number of periods (here, quarters of construction);
- C_j = cash flow for quarter j , reflecting beginning-of-period borrowing;
- r = discount rate or expected return (WACC), here expressed quarterly;
- t_{op} = quarter of commercial operation.

Overnight construction cost for the Nuclear Island (NI), the Turbine Island (TI or T/G) and the Balance of Plant (BOP) have been translated into cash flow by postulating construction costs

have been spread following a S-Curve (over 3 years).

Overnight construction costs of each six modules have been translated into cash flow by postulating construction costs have been spread equally across quarters (because of factory manufacturing).

Figure 9. Pattern for construction cash-flow spending

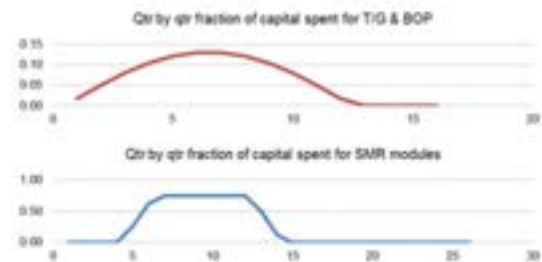


Table 6. Interests During Construction

Category	IDC [MUSD]
Conventional island and balance of plant	268
Nuclear island (or SMR modules)	49

Total Investment Capital Cost

Applying methodology in §0, the CAPEX contingency is calculated to be **230MUSD** that is added to the cost account “60s”, together with the IDC to form the financial cost:

Table 7. Total Capital Investment Cost breakdown summary

Code	Category	Result [MUSD]
	Overnight Construction Cost	= 2.822
+60s	Financial Costs (i.e. IDC + Contingencies)	547
=	Total Capital Investment Cost (TCIC)	= 3.369

¹³ The author has chosen to include the first core cost into the fuel cost account.

Operation and maintenance costs [25]

Little is available in the public domain regarding the O&M costs of the currently operating light water reactors (LWRs). Unfortunately, the best data on NPP O&M costs are proprietary. These data are collected by EUCG (formerly known as the Electric Utility Cost Group) and are available on a 'give-to-get' basis among members.

Without access to those data, the following model is proposed:

$$O\&M = O + M + PIN$$

Where:

- **O**: is the labour cost for operation and maintenance activities;
- **M**: miscellaneous cost including maintenance materials, supplies, operating fees, property taxes and insurance (not including accidental off-site nuclear damages);
- **PIN**: premium for accidental off-site nuclear damages.

Literature proposes:

- A base of 250 employees and an additional 50 persons per 180 MW. In the present situation, this leads to a total of ≈ 420 employees (total power considered being 6×100 MWe);
- Mean annual salary is set at 80.000 USD /employee;
- A share of 60/40 between O costs and M costs respectively;
- Premium for accidental off-site nuclear damages (PIN) has been estimated to 1USD /MWh¹⁴;
- O&M costs are decorrelated from the discount factor.

Which leads to:

$$O\&M = \frac{420 * 80.000}{600 * 89\% * 365 * 24} * \left(1 + \frac{40}{60}\right) + 1 = 12,97 \text{ USD /MWh}$$

14 Considering a nuclear disaster (INES 7 type event [31]) happens once every 25 years (Chernobyl in 1986 and Fukushima in 2011) with a cost of 100 billion euros. Additionally, assuming that 'a nuclear power plant accident in one country is an accident in all countries' [25] (meaning that the risk is spread across the 450 reactors actually in

Fuel costs [25]

Figure 10. Upstream fuel cycle - Fuel Fabrication



Source: Synatom [28]

Figure 11. Downstream fuel cycle - Waste Management



Source: Synatom [28]

Under the assumption that fuel is paid in a uniform stream over the life of the plant, without regard to the changing nature of a reactor's set of irradiated fuel, fuel costs can be decomposed as follow:

$$Fuel = FC + Waste$$

$$FC = Ore + Enrichment + Fabrication$$

- **Ore**: include price of natural uranium and the cost of its conversion in UF_6 prior to its centrifugation;
- **Enrichment**: is the cost of centrifugation of UF_6 ;
- **Fabrication**: is the price of fabrication of UO_2 fuel from enriched UF_6 ;
- **Waste**: is the interim storage cost per MWh (cost to manage used fuel) plus geological disposal costs.

Manual calculation from UxC's tool for fuel cost calculation [31] leads to value twice as low as those from literature [25], mainly due to significant decrease in Separative Work Unit¹⁵

operation [32]) and that the nuclear insurance premium may be estimated through the mathematical expected associated damages, it comes for a typical a large-scale water reactor: $10^{11}/(25*450*365*24*0,89*1200) < 1\$/MWh$.

15 Parameter of the uranium enrichment process [64].

(SWU) costs¹⁶. Therefore, fuel cost is calibrated from a third source [19]:

Table 8. Fuel Cost breakdown

Category	Cost [USD /MWh]
Fuel Cost	15,00
Interim storage	0,72
Long term geological disposal	1
Total Fuel costs	16,72

Decontamination and decommissioning

Decontamination and decommissioning cost (D&D) include all the costs necessary for area restoration and its restitution to the owner. These future costs are therefore mainly found under the form of provisions.

As an example, in Belgium, the amount required to be provisioned are not left to the plant staff expertise but decided by the Commission des Provisions Nucléaires thanks to a sector analysis every 3 year. This board and its prerogatives are defined by 11th April 2003 law [26][27].

Furthermore, Synatom is another agency which takes part to the nuclear fuel cycle management. Thus, Synatom is the entity that is provisioning for future D&D costs of nuclear plant on the Belgian territory. To collect these amounts, they also levy an activity-based tax from operators [28][29].

Amounts provisioned could be widely impacted by a revision of the updating rate used. Such as shown by the tremendous increase of Synatom reserves in 2016, from 8 to 9.2 billion of euros due to a change of updating rate [29]. These future possible modifications are not either considered in the present model.

The Cost Estimating Guidelines for Generation IV Nuclear Energy Sources published by the Economic Modelling Working Group (EMWG) recommends for D&D costs an estimation between 25 and 35% of the initial overnight capital costs [10]. But M.A. Moore argues that despite D&D facilitation in lead-cooled SMRs, the loss of economy of scale will increase the costs nevertheless. Thus, he recommends an estimation of 40% of overnight capital costs [30].

The total amount of D&D costs has been calculated by limiting us to two borders (min 35%; max 40%). Used rate is the best estimate of 38%

of overnight capital costs and the total amount was distributed on the business year's numbers to obtain a constant amount to be funded.

Here, D&D funding is treated as a sinking fund. Annual contributions to a 'nuclear decommissioning trust fund' earn a rate of return, rd , during the life of the facility. For ease of calculation this rate of return of this fund (rd) is postulated equal to the escalation rate of D&D costs [25]. The annual provision for D&D costs becomes:

$$D\&D = \frac{38\% * OC}{\frac{T * E}{38\% * 2,82 BUSD}}$$

$$= \frac{40years * 600MW * 365 * 24 * 89\%}{38\% * 2,82 BUSD}$$

$$= 5,73 USD /MWh$$

Financial aspects

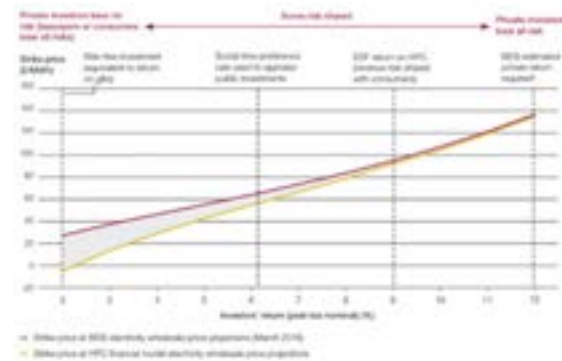
To paraphrase the author's finance professor:

"[...] the best way to kill a project is to challenge its discount rate [...]"

Schmit M., Solvay Business School

It is particularly true for nuclear projects as highlighted by the UK National Audit Office: the LCOE of nuclear projects is highly sensitive to the investors' expected return¹⁷.

Figure 12. LCOE sensitivity to investors' return. Source: UK National Audit Office [44]



The following sections deal with the determination of cost of money through (1) a bottom-up approach using the theory of the Capital Asset Pricing Model (CAPM) and (2) a wealth-based approach.

The aim of these sections is not to determine the unique and "true" price of capital but rather

16 <https://www.uxc.com/p/prices/UxCPriceChart.aspx?chart=spot-swu-full>

17 Which is peculiar to capital intensive projects including also, for example, water dam projects.

to give leads on what parameters influences it and, in turn, insights on how to exploit it.

Bottom-up approach [41][45]

The bottom-up methodology uses the standard formulae of the WACC (Weighted Average Cost of Capital) and estimates its parameters from database:

$$WACC = \frac{D}{D+E} * (1-t) * R_d + \frac{E}{D+E} * R_e$$

Where: D and E are the amount of debt and equity, R_d and R_e denote the costs of debt and equity respectively and t is the corporate tax rate.

$$R_d = R_f + (R_d - R_f)$$

Where R_f denotes the risk-free rate in the market of interest¹⁸ and $(R_d - R_f)$ denotes the bond premium in the market.

In turn, the cost of equity will be determined by the standard CAPM formula:

$$R_e = R_f + \beta * (E(R_m) - R_f)$$

Where R_f denotes the risk-free rate in the market. $(E(R_m) - R_f)$ denotes the equity market risk premium and β (beta) is a measure of the idiosyncratic, diversifiable (or specific) risk of the project (see §0).

Values of the parameters are extracted from two sources that are widely recognised and used in the finance and business world:

- The global equity risk premium database established by Professor Damodaran [46];

- The market risk premium database set-up by Professor Fernandez [47].

Results¹⁹ are summarised in the following tables for the 2017 year:

Table 9. Equity Risk Premium - Bottom-up approach

Source	Equity Risk Premium	Risk Free
Damodaran	5.45% ²⁰	2.41% ²¹
Fernandez	6.04% ²²	1.92% ²³
Average	5.75%	2.17%

Table 10. WACC computation: bottom-up approach

Parameter	Value
Risk free rate	2,17%
Equity risk premium	5,75%
Beta ²⁴	1,01
Nuclear risk premium ^{25,26}	2%
Return on equity	9,98%
Commercial debt risk premium ²⁷	2,02%
Before tax return on debt	4,19%
Corporate tax rate ²⁸	25,51%
After tax return of debt	3,12%
Leverage scenario I: (D/(D+E))	50%
Leverage scenario II: (D/(D+E))	40%
WACC (scenario I)	6,55%
WACC (scenario II)	7,24%
WACC range	6,55%-7,24%

18 As recalled by the European Union to the Hungarian government that used the sovereign long-term bond rate of Germany instead of its own (way higher) to establish its cost of capital [41].

19 Rates are adjusted for inflation.

20 Average of Germany (5.08%), France (5.65%), United Kingdom (5.65%), Belgium (5.78%) and USA (5.08%). For information purpose, other Market Risk premium are: China (5.89%), Russia (7.96%) and Greece (15.46%). Data may be downloaded from:

http://pages.stern.nyu.edu/~adamodar/New_Home_Page/datacurrent.html

21 USA long term Treasury bond rate.

22 Average of Germany (5.7%), France (6.5%), United Kingdom (5.9%), Belgium (6.4%) and USA (5.7%) Market Risk Premium. For information purpose, other Market Risk premium are: China (7.5%), Russia (7.7%) and Greece (16.2%). Data may be downloaded from:

https://papers.ssrn.com/sol3/papers.cfm?abstract_id=2954142

23 Average of Germany (1.4%), France (1.8%), United Kingdom (2.2%), Belgium (1.7%) and USA (2.5%).

24 From Damodaran Database (Western Europe): <http://www.stern.nyu.edu/~adamodar/pc/datasets/totalbetaEurope.xls>

25 Moody's (2009) study, to the announcement of a nuclear power plant construction project by American generation companies implies an average downgrade of 4 notches. In turn, Damodaran in his databases estimates that a credit rating difference of 4 notches, e.g. A3 and Ba1, translates into a total equity risk premium of 2.0% ([41] footnote n°70).

26 Literature suggest that this premium may rise up to 5% in deregulated market [25].

27 From Damodaran Database (Western Europe): <http://www.stern.nyu.edu/~adamodar/pc/datasets/waccEurope.xls>

28 From Damodaran Database (GDP-based weighted average for Western Europe): www.stern.nyu.edu/~adamodar/pc/datasets/ctryprem.xls

Wealth-based model

Most financial models assess project risk factors independently of project size. The Chicago University's study team analysis of the risk premium associated with large scale and SMRs led to the view that risk premium, by whatever measure, depends on the size of the project [11].

Rothwell has proposed a model for quantifying this relationship [25], postulating that the risk premium associated with a project is a function of the wealth of the sponsoring entity: "In particular, the cost of capital in financial markets is a function of the decision maker's preproject wealth (e.g. net present value) and debt to equity ratio, and the decision maker's anticipated (contingency-adjusted) post-project wealth and debt to equity ratio".

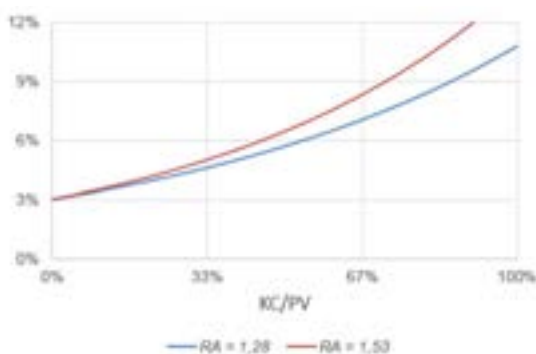
Rothwell developed a mathematical expression for this relationship, parametrised by the risk aversion of the sponsor:

$$r = (3\%) * \exp\{RA * (CK/PV)\}$$

Where:

- **RA:** is a measure of risk aversion;
- **KC:** is the total construction cost of the project;
- **PV:** is the present value of the sponsoring company before the project.

Figure 13. Risk premium and the ratio of construction cost (KC) to PV. Source: reproduced from [25]



29 British Pound to Euro. Value extracted from: <https://www.xe.com/currencycharts/?from=GBP&to=USD&view=10Y>

30 The period ranging from 2012 to 2013 has been considered in the evaluation because the deal

With as exemplary parameters 1,29 and 1,53 for the investor's risk aversion.

Those results suggest that SMRs should be viewed more favourably by utilities and by the investment community; hence, having a lower risk premium than large scale nuclear power plant because of the smaller size of the project relative to the market value of SMR project sponsors [11].

- Case study – EDF & Hinkley point c

Figure 14. Artist's impression of Hinkley Point C nuclear power station



Source: EDF Energy/PA

- The total construction cost of Hinkley Point C in UK is about 22B£;
- With a 66,5% participation of EDF in the project [44];
- The exchange rate (EUR/£) varied between [1,15-1,27] during the 2012-2013 period^{29,30};
- The total equity of EDF was about [30,7-38,9] BEUR in the 2012-2013 period [49][50].

Hence, the KC/PV ratio of the project ranged roughly between [40%-60%] leading to an expected return comprised between [7%-9,5%] which overlay the 9% return negotiated by EDF on the project [44].

has been signed in 2013 [44]. Hence, the period of negotiation is arbitrarily set to start the year prior to signature.

Market segmentation [52]

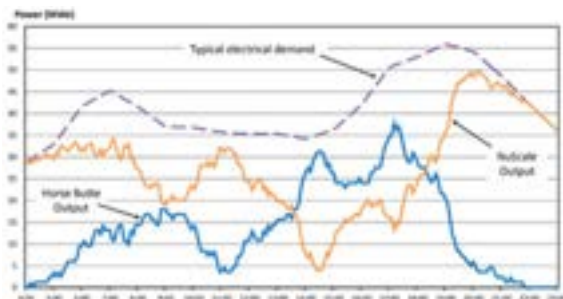
The SMRs open new market opportunities, both in term of:

- Market **location**: remote and off-grid communities such as in Canada [51] and in emerging countries;

Industrial applications:

- **Load following** and grid balancing as demonstrated by NuScale Power:

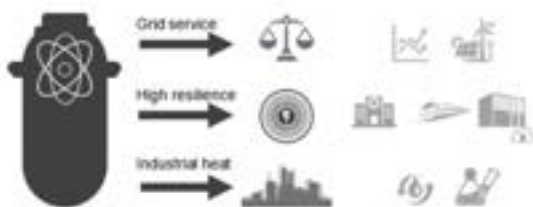
Figure 15. Example of NuScale module load-following to compensate for generation from the Horse Butte wind farm and daily



Source: NuScale Power [53]

- Direct **heat** uses such as district heating, sea water desalination, hydrogen production or industrial heat application [54][55].
- Those are better suited for SMRs concepts because the lower nominal power output inherently seeds flexibility and versatility of applications.

Figure 16. Illustration of SMRs market versatility



Source: author creation

The key message here is that the SMR approach broaden the range of opportunities of nuclear energy with different market segmentation depending of the SMR concept.

The analysis of the economic benefit of such versatility and flexibility exceed the framework of the present study. Locatelli open the path to such study through real options analysis [56].

IV. Results

The following sections successively present the results of the analysis, discuss them (benchmark and additional contextualisation) and suggest ways to bring improvement to the project.

Cost breakdown summary

Table 11. Capital and Operational Expenditures summary

Category	Sub-categories		Value
CAPEX	Direct (equipment supply)	NSSS	1.986
		T/G	483
		BOP	1.066
	Indirect cost	Owner's Cost	333
		Service Cost	833
	Financial Cost	IDC	528
Contingency		383	
			≈5.600 USD /kW
OPEX	Fuel		16,72
	O&M		12,91
	D&D		5,73

Normalised **investment cost** (USD /kW) of lead-cooled SMRs appears:

- in the higher range of nuclear technologies (in OECD countries, excluding Korea);
- in the range of offshore wind technologies [68];
- Higher than most other energy technologies (including fossil fuel generation).

This result tells us that while some design simplification may have reduced some equipment and structure requirements, lead-cooled SMRs remain a capital-intensive technology.

Operating cost (USD /kWh) of lead-cooled technology:

- Is high in comparison to current nuclear technologies (water-cooled), mainly due to higher enrichment requirement of fast reactors (see §0);

- Is in the range of renewable technologies³¹ depending on the location and the technology: commercial PV is cheaper to maintain than residential PV and offshore wind is more expensive than onshore wind due to lower accessibility;
- Outperforms fossil-fuel sources [62].

This result tells us that on a liberalised open-traded market, lead-cooled based SMRs would be price taker rather than price maker.

As explained by IAEA, “in liberalised electricity markets, the spot market price is usually determined by the marginal variable cost of the most expensive unit of generation required to meet demand. In other words, under marginal cost pricing, generators are operated according to a ‘merit order’ from lowest to highest marginal cost” [57] (see figure below):

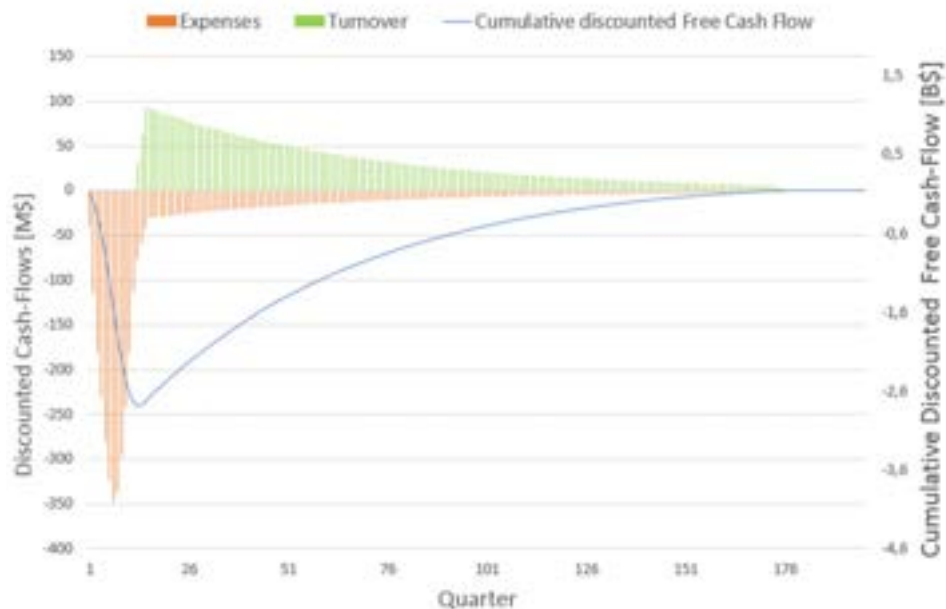
Figure 17. Merit order and marginal cost pricing. Source: adapted from [57]



Cash-flow

As discussed in previous section, nuclear projects are characterised by high up-front capital investment, counterbalanced by relatively low operating expenses. The discounted cash-flows (expenses and revenues³²) and cumulated discounted free cash-flow, plotted on the following graph, illustrate this concept.

Figure 18. Project cash flow: discounted expenses and revenues (left) and cumulated discounted free cash flow (right)



31 Fuel cost for renewable is zero (sun and wind) but proportionally require high O&M costs due to diseconomies of scales.

32 These cash-flows are constant in amount over time (when indexed for inflation and escalation) but their *value* decreases over time because of their future uncertainty.

Sensitivity analysis

Sensitivity studies aim to check the robustness of the model by simulating changes in all the relevant parameters of the model and emphasise the most critical ones.

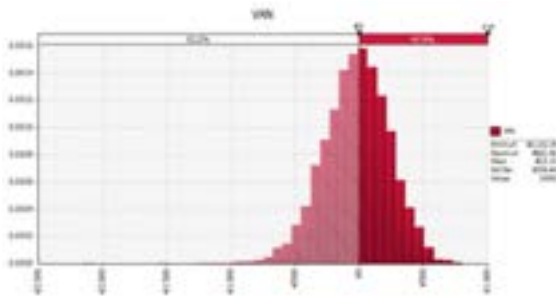
Histogram

From the Monte Carlo simulation (using @Risk), it appears that, at a cost of electricity equal to the LCOE (which includes a provision for contingencies), almost half of the scenarii display positive NPV (fr: VAN); meaning that the project creates values for the investors. For a greater range of confidence, the analysis would require: (1) greater project and technical details concerning the SMR and (2) an additional margin on the electricity price.

Input influence ranking & mitigation strategy

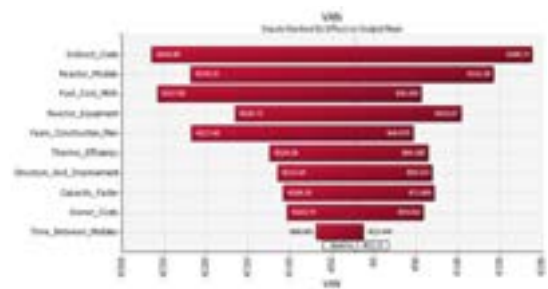
The sensitivity analysis highlights the parameters that should require additional attention. Because of their potential negative impact (or their potential benefits), special means should be tailored in order to mitigate the influence of those parameters and/or exploit their potential improvements capabilities.

Figure 19. Histogram of Monte Carlo 10.000 simulated scenarii



@Risk output from author's model

Figure 20: Tornado chart displaying sensitivity to input uncertainties



@Risk output from author's model

- Indirect cost

As highlighted by McKinsey [59] a frozen and proven design is essential. Delaying the start of the project prior to such evidences may be recommended and switch of technology (i.e. going for FOAK project) must be undertaken solely under strong reasons.

Countries with low (or no) recent experience in nuclear construction projects³³ should consider importing experienced project management teams to further reduce the contingency regarding engineering and project management costs.

- SMR modules

At this stage of the study (conceptual screening), the uncertainty surrounding the SMR modules (or more broadly, the NSSS) are due to lack of empirical data regarding such technologies. With evolution of the design, the uncertainties shall be lessened.

It is the level of design simplification and optimisation, together with the modularity capabilities that shall determine whether the cost implemented is over or underestimated.

Nevertheless, the general philosophy of SMR construction through mass manufacturing on assembly lines, aims to induce both efficiency and lower contingencies on manufacturing costs.

- Fuel cost

The uncertainty surrounding fuel costs are conditioned by (1) uranium ore price and (2) SWU price which depend (a) of the choice of

33 New entrants (United Arab Emirates, Egypt, Turkey...) and countries without continuity in their nuclear construction (Europe, U.S.A...).

technology for enrichment and (b) the bottleneck at the enrichment facilities, adding pressure to the market.

Optimising the diversity of providers leads to substantial gain from competition. In Europe it is one of the mandate of Euratom to guarantee such security of supply [71].

- Construction lead time & project management skills

In the continuity of what has been proposed to mitigate indirect costs, construction schedule may be kept under control when “decision makers” understand that their project management teams prevail on the choice of tools (e.g. data and project management software) and reactor design.

“Paying or waiting for the right team” and “avoiding the substitution of fancy system for successful proven people” are the key messages [59].

- Capacity factor

The ultimate economy of power is found to be substantially affected by the quality of the operator. The scale of large utilities has historically not demonstrated benefit to operation performance.

The choice of the operator must be rational and based on evidence of past performance. If the required standard is not (yet) available in the country, a new operating company should be created, and operators trained by capable operator (from abroad) [59].

- Cost of capital

As discussed in §0, the cost of capital is not a variable but a parameter that is decided/negotiated upon the launch of the project. It is conditioned by the project’s perceived risk by the sponsors: the higher the risk, the higher the expected return.

Its influence is rather important: an increase of 1% of the cost of capital (WACC) leads to an increase of the LCOE of ~9-10%. The section 0, provides additional strategies to lessen the total risk of a new nuclear construction.

Hedging risks

The theory of CAPM tells us that the market does not focus on the specific risk of a project because (1) specific risks of a project should already be considered in the cash flows forecast³⁴ and (2) a well-diversified portfolio of investments protects against specific risks of a project. Hence, the return that the market could legitimately expect is the non-idiosyncratic (non-diversifiable) risk [45].

Figure 21. Effect of diversification on the total risk of a portfolio of investments.

Source: adapted from [45]



When a manager (of a utility for example) considers a new nuclear project, this specific investment adds risk to its portfolio of generating assets³⁵. Hence, it is wise looking for strategies to mitigate them.

There are four types of risks surrounding nuclear projects:

- **Market** risk linked to the volatility of electricity prices that fosters the uncertainty regarding future operating cash flows;
- **Execution** risk composed of construction issues (delays and costs overrun) and the financial burden³⁶ of “mega-projects”;
- **Operational** risk concerning the future availability of the plant (efficient preventive maintenance, well-organised

34 See §3.2 that deals with uncertainties surrounding project (1) construction cost, (2) schedule (3) operational performance.

35 Informal interview with senior financial advisor.

36 The stop of VC Summer (U.S.), because of delays and costs overrun, led Westinghouse into bankruptcy [37]. Failing a smaller project would not necessary mean the fall of a company as an all; hence, increasing lenders confidence.

outages and refuelling, major component failure...);

- **Regulatory** risk both environmental (water access in context of climate change and nuclear wastes management mainly) and political because of majority shift following a bad public perception of nuclear energy³⁷.

The following sections present strategies to hedge all these kinds of risk. The side consequence of reducing the risk of the project is a greater confidence of its sponsors, leading to a lower expected return (i.e. WACC).

Revenue assurance [57]

Measures to mitigate market risk require guarantee on the price and the amount of electricity purchased. While those measures are widely used in regulated market they are used in liberalised market under many restrictions.

At the end of the day, the risk is shifted to the consumer and/or taxpayer, away from the investors.

- Long term power purchase agreement (PPA) [58]

Long term power purchase agreements are typically take-or-pay contract where a purchaser (host government, large energy intensive use company...) agrees to take a certain volume of electricity at a given price covering the cost of the project plus margin. Sovereign guarantees are an additional protection against the purchaser default.

A non-exhaustive list of countries applying such mechanism are: Turkey (Akkuyu and Sinop project), United Arab Emirates (Barakah project), Canada (refurbishment of Bruce A 3&4), France (Flamanville project)...

- Contract for difference (cfd)

A CfD is "a contract between two parties, typically described as "buyer" and "seller", stipulating that the seller will pay to the buyer the difference between the current value of an asset and its value at contract time (if the difference is negative, then the buyer pays instead to the seller). In effect CfDs are financial derivatives that allow traders to take advantage of prices moving up (long positions) or prices moving down (short positions) on underlying

financial instruments and are often used to speculate on those markets" [58]

The CfD instrument has been implemented at Hinkley Point C in UK which will provide a strike price of 92,50€/MWh (2012 price) to EDF [44].

It is worth mentioning that this mechanism, implemented in a liberalised market, has been approved by the European Commission [61].

Contractual ownership structures [58]

A mean to mitigate construction risk could be achieved through contracting schemes aimed to better split the risk and responsibilities between the contractors of the project. At a cost of greater margin on the construction cost, (part of) the risk of construction may be shifted toward the vendor.

- EPC turnkey contract

An Engineering-Procurement-Construction (EPC) turnkey contract is signed between the future owner (often the investor) with the vendor (technology supplier) for building the Nuclear Power Plant turnkey [58].

Some of the advantages are minimisation of cost impact and reduced risk of overall schedule delays which are on the EPC contractor. Nevertheless, such scheme requires significant financial capabilities from the owner of the NPP. The author believes that because of the lower up-front capital requirement of SMRs, this kind of EPC contract may be eased.

- Hybrid approach [58]

As described in §0, an NPP may be split in the (1) Nuclear Island, (2) the Turbine & Generator and (3) the Balance Of Plant. The idea would be to split the EPC contract into several packages, each handled by a separate sub-contractor. The idea pursued is to diversify the risk of construction by diversifying suppliers.

An alternative would be to use a "cost reimbursable pricing" for the nuclear island that is viewed as carrying more risk (less standard components, higher quality and regulatory requirements...). The author believes that the SMRs approach may lessen that perception because of (1) modularisation & factory production, (2) standardisation and (3) series effects.

³⁷ E.g. Belgium, Germany...

Financing models

The way the contracts are settled and how the risk is spread among investors is also of key importance. Depending of the market, the government involvement may be significant.

▪ Corporate model

Utilities with strong balance sheet can finance large projects by raising equity and borrowing money (debt). Creditors may claim their loan against the company's assets as a whole.

While the advantage of such financing model is its simplicity, it is also expensive and is accessible only to a handful of corporation with broad shoulder. As discussed in §0, the author believes that the SMR approach may expand the number of private financial actors able to take part in nuclear power project (because of the lower up-front capital requirements).

An alternative exists (also known as "Project financing") where a Special Purpose Vehicle (SPV) is created which establish a legal separation from sponsors' other assets. Hence, "lenders have recourse only to the revenues and/or assets of the project" [58] which appears off-balance sheet for the project sponsors. While being burdensome for large nuclear project³⁸, the author believes that, providing power purchase agreement, the SMR approach may be more suited to such type of financing.

Government to government financing

Government involvement in the financing process of large infrastructure projects (such as NPP) is largely known as of key importance because: it reduces the associated financial burden of "mega-project". This participation may be domestic (from the host country) or from the vendor's country.

It is worth mentioning that in Europe, the European Commission accepted the claims stating that there is market failure regarding electricity generation (see §0 on merit order principle and §0 about the externalities not considered in the LCOE approach), in particular for nuclear investment [41][61]. Hence, the

European Commission endorsed the state aid scheme established for HPC and Paks II.

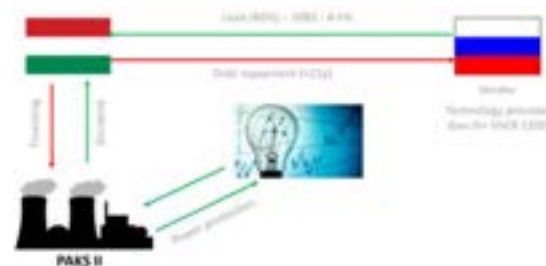
Host government involvement

The host government may participate in two non-exclusive ways: (1) direct financing of the project (capital, domestic bond issue, credits from public entities...) (e.g. Angra 3 in Brazil, Qinshan I&II in China, Paks II in Hungary...) and/or (2) financial supports (production tax credit, federal risk insurance, federal loan guarantee³⁹...).

Vendor's government involvement

State owned vendors companies⁴⁰ in countries where nuclear is part of national plan may attract investment for nuclear export. In Europe, the nuclear construction project of Paks II (Hungary), benefit from this scheme [41].

Figure 22. Paks II financing scheme



Source: Author creation from information in [41]

Technology choice

The author believes that the choice of technology itself, already significantly contribute to mitigate the regulatory risk:

- Lead-cooled technology and its ability to transmute long living nuclear waste (see §2.1.1) reduces exposure to cost escalation of nuclear waste management;
- The lower nominal power of SMRs lessen its waters access limitations which increase the confidence regarding environmental constraints;

38 Arthur D. Little helped the Swiss Nuclear New-Build Program to realize organizational readiness for the construction of two replacement plants: <http://www.adlittle.it/en/career/case-studies/organizational-structuring-swiss-nuclear-new-build-program>. In 2017, a referendum

confirmed the gradual nuclear power phase-out [73].

39 Mechanism implemented, for example, in the U.S. (Volgte) and U.K. (Hinkley Point C).

40 CNNC (China), Rosatom (Russia), EDF/AREVA (controlled by the France government), KEPCO (controlled by the South Korean government).

- The inherent safety capabilities of lead-cooled technologies, enhanced by the SMR approach, may spark a better public acceptance of nuclear energy. To paraphrase a famous nuclear scientist:

“[...] to be accepted by the public opinion, the safety principles of a nuclear reactor must be simple to explain [...]”

Dr D. Heuer, CNRS (France)⁴¹

LCOE

The Net Present Value (NPV) of the project is calculated by adding all the Free Cash Flow⁴² generated throughout the life of the project and discounted for the level of risk (or expected return) imposed by the investors (the WACC, see §0).

$$NPV = \sum_{t=1}^N \frac{FCF_t}{(1 + WACC)^t}$$

By definition, the LCOE is the Price of Electricity for which the project's NPV= 0 and it is on this base that electricity sources are compared to each other.

Reference model

Considering a corporate type of financing (see §0) where the total risk of the project is borne by private investment solely, while taking several conservative design parameters (see §0⁴³, §0⁴⁴ and §0⁴⁵) and keeping the nuclear risk premium⁴⁶. It comes:

$$LCOE_{7,3\%} = 103 \text{ USD /MWh}$$

Government involvement

As discussed in §0, the government involvement can significantly reduce financing costs (i.e. the WACC) as a side-consequence of reducing the financial burden of the project (i.e. its risk).

Considering: (1) a sovereign loan guarantee with (2) a greater leverage, (3) a modified accelerated recovery system⁴⁷ and (4) a power purchase agreement (CfD type, see §0), we have:

Table 12. Optimised financial structure, consequence of government involvement

Changed parameters	New values
Cost of equity ⁴⁸	7%
Cost of debt ⁴⁹	3%
Leverage	60% debt

It comes:

$$LCOE_{4,1\%} = 75 \text{ USD /MWh}$$

Design optimisation

When relaxing some conservatism⁵⁰ (e.g. contingencies, design life, operational performance...) which can be interpreted as a better design knowledge and/or more optimistic cost projections, we have:

Table 13. Optimised costs analysis, consequence of more optimistic projections

Changed parameters	New values
SMR operational life	60 years
Reactor Average Capacity Factor	90%
Contingencies	0 MUSD
Nuclear Steam Supply System & SMR modules	↘ 20%
Engineering and project management costs	↘ 20%

$$LCOE_{4,1\%}^{opt} = 63 \text{ USD /MWh}$$

It is worth mentioning that the vendor developing the SVBR-100, the SMR from which is inspired this study, forecast LCOE between 40-50 USD /MWh [65].

41 <https://www.youtube.com/watch?v=M4MgLixMrz8>

42 The Free Cash flows are the money available of shareholders, either for investment or dividend distribution.

43 Plant design life, operational performance, depreciation rate...

44 Regarding contingencies as an additional expense.

45 Lower end leverage ratio leading to the upper end of WACC range: 7,3%.

46 As discussed in §3.4.2, the nuclear premium may be linked to the size of large-scale nuclear project; hence, it may not be applicable to SMR projects. The premium has been conservatively kept.

47 It allows to shorten the depreciation period; hence, increasing the value of the associated cash-flow (20y instead of 35y)

48 The nuclear risk premium has been dropped (see §3.4.2) and an additional 1% reduction has been arbitrarily implemented because of the market risk suppression (CfD).

49 Because the debt repayment is backed by the government, the rate has been arbitrarily to ≈1% above the risk-free rate. The U.S., the Energy Policy Act of 2005 [72] allows to borrow from the state up to 80% of the investment of the project. Rothwell mention a rate of 3/8% above the long-term treasury bond rate for a 20 years term [25].

50 Based on data issued in [65].

Riskier markets

On the other hand, launching projects in riskier markets (such as emerging countries and remote off-grid areas) would lead to substantially higher expected returns due to geographical-related uncertainties (construction difficulties, supply chain and low productive workforce, political instabilities in the country...). Considering, arbitrarily, the following parameters:

Table 14. Project launched in riskier markets, consequence on financing costs

Changed parameters	New values
Cost of equity ⁵¹	16%
Cost of debt ⁵²	8%
Leverage	50% debt

It comes:

$$LCOE_{11\%} = 141 \text{ USD /MWh}$$

Almost twice as high as the same project (i.e. the same nuclear power plant) in favourable market with sovereign supports.

Discussion

This section benchmark competitiveness of the lead-cooled SMR with other energy alternatives while keeping reserve toward its.

▪ LCOE DOWNFALL

The LCOE projection is conditioned (i.e. sensitive) to its underlying hypotheses; hence, resulting in broad range of cost estimation when compiling the results found in the literature. Reasons for this disparity of results are wide: (1) for geographical reason (sun and wind exposure, maturity of local supply chain, labour cost, indigenous access to fossil fuel...), (2) federal supports mechanisms (e.g. influencing cost of money), (3) penalty toward greenhouse gas emission... The aim of the present study is not to challenges those underlying hypotheses but rather to provide a first guided and reasoned comparison from two different sources [62] & [66].

Additionally, it is worth keeping in mind that the LCOE is the projected cost of generating electricity up to the “the gate of the utility”. As highlighted by the Organisation for Economic Co-operation and Development (OECD) and the Nuclear Energy Agency (NEA), the full cost of electricity includes (1) system cost and (2) provision for external impacts:

Figure 23. Different cost categories composing the full costs of electricity provision

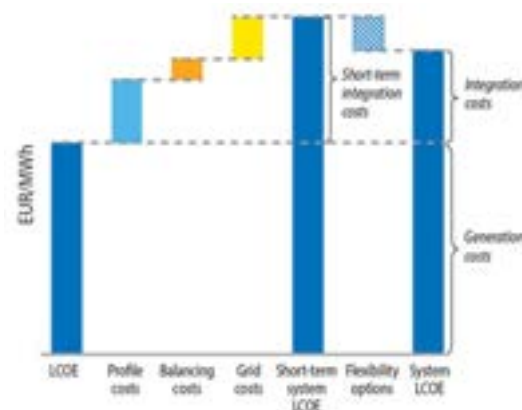


Source: reproduced from [62]

While they may be relatively high for non-dispatchable energy sources (e.g. intermittent renewable)

(15-45 USD /kWh), they are fairly low for dispatchable energy sources (coal, gas and nuclear) (< 5USD kWh) [68].

Figure 24. Illustration of system costs approach



Sources: from [62]

51 The nuclear risk premium has been dropped (see §3.4.2) and an additional 1% reduction has been arbitrarily implemented because of the market risk suppression (CfD).

52 Because the debt repayment is backed by the government, the rate has been arbitrarily to ≈1%

above the risk-free rate. The U.S., the Energy Policy Act of 2005 [72] allows to borrow from the state up to 80% of the investment of the project. Rothwell mention a rate of 3/8% above the long-term treasury bond rate for a 20 years term [25].

Finally, external costs may include: (1) climate change impact (greenhouse gas emission (e.g. CO₂)), (2) air pollution (NO_x, SO_x, micro-particles, radio-nuclides...), (3) major accidents (water-dam break, nuclear disaster, ground mine collapse, explosion and fossil fuel-related fire...), (4) land-use and natural resource depletion and (5) security of energy and electricity supply. Nuclear energy appears in the lower range for each of those cost categories [67][68].

▪ Lazard's study (US)

It appears from Lazard study [66] that lead-cooled SMRs may be competitive in the U.S. with large scale Pressurised Water Reactors. The main reason being the issues associated with the current constructions (see §0). While the costs projected in the present study are of NOAK, meaning that (1) the reactor is fully licensed, (2) detailed design is frozen and (3) the supply chain is mature. Which was not the case when the Westinghouse's AP1000 reactors started construction; hence, inflating its cost [69].

Moreover, in a corporate-type finance model, lead-cooled SMRs are not competitive with Gas Combined Cycle (GCC) but are, providing government involvement (that may be justified because of CO₂ emission concern for example).

Additionally, the studied SMR fits in the range of coal-based generating asset and offshore wind but does not compete with onshore wind and utility-scale solar assets in south (i.e. sunny regions (<60USD /MWh).

Finally, in remote areas with no access to the electricity grid or gas network, riskier projects appear to substantially outperform diesel reciprocating engines (>200USD /MWh), the typical electricity generating asset of such isolated regions.

▪ IEA & NEA study (OECD)

It appears from IEA and OECD/NEA study [67] that, at same discount rate (7%), lead-cooled SMRs (1) compete in the upper range of nuclear technologies, (2) fit in the range of fossil-fuelled generating assets (coal and gas) and (3) outperform intermittent renewable energies except for onshore wind.

It is worth mentioning that those conclusions results from world-wide analyses; hence,

obscuring regional variations and at a more granular level, it appears that:

- Lead-cooled SMRs is not competitive with water reservoir in Brazil;
- Lead-cooled SMRs does not meet parity with large scale pressurised nuclear water reactor in China and Korea, Known to have benefited from an uninterrupted construction program in the recent decades;
- Lead-cooled SMRs outperform gas plants in all OECD countries except for the U.S.A., Known to have large cheap indigenous reserves of shale gas.

Financial statements

The complete financial statements covering the 44 years of construction and operating life of the plant is displayed in Appendix A.

Income statement

The income statement reports the company's financial performance of a specific accounting period [74].

▪ Hypotheses

- Contribution to cost of goods (fuel), labour (O&M) and general expenses (such as D&D provision) are spread equally between modules;
- Values are expressed in constant 2017 dollar;
- Depreciation is linear over 35 years;
- Financial costs are calculated based on the debt rate of 4,2%;
- Negative treasury is financed by debt at a rate of 4,2%;
- No credit has been given to treasury⁵³;
- Losses are accumulated to benefit from tax rebate;
- Tax rate is constant and set to 25,51⁵⁴%.

▪ Analysis

Reactor starts operation the fourth year with a first turnover of 362 MUSD annually and reach full power the following year with a total turnover of almost ½ BUSD annually.

53 Either the bank interest rates are almost null or negative [39], distributed as dividend or are reinvested (see §0).

54 See §3.4.1.

A net positive operating income is reached on the first year of operation; 4 years after the begin of construction.

Gross margin is relatively important (>80%) which is typical of nuclear power assets.

Balance sheet

The balance sheet reports the company's assets, liabilities and shareholders' equity at a specific point in time [75].

- Hypotheses
 - Tangible assets are investments minus depreciation;
 - Nuclear core is refuelled once each 18 months and 1/3 of the core is replaced. Stocks correspond to the fuel stored in prevision of the next refuelling;
 - Clients pay their bill under one month;
 - Construction is financed 40% by debt and 60% by equity;
 - Suppliers are paid under one month.

- Analyses

Assets are built in two times; first because of the investment and the construction of the plant, reaching 2,8 BUSD (when accounting for depreciation) then because of the huge amount of cash generated by the electricity production: total reserves reaches **11 BUSD** at the end of commercial operation.

Rem: reserve does not decrease afterward because cost of Decontamination and Decommissioning (D&D) has already been provisioned during operational life of the plant (see §0).

Financing table

The financing table displays cash and cash-equivalents being transferred into and out of a business [76].

- Hypothesis

Long term debts are repaid under 21 years after being contracted.

- Analyses

The project generates net positive cash flow on the second year after start of commercial operation; which is 3 years after beginning of construction⁵⁵.

Change in working capital is fairly low.

Net cash flow rises as high as 400 MUSD per year when all modules are operating.

V. Conclusion

With respect to the uncertainties surrounding these estimates, the following conclusions can be drawn about SMR, nuclear projects in general and the lead-cooled technology:

SMR

- Because of the lower power output of SMRs, diseconomies of scale induce higher specific cost (USD /kWe) than conventional large-scale water reactor⁵⁶;

However, the SMR approach presents a lower financial risk due to:

- Reduced up-front total capital investment requirement; which are directly linked to the smaller size of SMR projects;
- Lowered execution risk during construction due to design simplification induced both by reduction in size of the plant and inherent safety capabilities offered by lead-cooled reactors.

Hence, this compensation should allow lead-cooled SMR to reach parity with conventional large-scale reactors in term of cost of production (USD /kWh), in markets with low or no nuclear construction record in the recent decades (Europe, North and South America, nuclear new entrants...);

Lead-cooled are expected to compete and even outperform several other sources of electricity production depending of the local market conditions, in particular for remote areas disconnected from the grid.

Nuclear projects

In parallel, because nuclear projects are capital intensive, their competitiveness heavily rely on

55 First concrete pouring. Moreover, site preparation and initial mobilisation starts sooner but require low of investment.

56 Unless proven otherwise by further design simplifications (specific footprint reduction),

economies of mass production or tremendous cost reductions because of alternative disruptive technology (such as expected from Molten Salt Reactors [70], see §6).

the rate at which capital is invested and on the timing at which cash-flows arise;

Because the cost to access capital is inherently tight to the total risk of a project, strategies exist to mitigate it and further improve the competitiveness of such project, from a government perspective the leverages are:

- Federal loan guarantees mechanically lower capital rate by lending money slightly above sovereign bond rate;
- Long term purchase agreement -such as Contract For Difference (CfD)- tackles market risk by removing the uncertainties surrounding the electricity sell prices;
- Accelerated depreciation and investment tax credit are mechanisms that improve profitability by bringing tax shields sooner in the project.

A fancy new technology should not be thought to replace experienced management team and one should be willing to invest in human resources development.

Lead-cooled technology

Federal supports are typically exclusive to infrastructures and assets that government perceive as strategic. The author believes that transmutation of long living wastes and inherent safety properties of lead-cooled reactors may back the public acceptance of such support.

VI. Recommendations for Future Study

In the continuity of the present study, it is recommended to launch complementary analyses to assess:

- The profitability of other SMRs technologies, in particular, Molten Salt technology that are claimed to be highly promising. Such study could be performed using the same methodology as detailed in the present report and re-using turnkey the excel-based model developed,
- The potential benefit of alternative energy production schemes (e.g. load following and heat application) using, for example, real option analysis.

Appendix A: Financial Statements

Acknowledgements

This report has benefitted greatly from the substantial contributions provided by colleagues at Tractebel and outside experts that I would like to thank:

Christian Pierlot, former General Manager of the nuclear entity at Tractebel, who was the first to believe in my project and sponsored me at Tractebel. Dr Geoffrey Rothwell, Principal Economist in the Division of Nuclear Development at the Nuclear Energy Agency, whose book and interviews projected me years ahead in my work. Dr Janne Wallenius, CEO of LeadCold Reactors, who gave me key insights about the analysis process I have followed. Philippe Monette, Manager of the Nuclear New Build department, who sponsored my numeric tools and connected me with relevant experts inside our organisation. Gregory Tilte, Senior Financial Advisor at Engie, whose business insights substantially helped me articulate my way of reasoning and shape my financial acumen. Michèle Auglaire, Head of Department Safety and Modelling expertise at Tractebel, who sponsored my accelerated training on lead-cooled reactor at the SCK-CEN, where I acquired a deep knowledge of the technology and connected with invaluable contacts. Alessandro Alemberti, Head of the Nuclear Science and Development Department of Ansaldo Nucleare, who helped me in my literature researches. Arnaud Meert, Head of Service Fuel Management Corporate at Engie, who advised me on the structure my methodology when I started my study from scratch. Jean-Paul Poncelet, former Belgian Minister of Energy and Director General of Foratom, who initiated me to European regulation regarding government involvement in nuclear projects and with whom I hope pursuing this path. François Gruselle, colleague who mentored me on the numeric tools I used. Bernard Dereeper, Marketing & Sales Manager of the Nuclear entity at Tractebel whose feedbacks kept me focused on striving for the highest standard in business writing.

Dr Mathias Schmit, my Professor of Finance at Solvay and promotor of my master thesis, who

has helped me build my strategy for investigating and exploiting the results of my analysis.

And last but not least, Anicet Touré, SMRs expert at Tractebel, colleague and close friend who has unconditionally supported me during this project that I have started more than a year ago now. His challenging feedbacks have brought out the best I could offer for this work. I could not tell how many times we remade the world at the coffee machine, but I am deeply convinced that the present work is my first path on our starting journey...

Nomenclature

ALFRED	Advanced Lead Fast Reactor Demonstrator
BOP	Balance Of Plant
CNNC	China National Nuclear Corporation
D&D	Decontamination and Decommissioning
EP	Electricity Price
EPC	Engineering Procurement and Construction
FOAK	First Of A Kind
HPC	Hinkley Point C
IAEA	International Atomic Energy Agency
LCOE	Levelised Cost of Electricity
SMR	Small Modular Reactor
NI	Nuclear Island
NOAK	Nth Of A Kind
NPP	Nuclear Power Plant
NPV	Net Present Value
O&M	Operation and Maintenance
PPA	Power Purchase Agreement
RPV	Reactor Pressure Vessel
T/G	Turbine & Generator
WACC	Weighted Average Cost of Capital

References

- [1] Furfari S., Politique et Géopolitique de l'énergie, 2012, Edition TECHNIP
- [2] EIA, International Energy Outlook 2017, [https://www.eia.gov/outlooks/ieo/pdf/0484\(2017\).pdf](https://www.eia.gov/outlooks/ieo/pdf/0484(2017).pdf)
- [3] Tractebel report: DDN/4NT/0027142/000/01, Characteristics and comparison of Small Modular Reactors
- [4] Tractebel report: DDN/4NT/0004598/000/00, Characteristics and Comparison of Generation IV systems
- [5] Berthélemy M., Nuclear reactors' construction costs: The role of lead-time, standardization and technological progress, (March 2014) <https://hal.archives-ouvertes.fr/hal-00956292/document>
- [6] Tractebel report: TIERSPR/4AR/0001535/000/00, International SMR and Advanced Reactor Summit, April 14-15, 2016, Atlanta, USA
- [7] Tractebel report: TIERSPR/4N/0001547/000/00, SMR Market analysis
- [8] UK National Nuclear Laboratory, "Small Modular Reactors (SMR) Feasibility study", (December 2014) <http://www.nnl.co.uk/media/1627/smr-feasibility-study-december-2014.pdf>
- [9] OECD/NEA, Current Status, Technical Feasibility and Economics of Small Nuclear Reactors, (June 2011) <https://www.oecd-nea.org/ndd/reports/2011/current-status-small-reactors.pdf>
- [10] Generation IV International Forum, "Cost estimating guidelines for generation IV energy systems", (September 2007) https://www.gen-4.org/gif/upload/docs/application/pdf/2013-09/emwg_guidelines.pdf
- [11] The University of Chicago, "Small Modular Reactors – Key to Future Nuclear Power Generation in the U.S.", (November 2011) <https://www.energy.gov/sites/prod/files/2015/12/f27/ECON-SMRKeytoNuclearPowerDec2011.pdf>
- [12] EIRP – Energy innovation Reform Project, "What will advanced nuclear power plants cost?" https://www.eenews.net/assets/2017/07/25/document_gw_07.pdf
- [13] GE Nuclear Energy Division, "Economic Assessment of S-PRISM including development and generating costs"
- [14] ELSEVIER, Nuclear Engineering and Design, "Nuclear Air Brayton Combined Cycle and Mark 1 Pebble Bed Fluoride-Salt-Cooled High Temperature Reactor economic performance in a regulated electricity market", (2017)
- [15] Canadian Nuclear Laboratories, 4th International Technical Meeting on Small Reactor (ITMSR-4), "Economics of very small modular reactors in the North", (November 2016)
- [16] Idaho National Laboratory, "Small Modular Reactor: First-of-a-Kind (FOAK) and Nth-of-a-Kind (NOAK) Economic Analysis", (August 2014) <https://inldigitallibrary.inl.gov/sites/sti/sti/6293982.pdf>
- [17] Illinois Institute of Technology, "Small Modular Reactors: Parametric Modelling of Integrated Reactor Vessel Manufacturing Within A Factory Environment – Volume 1", (August 2013)
- [18] SMR Start, "The Economics of Small Modular Reactors", (September 2014) <http://smrstart.org/wp-content/uploads/2017/09/SMR-Start-Economic-Analysis-APPROVED-2017-09-14.pdf>
- [19] Oak Ridge National Laboratory, Advanced High Temperature Reactor Systems and Economic Analysis, September 2011 <https://info.ornl.gov/sites/publications/files/Pub32466.pdf>

- [20] IAEA Nuclear Energy Series, “Financing of New Nuclear Power Plants”, (2008) https://www-pub.iaea.org/MTCD/publications/PDF/Pub1345_web.pdf
- [21] World Nuclear Association, “Nuclear Power Economics and Project Structuring”, (2017) http://www.world-nuclear.org/getmedia/84082691-786c-414f-8178-a26be866d8da/REPORT_Economics_Report_2017.pdf.aspx
- [22] IAEA Advanced Reactors Information System (ARIS), “Advances in Small Modular Reactor Technology Developments”, (2016) https://aris.iaea.org/Publications/SMR-Book_2016.pdf
- [23] IAEA Advanced Reactor Information System (ARIS) website (Last consulted 22nd October 2017): <https://aris.iaea.org/sites/LFR.html>
- [24] FOREN, “ALFRED feasibility in Romania: main outcomes of the arcadia project”, (2016)
- [25] Rothwell, G., 2015 The Economics of Future Nuclear Power: An Update of the University of Chicago’s 2004 The Economic Future of Nuclear Power
- [26] Commission des Provisions Nucléaires, Rapport annuel 2016 <https://economie.fgov.be/sites/default/files/Files/Energy/CPNucl-Rapport-2016.pdf>
- [27] ETAAMB website, http://www.etaamb.be/fr/loi-du-11-avril-2003_n2003011326.html, (Last Consulted 15th December 2017)
- [28] SYNATOM website, <http://synatom.be/fr/>, (Last Consulted 16th December 2017)
- [29] SYNATOM, Rapport annuel 2016 http://synatom.be/uploads/files/rapports/Synatom_2016_FR_web.pdf
- [30] MOORE M.A., The Economics of Novel vSMRs in the North, CNS Bulletin, Vol.38 No. 2, 2017
- [31] Wikipedia The Free Encyclopedia, International Nuclear Event Scale (INES), (Last Consulted 20th May 2018) https://en.wikipedia.org/wiki/International_Nuclear_Event_Scale
- [32] IAEA, PRIS Power Reactor Information System, (Last Consulted 20th May 2018) <https://www.iaea.org/pris/>
- [33] UxC, Fuel quantity and Cost calculator: <https://www.uxc.com/p/tools/FuelCalculator.aspx>, (Last Consulted 5th January 2018)
- [34] <http://www.world-nuclear-news.org/NN-British-MPs-question-value-of-Hinkley-Point-project-23111701.html>
- [35] <http://www.world-nuclear-news.org/NN-Olkiluoto-3-commercial-operation-rescheduled-0910177.html>
- [36] <http://www.world-nuclear-news.org/NN-EDF-confirms-Flamanville-EPR-start-up-schedule-1207174.html>
- [37] <http://www.world-nuclear-news.org/C-Westinghouse-files-for-US-bankruptcy-protection-29031702.html>
- [38] <http://www.nuscalepower.com/>
- [39] <http://www.lalibre.be/economie/conjoncture/la-bce-laisse-ses-taux-directeurs-inchanges-5901de0acd70812a65adc7bf>
- [40] Alemberti A., Ansaldo Nucleare, Lead cooled Fast Reactor Development, SCK-CEN conference (2017)
- [41] European Commission, Commission decision on the measure/aid scheme/state aid which Hungary is planning to implement for supporting the development of two new nuclear reactors at Paks II nuclear power station, S.A. 38454 – 2015/C (ex 2015/N). (March 2017)
- [42] Juha P., Fennovoima, Energy production in Nordic area and Finland, Mankala principle, project valuation and risk management. IAEA Technical Meeting on Nuclear Power Cost Estimation and Analysis Methodologies. Vienna (April 2018).
- [43] IAEA Power Reactor Information System (PRIS) website last consult (18th May 2018) <https://www.iaea.org/pris/>
- [44] National Audit Office (UK), Hinkley Point C (June 2017). <https://www.nao.org.uk/wp-content/uploads/2017/06/Hinkley-Point-C.pdf>
- [45] Jonathan Berk & Peter DeMarzo, Corporate Finance, Pearson (Fourth Edition).
- [46] Damodaran, Aswath, Equity Risk Premiums (ERP): Determinants, Estimation and Implications – The 2017

- Edition (March 27, 2017). Available at SSRN: <https://ssrn.com/abstract=2947861> or <http://dx.doi.org/10.2139/ssrn.2947861>
- [47] Fernandez, Pablo and Pershin, Vitaly and Fernández Acín, Isabel, Discount Rate (Risk-Free Rate and Market Risk Premium) Used for 41 Countries in 2017: A Survey (April 17, 2017). Available at SSRN: <https://ssrn.com/abstract=2954142> or <http://dx.doi.org/10.2139/ssrn.2954142>
- [48] Fernandez, Pablo and Aguirreamalloa, Javier and Linares, Pablo, Market Risk Premium and Risk Free Rate Used for 51 Countries in 2013: A Survey with 6,237 Answers (June 26, 2013). Available at SSRN: <https://ssrn.com/abstract=914160> or <http://dx.doi.org/10.2139/ssrn.914160>
- [49] EDF, Consolidated Financial Statements at 31 December 2012. https://www.edf.fr/sites/default/files/uploads/2012EDFGroupCptesCons_v3_va.pdf
- [50] EDF, 2013 Consolidated Financial Statements. https://www.edf.fr/sites/default/files/uploads/EDF2013_rapport_financier_comptes_consolides_va.pdf
- [51] Canadian Nuclear Laboratories, Perspectives on Canada's SMR opportunity, Summary Report: Request for Expressions of Interest (REOI) – CNL's Small Modular Reactor Strategy (2018). http://www.cnl.ca/site/media/Parent/CNL_SmModularReactor_Report.pdf
- [52] World Nuclear Association website, Small Nuclear Power Reactor, (Last Consulted 20th May 2018). <http://www.world-nuclear.org/information-library/nuclear-fuel-cycle/nuclear-power-reactors/small-nuclear-power-reactors.aspx>
- [53] D.T. Ingersoll, NuScale Power LLC, Can Nuclear Power and Renewables be Friends? (2015). http://www.nuscalepower.com/images/our_technology/nuscale-integration-with-renewables_icapp15.pdf
- [54] Locatelli et al, Cogeneration: An option to facilitate load following in Small Modular Reactors, Elsevier, Progress in Nuclear Energy (2017)
- [55] World Nuclear Association website, Nuclear Process Heat for Industry, (Last Consulted 20th May 2018). <http://www.world-nuclear.org/information-library/non-power-nuclear-applications/industry/nuclear-process-heat-for-industry.aspx>
- [56] Locatelli et al, Load following with Small Modular Reactors (SMR): A real options analysis, Elsevier, Energy (2015)
- [57] IAEA, Financing Nuclear Power in Evolving Electricity Markets, Vienna (April 2018)
- [58] IAEA, Financing NPP in evolving market – A reference book, Vienne (April 2018)
- [59] McKinsey&Company, Key success factors in cost management for nuclear new builds, Vienna (April 2018)
- [60] World Nuclear Association, Lesson-Learning in Nuclear Construction Projects, (April 2018) <http://world-nuclear.org/getattachment/e9c28f2a-a335-48a8-aa4f-525471a6795a/REPORT-Lesson-learning-in-Nuclear-Construction.pdf.aspx>
- [61] European Commission, Commission Decision of 08.10.2014 on the aid measure SA.34947 (2013/C)(ex 2013/N) which the United Kingdom is planning to implement for Support to the Hinkley Point C Nuclear Power Station http://ec.europa.eu/competition/state_aid/cases/251157/251157_1615983_2292_4.pdf
- [62] NEO/OECD, Projected Costs of Generating Electricity, 2015 Edition <https://www.oecd-neo.org/ndd/pubs/2015/7057-proj-costs-electricity-2015.pdf>
- [63] ASCPE Les Cahiers des Entretiens Européens, Les investissements dans le nucléaire en Europe – Bâtir un cadre de long terme pour la valorisation et le financement des projets (Octobre 2016) [http://www.entretiens-europeens.org/attachments/article/78/INVTATION-RR-EE-20%20OCTOBRE%202016-FRANCAIS%20\(2\).pdf](http://www.entretiens-europeens.org/attachments/article/78/INVTATION-RR-EE-20%20OCTOBRE%202016-FRANCAIS%20(2).pdf)
- [64] World Nuclear Association website, Uranium Enrichment, (Last Consulted 21th May 2018) <http://www.world-nuclear.org/information-library/nuclear-fuel-cycle/conversion-enrichment-and-fabrication/uranium-enrichment.aspx>
- [65] AKME, SVBR-100: New Generation Nuclear Power Plants for Small and Medium-Sized Power Applications. <http://www.akmeengineering.com/assets/files/SVBR->

- 100%20new%20generation%20power%20plants.pdf
- [66] Lazard, Lazard's Levelized Cost of Energy Analysis – Version 11.0 (November 2017) <https://www.lazard.com/media/450337/lazard-levelized-cost-of-energy-version-110.pdf>
- [67] World Nuclear Organisation website, Externalities of Electricity Generation, (Last Consulted 22nd May 2018), <http://www.world-nuclear.org/information-library/economic-aspects/externalities-of-electricity-generation.aspx>
- [68] OECD/NEA, The Full Costs of Electricity Provision, 2018 <https://www.oecd-neo.org/ndd/pubs/2018/7298-full-costs-2018.pdf>
- [69] <https://www.reuters.com/article/us-toshiba-accounting-westinghouse-nucle/how-two-cutting-edge-u-s-nuclear-projects-bankrupted-westinghouse-idUSKBN17Y0CQ>
- [70] Terrestrial Energy website, <https://www.terrestrialenergy.com/technology/competitive/> (Last Consulted 25th May 2018)
- [71] European Union, The Euratom Treaty – Consolidated Version, (2016) <http://www.consilium.europa.eu/media/29775/qc0115106enn.pdf>
- [72] U.S. Government, Public Law 109-58-AUG. 8, 2005, Energy Policy Act of 2005, Chapter XII, <https://www.ferc.gov/enforcement/enforce-res/EPAct2005.pdf>
- [73] World Nuclear Association website, Nuclear Power in Switzerland, (Last Consulted 30th May 2018), <http://www.world-nuclear.org/information-library/country-profiles/countries-o-s/switzerland.aspx>
- [74] Investopedia, Income Statement, (Last Consulted 30th May 2018) <https://www.investopedia.com/terms/i/incomestatement.asp>
- [75] Investopedia, Balance Sheet, (Last Consulted 30th May 2018) <https://www.investopedia.com/terms/b/balancesheet.asp>
- [76] Investopedia, Cash Flow, (Last Consulted 30th May 2018) <https://www.investopedia.com/terms/c/cashflow.asp>

The Generation IV International Forum (GIF) is a co-operative international endeavour that was set up to carry out the research and development needed to establish the feasibility and performance capabilities of the next generation of nuclear energy systems. The Generation IV International Forum has fourteen members that are signatories of its founding document, the GIF Charter. The goals adopted by GIF provided the basis for identifying and selecting six nuclear energy systems for further development. The selected systems are based on a variety of reactor, energy conversion and fuel cycle technologies. Their designs include thermal and fast neutron spectra cores, as well as closed and open fuel cycles. The reactors range in size from very small to very large. Depending on their respective degree of technical maturity, the first GEN IV systems are expected to be deployed commercially around 2030-2040.

The GIF Symposia are public scientific events aimed at disseminating the results of international collaborative research performed within the Forum. The first GIF Symposium was held in Paris, France in 2009, the second in San Diego, United States in 2012 and the third in Chiba, Japan in 2015. This fourth GIF Symposium, held in Paris on 16-17 October 2018, is designed to inform and educate audiences beyond the GIF community. Its objective is to report the achievements of the Forum in developing nuclear energy systems that are aligned with today's global sustainable development goals. In particular, the fourth GIF Symposium outlines a credible GIF path towards achieving the goals of the updated GIF R&D Roadmap, leading to the demonstration and deployment of innovative nuclear energy systems that will establish nuclear energy as a valuable part of the global, long-term sustainable carbon-free energy mix.